UNIVERSITÉ DU QUÉBEC

THÈSE PRÉSENTÉE À
L'UNIVERSITÉ DU QUÉBEC À TROIS-RIVIÈRES

COMME EXIGENCE PARTIELLE DU
DOCTORAT EN GÉNIE PAPETIER

PAR
RUIJUN GU

MECHANICAL PROPERTIES AND MICROSTRUCTURES FORMATIONS OF WOOD THERMOPLASTIC COMPOSITES/ PROPRIÉTÉS MÉCANIQUES ET FORMATIONS DES MICROSTRUCTURES DANS LES COMPOSITES BOIS-THERMOPLASTIQUES

JUIN 2010

UNIVERSITÉ DU QUÉBEC À TROIS-RIVIÈRES

DOCTORAT EN GÉNIE PAPETIER (PH.D.)

Programme offert par l'Université du QUÉBEC À TROIS-RIVIÈRES

MECHANICAL PROPERTIES AND MICROSTRUCTURES FORMATIONS OF WOOD THERMOPLASTIC COMPOSITES/PROPRIÉTÉS MÉCANIQUES ET FORMATIONS DES MICROSTRUCTURES DANS LES COMPOSITES BOIS-THERMOPLASTIQUES

PAR

RUIJUN GU

Bohuslav V. Kokta, directeur de recherche	Université du Québec à Trois-Rivières
Daniel Montplaisir, président du jury	Université du Québec à Trois-Rivières
Kwei-Nam Law, évaluateur	Université du Québec à Trois-Rivières
Bernard Riedl, évaluateur externe	Université Laval

Thèse soutenue le 16 juin 2010

Part A: General Declaration

Université du Québec à Trois-Rivières

Declaration for thesis based on conjointly published/unpublished/ submitted works

General Declaration

In accordance with Université du Québec à Trois-Rivières Doctorate Regulation 138 (Rédaction sous forme d'articles scientifiques) the following declarations are made:

I hereby declare that this thesis contains no material which has been accepted for the award of any other degree or diploma at any university or equivalent institution and that, to the best of my knowledge and belief, this thesis contains no material previously published or written by any other person except where due acknowledgement has been made in the text of the thesis.

This thesis includes five original papers published in peer reviewed journals, and eight refereed proceeding articles & posters, three unpublished publications, and two submissions. The core theme of the thesis is how to achieve high impact strength of wood plastic composite reinforced with nanofillers. The ideas, development and writing up of all the papers in the thesis were the principal responsibility of myself, the candidate, working within the department of chemical engineering under the supervision of Prof. B.V. Kokta.

In the case of chapter 3-12 my contribution to the work involved the following:

Chapter	Publication title	Publication status	Candidate's contribution
Chapter 3	Effect of Independent Variables on Mechanical Properties and Maximization of Aspen-Polypropylene Composites	Published	100%
Chapter 4	Maximization of the Mechanical Properties of Birch-Polypropylene Composites with Additives by Statistical Experimental Design	Published	100%
Chapter 5	Effect of Variables on the Mechanical Properties and Maximization of Polyethylene-Aspen Composites by Statistical Experiment Design	Published	100%
Chapter 6	Optimization of Mechanical Properties of PE Composites via Central Composite Design and Deposition Formation of Nanofiller	Published	100%
Chapter 7	Mechanical Properties of PP composites Reinforced with BCTMP Aspen fiber	Published	100%
Chapter 8	Effects of Coupling agent, Initiator and Nanofiller on the Properties of Polyethylene Composites	Prepared	100%
Chapter 9	Effect of Antioxidant and Initiator on the Mechanical Properties of Polypropylene-Aspen Composites	Published	100%
Chapter 10	Water behaviors and Mechanical Characteristics of Wood Plastic Composites Reinforced with Organo-Nanoclays	Published	100%
Chapter 11	Morphological Structures and Functionalization of Wood fiber in Wood Plastic Composites	Submitted	100%
Chapter 12	Bacterial cellulose reinforced thermoplastic composites: Fabrication and performance evaluation	Accepted	100%

I have renumbered sections of submitted, unpublished or published papers in order to generate a consistent presentation within the thesis.

Signed: 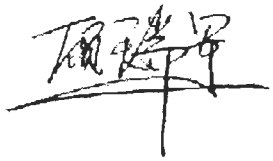 .....Date:.....27 February 2010

Part B: Suggested Declaration for Thesis Chapter

Université du Québec à Trois-Rivières

Declaration for Thesis Chapter 3-11

Declaration by candidate

In the case of Chapter 3-12, I'm the first author on the papers which submitted, published or in press. I'm confident that both Composites Part A and Journal of Reinforced Plastics and Composites would accept the papers. I can claim credit to 100% of the work since I undertook the experimental and data analyses that are reported in the papers. I also wrote the initial drafts of the manuscripts. No other authors will be submitting these works as parts of my thesis submissions and publications, with the exception of UQTR who will be including the pedigree workup and analysis in my thesis. The study was conceived and conducted under the supervision of Prof. Kokta. To date, my director and I have indicated that I would to submit the manuscripts and my publications as parts of my Ph.D.

Candidate's Signature 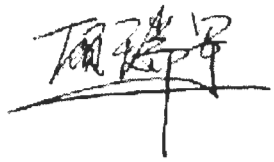 **Date** 27 February 2010

Declaration by director & co-author

The undersigned hereby certify that:

The above declaration correctly reflects the nature and extent of the candidate's contribution to this work;

He meets the criteria for authorship in that he has participated in the conception, execution, or interpretation, of at least that part of the publications in his field of expertise;

He takes public responsibility for his part of the publications, except for the responsible author who accepts overall responsibility for the publications;

There are no other authors of the publication according to these criteria;

Potential conflicts of interest have been disclosed to (a) granting bodies, (b) the editor or publisher of journals or other publications, and (c) the head of the responsible academic unit; and

The original data are stored at the following location(s) and will be held for at least five years from the date indicated below:

Location(s)

Integrated Pulp and Paper Center
Pulp and Paper Research Center
Department of Chemical Engineering
University of Quebec at Trois-Rivieres

B.V. Kokta 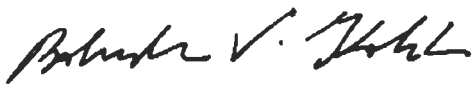 **Date** 27 February 2010

List of Realizations

Refereed journal paper 1

Ruijun Gu and B.V. Kokta. Effect of Independent Variables on Mechanical Properties and Maximization of Aspen-Polypropylene Composites. Journal of Thermoplastic Composite Materials. 2008, 21(1): 27-50.

Refereed journal paper 2

Ruijun Gu and B.V. Kokta. Effect of Antioxidant and Initiator on the Mechanical Properties of Polypropylene-Aspen Composites. Journal of Thermoplastic Composite Materials. 2008, 21(2): 175-189.

Refereed journal paper 3

Ruijun Gu, B.V. Kokta and Gabriela Chalupova. Effect of Variables on the Mechanical Properties and Maximization of Polyethylene-Aspen Composites by Statistical Experiment Design. Journal of Thermoplastic Composite Materials. 2009, 22(6): 633-649.

Refereed journal paper 4

Ruijun Gu and B.V. Kokta. Maximization of the Mechanical Properties of Birch-Polypropylene Composites with Additives by Statistical Experimental Design. Journal of Thermoplastic Composite Materials. 2010, 23(2): 239-263.

Refereed journal paper 5

Ruijun Gu and B.V. Kokta. Mechanical Properties of PP composites Reinforced with BCTMP Aspen fiber. Journal of Thermoplastic Composite Materials. 2010, 23(4): 513-542.

Referred journal paper 6

Ruijun Gu, B.V. Kokta, D. Michalkova, B. Dimzoski, I. Fortelny, M. Slouf and Z. Krulis. Characteristics of Wood Plastic Composites Reinforced with Nanoclays. Journal of Reinforced Plastics and Composites. JRP-10-0178. In press.

Referred journal paper 7

Ruijun Gu, B.V. Kokta and K. Law. Optimization of PE Composites and Deposition Formation of Nanoclay Particles. Journal of Composite Materials. JCM-10-0215. Accepted.

Referred journal paper 8

Ruijun Gu, B.V. Kokta, Katrin Frankenfeld and Kerstin Schlufter. Bacterial cellulose reinforced thermoplastic composites: Fabrication and performance preliminary evaluation. BioResources. #1071. Accepted.

Refereed proceedings 9

Ruijun Gu, B.V. Kokta and Kwei-Nam Law. Optimization of Mechanical Properties of PE Composites via Central Composite Design and Deposition Formation of Nanofiller. 24th ASC conference, 15-17 September 2009, Newark, DE, USA. #312.

Refereed proceedings 10

Ruijun Gu and B.V. Kokta. Water behaviors and Mechanical Characteristics of Wood Plastic Composites Reinforced with Organo-Nanoclay. 96th PAPTAC. Montreal, Canada. 2-3 Feburary 2010: D126-D136.

Refereed proceedings 11

Ruijun Gu, B.V. Kokta and G. Chalupova. Effect of Variables on the Mechanical Properties and Maximization of Polyethylene-Aspen Composites by Statistical Experiment Design. 94th PAPTAC. Montreal, Canada. 5-7 February 2008: A77-A82.

Submission 12

Ruijun Gu and B.V. Kokta. Functionalized Wood fiber in Wood Plastic Composites: Evaluation of Morphological Structures via FQA and SEM (Part 1). Journal of Applied Polymer and Science. Preparation.

Submission 13

Ruijun Gu and B.V. Kokta. Functionalized Wood fiber in Wood Plastic Composites: Evaluation of Esterification via FTIR and XPS (Part 2). Journal of Applied Polymer and Science. Preparation.

Submission 14

Ruijun Gu and B.V. Kokta. Effects of Coupling agent, Initiator and Nanofiller on the Properties of Polyethylene Composites. Journal of Composite Materials. Preparation.

List of Additional Realizations

Scientific posters

Ruijun Gu, B.V. Kokta and Kwei-Nam Law. Optimization of Mechanical Properties of PE Composites via Central Composite Design and Deposition Formation of Nanofiller. APMA-AUTO21 Annual Conference and Exhibition and HQP Poster Competition, 26-28 May 2009, Hamilton, Ontario, CANADA. (Poster)

Ruijun Gu and B.V. Kokta. Mechanical properties of PP hybrid nanocomposites reinforced with Bleached Aspen CTMP fiber. 10th International Conference on Wood & Biofiber Plastic Composites. 11-13 May 2009, Madison, USA. (Poster)

Ruijun Gu and B.V. Kokta. Effects of Coupling agent, Initiator and Nanofiller on the Properties of Polyethylene Composites. Scientific contest of posters of UQTR 2008. (Poster)

Ruijun Gu and B.V. Kokta. Effect of Independent Variables on Mechanical Properties and Maximization of Aspen-Polypropylene Composites. 6th International Symposium "Materials made of Renewable Resources". Erfurt, Germany. 6-7 September 2007. (Poster)

Acknowledgements

This Ph.D. dissertation is based on experimental and theoretical work carried out at the Department of Chemistry Engineering, UQTR and at the Centre de recherche en pâtes et papiers, UQTR.

I would like to express my best sincere thanks to my supervisor Prof. B.V. Kokta. This work has been carried out under his supervision and I'm very grateful for all his guidance and his permissions for conference attendance during my works and studies at the UQTR. I also thank to Prof. Bernard Riedl for his professional translation and corrections, Dr. Kwei-nam Law for helping and Prof. Claude Daneault for leading the efforts and creating an uncomplicated environment to conduct the research. I thank all committee members from the bottom of my heart for their suggestions, supporting and understandings. I also wish to thank the Centre de recherche en pâtes et papiers and its staff for their assistance.

I would like to thank Dr. Ivan Fortelny at the Institute Macromolecular Chemistry, Czech for help with impact measurements and TEM & SEM images, and Ms. Agnès Lejeune at UQTR for help with the SEM and XPS observations. I also thank Ms. Isabelle Boulan and Mr. Michel Paquin for their support throughout my work and studies.

The financial support from the Natural Science and Engineering Research Council of Canada (NSERC), Fonds Nature et Technologie du Québec (FQRNT), AUTO21 NCE, Foundation de l'UQTR, Kruger Inc. and Canadian Association for Composite Structures and Materials is really appreciated. NOVA chemicals, Phillips Sumika Polypropylene Company, and Research Center of Medical Technology and Biotechnology (fzmb, GmbH, Bad Langensalza, Thüringen, Germany) are also appreciated for their materials donations.

Finally, I truly thank my wife for her support during my studies and also honor my son and my daughter for their sweetness.

Summary

Currently, much effort has been undertaken to replace glass fibers with wood fibers to reinforce thermoplastic composites in order to produce biomaterials. In this study, four wood fibers, namely CTMP birch, CTMP aspen fiber, BCTMP aspen fiber and bacterial cellulose, were employed as reinforcement materials in polypropylene or polyethylene matrix. The most important problem encountered with wood composites is the inherent incompatibility between hydrophilic fiber materials and hydrophobic polymer matrices. Chemical coupling plays an important role in improving interfacial bonding strength in wood composites. In this study, the effects of coupling agent type and structure, graft polymerization of coupling agents and coupling process on chemical coupling were investigated. Coupling mechanisms were established both for maleated PP and maleated PE. In addition, the effect of the initiator on resulting strength was also investigated.

Surface treatments of wood fibers were carried out with two kinds of maleated polyolefins: MAPE and MAPP. The blending time as well as the addition sequence of wood fiber and initiator was optimized. Maleated coupling agents were compounded with wood fiber during melt blending. The composites were prepared in a standard mold equipped with rollers, an adjustable temperature oil bath and a changeable mixing rate. The composites were prepared at a variable temperature, with 170°C for PE and 190°C for PP, 60rpm mixing rate and an optimium blending time.

It was found that the composite could achieve optimum impact strength without weakening tensile strength after compounding 30-35min. In addition, the bulk mixing method (no-premixing method) could lead to superior impact and tensile strength compared to pre-mixing method with wood fiber pre-coated by the mixture of the maleated polymer and small amount of polymer matrix. The addition sequence of DCP at final-step is the best method to achieve higher impact strength without tensile strength decrease for wood composite due to the difference in the oxidation and grafting reaction time in presence of initiator.

It is well known that the mechanical properties of wood composites were significantly enhanced by employment of coupling agents and affected by their characteristics. However, the properties deteriorated with excess coupling agent employment due to its entanglements and slippages. The optimum concentration of

coupling agent was found to be 3wt% for wood composites which was reinforced with 30wt% wood fiber and 0.2wt% DCP.

Wood fiber showed different strength behaviors in incompatibilized and compatibilized systems. Generally, both impact and tensile strength decreased with an increase of wood fiber content without compatibilizer presented. Oppositely, the strength was improved in the presence of a compatibilizer as wood fiber concentration increased due to the increased bonding on more reactive sites. The extent of interfacial interactions was evaluated with the addition of 1wt% bacterial cellulose exhibiting superior impact strength based on traditional wood composites.

It was an interesting finding that the introduction of NC at low content (<2wt%) could increase the impact and tensile strength of both polymeric nanocomposites and wood composites, but weakens the strength at high content (up to 20wt%). Different organo-NC exhibited different behaviors due to the different nature of surfactants, and the differences would be magnified after the system was compatibilized by coupling agent and initiator. Moreover, natural NC led to better performance than concentrates-NC as well as other modified NC except I.34TCN which has reactive pendant groups –OH ready to react with coupling agent.

It was also found that initiator-DCP showed a positive effect on PE composites but negative effect on PP ones.

In another study, moisture uptake, water uptake and water loss of the composites were evaluated. It was found that moisture uptake, water uptake and water loss of the composites decreased with employment of coupling agent due to the interfacial adhesion improvement and hydrophobic polymer deposition on fiber surface leading the decrease of void fractions and penetrating channels blocked. Moreover, NC would improve the water resistance and water loss property of wood composites via the actions of blocking and bulking, which was a function of NC amount and its surface modification by surfactant. Surfactants play an important role by their morphological structures as well as chemical reactions, and are also a source of wood composites anti-discoloration. Considering the strength and water behaviors, I.34TCN modified by ammonium with 2 hydroxyl groups was the best ones as well as natural NC.

Stress-strain behavior of PE nanocomposites was studied. Comparing the changes of stress-strain curves of the materials based on PE, the effects of wood fiber, coupling agent and initiator on the morphologies were predictable. Normally, the

compatibilized composites became more brittle as wood fiber and NC were introduced while the compatibilizer showed converse effects in the presence of wood fiber, showing high modulus with fiber addition.

Considering the importance of chemical coupling, the chemical changes were systemically illustrated by FQA, SEM, FTIR and XPS.

FQA and SEM were used to monitor the morphological changes of wood fiber and their fracture modes. In addition, FTIR and XPS analyses revealed the decrease in hydrophilicity of wood fiber with maleated polyolefin treatments and new bond formation with employment of coupling agent because of chemical bonding occurring at the interface.

For melt-blending process, driving and shear force were applied to wood composites. The interfacial morphology was illustrated with the break-off, cracking, curling, extruding, twisting, fibrillations, and pinwheels models. The changes of the morphologies were mainly related to the characteristics of the matrix and maleated polymer, where PE and/or MAPE could functionalize wood fiber more efficiently than PP and/or MAPP while exhibiting shorter and serious fractures. The morphologies were also related to the Mw of maleatd polymer and their amounts which were evidenced by FQA and SEM analyses.

The interfaces among the composites displayed covalent bonding formed by esterification and carbon-carbon bonding, strong secondary bonding (e.g. hydrogen bonding), macromolecular chain entanglement, and mechanical interblocking. With FTIR analysis, the evidence of chemical bonds at the interface was confirmed. The performances of maleated coupling agents were mainly related to their Mw, maleic anhydride groups, backbone structure, and concentration. For coupling agents, both MAPP and MAPE with large Mw were preferred because of better performance at the interface. Based on the entirely bonded experimental results, maleic anhydride graft has an important impact on the esterification reaction, where high MA% formed high chemical bonding capacity. However, MAPE has higher reactivity than MAPP after normalization at the same MA% level. Unlike in entirely bonded experiments, the results of partly bonded experiments indicated that the amount of coupling agent had impact on the formation of chemical bonding at an optimal concentration. For both MAPP and MAPE, the reactive efficiency decreased if excess coupling agent was employed.

The chemical reactions between maleated polyolefins and wood fibers in a blender process were also determined by XPS with the goal to evaluate the grafting efficiency and the formation of ester links. First, the modified and extracted wood fibers were similar compared to initial wood fiber, which implied their similarities in surface morphologies. But the changes of the carbon and oxygen concentration varied as a function of the sampling depth which indicated its inhomogeneous structure-fractional coated structure. A little difference of binding energy as well as the concentration of oxygen and carbon among bonded fiber was found as a function of depth profiles. Significant difference in surface elemental compositions of the bonded fibers evidenced the occurrences of ester bonds by increasing the O/C ratio. The high resolution spectra of C1s gave us more information on the type of bonding formed and also used to determine hydroxyl index, carbonyl index, grafting index as well as $C_{ox/unox}$ effect on the reactive efficiency, even the depositions of maleated polymer led to the chemical shifts of oxygen upward and all deconvoluted C1s downward. XPS results also proved the difference in maleic anhydride resulting in the modified fiber with different kind of oxygen-carbon bonds. High MA% maleated polymer achieved high oxygen-carbon bonds compared to low ones. Still, MAPE could accomplish superior reactivity in contrast to MAPP after normalizing at the same level by comparison of hydroxyl index, grafting index as well as carbonyl index calculated by XPS.

There was also an interesting finding that the shake-up effect of surface lignin was eliminated after maleated polymer was employed regardless of the type and MA% of maleated polymer used as well as the fact that the nitrogen band was missing. As an engineering material, wood composites reinforced with CTMP wood fiber could achieve good performance due to rich surface coverage by lignin and extractives which acted as internal lubricant and natural antioxidant during high temperature process.

Keywords: FQA, FTIR, Impact strength, Tensile strength, Maleated polymer, Mechanical properties, Polymeric nanocomposites, Polyolefin, SEM, Water loss, Water uptake, Wood composite, Wood fiber, XPS

Résumé

Actuellement, un effort particulier a été entrepris afin de remplacer les fibres de verre par de la fibre de bois et améliorer les points techniques qui accélèrent le développement des matériaux composites thermoplastiques avec fibres naturelles afin de produire des biomatériaux. Dans cette étude, quatre fibres ont été utilisées comme renfort des composites à matrices de polypropylène ou de polyéthylène: il s'agit des fibres de CTMP (pulpe chimico-thermo-mécanique) de bouleau, CTMP et BCTMP (pulpe blanchie-chimico-thermo-mécanique) de tremble et de cellulose bactérienne. Le plus important problème rencontré dans ces composites est l'incompatibilité inhérente entre les fibres hydrophiles et les matrices de polymère hydrophobe. Le couplage chimique joue un rôle important dans l'amélioration des liaisons covalentes et autres à l'interface dans les bois composites, ce qui devrait améliorer les propriétés. Les effets de type et structures d'agent de couplage, le greffage polymère d'agents de couplage et le couplage chimique ont fait l'objet d'une enquête dans nos études.

Les traitements de surface de fibres de bois ont été effectués avec deux types de maléate de polyoléfines: le maléate de polypropylène (MAPP) et le maléate de polyéthylène (MAPE), lesquels sont des agents de couplage, donc des agents compatibilisants ou émulgateurs. Le temps de mélange ainsi que la séquence d'ajout de fibres de bois et de l'initiateur ont été optimisés. Les maléates ont été ajoutés à la fibre de bois suite à la fonte du mélange. Les matériaux composites ont été préparés dans un moule standard équipé de rouleaux, d'un bain d'huile de température réglable et à taux de mélange variable. Les matériaux composites ont été préparés à une température variable, soit à 170°C pour le PE et 190°C pour le PP, à 60rpm, à des taux de mélange et un temps de mélange optimal. Il a été trouvé que le composite pourrait atteindre une résistance aux chocs optimale sans affaiblir sa résistance à la traction après environ 30-35 minutes de malaxage (compounding en anglais). De plus, la méthode de mélange en vrac (sans pré-mélangeage) conduit à une résistance à l'impact et une résistance à la traction supérieures comparé à la méthode avec mélange préalable de la fibre de bois pré-enduite de polymères maléatés et une petite quantité de la matrice polymère. La séquence d'ajout du peroxyde de dicumyle (DCP) à l'étape finale est la meilleure méthode pour obtenir la résistance aux chocs la plus élevée sans diminution de résistance en tension pour les composites en raison

de la différence dans le temps de la réaction d'oxydation et de greffage en présence d'initiateur.

Il est bien connu que les propriétés mécaniques des composites de fibres de bois sont considérablement augmentées par l'emploi d'un agent de couplage et affectées par leurs caractéristiques. Les propriétés ont été détériorées avec la présence excessive d'agent de couplage employé en raison des enchevêtrements et de la lubrification. Il est à noter que la concentration optimale pour l'agent de couplage a été à 3% en poids pour la polyoléfine maléatée dans des composites renforcés avec 30% en poids de fibre de bois et 0.2% en poids de DCP.

La fibre de bois a montré des contributions différentes à la force de résistance dans les systèmes compatibilisés et non-compatibilisés. Généralement, la résistance à l'impact et à la traction diminuent avec l'augmentation du contenu en fibres sans compatibilisation. La résistance a été améliorée en présence d'agents compatiblisants lorsque la concentration de la fibre de bois a augmenté en raison de l'augmentation des liaisons sur des sites réactifs L'ampleur des interactions interfaciales a été évaluée suite à l'addition de 1% poids de cellulose bactérienne ce qui a entraîné une résistance à l'impact supérieure comparativement à celle des composites traditionnels.

Il était un intéressant de constater que l'introduction de la nano-argile (NC) à bas contenu (<2% poids) augmente la résistance à l'impact et à la traction des nanocomposites polymères et des composites de fibres de bois, mais affaiblit leur résistance mécanique à un contenu élevé (jusqu'à 20% poids). Différents NC modifiés à l'aide de surfactants organiques montrent différents comportements dus à la nature différente des surfactants, et ces différences sont amplifiées après que les systèmes aient été compatibilisés par l'agent de couplage et l'initiateur. De plus, la NC non-modifiée conduit à de meilleures performances que la NC sous forme de concentré ainsi que l'autre NC modifiée sauf la variété I.34TCN qui a des groupements réactifs latéraux –OH prêts à réagir avec l'agent de couplage.

On a également constaté que l'initiateur (DCP) a montré un effet positif sur le composite à base de PE mais négatif sur ceux à base de PP.

Dans une autre étude, le contenu en humidité, l'absorption et la désorption d'eau des composites ont été évalués. Il été trouvé que le contenu en humidité, l'absorption et la désorption d'eau ont diminué avec l'emploi d'agents de couplage en raison de l'adhérence interfaciale améliorée et le caractère hydrophobe des polymères déposés

sur les surface des fibres, ce qui conduit à une diminution des fractions de vides ou pores et les blocages des canaux et capiullaires. D'ailleurs, le NC améliorerait la stabilité dimensionnelle des composites de fibre de bois via des actions de blocage et d'empêchement stérique, qui était une fonction de la quantité de NC et sa modification de surface par des surfactants. Il convient de noter que les surfactants jouent un rôle important de par leurs structures morphologiques aussi bien que suite à leurs réactions chimiques, et sont aussi une source de anti-décoloration de composites de fibres de bois. Considérant les résistances des composites et leur stabilité dimensionnelle, le I.34TCN modifié par le groupement ammonium avec 2 groupes hydroxyles aussi bien que la NC naturelle non-modifiée sont les meilleures.

Le comportement en tension-élongation de nanocomposites à base de PE a été étudié. Comparant les changements des courbes de tension-élongation des matériaux à base de PE, les effets de la fibre de bois, de l'agent de couplage et de l'initiateur sur les morphologies étaient clairs. Normalement, les composites deviennent plus fragiles lorsque la fibre de bois et la NC sont introduites dans le composite tandis que l'agent compatiblisant a montré l'effet inverse en présence de fibre de bois, en augmentant le coefficient modulo.

En raison de l'importance du couplage chimique, les changements chimiques ont été systématiquement caractérisés par les mesures de distribution de taille des fibres (FQA), la microscopie électronique à balayage (SEM), la spectroscopie infrarouge à transformée de Fourier (FTIR) et la spectroscopie des photoélectrons (XPS).

Le FQA et la SEM ont été utilisés pour suivre les changements morphologiques de la fibre de bois et leurs modes des ruptures. En outre, les analyses FTIR et XPS ont révélés l'augmentation du caractère hydrophobe de la fibre de bois traitée aux polyoléfines maléatées et la nouvelle formation de liens créés par l'agent de couplage suite à la formation de liaisons chimique à l'interface.

Pendant les processus de mélange et mise en forme à l'état fondu, des forces des cisaillements sont été appliquées aux composites de fibres de bois. La morphologie interfaciale est illustrée avec les modes des ruptures, des fissurations, des extrusions, des torsions et des fibrillations. Les changements des morphologies ont été principalement liés aux caractéristiques de la matrice et du polymère maléaté, où le PE ou MAPE pouvaient fonctionnaliser la fibre de bois plus efficacement que le PP ou le MAPP lesquels ont donné des fractures plus courtes et importantes. Il convient de noter que les morphologies ont été également liées aux masses moléculaires des

agents couplants et leurs quantités ajoutées ce qui a été mis en évidence par les analyses de FQA et SEM.

Les interfaces dans ces composites comportent des liaisons covalentes, dues à l'estérification et aux liens carbone-carbone, des liaisons secondaires fortes (liaisons hydrogènes), des enchevêtrements des chaînes polymères, et une adhésion mécanique. Les analyses FTIR viennent démontrent l'existence de liens chimiques entre les surfaces. Les performances des agents de couplage, donc des polymères maléatés, sont liées principalement à leur masse moléculaire (Mw), leur contenu en anhydrides, leur structure de chaîne principale, et leur concentration. Les agents de couplage MAPP et MAPE avec grandes masses molaires, M_w, ont une meilleure performance au niveau de l'interface. Basé sur les résultats expérimentaux, le greffage de l'anhydride maléique (MA%) a un impact important sur l'estérification, où le MA% le plus élevé à donné le plus de liaisons chimiques. Cependant, le MAPE a une réactivité plus élevée que celle du MAPP après une normalisation au même niveau de MA%. Les résultats des mesures sur les surfaces partiellement liées ont indiqué que la quantité d'agent de couplage a un impact sur la formation de la liaison chimique à une concentration optimale. Pour les MAPP et MAPE, l'efficacité de la réaction a diminué si trop d'agent de couplage est employée.

Les réactions chimiques entre les polyoléfines maléatées et les fibres des bois pendant le processus du mélange ont été également déterminées par XPS dans le but d'évaluer l'efficacité du greffage et la formation de liens esters. D'abord, les fibres de bois modifiés et extraites étaient similaires comparées aux fibres de bois initiales ce qui était impliqué par leur similarité de morphologie de surface. Des changements de la concentration de carbone et d'oxygène en fonction de la profondeur d'échantillonnage indiquent une structure de surface non-homogène. Une petite différence d'énergie de liaison et de concentration du carbone et de l'oxygène a été trouvée en fonction des profils de profondeur sur les fibres modifiés. Des différences significatives des compositions élémentaires de surface des fibres modifiées sont une évidence de la présence de liens esters comme le montre le rapport O/C. Les spectres de haute résolution de C_{1s} nous donnent plus d'informations sur le type de liaisons formées et sont aussi utiles pour déterminer le taux d'hydroxyles, le taux de carbonyles, le taux de greffage ainsi que le rapport $C_{ox/unox}$ et leur effet sur la réactivité, alors que le dépôt sur les surfaces de polymères maléatés sont corrélés avec un taux croissant d'oxygène en surface et une diminution de C_{1s}. Les résultats

d'XPS ont prouvé également que la quantité d'anhydride maléique déposée sur la fibre a un effet sur le type de liens oxygène-carbone. Beaucoup de MA en surface amène une hausse des liens oxygène-carbone détectés en surface. L'utilisation du MAPE se traduit par une réactivité supérieure par rapport au MAPP après normalisation en comparaison au taux d'hydroxyles, le taux de greffage, le taux de carbonyles obtenus de l'XPS au même MA% (1.5%).

L'effet de la liaison de la lignine de surface été éliminé après que le polymère maléaté ait été employé sans regard à sa nature et son pourcentage et de plus, il n'y a aucun signe d'azote en surface. Comme matériel d'ingénierie, les composites de fibres de bois renforcés avec de la fibre CTMP montrent une bonne performance en raison de leur riche couverture en surface par la lignine et des extractibles qui agissent en tant que lubrifiants internes et antioxydants naturels pendant les traitements à haute température.

Mots-clés: FQA, FTIR, résistance aux impacts, résistance à la traction, polymère maléatés, propriétés mécaniques, nanocomposites polymères, polyoléfine, SEM, désorption d'eau, absorption d'eau, composites du bois, fibre du bois, XPS

Résumé substantiel

PROBLÉMATIQUE

Les polyoléfines constituent un type de polymères avec un bon rapport qualité-prix et une grande facilité de transformation. Cependant, les composites bois-polymères (WPC) fabriqués à partir de polyoléfines et de fibre de bois ont besoin d'amélioration côté résistance à l'impact, aux températures ambiantes ou basses, pour répondre aux besoins industriels. En général les forces d'impact et d'effort doivent être transférées de la matrice aux fibres renforcées par une interface de fibre-matrice afin de supporter des charges lourdes. Le défi de composites du bois est leur basse ductilité et leur résistance aux chocs inférieure dues à (I) la mauvaise compatibilité entre la fibre de bois hydrophile et le polypropylène hydrophobe ce qui donne une faible adhérence interfaciale; (II) la mauvaise dispersion de la fibre de bois dans la polyoléfine en raison des fortes interactions fibre-fibre causées par les liaisons hydrogène; (III) l'allongement limité de la fibre de bois en raison de sa haute cristallinité. Actuellement, la résistance à l'impact a été augmentée en renforçant l'adhésion interfaciale et la compatibilité à l'aide d'un agent compatibilisant de façon à transférer efficacement la force entre les fibres de bois hydrophiles et les polymères hydrophobes ce qui donne également une amélioration des propriétés en traction.

OBJECTIF

En général les forces d'impact et les efforts doivent être transférés de à la matrice aux fibres par une interface fibre-matrice afin de supporter les charges importantes. Une interface plus forte transférera la charge plus efficacement vers la matrice alors que les inconvénients des WPC sont la mauvaise adhésion interfaciale entre les fibres de bois hydrophiles et les polymères hydrophobes qui conduiront à une force de transfert plus faible ayant pour résultat des propriétés décroissantes de force et d'impact. L'adhésion interfaciale entre la matrice et les fibres de bois est augmentée suite à la compatibilisation pour augmenter la résistance à la traction aussi bien que la résistance à l'impact.

Ce type de polymères pseudo-ductiles comme le PE et le PP, ont une température de transition fragile à ductile et des résistances à l'impact limitées.

Bien que les fibres de bois plus rigides contenant un haut pourcentage de lignine pourraient augmenter la résistance dû à la formation des stéréo-structures en renforçant l'adhésion interfaciale et améliorant les propriétés telles la stabilité thermique, l'amélioration est encore limitée parce que les fibres de bois rigides entraînent une déformation inférieure et affaiblissent la résilience. En conséquence, la plupart des WPC devra être améliorée afin de satisfaire aux exigences des applications finales.

L'objectif principal de ces travaux est d'étudier la fibre de bois fonctionnalisée à l'aide d'un système de mélange à rouleaux ainsi que les modèles de rupture de la fibre de bois et la rhéologie de la matrice. Avec cette compréhension, la fabrication et la conception de produits peut mener à de meilleures performances menant à la création des nouveaux matériaux verts. Plus précisément, ce travail est prévu pour mettre en évidence des relations entre les microstructures de la fibre de bois et les fonctions structurales interfaciales employées dans les diverses conditions

Dans ce travail les quatre principaux aspects suivants seront examinés.

1. Les comportements mécaniques des nanocomposites et des composites de composition variable, des méthodes de mélange et de thermo-oxydation *etc.*
2. Les comportements mécaniques et morphologiques du nanorenfort (NC) modifiés avec différents surfactants organiques.
3. Les comportements fonctionnels de la fibre de bois entièrement et partiellement recouverte avec les polymères maléiques.
4. L'étude exploratoire des comportements du renfort à base de cellulose bactérienne.

MÉTHODOLOGIE

Préparation des échantillons de WPC

Tous les composites ont été préparés en mélangeant la fibre de bois et le polymère dans un mélangeur à rouleaux de type Brabender avec quelques additifs selon les conditions suivantes: 20% poids de la matrice polymère a été fondu sur les rouleaux à 190°C ou 170°C avec addition de polyoléfine maléatée. La fibre de bois (CTMP de tremble, BCTMP de tremble ou CTMP de bouleau) et le polymère résiduel ont été alors ajoutés et mélangés durant 7 minutes à 60rpm avec ou sans NC, puis

récupération du mélange des rouleaux et ré-malaxage aux rouleaux 5 fois, 3-5 minutes chaque fois, afin d'obtenir des feuilles de composite uniformes.

Enfin, les feuilles de composites sont récupérées des rouleaux et transformés en bandes avec un couteau selon la taille du moule après que le DCP (péroxyde de dicumile ou de son vrai nom: Bis (α,α- diméthyl benzyle) ***péroxyde***) supplémentaire ait été ajouté, pour 3 minutes.

Les bandes de composites sont alors moulés en forme d'haltères (ASTM D638 Type V). 24 spécimens (12 pour l'essai de tension et 12 pour les tests de résistance d'impact) ont été simultanément mis dans un moule couvert par des plaques métalliques des deux côtés et qui ont été chauffées à 192±2°C ou 171±1°C dans une presse DAKE et durant 15 minutes sous une pression de 20MPa (25-26 tonnes), et alors refroidi au-dessous de 100°C ou 60°C en circulant de l'eau froide dans les plaques de la presse.

Les dimensions approximatives des spécimens ont été mesurées après avoir été conditionnés et polis. Les propriétés mécaniques ont été examinées à l'aide d'un appareil Instron et un testeur d'impact selon la méthode d'ASTM D638 et ASTM D1822 (DIN 53448), respectivement.

Préparation des fibres des bois modifiées

Des composites comportant le polymère maléaté avec 10, 20, 30, 40, 50 et 60 w% en poids de fibres de CTMP de bouleau ont été faits, pour obtenir des fibres couvertes entièrement selon la méthode 1 du schéma 1 du chapitre 11. Des composites de polyoléfine avec les fibres de CTMP de bouleau à 30 % en poids en présence de 0, 1, 2, 3, 5, 8 et 10% en poids de polymère maléaté ont aussi été faits pour obtenir les fibres couvertes partiellement par la méthode 1 de schéma 1 du chapitre 11.

Tous les composites ont été préparés par moulage avec le moulin à deux rouleaux (Roll-Mill). La température pour le PE est 170°C et pour le PP de 190°C. Des tranches ou feuilles minces sont obtenues après récupération des rouleaux et stockées à la salle de conditionnement pour les prochaines étapes. Les spécifications pour le moulin à deux rouleaux ont été comme suit: 30 cm longueur, 15 cm de rayon, 0.6 de rapport de vitesse et 60 rpm pour la vitesse du rouleau.

Ensuite toutes les tranches minces des composites conditionnées sont dissoutes dans le xylène bouillant. Les fibres de bois traités brutes sont séparées de la solution (le mélange de polymère ou le polymère maléaté) au moyen d'un filtre métallique (100

mailles au pouce). Les fibres brutes sont extraites par l'appareil d'extraction de Soxhlet avec le xylène au reflux 48h. Les fibres traitées sont obtenues après purification à l'acétone.

Les fibres traitées ainsi qu'une centaine de fibres de bois traitées brutes sont obtenues par dissolution-filtrage pour éliminer le polymère résiduel. La séparation-purification est répétée 4 fois en raison de sa viscosité élevée de la solution de PE. Enfin, les fibres sont dispersées dans le xylène sous ébullition de nouveau, et versées dans l'acétone pour précipiter et laver. Touts les fibres modifiées sont séchées à l'air.

Caractérisation des échantillons et des fibres modifiées

Les caractéristiques physiques de la fibre de bois traité ont été déterminées par le FQA selon la meilleure méthode ISO 16065 et TAPPI T271. Les caractéristiques chimiques ont été déterminées par FTIR (System 2000 FTIR) et XPS (Kratos Axis, HIS 165). Les microstructures morphologiques ont été observées par SEM pour indiquer les modes de fractures.

RÉSULTAS ET DISCUSSION

Caractéristiques des conditions des composants

Dans ces études, nous nous concentrons sur l'estérification et ses conséquences importantes. Avant l'étude du mécanisme de couplage, les conditions opératoires du mélanges des composites et nanocomposites polymères ont été optimisées tel que décrit en section 1-4.

1. Le temps de mélange a été établi autour de 30-35 minutes pour obtenir la résistance à l'impact optimale sans affaiblir la résistance en tension.
2. La méthode de mélange en masse (sans mélange préalable) pourrait mener à une résistance à l'impact supérieure comparé à la méthode avec mélange préalable où la fibre de bois a été pré-enduite à l'aide des polymères maléatés et un peu de la matrice polymère (20% en poids).
3. La séquence avec l'ajout des DCP à l'étape finale est la meilleure méthode pour obtenir une meilleure résistance aux chocs sans diminution de la résistance tension des WPC en raison de la différence dans le temps de la réaction de greffage et d'oxydation en présence de l'initiateur.
4. L'agent d'antioxydant peut empêcher la thermo-dégradation des WPC en présence de DCP. Sinon, il a agi en tant comme un remplisseur inorganique

résultant en une résistance à l'impact et à la traction plus basses. On a conclu que le DCP accélère la thermo-dégradation des WPC à base de PP.

Propriétés mécaniques des WPC et des nanocomposites polymères

En second lieu, après préparation des nanocomposites et des WPC avec des conditions optimisées, les effets de la fibre de bois, de l'agent de couplage, du NC et du DCP ont été étudiés. Selon les études sur les changements associés à chaque composant, quelques conclusions ont été faites comme suit (section 5-9).

5. La fibre de bois a montré différents comportements en résistance dans les composites sans ou avec agents compatibilisants. Les résistances à l'impact et à la traction ont diminué avec l'augmentation du contenu en fibre sans l'addition d'agents compatiblisants en raison de la mauvaise adhésion interfaciale. Les résistances se sont améliorées lorsque les agents compatiblisants ont été utilisés en fonction de la concentration croissante en fibre en raison de la compatibilité améliorée. De plus, la taille de la fibre de bois sélectionné (20-60 mailles au pouce, 60-80 mailles au pouce, and 80+ mailles au pouce) n'a eu aucun effet sur les propriétés mécaniques des composites de PP sans agent de couplage. Cette conclusion a été confirmée par les résultats du FQA, montrant que la fibre de bois était fracturée au cours de mélange et moulage Lorsque 1% en poids de cellulose bactérienne a été ajoutée au WPC, les interactions interfaciales ont été accentuées et la résistance à l'impact et à la traction ont été améliorées parce que la cellulose bactérienne peut se lier in situ à la fibre de bois suite à la forte adhésion causée par la haute affinité de la cellulose via la liaison hydrogène.
6. On sait maintenant que les propriétés mécaniques des WPC ont été sensiblement augmentées par l'emploi de l'agent de couplage et affectées par leurs caractéristiques, où le MAPP de haute M_w et bas pourcentage en groupements maléatés a pu contribuer a donner aux WPC hybrides homo-PP de meilleures performances. Cependant, il convient de noter que les propriétés ont été détériorées avec l'utilisation excessive de l'agent de couplage en raison de ses enchevêtrements et de la lubrification excessive qui ont été observés sur les micrographies SEM. La concentration optimale pour l'agent de couplage se trouve à 3% en poids pour les WPC à base de polyoléfines maléatées et 0.2% en poids de DCP.

7. C'est une aussi une conclusion intéressante que suite à l'introduction de la NC en bas contenu (<2% en poids), on constate une augmentation de la résistance à l'impact et les forces de traction, mais on affaiblit ces propriétés avec un contenu élevé (jusqu'à 20% en poids). L'addition de différentes variétés de NC modifiées à l'aide de surfactants organiques a entraîné des comportements différents en raison de la nature différente des surfactants, et ces différences ont été amplifiées après que le système ait été compatibilité avec l'agent de couplage et l'initiateur. Bien que l'addition de NC sous forme de concentrés mène facilement à des feuilles uniformes, l'addition de NC non modifiées a conduit à une meilleure performance mécanique que le NC sous forme de concentrés ainsi que les autres NC modifiés excepté celui de type I.34TCN qui a des groupements réactifs latéraux –OH prêts a réagir avec l'agent de couplage, alors que le NC- sous forme de concentrés n'a aucune interaction avec la matrice polymère ; la NC-non modifiée se dépose sur la surface de la fibre de bois, et on la retrouve même dans les lumens du bois. Les interactions fortes entre NC non-modifié et le polymère polaire sont vérifiées par les images des SEM.
8. Dans le système de moulage avec deux rouleaux, l'utilisation du DCP a diminué les forces d'impact/traction des WPC à base de PP suite à une thermo-oxydation accélérée aux températures près de 200°C. Toutefois, l'utilisation du DCP a montré un effet positif sur les WPC à base de PE impliquant que la dégradation de la fibre de bois et le polymère de PE a été compensée par des copolymérisations et réticulations.
9. Par l'étude statistique utilisant un modèle de type composite centrale (CCD), la concentration optimale des additifs ont été déterminée afin de maximiser la résistance aux chocs aussi bien que les propriétés en traction. L'effet relatif de chaque composant a été indiqué, où l'agent de couplage a eu un effet positif, le NC a joué deux rôles sur les propriétés selon son contenu, et le DCP a un effet positif sur les composites de PE mais un effet négatif sur les composites de PP.

Caractéristiques des comportements en présence d'humidité

L'humidité, la prise d'eau et l'absorption des composites ont été évaluées .Les résultats des comportements de l'eau en fonction des changements des fibres des bois et des NC ont été présenté dans les sections 10-12.

10. L'absorption et la désorption d'humidité ont diminué avec l'emploi d'agents de couplage en raison de l'adhésion interfaciale améliorée et la présence de polymère hydrophobe à la surface des fibres menant à la diminution des espaces vides et les voies de pénétrations bloquées dans le WPC ainsi que l'élimination des groupes –OH en surface et la présence des chaînes polymères hydrophobes autour des fibres de bois menant à un caractère plus hydrophobe. Avec l'augmentation du temps de trempage dans l'eau, l'absorption d'eau a augmenté puisque que les molécules d'eau pénètrent davantage dans les interstices de fibres du bois. D'ailleurs, la vitesse d'absorption sera accélérée par le gonflement de la paroi cellulaire, où certaines fissures agissent comme des voies d'accès à l'eau. À l'opposé, la vitesse d'absorption est ralentie par le polymère hydrophobe déposé en surface dans les WPC comportant des agents de couplage hydrophobes.
11. L'absorption et la désorption d'eau ont augmenté avec l'augmentation du chargement en fibre de bois. Car plus les fibres sont présentes, plus les fibres sont exposées aux molécules d'eau, ce qui fera pénétrer l'eau via les pores non remplis, les ponctuations non remplies, et même les points de contact entre les fibres et avec la matrice. De plus s'il y a plus de fibres, il y a plus de groupements hydrophiles pour se combiner avec l'eau. Il a été également estimé que plus de fibres raccourcira le temps de trempage pour atteindre la saturation avec une quantité limitée d'agent de couplage.
12. Dans les études des comportements de stabilité dimensionnelle des WPC, il a été trouvé que les NC amélioreraient la résistance à l'eau des WPC via les actions de bloquage qui sont fonction de la quantité de NC et sa modification de surface par le surfactant. Les surfactants jouent un rôle important par leurs structures morphologiques aussi bien que par leurs réactions chimiques, et ils sont également une source d'anti-décoloration des WPC. Il était original de trouver que les WPC comportant des NC ont une coloration différente. C'est aussi le cas de nos résultats sur la stabilité dimensionnelle des WPC comportant des NC.

Caractéristiques des comportements en tension-élongation

Le comportement en tension-élongation des WPC de PE a été étudié. L'ajout de NC non-modifié rend les nanocomposites polyméres plus fragiles si leur contenu est augmenté. Le comportement en tension–élongation des WPC suite à l'ajout de fibre de bois, d'agent de couplage et l'initiateur sur les morphologies est bien régulier et interprétable. Le composite devient plus fragile avec addition de fibre de bois s et NC tandis que l'agent compatibilisant a montré l'effet inverse en présence de fibre de bois, avec dans ce dernier cas, un haut coefficient modulo. L'I.34TCN modifié au tensio-actif comportant un site ammonium avec 2 groupes hydroxyles ainsi que NC-naturel étaient les meilleurs additifs pour augmenter la résistance mécanique et la résistance à l'humidité.

Caractéristiques des fibres traitées

Finalement, les mécanismes de couplages ont été établis pour les additifs MAPP et MAPE avec M_w variable. Des traitements des surfaces des fibres des bois ont été effectués avec deux types des polyoléfines maléatés (MAPE et MAPP) via mélange et moulage à l'état fusion. Le FQA et le SEM ont été employés pour étudier les modifications morphologiques des fibres des bois et leurs modes des fractures. En outre, les analyses FTIR et XPS ont suivi l'augmentation de l'hydrophobicité de la fibre de bois traitée par les polyoléfines maléatés et la nouvelle formation de liens chimique suite à leur emploi. Ces changements chimiques sont systématiquement expliqués par FQA, SEM, FTIR et XPS dans les sections suivantes 13-18.

13. Pour les expériences avec les fibres enduites entièrement, les morphologies interfaciales de la fibre de bois modifié ont été illustrées avec les modes de détachement, craquement, retroussement, extrusion, torsion, fibrillation et de roues à taquets. Les changements des morphologies ont été principalement liés aux caractéristiques de la matrice polymère combinée au polymère maléaté, où dans le cas du PE ou MAPE il y a eu attrition des fibres comparé au cas du PP et MAPP. Les morphologies ont été également liées aux M_w des polymères maléatés et leurs concentrations, mises en évidence par les analyses de FQA et de SEM. À l'opposé des changements dus aux tailles des fibres de bois, l'emploi de MAPP de M_w élevé a contribué à faire apparaître des fibres des bois avec plus de vrillons, boucles et coudes et cela semble lié à la présence de sites hydrophiles latéraux sur le MAPP tandis que l'emploi

du MAPE de bas M_w est lié à l'apparition de plus de boucles et coudes chez les fibres, liées à la présence d'interactions plus fortes. Il est conclu que le M_w a un impact important sur la morphologie des fibres, surtout suite à l'emploi de MAPP. Toutefois, le M_w a un effet important sur la morphologie dans le cas où le MAPE est ajouté dans le fondu. De toute évidence, l'emploi de MAPE entraîne des morphologies en boucles chez les fibres alors que le MAPP entraîne plutôt des fractures.

14. Dans les expériences avec des fibres partiellement recouvertes, la longueur et la largeur de la fibre optimale ont pu être réalisées à une concentration optimale d'agent de couplage. Les résultats de FQA ont démontré que 3% en poids de MAPP serait suffisant pour solliciter 30% en poids des fibres de la charge, ce qui produit les fractures plus complexes, par exemple des fibrillations entraînant des boucles et des coudes confirmées par les données de FQA et les images de SEM.
15. Basé sur les résultats expérimentaux avec des fibres entièrement recouvertes, le greffage maléique d'anhydride consiste en une estérification, où les polymères forment plus de liaisons chimiques comme démontré par leur spectre FTIR avec un haut degré de carbonyles comme le démontre l'intégration des pics. D'ailleurs, la réactivité de MAPE était plus haute que celle du MAPP après normalisation au même niveau de contenu en anhydrides. Contrairement aux expériences avec des fibres entièrement recouvertes, les résultats des expériences avec des fibres partiellement recouvertes ont indiqué que la quantité d'agent de couplage a eu un impact sur la formation des liaisons chimiques à la concentration de 3% en poids. Pour le MAPP et MAPE, l'efficacité de la réaction a diminué si l'agent de couplage est employé de façon excessive ce qui mène à une diminution de l'intensité de la bande carbonyle.
16. L'XPS a été utilisée pour évaluer l'efficacité du greffage et la formation de lien ester entre la fibre de bois et le polymère maléaté dans le procédé de mélange. Les fibres modifiés étaient similaires comparées, extraites ou vierges, tel que démontré par les observations de leurs spectres de survol. Cependant, les concentrations de carbone et d'oxygène ont varié en fonction de la profondeur d'échantillonnage ce qui indique des structures non-homogènes, tel des structures en couches fractionnées. Une petite différence

d'énergie de liaison ainsi que dans la concentration de carbone et d'oxygène dans les fibres recouvertes a été trouvée en fonction des profils de profondeur. Une différence significative dans les compositions élémentaires de surface des fibres recouvertes a démontré la présence de liaisons esters tel que constaté avec un rapport O/C croissant, où le rapport O/C de la fibre extraite, à 0.448, a diminué à 0.047 et 0.071 pour les fibres modifiés par MAPE et MAPP, respectivement. D'ailleurs, les spectres de haute résolution C1s nous ont donné plus d'informations sur le type de liaison formé et également ont été utilisés pour déterminer l'index hydroxyle, l'index carbonyle, le taux de greffage ainsi que le rapport $C_{ox/unox}$ et leur effet sur l'efficacité de la réaction; même les dépôts de polymère maléaté entraînent un accroissement dans le pourcentage atomique de surface d''oxygène tout en diminuant le pourcentage de C_{1s}. Les résultats d'XPS ont également prouvé que les différences en concentrations initiales d'anhydride maléique ont entraîné des changements sur la fibre modifiée en surface concernant la nature des liens oxygène-carbone, lesquels sont identifiés par des changements de la surface du pic deconvolué du carbone, ce qui donne un rapport $C_{ox/unox}$ qui varie de 1.72 pour la fibre extraite jusqu'à 4.57 et 4.53 pour les fibres modifiés au MAPE et MAPP, respectivement. L'utilisation du MAPP à haut taux d'anhydrides a donné un taux élevé de liens oxygène-carbone comparativement au MAPE moins maléaté, suivant la concentration de C_3 et C_4. Néanmoins, l'utilisation du MAPE a pu donner un contraste de réactivité supérieur à celui du MAPP selon l'index hydroxyle, le taux de greffage et l'index carbonyle, qui calculé par XPS, a été normalisé au même niveau.

17. Suite à l'emploi d'agents de couplages, soit les polymères maléatés, quelque soit leur type ou degré d'anhydrides, l'effet 'shake-up' adhésif de la lignine de surface aussi bien que la bande d'azote étaient absentes en raison de la suppression des extractibles à base d'azote après la procédure de modification, qui a fait que les extractifs hydrophiles contenant l'azote se sont déplacés aux surfaces des fibres modifiées et puis ont disparu à température plus haute des surfaces des fibres.
18. Les bois composites renforcés avec la fibre CTMP fibre ont pu réaliser de bonnes performances en raison de la riche couverture en surface de lignine

(75-76%) et d'extractibles (37-49%) ce qui agi en tant que la lubrifiants internes et antioxydants naturels pendant le processus de moulage et mise en forme.

Contents

List of Figures

List of Tables

List of Schedules

List of Equations

List of Symbols & Abbreviations

WPC	Wood plastic composite
TMP	Thermomechanical pulp
CTMP	Chemothermomechanical pulp
BCTMP	Bleached Chemothermomechanical pulp
Tg	Glass transition temperature
PE	Polyethylene
PP	Polypropylene
PVC	Polyvinyl chloride
PU	Polyurethane
MOE	Modulus of elasticity
MOR	Modulus of rupture
MFI	Melt flow index
LLDPE	Linear low density polyethylene
LDPE	Low density polyethylene
MDPE	Medium density polyethylene
HDPE	High density polyethyene
MAPP	Maleated polypropylene
MAPE	Maleated polyethylene
TPO	Thermoplastic olefin
EVA	Ethylene vinyl acetate
EVOH	Ethylene vinyl alcohol
PSt	Polystyrene
PBNCO	Polybutadiene isocyanate
TGA	Thermogravimetric analysis
DCP	Dicumyl peroxide
CCD	Central composite design
NC	Nanoclay
Mw	Weight average molecular mass
MA%	Maleic anhydride graft
FTIR	Fourier Transform Infrared Analysis
XPS	X-ray photoelectron spectroscopy
SEM	Scanning Electron Microscopy
FQA	Fiber quality analysis

Chapter 1 - Introduction

Typical hybrid composites are composed of a heterogeneous combination of natural fibers, the polymer matrix and other components on a macroscopic scale to form a single structure to achieve specific physical, chemical and mechanical characteristics which could not be obtained with the separate components. Based on the characteristics of reinforcement, common composite materials can be classified as follows.

1.1 Nanocomposites

Nanocomposites materials are engineering materials made from the matrix compounded with inorganic fillers [1], such as talc [2], mica [3, 4], glass fiber [5, 6, 7, 8, 9], calcium carbonate [10, 11, 12, 13], clays [14, 15, 16, 17, 18, 19, 20, 21, 22, 23] and organically modified clays [24, 25, 26, 27, 28, 29, 30, 31, 32, 33, 34] which are incorporated into polymer composites. The composites filled with organic modified clays may increase strength and modulus[35], give thermo-oxidative stability[31, 36, 37, 38], enhance barrier properties [39], improve solvent resistance [28, 40], reduce thermal expansion coefficient [39], increase flame retardancy [41], increase ionic conductivity [42, 43, 25] and control biodegradability [44].

1.2 Wood-based composites

Until recently the term "reinforced plastics" has usually meant glass, carbon, aramid or polyethylene fibers, incorporated in petroleum-based resins. Several factors are now stimulating interest in plant based fibers and bioplastics for composites manufacture. These factors include the drive for sustainable technology, legislation on the recycling of end-of-life vehicles and the automotive industry's continuing demands for weight reduction and control of material costs. Geoffrey Pritchard highlighted some of the developments at a recent conference on wood and biofiber Plastic Composites [45].

Wood-based composites are created by combining matrix with wood materials, such as agro-based fiber [46, 47, 48, 49, 50, 51, 52, 53, 54, 55, 56], wood flour [57, 58, 59, 60, 61, 62, 63, 64, 65, 66, 67, 68, 69, 70, 71, 72] and wood fiber [73, 74, 75, 76, 77, 78, 79, 80, 81, 82, 83, 84, 85, 86, 87, 88, 89, 90, 91, 92, 93, 94]. Wood plastic composites became more popular due to their availability and abundance because of being renewable resources [95, 96], with low cost [56, 97], high relative strength [96]

and stiffness [98, 99, 100] , low density [100], greater thermal stability [101, 102], high biodegradability [103, 104, 105, 106] as well as excellent mechanical and physical properties [102, 107, 108]. Wood-based composites are classified into three kinds according to the different characteristics of the basic matrices.

An early example of a wood filled plastic is Bakelite, which was developed in the early 1900's. One of the first commercial uses of wood plastic composites based on thermoplastic polymer resins was the use of wood flour and PVC to manufacture flooring tiles, first produced in the mid 1950's.

Wood composites are interesting reinforcement for polyolefins, such as thermoplastics, thermosets and elastomeric polymers while thermoplastics are the most popular [109].

1.2.1 Wood thermoplastic composites

Wood thermoplastic composite is an alternative material for wood and engineering materials [110, 111, 112, 113], where wood fibers provide more efficient stress force-transfer to the composite materials [87, 113, 114, 115, 116] than conventional reinforcing materials. WPC has been widely used to replace impregnated wood in many outdoor and plastic and biomedical applications [110] as indicated in Figure 1.1.

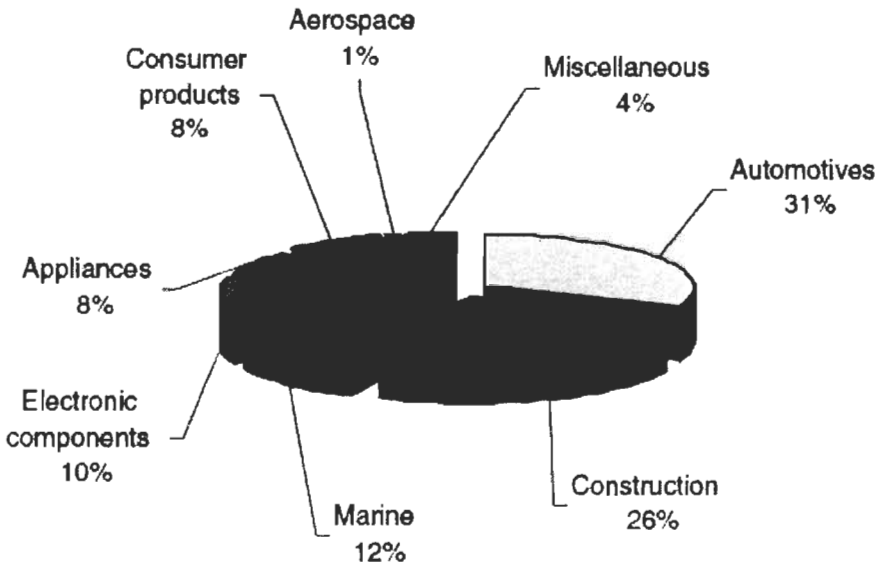

Figure 1.1 Wood plastic composites used in 2002 [99]

Global use of composite materials has reached 13.5 billion lb in 2004 with growth rate of 8.7 percent and could increase to 17.5 billion lb per annum globally by 2010

[117]. To put this in perspective, a recent study from Freedonia suggests an 11% annual growth through 2009 for the combined WPC and plastic lumber sector in the USA to reach a value of to US$3.8 billion. According to a new study from Freedonia, *Composite & Plastic Lumber* (#2027), moulding and trim will remain the largest end use but will lose share to other applications, while residential building will remain the top US market during the forecast period. Among the major product categories, windows and doors applications are anticipated to post the fastest gains up to 2009 (but from a small base), with demand expected to exceed $200 million [118].

Table 1.1 Total USA WPC Demand to 2011 [110]

USA Composite &Plastic Lumber Demand By Applications &Materials-$ million (£ million)					
Composite and Plastic Lumber Demand	1992	1996	2001	2006	2011
Decking	97(59)	195(118)	410(248)	900(545)	2485(1506)
Moulding &Trim	115(70)	218(132)	330(200)	430(261)	580(352)
Fencing	12(7)	55(33)	160(97)	315(191)	560(339)
Windows & Doors	1(1)	15(9)	65(39)	135(82)	240(145)
Miscellaneous	47(28)	75(45)	105(64)	170(103)	245(148)
Total Demand	272(165)	558(338)	1070(648)	1950(1182)	4110(2491)
Total WPC	54(33)	148(70)	375(227)	880(533)	2445(1482)
Total Plastic Lumber	218(132)	410(248)	695(421)	1070(648)	1665(1009)

Source: The Freedonia Group Inc 2002-Composite and Plastic Lumber in the United States

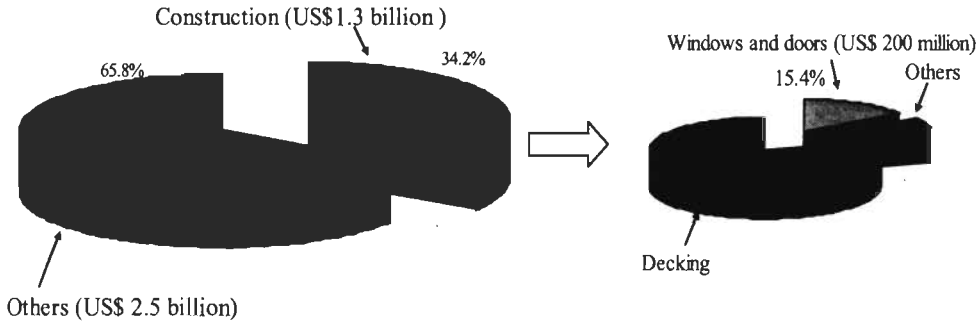

Source: The Freedonia Group Inc 2006-Composite&Plastic Lumber to 2009

Figure 1.2 The perspective values of WPC to 2009 in USA [111]

A common wood composite means wood thermoplastic composites [79, 119, 120, 121, 122, 123, 124] while polyethylene (PE) and polypropylene (PP) are important engineering thermoplastics used widely in the field of the composites today (Figure

1.3 Wood Plastic Composites Demand by Matrix Resin in 2004 [109] and Figure 1.4).

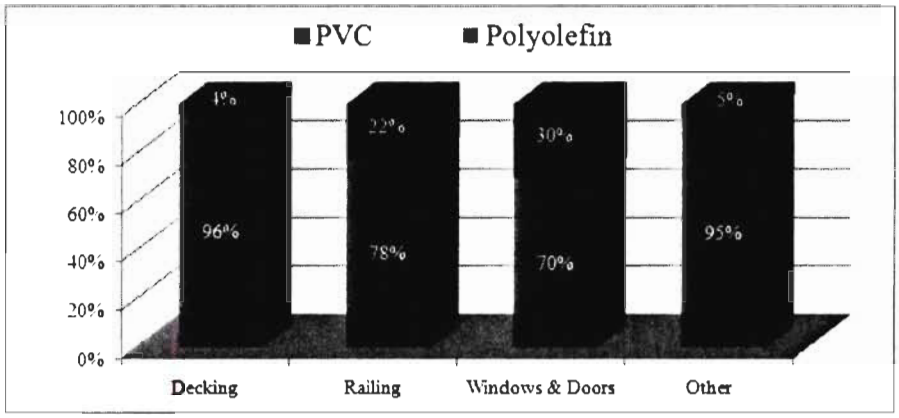

Figure 1.3 Wood Plastic Composites Demand by Matrix Resin in 2004 [109]

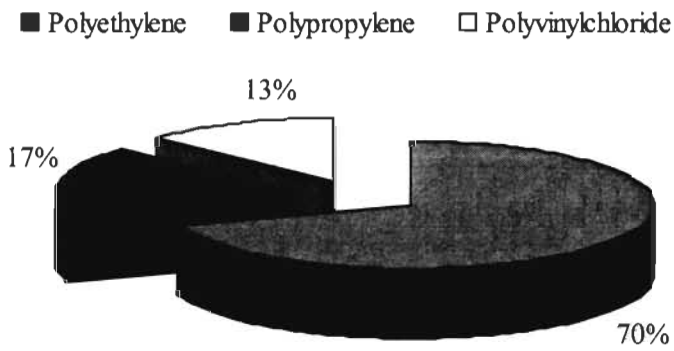

Figure 1.4 Polymer Use in Wood Plastic Composites to 2011 [110]

1.2.2 Wood elastomer composites

Wood elastomer composites were obtained by compounding rubber matrix and wood fiber with coupling agents to improve flexibility, high low strain modulus, stiffness and damping and processing economy by two-roll laboratory mill and then crosslinked by peroxide after being conditioned as described in Figure 1.5. In addition, wood fibers have advantages due to their renewable nature, low cost, easy availability and ease of chemical and mechanical modification. Many researchers have reported improvements in the mechanical properties of short fiber reinforced rubber composites [125, 126, 127, 128, 129, 130].

Wood elastomer composites were prepared by blending wood fiber into natural rubber by two-roll laboratory mill (or rubber latex emulsion) to obtain the sheeted rubber compound to be cured by peroxide after conditioning.

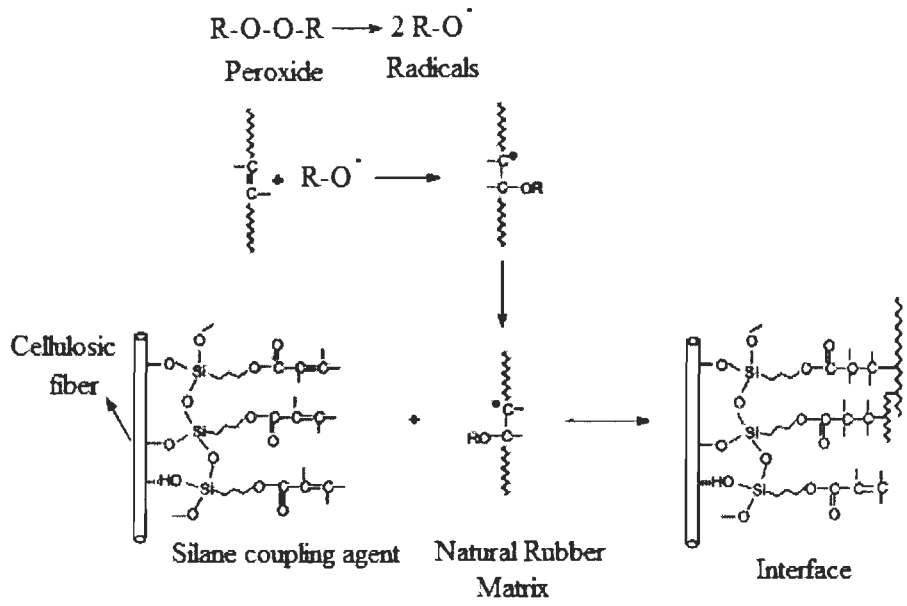

Figure 1.5 Schematic illustration of the interfacial reaction between natural rubber and grafted wood fiber with an initiator [126]

1.2.3 Wood thermoset composites

Wood thermoset composites refers to any composites that contain wood fibers and thermosets which are crosslinkable polymers that can't be melted once cured, such as epoxies, unsaturated polyesters and phenolices. Wood thermoset composites were obtained by compounding wood fiber with resins in a Brabender type mixer at ambient temperature, and molded at high pressure and temperature after degassing for several hours and then postcured. Coupling agent could be used to improve the interfacial adhesion between the resins and wood fibers [131, 132, 133, 134].

1.3 Literature review

Wood thermoplastic composites are mainly polyolefins reinforced with wood fiber and their characteristics originate from the characteristics of wood fibers, polyolefins and their interactions [56, 135].

1.3.1 Morphology and characteristics of WPC

There are mainly three kinds of reactions occurring among the composites including wood fiber and polyolefin grafted/coupled by coupling agent [136, 137] or copolymerized and/or crosslinked by initiator [137]. It is sensible to assume that the local shear stress distribution depends on wood fiber l/d and on wood fiber strength as well as on matrix.

1.3.1.1 Failure modes

Generally, wood fibers are not well oriented in the reinforced composites. Therefore, no single failure mode will occur in the composite but rather a combination of all possible modes. Four different damage modes can be identified during the failure of the hybrids as described in Figure 1.6 [138, 139, 140, 141, 142]: yielding of matrix see Figure 1.7 (a), fiber pull-out (b) and fiber debonding (b-c), and fiber fracture (d).

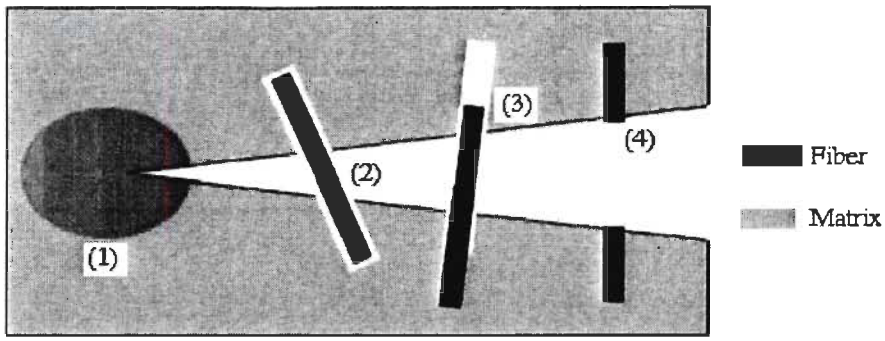

Figure 1.6 Damage modes observed in short fiber composites during failure [138]

(1) Yielding of matrix, (2) fiber debonding, (3) fiber pull-out and (4) fiber fracture

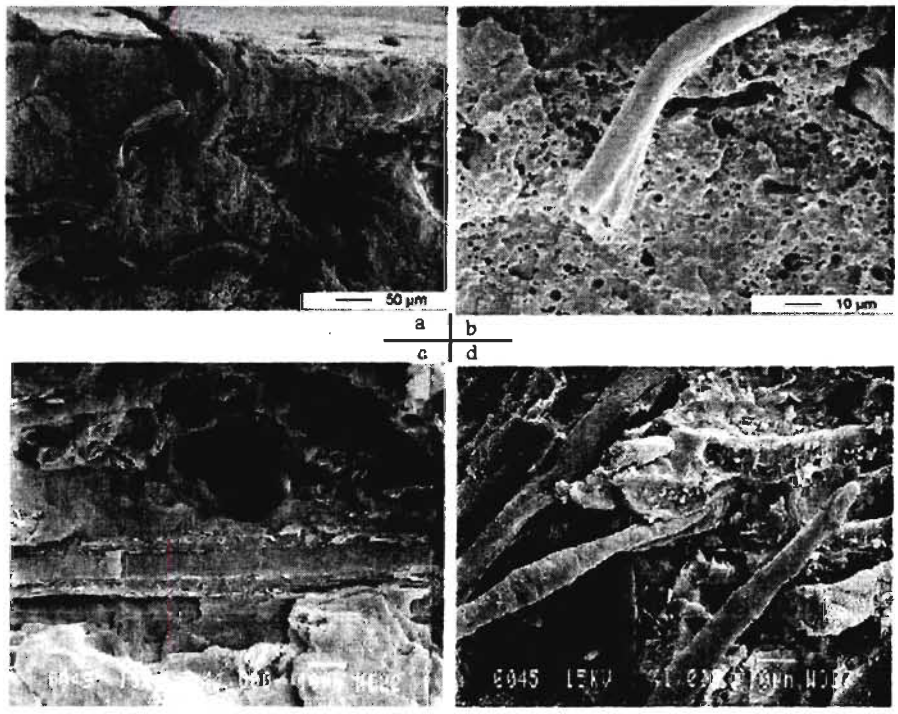

Figure 1.7 Fractured surface of hybrid composite

a- matrix twisted and broken wood fibers, and b-Fiber pull-out and debonding [140]; c-Fiber debonding and d-Fiber breakages [143]

1.3.1.2 Problems

A polyolefin is a polymer exhibiting very attractive cost-performance balance and easy processability. However, WPC made from polyolefin and wood fiber need impact resistance improvement at ambient or low temperatures to fulfill the industrial requirements [144]. For the reinforcement to be effective stress/impact force must be transferred from the matrix to the reinforced fibers through a fibers-matrix interface in order to carry heavy load [113, 116]. The challenges of WPC is lower ductility and lower impact strength due to (I) the poor compatibility between polar hydrophilic wood fiber and non-polar hydrophobic polyolefin which may result in weak interfacial adhesion [145]; (II) poor dispersion of wood fiber in the polyolefin because of strong fiber-fiber interactions resulting from hydrogen bonding [146]; (III) the limited extension of wood fiber because of high crystallinity [147, 148]. Presently, the impact strength was enhanced by strengthening interfacial adhesion and compatibility when compatibilizer was used to transfer more force effectively between the hydrophilic wood fibers and the hydrophobic polymers resulting also in the enhancement of tensile properties [84, 149, 150, 151].

1.3.2 Traditional strategies for composite strength improvement

Due to the fact that strength originates from the strength of the matrix and wood fiber, the quality of the wood fibers-matrix interface is significant to the properties of composites. The modification of matrix or wood fiber by physical and/or chemical methods could lead to composites with superior impact strength due to the strengthened interfacial adhesion. Among the strength modification methods available today, coupling agents and polymeric impact modifiers known as functionalized polymers, offer a full range of toughening performance [152]. However, the efficiency of the adhesion between the matrix and wood fiber is different for different modification techniques used [56].

1.3.2.1 Modification of wood fiber

As mentioned above, the characteristics and properties of wood thermoplastic composite come from the characteristics of matrix and fiber as well as the interfacial adhesion between them. Low adhesion between both layers causes a considerable decrease in the mechanical behavior of the material, as the interface becomes a weak point in the material. Consequently, it is necessary to modify the matrix and/or wood fiber to obtain wood plastic composites with high performance while the easiest and

most economic way is to modify wood fiber due to presence of many hydroxyl groups in cellulose and lignin. The characteristics and properties of wood fiber can be changed or modified by physical and chemical method.

1.3.2.1.1 Physical modification

Physical modifications include stretching [142], calendaring [153], thermo-treatment [154], alkaline treatment [78, 155] to improve the tenacity [156, 157, 158], acid treatment [159] to enhance the porous surface [160], solvent extraction [161, 162, 163, 164] to create high pore spaces in the surface of wood fiber as well as to remove volatile organic compounds/pitch components, electric discharge (corona, cold plasma) [165, 166] to change the surface energy of the cellulose fibers [167] and produce reactive free radicals [167] etc.

The physical modification changes the structural and surface properties of the wood fiber to influence the mechanical bonding with the matrix, but does not change in main chemical compositions of wood fibers resulting in no fundamental changes of the strength improvement.

1.3.2.1.1.1 Alkaline treatment

Sodium hydroxide could dissolve some lower molecular impurities, such as pectin and hemicellulose *etc* while not changing the chemical structures of the main part of cellulose. Alkaline treatment could decrease the fibrillar rotation angle and increase the X-ray orientation degree of the molecule to decrease the extension at breakage and improve the tenacity [157, 158, 168]. The type of the solution of alkali metals and the concentration of the solution has an important influence on the effects of the treatment.

1.3.2.1.1.2 Acid treatment

The treatment of xylogen with a low concentration acid solution could remove the impurities, such as pectin *etc*, and improve the porous surfaces which affect the mechanical properties [160].

1.3.2.1.1.3 Solvent extraction

Solvent extraction can remove the extractives to create pore spaces in the cell wall of fiber and lower the fiber saturation point of aspen wood while increase the fiber

saturation point of southern pines [162] as well as remove volatile organic compounds and pitch components of the wood to enhance the strength properties and the adhesion between xylogen and matrix to improve tensile, stiffness *etc* [163]. Moreover, solvent extraction could also increase the heavy metal irons removal capacities of lignocellulosic fiber, such as removal of copper, nickel and zinc ions from aqueous solutions as well as extractives due to changed cell wall chemistry and architecture [164].

1.3.2.1.1.4 Electric discharge

Electric discharge (corona, cold plasma) is another way of physical treatment. Corona treatment is one of the most interesting techniques for surface oxidation activation. This process changes the surface energy of the cellulose fibers [167] and in case of wood surface activation increases the amount of aldehyde groups [169].

The same effects are reached by cold plasma treatment. Depending on type and nature of the used gases, a variety of surface modification could be achieved. Surface crosslinkings could be introduced, surface energy could be increased or decreased, reactive free radicals [167] and groups [170] could be produced.

Electric discharge methods are known to be very effective for "non-active" polymer substrates as polystyrene, polyethylene, polypropylene *etc*. They are successfully used for cellulose-fiber modification, to decrease the melt viscosity of cellulose-polyethylene composites [171] and improve mechanical properties of cellulose-polypropylene composites [167].

1.3.2.1.2 Chemical modification

Chemical modifications are used to improve the interfacial compatibility between the anionic wood fiber and hydrophobic polyolefin by introducing a third material. There are many methods to improve the strength of matrix, wood fiber and their interfacial adhesion.

1.3.2.1.2.1 Chemical coupling

Coupling is an important chemical modification which improves the interfacial adhesion. The development of a definitive theory for the mechanism of bonding by coupling agents in composites is a complex problem. The main chemical bonding theory alone is not sufficient. The consideration of other concepts appears to be

necessary, including the morphology of the interphase, the acid-base reactions at the interface, the surface energy and the wetting phenomena. There are several mechanisms of coupling in materials [172, 173, 174] as follows:

- ✓ Weak boundary layers: coupling agents eliminate weak boundary layers [175].
- ✓ Deformable layers: coupling agents produce a tough, flexible layer [176].
- ✓ Restrained layers: coupling agents develop a highly crosslinked interphase region with a modulus intermediate between that of substrate and of the polymer [177].
- ✓ Surface wettability: coupling agents improve the wetting between polymer and substrate (critical surface tension factor) [178].
- ✓ Chemical bonding: coupling agents form covalent bonds with both materials [179].
- ✓ Acid-base effect: coupling agents alter acidity of substrate surface [180].

Overall, the most important thing for chemical modification is to improve the interfacial adhesion among the components, especially by chemical bonding. It is possible to form a bridge of chemical bonds between the fiber and matrix by treating the surface of wood fibers with a polymeric compound.

1.3.2.1.2.1.1 Isocynates treatment

The mechanical properties of composites reinforced with wood-fibers and PVC or PS as resin can be improved by an isocyanate treatment of those cellulose fibers [181, 182], the polymer matrix [183, 184, 185, 186, 187] or the elastomer [188, 189], such as polybutadiene isocyanate. Polymethylene–polyphenyl–isocyanate (PMPPIC) which was chemically linked to the cellulose matrix through strong chemical bonds [184, 185, 186]. As isocyanated elastomer, polybutadiene isocyanate (PBNCO) can significantly enhance the impact strength of the composite by forming the urethane bonds with –NCO groups of PBNCO reacting chemically with –OH groups of the fibers with the presence of DCP [189].

The behavior of the strength benefits from the chemical linkage with wood fiber and the crosslink and/or entanglements with the matrix. It also benefits from the large extension of elastomer as the functionalized elastomer introduced. However, if the coupling agent is incompatible to the matrix or without the presence of initiator, the improvement of impact strength is small. A serious weakness is the difficult storage

and poor processability because the isocyanate coupling agent is highly self-reactive and highly reactive to H_2O which increases the production costs.

1.3.2.1.2.1.2 Silanes treatment

Silanes are the main group of coupling agents for glass-fiber reinforced polymers [190]. They have been developed to couple virtually any polymer to the minerals, which are used in reinforced composites [62, 121, 124, 191, 192].

Silanes have been developed virtually to couple the composites by pumping the solution of silanes and DCP into the extruder to enhance its impact strength [67, 124]. The reaction of a silane treated substrate enhances the wetting by the resin. The general mechanism of how vinyltrimethoxy silanes form bonds with the fiber surface which contains hydroxyl groups is shown in Figure 1.8.

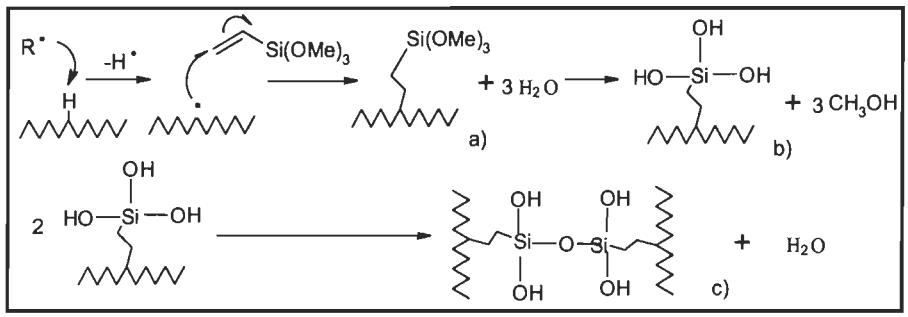

Figure 1.8 Reaction mechanism of silane onto polyolefin by peroxide [124]

a)-Peroxide induced vinyltrimethoxy silane onto polyolefin; b)-Condensation step; c)-Silane crosslinking

Similar to an isocyanate coupling agent, it could be co-polymerized to form inter-penetrating networks in the presence of initiator, and the behavior is also affected by the compatibility with the matrix. Although silane consumes H_2O and lowers the moisture, the formation of CH_3OH could flaw the appearance while the applications would also be restrained by the manufacturing technique.

1.3.2.1.2.1.3 Maleated polyolefin

Maleated polyolefins are very popular in polyolefin use today due to the easiest and economic techniques while having good compatibility to the matrix polymer. The dominant resins used in the production of WPC are PE and PP [109, 110], even 95% composites being produced with virgin or recycled PE or PP in North American market (see Figure 1.9) due to their availability and cost as well as their final properties.

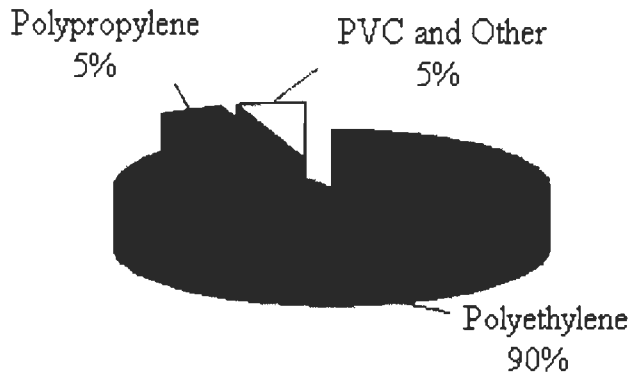

Figure 1.9 North American Wood Plastic Composite Resin Use in 2006 [193]

The reaction mechanisms of maleated polyolefin coupling the matrix have been illustrated in Figure 1.10. However, as incorporating of maleated polyolefin, the deformation of WPC was increased [194] as well as the damping index [195].

Maleated polyolefin can be used as coupling agent in hybrids to improve interface between the hydrophilic wood fiber and the hydrophobic matrix. Moreover, natural fibers have abundant hydroxyl groups that can react with the maleic anhydride groups of maleated polymer and allow the hydrophobic portions of the molecule to incorporate into the bulk matrix. Maleated polyolefins preferred are maleated PP (MAPP) and maleated PE (MAPE), used in the field of the composites widely for polypropylene and polyethylene. The structure of MAPP and MAPE are shown in Figure 1.11.

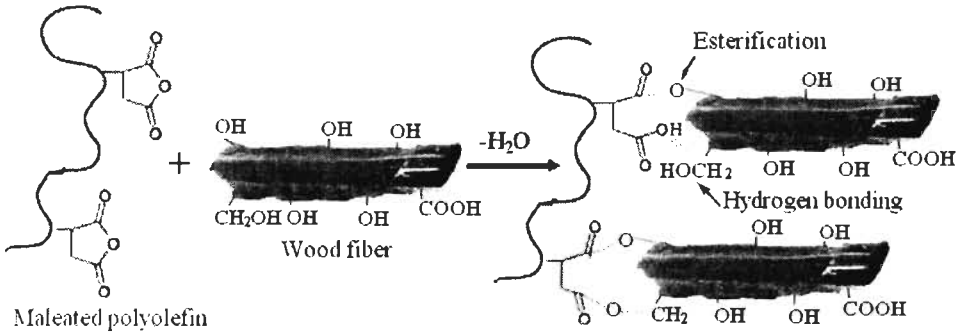

Figure 1.10 Proposed reaction schemes between hydrophilic wood fiber and hydrophobic polymer [136]

Due to the poor adhesion between polar wood fiber and nonpolar polyolefin, wood fiber is embedded in the polyolefin matrix phase and there are no clear gaps in the interfacial area between wood fiber and the polymeric matrix with the addition of coupling agents (Figure 1.10). This suggests that coupling agents improved the interfacial adhesion between matrix and wood fiber because maleic anhydride group

is directly grafted onto the polyolefin backbone and is accessible for attachment to the surface of wood fiber with covalent bonding by esterification [136]. Otherwise, there are hydrogen bonding, polymer entanglement and mechanical interbonding resulting in the strength enhancement of the composites [136, 137].

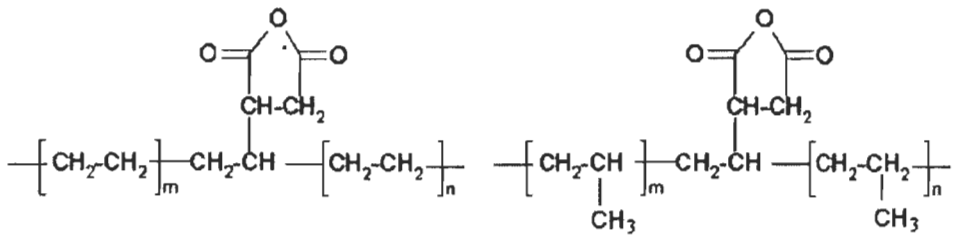

Figure 1.11 Chemical structure of maleated polyolefin

1.3.2.1.2.2 Graft copolymerization

Graft copolymerization is an effective chemical modification of wood fibers [196]. The cellulose fiber is treated with an aqueous solution with selected ions and is exposed to a high energy radiation to form free radicals after the cellulose molecule reacts [197], and then can be copolymerized with a suitable monomer which is compatible to the matrix polymer [198, 199, 200, 201]. The resulting co-polymer possesses the characteristic properties of both fibrous cellulose and grafted polymer. However, the production of free radical may shorten the fiber length resulting in inferior strength without considering other factors [202].

1.3.2.1.2.3 Plasma polymerization

Plasma technologies have been applied to improve the surface properties of fibers in wood plastic composite [203]. Plasma-initiated graft polymerization is discussed to highlight very recent developments. The influence of various plasma treatments on the chemical and mechanical properties of different fibers as well as fiber-reinforced composites is described [204, 205, 206, 207]. Similar to graft copolymerization, plasma polymerization are used to modify wood fiber by grafting polymeric chain with the initiation [208, 209]. However, results obtained by rather expensive plasma treatment technique could be obtained by using coupling agents.

1.3.2.2 Strength modifier

1.3.2.2.1 Traditional modifier

Traditional modifier is usually an elastomer or a plastic incorporated in a plastic compound to improve the impact resistance of the finished products, such as functional ethylene copolymers [210] and acrylate based copolymers [211]. Impact strength and elongation at break could be improved by adding impact modifiers with mechanisms shown in Figure 1.12.

Several technical approaches can be divided in three categories all based on the incorporation of an elastomeric damping phase: the introduction of elastomer during polymerization [212]; the dispersion of elastomer phase during compounding and the incorporation of elastomeric core-shell particles is possible [213].

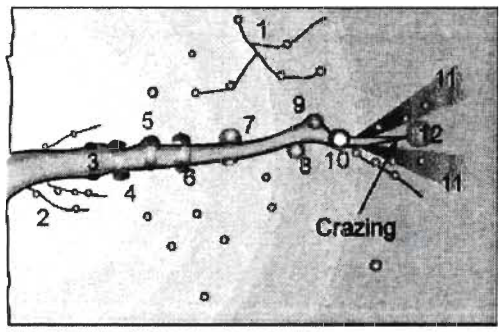

1. Shear Yielding/Craze interaction
2. Shear band formation near rubber particles
3. Fracture at rubber particle after cavitation
4. Stretching
5. Debonding of rubber particles
6. Tearing of rubber particles
7. Transparticle failure
8. Debonding of particles
9. Craze deflection
10. Voided or cavitated particles
11. Diffuse shear yielding
12. Plastic zone at crack tip

Figure 1.12 Toughening mechanism combination and interactions [214]

1.3.2.2.2 Core shell modifiers

Core-shell particulates can be considered as filler and attributes the composites with superior strength with the changes of its morphologies. Generally, most of core-shell modifier is composed of the rigid-shell and the rubbery-core. Chemical combinations are possible concerning the composition of the core or the shell to produce the rigid-shell and rubbery-core functional particulates to achieve specific applications. Still, the rigid shell/core plays important roles to the improvement in the system due to its excellent recovery and handling, compatibility with the matrix and indirectly effects. Moreover, core-shell particulates could be delivered as powder or pellets through a melt or agglomeration process depending on the application.

1.3.2.3 Traditional foamed techniques

The foam-core technology has been attended in both scientific and industrial communities to achieve lower density higher deformation impact strength polymer Nanocomposite foams have received increasing attention in both scientific and industrial communities to achieve lightweight, high strength and multifunctional

materials [215, 216, 217]. Recently, microcellular WPC has become popular due to increasing toughness and ductility. A lot of foam-cores could effectively prevent the cracks or fractures from spreading and let the points of cracks become dull. So, the foam technology was used on hybrid composite [218, 219] to lower the density [86, 215], enhance the tensile properties [220, 221, 222] and improve the impact strength [223]. Lower foamed density (the density of foamed materials > $0.4g/cm^3$) is more popular in order to achieve specified rigidity [220], higher deformation [224] and higher rebound resilience [225].

Incorporating a fine-celled structure into WPC significantly improves their impact strength and reduces their weight and cost [226]. The chemical blowing agent could be cold mixed with the matrix to obtain the mixed granules. However, it is difficult to achieve a fine-celled microcellular structure with either injection processing [221, 222, 223] or extrusion foaming [227, 228] because the blowing agent was not uniform in cold agglomerate granules made by cold mixing. The non-uniform distribution of the chemical blowing agent releases gas rapidly [217] and leads to the irregular distribution of cell and its size resulting in a large average cell size (see Figure 1.13) even with exothermic foaming agent. Indeed some pores are large enough to form big large volume voids which would induce stress concentration such as to be damaged easily.

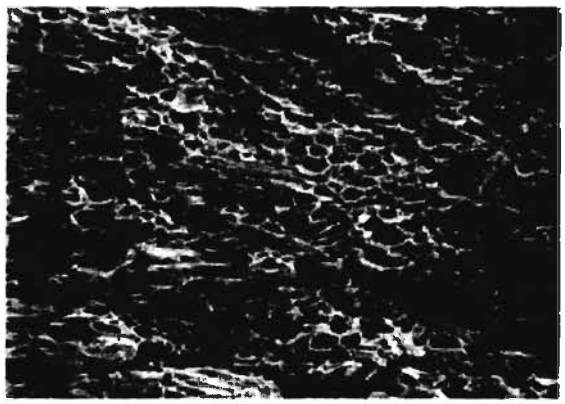

Figure 1.13 Typical cell morphology of the microcellular wood composites [221]

Although exo-endothermic blowing agent released gas smoothly to obtain a relatively uniform and closed cell structure by a continuous extrusion process [229] or injection molding process [86], it always achieves microcellular structures due to the cell expansion and the volume to form larger foams with open structure leading to poor microcellular structures as rough surface and larger void resulting in

lowering the properties [222] with presence of wood fiber [229] and increasing blowing agent loading [221, 223, 231].

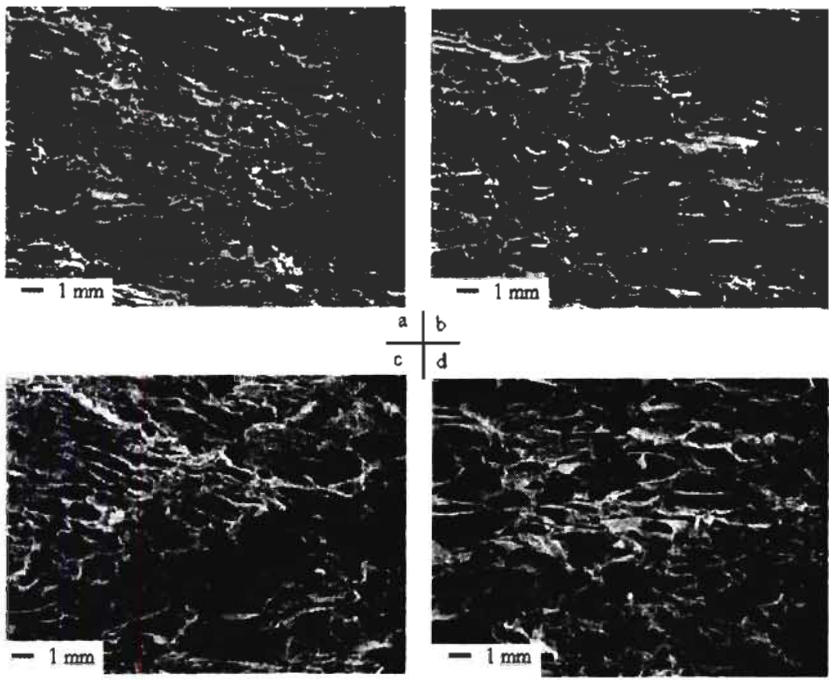

Figure 1.14 Cell morphology of microcellular WPC with various content of chemical blowing agent a-2wt%, b-3wt%, c-4wt%, d-5wt% [221]

Moreover, the inherent moisture and other volatiles, present in the wood fiber, are released during the subsequent stages of WPC processing and heating, particularly in extrusion which leads to gross deterioration in the cell structure and rough surface quality of the extrudate [227, 230] to deteriorate the properties even after online devolatilization [227, 231] and air circulating oven drying [221, 222, 223] *etc* because even the dried wood fiber gradually releases volatiles too [232] as it is being further heated at the processing temperatures of the plastics, which is typically around 200°C, and adversely affects the morphology of the composites materials due to the decomposition of wood fiber [231, 232]. When the quantity of these emissions from wood fiber is very low, the cellular structure is not affected severely [227]. Otherwise, it is extremely difficult to properly control the density of the extrudate [227, 230]. Strategies for reducing volatile emissions during WPC processing have been investigated recently to improve the cell morphology of the final product [231, 232].

Still, foamed WPC products have been commercialized, the coarse and non-uniform cell morphology still inhibits the potential utility of these products. However, these

faults could be improved by nanocellular structures research which will be carried out in another project.

1.4 Objectives

Wood plastic composites are interesting reinforcement for polyolefins, as well as other thermoplastics, thermosets and elastomeric polymers. The wood thermoplastic composites are very popular [109]. Wood plastic composites are an alternative material for neat wood and engineering materials [110, 111, 112], and wood fibers provide the more or less efficient stress force-transfer to the composite materials [87, 113, 114, 115, 116] over conventional reinforcing materials. But challenges of wood plastic composites include lower ductility and lower strength due to the poor compatibility between wood fibers and matrix.

For the reinforcement to be effective, the stress/impact force must be transferred from the matrix to the reinforced fibers through a fibers-matrix interface in order to carry heavy load [113, 116]. Stronger interface will transfer more force effectively among the matrix while the drawbacks of wood plastic composites which are the poor interfacial adhesion between hydrophilic wood fibers and hydrophobic polymers leading to weaker transfer force resulting in decreasing strength, impact and creep properties. The interfacial adhesion between matrix and wood fibers should be improved with compatibilizer to increase the tensile strength as well as impact properties [84, 149, 150, 151].

Pseudo-ductile engineering polymers, such as PE and PP, exhibit a brittle-to-ductile transition temperature and limited impact strength. Although stiffer, wood fibers, in general containing high content of lignin, could increase the strength due to forming more stereo-structures easily by strengthening the interfacial adhesion [233, 234] and improve thermal stability performance [235, 236, 237, 238], the improvement is still limited because the rigid wood fibers mean lower deformation and weaken the rebound resilience. In consequence, most wood plastic composites have to be improved in order to satisfy end-use requirements for rigid applications. So there are big challenges for improving the strength under the increase of the resistance of deformation as well as the functions occurred among wood plastic composites.

As aforementioned above, a literature survey indicates no systematical studies concerning the effect of wood plastic composites preparation and composition on the

mechanical properties, especially to impact strength, and the morphological formation.

The main objective of this work is to study the mechanism of wood fiber functionalized under a roller blending system revealing the fracture modes of wood fiber and the rheology of the matrix. With this understanding, the manufacture and product design could be directed to achieve best performance leading to creation of green materials. More precisely, this work is intended to show an evidence between the microstructures of wood fiber and the interfacial structural functions employed under various conditions. In this work the following four principal aspects will be examined.

1. The mechanical behaviors of the nanocomposites and the composites varying compositions, compounding method and thermal oxidization *etc.*
2. The mechanical and morphological behaviors of the composites after the introduction of nanofiller.
3. The functional behaviors of wood fiber under the entirely and partly bonded condition.
4. The exploratory study of the reinforcement with bacterial cellulose fibers.

1.4.1 Justification

Despite its beneficial effect in the composite, the influence of coupling agent and compounding method on the mechanical behaviors receive little attention. The behavior of the composites made with an excess coupling agent will be examined and defined.

Secondly, the behavior of wood fiber has an influence on the distribution of inorganic particles leading to superior water resistance rather than the increase of modulus for organo-nanoclay with different modification.

Further, wood fiber is a complex hydrophilic material. Mainly the hydroxyl groups of wood fiber respond to the modification reactions. Our experiences indicate that the fractures behaviors are different when wood fiber is grafted entirely or partly. Thus, a systematic study on wood composites could provide us with new information on the performance of wood composites.

Additionally, the failure of wood fiber in wood composites is directly related to fractures induced by compounding, but this fact has received little research attention. It is known that fiber length and the compatibility are the two principal factors

involved in wood plastic composites manufacturing. It would be of great interest to examine the changes of fiber characteristics (fibrillation and fiber size) on the strength of wood plastic composites as a function of the consumed energy.

The repeated works on the composites made with different wood fiber and the matrices are investigated to show corresponding behaviors. It is widely accepted that the final fiber characteristics are mainly determined by the initial matrices conditions and the grafting manner. Such information may shed some lights on the mechanism of esterification, and hopefully it might lead to energy saving by optimizing the compounding functions.

1.4.2 Thesis content

This thesis consists of thirteen chapters. Chapter 1 describes the history of wood composites and gives an insight of the advantage of wood plastic and their shortcomings. Chapter 2 reviews briefly the natural source of wood, the characteristics of wood fiber and the polymer used. Chapter 3 to Chapter 11 present the results and the discussions concerning our publications. Chapter 12 is an exploratory study on bacterial cellulose used in biomedical applications. Finally, Chapter 13 gives a general conclusion. The research works presented in Chapter 3-11 are divided in four sections.

1.4.2.1 Strategies for improving mechanical properties of both the nano-composite and the composites (Chapter 3-7)

Except the studies on the traditional modification including coupling agent and initiator, nano-particles are used to improve the strength due to the stress transferred via junction points [239]. However, many publications were reported on polymeric nanocomposite materials [239, 240, 241, 242, 243, 244, 245, 246, 247, 248], but very little was published on its applications in wood plastic composite. Challenges for improving the strength include adding nanoclay to investigate the improvement of the compatibilities with the wood composites components. A series of methods of compatibilisation and modification of wood fibers and the maximization of the properties are performed and compared using nanofiller and coupling agents as well as initiator.

In addition, the influence of the type of matrix, the fiber size, the graft level of maleic anhydride groups and molecular weight of coupling agents on the mechanical

properties are investigated. The distribution and deposition of nanofiller is also shown as function of the cationic nanofiller and anionic wood fiber.

1.4.2.2 The behaviors of the thermal degradation during the compounding (Chapter 8-9)

The thermal behaviors of the composites are evidenced by incorportating of anti-oxidant after the investigation of virgin matrix.

1.4.2.3 The water and mechanical behaviors of the composites reinforced with organo-nanoclay (Chapter 10)

The dimensional stability and mechanical behaviors of the composites reinforced with organo-nanoclay (Chapter 10).

As indicated that organic surfactant has impact on the surface chemical of nanoclay, the studies are performed to disclose the effects of nanolcay particles on the improvement of either polymeric nanocomposites or the wood composites. Moreover, the dimensional stability of wood composites are studied and the resulting mechanisms are clarified.

1.4.2.4 The morphological structure of functionalized wood fiber in wood composites (Chapter 11)

Several measurements are used to evidence the reactions in wood composites. The physical morphologies of wood fiber are also quantified and imaged. With these findings, the occurrences of the fractures and the esterifications are well documented and related to the mechanical performance.

Chapter 11 fully details the esterification when wood fiber was grafted by coupling agent, and even the fractional bonded polymer is characterized by a new way.

Chapter 2 - Background

Wood plastic composite lumber is composed of natural fibers and virgin/recycled thermoplastics including PE, PP, PVC, PSt *etc.* While thermosets include epoxies, polyesters, phenolics, silicones and elastomers include rubber and PU. The characteristics of wood fibers and the matrix affect the properties and microstructures of wood composite.

2.1 Natural resources of wood

In Canada, forests occupies 45% of the territory, representing 417.6 million hectares of the total Canadian continental area of 921.5 million hectares. Forests stretch from the Atlantic to the Pacific coasts, and to the north up to the Arctic treeline limit as shown in Figure 2.1. Canada is home to about 180 species of trees. Tree species are typically grouped into deciduous and coniferous. Some deciduous species such as birch and willow are found in most Northern areas where trees are found.

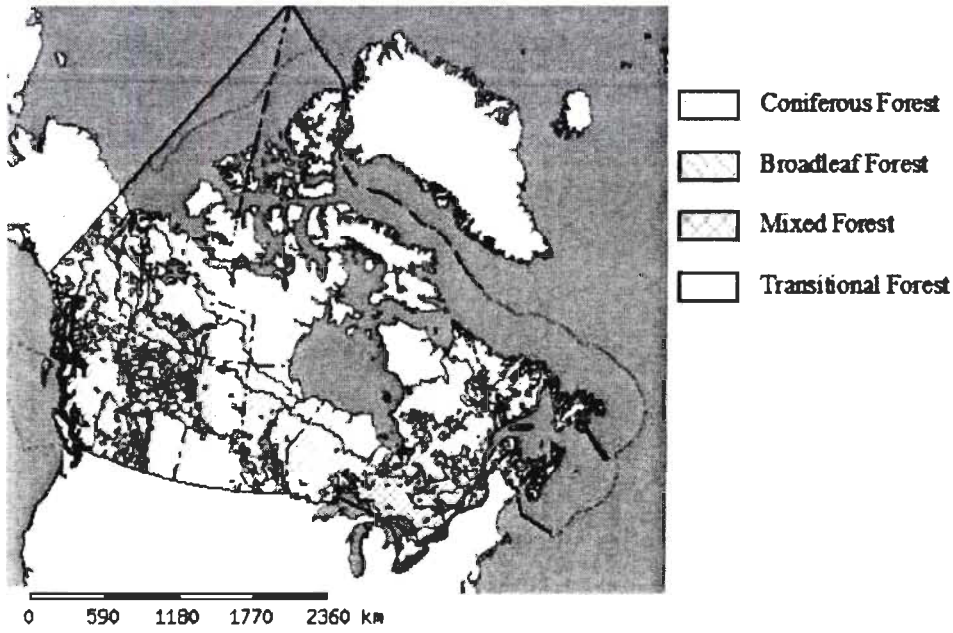

Figure 2.1 Distribution of tree species in Canada [249]

Figure 2.1 shows the number of tree species by ecoregion. Due to the warmer climatic conditions, more tree species live in the Southern part of Canada than in the north. The highest numbers of tree species are found in the Mixwood Plains ecozone and the southern part of the Boreal Shield, located in Southern Ontario and along the St. Lawrence River. The ecoregion that contains the highest number of tree species is

the Lake Erie Lowlands, located in the Mixwood Plains Ecozone, with 95 tree species. Figure 2.2 shows the tree species in the province of Quebec. Two kind of wood fibers from hardwood in Quebec are very popular and were studied here.

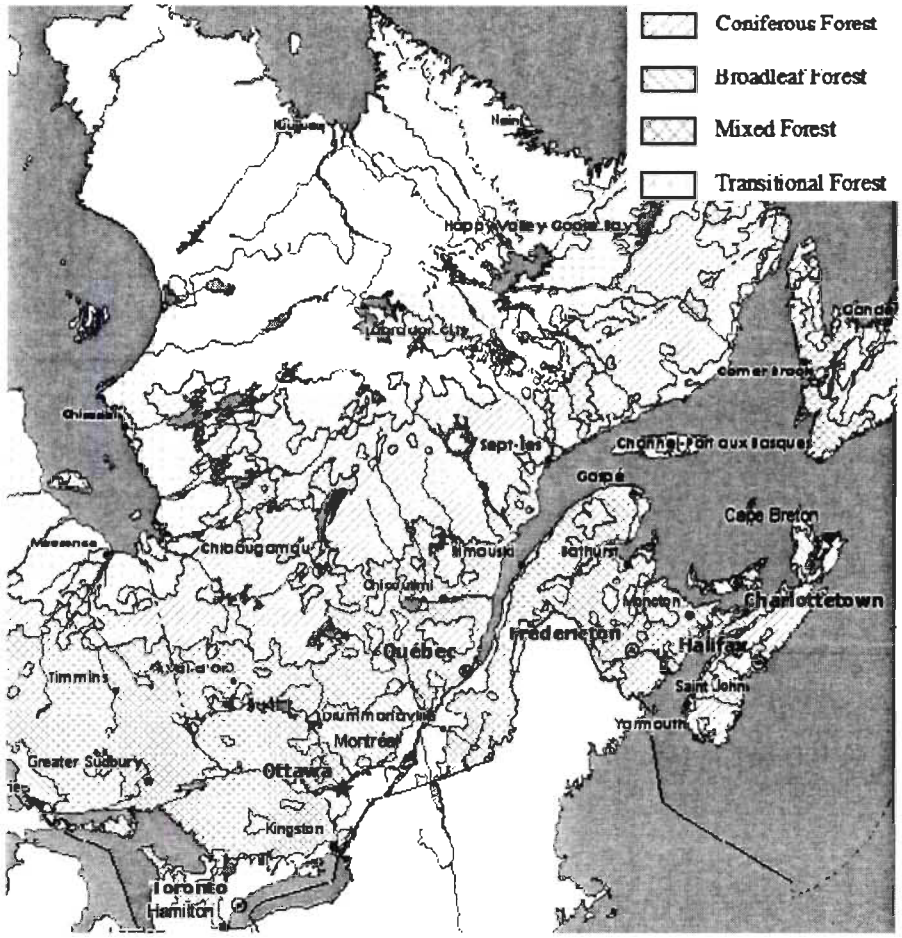

Figure 2.2 Distribution of tree species in Quebec [249]

➢ **Trembling aspen** (*Populus tremuloides*) one of the broadleaf species growing in the boreal area, is a hardwood tree that has the widest range of any tree in North America, extending from the North Eastern United States through Canada to Alaska, as well as throughout the forested areas of Canada and the province east of the Coast Ranges（Figure 2.3 insert No.2）. The sapwood is white to light cream in color and merges gradually into the heartwood, resulting in a boundary that is very hard to distinguish.

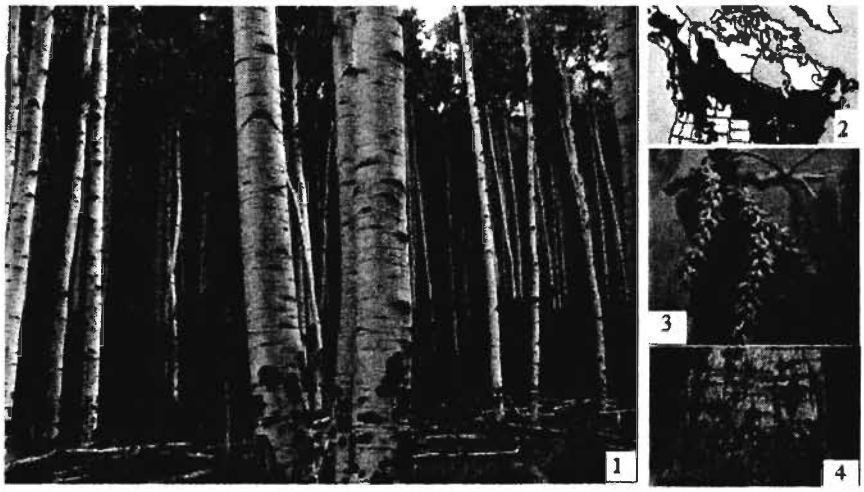

Figure 2.3 Photos of trembling aspen [250]

Note: 1) Young bark smooth, pale green to whitish; 2) Mature dark becomes dark and furrowed, trunk cylindrical and smooth; 3) Distribution of aspen in North America; 4) Seed catkins, fruits capsules will split into two parts

Aspen tree is a deciduous tree quick growing to 20-25m at maturity with a trunk 20-80cm diameter, but with short life (around 50 years). It can be propagated by cuttings, which can't tolerate strong wind and root very easily, and also highly susceptible to fire and insects damage. Aspen wood is soft and brittle and not very durable, and is a very common hardwood to be used for pulp in Canada, especially in Quebec.

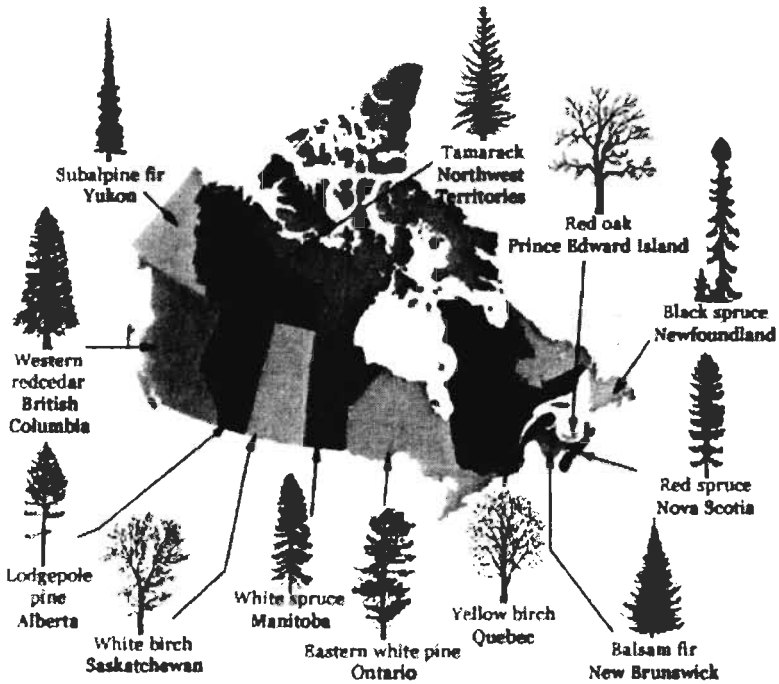

Figure 2.4 Canada's official provincial and territorial trees [251]

➢ **Yellow birch** (*Betula alleghaniensis*) is a slow-growing, medium-sized (>20m) hardwood tree. The bark has conspicuous lenticels (long horizontal markings), is yellowish or bronze during the early stages of its life, and takes on dark reddish colors as it matures. Ungulates and hares forage on leaves and young twigs during the summer and winter. Yellow birch is one of the most widely distributed species in North America （Figure 2.5 insert No.2), especially in Quebec. It is the provincial tree of Quebec [251, 252].

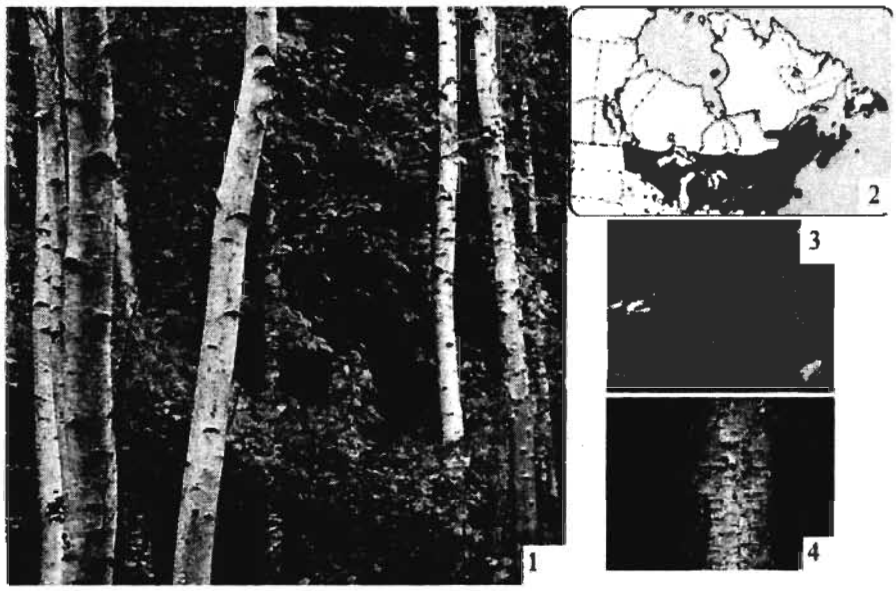

Figure 2.5 Photos of yellow birch [253]

Note: 1) Young bark; 2) Distribution of aspen in North America; 3) Yellow birch leaf; 4) Mature bark

2.1.1 Characteristics of wood fibers

All wood is composed of cellulose, lignin, hemicelluloses, and minor amounts (5% to 10%) of extraneous materials contained in a cellular structure [254] and the layers of wood are shown in Figure 2.6.

Normal juvenile and mature wood fibers are approximately rectangular in cross-section with the wall thickness varying from 10% of the total cross section in early-wood to about 80% of the cross section in late-wood. Wood fiber is composed of layers of crystalline cellulose (fibrils) wrapped in a cylindrical shape with an open center, or "lumen". The gross wood structure is composed of fibers in the longitudinal direction bound together by lignin "glue" and bundles of ray cells oriented in the radial direction in the wood which act as reinforcement rods to increase the radial strength.

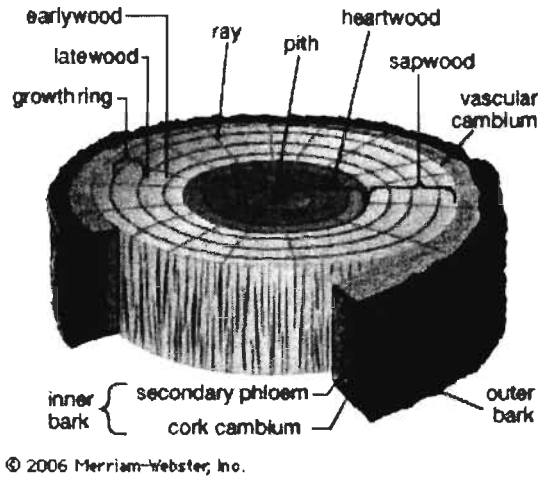

Figure 2.6 Cross section of a tree trunk [255]

The imaging of poplar wood cell walls by Raman microscopy cross-section is shown in Figure 2.7. There are two kind of methods to produce wood fiber in industry: mechanical pulping [256] and chemical pulping [257]. Variations in the characteristics and volume of these components and differences in cellular structure make woods heavy or light, stiff or flexible, and hard or soft. However, to use wood to its best advantage and most effectively in engineering applications, specific characteristics or physical properties must be considered.

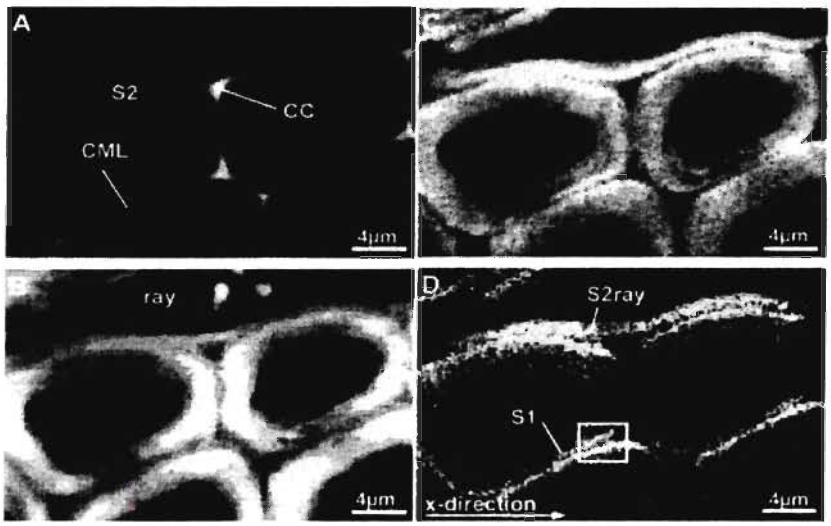

Figure 2.7 Raman images (30×20μm) of a cross section of poplar latewood [258]

Note: CML-Compound middle lamella; CC-Cell corner

2.1.2 Wood fibers

The effects of fiber morphology on mechanical properties of wood plastic composites are applicable to any type of fiber, regardless of source. Many areas of

the world do not possess indigenous supplies of wood fiber. The demand for pulp fiber has grown fast in China market, and plenty of non-wood plant fiber is available in these areas. For example, China is the biggest producer of straw pulp in the world and import largest amounts of pulp [259]. Although there were many fibrous sources, the fibers are mainly from softwoods and hardwoods, comprising 94% of the market [260].

Wood fibers properties could be divided into three parts:

1. Structural properties (ML, S1, S2, fibril angle etc);
2. Chemical properties (chemical composition and structure);
3. Morphological properties (cell wall thickness, fiber width and fiber length).

2.1.2.1 Structure of woody cell

Wood is a cellular materials built up by tube-shaped cells oriented fairly parallel to stem or branch axis. The wood cell walls organized in several layers including the middle lamella (ML), primary cell wall (P), secondary cell wall (S1, S2 and S3) and warty layer (W) illustrated in Figure 2.8 (a) as well as their thickness. The wood cell wall consists of crystalline cellulose fibrils with 2.5nm diameter embedded in an amorphous hemicelluloses-lignin matrix where lignin acts as adhesive described in Figure 2.8 (b-c).

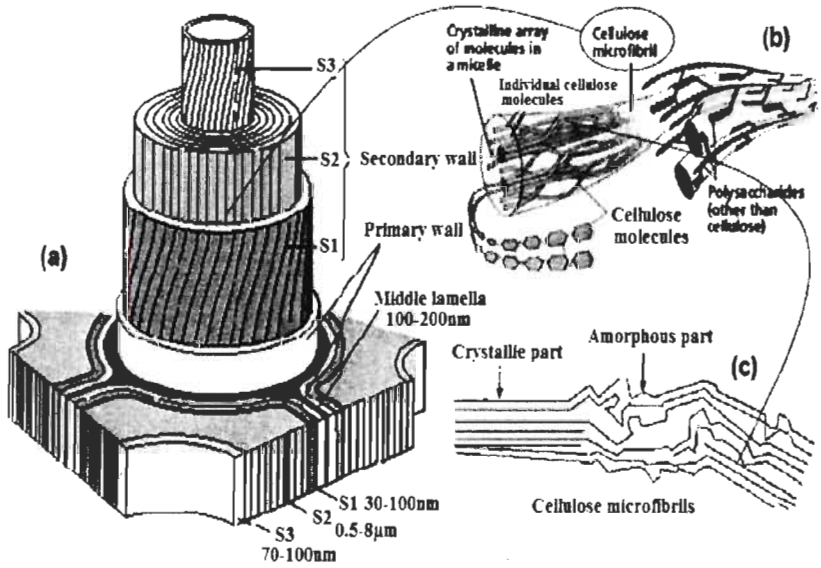

Figure 2.8 (a) Simplified composition of the wood cell wall. (b) A schematic representation of the cellulosic mircrofibrils. Amorphous hemicellulose and some lignin are located between the crystalline cellulose microfibrils; (c) Schematics of a cellulose microfibril [261].

The S2 layer comprises the major part of the cell wall and the cellulose fibrils are aligned fairly parallel and trace a steep spiral around the cell (Figure 2.8 b) and while angle is sharply defined as the tilt angle versus the longitudinal axis of the cell usually differs according to different layers [260]. The tilt angle of cellulose fibrils in tissue plays a key role in determining the mechanical properties of wood and this angle could be determined by a scanning X-ray microdiffraction technique in non-destructive determination.

2.1.2.2 Chemical compositions of wood fiber

Wood fiber is mainly built up of cellulose, hemicellulose and lignin (Table 2.1), and also including some inorganic compounds and minor extractives.

Table 2.1 Molecular structure and natural composition of wood fiber [262]

Components	Composition, % Hardwood	Softwood	Polymeric Nature	DP	Building Molecular	Role
Cellulose	40-50	40-50	Linear molecule Crystalline	5000-10000	Glucose	Framework
Hemicellulose	25-35	25-30	Branched molecule Amorphous	150-200	Primarily non-glucose sugars	Matrix
Lignin	20-25	25-35	3D molecule Amorphous	100-1000	Phenyl propane	Matrix
Extractives	0-10	0-10	Polymeric	----	Polyphenols	Encrusting

2.1.2.2.1 Cellulose

Cellulose is the most abundant biopolymer on earth. Around 40% of the dry weight of wood consists of cellulose. Cellulose is a linear polymer (homopolysaccharide) composed of D-glucose units linked together by β-1-4 glycosidic bonds (Figure 2.9) and the degree of polymerization (DP) is up to10000 glucose units [263] and following drop in chemical pulping around 500-2000 while mechanical treatment of fibers has very little effect on the DP [264]. Most of the cellulose found in wood fibers has approximately the same molecular size, i.e. a very low polydispersity [263].

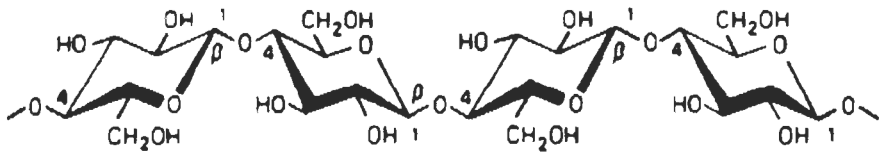

Figure 2.9 Molecular structures of cellulose

Cellulose has a strong tendency to form intra- and inter-molecular hydrogen bonds by the hydroxyl groups on these linear cellulose chains and aggregated bundles of

molecules, which stiffen the straight chain and promote aggregation into a crystalline structure and give cellulose a multitude of partially crystalline fiber structures and morphologies illustrates in Figure 2.8 (b) and (c). The crystallinity decreases with increasing height above the ground. However, the degree of crystallinity of cellulose was 50-56% in kraft pulp, about 50% in normal wood, and 50–60% in compression wood [261] as presented in Table 2.2.

Table 2.2 X-ray Crystallinity of some cellulose materials [265]

Samples	X-ray crystallinity, %
Cotton linters	56-63
Sulfite dissolving pulp	50-56
Prehydrolyzed sulfate pulp	46
Viscose rayon	27-40
Regenerated cellulose film	40-45

2.1.2.2.2 Hemicelluloses

Hemicelluloses constitute about 25-35% of the wood material and are a group of branched polysaccharide polymers (heteropolysaccharide) built up of xylan, glucomannan, galactoglucomannan, arabinogalactan and galactan, with low molecular weight, the degree of polymerization is 150-200 in Table 2.1.

Galactoglucomannans (about 20%) are main hemicellulose in softwoods (Figure 2.10) and contain 5-10% arabinoglucuronoxylan (Figure 2.11), arabinogalactan and other polysaccharides while glucuronoxylans (about 16% of the dry weight of the wood) are main hemicellulose in hardwoods (Figure 2.12) and contain 15-30% xylan of the dry wood, 2-5% glucomannan and other polysaccharides in hardwood glucuronoxylan.

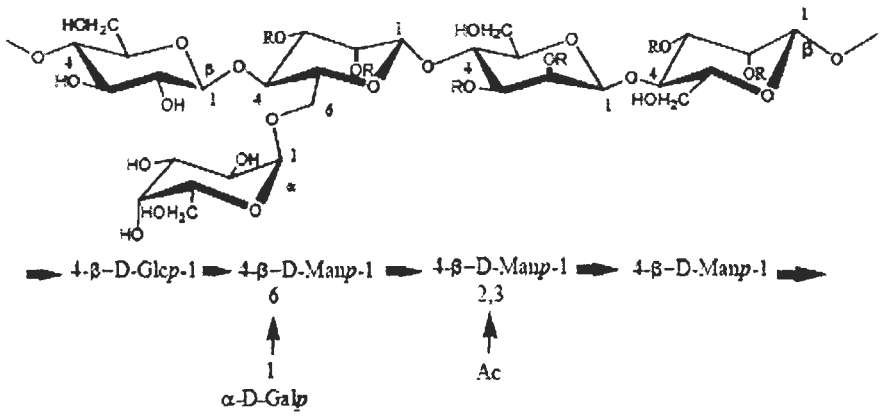

Figure 2.10 Principal structures of Galactoglucomannans in softwood [265]

Sugar units: β-D-glucopyranose(Glc*p*); β-D-mannopyranose (Man*p*); β-D-galactopyranose (Gal*p*); R=CH_3CO or H. The lower representation is the abbreviated formula showing the proportions of the unites (galactose-rich fraction)

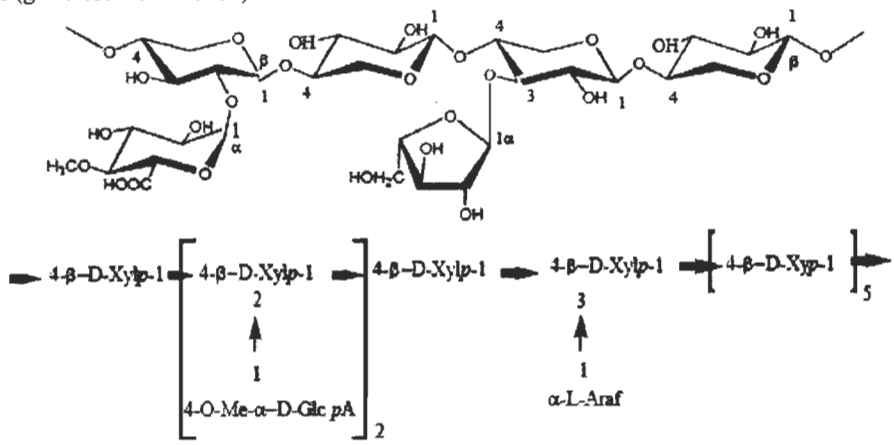

Figure 2.11 Principal structure of Abrabinoglucuronoxylan in softwood [265]

Sugar units: β-D-xylopyranose(Xyl*p*); 4-O-methyl-α-D-glucopyranosyluronic acid (Glc*p*A); α-L-Arobinofuranose (Ara*f*). The lower representation is the abbreviated formula showing the proportions of unites.

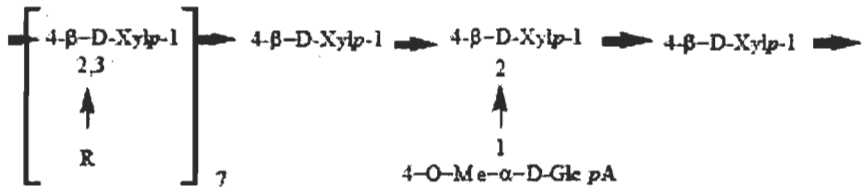

Figure 2.12 Principal structure of Glucuronoxylan in hardwood [263]

Sugar units: β-D-xylopyranose(Xyl*p*); 4-O-methyl-α-D-glucopyranosyluronic acid (Glc*p*A); R=Acetyl group (CH_3HO).

Principal chemical compositions and structural features of hemicelluloses in softwoods and hardwoods are summarized in Table 2.3 [266].

Table 2.3 The main hemicellulose in hardwoods and softwoods [266]

Species	Polysaccharide	Amount %	Composition (molar ratios)						
			Xyl	GlcA	Ara	Man	Glc	Gal	Ac
Hardwood	Glucuronoxylan	15-30	10	1	--	--	--	--	7
	Glucomannan	2-5	--	--	--	1-2	1	--	--
Softwood	Arabinoglucuronoxylan	7-10	10	2	1.3	--	--	--	--
	(Galacto)glucomannan	10-15	--	--	--	4	1	0.1	1
	Galactoglucomannan	5-8	--	--	--	3	1	1	1

Abbreviation: Xyl=xylose; GlcA=4-O-methyl- α-D-glucuronic acid; Ara=arabinose; Man=mannose; Glc=glucose; Gal=galactose; Ac=acetyl group.

2.1.2.2.3 Lignin

Lignin, makes-up 15-30% of wood, is the second most abundant biopolymer in the plant after cellulose. Lignins are complex heterogeneous polymers of phenylpropane unite, such as *trans*-coniferyl, *trans*-sinapyl and *trans-p*-coumaryl alcohols, which are the precursors of lignin [267, 268, 269, 270]. Lignin binds the wood cell together with cellulose and hemicellulose to form lignin-cellulose complex and lignin-hemicellulose complex resulting in network polymer with hydroxyl phenylpropane groups as the glue of wood.

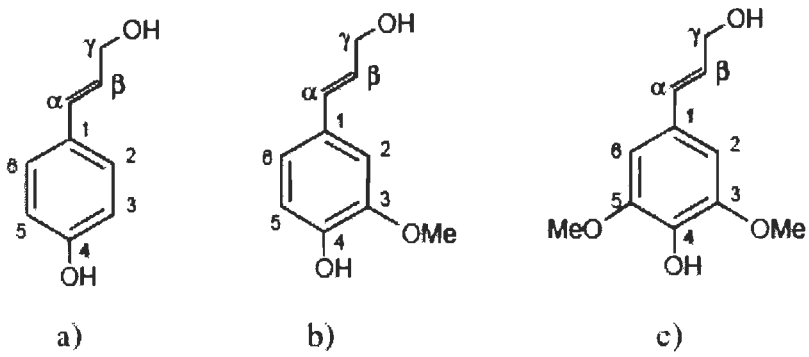

Figure 2.13 Three type precursors of lignin during the formation of cell wall [271]

a) trans-*p*-coumaryl alcohols; b) trans-coniferyl (guaiacyl unit); c) trans-sinapyl alcohol (syringyl unit)

2.1.2.2.4 Extractives

Extractives make-up about 3-10% of the dry wood grown in temperate climates while higher quantities are found in tropical climates [272]. Although these extractives are small in quantity, they have significant influences on the properties of wood, such as color, odor and decay resistance [272, 273]. Extractives are encrusting polyphenols, e.g. terpenes, terpenoids, esters of fatty acids (fats and waxes), phenolic compounds and several other compounds which could be extracted from wood with polar or nonpolar solvents [274].

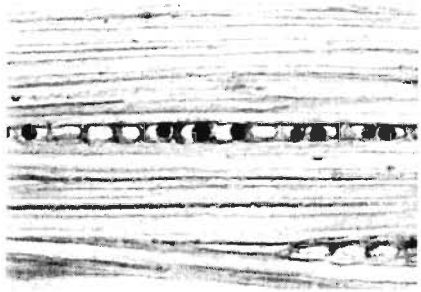

Figure 2.14 Extractives droplets in a wood section [275]

2.1.3 Softwood and Hardwood

Throughout history, the unique characteristics and comparative abundance of wood have made it a natural material for homes and industrials [254]. Wood fibers come from wood chips by pulping. The characteristics of wood have important effects on the fiber. Common to the two species groups is that the main cell type (tracheid /fiber) in the wood has at least some supporting function that gives mechanical strength to the tree. Hardwoods, which developed much later than softwoods, have a different arrangement of the cells building up the trees and there are differences in both their general function and their chemical composition [254]. However, this thesis has focused on hardwoods and the concentration will be on the mechanical properties of these species.

Softwood trees are softer than hardwood with the exception of Douglas fir which is harder and stronger than many hardwoods while balsa is much softer than most softwoods as a hardwoods [276]. The difference between softwood and hardwood is found in the microscopic structure and chemical components of the wood.

2.1.3.1 Difference in woody cell

The difference between softwood and hardwood is found in the microscopic structure of the wood. Softwood contains only two types of cells: 90-95% longitudinal wood fibers (or tracheids) and 5-10% transverse ray cells. Longitudinal wood fiber functions in water conduction and support mechanical strength to the tree. Softwoods lack vessel elements for water transport that hardwoods have. These vessels are manifested in hardwoods as pores. In softwood water transport within the tree is via the tracheids only. Hardwoods have vessel elements for water transport that softwoods lack; these vessel elements are evident in hardwoods as pores. SEM images show the presence of pores in hardwoods and absence in softwoods in Figure 2.15 [277, 278].

2.1.3.2 Difference in physical and chemical properties

Hardwoods, that developed much later than softwoods, have a different arrangement of the cells building up the trees in Figure 2.16 and there are differences in both their general function and their chemical composition, illustrated in Table 2.2 and Table 2.3 and have different structure of hemicelluloses as shown in Figure 2.10, Figure 2.11 and Figure 2.12.

Figure 2.17 and Figure 2.18 illustrate the difference of the microscopic structures between softwood fiber and hardwood fibers that the softwood fibers are longitudinal tracheids formed from a single hollow (dead) spindle-shaped cell connunicated by pits pairs in Figure 2.17(1) while the difference between earlywood and laterwood is obvious from Figure 2.17(3). There are no vessels among the woody cell.

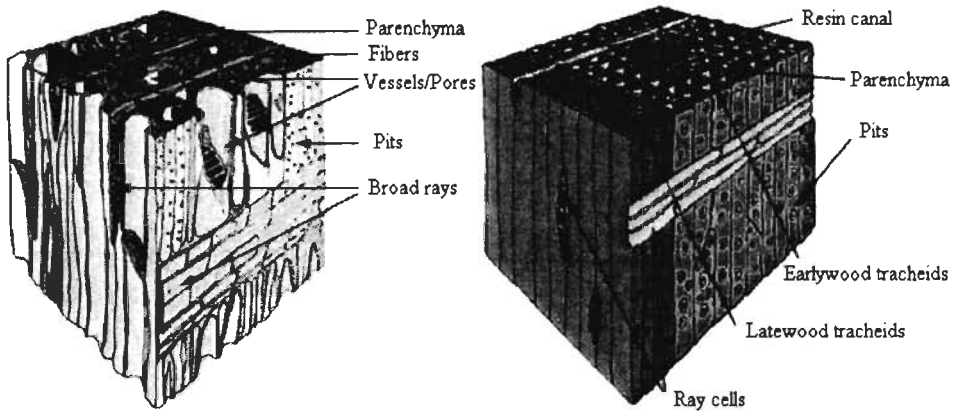

Figure 2.15 Three-dimensional cell level comparisons between hardwood (left) and softwoods (right) [277]

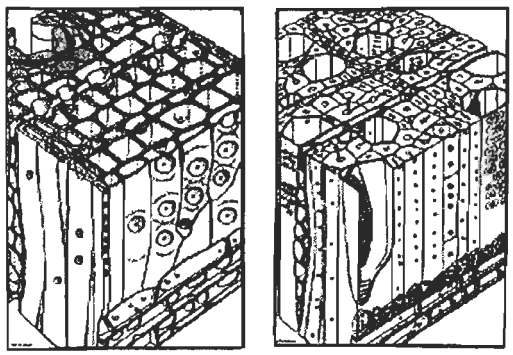

Figure 2.16 Cell wall–Softwood (left) and Hardwood (right) [278]

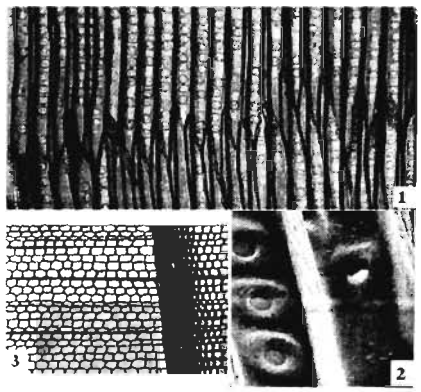

Figure 2.17 Microscopy of softwood fiber [279]

Note: 1-Radical section; 2-Windows pits and holes; 3-Cross section

Hardwoods are the timber of dicotyledonous angiosperms composed of vessels, few tracheids and lots of parenchyma as in Figure 2.18(1). Vessels are wide tubes composed of several stacked vessel element cells perforates or with perforation plates to help stop cavitations from spreading from vessel to vessel shown in Figure 2.18(2). Hardwoods are broadly classified into two groups. The first are termed ring-porous such that the vessels are much wider and more numerous in earlywood resulting in clear annual rings as shown in Figure 2.18(3) e.g. ash. While the diffuse porous hardwoods, on the other hand, show little variation in the quality and quantity of vessels through the year, so the annual rings are much less obvious, e.g. beech as shown in Figure 2.18(4). However, since this thesis has focused on hardwoods, the concentration will be on the structure of these species.

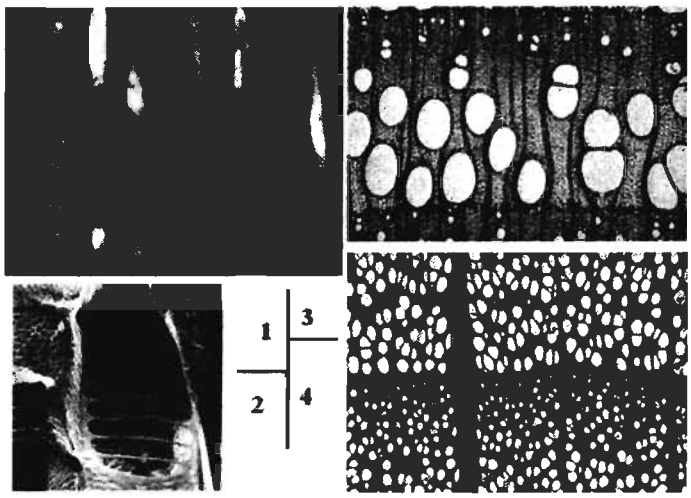

Figure 2.18 Microscopy of hardwood fiber [279, 280]

Note: 1-Radical section of Bitternut hickory (Carya cordiformis); 2-Vessels; 3-Cross section of Ash; 4-Cross section of Beech.

2.1.3.3 Physical and mechanical properties of wood fibers

Wood is far from being homogenous materials due to large natural variation between various wood species and within a specified species. Even in same species, wood properties are found to be variable due to the genetic inheritance and environmental condition in a tree stem at a certain age.

Therefore, fiber properties are also different resulting in the raw wood entering the pulping process pulping method. Because the wood polymer composites are largely filled with wood fibers, the fiber morphological characteristics of the original woods could be expected to attribute the basis for final properties of the products, such as

strengths and modulus. Physical and mechanical properties of natural fibers are shown in Table 2.4.

Table 2.4 Physical and Mechanical properties of some natural fibers [281]

Species	Density g/cm³	Tensile strength MPa	Young's modulus GPa	Specific strength Pam³/g	Specific Young's modulus kPam³/g
Flax	1.4-1.5	500-900	50-70	357-600	36-47
Hemp	1.48	300-800	30-60	203-541	20-41
Jute	1.3-1.5	200-500	20-55	154-333	15-37
Sisal	1.45	100-800	9-22	69-552	6-15
Banana	1.4	500-700	7-20	375-500	5-14
Softwood	1.4	100-170	10-50	71-121	7-36
Hardwood	1.4	90-180	10-70	64-129	7-50

2.1.3.4 Physical and mechanical properties of softwoods and hardwoods fiber in WPC

There are many kinds of natural fibers suitable to reinforce plastics due to their relative high strength and stiffness, and low density [282]. Natural fibers can be processed in different ways to yield different mechanical properties. Modulus of elasticity (MOE) of cellulose fiber could be up to 40GPa obtained from bulk wood and about 10GPa for fibers from chemical pulping processes. The separated fiber can be hydrolyzed into microfibrils with MOE of 70GPa following mechanical disintegration. Although the theoretical value of the MOE of cellulose chains is up to 250GPa, there is no suitable technology to separate the chains from microfibrils [283, 284]. Figure 2.19 compares the specific strength and modulus of some popular materials.

Wood pulp fiber is one promising and often-used wood fiber among the different types of fibers used in wood-based composites due to the distinct advantages [143]. The characteristics of wood fibers pulping from different species of wood are different due to the climatic conditions, age and the digestion process as well as the pulping technique, e.g. chemical or mechanical pulping method [285, 286]

Some results have been reported concerning the effect of hardwoods and softwoods pulp fiber on the mechanical properties of WPC. Stark [143] found that although both notched and unnotched impact strength were lowered as well as tensile strength for plastics filled with wood fibers from either hardwood fibers or softwood fibers, the reinforcements by hardwood fiber were a little better than softwood fibers which was opposite to tensile strength at 20wt% level loading. Stark also found

enhancements in flexural properties, e.g. flexural strength and MOE, using softwood fibers to reinforce PP composites compared to hardwood fibers [143], which are typically longer and slimmer than hardwood fiber due to the higher aspect ratio and length of softwood pulp fibers [287, 288, 289].

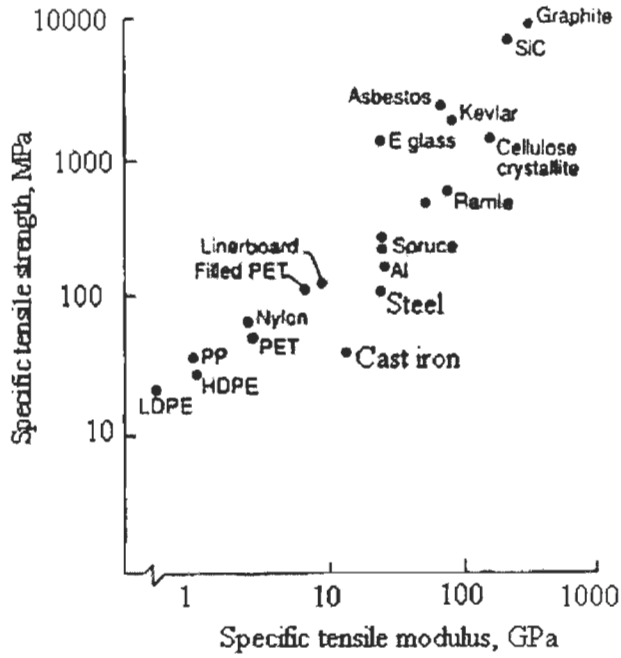

Figure 2.19 Comparison of specific tensile and modulus of various materials [46]

However, some contradictory results have been reported that MOE of PP composites reinforced with 20wt% hardwood fibers, those being slightly inferior to softwood fibers while vice versa at 40wt% level [143]. Regardless of the concentration of fibers, Stark [143] examined that the added hardwood fibers decreased elongation and mold shrinkage compared to softwood due to the shorter fiber length and thinner cell wall of hardwood as well as lower aspect ratio similar to that of wood flour.

Wood pulp fibers are different according to the pulping technique listed in Table 2.5. TMP fiber (length approximately 1-2mm) tensile strength is approximately 50-70% that of kraft fibers which are approximately 3-5mm in length [290]. TMP fibers typically contain less cellulose (16-36%) than kraft fibers (78-88%) [291]. Typically, unbleached kraft fibers consist of 78-88% carbohydrates and 12-22% lignin, while bleached kraft fibers contain 94-96% carbohydrates and 1% lignin [291]. The removal of lignin from the fiber has the potential to increase fiber-matrix adhesion due to more open or rougher fiber surface leading to increased physical bonding with

the matrix [292].However, kraft fibers display lower reactivity with coupling agents due to the low amount of aromatic hydroxyl groups as well as lower MOE.

Table 2.5 Summary of major pulping process [293]

Process	Treatment		Pulp yield	Relative strength	
	Chemical	Mechanical	%	Softwood	Hardwood
TMP	Stream	Disk refiner (Pressure)	80-90	6-7	---
CTMP	Sodium sulfite or Sodium hydroxide	Disk refiner (Pressure)	80-90	---	5-8
Kraft	Sodium hydroxide +sodium sulfite	None	45-55	10	7-8

Although the thermal stability of lignin is below that of cellulose [294] and accelerates the degradation of phenolic resin composite reinforced with vegetable fibers in the beginning of decomposition, the rate of degradation is lower resulting in producing a more progressive degradation of fibers [295]. Furthermore, wood pulp fibers undergo photo-degradation resulting in the breakdown of lignin to form free radicals and then attack the polymer chains leading to reducing the flexural strength of hybrid composite [296, 297] and greater deterioration of elongation while decreasing impact strength and tensile properties contrary to the enhancement of modulus [297, 298].

It is important to note that lignin hindered phenolic hydroxyl groups can act as stabilizer of reactions induced by oxygen and its radicals, and the reactivity is influenced by limited diffusion into polyolefins. Pouteau *et al.* studied PP samples filled with 15 kind of lignin to characterize their antioxidant properties and it was revealed that lignin has an antioxidant activity and the reactivity increases with the decrease of molecular weight as well as the increase of concentration. Even higher molecular weight lignins have an antioxidant activity [299].

Košíková *et al.* examined the stabilizing effect of sulphur-free lignin in Styrene-Butadiene rubber and natural rubber with improvement of physicomechanical properties of prepared vulcanizates, e.g. stress at 100% elongation, tensile strength at break and elongation at break, to confirm that lignin acts as an active filler [300]. Moreover, the thermo-oxidative degradation of natural rubber vulcanizates was considerably improved by addition of lignin as shown by TGA and DSC analysis due to the chemical reaction between lignin and the sulphur-based vulcanization system [301] which is an accordance with the observation of natural rubber filled with carbon black with lignin acting as an antioxidant [302]. Gregorová *et al.* have studied

the stabilization effect of lignin in PP and recycled PP blends and revealed that the antioxidant effect increased with lignin concentration, and also enhances the antioxidant effectiveness (AEX) of commercial antioxidant Irganox 1010 [303], leading to a rigidity increase. In addition, hardwoods are generally far more resistant to decay than softwoods when used for exterior work [304], so hardwood mechanical pulp fiber could be a suitable choice.

2.1.3.5 Morphological properties of selected hardwood fiber

Due to aspen and birch fibers use in this thesis, some morphological properties are shown in this section. WPCs contain fibers of different origin with diverse properties. The fiber selection is normally based on the requirements of the final product. The morphologies properties of fibers including length, width and wall thickness etc are well presented in the Table 2.6.

Table 2.6 Morphological properties for wood kraft pulp fibers [305, 306]

Species	Density kg/m³	Length mm	Width μm	Wall thickness μm	Coarseness mg/m
Aspen	582	1.0-1.3	18-19	2.0-3.0	86
Birch	740	1.1-1.5	16-22	3.0-3.6	114

An approximate perceptual distribution of the chemical components in different tracheid resctions is plotted in Figure 2.20 and the general compositions are defined in Table 2.7. Due to the fact that the decomposition temperature of the hemicellulose (about 200-350°C) is lower than that of cellulose (about 240-350°C) and the amount of hemicellulose in hardwood is higher than in softwood [307], its degradation is easier in hardwoods than softwoods. However, the breaking of a hemicellulose chains does not reduce as much the strength of the wood as breaking of cellulose chains [308].

Table 2.7 Typical properties of Aspen and Birch wood [265]

Hardwood	Density† kg/cm³	Lignin %	α-Cellulose %	Pentosan %	Extractives %	Ash %
Yellow birch	657	21.2	49.4	21.4	2.6	2.9-1.7
Trembling aspen	400	18.2	50.2	17.5	2.4	4

† Oven dry density

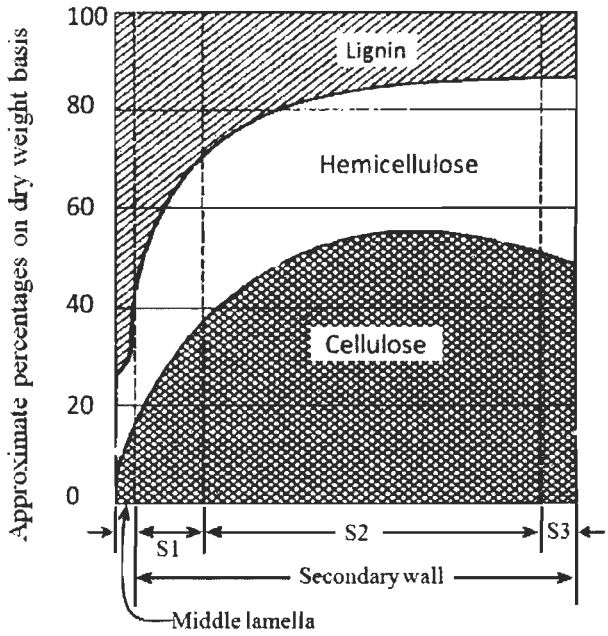

Figure 2.20. Distribution of the principal chemical constitutes within the various layers of the cell wall in conifers [309]

2.1.4 Grades of pulp fibers

Pulps were classified mainly according to their pulping process [305]. Pulping is nothing but breaking/removing lignin to separate fibers. The properties of various pulp fibers have different characteristics. Two type of pulping process used to prepare fibers used in our research are described below.

Aspen wood has a relatively low lignin content compared to that of other pulped hardwoods which makes the pulp easier to bleach. Like birch kraft, aspen kraft pulps refine quickly producing a dense, smooth paper, but with less strength compared to birch pulp. Birch hardwood kraft pulps are thin walled and the pulped wood has relatively high hemicellulose content. These pulps refine quickly, producing a pulp which tends to be lower in opacity and bulk compared to eucalyptus hardwood kraft pulps, but higher in burst and tensile strength.

2.1.4.1 Chemi-Thermo-Mechanical Pulp (CTMP)

CTMP process is used both for pulping hardwood as well as softwood to obtain high yield pulp. The sequence of actions of CTMP preparation is: Soaking wood chips in chemicals →Steaming →Refining.

2.1.4.2 Bleached Chemi Thermo Mechanical Pulp (BCTMP)

High yield Bleached CTMP is obtained by bleaching using i.e. ozone or peroxide. Softwood BCTMP is produced at a similar yield (>85%) to Hardwood BCTMP. Although hydrogen peroxide is the sole bleaching agent, hardwood pulps could be produced with up to 88% ISO brightness which is slightly higher than brightness of softwood pulps (60-80% ISO brightness) due to the lower lignin levels.

2.1.5 Grades of pulp fibers

Chemical mechanical pulping (CTMP), where almost no fiber wall are destroyed compared to that obtained solely by mechanical pulping processing including TMP and RMP is illustrated in Figure 2.21, where wood fibers are separated from the wood bundle by removing the lignin-rich surface material

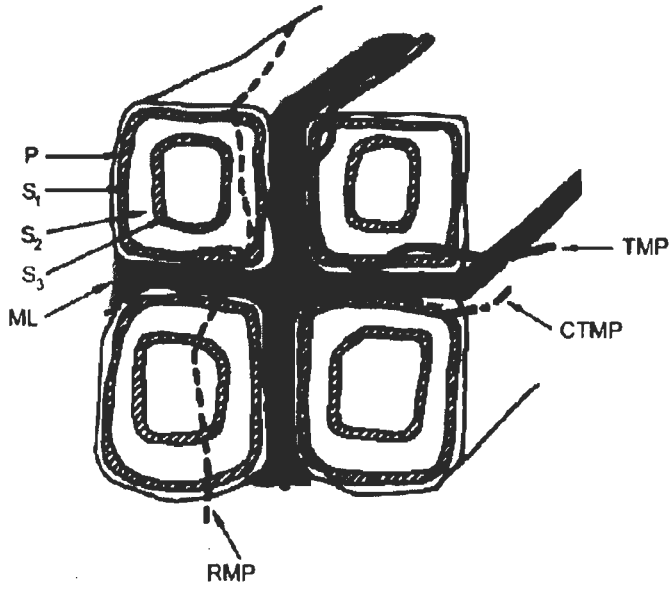

Figure 2.21 Breakdown of the wood matrix as a function of refining temperature

RMP 20–95°C, TMP 110–150°C, MDF 170–190°C (Franzén 1986 310).

2.2 Matrix polymer

Matrix may be categorized in many ways, they can be classified into three kinds based on the ways in which they respond to heat. Thermosets are marcomolecules which undergo a permanent chemical reaction when heated while thermoplastics undergo a temporary physical change. Moreover, elastomers are amorphous polymers existing above their glass transition temperature (Tg) and have the property of elasticity.

2.2.1 Thermoset

A thermoset is a material that cures or hardens into a given shape by heating or curing. The reaction of thermosets is irreversible by which permanent connections are made between the molecular chains which give the cured polymer a three-dimensional structure as well as a higher degree of rigidity. Thermosets can't be melted once they are cured since they are chemically crosslinked. But these matrices usually outperform thermoplastics by having good mechanical properties, chemical resistance, thermal stability, overall durability and very low creep.

2.2.2 Elastomer

Elastomers are usually thermosets (requiring vulcanization) but may also be thermoplastic, defined as thermoplastic elastomer, with high elasticity manipulated at temperature higher than the Tg of the polymer. Elastomers could bear strong tensile impact and stress force due to their long chains and capacity to reconfigure them to distribute an applied stress leading to extreme flexibility with a reversible elongation from 5-700%, depending on the specific material, which are widely used to modify the properties of rigid thermoplastics, usually improving impact strength. This is quite common for sheet goods and general molding compounds, e.g. WPC with high impact strength.

2.2.3 Thermoplastics

A thermoplastic softens when heated, but it does not cure or set. A thermoplastic often begins in pellet form, and then becomes softer and more fluid as heat increases. This fluidity allows it to be injected or molded under pressure. As it cools, the thermoplastic will harden in the shape of the mold, but there is no crosslinking reaction occurring which is not similar to the thermoset material. The changes in the thermoplastic are only physical and wholly reversible by heating. A thermoplastic material can be reprocessed many times and is popular as used in wood polymer composite.

2.2.3.1 Polymerization and Structures

The most frequently used thermoplastics are PP and PE with low melting point resulting in better fluidity leading to be injected or molded below 200°C. Wood fiber can be thermo-degraded seriously over this temperature. Both PP and PE are the most ones used in WPC which are polymerized as described below.

2.2.3.1.1 Polypropylene

Polypropylene is a thermoplastic polymer and a linear structure based on the monomer CnH_2n made by chemical industry in 1957 (see Figure 2.22) and used in wide variety of applications, including WPC.

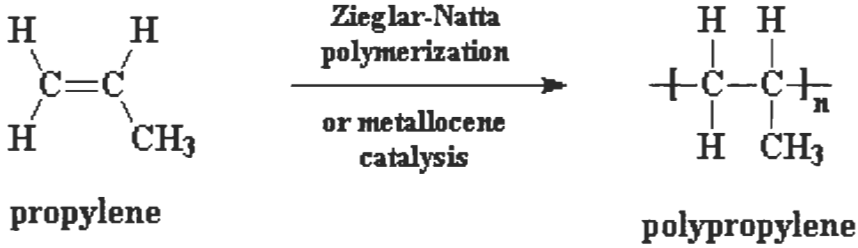

Figure 2.22 Synthesis of polypropylene [311]

Polypropylene can be made with different tacticities. Most commercial polypropylene is isotactic (see Figure 2.23) and has an intermediate level of crystallinity between that of low density polyethylene and high density polyethylene, opposite to amorphous thermoplastics, such as polystyrene, PVC, polyamide, etc. On the other hand PP has higher working temperatures and tensile strength than polyethylene. Polypropylene is rugged, often somewhat stiffer than some other plastics, reasonably economical.

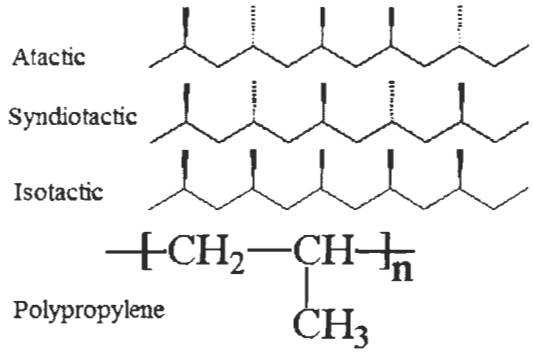

Figure 2.23 Polypropylene structure

2.2.3.1.2 Polyethylene

Polyethylene is the most popular plastic in the world and is used in WPC widely. Sometimes it's a little more complicated. Sometimes some of the carbons, instead of having the hydrogens attached to them, will have long chains of polyethylene attached to them. This is called branched, or low-density polyethylene, or LDPE. When there is no branching, it is called linear polyethylene, or HDPE. Linear

polyethylene is much stronger than branched polyethylene, but branched polyethylene is cheaper and easier to make (see Figure 2.24).

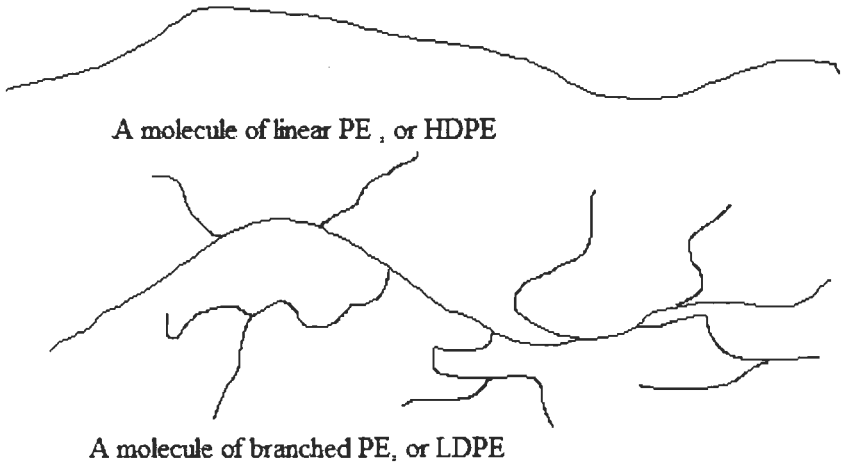

Figure 2.24 Morphological structure of Polyethylene [311]

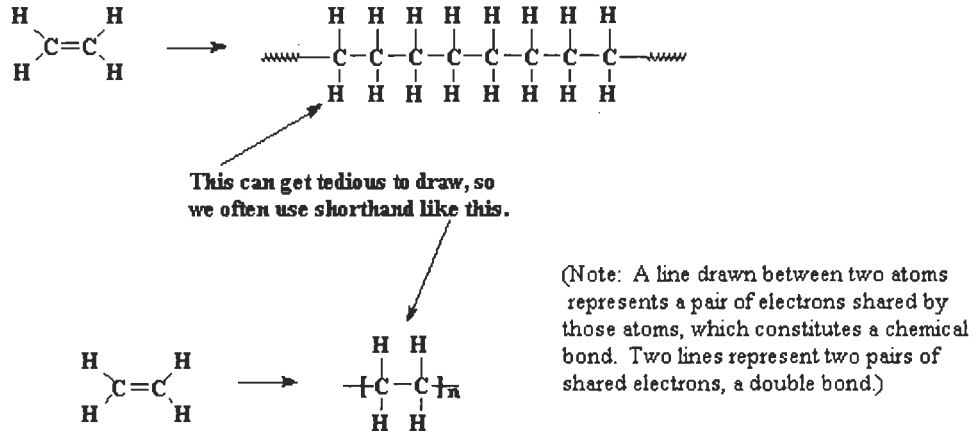

And when we're feeling really lazy we just draw it like this:

$$CH_2{=}CH_2 \longrightarrow -\!\left[CH_2\text{-}CH_2\right]\!-_n$$

Figure 2.25 Synthesis of linear polyethylene [311]

Polyethylene is vinyl polymer, made from the monomer ethylene. Linear polyethylene (HDPE) is made by a more complicated procedure called Ziegler-Natta polymerization (see Figure 2.25). Branched polyethylene is often made by free radical vinyl polymerization (see Figure 2.26). UHMWPE is made using metallocene catalysis polymerization (see Figure 2.27).

HDPE is normally produced with molecular weights in the range of 200000 to 500000, but it can be made even higher. If the molecular weights reach 3-6 million, it is referred to as ultra-high molecular weight polyethylene (UHMWPE) which has similar strength as Kevlar for use in bullet proof vests etc.

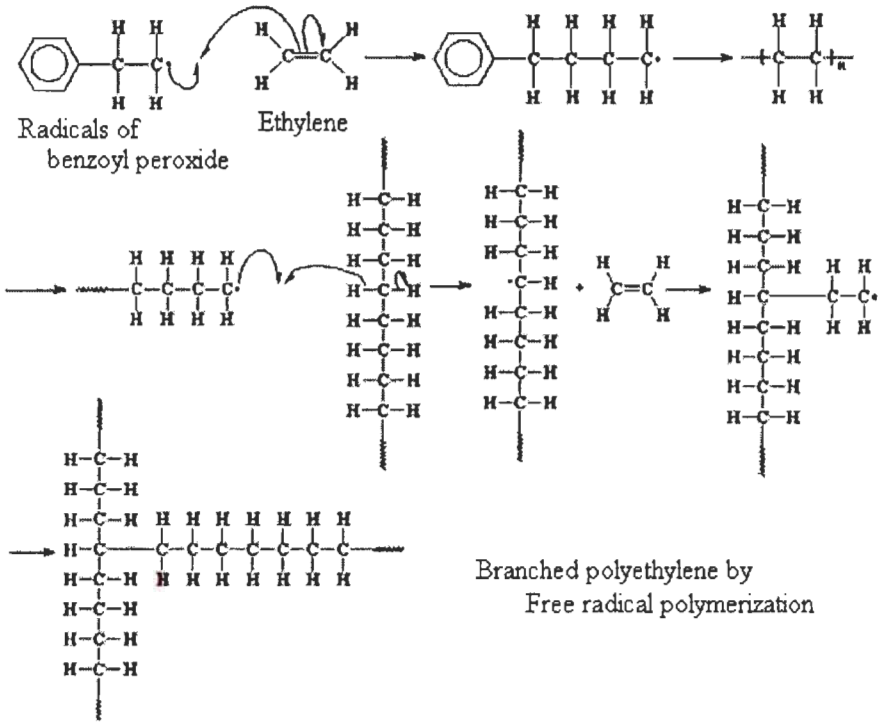

Figure 2.26 Synthesis of branched polyethylene [312]

Branched polyethylene (LDPE) can be produced by Ziegler-Natta polymerization by copolymerizing ethylene monomer with an alkyl-branched co-monomer to get short hydrocarbon branches (see Figure 2.27). Ziegler-Natta polymerization produces linear low-density polyethylene (LLDPE) using a co-monomer with the catchy name 4-methyl-1-pentene indicated in Figure 2.27.

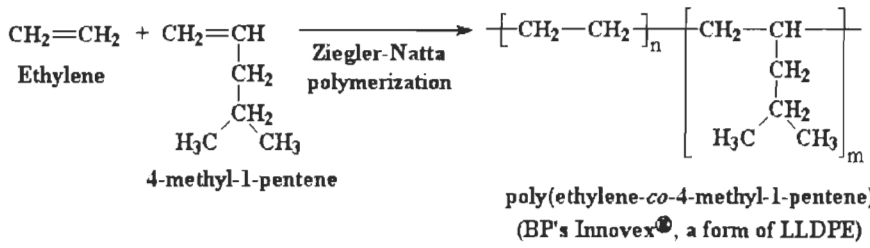

Figure 2.27 Synthesis of linear low density polyethylene [311]

Their typical properties are listed in Table 2.8. Melting point of commercial PP is 174°C and it doesn't melt below 160°C while PE is a more common plastic, which

will anneal at around 100°C. In general, the crystallinity level of PP is around 50-60%, but not very dense and it behaves as an elastomer while the crystallinity level of PE varies according to their type (see Table 2.9).

Table 2.8 Typical properties of polypropylene and polyethylene [311]

	Polypropylene	Polyethylene
Monomer:	Propylene	Ethylene
Polymerization:	Zieglar-Natta metallocene catalysis	Free radical chain Ziegler-Natta metallocene catalysis
Morphology:	highly crystalline (isotactic) highly amorphous (atactic)	highly crystalline (linear) highly amorphous (branched)
Melting temperature:	174°C (100% isotactic)	137°C
Tg:	-17°C	-130°C to -80°C

2.2.3.2 Rheology and Morphology

Melt Flow Index (MFI) is an approximate measure of melt viscosity or the polymer Mw and gives an indication of polypropylene's molecular weight and helps to determine how easily the melted raw material will flow during processing. Typical physical properties are stated in Table 2.9. Polymer with higher MFI fills the mold more easily during the injection or molding production process exhibiting good processability.

Table 2.9 Typical physical properties of PP and PE [313]

Products	MFI, g/10min	Density, g/cm³	Crystallinity, %
LLDPE	0.1-100.0	0.900-0.939	35-60
LDPE	0.2-20.0	0.916-0.925	35-55
MDPE	0.1-35.0	0.926-0.940	70-80
HDPE	0.2-5.0	0.942-0.965	85
PP	2.0-50.0	0.890-0.905	50-60

2.3 Main additives

2.3.1 Coupling agent

Due to the incompatibility between the matrix and wood fiber, coupling agents should be employed into WPC to improve the weak adhesion, poor dispersion and incompatibility between the hydrophilic natural fibers and the hydrophobic polyolefin [151, 314, 315] as illustrated in Figure 2.28. So far, many coupling agents have been used in production and research. Popular coupling agents currently being used include isocyanates, anhydrides, silanes, and anhydride-modified copolymers. In addition, maleated polyolefins are excellent compatilibizers to improve the

combination of the matrix polymer and wood fiber to bear strong impact [195, 316, 317, 318, 319, 320] and transfer stress effectively [113, 114, 115, 116] by coating the surface of wood fiber, polymer or both by compounding, blending, soaking, spraying, or other methods.

In addition, DCP would produce chemical bonds among the polymer molecules, maleated polymer and wood fiber [137, 321] to enhance the impact strength[322]. Thereby, in most cases, our reasearch would incorporate the presence of maleated polyolefin and DCP. The role of maleated polyolefin in fiber–matrix is indicated in Figure 1.10.

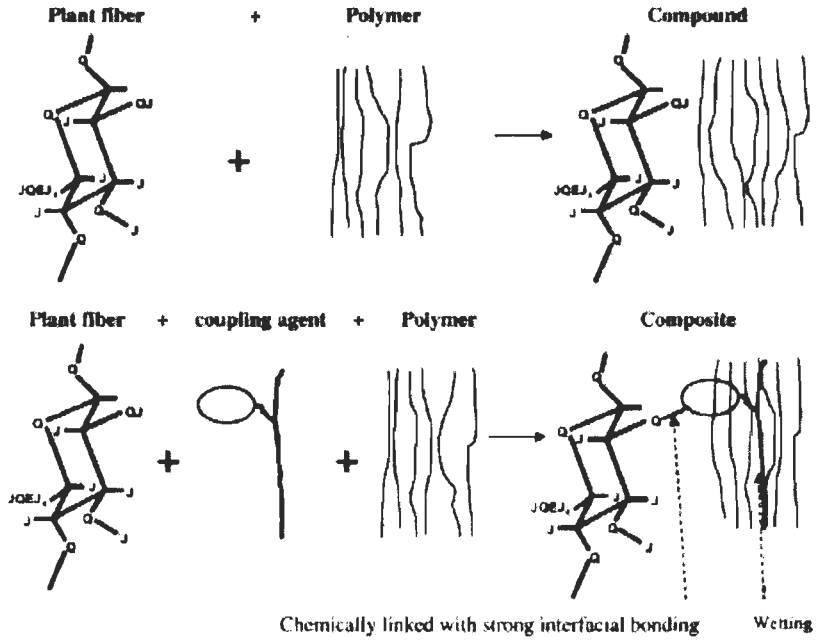

Figure 2.28 Mechanism of coupling agent between hydrophilic wood fiber and hydrophobic the matrix polyolefin [99]

2.3.2 Initiator

Dicumyl peroxide (DCP) can be broken down into three radicals type (see Figure 2.29) to radicalize the matrix to polymerize themselves and maleated polymer as indicated in Figure 2.30 (a-b) and graft to wood fiber indicated in Figure 2.30 (c) [137]. The stereo-structure formed would enhance the mechanical properties of the composites.

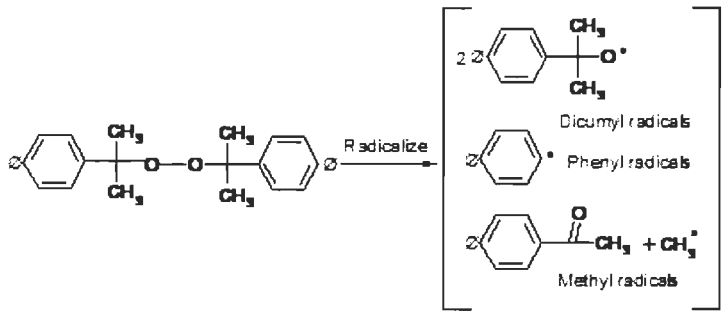

Figure 2.29 Radicalization of dicumyl peroxide

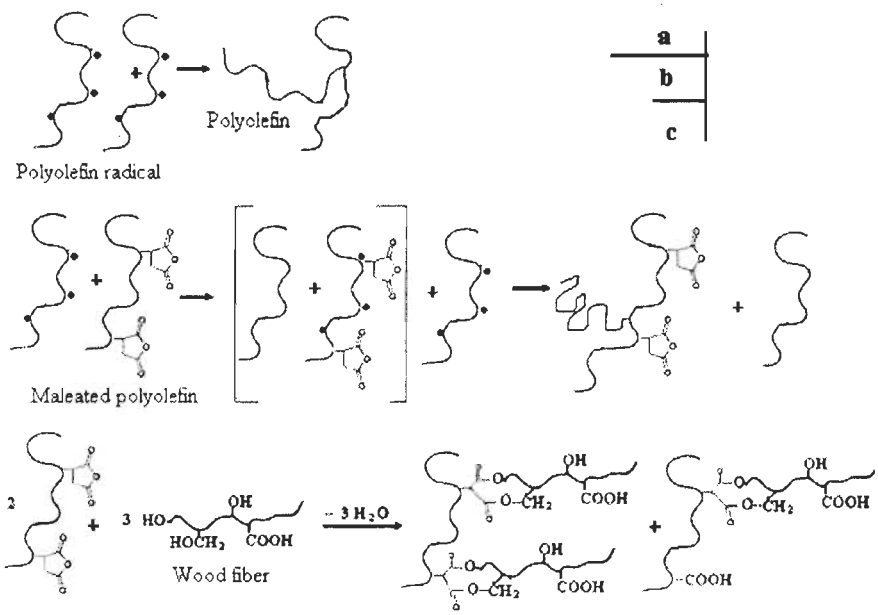

Figure 2.30 Crosslinking mechanisms in maleated hybrid by DCP [137]

2.3.3 Nanofiller

Incorporating small quantities of inorganic nanofillers could also upgrade mechanical strength and stiffness of nanocomposite as well as helping with its barrier, flame resistance, thermal and structural properties where the reinforcing particles could be distributed in the polymeric matrix at the nanometer level as stated in Figure 2.31. Depending on the nature of the filler distribution within the matrix, the morphology of the generated composites can evolve from the so-called intercalated nano-composites with a regular alternation of the layered silicates and polymer monolayers to the exfoliated (delaminated) type of nanocomposites where the layered silicates are randomly and homogeneously distributed within the polymer matrix (Figure 2.32).

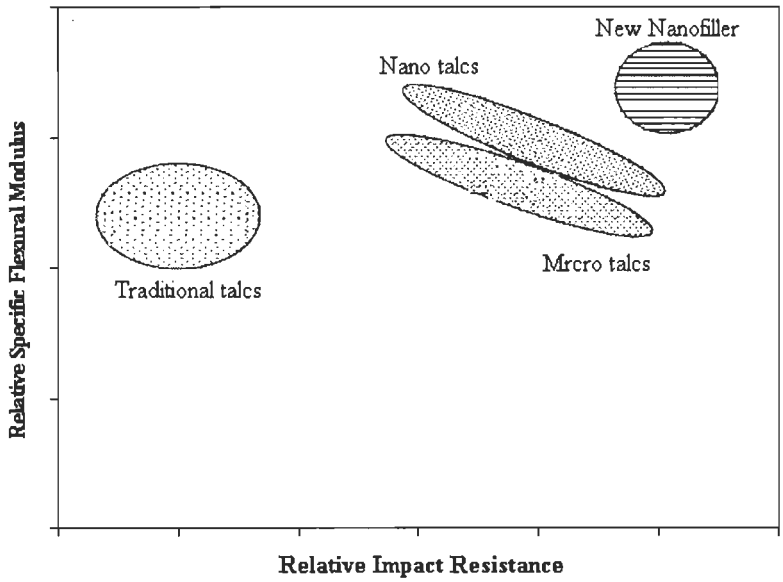

Figure 2.31 Relative impact modulus balance of various fillers used in TPO [323]

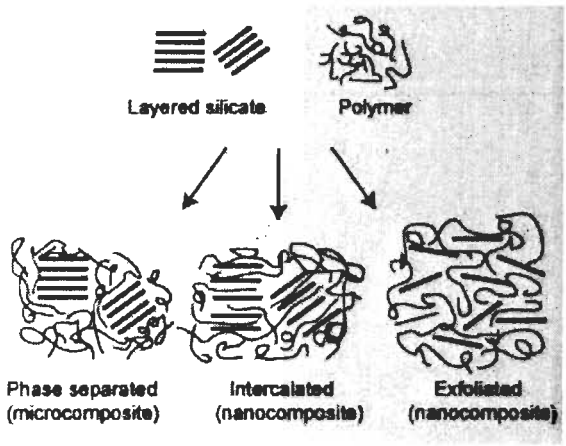

Figure 2.32 Different morphologies during dispersion of filler [324, 325]

The easiest and economic most interesting way to produce these types of materials is kneading the polymer in the molten state with nanofiller. With polar matrix, this technique is workable, such as in PS, EVA or EVOH. However, with non-polar polyolefin, e.g. PE and PP, cannot easily disperse the particles into nanometer level by this method due to fundamental thermodynamic laws [325].

Therefore, formulators desiring to use WPC with nanofiler must consider both formula and process in capturing the benefits. But the generations of nanocomposites with these non-polar polyolefins are very difficult. New synthesis routes by pre-dispersed master batch versions or usage of modified polymers (maleic anhydride grafted polymers) are possible ways as reported by Dr. Lan from Nanocor. One

further improvement for nanocomposites with high polymer processing temperatures (>260°C) is the usage of oligomer treated organoclays which avoids the unwanted thermally induced side-reaction of Hofmann-elimination generating olefins from the quaternary ammonium compounds [325] and the polarity of wood fiber would help with the distribution of nanofiller in nanometer [326].

Chapter 3 - Effect of Independent Variables on Mechanical Properties and Maximization of Aspen-Polypropylene Composites

Ruijun Gu and Bohuslav V. Kokta
Journal of Thermoplastic Composite Materials. 2008, 21(1): 27-50
DOI: 10.1177/0892705707085347
http://jtc.sagepub.com/cgi/content/abstract/21/1/27

Abstract: A study on the effect of concentration of maleated polypropylene (MAPP), dicumyl peroxide (DCP), nanoclay (NC) and aspen fiber loading on the mechanical properties of Aspen-PP composites was undertaken with the objective to protect or increase the impact strength without losing or weakening tensile strength. The central composite design of Statgraphic plus was used to determine the optimum concentration of additives and to maximize both the impact as well as tensile strength properties to be superior to that of pure polypropylene. Finally the price of PP-composites with an optimal composition of filler (aspen fiber and NC), coupling agent (MAPP) and initiator (DCP) was compared to that of pure PP and PP reinforced with glass fibers.

Keywords: Wood fiber, Polypropylene, Impact, Nanoclay, Nanocomposites, Composites, Aspen fiber, MAPP, DCP

3.1 Introduction

Wood plastic composites (WPC) are used to replace impregnated wood in many outdoor and neat plastics applications, and also in biomedical areas [327] due to their abundant availability, low cost, high relative strength, and stiffness, low density and renewable nature [135, 328, 329, 330, 331]. WPC could be prepared with recycled polyolefin and wood fibers helping to reduce waste disposal burdens [91] as well as excellent mechanical and physical properties, such as low cost/high volume etc. Wood fibers could also reinforce green composites on mechanical, thermo-mechanical and morphological properties, e.g. PHBV based biocomposites due to its natural and renewable [82].

In general, in the composites reinforced with cellulosic fibers the compatibility between composite components have to be improved using either physical or chemical modification of the thermoplastics or wood fiber by using coupling agent [167, 332, 333, 334]. Popular coupling agent like maleated polyolefins based on anhydride [319, 328, 335, 336, 337, 338] such as maleated polypropylene, maleated

polyethylene and silanes [92, 124, 339, 340, 341, 342, 343, 344, 345], sodium benzoate [346, 347], and dicumyl/benzoyl peroxide [348, 349] improve the linkage between matrix and fiber. Wood fiber could be treated with some chemicals, such as alkali, isocyanate [343, 344, 345, 348] and peroxide [349] to create more reactive sites. The properties of composite materials are also determined by the characteristics of the polymer matrices themselves, together with reinforcement, and the adhesion fiber/matrix interface that mainly depends on voids and the bonding strength at the interface. Moreover, wood fibers are rich in lignin with abundant hydroxide group which could react with -OH to form branched structures which can improve the strength of the composites. Because lignin is a solid polymer with high molecular weight, lignocelluloses fiber may also produce more solid point in matrix to enhance the composites' impact strength [223].

3.2 Experimental material and methods

3.2.1 Materials

Polypropylene was supplied by Montell Canada Inc. Air-dried wood fiber is aspen fiber (CTMP, 20-60 mesh) which prepared in Centre Recherche en Pâtes et Papiers laboratory of Centre Intégré en Pâtes et Papiers. Maleated polypropylene was supplied by Eastman chemical company as coupling agent under the name Epolene G-3003 polymer with 9% acid anhydride. Dicumyl peroxide (98% active DCP) was supplied by Sigma-Aldrich Chemical Co. and was used as the initiator, the halftime at different temperature was listed in Table 3.1. Cloisite®10Å is a natural montmorillonite modified with a quaternary ammonium salt received from Southern Clay Products Inc. was used as filler. The typical properties were illustrated in Table 3.2.

Table 3.1 The halftime of DCP at different processing temperature

Temperature, °C	100	115	125	130	145	150	175	180	190
Halftime, min	3000	744	138	108	18	9	0.9	0.4	0.2

3.2.2 Experimental

3.2.2.1 Effect of independent variables on the properties of the composites based on PP

In order to study the effect of blending time on the mechanical properties, PP was blended with 2wt% NC varying from 10-40min under same procedure. All

composites were compounded in a two-roll C.W. Brabender as the independent variables (aspen fiber, MAPP, DCP and NC) introduced stepwise according to the following procedure to study their effects on the mechanical properties of the correspondence composites.

Table 3.2 Typical physical properties of Nanoclay

Treatment/Properties		Cloisite®10Å
Organic Modifier		2MBHT(1)
Modifier Concentration		125 meg/100g Clay
Moisture, %		<2%
Weight loss on Ignition, %		39%
Density, g/cc		1.90
Dry particle sizes, volume	10%	<2μm
	50%	<6μm
	90%	<13μm
X Ray Results: d_{001}		19.2 Å

Note: (1) 2MBHT: Dimethyl, benzyl, hydrogenated tallow, quaternary ammonium

3.2.2.2 Statistical experiment design

There are numerous independent variables including processing conditions that affect the resulting properties of the composites. We have minimized the independent variables in previous works [350, 351, 352] and our exploratory studies in this paper.

Table 3.3 Coding of the independent variables

Factors	-1.682	-1	0	+1	+1.682
NC, wt%	0	0.81	2	3.19	4
MAPP, wt%	0	1.01	2.5	3.99	5
DCP, wt%	0	0.041	0.1	0.16	0.2

We chose central composite design (CCD) for 3 factors with 3 levels each-NC, MAPP and DCP concentrations, one from each being at center. The levels were set on the basis of certain limits as indicated in Table 3.3.

We created a central composite design: 2^{3+} star design which will study the effects of 3 experimental factors in 16 runs, including 9 experiments which were set at the center points of the factor indicated in Figure 3.1. The design is to be run in a single block with aspen fiber content at 30wt%. The order of the experiments has been fully randomized which would provide protection against the effects of hidden variables.

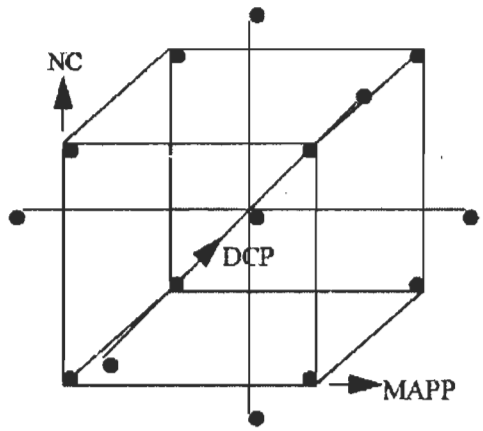

Figure 3.1 Diagram of central composites design with the composition of the samples for each experiment

3.2.3 Compounding

All the blends were prepared by blending the components with Thermotron-C.W. Brabender (Model T-303) according to the conditions as follows. Twenty weight percent PP with or without MAPP was melted on rollers at 190°C. Aspen fiber and the residual (80wt%) PP with or without NC were then added and blended in 7 min at 60 rpm, then peeling mixture from the roller and re-blended for 5 times, each time for 5 min to obtain the uniform composite sheet.

Finally, removing the composites sheet from the roller and making into strips with knife according to the molder size after DCP added and blending for 3min.

3.2.4 Compression molding

The composite strips were molded to dog-bone shape specimens (ASTM D638 Type V). 24 specimens (12 for tensile testing and 12 for impact strength testing) were simultaneously put in a molder covered by metal plates on both sides, heated at 192±2°C DAKE, pressed for 15mins under the pressure of 20MPa (25-26 tons), and then cooled below 100°C by circulating cold water in the press. The approximate dimensions of tensile specimen were as follows: width 0.28-0.30cm and thickness 0.31-0.33cm. And the width of impact was 0.28-0.30cm and thickness 0.15-0.17cm.

3.2.5 Mechanical tests

All the specimens were conditioned in testing room overnight, measured with micrometer after polishing. Mechanical measurements were made on an Instron tester (Model 4201) at 23°C and 50% level of relative humidity. Samples properties

were automatically determined by the Series IX Automated Materials Testing system-Version5.20 under ASTM D638.

3.2.6 Determination of tensile impact

Tensile impact strength (un-notched) was measured at 23°C using a TMI impact tester (TMI No.43-01) which was equipped with a special fixture for test specimen according to ASTM D1822. The maximum energy of the pendulum was 2J. Test specimens were obtained from compression-molded plates.

3.3 Results and Discussions

3.3.1 Effect of blending time on the properties of PP/NC composites

In order to seek the effects of blending time for PP/NC composite, we first employed a roller mixer-thermotron Brabender for melt compounding of the composite of polypropylene and NC. Impact and Stress properties of PP/NC composite with different blending time are shown in the following Figure 3.2-Figure 3.3. We concluded that impact strength reach its highest value point (216.83-220.63kJ/m²) between 30-40min while its stress at max load was increasing slightly from 30.52MPa to 31.52MPa.

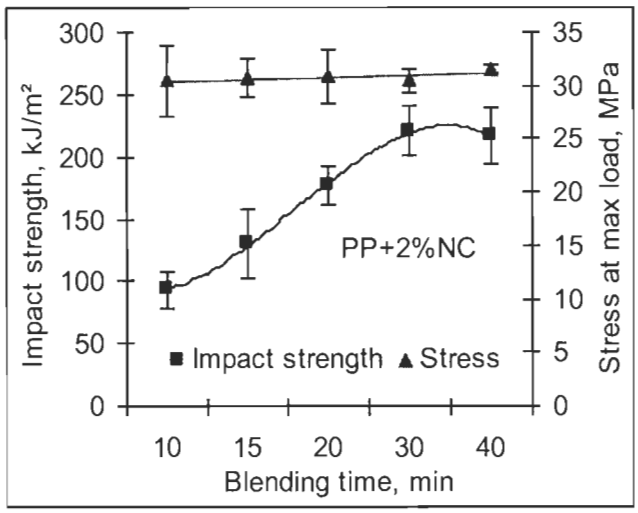

Figure 3.2 Effects of Blending time on the Impact strength and max Stress of the PP/NC composites

Figure 3.2 shows the effect of blending time on impact strength and tensile properties. Impact strength increased with increasing blending time until a peak point was reached at around 35min, and then impact strength decreased slightly due to

more degradation of fiber and polymer at high blending temperature in particular for wood fiber [353].

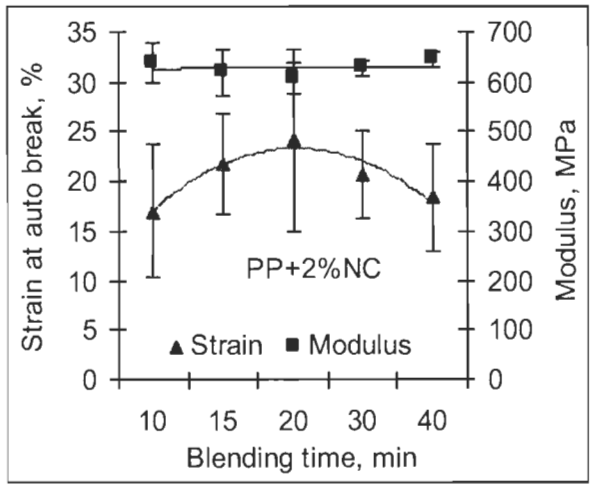

Figure 3.3 Effects of Blending time on the Strain at auto break and Modulus of the PP/NC composites

Meanwhile, strain at auto break point increased at first due to plus uniform dispersion, and then a decrease is obvious consequence of the oxidative degradation of PP takes place at 190°C as processing time extended more than 20 minutes shown in Figure 3.3. In order to obtain the composites with higher impact strength, and tensile strength 35min experimental blending time was chosen. The increase of modulus was a bit within the limits of errors. Because the thermo-oxidative degradation takes place at open roll mills, it is necessary to define stabilizing system, as was done in another paper. We investigated the influence of mainly independent variables without thermal antioxidants.

3.3.2 Effects of Independent variables on the mechanical properties of PP/Aspen composites

Figure 3.4 shows the effect of the impact strength of the composites with aspen fiber, MAPP, DCP and NC introduced step by step. For PP matrix composites, the impact strength increased and reached an optimum value at 30wt% level of aspen fiber introduced due to matrix fiber debonding and fiber pull-out as similar to the previous research [354]. Chuai *et al* [318] studied the MAPP grafting which was conducted in the solution of MAPP in hot xylene with sodium hypophosphite as an esterification catalyst and extracted with xylene to remove free MAPP and compared to MAPP treatment which was carried out by simply melt mixing with fiber in a two-roll mill to investigate that MAPP grafting. MAPP treatment has similar effects on the

mechanical properties and morphology of PP/Conifer fiber composites. So, MAPP treatment was carried out by melt mixing with PP and fiber in a two-roll thermotron in our experiment. Figure 3.3 also shows the relationships between the impact strength and MAPP, DCP and NC loading. The maximum impact strength of the composite specimens reinforced with MAPP at 30wt% aspen fiber loading was 179kJ/m² higher than PP/Aspen and pure PP which were 91kJ/m² and 71kJ/m². It was found that the impact strength of the composites with DCP concentration decreased from 179kJ/m² down to 48kJ/m² (down 2.7 times) because the impact strength depends on molecular weight directly [355] due to the degradation of PP matrix [356, 357] and wood fiber [353]. The impact strength increased slightly with NC added within lower content with fiber existence.

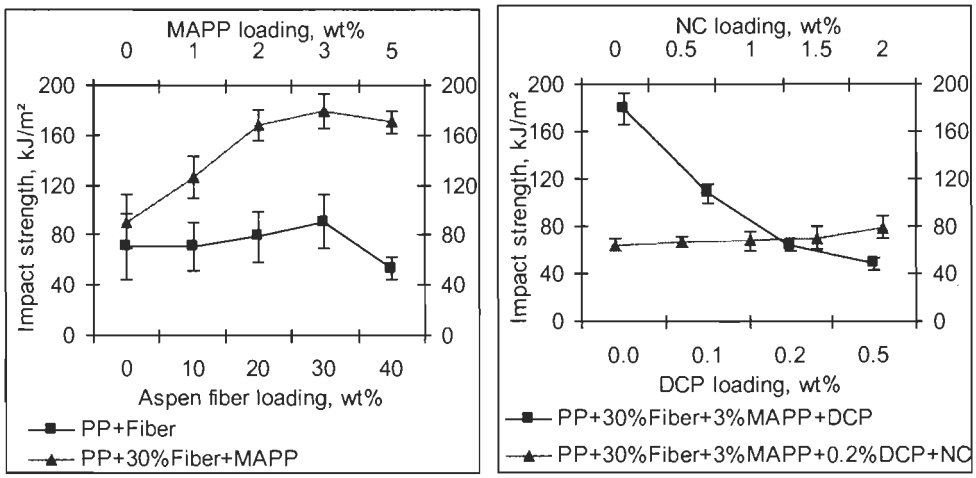

Figure 3.4 Effect of independent variables on the impact strength of the Aspen-PP composites

The results obtained from Figure 3.5 show that both aspen fiber and DCP have had negative influence on the tensile strength of the composites. The effect of DCP dropped abruptly down (almost 73%) from 46MPa to 27MPa while MAPP showed the opposite effect from 26MPa up to 46MPa with an optimum value at 3wt% with the reinforcement of 30wt% aspen fiber. The presence and decomposition of DCP is speeding up the oxidation. In contrast to pure PP, the optimum value of tensile strength of the composite reinforced with MAPP at 30wt% fiber was up 39.89% (from 46MPa versus 33MPa). These improvements are due to the enhanced stress transfer from the matrix to the fiber via the compatibilizer [358, 359]. Moreover, MAPP used has a higher amount of maleic groups per chain length (9mg KOH/g) and higher molecular weight (M_w=52,000) to make more MAPP chains involved in

inter-chain entanglements and to contribute to the mechanical continuity of the composites [317].

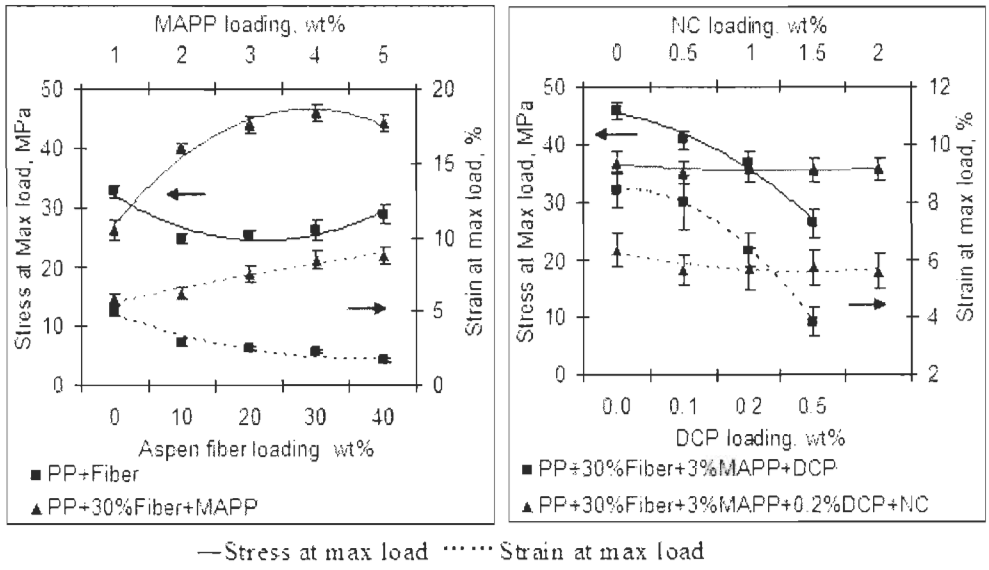

Figure 3.5 Effects of independent variables on the max stress and strain of the Aspen-PP composites

NC in lower content has almost no influence of the tensile of the composites. Although the scatter of the values is taken in account, the strain of Aspen-PP composite filled with NC was down slightly due to the clay particles that could make the matrix more flexible and reduce the entanglements of MAPP chains with PP as mentioned previous. With specimens reinforced with fiber, the steep decline in strain immediately on fiber addition is obvious, because which fiber has low elongation at break restricts the polymer molecules flowing past one another. This behavior is typical of reinforced thermoplastics in general and has been reported by many researchers [56, 84, 337]. The addition of fiber had a positive effect on the rigidity of the composite because birch fiber was less flexible than PP fiber which restricted the mobility of matrix and made more stiffness. The strain was decreased obviously as aspen fiber was introduced from 12.6% (PP) to 4.2% (with 40wt% fiber loaded) which was different from the previous works [69, 91, 360, 361]. The results might be attributed to the increase of blending time in this paper. Longer blending time results in a better dispersion of fiber in the matrix which also improves the interface strength between matrix and fiber. Although most thermoplastics are non-polar substances which are not compatible with polar fiber which leads to poor adhesion at the fiber-

matrix interface, higher fiber content and more homogeneity means more resistance to tension on fiber that could enhance the tensile strength of composite.

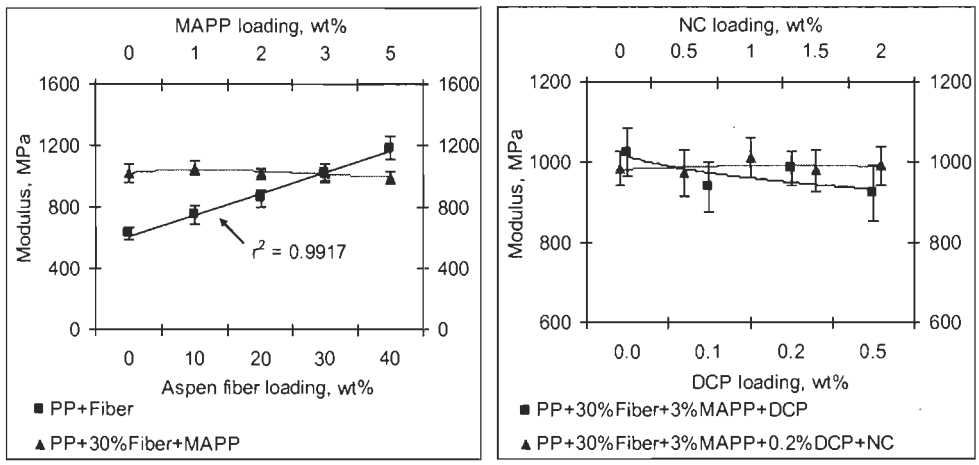

Figure 3.6 Effects of independent variables on the modulus of the Aspen-PP composites

The strain at break also decreased steadily as DCP and NC loading increased in the composite. The strain at break of the composites with DCP decreased more strongly (120%, from 0 to 0.5wt %) than the composites with NC (14%, from 0 to 2.0wt %).

The modulus increased significantly with the increase in fiber content of composites as presented in Figure 3.6. Moreover, the modulus of the composites slightly decreased as MAPP and DCP were introduced. The positive influence of MAPP was counteracted by the negative influence of DCP shown in Figure 3.6. Moreover, the modulus of the composite has a relationship with fiber loading in a term of a linear equation as shown in Figure 3.6 according to A. Karmarkar *et al* [84].

Figure 3.7 shows energy at break point of the composites reinforced with aspen fiber with MAPP, DCP and NC. Fracture energy decreased sharply as fiber was introduced into the matrix, and increased slightly with MAPP content due to the surface energy increases with an increase in the MAPP content due to the number of the high energy sites introduced graducally as the content of MAPP increased [362]. The result of PP reinforced with CTMP aspen fiber was also agreed with our previous researches [181, 182, 184, 185].

As NC was added within a lower content, the fracture energy decreased slightly due to the particles of filler weakened the interfacial strength among fillers, fibers and matrix as shown in Figure 3.7. The surface energy of the particles of NC was lower than reactive component. Moreover, the particles of NC were solid as contact points

which made the composite more fragile due to its harder phase and its restriction of wood fiber and matrix fiber to entangle each other. As the increase of NC content, more particles were dispersed in the composite which leads to some defects.

We also conclude from Figure 3.7 that the energy was reduced sharply as DCP was added, from 0.37J to 0.08J, down 390%.

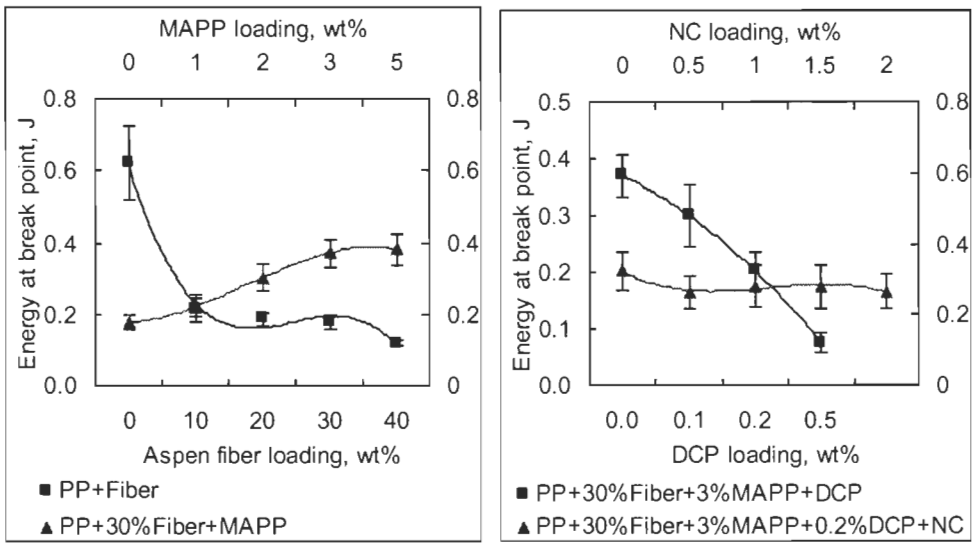

Figure 3.7 Effects of independent variables on the break energy of the Aspen-PP composites

3.3.3 Results obtained using Statistical Experimental Design

Using Statgraphic plus, the conditions (independent variables) to obtain the best mechanical properties were calculated and then compared at aspen fiber loading at 30wt%. The physical and mechanical properties are presented in Figure 3.8, Figure 3.9 and Figure 3.10. Considering the results above, we adopted Statagraphics plus software to evaluate the optimum values of the mechanical properties, and determined the optimum values as the final studies in following parts. Response surface diagram for impact strength as a function of the concentrations of MAPP and NC is presented in Figure 3.8 as well as the max tensile strength. It is clear from the picture that the impact strength is a function of MAPP content as well as DCP content and their synergistic reaction, and approaching max values around 154kJ/m^2 at the optimum values of DCP (0wt%) with concentration corresponding to level – 1.682, MAPP (5wt%) to level 1.682 and NC (0.76wt%) to level -1.043 according to Table 3.3.

The value of DCP at the above mentioned concentration was chosen at optimal level because Standardized Pareto Chart for Impact at 30wt% fiber loading on Figure 3.9 indicates that DCP content is the most important factor in determining the impact strength under conditions used, which was negative, while MAPP content which is the second important factor to determine the impact strength was positive.

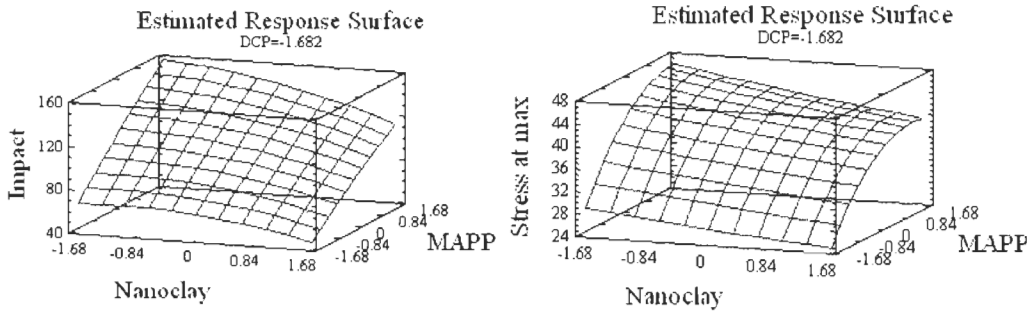

Figure 3.8 Response surface diagram for impact strength and max stress as a function of the concentrations of MAPP content and NC content at the optimum DCP level with 30% fiber loading

The tensile strength is a function mainly of MAPP content and approaching max values around 46MPa at the optimum value of DCP with concentration corresponding to the level -1.682. The maximum values of the composite yield tensile strength of about 46MPa which are much higher than that of PP being 33MPa which indicates good fiber matrix adhesion as evaluated by Statagraphics plus.

We also conclude that MAPP was the most positive factor in determining the stress strength under various conditions while DCP addition was negative factor to stress strength of composites, taking second position. At same time, the NC content also has influence on stress just in secondary.

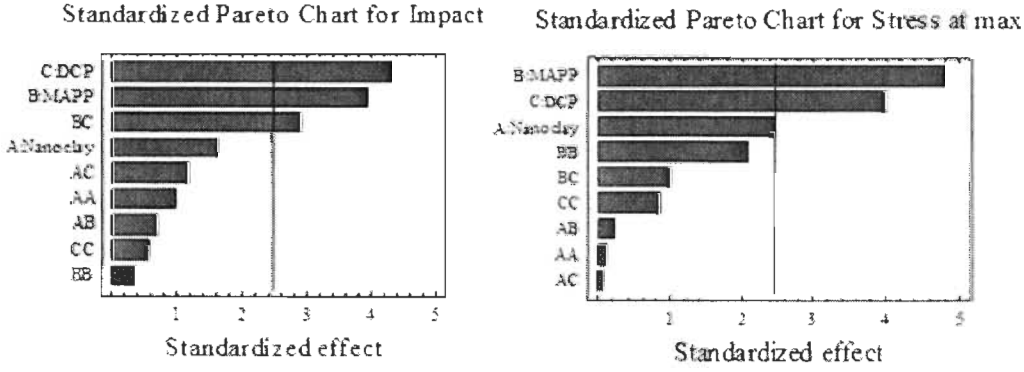

Figure 3.9 Standardized Pareto Chart for Impact and max stress at 30% fiber loading

Response surface diagrams for strain at maximum and modulus as a function of the concentrations of MAPP and NC is presented in Figure 3.10. In the case of modulus, max values around 1032MPa, was slightly higher than for PP filled with 30% aspen fiber (1019.0MPa) and slightly lower than the composite with 40% fiber (1183MPa) regardless of deviation.

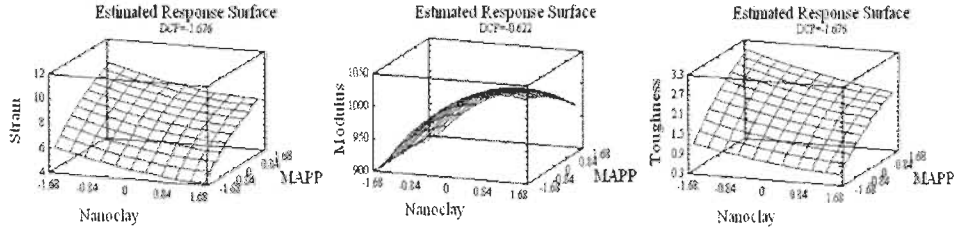

Figure 3.10 Response surface diagram for max strain, max strain and toughness as a function of the concentrations of MAPP and NC at the different optimum DCP level with 30% fiber loading

Note: The optimum coded levels of DCP are -1.676, -0.622 and -1.676 corresponding to the optimum actual amounts of DCP are 0wt%, 0.063wt% and 0wt%, respectively

Finally, Stagraphic plus enabled us to estimate the maximum values of the mechanical properties as well as the optimum values of independent variables. It is possible to achieve the composite with the maximization of the mechanical properties. The maximum obtainable values are presented in Figure 3.11, Figure 3.12, Figure 3.13, Figure 3.14 and Figure 3.15. The results from Figure 3.11-3.15 are in agreement with the results achieved in exploratory research presented in Figure 3.2 to Figure 3.7. It suggests that Aspen-PP composites could be made to achieve superior impact as well as simultaneously best tensile strength.

We chose the compositions optimum on impact strength in exploratory group and CCD respectively as showed in Figure 3.11. The addition of fiber could provide the composites with superior impact strength as well as MAPP introduced, from 71kJ/m^2 up to 91kJ/m^2 and final reached 179kJ/m^2 as 3wt% MAPP added. But as DCP added, the impact strength dropped from 179kJ/m^2 to 108kJ/m^2, and decreased in step to 79kJ/m^2 as 2wt% NC added. From Figure 3.11, we also determined that the presence of initiator could damage the impact strength of the composites due to emanation a lot of simple chemicals during its degradation. That is to say DCP has a negative influence on the impact strength of the composites prepared in open-air roller Brabender with MAPP and NC, while MAPP has a positive influence on the impact strength due to production more reactive point between matrix and fiber.

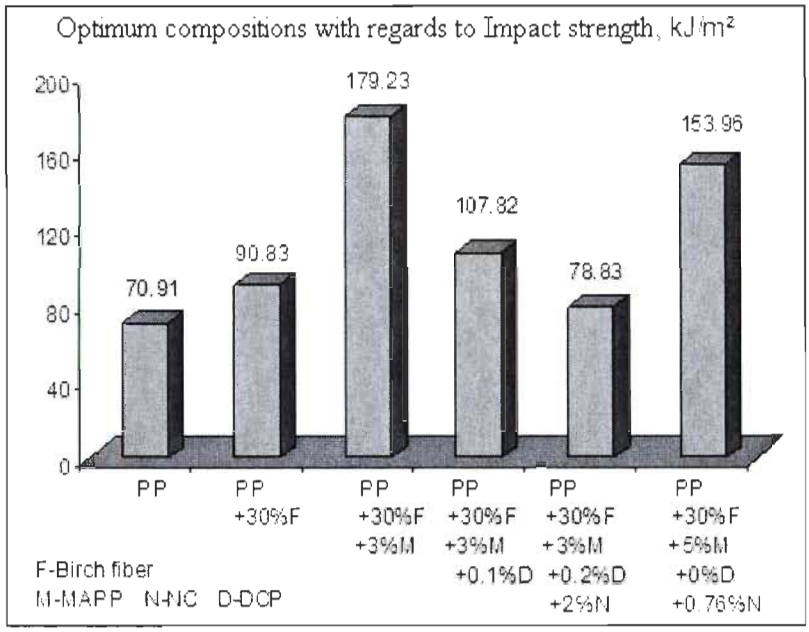

Figure 3.11 Effect of compositions on the impact strength of the composites

The conditions to obtain the best maxmium stress were calculated and then compared with the exploratory results indicated in Figure 3.12. The optimum values of maximum stress would reach 46MPa with 4.85wt% MAPP at 30wt% aspen fiber loading which was much higher than pure PP (33MPa), the composites reinforced with MAPP, NC and fiber respectively. We also concluded that NC and DCP have negative effect on the maximum stress of the composites as to maximum strain.

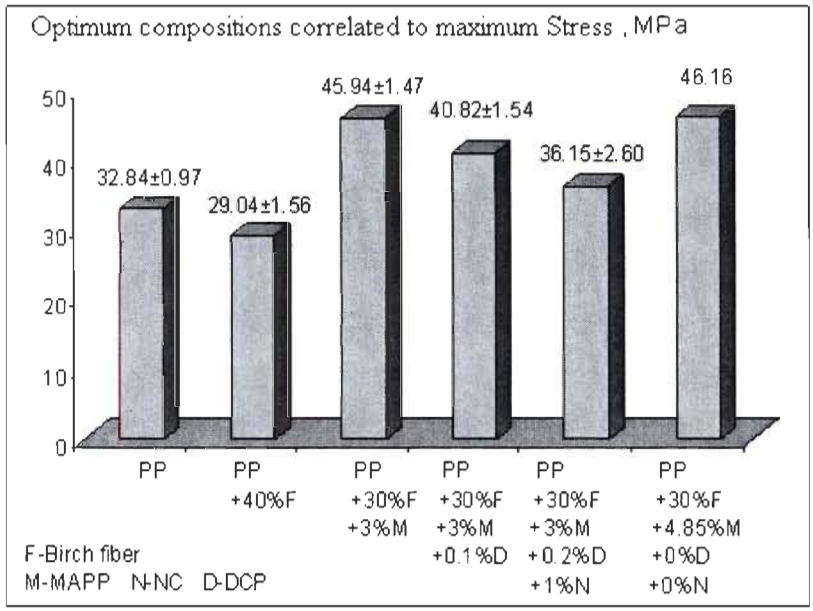

Figure 3.12 Effect of compositions on the max stress of the composites

From Figure 3.13, pure PP with highest strain (12.6%) among the composites was introduced with fiber, MAPP, DCP and NC and lead to more fragile composites. The decrease of strain caused by DCP was flarser than fiber or NC due to the degradation of DCP which produced some lower molecular weight chemicals as confirmed in Figure 3.5. The strain of Aspen-PP composite with reinforcement of 30wt% fiber was increasing up 52.6% at MAPP content at 5wt% content than the composite without MAPP.

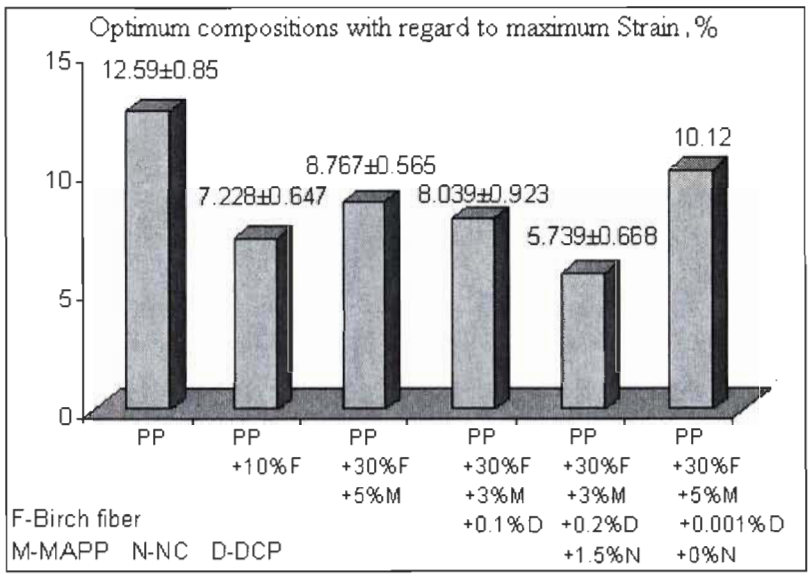

Figure 3.13 Effect of compositions on the max strain of the composites

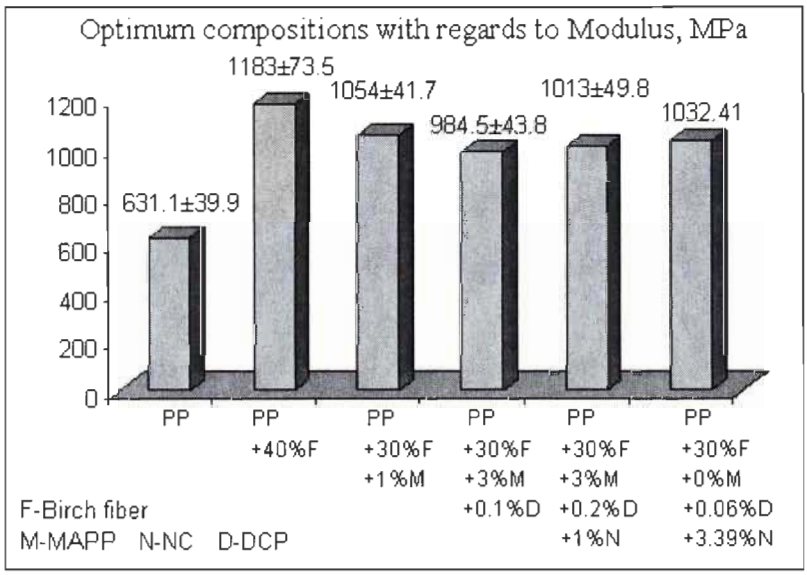

Figure 3.14 Effect of compositions on the modulus of the composites

The effect of fiber loading and additives on the modulus and toughness at constant optimum compositions of MAPP, NC and DCP at 30wt% fiber loading levels were clearly seen in Figure 3.14 and Figure 3.15. It's evident that fiber was giving a modulus superior to that of pure PP, up about 87.5% at 40wt% level. Although DCP has negative effect n modulus, the modulus of the composite filled with 1wt% NC was up from 984.5MPa to 1013MPa from Figure 3.14. It confirmed that the conclusion from Figure 3.6 that NC has positive effect on the modulus, similar results to previous report [349].

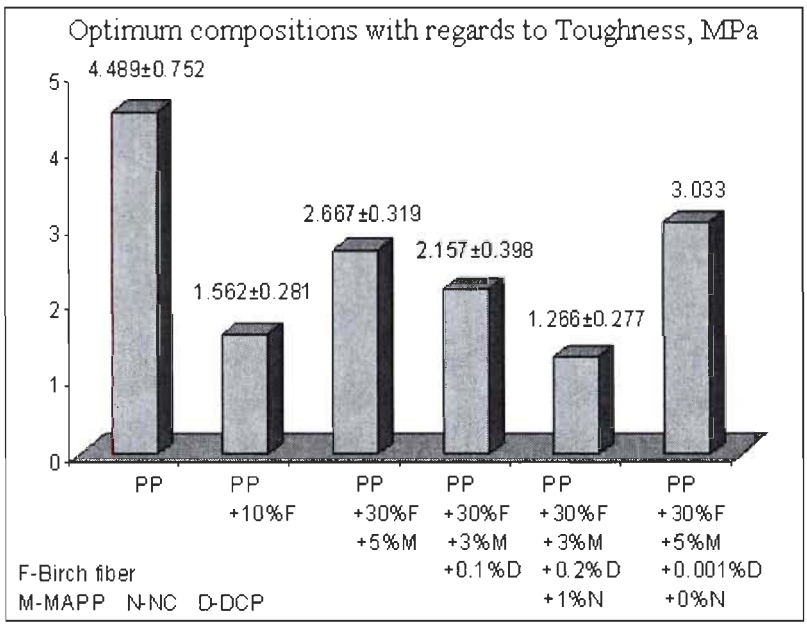

Figure 3.15 Effect of compositions on the toughness of the composites

The similar effect of fiber loading on the toughness at constant optimum compositions of MAPP, NC and DCP was clear from the following Figure 3.15. In that case, the optimum toughness with optimal MAPP loaded was reached 3.0MPa which was superior to that of the composite at 30wt% fiber (1.2MPa) and 5wt% MAPP additional (2.7MPa).

We always considered the costs of materials, especially to engineering materials as well as their properties. We chose some classic composites listed in Figure 3.11-Figure 3.15 to estimate the cost of products presented in Figure 3.16.

The cost of the composites reinforced with aspen fiber and NC were economic compared with the composite filled with glass fiber at 30% loading level. From Figure 3.16, we also proved that the thermoplastics reinforced with wood fiber could decrease the cost for its lower price and rich resources. Considering both the

mechanical properties and their cost, we recommended that the composite with optimum compositions with 30wt% fiber loaded with certain content of MAPP was the best choice.

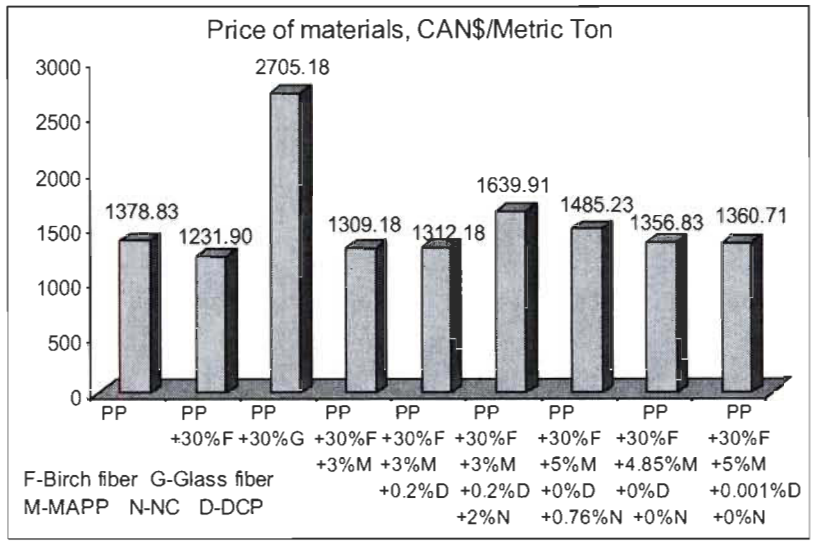

Figure 3.16 PP/Aspen composites price comparison with pure PP in February 2007

3.4 Conclusions

In this study, it was found that the composite could achieve optimum impact strength at the optimum blending time. The exploratory research was carried out with aspen fiber, MAPP, DCP and NC loaded based homo-PP to investigate the methodology and mechanical properties of WPC.

Table 3.4 Optimizations of mechanical properties of the composites using CCD

Mechanical Properties	The increase of physical properties of PP composites in comparison with PP		
	30% Fiber	30% Fiber+3%MAPP	CCD at 30% Fiber
Impact strength, kJ/m²	28.09%	152.76%	117.12%
Stress at max load, MPa	-19.67%	39.89%	40.56%
Strain at max load, %	-54.38%	-32.97%	-19.62%
Modulus, MPa	61.46%	62.41%	63.59
Toughness, MPa	-72.84%	-41.81%	-32.43%

It can be concluded that the addition of DCP and NC results in worsening the mechanical properties of WPC while the application of MAPP with high content of maleic anhydride grafted to fiber could improve the impact as well as tensile strength. It was also found that the Modulus of WPC without any additives has an increasing linear relationship with the content of wood fiber loaded. CCD was used

to determine the optimum concentration of additives and to maximize both the impact strength as well as tensile properties. The comparisons of results were listed in Table 3.4.

3.5 Acknowledgment

The authors wish to thank the NSERC and National Centers of Excellence of Canada-Auto 21 for its financial support.

Chapter 4 - Maximization of the Mechanical Properties of Birch-Polypropylene Composites with Additives by Statistical Experimental Design

Ruijun Gu and Bohuslav V. Kokta
Journal of Thermoplastic Composite Materials. 2010, 23(2):239-263.
DOI: 10.1177/0892705708103402
http://jtc.sagepub.com/cgi/content/abstract/23/2/239

Abstract: A systematic study of effects of concentrations of maleated polypropylene(MAPP), dicumyl peroxide (DCP), Nanobelnd™ concentrate (MB1001) and Birch fibers on the mechanical properties of Birch-PP composite was undertaken with the objective to protect or increase the impact strength without losing tensile strength. Using Stagraphic Plus, a Central Composite Design made it possible to determine the optimum concentrations of additives and to maximize both the impact as well as tensile properties to reach values well above that of virgin polypropylene.

Keywords: Wood fiber, Birch fiber, Polypropylene, Impact, Nanoclay, Nanoblend, Composites, Nanocomposites

4.1 Introduction

Composites materials are engineering materials made from two or more components on a macroscopic scale to form a useful material. It's not simply a mass of fibers dispersed within a matrix. A "true" composite might be considered to have a matrix material completely surrounding its reinforcing material in which the two phases act together to achieve superior characteristics not attainable by either constituent acting alone. Composites are composed of a heterogeneous combination of components differing in a composition, morphology and usually physical properties, made to produce specific physical, chemical and mechanical characteristics. Composites are not only used in outdoor/engineering materials but also applied in biomedical [327]. The use of reinforcing fillers, which can reduce material costs and improve certain properties, is finding increasing use in thermoplastic polymer composites. Currently, various inorganic materials such as talc, mica, clay, glass fiber , calcium carbonate and organic modified clays are being incorporated into thermoplastic composites [363, 364, 365]. The composites filled with organic-modified clays can increase strength and modulus [35], thermo-oxidative stability [36, 37], enhance barrier properties [39], improve solvent resistance [40], reduce thermal expansion

coefficient [39], increase flame retardancy [41], increase ionic conductivity [42, 43] and controle biodegradability [36, 44].

Nowadays, lignocellulosic fibers have renewed interest in natural materials as they are biodegradable, renewable and environmentally friendly and low cost. Lately, interest has grown in composites made from wood fiber in thermoplastic matrices, particularly for low cost/high volume applications. The composites filled with wood fiber being biomaterials will certainly reduce waste disposal burdens [91]. Wood and cellulosic fibers offer a number of benefits for wood-thermoplastic composites including low hardness, relatively low density, biodegradability, low volumetic cost, and are less abrasive to processing equipment. Composites reinforced with lignocellulosic fibers show an improvement in tensile strength, but a sharp drop in the impact strength and the elongation. The presence of impact modifiers leads to tensile properties decrease while preserving or improving the impact strength. Oksman *et al.* [366 , 367 , 368] investigated the mechanical properties and morphology of PE/WF composites modified with a styrene-ethylene/butylene-styrene triblock copolymer grafted with maleic anhydride (SEBSgMA) and showed enhancement both in the tensile and impact strength of the resulting composites due to the improved adhesion between filler and matrix. Therefore more interfacial bonding between wood fibers and the matrix may lead to composite tensile and impact strength improvement. However, wood fiber/polyolefin composites are often unable to take full advantage of the reinforcement potential due to the poor adhesion between the matrix and the wood fiber because of a hydrophilic nature of natural fiber that lowers the compatibility with hydrophobic polymeric matrices during fabrication. Interaction between the anhydride groups of maleated coupling agents and hydroxyl groups of natural fibers can overcome the incompatibility problem and lead to the increase tensile and impact strength of wood fiber thermoplastic composites. Coupling agent based on anhydride could improve the bonding strength between matrix and fiber, especially, maleated polypropylene, maleated polyethylene and silane [92, 339, 340, 341, 342] or sodium benzoate [346, 347] and dicumyl/benzoyl peroxide [348, 349] as a crosslinking agent being the most utilized. Wood fiber could be pretreated with alkali, isocyanate or peroxide [348, 349] to create more reactive sites. The properties of composite materials are not only determined by the characteristics of the polymer matrices themselves but also by voids and the bonding strength or adhesion at the interface.

Wood fibers contain numerous hydroxyl groups resulting in its strong hydrophilic character which made the thermoplastics reinforced with wood fiber sensitive to environmental and dimensional stability [317, 342, 369, 370, 371, 372] and may also lead to microcracking [369].

In the present work a way is explored to modify the natural fiber by coupling with a matrix in order to obtain an excellent composite in which a strong fiber with high strength and modulus is bonded with matrix to carry heavy load [113]. Fibers serve to resist tension, the matrix serves to resist shear in terms of stress, and all materials present serve to resist compression, including any aggregate. Moreover, natural fibers are rich in lignin with abundant hydroxide group able to react with maleic anhydride groups to form branched structures. Lignocellulosic fiber could also produce more solid bonding in a matrix to enhance higher impact strength [233]. Moreover nanoblend concentrate was also used alongside with fibers to reduce the effects of deformation.

4.2 Experimental materials and methods

4.2.1 Materials

Polypropylene was supplied by FINA Chemicals Inc. branded as FINA 3622 with the melt flow of 12.0g/10min (ASTM D1238L). Air-dried Birch fiber (CTMP, 20-80 mesh) was prepared at laboratory of CRPP, UQTR. Maleated polypropylene (Epolene G-3003) was supplied by Eastman chemical company (Kingsport Tenn.) as coupling agent. Its maleic acid graft is 1.5% and the molecular weight is 52,000. Dicumyl peroxide (98% active DCP) supplied by Sigma Chemical Co. was used as an initiator. Its halftime is 0.2min at 190°C. Concentrate MB1001 received from PolyOne Corporation was used as filler based polypropylene with 40±2wt% natural montmorillonite in exfoliated distribution. Its specific gravity is 1.10.

4.2.2 Experimental methods

4.2.2.1 Effects of main factors on the mechanical properties of PP/Birch composites

All blended composites were compounded in a two-roll C.W. Brabender according to the compositions listed on Table 4.1 in order to study the influence of birch fiber, MAPP, DCP and MB1001 on the mechanical properties.

Table 4.1 Diagram of Birch fiber, MAPP, DCP and MB1001 loading on the PP/Birch composites

Code	PP, g	Birch, g	MAPP, g	DCP, g	MB1001, g
PP	100	0	0	0	0
PPN5	95	0	0	0	5
PPN10	90	0	0	0	10
PPN15	85	0	0	0	15
PPN100	0	0	0	0	100
PPF10	90	10	0	0	0
PPF20	80	20	0	0	0
PPF30	70	30	0	0	0
PPF10M3D0.2	86.8	10	3	0.2	0
PPF20M3D0.2	76.8	20	3	0.2	0
PPF30M3D0.2	66.8	30	3	0.2	0
PPF30M3D0.2N10	56.8	30	3	0.2	10

4.2.2.2 Statistical experiment design

There are numerous independent variables including processing conditions that affect the resulting properties of the composites [350, 373, 374].

Table 4.2 Coded factor levels corresponding to actual factor levels in experiments

Coded factor levels / Actual factor levels	-1.682	-1	0	+1	+1.682
MB1001, wt%	0	0.81	2	3.19	4
MAPP, wt%	0	1.01	2.5	3.99	5
DCP, wt%	0	0.041	0.1	0.16	0.2

A central composite design (CCD): 2^3+star design was chosen for three experimental factors (MB1001, MAPP and DCP) which is presented in Figure 4.1. The actual and coded factor levels were set on the basis of certain limits as indicated in Table 4.2. The experiments generated by *Statgraphic Centurion*® software consist of 16 runs (two runs were set at center points, 6 runs were set at axial points and 8 runs were set at cube points) for 3 factors in coded units as shown in Table 4.3. The design is to be run in a single block for a chosen content of wood fibers. Wood fibers were added to each single block at 10 or 30wt% level. The order of the experiments has been fully randomized in order to provide protection against the effects of hidden variables.

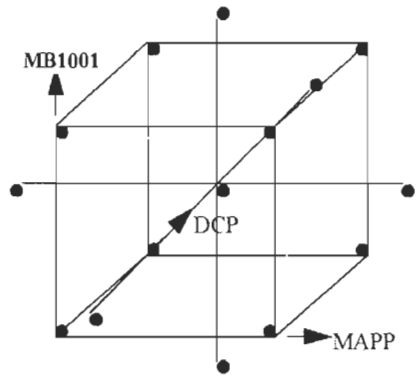

Figure 4.1 Diagram of central composites design with the composition of the samples for each experiment

Table 4.3 Diagram of Central composites design: 2^3+ star Design with one block in term of coded factor levels generated by the Statgraphics Centurions software

Run No.	Block	MB1001	MAPP	DCP
1	1	-1	1	-1
2	1	1	-1	1
3	1	1.682	0	0
4	1	-1	1	1
5	1	1	1	-1
6	1	0	0	-1.682
7	1	0	1.682	0
8	1	0	0	0
9	1	-1	-1	1
10	1	0	0	0
11	1	-1	-1	-1
12	1	1	-1	-1
13	1	1	1	1
14	1	0	-1.682	0
15	1	-1.682	0	0
16	1	0	0	1.682

4.2.3 Compounding

All the blends were prepared by blending the components with Thermotron-C.W. Brabender (Model T-303) according to the conditions as follows. Twenty weight percent PP with or without MAPP/MB1001 was melted on rollers at 190°C. Birch fiber and the residual (eighty weight percent) PP were then added and blended within 7 min at 60 rpm, then peeling mixture from the roller and re-blended for 5 times, each time for 3 min to obtain the uniform composite sheet.

Finally, removing the composites sheet from the roller and making into strips with knife according to the molder size after DCP added and blending for 3min.

4.2.4 Compression molding

The composite strips were molded to dog-bone shape specimens (ASTM D638 Type V for tensile and ISO 8256 Type II for impact testing). 22 specimens (10 for tensile testing and 12 for impact strength testing) were simultaneously put in a molder covered by metal plates on both side, heated at 192±2°C DAKE, pressed for 15mins under the pressure of 20MPa, and then cooled below 100°C by circulating cold water in the press. The approximate dimensions of tensile specimens were as follows: width 0.28-0.34cm and thickness 0.29-0.34cm. And the width of impact was 0.28-0.34cm and thickness 0.14-0.19cm.

4.2.5 Mechanical tests

All the specimens were conditioned in testing room overnight, measured with micrometer after polishing. Measurements were made on an Instron tester (Model 4201) at 23°C and 45% level of relative humidity according to ASTM D638.

4.2.6 Determination of tensile impact

Tensile impact strength (un-notched) was measured at ambient temperature (23°C) using a TMI impact tester (TMI No.43-01) according to ASTM D1822. The maximum energy of the pendulum was 2J. Test specimens used were that taken from compression-molded plates.

4.3 Results and Discussions

4.3.1 Functional factors and mechanical properties of PP/Birch composites

4.3.1.1 Effects of Nanoblend concentrate MB1001 on the mechanical properties of pure PP

In order to seek the effects of MB1001 loading for nanocomposites, the composite of PP and MB1001 was studied employed a roller mixer-thermotron Brabender with melt compounding. Mechanical properties of PP/MB1001 composite are shown in Figure 4.2, Figure 4.3 and Figure 4.4. Figure 4.2 shows the effect of MB1001 on impact strength properties. Impact strength increased with increasing MB1001 content until a peak point was reached at around 5wt%.

Strength at max load and Z-slp point was just increased slightly and then dropped suddenly as well as its strain showed in Figure 4.3. But to auto break point, especially at 10%, the stress dropped much while strain increased. That is to say a limited amount of concentrates affect the stress and strain. Obviously, the composites

of PP/MB1001 has a good strength and tensile at 5-10wt% or at 1.9-4.2wt% of MB1001.

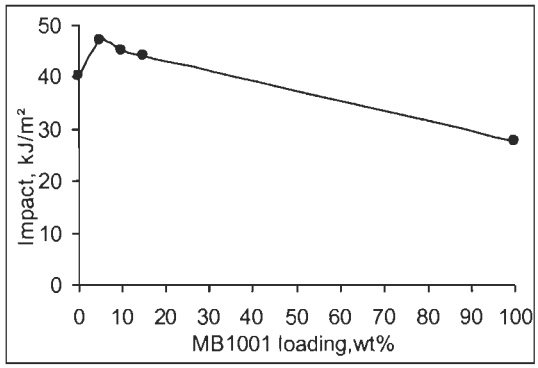

Figure 4.2 Effects of MB1001 loading on Impact strength of PP/MB1001 composites

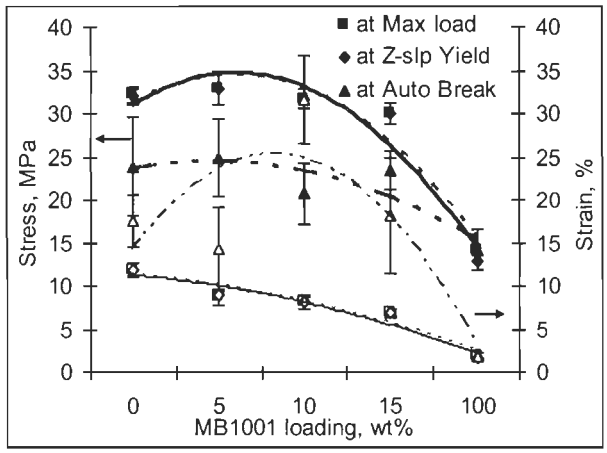

Figure 4.3 Effects of MB1001 loading on stress and strain of PP/MB1001 at different point

The improvement in tensile strength was quite gentle at low clay amount present. The trend is reported by others [233]. The role of the clay as a reinforcer in the matrix as shown in Figure 4.4 is quite evident. Polymer chains restricted in mobility contribute to the improvement of the modulus in a polymer-clay hybrid. Increasing the clay content will greatly constrain the polymer chain's mobility and the modulus is improved. An observed decrease in the strain at break could be explained by the same reasoning because the plastic deformation of the matrix is greatly limited by an increase in the clay loading which was described in previously reports [233].

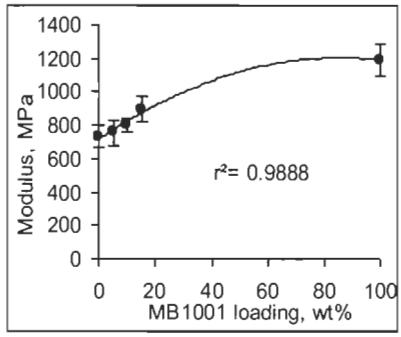

Figure 4.4 Effects of MB1001 loading on Modulus of PP/MB1001 composites

4.3.1.2 Effects birch fiber on the mechanical properties of the composites

The physical properties of the composite reinforced with birch fiber with or without additives were investigated. MAPP addition was carried out by melt compounding with PP and fiber in a two-roll thermotron as coupling agent in our experiment since MAPP grafting and MAPP treatment has similar effects on the mechanical properties of PP/Birch fiber composites [318].

Figure 4.5 shows the relationship between the impact strength and the fiber loading with/without MAPP and DCP. The maximum impact strength of the composite specimens without MAPP and DCP was 34kJ/m² lower than pure PP which was 40kJ/m² due to its thermo-plasticity. It was found that the impact strength of the composites with additives was lower than the composites specimens without additives at same fiber loading.

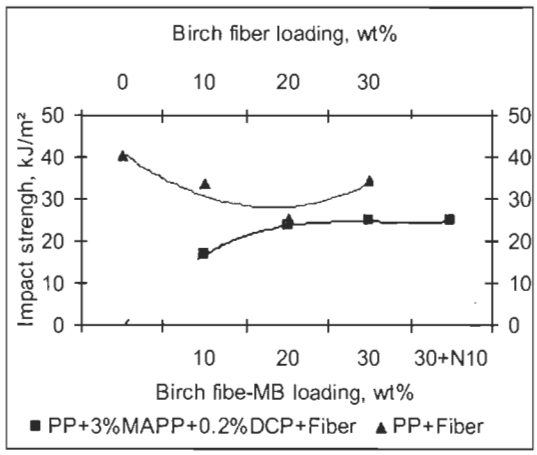

Figure 4.5 Effects of birch fiber loading on Impact strength of the composites with and without additives

Both impact strength and tensile increased with increasing fiber content until a peak reached. With an addition of MAPP/DCP leading to similar trends in the composites,

the impact and tensile could be seen from Figure 4.5 and Figure 4.6. These improvements are due to the enhanced stress transfer from the matrix to the fiber via the compatibilizer [358, 359].

Results for stress and strain of the composites are compared in Figure 4.6. As can be seen, performance of composites with additives was better than that of the composites without additives. With specimens with coupling agent, the stress increased with an increase in the fiber content due to the number of bonding point continuously as the content of birch fiber increased, although DCP addition resulted in severe degradation of PP. Higher processing temperatures clearly caused more degradation of PP during processing, especially in an open-air roller [356]. So we think DCP has a negative influence on the mechanical properties in our experiment and MAPP addition mainly leads to the enhancement of impact and tensile from Figure 4.5 and Figure 4.6.

MAPP which having a higher amount of maleic groups per chain length and higher molecular weight (M_w=52,000) allows more MAPP chains be involved in inter-chain entanglements and to contribute to the mechanical continuity of the composites [317]. In the presence of MAPP and DCP, more fibers lead to more hydroxyl groups bonding with maleic anhydride and enhancing the interfacial birch fiber/PP matrix adhesion. MB1001 when added at 30wt% fiber loading decreased the impact strength because the nanoparticles could make the matrix more flexible and reduce the entanglements of MAPP chains with PP.

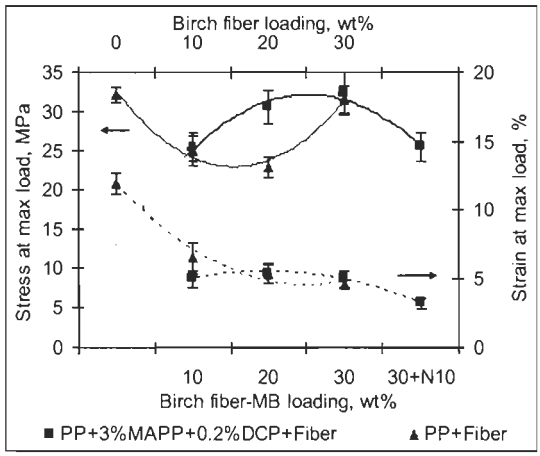

Figure 4.6 Effects of birch fiber loading on stress and strain of the composites with and without additives

For specimens without compabitilizer, the tensile strength decreased at 10% birch fiber content, but then increased at 30wt% fiber content, which was different from the previously reported works [69, 360, 361, 375]. This may be attributed to the increase of blending time used in the present work. Longer blending time achieved a better dispersion of fiber in the matrix and improved the interface strength. Although most thermoplastics are non-polar substances which are not compatible with polar fiber which contributes to a poor adhesion at the fiber-matrix interface, higher fiber content homogeneously dispersed means that the fiber could better enhance the tensile strength.

The strain at max load decreased steadily as the fiber loading increased in the composite. But there are significant differences in the strain of hybrid composites with and without additives. The strain of the composites without additives decreased more strongly (113% max.) than the composites containing MAPP and DCP (27% max.). The steep decline in strain immediately upon fiber addition is obvious, because fiber has low elongation at break restrict the polymer molecules flowing past one another. This behavior is typical of reinforced thermoplastics in general and has been reported by many researchers [56, 84, 337]. The addition of fiber had a positive effect on the rigidity of the composite because birch fiber was less flexible than PP which restricted the mobility of matrix and made more stiffness.

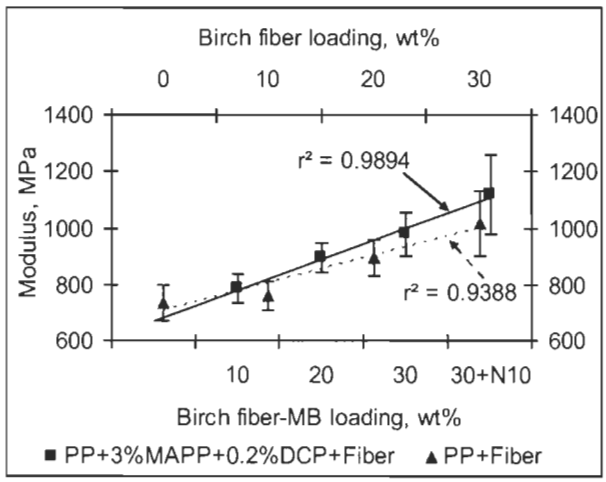

Figure 4.7 Effects of birch fiber loading on modulus of the composites with and without additives

The modulus increased significantly with the increase in fiber content of composites both with and without additives and 10wt% MB1001 as presented in Figure 4.7. Coupling agent and initiator can change the molecular morphology of the polymer

chains near the fiber-polymer interphase. Yin *et al.* [376] reported that the addition of coupling agent (MAPP) even at low levels (1-2%) increased the nucleation capacity of wood fibers for PP and dramatically changes the crystal morphology of PP around the fibers. When MAPP is added, surface crystallization dominates over bulk crystallization and a transcrystalline layer can be formed around the wood fibers. More crystallites give much higher modulus and increase the modulus contribution of the matrix to the composite modulus [84, 377]. But the degradation of matrix caused by the presence of DCP could hurt the modulus of the composites after DCP. The positive influence of MAPP was been counteracted by the negative influence of DCP shown in Figure 4.7. Moreover, both of them has a relationship with fiber loading in a term of a linearly equation as shown in Figure 4.7 such that similar results were also observed on wood fiber/polypropylene composites compatibilized with m-TMI-g-PP by A. Karmarkar *et al.* [84] and aspen/polypropylene composite without coupling agent by Gu *et al.* [378].

Figure 4.8 shows energy at break point and toughness at break point of the composites with and without additives. The experimental results showed that the energy and toughness has similar trends and could be interpreted with same reasons respectively. Fracture energy decreases sharply as fiber was loaded with specimens untreated with MAPP and DCP and increases slightly with treatment because the surface energy increased with an increase in the MAPP content due to the number of the high energy sites introduced continuously as the content of MAPP increased [362]. The result of PP reinforced with untreated wood fiber was also in agreement with our previous work [181, 182, 184, 185].

As the clay (MB1001) was added, the fracture energy decreased obviously due to the particles of filler weakening the interfacial strength among fillers, fibers and matrix as shown in Figure 4.8. The surface energy of the particles of clays was lower than that of reactive component. On the other hand, the clays solid particles negatively affected absorption of the fracture energy and made the composites more fragile due to its harder phase and its restriction for wood fiber and matrix to entangle. Moreover, more MB1001 means more particles dispersed in the composites probably leading to some flaws which have been proved during the test. During the test of same identical sample, there were 1-2 specimens broken beyond the domain of standard devriation which resulted from the shortcomings of the structures and distributions of wood fiber and clays, especially to clays in the matrix. Though we

employed clays in form of MB1001 which was prepared by special technique, it's still difficult to disperse particle by particle. The interpretations of toughness were similar to those of energy because toughness was calculated from energy.

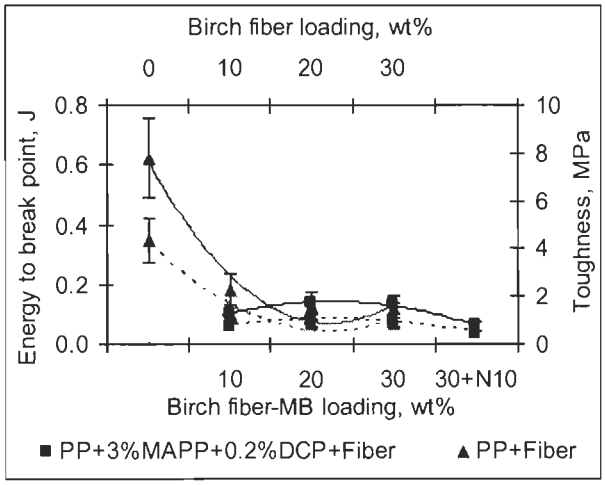

Figure 4.8 Effects of birch fiber loading on energy and toughness of the composites with and without additives (·····Toughness —Energy to break point)

4.3.2 Results obtained using statistical experimental design

Comparing the systematic results on the impact and tensile properties of the composites designed by CCD with different content of fiber as the single block, the composite with higher fiber loading achieved superior properties although the compositions were same excepting of the content of fiber from Figure 4.9 and Figure 4.10. So, it was chosen to calculate the optimum composites compositions and evaluate their optimum properties as well as the final cost of composites at the thirty weight percent of fiber from Figure 4.11 and Figure 4.13-Figure 4.16.

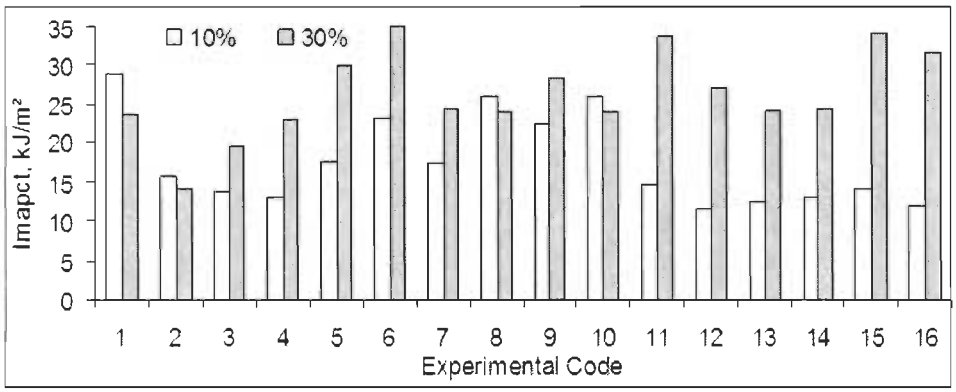

Figure 4.9 Effects of the difference of birch fiber loading on impact strength of the composites

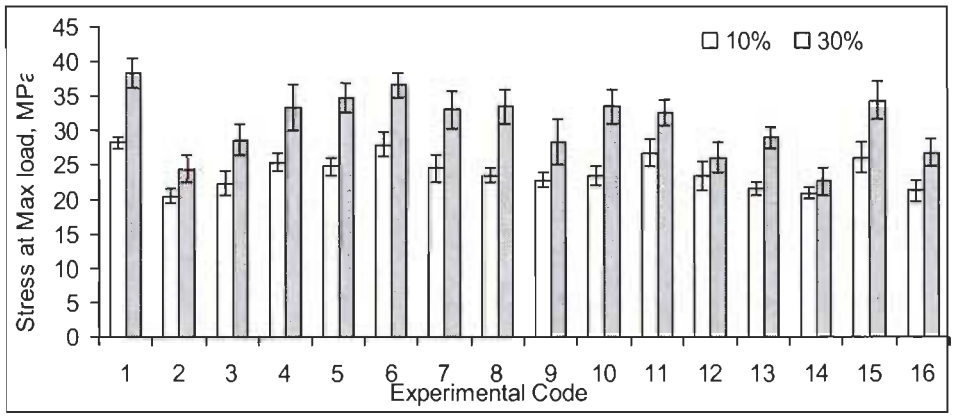

Figure 4.10 Effects of the difference of birch fiber loading on tensile property of the composites

Statagraphics plus is a very powerful program for the statistical evaluation. It's used to determinate the effects (main and interactions) which could be visualized and optimized the correlations between independent variables (MB1001, MAPP and DCP) and dependent variables (properties) with response surface plot. Response surface diagram for impact strength as a function of the concentrations of MAPP and MB1001 is presented in Figure 4.11. It is clear from the picture that the impact strength is a function of MB1001 as well as its synergistic reaction with MAPP, and approaching max values around 50kJ/m^2 at the optimum value of DCP with concentration corresponding to the factor level -1.682 at 30wt% fiber loading.

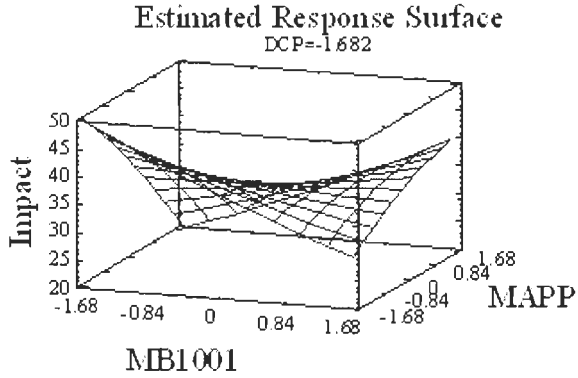

Figure 4.11 Response surface diagram for impact strength as a function of the concentrations of MAPP and MB1001 at the optimum DCP level with 30% fiber loading

The value of DCP at the above mentioned concentration was chosen at optimal level because Standardized Pareto Chart for Impact at 30 % fiber loading on Figure 4.12

indicates that MB1001 is the most important factor in determining the impact strength.

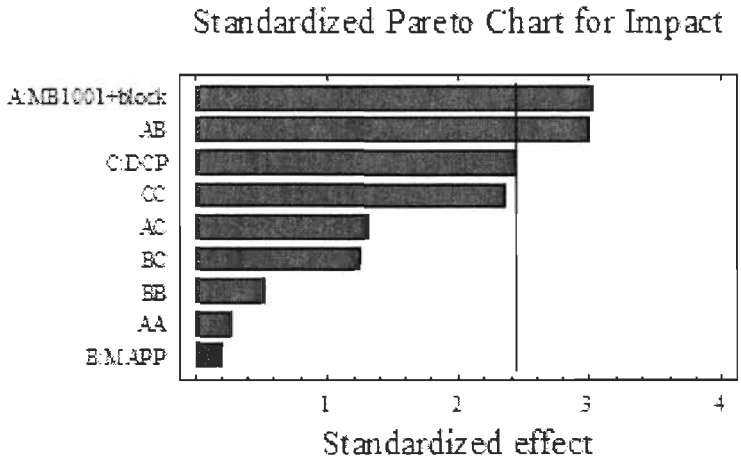

Figure 4.12 Standardized Pareto Chart for Impact strength at 30 % fiber loading

Response surface diagram for max tensile strength as a function of the concentrations of MAPP and MB1001 is presented in Figure 4.13. It is evident from the picture that the tensile strength is mainly function of MAPP content and approaches to maximum values of 40MPa by setting DCP at the optimum concentration which is corresponding to the coded level of -1.682. The maximum values of the composite max tensile strength of about 40MPa are higher than that of PP being 33MPa which indicates good fiber matrix adhesion.

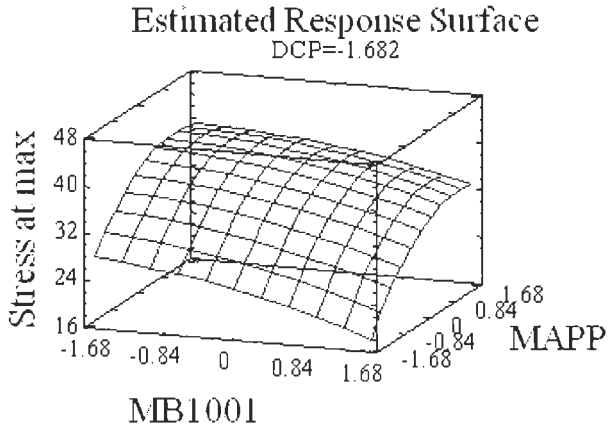

Figure 4.13 Response surface diagram for max tensile strength as a function of the concentrations of MAPP and MB1001 at the optimum DCP level with 30% fiber loading

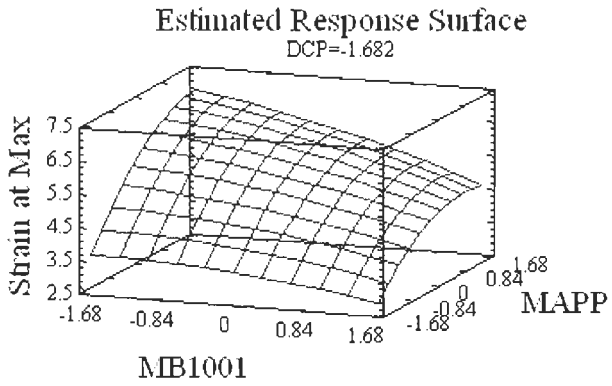

Figure 4.14 Response surface diagram for max strain as a function of the concentrations of MAPP and MB1001 at the optimum DCP level with 30% fiber loading

Response surface diagram for maximum strain and modulus as a function of the concentrations of MAPP and MB1001 is indicated in Figure 4.14 and Figure 4.15. In the case of strain (Figure 4.14) max values reaching 6.9% at the optimum value of DCP which are lower than that of PP being 11.9% could be explained by higher fiber stiffness. Optimum value of modulus, Figure 4.15, reached 1.1×10^{3}MPa, higher than that of the pure PP (733MPa) were reached in the absence of MAPP and DCP. These results are in agreement with our previously reported ones [135, 336, 379] which showed that the existence of coupling agent or initiator usually leads to modulus decreased when compared to the composites without them and increased due to the addition of clay.

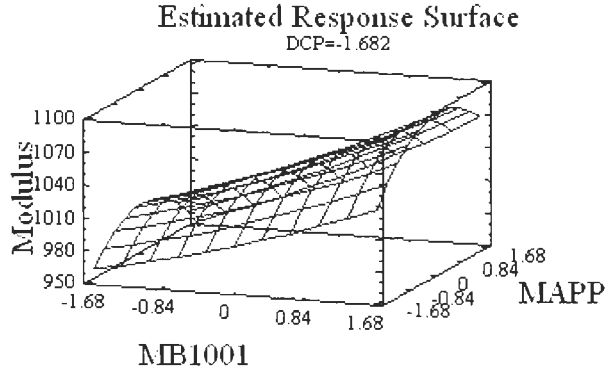

Figure 4.15 Response surface diagram for modulus as a function of the concentrations of MAPP and MB1001 at the optimum DCP level with 30% fiber loading

Response surface diagram for Toughness as a function of the concentrations of MAPP and MB1001 is described in Figure 4.16. The maximum values of toughness

could reach 1.83J. with DCP, MB1001 and MAPP corresponding to the level of -1.682, -1.682 and 1.355.

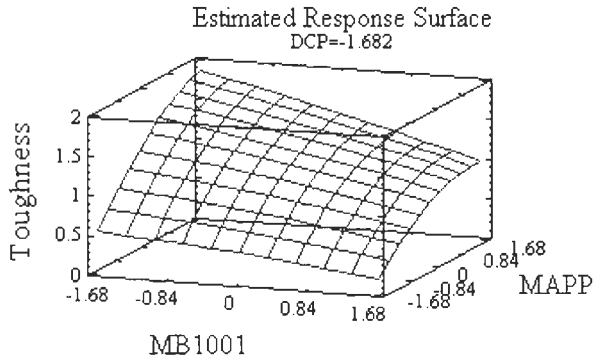

Figure 4.16 Response surface diagram for Toughness as a function of the concentrations of MAPP and MB1001 at the optimum DCP level with 30% fiber loading

Statgraphic Centurion software not only enabled us to estimate maximum mechanical properties values but also estimate the values of independent variables necessary to maximize properties from Figure 4.11-Figure 4.16. Results in Figure 4.17-Figure 4.21 confirmed the trend found in exploratory part of the work presented in Figure 4.2-Figure 4.8.

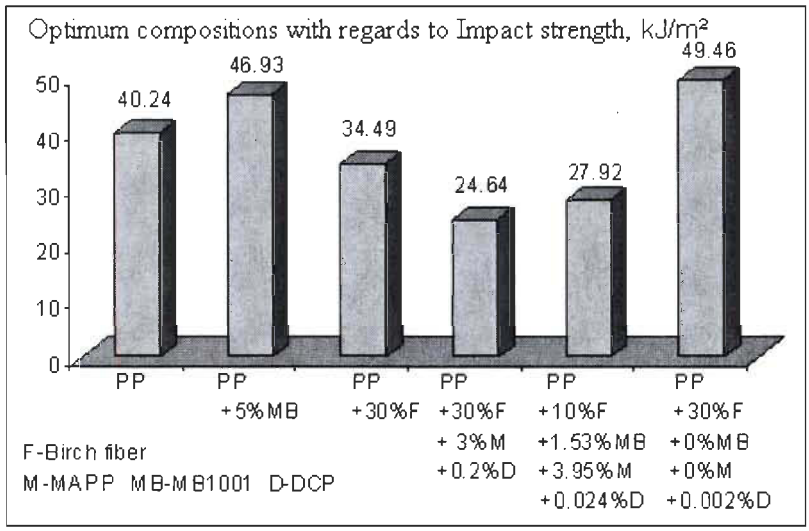

Figure 4.17 Effect of compositions on the impact strength of the composites

We chose the compositions optimum on impact strength found in previous exploratory part and CCD respectively as showed in Figure 4.17. The addition of nanoblend concentrate clay could provide nanocomposites with superior impact strength but without fiber load, with the increase from 40kJ/m² of pure PP up to

47kJ/m². In the presence of fibers the impact strength could reach 49kJ/m² at optimum compositions found using the statistical design for 30wt% birch fibers.

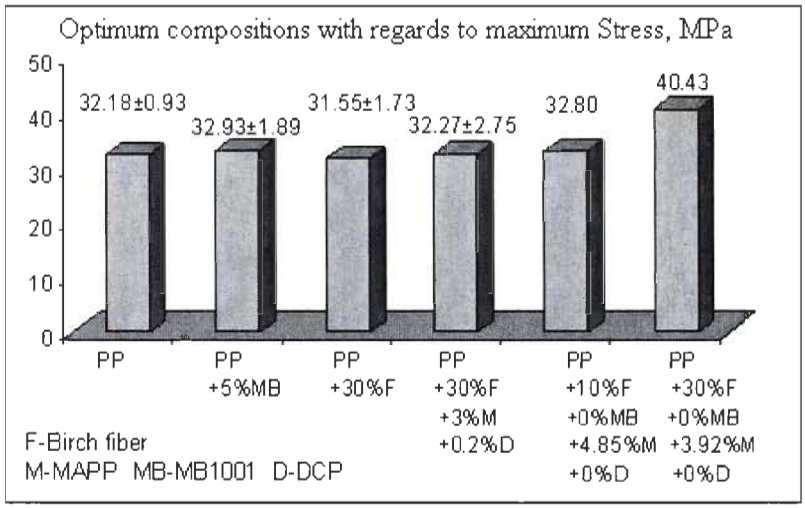

Figure 4.18 Effect of compositions on the max stress of the composites

DCP has a negative influence on the impact strength of the composites prepared in open-air roller Brabender with MAPP and MB1001. The effect of additives on the max stress of composites is presented in Figure 4.18. The optimum values of max stress would reach 40MPa with 3.92wt% MAPP at 30wt% birch fiber loading which was higher than that of pure PP (32MPa). Both MB1001 and DCP have negative effect on the max stress of the composites.

Effect of additives on the max strain of the composites is shown in Figure 4.19. In general, strain has decreased in presence of additives due to the morphology phase stiffening.

The effects of fiber loading and additives on the modulus and toughness at constant optimum concentrations of MAPP, MB1001 and DCP at 10wt% and 30wt% fiber loading levels are clearly seen in Figure 4.20 and Figure 4.21. It's evident that fiber is giving a modulus superior to that of pure PP, up about 35-50%. Fiber loading levels 10wt% as well as 30wt% are both leading to the modulus increase, slightly higher at 30wt% level (1092MPa versus 994MPa comparing to 733MPa for PP). It was also shown that MB1001 which contained 40% clay in matrix PP has higher modulus than PP, 1.2×10^3MPa versus 733MPa for pure PP as was also presented in a previous report [233].

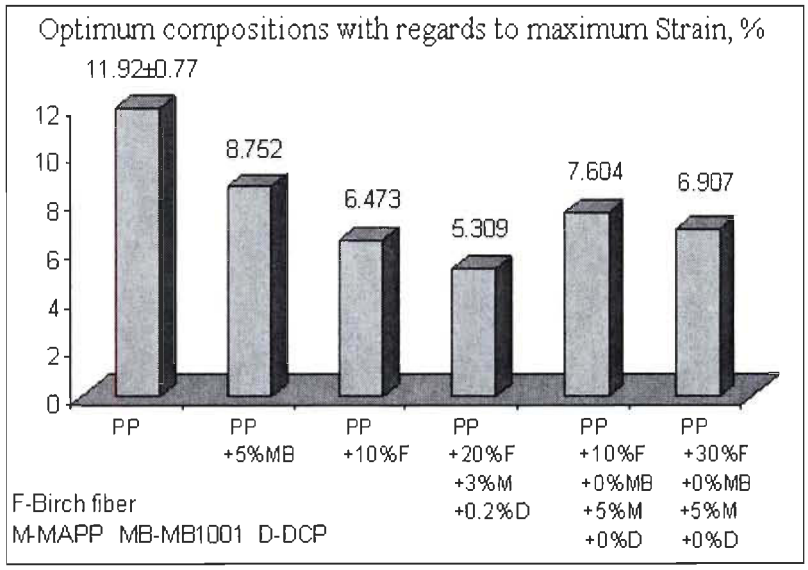

Figure 4.19 Effect of compositions on the max strain of the composites

The effect of fiber loading on the toughness at constant optimum compositions of MAPP, MB1001 and DCP at 10wt% and 30wt% levels is shown in the following Figure 4.21.

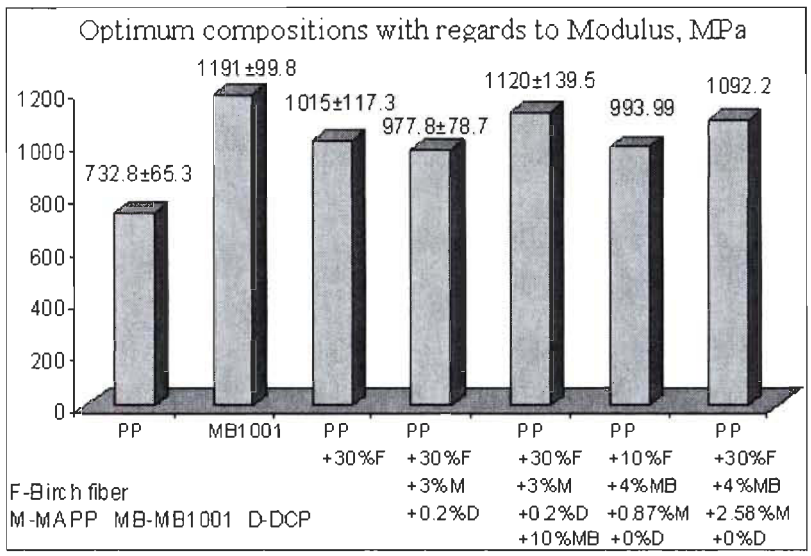

Figure 4.20 Effect of compositions on the modulus of the composites

Toughness at break point has a dramatically increasing at 10wt% level of MB1001 valued 8.28MPa. The optimum toughness of the composites both at 10wt% fiber loading and 30wt% fiber loading were inferior to that of the nanocomposites filled with 10wt% MB1001 only as well as pure PP (4.37MPa).

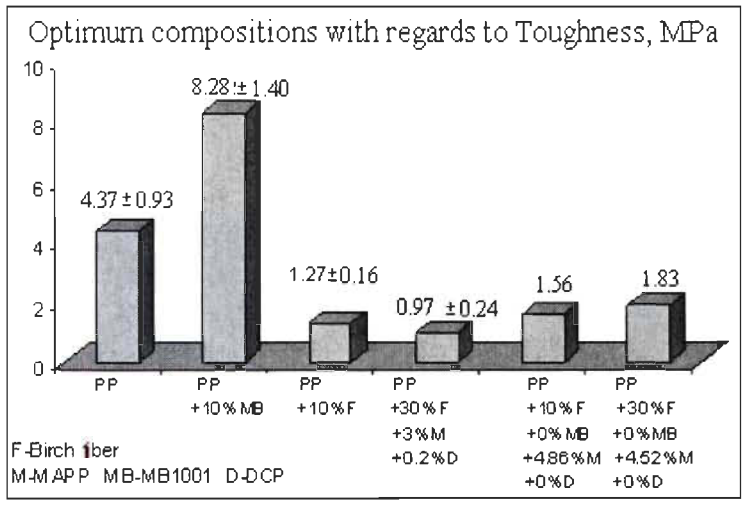

Figure 4.21 Effect of compositions on the toughness of the composites

The comparison of results was summarized in Table 4.4. It was concluded that the central composite design made it possible to determine the optimum concentration of additives and to maximize both the impact as well as tensile properties. It was also found, that birch fiber reinforcement of PP composites at 30wt% level could lead to improvement both the impact as well as the tensile strength properties increasing as presented in the Table 4.4.

Table 4.4 Optimizations of mechanical properties of the composites designed by CCD

Property	The increase of physical properties of composites based PP comparing with PP		
	30wt% Birch fiber	10wt% Birch fiber+additives	30wt% Birch fiber +additives
Impact strength	-14%	-31%	**23%**
Stress at max load	-2%	**2%**	**26%**
Strain at max load	-62%	-36%	-42%
Modulus	**39%**	**36%**	**49%**
Toughness	-81%	-64%	-58%

Considering the cost of out-doors materials as well as their properties, we chose all the composites listed in Figure 4.17 and Figure 4.18 to estimate the cost of products presented in Figure 4.22. The cost of the composites reinforced with birch fiber and MB1001 were economic compared with the composite filled with glass fiber at 30% loading level. Values from Figure 4.22 also show that the thermoplastics reinforced with wood fiber have lower cost than pure PP cost. Considering the mechanical properties as well as their cost, we regarded that the composites with optimum compositions with 30wt% fiber loaded was the best choice and the second was the composite reinforced with 30wt% birch fiber without any additives.

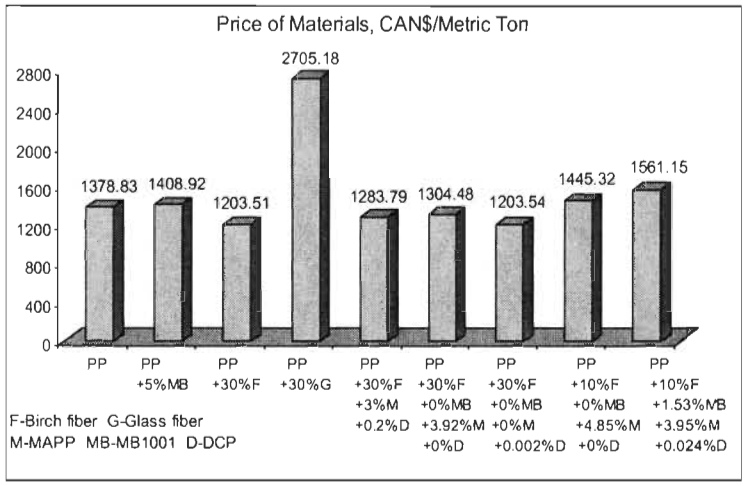

Figure 4.22 PP/Birch composites price comparison with pure PP

4.4 Conclusions

The exploratory and systematic research were carried out with birch fiber, MAPP, DCP, and MB1001 loaded based homo-PP to investigate the methodology and mechanical properties of nanocomposite and hybrid composite. The following conclusions were drawn from the above results:

(1) MB1001 improved impact, tensile and deformation properties of Nanocomposite which could achieve optimum properties on both impact strength and tensile properties at 5% loading level.

(2) Hybrid composite with fiber only has superior impact strength compare to the composites with the addition of MAPP, DCP and MB1001 resulting from the degradation of PP and wood fibers speeded up in the presence of DCP during the thermal processing. However, the tensile property was conversed because the improved interfacial adhesion/compatibility and the formed networks functioned by MAPP and DCP among the composites leading to transferring force effectively.

(3) Whether the hybrid composite with additives or not, the Modulus has an increasing linear relationship with the fiber loading.

(4) It's possible to carry out the hybrid composite to protect or increase the impact strength without losing tensile properties at optimum compositions to lead to lower cost by central composite design.

Chapter 5 - Effect of Variables on the Mechanical Properties and Maximization of Polyethylene-Aspen Composites by Statistical Experiment Design

Ruijun Gu, Bohuslav V. Kokta and Gabriela Chalupova
Journal of Thermoplastic Composite Materials. 2009, 22(6): 633-649.
DOI: 10.1177/0892705709105965
http://jtc.sagepub.com/cgi/content/abstract/22/6/633

Abstract: Systemic studies of the effects of the concentrations of maleated polyethylene (MAPE) loading, the content and addition sequence of dicumyl peroxide (DCP), the content and type of Nanoclay (NC) and Aspen TMP fiber loading on the mechanical properties of PE-Aspen composite were undertaken with the objective to increase the impact strength as well as the tensile properties. In this paper, the formation of an optimal compatibilizing system for the hybrid composite PE-Aspen-NC by combining basic principles for compatibilization was investigated. Statistical approach experimentation using *Statgraphics Centurion*® with the objective to maximize both the tensile strength as well as the impact properties of natural fiber and nanoclay filled PE was applied to reach values well above that of virgin PE.

Keywords: Aspen fiber, Central composite design, Composite, NC, PE, Wood fiber

5.1 Introduction

Wood plastic composites are hybrid materials that combine the performance and cost attributes of both wood and thermoplastics. Wood fiber is available worldwide and biodegradable[82] due to low cost and easy disposal [91]. Due to these particular attributes this hybrid composite material is gaining an increasing niche in the market place, particularly in North America. According to the projection of Freedonia (Study #1929, www.freedoniagroup.com) the demand for reinforced plastics in the USA is expected to grow nearly 3% annually, from about 1.7 million tones in 2004 to 1.9 million tones in 2009 with a total value of US$7.2 billion.

But interfacial modifiers should be used to improve the interfacial compatibilization and its adhesion to hydrophobic matrix. MAPE was used as a coupling agent in the hybride composite [81, 92, 316] while DCP used as a crosslinking agent [380, 381, 382, 383] being most utilized for chemical bonding to both the wood fiber and the polymer matrix [321]. Moreover, natural fibers are rich in lignin with abundant multi-functional hydroxyl groups to react with maleic anhydride group to form

branched structures. Lignocelluloses fiber would also produce more anchorage point in matrix to enhance higher impact strength because lignin is a solid macromolecule [233].

The main focus on this study is to investigate the effects of varied independent variables, i.e. MAPE, DCP, and Nanoclay content, on the mechanical properties of the PE-Aspen composite.

5.2 Experimental

5.2.1 Materials

Thermoplastics: Linear low density polyethylene (LLDPE) (NOVAPOL® GF-0218-F, powder) was supplied by NOVA Chemicals Inc. Its melt flow index is 2.0g/10min.

Wood fiber: Industrial Chemical Thermo-Mechanical Pulp of trembling aspen (*Populus tremuloides* Michx.) was employed. The wood pulp fibers were air-dried and ground at our laboratory to produce fine particles. Particles that passed through a 20-mesh but retained on a 60-mesh screen were employed in this study.

Coupling agent: Maleated polyethylene (Eastman G-2010, Kingsport Tenn.) was supplied by Eastman chemical company and contains 1.5% maleic anhydride.

Initiator: Dicumyl peroxide (98% active DCP) whose halftime is 1 min at 171°C, supplied by Sigma Chemical Co. was used as a crosslinking agent.

Fillers: Cloisite®10Å and Cloisite® Na^+ Nanoclay were used as received from Southern Clay Products Inc. The typical physical properties are shown in Table 5.1.

Table 5.1 Typical physical properties bulletin

Physical Properties		Cloisite® 10 Å	Cloisite® Na^+
Treatment	Organic modifier	2MBHT(1)	None
	Modifier concentration	125meq/100g	
Moisture, %		<2%	4-9%
Density, g/cc		1.90	2.86
Dry particles size (by volume)	10%	<2μm	<2μm
	50%	<6μm	<6μm
	90%	<13μm	<13μm
d_{001} X-Ray		19.2Å	11.7 Å

Note: (1) 2MBHT- dimethyl, benzyl, hydrogenated tallow, quaternary ammonium

5.2.2 Experimental and compounding

5.2.2.1 Effect of different adding-method of DCP on the mechanical properties of PE-Aspen composite

PE-Aspen composite containing 2.5% MAPE, 2% Cloisite® 10Å NC and 0.2% DCP at 30% content of fiber was chosen as a reference sample to study the mixing sequence for DCP. The addition of DCP was done as illustrated in Schedule 5.1.

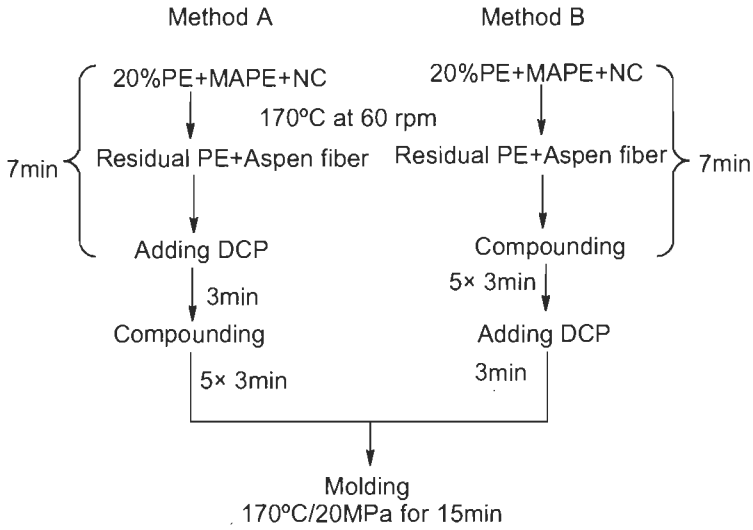

Schedule 5.1 Compounding and molding conditions

5.2.2.2 Effects of independent variables on the mechanical properties of PE-Aspen composite

All composites were compounded in a two-roll Brabender to study the influence of Cloisite® Na^{+}, MAPE and DCP on the mechanical properties by method B in Schedule 5.1.

5.2.2.3 Statistical experiment design logic

A central composite design (CCD): 2^3 + star design was used to study the three experimental factors (NC, MAPE, and DCP) in 16 tests with one single block. The order of the experiments was randomized. The CCD for three factors, with extremes of +1 to -1, was determined at 1.682 distances by a *Statgraphic* Centurion® software as shown in Table 5.2 CCD for three experimental factors†. Wood fibers were added to single block at 30wt%. All blended composites were compounded by method B in Schedule 5.1.

5.2.3 Compression molding

The composite strips were pressed into dog-bone shaped mould (ASTM D638 Type V for tensile and ISO 8256 Type II for impact testing). A total of 22 specimens (10 for tensile testing and 12 for impact testing) were simultaneously prepared in the same mould. The mould was maintained at 170 ± 2 °C by means of a Dake Press and held for 15min under a pressure of 20MPa. After the high pressure stage, the mould was cooled below 60°C by circulating cold water in the platens. The approximate dimensions of specimens for tensile test were 0.28-0.31 cm wide and 0.32-0.36 cm thick, whereas those of impact test specimen were 0.28-0.30 cm wide and 0.18-0.21 cm thick. All the specimens were polished, then equilibrated overnight in a testing room, and then the width and the thickness was measured with a micrometer.

Table 5.2 CCD for three experimental factors†

Run No.	Block	‡NC	MAPE	DCP
1	1	**-1** (0.81)	**1** (3.99)	**-1** (0.041)
2	1	**1** (3.19)	**-1** (1.01)	**1** (0.16)
3	1	**1.682** (4)	**0** (2.5)	**0** (0.1)
4	1	**-1** (0.81)	**1** (3.99)	**1** (0.16)
5	1	**1** (3.19)	**1** (3.99)	**-1** (0.041)
6	1	**0** (2)	**0** (0.25)	**-1.682** (0)
7	1	**0** (2)	**1.682** (5)	**0** (0.1)
8	1	**0** (2)	**0** (2.5)	**0** (0.1)
9	1	**-1** (0.81)	**-1** (1.01)	**1** (0.16)
10	1	**0** (2)	**0** (2.5)	**0** (0.1)
11	1	**-1** (0.81)	**-1** (1.01)	**-1** (0.041)
12	1	**1** (3.19)	**-1** (1.01)	**-1** (0.041)
13	1	**1** (3.19)	**1** (3.99)	**1** (0.16)
14	1	**0** (2)	**-1.682** (0)	**0** (0.1)
15	1	**-1.682** (0)	**0** (2.5)	**0** (0.1)
16	1	**0** (2)	**0** (2.5)	**1.682** (0.2)

† Figures in brackets are weight percent for NC, MAPE and DCP
‡ NC incorporated is Cloisite®10Å and Cloisite® Na+ respectively

5.2.4 Mechanical tests

The tensile tests were performed using an Instron machine (Model 4201) at 23°C and 50 % relative humidity according to ASTM D638 while the impact tests were performed by means of a TMI impact tester (TMI No 43-01) at ambient temperature (~ 23°C) following the ISO 8256 method.

5.3 Results and Discussions

5.3.1 Addition sequence of DCP based on the mechanical properties of PE-Aspen composite

The results of the effect of DCP introduction method on the impact and tensile properties of PE-Aspen composite composed of 30wt% aspen fiber, 2.5wt% MAPE, 2wt% NC and 0.2wt% DCP as a function of DCP addition sequence are shown in Figure 5.1. The impact properties of the composite initiated with DCP at final-step (DCP added method B) is superior to that initiated at early-step. During longer compounding time in the DCP presence, the effect of inhibitory action becomes clearer.

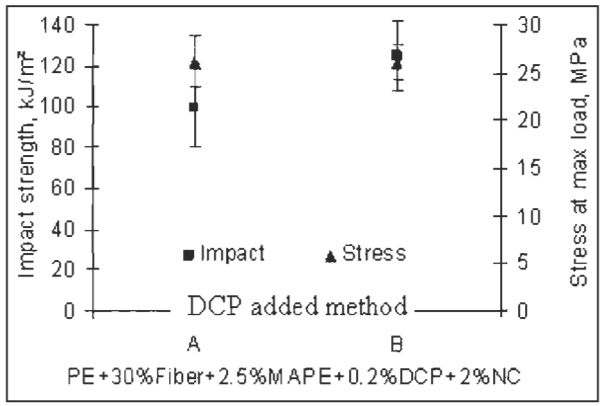

Figure 5.1 Effects of DCP adding method on the impact/stress of PE-Aspen composite

The observed difference in strength properties of the composite with DCP added in final-step is attributed to different functions. From Figure 5.1, it's obvious that the impact strength is different between the addition of DCP at final-step (125kJ/m²) and early-step (99kJ/m²) while the stress at max load is nearly unchanged. In both methods, the rate of DCP decomposition is too high and yields high radical concentration at the beginning of the process [384] at near 200°C, and these maximum amounts of radicals [385, 386] would abstract hydrogen atoms from matrix molecules to produce alkyl radicals which will be reformed with wood fiber and itself [387]. Unfortunately, lots of free radicals of DCP escape easily due to operating at an open-air roller. Moreover, very little residual DCP is left to crosslink the matrix when molding after longer compounding. In consequence, in order to minimize the degradation of matrix and grafted matrix with fiber and maximize the residual DCP content, we adopted method B in our following experiments. In

addition, the DCP should be mixed with polymer and fiber under its decomposition temperature or an injection method should be used in industrial prodution.

5.3.2 Effects of Cloisite® Na^+ NC on the properties of PE-Aspen composite

Impact and tensile strength of virgin PE and PE-Aspen composites composed of 30wt% aspen fiber, 3wt% MAPE and 0.1wt% DCP as a function of NC addition are shown in Figure 5.2 and Figure 5.3. The addition of NC increases the tensile strength and decreases the impact strength because NC leads to the increase of crystallinity [194, 388]. The maximum impact strength of the composite specimens reinforced with MAPE (3%) and DCP (0.1%) at 30% aspen fiber loading is 165kJ/m² lower than pure PE which is 202kJ/m². It is also found that the impact strength of the composites decreased by 73.3% (from 202kJ/m² down to 116kJ/m²) when the nanocomposite with NC was added for a low concentration of coupling and nucleating agents. Lei *et al.* [194] have obtained similar results with HDPE/Pine composites.

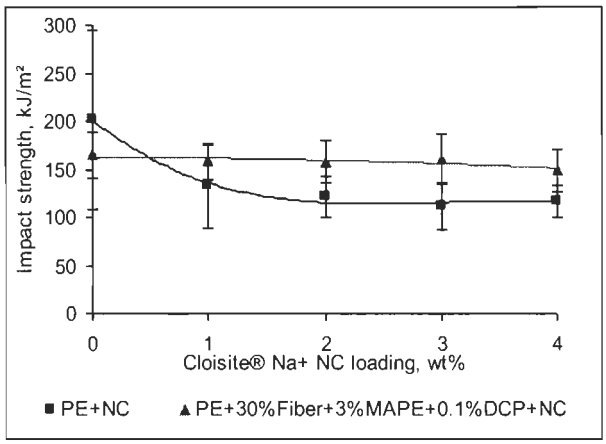

Figure 5.2 Effects of NC on impact of PE Nanocomposite and PE-Aspen composite

When 4% NC is added, the tensile strength increases by 12% from 28MPa to 31MPa with 4% NC as shown in Figure 5.3. Meanwhile there is no influence on the tensile strength when nanocomposite are added to PE alone. In contrast to virgin PE for same property, PE-Aspen composite reinforced with MAPE and DCP at 30% fiber is up 161% (from 28MPa versus 11MPa). MAPE used has a higher amount of maleic groups per chain length to make more MAPE chains involved in inter-chain entanglements and to contribute to the mechanical continuity of the composites [92, 316].

To PE-Aspen composites, because the degree of crystallinity in the composite reinforced with wood fiber would increase [194, 388] due to acting as a nucleating agent [389, 390] as well as the particles acting as a lubricant to reduce the entanglement of MAPE chains with PE following the introduction of NC, the strain is improved up 21% (from 22% to 17%) with the increase of NC from 0% to up to 4% NC resulting in good deformation resistance, but the strain of PE nanocomposites increases slightly from 156% to 174% as NC loading increased due to more network-point within the matrix and the content of crystalline of matrix decrease due to the particles of NC inserted (see Figure 5.3).

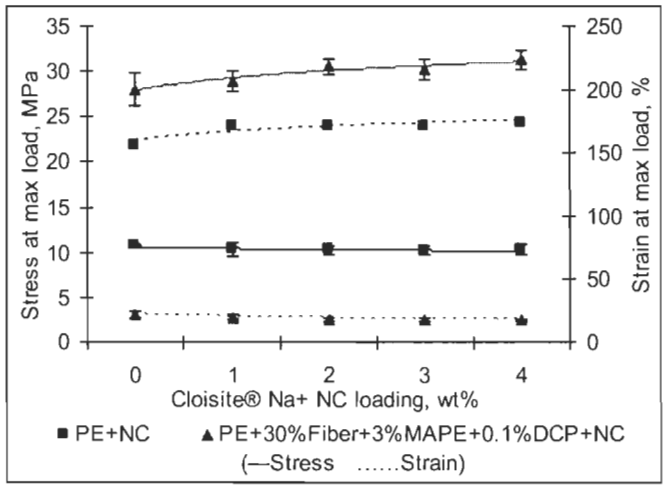

Figure 5.3 Effects of NC on stress and strain of PE Nanocomposite and PE-Aspen composite

With the employment of MAPE and DCP, the strain at maximum decreases when aspen fiber are incorporated from 156% of virgin PE to 22% of PE-Aspen composites with 30wt% fiber employed which is in agreement with the previous works [315, 360, 391] because the fiber low elongation at break restricts the polymer molecules flowing past one another [56]. The addition of fibers had a positive effect on the rigidity of the composite because aspen fiber lower flexibility compared to PE. Mobility of the matrix was restricted and resulted in a stiffer composite.

5.3.3 Effects of MAPE loading on the properties of PE-Aspen composite

The hydroxyl and the other polar groups in wood fibers are the active sites of water absorption resulting in incompatibility with the hydrophobic polyethylene matrix [145] as well as poor dispersion of wood fiber in the polyethylene matrix due to strong fiber-fiber interactions resulting from hydrogen bonding [146] leading to poor

mechanical properties of the composites. MAPE acts as an excellent compatilizer [92] which improves the combination of matrix polymer and wood fiber to transfer more stress from matrix to wood fiber. The coated wood fibers reduce the surface hydrophilicity by forming an ester linkage at interface of maleated compolymers [137]. Furthermore, the nonpolar part of MAPE becomes compatible with the virgin matrix to lower the surface energies of the fibers and increase its wettability and dispersion as implied from the test results reported in Figure 5.4, Figure 5.5 and Figure 5.6. All the treated composites with reinforced 30wt% aspen fibers exhibit the improvement in impact and tensile strength with the increase of MAPE in comparison to the unfilled composites, but the growth rate remains at the same level with the content of MAPE at more than 3wt% in Figure 5.4. This behavior may be attributed to the migration of excess MAPE around the fibers to cause agglomerating among nonpolar hydrophobic matrix resulting from relative polarity difference and thus not entangling with polymer matrix which leads to slippage [92, 316].

Figure 5.4 shows that the impact strength increases 80% from 89.8kJ/m² without feeding coupling agent to 161kJ/m² of the composite with 3wt% MAPE at optimum value due to enhanced adhesion between matrix and wood fiber which is similar to the previous research [81, 91, 92, 316, 392], but decreases to 151kJ/m² as excessive amount of MAPE is added. MAPE is introduced by melt mixing with PE and fiber in a two-roll thermotron as a coupling agent in our experiment. The maximum impact strength of hybrids reinforced with G2010 at 3% level is 161kJ/m² which is higher than the reference PE-Aspen composite (90kJ/m²) due to the better wettability of the PE based maleic anhydride to the LLDPE matrix polymer, however inferior to that of virgin PE (202kJ/m²). It is found that the compatibilizer migration around the fibers act as a damper to the shock wave, being imparted during shocking transferred onto the surface of wood fibers evenly [358, 359] due to more MAPE introduced leading to a more effective stress transfer and a more uniform stress distribution when the ends of fibers are bonded to the matrix [116].

The results obtained from Figure 5.4 also show that MAPE has a positive influence on the tensile strength at maximum load of the composites as well as strain (see Figure 5.5). Tensile increases 21.4% to reach 31.7MPa at 5wt% MAPE with the addition of 30wt% aspen pulp fiber, 3wt% NC and 0.1wt% DCP. In contrast to virgin PE, the tensile strength of the composite reinforced with MAPE is up almost 3 times at maximum (from 11MPa versus 31.7MPa).

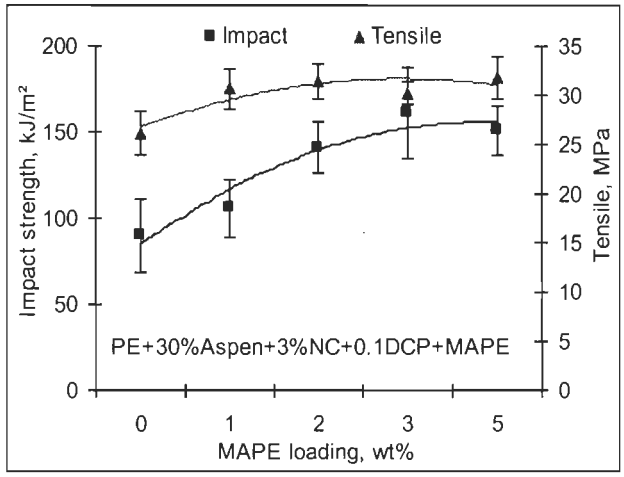

Figure 5.4 Effects of MAPE loading on impact and tensile properties of PE-Aspen composite

The modulus increases a little with the increase of MAPE concentration due to the improved interfacial adhesion and interaction between plastic and wood fibers, reaching 622MPa at 2wt% MAPE, and then decreases to 590MPa with 5wt% as more MAPE is introduced (as presented in Figure 5.5) resulting from excess MAPE leading to slippages acting as a lubricant. Similar results for other wood flour filled PE composites were also reported [393, 394]. Anyway, in the case of the modulus, coupling agent has no significant effect on composites which is similar to HDPE-wood flour composites reported by Li *et al.* [136].

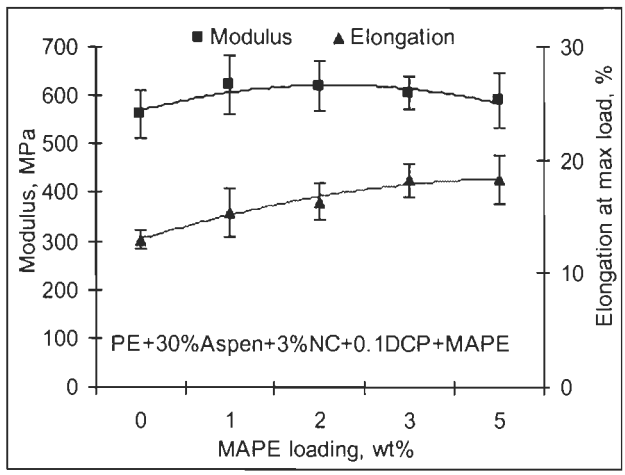

Figure 5.5 Effects of MAPE loading on modulus and elongation of PE-Aspen composite

The elongation at max load increases up 40% to withstand much more fracture energy with the content of MAPE increased because the increase of MAPE is

lowering the crystallinity level due to the crystal imperfection due to MAPE in spite of increasing the crystallization rate [194] to achieve highly amorphous morphology. With the improvement of the compatibility among the matrix and more polymers impregnated into the fiber, the elongation of the composites increases which is contributing to the toughness as well as the plasticity in Figure 5.6.

Figure 5.6 shows that the composite with higher MAPE could bear and absorb strong shocking force to reveal good plasticity with the ratio increasing steadily from 1.2 up to 1.4 similar to the composite with varying NC concentration. The toughness increases sharply as MAPE is introduced into the matrix which leads to stronger interfacial bonding between the fiber and matrix polymer due to the better compatibility to the matrix polymer coupling with MAPE [393].

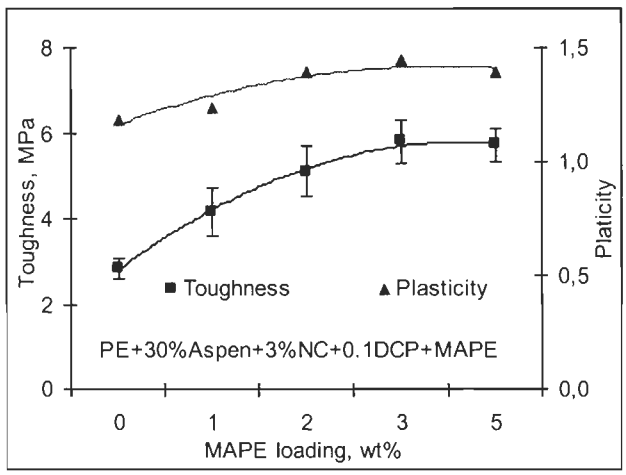

Figure 5.6 Effects of MAPE loading on toughness and plasticity of PE-Aspen composite

(Plasticity is defined as the ratio of $E_{Facture}/E_{Yield}$)

As summarized, tensile properties including tensile strength, tensile modulus and elongation at max load are significantly improved as well as the impact resistance. It is believed that the better wetting and polymer entanglement of MAPE and wood fiber to the matrix polymer by a coupling agent is responsible for improved results, improved plasticity following the incorporation of coupling agent. Similar result for other lignocellulosic filler filled PE composites on the improvement of impact resistance, tensile strength and elongation were also reported [335, 395], but were opposite for modulus. Some reports show that coupling agent has negative effect on impact strength of wood flour-LDPE composites by Yang *et al.* [393] and for Eucalyptus wood residue-HDPE composite by Mengeloglu *et al.* [394], while in our

case, addition of MAPE coupling agent significantly improves the impact, tensile strength, elongation at maximum load as well as slightly increases modulus due to reinforcement with pulp fiber, not wood flour, due to higher aspect ratio and higher content of active groups on the surface of fiber, resulting in more positive effect on tensile properties, impact resistance and toughness.

5.3.4 Effects of the NC type on the properties of the composites blocked with aspen fiber

Cloisite® Na^+ is a natural montmorillonite while Cloisite® 10A is a natural montmorillnite modified with a quaternary ammonium salt. Although the compositions are same, the Impact strength of PE-Aspen composite is different due to the application of different kind of NC as shown in Figure 5.7, Figure 5.8 and Figure 5.9. The difference depended on the difference of the content. Both impact and tensile properties of the composites filled with Cloisite® Na+ are superior to Cloisite® 10A from Figure 5.7 due to the difference in basal spacing and density as well as their polarity.

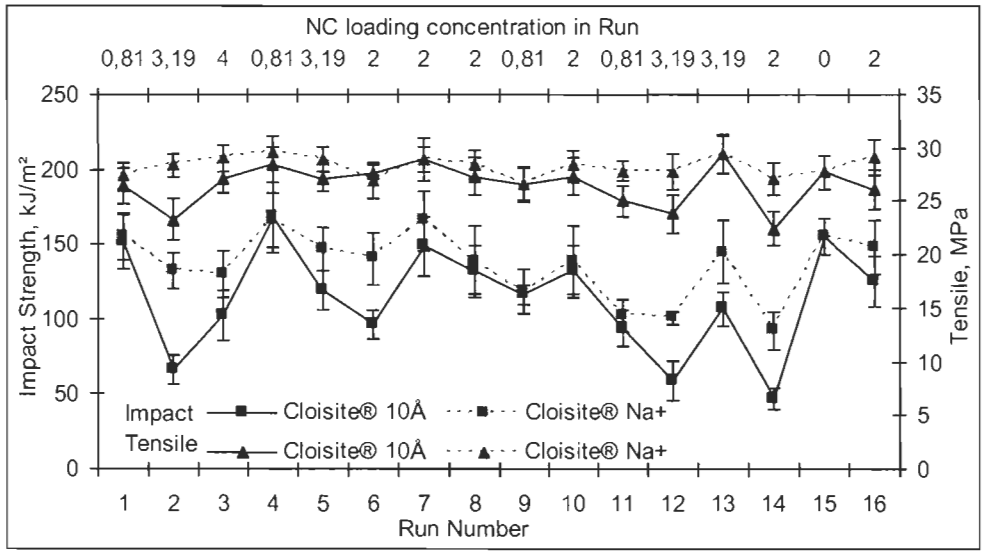

Figure 5.7 Effects of NC kind on impact and tensile of PE-Aspen composite

Although interaction between the modified clays and the matrix increase due to its weaker polarity and having larger basal spacing leading to more number of the matrix polymer chains enter into the gallery-gap and reside in a restrained form. But considering aspen fiber is anionic and easier to be dispersed than inorganic nanofiller, the stronger cationic Cloisite® Na^+ is dispersed better than Cloisite® 10A due to stronger polymer/monomer hydrophobicity and surface hydrophobicity [396].

Similar results were observed by Maiti *et al.* [397]. Thus the matrix polymer chains enter easily into the smaller gallery-gap of Cloisite® Na^+ and break the layered structures of the clays to form exfoliated structures because the exfoliation formations Cloisite® Na^+ is achieved easier than Cloisite® 10A due to its stronger function with fiber for their cations as well as its higher density but smaller particle sizes. As a result, PE-Aspen composite with natural clay will be more favorable than that of the modified one. Mechanical properties depend on the number of filler particles and on the filler-matrix interaction. Hence, the smaller particles disperse in the matrix and reflect in the mechanical properties.

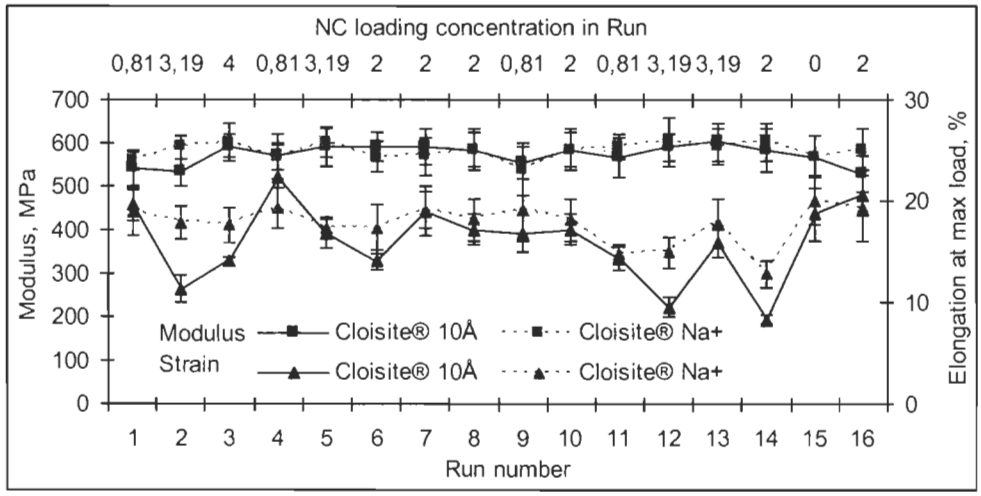

Figure 5.8 Effect of NC kinds on modulus and elongation of PE-Aspen composite

Although the unmodified clay could contribute to the increase of modulus due to better polymer-filler interaction and filler dispersion in the matrix [397], the modulus in the experiment was not improved in Figure 5.8 because the main contribution to the modulus came from the wood fiber as stated above. Meanwhile the plasticity of hybrid composite filled with Cloisite® Na+ is enhanced resulting in superior extension to absorb more force leading to better toughness than modified clay shown in Figure 5.9.

The above-described results indicate that the unmodified clay, that is Cloisite® Na^+, provides better mechanical properties in hybrid composite than the modified clay which is accordance with the results of Fluoroelastomer/Clay Nanocomposite reported by Maiti *et al.* [397] due to the effect of hydrophilicity of wood fiber and the matrix modified by coupling agent as well as initiator. The distribution of inorganic

nanofiller along the alignment of wood fiber in the matrix polymer is also expected due to the opposite polarities resulting in attracting each other. Whatever, Cloisite® Na^+ is chosen as a nanofiller in most of our experiments considering the mentioned virtues.

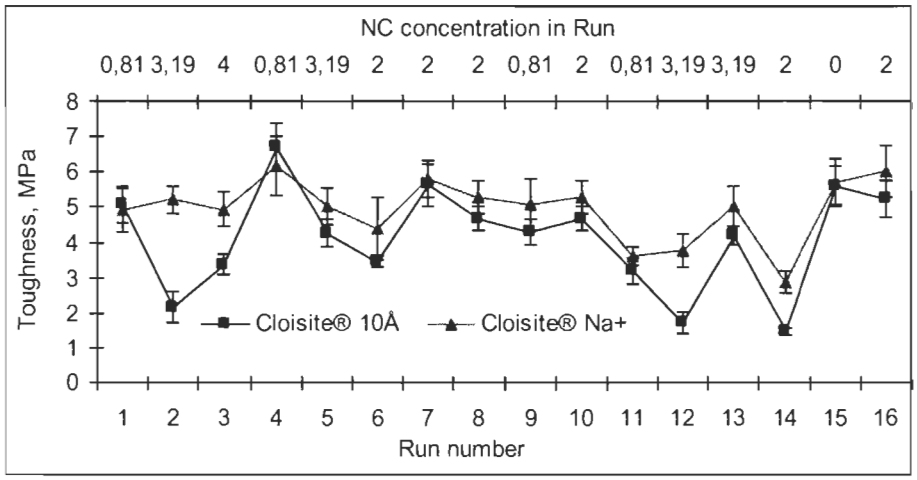

Figure 5.9 Effect of NC kinds on toughness of PE-Aspen composite

Statagraphics Centurion software is used to determinate the effects (main and interactions) which could be optimized the correlations between independent variables and dependent variables with response surface plot (not shown). After running the optimizations, the optimized compositions settings are summarized in Table 5.3 that maximize the impact and tensile properties in the actual levels. The increase is defined as the increased value divided by the corresponding value of PE reinforced with 30wt% aspen fiber.

Whether filled with Cloisite® Na^+ or Cloisite® 10A, the impact and tensile of hybrid composite could be improved greatly by changing the content of coupling agent and initiator compared with the composite reinforced with fiber at the same level.

5.4 Conclusions

(1) The addition sequence of DCP at final-step is best method to achieve higher impact strength without tensile damaging for PE-Aspen composite due to the difference in the oxidation and grafting reaction time in presence of DCP.

(2) Inorganic NC enhances the tensile strength of PE composites with addition of coupling agent and initiator a bit and impairs their impact strength slightly, and shows a similar behavior of impact strength exhibiting unchanged impact

as well tensile of PE nanocomposite. In general, the strain of PE-Aspen composite decreases while increases a bit to PE nanocomposite.

(3) MAPE, e.g. G2010, is employed to enhance the interfacial adhesion between wood fiber and PE to achieve maximal compatibilities due to the similar morphologies in the presence of initiator and nanofiller. MAPE provides significant improvements on impact and tensile strength of PE-Aspen composites due to the stronger adhesion and sufficient linkages between wood fiber and the matrix by coupling. It was also concluded that MAPE offer the PE-Aspen composite with increasing elongation which will weaken the resistance of deformation of the materials. However, this decrease could be filled up by introducing NC.

(4) Comparing each series of 16 runs designed by central composite design, the properties of the composites filled with Cloisite® Na^+ are superior to that filled with Cloisite®10Å at the same concentrations because of its smaller basal spacing and higher density as well as its stronger polarity to increase interaction due to the uniform dispersion alongside with fiber. Furthermore, the impact and tensile strength could be optimized by Centurion for optimum concentrations of MAPE, NC and DCP.

Table 5.3 Numerical optimization of the hybrids compared to PE incorporated of 30wt% fiber

Properties	Predicting values by CCD		Real values	
	Cloisite®10A	Cloisite®Na^+	+30wt%Aspen +3wt%MAPE	+30wt%Aspen
Impact, kJ/m²	183	181	140	30
Increase	**5**	**5**	**3.6**	---
G2010	4.1	5	---	---
DCP	0.15	0.13	---	---
NC	0	0	---	---
Tensile, MPa	30	31	30	17
Increase	**81%**	**86%**	**78%**	---
G2010	5	5	---	---
DCP	0.16	0.17	---	---
NC	4	4	---	---

5.5 Acknowledgements

The authors would like to thank the NSERC, Natural Centers of Excellence of Canada and Auto 21 for the financial support.

Chapter 6 - Optimization of Mechanical Properties of PE/Wood Composites using Central Composite Design and Deposition Formation of Nanofiller

Ruijun Gu, B.V. Kokta and Kwei-Nam Law

Some parts were presented in Proceedings of the American Society for Composites-24th Technical Conference, 15-17 September 2009, Newark, DE, USA. Paper #312
Revised full manuscript is accepted by Journal of Composite Materials

Abstract: Systematic studies on the effects of maleated PE (MAPE), initiator (DCP) and Nanofiller (NC) or Nanoblend concentrates (MB2001) on the mechanical properties of wood fiber reinforced PE composites were undertaken with the objective to obtain optimum impact strength while protecting tensile strength. A central Composite Design (CCD) was used to evaluate the relative importance of each independent factor, i.e. MAPE, NC or MB2001 and DCP, for the properties studied as a function of wood fiber content.

The deposition of NC particles on the surface of wood fibers as well as inside fiber lumen and the formations of bonds due to MAPE and/or DCP were confirmed by SEM microscopy. In addition, the differences between NC-natural and NC-concentrates were also ascertained.

6.1 Introduction

Wood plastic composites are hybrid materials that combine the performance and cost attributes of both wood and thermoplastics. Due to these particular attributes this hybrid composite material is gaining an increasing niche in the market place, particularly in North America [111, 117]. Wood fibers help reinforce the thermoplastics and replace the mineral or glass filler in thermoplastics to reduce cost, enhance appearance and improve properties [155, 398, 399, 400, 401, 402] and help environmental recycling [81, 121, 403, 404]. In recent years, the adoptions of small quantities of nanofillers in PE composites [56, 194, 315, 360, 388, 389, 390, 391, 405] are driven by the upgraded mechanical strength and stiffness of nanocomposite [323, 406, 407, 408, 409, 410, 411, 412, 413, 414, 415].

In statistics, a CCD is a powerful statistical approach to model and optimize the response of interest influenced by several independent variables [416, 417, 418] and could be applied in the field of wood plastic composite to minimize number of trials and the independent variables because of numerous independent variables including processing conditions resulting in the properties of the composites [405, 419, 420].

Microscopy was used to analyze the morphology of wood plastic composite to verify the improvement of compatibility between hydrophilic wood fiber and hydrophobic PE [59, 202, 391, 421, 422, 423, 424]

The main objective of this work was to investigate the effects of the independent factors such as MAPE, NC and DCP on the resulting composite materials as a function of wood fiber loading. The morphology of wood plastic composite filled with NC was also analysed by SEM to indicate the distribution of NC particles as well as the existence of chemical bonding in the presence of MAPE and DCP and its influence on the properties.

6.2 Experimental and materials

6.2.1 Materials

Thermoplastic: Linear low density polyethylene (LLDPE, Novacor® HI-0753-H) was supplied by Novacor chemicals Ltd. Its melting mass-flow rate is 1.0g/10min.

Wood fiber: Industrial CTMP of white birch (*Betula papyrifera* Marsh.) was employed. The wood pulp fiber was air-dried and ground at our laboratory to produce fine particles. Particles that passed through a 20-mesh but retained on a 60-mesh screen were employed in this study.

Coupling agent: MAPE (G2010) was supplied by Eastman chemical company (Kingsport Tenn.). Its maleic acid graft content is 1.5% and the molecular weight is 15,000.

Initiator: Dicumyl peroxide (98% active DCP) with its halftime is 1min at 171°C, supplied by Sigma Chemical Co. was used as an initiator.

Nanofiller: NC-natural (Cloisite® Na^+) was received from Southern Clay Products Inc. The typical physical properties are: moisture content 4-9%; density 2.86 g/cm^3; particle size (v) 10% <2μm, 50% <6μm, 90% <13μm; d_{001} X-ray 11.7 Å. NC-concentrates (MB2001) received from PolyOne Corporation was used as Nanoblend concentrate based low density PE with 38-42% natural montmorillonite in exfoliated distribution. Its specific gravity is 1.10.

6.2.2 Experimental design

A central composite design (CCD): 2^3 + star design was used to study the three experimental factors (Nanofiller, Coupling agent-MAPE and DCP) in 16 experiments with one single block indicated in Figure 6.1. The actual and coded factor levels were set on the basis of certain limits as indicated in Table 6.1.

Table 6.1 Coded factor levels corresponding to actual factor levels in experiments

Coded factor levels / Actual factor levels	-1.682	-1	0	+1	+1.682
†Nanofiller, wt%	0(0)‡	0.81(2)	2(5)	3.19(8)	4(10)
G2010, wt%	0	1.01	2.5	3.99	5
DCP, wt%	0	0.041	0.1	0.16	0.2

† Cloisite® Na^+ or MB2001; ‡ Figures in brackets are wt% forMB2001

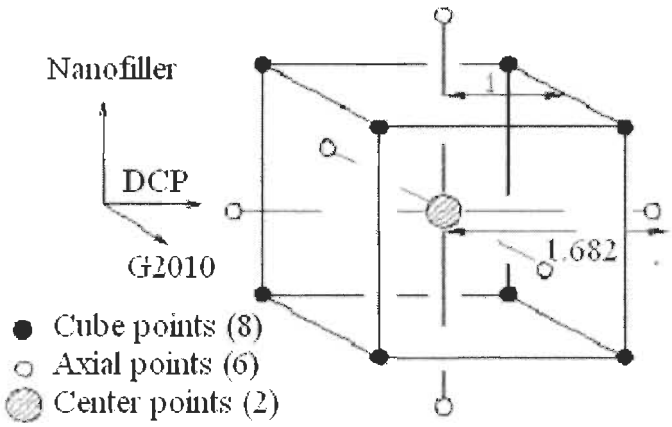

Figure 6.1 Schematic of a Central composite design for 3 factors

The CCD consisting 16 runs for 3 factors in coded units as shown in Table 6.2 which generated by Statgraphic Centurion® software. Wood fibers were added to each single block at 10, 20 or 30% (wt). The order of the experiments was randomized.

Table 6.2 CCD for three experimental factors

Run No.	†Block	‡Nanofiller	G2010	DCP
1	1	-1	1	-1
2	1	1	-1	1
3	1	1.682	0	0
4	1	-1	1	1
5	1	1	1	-1
6	1	0	0	-1.682
7	1	0	1.682	0
8	1	0	0	0
9	1	-1	-1	1
10	1	0	0	0
11	1	-1	-1	-1
12	1	1	-1	-1
13	1	1	1	1
14	1	0	-1.682	0
15	1	-1.682	0	0
16	1	0	0	1.682

† Birch fiber incorporation rate for each series of 16 runs: 10, 20 and 30wt%.
‡ Incorporating NC (Cloisite® Na^+) or Concentrates (MB2001) respectively.

6.2.3 Compounding

All samples were compounded in a two-roll Brabender as illustrated in Schedule 6.1.

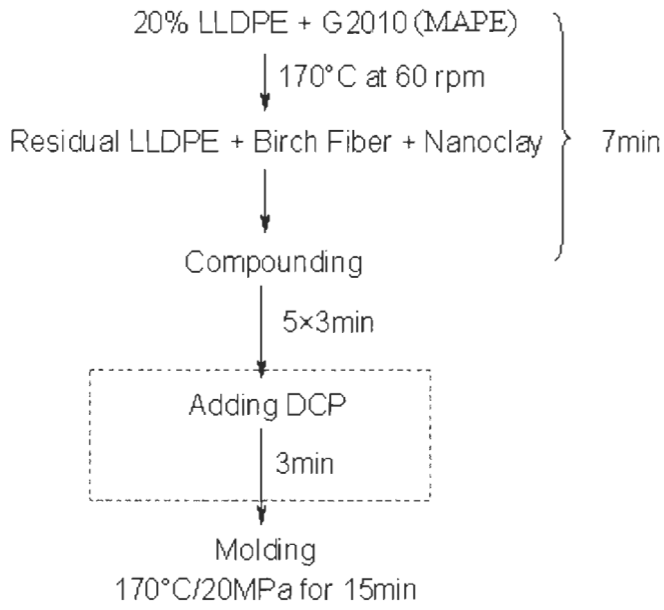

Schedule 6.1 Compounding and molding conditions

6.2.4 Compression molding

The composite strips were pressed into a dog-bone shaped mould (ASTM D638 Type V for tensile and ISO 8256 Type II for impact testing). A total of 22 specimens (10 for tensile testing and 12 for impact testing) were simultaneously prepared in the same mould. The mould was maintained at 170±2°C by means of a Dake Press and held for 15min under a pressure of 20MPa. After the high pressure stage, the mould was cooled below 60°C by circulating cold water in the platens. The approximate dimensions of specimens for tensile test were 0.30-0.315 cm wide and 0.27-0.30 cm thick, whereas those of impact test specimen were 0.27-0.29 cm wide and 0.14-0.16 cm thick. All the specimens were polished, then equilibrated overnight in a testing room, and then the width and the thickness were measured with a micrometer.

6.2.5 Mechanical tests

The tensile tests were performed using an Instron machine (Model 4201) at 23°C and 50% relative humidity according to ASTM D638 while the impact tests were performed by means of a TMI impact tester (TMI No 43-01) at ambient temperature (~23°C) following the ISO 8256 method.

6.2.6 Scanning electron microscopy

Samples were cut (with a saw) perpendicular to their thickness. From those cut surfaces, material was cut off using further cutting at the liquid nitrogen temperature with a glass knife whose angle was 90° (Cryogenic scratching). Surfaces obtained that way were mounted on a substrate (cutting to a proper size, fixing onto a microscope stub), surface-coated with platinum (4nm in thickness), and observed with a scanning electron microscope (JSM 6400, JEOL, Japan).

6.2.7 Transmission electron microscopy

Nanocomposite samples were characterized by transmission electron microscopy (TEM). All nanocomposites samples were treated as follows: 50nm ultrathin sections were prepared at cryo-conditions (ultramicrotome Ultracut UCT, Leica; diamond knife; sample temperature -85°C, knife temperature -50°C), transferred to a microscopic grid, covered with thin carbon layer and observed in a TEM microscope (Tecnai G2 Spirit Twin 12) at 120 kV using standard bright field imaging. Final micrographs showed light polymer matrix with characteristic cross-sections of wood fibers and dark nanoclay agglomerates and/or single sheets.

6.3 Results and Discussions

6.3.1 The morphological changes of NC particles in PE nanocomposites

The changes in morphology of NC particles in polymeric nanocomposite are shown in Figure 6.2. Due to poor compatibility between hydrophilic NC particles in hydrophobic matrices, NC particles are not wettable by polymer without hydrophilic components introduced (see Figure 6.2a). With incorporation of G2010 and DCP, the polarity of the system changes from hydrophobic to hydrophilic. Therefore, the proper exfoliated plaque is obtained easily by improving compatibility between NC particles and the matrices in concentrates resulting from the pre-exfoliated dispersion of NC particles. Polymeric nanocomposites reinforced with NC-concentrates exhibits one phase due to NC particles in concentrates packaged with hydrophilic polymer (Figure 6.2b-b') and it is difficult to distinguish the particles because of nanosized dispersion. However, though, NC-natural is difficult to be dispersed into nanosize even incorporating of G2010 and DCP, lots of clay craters formed by NC-natural particles interacting strongly with the matrix during fracturing which is verified by the inserted image in Figure 6.2c' while dispersed in

microsize, even nanosize (see Figure 6.2c). Polymeric nanocomposites employed NC-natural are also similar in gray color and there are strong interactions between NC-natural particles and the matrix and the color of the nanocomposites exhibits gray color in the presence of hydrophilic polymer created by incorporating of MAPE and DCP.

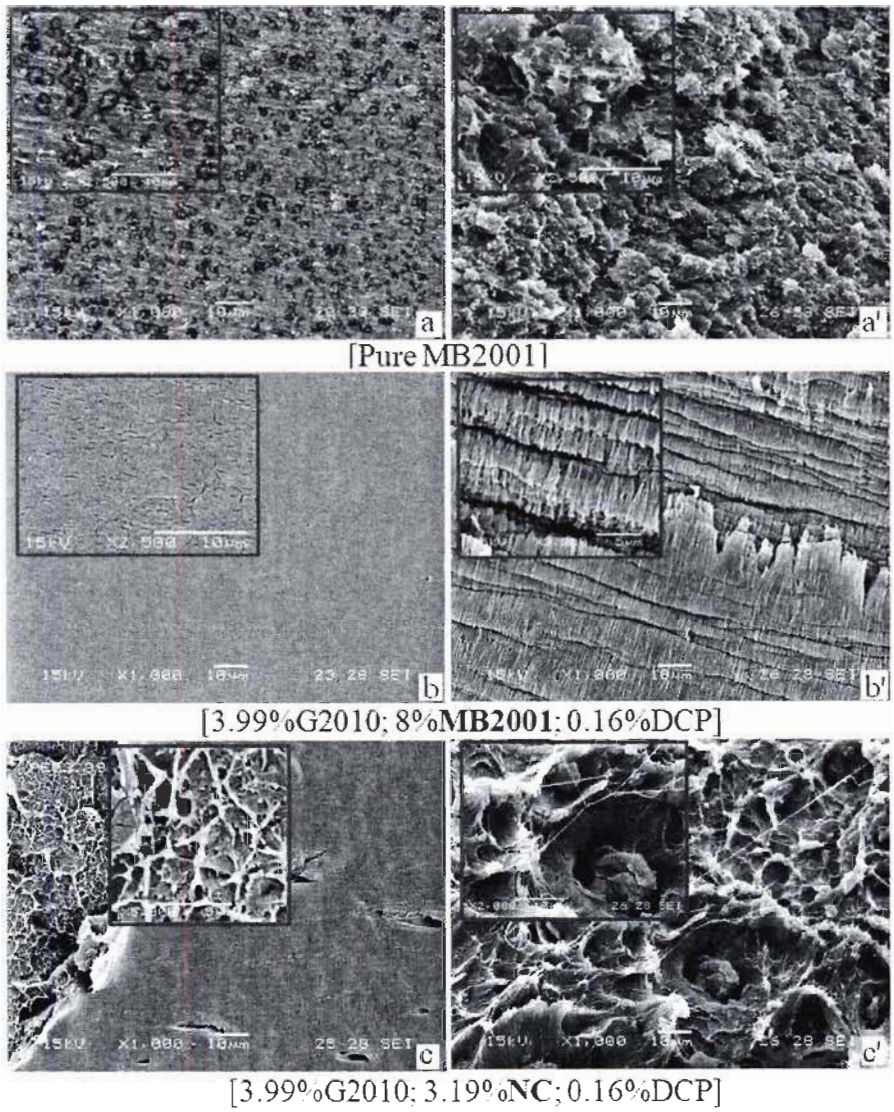

Figure 6.2 Cross (left) and fracture (right) sectional SEM images of the changes in morphology of NC-natural and NC-concentrates particles in the polymeric nanocomposite

So, it is concluded that NC-concentrates makes PE nanocomposites with MAPE and DCP present formed proper plaque easily because the most NC-concentrates particles are in nanomer level, but with weaker interactions while NC-natural leads to the nanocomposites with stronger interactions (rough

fractured surface meaning strong interactions), but less in nanomer level, and more still in microsize. It was known that NC-concentrates (pure MB2001) have exfoliated distribution (Figure 6.3a), where NC-concentrates could achieve an exfoliated distribution more easily than NC-natural (Figure 6.3b), which was intercalated distribution, even in exfoliated distribution as may be shown in Figure 6.3c in the compatibilized polymeric nanocomposites as coupling agent and initiator combined with it. However, as wood fibers are employed, the distribution of NC particles would be improved due to the influences of the polarity of wood fiber resulting in an exfoliated distribution as illustrated in Figure 6.3d, which indicates that NC-concentrates could achieve exfoliated dispersion as wood fiber employed with the presence of coupling agent and cross-linking agent as well as NC-natural.

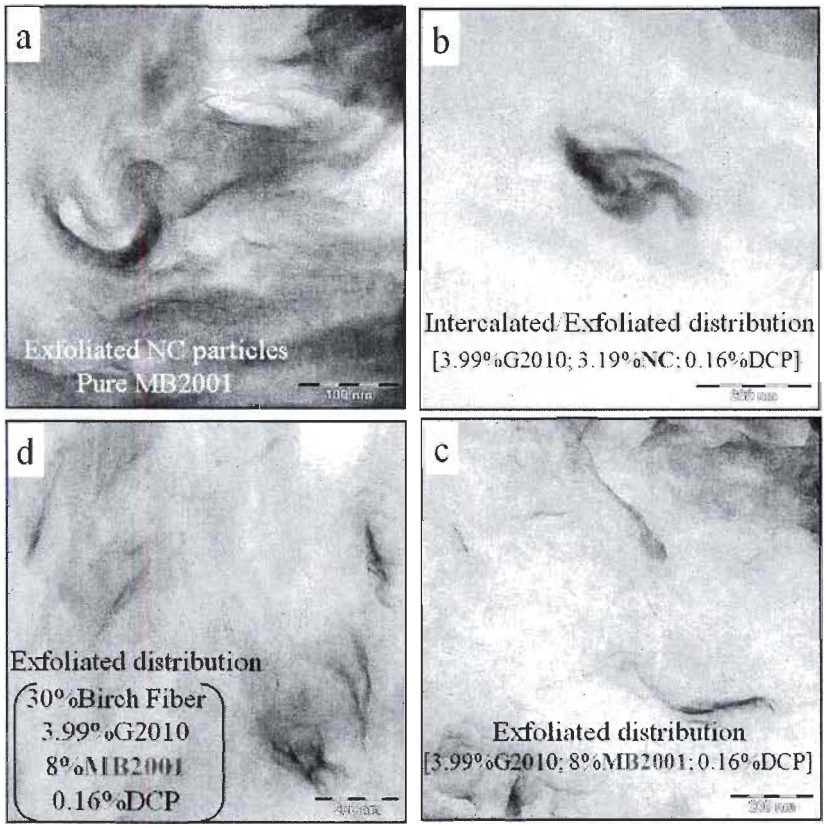

Figure 6.3 TEM images of the formation of NC-natural and NC-concentrates particles in polymeric nanocomposites and wood composite

6.3.2 Effects of birch fiber loading on the mechanical properties of PE composites via CCD

The incorporation of birch fibers had greatly improved the impact and tensile strength as illustrated in Figure 6.4. The improvement was particularly significant at 30% fiber loading. High impact strength could be obtained in the runs (7, 4, 13) containing high percent MAPE which ranged from 3.99wt% (+1) to 5wt% (+1.682) with moderate amount of DCP (0 and +1) or in the runs (16, 4, 13) containing high DCP which ranged 0.16wt% (+1) to 0.2wt% (+1.682) with moderate amount of MAPE (0 and +1) respectively. In these cases MAPE and DCP improve the compatibility between the matrix polymer and wood fiber, more wood fibers are employed in the matrix resulting in more stress or force transferred effectively from the matrix onto the surface of wood fiber by esterfication networks [59] with more wood fibers introduced.

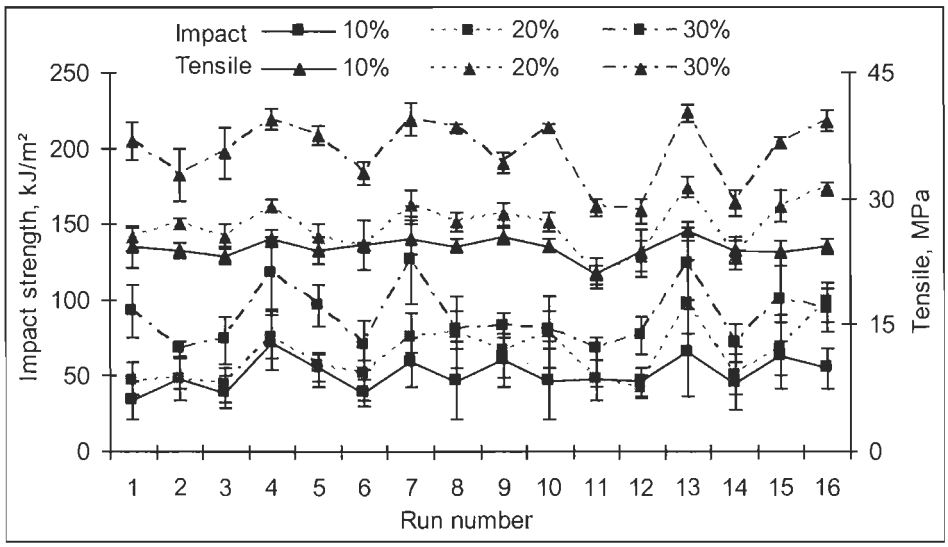

Figure 6.4 Effects of wood fiber loading on impact and tensile of PE composite

The result is verified by microscopy of run 13 (Figure 6.5a) which displays amounts of chemical bonding formed as high percent wood fiber is introduced in the presence of MAPE and/or DCP. Regardless of the amounts of wood fiber, less chemical bonding were formed as a result of low level of MAPE or DCP added as shown in Figure 6.5b which is similar to the studies of Yuan and coworkers [202]. In the presence of high level of MAPE and/or DCP, an excess of MAPE would cover the surface of wood fiber and cause agglomerating among nonpolar hydrophobic matrix resulting from relative polarity difference and thus not entanglement with polymer matrix which leads to slippage [92, 316]. These behaviors are displayed in Figure

6.5c-d and results in the composite with less matrix-MAPE-fiber networks formed leading to the decrease of impact and tensile strength.

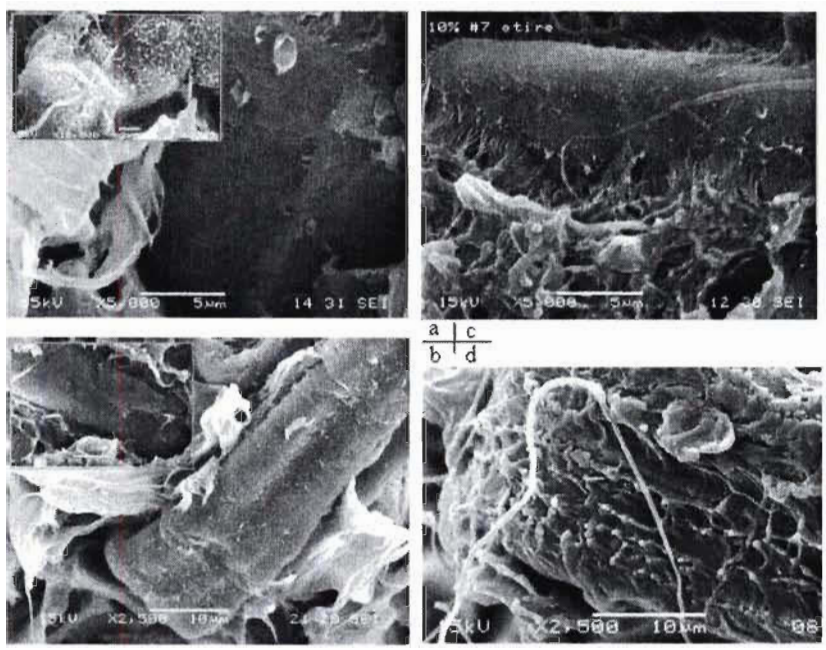

Figure 6.5 Imaging of bonding formation with SEM

a-Run 13 composite (30%Birch; 3.99%G2010;3.19%NC; 0.16%DCP);
b-Run 1 composite (30%Birch; 0.81%G2010;3.19%NC; 0.041%DCP);
c-Run 7 composite (10%Birch; 5%G2010; 2%NC; 0.1%DCP);
d-Run 13 composite (10%Birch; 3.99%G2010;3.19%NC; 0.16%DCP).

The relationship between impact/tensile strength and the significant main factors and their interactions could be better understood by examining the effects generated according to the prediction of the tested values of impact and tensile strength as shown in Figure 6.6 and Figure 6.7. Figure 6.6 and Figure 6.7 reveal that the influence of MAPE and DCP are the most significant. Figure 6.6 shows that impact strength increases with the content of G2010 and/or DCP regardless of the concentration of wood fiber. However G2010 had a little effect at lower fiber loading, but its effect becomes larger at higher fiber loading with different trends of the curves due to more fibers being involved into coupling reactions. NC improves impact strength at low content and then deteriorates at higher content with higher fiber loading acting as the orthogonal block.

The presence of NC-natural had negative effect on impact strength at low wood fiber amount while it showed inverse effects with higher amount of wood fiber. At high amount of wood fibers, NC particles would preferably deposit on the surface of wood fibers (see Figure 6.8b) and even enter the wood lumen [425] (see

Figure 6.8a) exhibiting no significant effect on the impact and tensile strength as indicated in Figure 6.6-Figure 6.7.

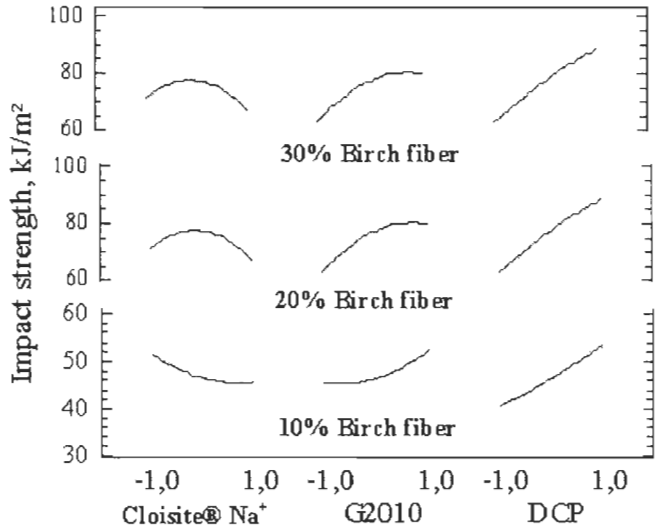

Figure 6.6 G2010, DCP and Cloisite® Na^+ dependences plots for Impact strength of PE composites on birch fiber loading

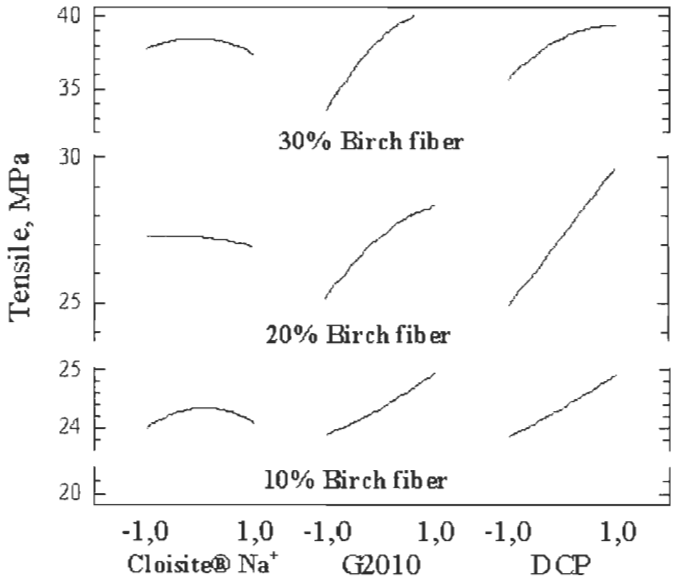

Figure 6.7 G2010, DCP and Cloisite® Na^+ dependences plots for Tensile strength of PE composites on birch fiber loading

Moreover, Figure 6.6-Figure 6.7 also indicates that high fiber loading could result in superior impact and tensile strength which concords with the conclusion in Figure 6.4. The influences of each independent variable were in an agreement with our previous results [405].

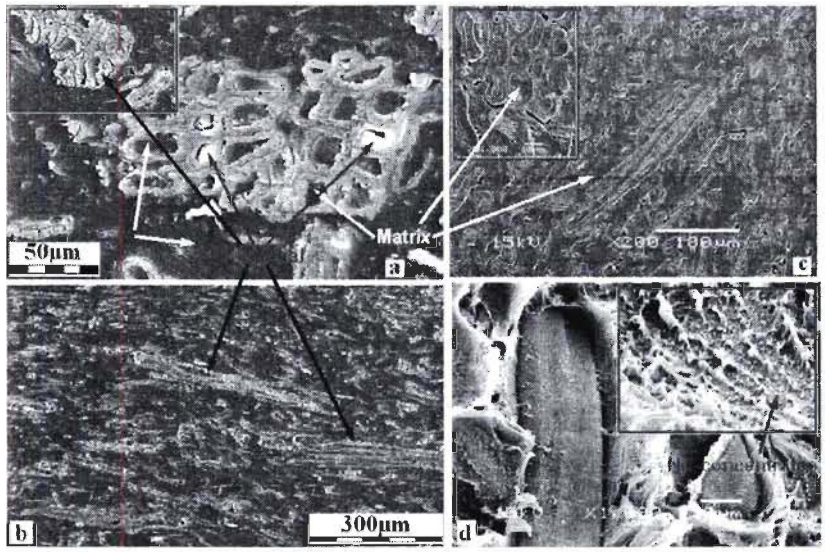

Figure 6.8 SEM images of NC particles distributed in PE composites

a, b-Cross and surface sectional SEM images of PE composite filled with NC-natural (Run 13: 30%Birch; 3.99%G2010; 3.19%NC; 0.16%DCP);
c, d- Cross | surface and fracture sectional SEM images of PE composite filled with NC-concentrates (Run 13: 30%Birch; 3.99%G2010; 8%MB2001; 0.16%DCP)

The improvement in modulus by the addition of wood fiber is remarkably evident as revealed in Figure 6.9. The effect of 30% addition of wood fiber is particularly pronounced in all experimental trials due to high MOR of wood fiber distributed uniformly in the matrix polymer with the presence of the compatibilizers [202]. Moreover, the increase of modulus results in forming the high bulk crystallization and transcrystalline due to the nucleation of NC as well as the acceleration of thermal oxidation of fiber and the matrix polymer due to the presence of DCP. Furthermore, the crystallites are very likely produced by changing the crystal morphology of the matrix polymer coating on the surface of wood fiber [376].

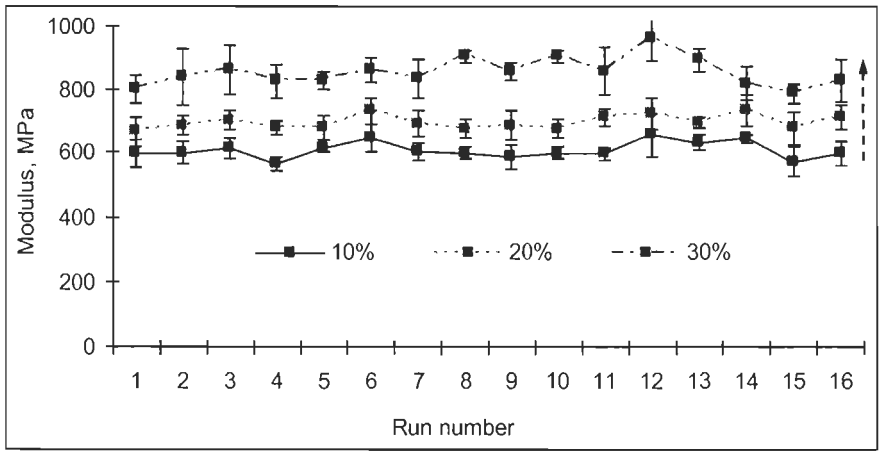

Figure 6.9 Effects of wood fiber loading on the modulus of PE composite

Although NC, G2010 and DCP had effects on the modulus, the improvement of modulus was principally originated from the attribution of the morphology of wood fiber, i.e. highly MOR, and the changes of the crystal morphology [376] by comparing with the increased modulus following the increase of wood fiber from 10phr to 30phr leading to the different level of the range of modulus described in Figure 6.10. Meanwhile, the trends of the curves in Figure 6.10 also indicate the main effect or interactions of G2010 and DCP are affected by the fiber loading level.

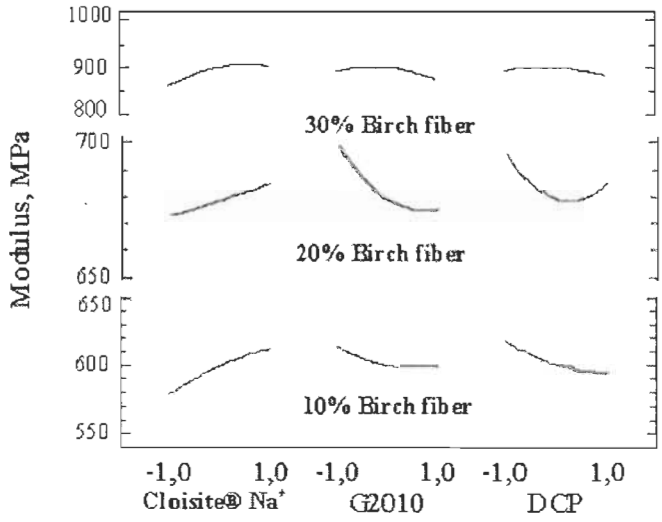

Figure 6.10 G2010, DCP and Cloisite® Na^+ dependences plots for Modulus of PE composites on birch fiber loading

The numerical optimization performed by Statgraphics Centurion is used to identify the optimal compositions which maximize certain properties of PE composites .In this computerized optimization method, optimization criteria for all variables are set according to the above-exploratory studies. Optimal values of some properties and the optimal compositions are predicted by the software as summarized in Table 6.3 through converting the coded factor levels to actual factor levels in experiments. The increase is defined as the increase value divided by the corresponding value of virgin PE.

After running the optimizations, the best set of experimental compositions that maximize the properties of PE composites are identified in Table 6.3. The results clearly suggests that PE composite with the improved impact could be achieved with the high fiber content in the presence of the compatibilizers, i.e. up 28.9% at 30phr fiber loading. When the content of fiber is at the lower level, the improvement of impact by the compatilizers could not counteract the impairment due to the

incompatibility and the stiffness of fiber resulting from lack of chemical bonding (Figure 6.5b). The tensile strength could be improved largely with the introduction of wood fiber from 5.3% to 62.7%. The described results are as expected because of the dependence of wood fiber on the amount of stress and force dispersing and transferring among the reinforced matrix polymer due to good compatibility and strong adhesion between wood fiber and the matrix polymer by coupling and crosslinking reactions. Similarly, the modulus could also be improved due to the stiffness of fiber and its high modulus of rupture (MOR) and modulus of elasticity (MOE).

Table 6.3 Optimized properties of PE composites compared to virgin PE

Composites		Optimum properties		Optimal actual factor setting and solutions, wt%			
		Value	Increase	G2010	DCP	NC-natural	NC-concentrates
		Impact strength, kJ/m²					
Virgin PE		134.2	--	--	--	--	--
PE+30%fiber		43.2	-67.8%	--	--	--	--
CCD	10% fiber	93.4	-30.4%	5	0.184	0	--
	20% fiber	109.8	-18.2%	5	0.2	2.69	--
	30% fiber	173	28.9%	5	0.2	0	--
		94.7	-29.4%	5	0.175	--	0
		Tensile, MPa					
Virgin PE		25.1	--	--	--	--	--
PE+30%fiber		21.8	-13%	--	--	--	--
CCD	10% fiber	26.4	5.3%	4.99	0.2	0.69	--
	20% fiber	32.2	28.4%	4.1	0.2	0.97	--
	30% fiber	40.8	62.7%	3.99	0.141	2.10	--
		33.4	33.1%	5	0.2	--	0.005
		Modulus, MPa					
Virgin PE		568	--	--	--	--	--
PE+30%fiber		697	22.8%	--	--	--	--
CCD	10% fiber	698	21.4%	0	0	3.89	--
	20% fiber	804	41.6%	0	0	3.88	--
	30% fiber	926	63.1%	0.51	0	2.99	--
		829	46%	0.51	0	--	2.99

A regression analysis is carried out to obtain the best-fit model to the optimal data. The regression analysis of the optimization suggests the relationship between the properties, i.e. impact, tensile and modulus, of PE composites and the block in Figure 6.11 to Figure 6.13 setting the dependent variables at optimal conditions.

The optimal impact, tensile and modulus can be expressed by Equation 1-3 in terms of the birch fiber content (%). The wood fiber content of the lowest impact strength is drawn at 15% which best fits with the curves in Figure 6.11. At less than 15% fiber

loading, wood fiber had negative effect on the impact strength. The composites could achieve superior impact strength with more 25wt% fiber employed compared to that of pure PE matrix. The increasing trend becomes larger following the introduction of wood fibers because of the amount of fibers involved in transferring the stress in the whole matrix.

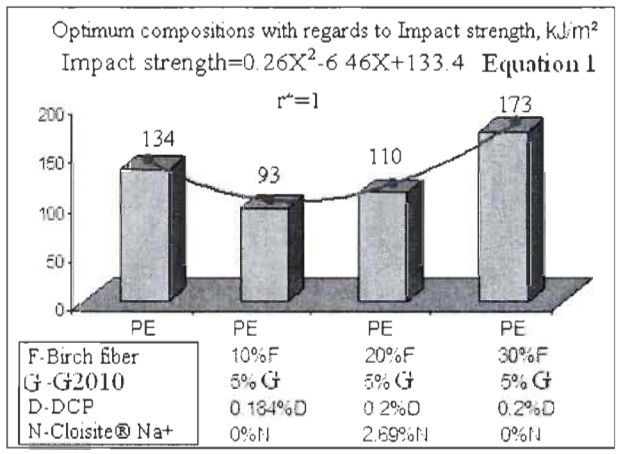

Figure 6.11 Relationships between optimal impact and wood fiber loading

The relationship between the tensile and the amount of fiber is described in Equation 2. The value of tensile of virgin PE could be obtained at 5wt% wood fiber content according to Equation 2. With the presence of the compatibilizers, wood fiber has negative effect on tensile in the range 0-5% and has positive higher than 5% as shown in Figure 6.12. Therefore, wood fiber has large effects on the mechanical properties of PE composite designed by CCD. Considering the improvement of impact and tensile, the loading of wood fibers should be higher than 25% with the optimal composition of additives as indicated in Table 6.3. Generally, PE composite reinforced with 30wt% of fibers is used widely in our experiments.

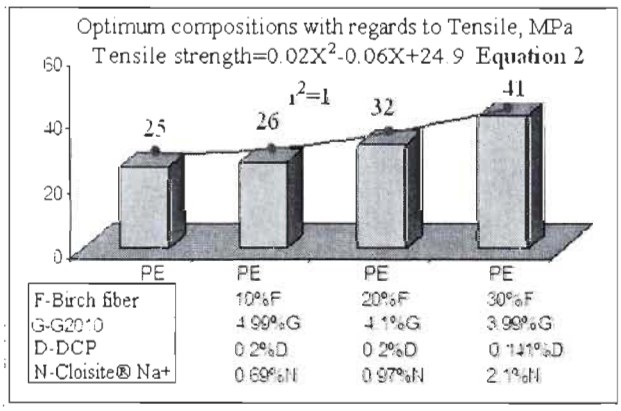

Figure 6.12 Relationships between optimal tensile and wood fiber loading

Similarly, the modulus of PE composite reinforced with wood fiber strongly depends on the level of the block as described in Equation 3 and curves in Figure 6.13. Equation 3 indicates that the effect of the block with different fiber loading is positive implying that the modulus is improved with the increase of wood fiber. This result is in an agreement with the work reported by A. Karmarkar *et al.* [84].

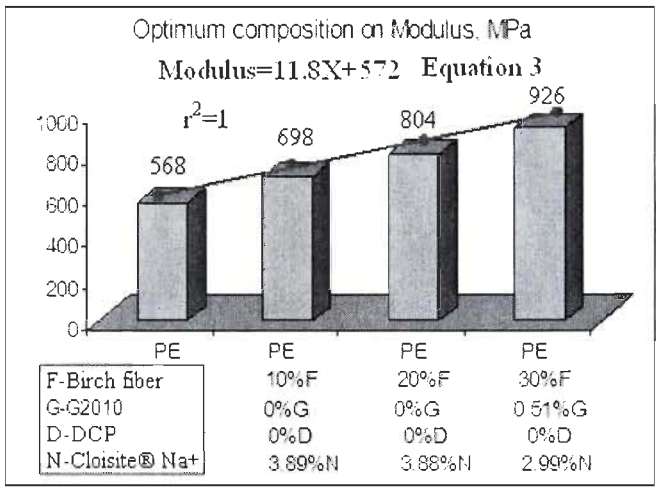

Figure 6.13 Relationships between optimal modulus and wood fiber loading

6.3.3 Effects of NC-natural and NC-concentrates on the mechanical properties of PE composites reinforced with 30wt% birch fiber using CCD

Although the actual levels of MB2001 (NC-concentrates) ranged in 0-10wt%, the actual content of natural montmorillonite involved in the experiments are similar to inorganic NC because MB2001 was already exfoliated natural NC in low density polyethylene which ranged 38% to 42% while Cloisite® Na^+ is a pure natural montmorillonite.

The composites filled with Cloisite® Na^+ (NC- natural) have superior impact and tensile strength compared to the composites prepared with MB2001 in each run shown in Figure 6.14 because Cloisite® Na^+ deposits on wood fiber during the changes of NC particles from microsize into nanosize because of its stronger cation content (Figure 6.8b) while less NC-concentrates particles attaches on the fiber surface and more NC-concentrates particles stay in the matrix as indicated in Figure 6.8c-d due to the weaker interactions between MB2001 and the matrix with exfoliated dispersion as compared to the microscopic images of PE composites filled with NC-natural in Figure 6.8a-b. It is also concluded that there are no NC-concentrates particles located in wood fiber lumen because of the surface chemistry and surface energy of NC-concentrates particles which has changed from hydrophylic to hydrophobic through

compounding process which prohibits the hydrophobic pre-exfoliated NC-concentrates particles from entering fiber lumen by pores or holes as shown in the inserted images of Figure 6.8c. Conversely, most NC-concentrates particles are present in the matrix as seen from the inserted image in Figure 6.8d.

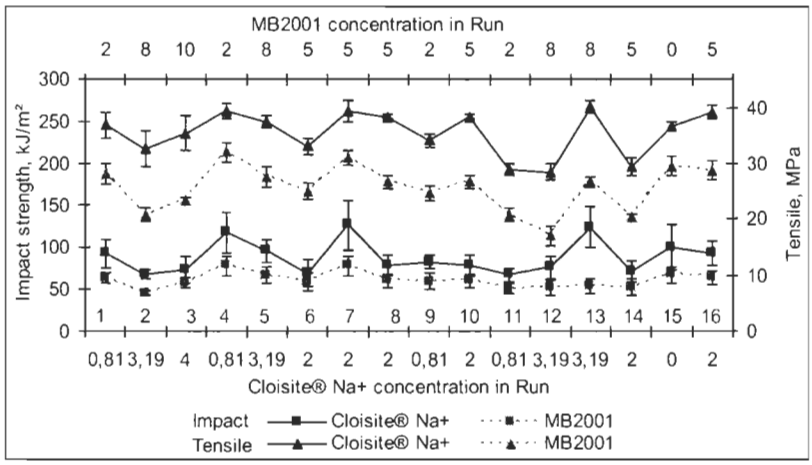

Figure 6.14 Effects of nanofiller type on impact and tensile of PE composite

SEM images in Figure 6.8 show that NC-natural is changed from microsize into nanosize by reactive processing which also adheres to the surface wood fibers and even enters into fiber lumens by driving force. In addition, the positive effect of NC-natural is observed in the case of impact strength (Figure 6.14) and Modulus (Figure 6.15). Moreover, the NC-natural particles would not prohibit the movements of molecule chains due to most of them depositing on wood fiber leading to higher elongation while having higher modulus.

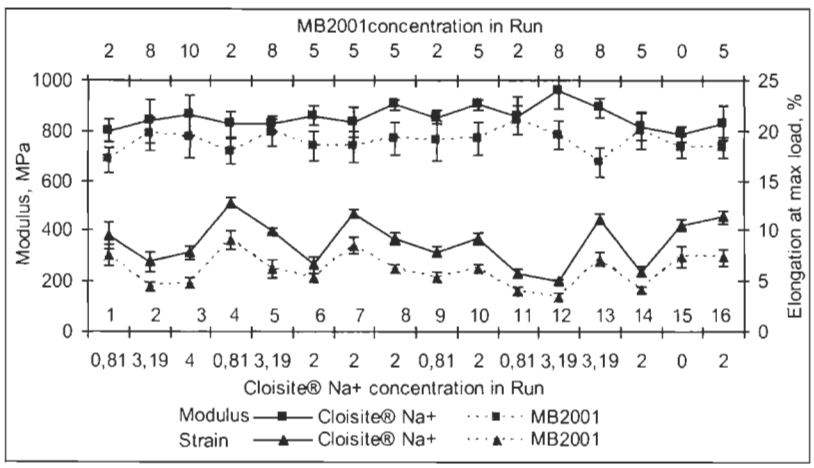

Figure 6.15 Effects of nanofiller type on modulus and elongation of PE composite

Although it is easier to obtain the proper exfoliated plaque using MB2001, the interactions between the NC-concentrates particles and G2010, DCP even wood fiber would be less effective because the NC-concentrates particles were already in the state of an exfoliated dispersion and it was difficult to release the interacted particles and re-joint with polarized molecule through replacing the former matrices during current compounding processing.

It should be noted that NC-concentrates will produce porous/fibrous structure as figured out in Figure 6.16a while NC-natural will not cause this happening (see Figure 6.16b). Obviously that porous morphology could cause the wood composites relative low strength due to weakened adhesion as indicated in Figure 6.16(a-2) which could be enlarged by the inserted images of Figure 6.16(a-3) and (a-4). The low modulus is reasonable due to these fibrous structures.

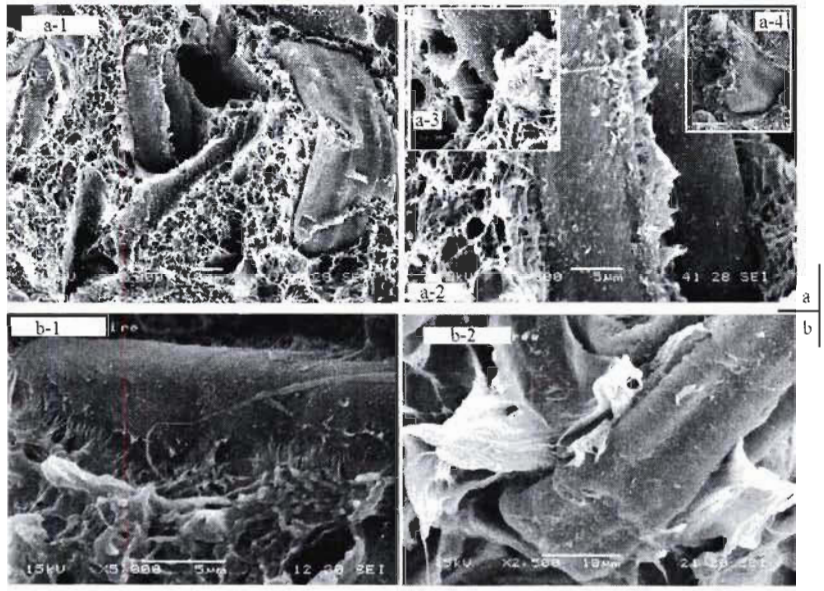

Figure 6.16 Fracture images of wood composites reinforced with NC in different morphology

a:Wood composites reinforced with NC-Concentrates
b:Wood composites reinforced with NC-Natural

Main effects of impact strength of PE composite on G2010, DCP and MB2001 are shown in Figure 6.17. The effect plot of MB2001 declines successively. The influence of G2010 has not changed significantly either NC-natural or NC-concentrates presented due to the polarity and alkalinity of the NC having no obviously influence on the interaction of G2010. The ranged values of the composites filled with NC-concentrates (Figure 6.17) are inferior to the composites

filled with NC-natural (Figure 6.5) resulting from low interactions caused by NC which is verified by the distribution of NC particles in Figure 6.8.

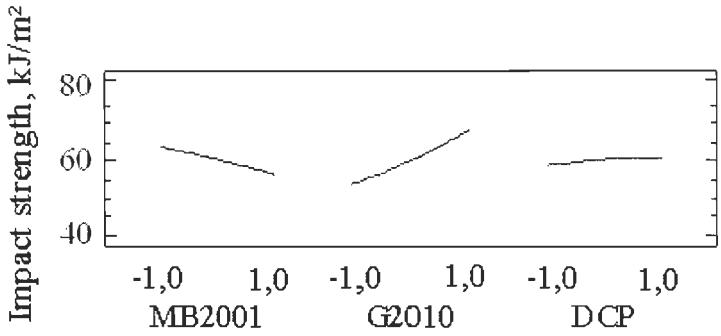

Figure 6.17 G2010, DCP and MB2001 dependences plots for Impact strength of PE composites incorporating of 30phr birch fiber

Similarly, MB2001 has negative effects on the tensile strength while there are no changes to G2010 and DCP (see Figure 6.18) comparing to the effect plots with Cloisite® Na^+ in Figure 6.7.

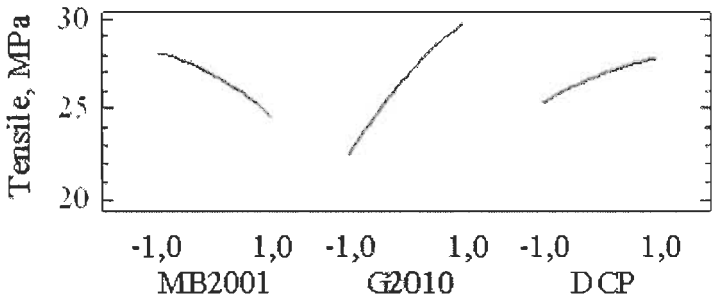

Figure 6.18 G2010, DCP and MB2001 dependences plots for Tensile of PE composites incorporating of 30phr birch fiber

It is also expected that G2010 prefers to react with the hydroxyl groups on the surface of wood fibers. NC-natural deposits and adheres the surface of wood fiber would lead to more G2010 molecules interacting with NC-natural particles forming stronger physical networks than NC-concentrates which was indicated in polymeric nanocomposites without fiber presented (Figure 6.2c'). Moreover, poor interaction leads to the modulus slight decline as shown in Figure 6.19. Regardless of the range of modulus, their main effects plot is similar to Cloisite® Na^+ (NC-natural). In theory, the aligning distribution of NC particles in PE composites would be changed due to the NC particles exhibiting hydrophobic not its hydrophilic characteristics. However, there were no related reports yet.

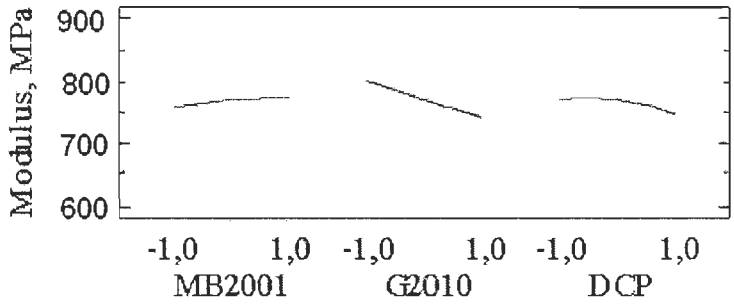

Figure 6.19 G2010, DCP and MB2001 dependences plots for Modulus of PE composites incorporating of 30phr birch fiber

Optimization of the correlations between main effects and the properties by *Statagraphics Centurion* in comparing to virgin PE and the composite with 30wt% birch fiber are presented in Table 6.3. Both impact and tensile strength of PE composites have increased when using compatibilizers due to the improvement of the interfacial adhesion and the interactions between wood fibers and the matrix which was helping the transmission of the impact force through the composite [87, 113, 114, 116] leading to improved tensile and modulus [420].

However, generally improved interfacial adhesion is also expected to decrease impact strength due to the synthetic effects between the reduction of the impact strength drastically by decreasing the elongation and forming a new stress concentration around fiber ends, and the enhancement of impact due to the fibers stopped crack propagation rate by forcing crack around fiber and bridging crack through fiber pullout [426, 427]. But the unnotched Izod impact strength of the composite are found to increase in almost every case as indicated in Table 6.3, around 2-4 times with optimal modifiers at 30wt% birch fiber loading compared to PE composites without modifiers employed. This indicates that birch fiber has positive effect on impact strength of LLDPE based PE composites with the presence of compatibilizers due to the contributions of interface modifiers which improved the dispersion of the wood fiber in the matrix [428, 429]. With the introduction of the modifiers, well dispersed and coupled wood fibers formed a dampening phase to stop the crack propagation through fiber pullout, and also formed a new stress concentration by strengthening fiber ends to the matrix resulting in transferring the stress more effective and distributing the force more uniform leading to an improved impact [116]. Similarly, modulus increases with the introduction of compatibilizers due to the fiber efficiency factor of the modulus and strength increased after addition

of the compatibilizers [427]. Comparing to virgin PE, it is possible to obtain superior impact strength by employment of Cloisite® Na^+, rather than MB2001.

6.4 Conclusions

In this section, a statistical model is established to reflect the relationships between the wood fiber reinforced composites and their compositions including G2010, DCP and NC in different nature and dispersed morphology. The statistical analysis and numerical optimization results demonstrate the following preliminary conclusions:

1. The CTMP white birch plays a remarkable role in enhancing the mechanical properties of PE composites in the presence of coupling agent, DCP and NC. The loading of 30% birch fibers yields better results when compared to the lower charges. Among the three experimental factors studied MAPE and DCP have the most influencing effect on the properties of the resulting composite while the NC has relatively little significant effect.
2. Both impact and tensile of the composites filled with NC-natural are superior to those of composites prepared with NC-concentrates due to NC-natural depositing on the surface of wood fiber, and even loaded in wood lumen. The strong interactions between NC-natural and polar polymer is verified by SEM images of PE nanocomposites, that is rough surface.

6.5 Acknowledgements

The author would like to thank the NSERC, FQRNT and AUTO21 for their financial support. The author also thanks Mme Agnès Lejeune for help with the SEM images. A version of small parts of this article was presented at Polymeric Materials P2008, Halle, Germany. 24-26 September, 2008.

Chapter 7 - Mechanical Properties of PP composites Reinforced with BCTMP Aspen fiber

Ruijun Gu and Bohuslav V. Kokta
Journal of Thermoplastic Composite Materials. 2010, 23(4): 513-542.
DOI: 10.1177/0892705709355232
http://jtc.sagepub.com/content/23/4/513

Absatract: In this work we investigated the effect of incorporating wood fibers (Bleached chemi-thermo-mechanical pulp of aspen, BCTMP) on the properties of a hybrid composite material made from maleated polypropylene (MAPP) and with or without Nanoclay (NC). The effects of morphological structure of polypropylene (PP), the maleic anhydride graft (MA%) and molecular mass (Mw) of MAPP were also performed to evaluate the improvements of each independent factor (MAPP, Dicumyl peroxide-DCP and NC).

In our case, the size of wood fiber had little effect on the impact and tensile strength. High Mw and low MA% MAPP contributes homo-PP hybrids with better performance either impact or tensile. In addition, wood fiber gives the hybrids, based on both homo-polypropylene (homo-PP) and co-polypropylene (co-PP) without the presence of coupling agent, similar behaviors of impact and tensile properties. However, the impact and tensile strength of the hybrids mentioned above are improved in the presence of coupling agent. NC weakens the impact strength of composites with/without the reinforcement of wood fiber, coupling agent and DCP. It shows different behaviors of tensile property with the improvement of tensile strength for hybrids with with wood fiber, coupling agent, and DCP but is impartial to nanocomposites without additives. Moreover, the behavior of tensile property is in concordance with the changes of elongation as well as toughness. Furthermore, DCP leads to negative effects on the impact and tensile of the hybrids when fiber presents as well as toughness, but exhibits better resistance to deformation and extension which is in concordance with the increase of modulus. In addition, there is a little increase in plasticity.

Keywords: Aspen fiber, BCTMP, MAPP, Polypropylene, Wood fiber, Wood plastic composite

7.1 Introduction

Global ecological concern has interested in biofiber plastic composite due to their local availability and for being renewable resource [45, 95], relatively low cost [56,

97], high relative strength [45], stiffness [98, 99, 100], low density [100], greater thermal stability [101, 102], high biodegradability [103, 104, 105, 106] as well as excellent mechanical and physical properties [102, 107, 108]. The ultimate tensile strength of cellulose is estimated to be 17.8GPa [56] which is 7 times higher than that of steel. Intrinsically, the very high elastic modulus and tensile strength imply that cellulose possesses the potential to replace glass fiber.

The typical polyolefin materials used in wood plastic composites (WPC) is PP having a lower melting point and a wide range of melt index [109, 110]. Global polyolefins demand exceeded 115 million tons in 2007, a growth of 5.3% over 2006 and would rise to just less than 250 million tons by 2025, as a report of ChemSystems [430]. PP is a semicrystalline thermoplastic polymeric material that has been widely used because of its light and recyclable saving weight and environmentally friendly and its attractive combination of good processability, mechanical properties, and chemical resistance. However, it has inadequate stiffness and brittleness which limits its versatile application which could be improved by compounding with inorganic clay. Introducing a certain content of NC could improve impact strength and toughness in higher temperature range resulting in the primary mechanism of plastic deformation by crazing and vein-type changing to microvoid-coalescence fibrillation process while increasing its modulus [431, 432]. The improvement in yield strength is due to stronger interfacial interaction between the clay platelets and the matrix and the improvement in modulus is attributed to effective load transfer between the matrix and the exfoliated clay platelets [17]. But there was a converse result on impact strength reported by Dong [433] that the impact strength is reduced due to the clay aggregation.

WPCs are widely used in many industries such as the aircraft, automobile, construction, and electronic industries [99]. Wood PP composites are found mainly in automotive and consumer products which is light and easily recyclable to save weight and environmentally friendly. Global demand for PP will grow for 6.9% a year until 2010 while North America will exhibits consumption growth rate of 4.5% according to the market research repot by Merchant Research & Consulting Ltd. As a biodegradable and natural resource, compounding with wood fiber could contribute to high utilization of WPC in the automotive industry by improving the adhesion between the fibers and the matrix [434].

Wood fiber is a hydrophilic porous composite of cellulose, lignin and hemicellulose polymers that are rich in functional groups, such as hydroxyls, and has a critical surface energy in the 40-60 mJ/m^2 range [435] leading commonly proposed adhesion mechanisms on wood substrates by mechanical interlocking, adsorption theory and chemical bonding. However, PP having very low surface energy owing to its hydrophobic nature lacks the suitable adhesion to the aluminosilicate surface of the NC and the hydrophilic wood fiber [436]. Thereby, adding a small amount of coupling agent or initiator may further complicate the adhesion properties of WPC as they are low molecular weight, mobile compounds which may migrate to the surface, improving the interfacial adhesion, and helping in making the synthesis of well exfoliated PP nanocomposites reinforced with wood fiber incorporating NC. But PP hybrids are still found to be highly hydrophobic, low surface energy material similar to polyolefins albeit having a high level of heterogeneity even with the presence of MAPP [79].

Wood fiber is well known not to melt, but shows thermal degradation at high temperature. However, the thermal degradation can occur during the melting compounding and molding process if the processing temperature reaches 200°C [437]. The mass loss steps of natural fibers occur under 200°C due to the loss of moisture and then decomposition of fibers from 200°C which is confirmed by Kim and coworkers [438, 439]. Although the mass loss steps of pure PP occurs very slowly under 500°C showing superior thermal stability to wood fiber [438], the thermal degradation of wood fiber should be considered in the processing [440], especially in the presence of initiator, that is dicumyl peroxide to degrade PP matrix [356, 357] and wood fiber [353]. Nanoclay gives the composite higher modulus [35, 441] as well as thermal properties [36], moisture resistance [28] and higher impact strength [378] to create a biodegradable composite materials [44].

The main objective of this work was to study the influence of wood fiber, MAPP, NC and DCP.on the mechanical properties of PP hybrids due to the changes of its morphological structures We also study the effects of wood fiber size and the use of different Mw of MAPP with different MA% as a coupling agent.

7.2 Experimental and materials

7.2.1 Materials

Thermoplastics: Two kind of PP were employed, and their molecular characteristics are summarized in Table 7.1.

Wood fiber: Industrial bleached chemi-thermo-mechanical pulp of aspen (BCTMP, Brightness 82-85% ISO) received as a pressed bale from Temcell Inc (Temiscaming division) was used. The wood pulp fibers were air-dried and grounded at our laboratory to produce fine fiber particles after soaked and loosened. Particles that passed through a 20-mesh but retained on a 60-mesh screen (20-60 mesh), passed through a 60-mesh but retained on a 80-mesh screen (60-80 mesh) and passed through a 80-mesh screen (80 + mesh) were employed in this studies.

Table 7.1 Typical properties bulletin of the matrix

Properties	Polypropylene		ASTM
	Homo-PP	Co-PP	
Manufacturer	Phillips Sumika	Basell	
Trade name	Marlex® HGZ-1200	Pro-fax SB642	
Density	0.910 g/cm^3	0.902 g/cm^3	D1505/D792
Melt flow index	120 g/10min	22 g/10min	D1238
Tensile strength, Yield,	36.9MPa	17.2 MPa	D638
Flexural Modulus	1.8×10^3 MPa	689 MPa	D790
Izod impact, Notched (23°C)	0.180J/cm	No break	D256

Coupling agent: Maleated polypropylenes (MAPP) supplied by Eastman chemical company (Kingsport Tenn.) were used as coupling agent. The typical physical properties of maleated polypropylenes are indicated in Table 7.2.

Table 7.2 Typical physical properties bulletin of maleated PP

Physical properties	G3003	G3015	G3216
Producer	Eastman	Eastman	Eastman
Polymer type	Ma-PP	Ma-PP	Ma-PP
MA graft, %	1.5	2.5	2.5
Mw	52000	47000	60000

Initiator: Dicumyl peroxide (98% active) supplied by Sigma Chemical Co. was used as an initiator as received. Its halftime is 0.2min at 190 °C.

Nanofiller: Cloisite® Na^+ Nanoclay received from Southern Clay Products Inc. was used as nanofiller. The typical physical properties are: moisture content 4-9%, density 2.86 g/cm^3; particle size (v): 10%<2 μm, 50%<6 μm, 90%<13 μm; d_{001} X-ray 11.7 Å.

7.2.2 Experimental methods

7.2.2.1 Measurement of aspect ratio

The aspect ratio of wood fiber was calculated by the arithmetic mean length divided by the arithmetic mean width measured by Fiber quality analyzer (Optest Equipment).

7.2.2.2 Effects of inorganic NC loading on the properties of PP Nanocomposites

Nanocomposites were based on homo-PP compounded with 0, 5, 10, 15 and 20% inorganic NC (based on total weight of the composite) described in Schedule 7.1 compared to PP hybrids reinforced with aspen fibers, MAPP and DCP to investigate its effects. The total 35 min blending time corresponds to the process time of the hybrids.

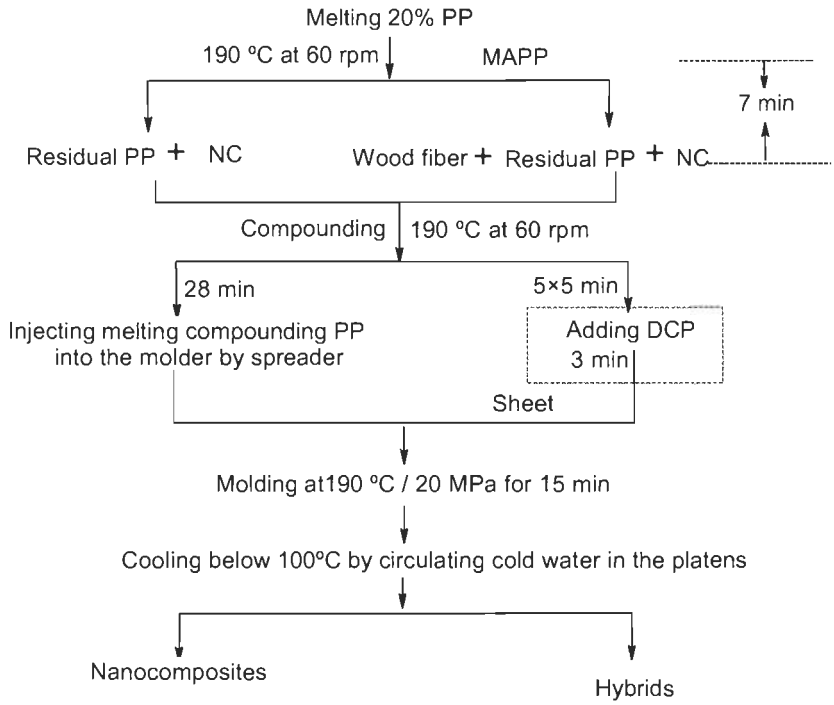

Schedule 7.1 Compounding and molding conditions

7.2.2.3 Effect of independent variables on the mechanical properties of PP hybrids

All the hybrids sheets were prepared by a two-roll mill according to Schedule 7.1 in order to study the influence of the characteristics and the content of wood fiber, MAPP, NC and DCP on the mechanical properties. The specifications of the used two roll mill were: 30 cm length, 15 cm radius, 0.6 gear ratio and 60 rpm roll speed.

7.2.3 Compounding and compression molding

The composite strips were pressed into the dog-bone shaped mould (ASTM D638 Type V for tensile and ISO 8256 Type II for impact strength testing). 22 specimens (10 for tensile testing and 12 for impact strength testing) were simultaneously prepared in the same mould.

7.2.4 Mechanical tests

All the specimens were conditioned in testing room overnight. Width and thickness were measured after being polished. The tensile tests was performed using an Instron machine (Model 4201) according to ASTM D638 while impact strength was performed by means of a TMI impact strength test machine (TMI No 43-01) following the ISO 8256 method.

7.3 Results and Discussions

7.3.1 Initial aspect ratio of wood fiber

Air-dried pulped wood fiber is grinded and screened into different mesh size. One variable used to characterize wood fiber in different mesh size is aspect ratio. According to the testing results, the aspect ratio of screened pulped fiber is 60-80mesh > 20-60mesh > 80+mesh at a similar width contributed from the grinded fibers (Table 7.3).

Table 7.3 Typical properties of screened BCTMP aspen fiber

BCTMP Aspen fiber	Mesh size					
	20-60mesh	sd	60-80mesh	sd	80+mesh	sd
Fine, %	22.11	0.07	8.74	0.53	53.31	0.15
Mean length, mm	**0.61**	0.00	**0.74**	0.04	**0.26**	0.00
Mean width, μm	**25.05**	0.15	**24.20**	0.28	**24.30**	0.00
Mean curl index	0.07	0.00	0.04	0.00	0.05	0.00
Mean kink index, 1/mm	1.01	0.07	0.74	0.07	0.97	0.03
Aspect ratio, l/d	**24.39**	0.07	**30.59**	1.67	**10.74**	0.04

Wood flour acts as filler, but wood fibers typically are employed to reinforce plastics except fill with to higher aspect ratios [341].

7.3.2 Effects of the characteristics of wood fiber and MAPP on the mechanical properties of PP hybrids

7.3.2.1 Effects of the size of wood fiber on the properties of homo-PP hybrids

The use of wood fibers as reinforcement materials for thermoplastics industry has been in the form of particles, fiber bundles or single fibers. In general, pulped wood

fiber used to reinforce rather than fill which results in the increase of strength as well as stiffness due to the transfer of stress from the matrix to the fiber [87, 113, 114, 116, 442] at a critical fiber length. This shortest fiber length (pull-out length) is called the critical fiber length (or the maximum value of load transfer length) [442]. Osswald also suggested stress is efficiently transferred only if the bond between the matrix and fiber is good by a shear transfer mechanism when the fibers are of finite length. If the fiber length is less than the critical length and the matrix can't effectively grip wood fiber to take the strain, wood fibers will slip and be pulled out, instead of being broken under tension. So, excepting there is a minimum fiber length required in case of a given fiber to build up the shear stress between fiber and the matrix to the value of tensile fracture stress of the fiber [443], it is reasonable to employ a coupling agent in the composite to ensure a strong bond. A coupling agent improves the bond between the plastic matrix and natural fiber by chemical and physical means [444, 445].

In the following discussion, wood fibers are referred to by their initial mesh size (Table 7.3). The results of impact strength, tensile strength, elongation, and modulus tests on hybrids made with different sizes of wood fibers are presented in Figure 7.1-Figure 7.4. Results show that using different fiber proportions and aspect ratio have an important effect throughout the WPC manufacturing processes.

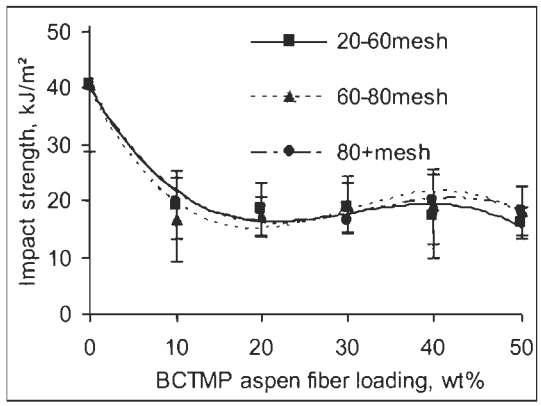

Figure 7.1 Effects of fiber mesh size on impact strength of homo-PP hybrids

Figure 7.1 shows that the values of unnotched impact strength decreased significantly with the changes of fiber content. This is consistent with the result reported by Karmarkar and coworkers [84] and Raj and coworkers [360]. The decrease of impact strength in hybrids compared to virgin PP came from the presence of fiber in the PP matrix providing points of stress concentrations, thus providing

sites for crack initiation. Another reason for decrease in impact strength may be the stiffening of polymer chains due to bonding between wood fiber and matrix to providing sites for crack initiation.

However, the effect of initial fiber mesh size on the impact strength is seen in Figure 7.1 and shows that the impact strength is not very much affected by mesh size in the range studied. The trend of the decrease of hybrid reinforced with aspen fiber in different mesh size is conversely at the point of 30wt% fiber loading. The worst value of impact is down 61% compared to virgin PP reinforced with 20-60mesh aspen fiber, and down 55.3-55.5% for the hybrids reinforced with 60-80mesh and 80+mesh fiber. The range of the decrease is different according to the fiber size because short fiber is the easiest to mix with PP exhibiting maximum torque [446].The result of unnotched impact strength of PP composite filled with 40% fiber is similar to the research reported by Stark and Rowlands [341] filled with wood flour showing higher mesh size leading to lower impact energy. It seems that the value of impact strength has no relationship to the aspect ratio.

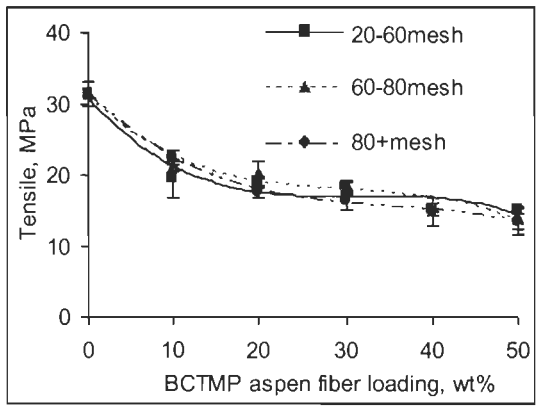

Figure 7.2 Effects of fiber mesh size on tensile strength of homo-PP hybrids

Tensile strength, modulus and elongation at max load provide an excellent measure of the degree of reinforcement provided by the wood fiber to hybrid composites [447]. Since the tensile strength depends on the weakest part of hybrid composites and the interfacial interaction between the matrix and wood fiber, the tensile strength of the PP hybrid composites decreases with incorporation of bleached aspen fiber due to the poor adhesion between hydrophobic PP and hydrophilic wood fiber in Figure 7.2. The effect of fiber on tensile strength is consistent with the report by Raj and coworkers [360]. However, tensile strength decreases 41-42% to 20-60 and 60-80 mesh while 48% to 80+ mesh at 30wt% fiber loading. Following wood fiber

introduced continuously, tensile strengths dropped 52-56% to 20-60mesh and 60-80mesh while 58% to 80+mesh at 50wt% fiber loading. The hybrid reinforced with 40wt% fiber in high mesh size has similar trend to Stark and Rowlands [341].

We conclude that the aspect ratio plays an important effect on the tensile at high fiber content exhibiting higher aspect ratio higher tensile strength while the length of fiber affects much at low fiber content due to the level of mixing with the matrix [446] and the distribution of fiber [448].

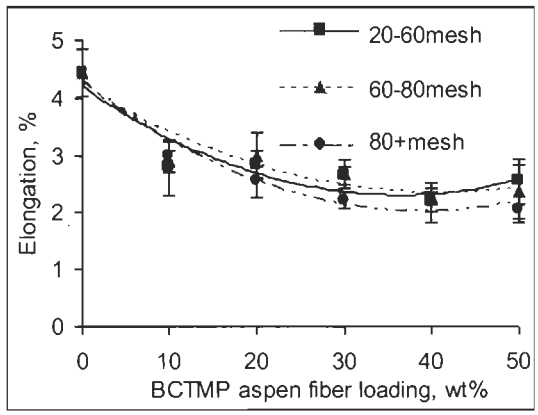

Figure 7.3 Effects of fiber size on elongation of homo-PP hybrids

Irregardless of fiber size, the elongation at maximum (Figure 7.3) decreases steadily, about 43-54% compared to virgin PP, with the changes of wood fiber content. There is a little difference in elongation at max for hybrids reinforced with wood fiber in different mesh size showing that the hybrid reinforced with highly aspect ratio (highly length) fiber has higher extension. The steep decline in elongation on wood fiber addition is obvious because wood fiber had low elongation and restricts the polymer molecules flowing past on another exhibiting better resistance deformation. This behavior is typical of reinforced thermoplastic in general and has been reported by many researchers [56, 84, 337, 360].

The effect of fiber loading and size on the tensile modulus is given in Figure 7.4. The trend of modulus increases slightly which benefits from the changes of molecular morphology of the polymer chains near the surface of wood fiber [376]. As fiber content above 40wt%, the decrease of modulus is coming from the bad distribution of fiber resulting in flaws not stiffening by fiber chains.

The effect of longer fiber is to lower modulus because increasing the length of wood fiber made it more difficult for polymer molecules to fully penetrate into the vessels of wood fiber. Conversely, short fiber is easily penetrated by the matrix leading to

more interaction and stronger adhesion between the matrix and wood fiber to grant the hybrid high tensile modulus [337] at same fiber content. Similar results were also reported by Stark and Rowlands [341], Raj and coworkers [360] and Yuan and coworkers [202].

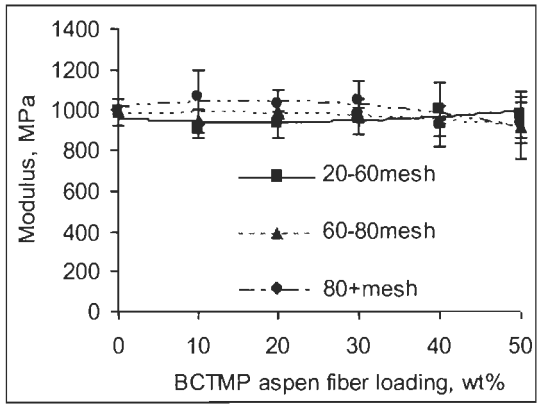

Figure 7.4 Effects of fiber size on modulus of homo-PP hybrids

7.3.2.2 Effects of the MAPP in different Mw and MA% on the properties of homo-PP hybrids

Due to strong hydrophilicity between fibers, they tend to agglomerate during the compounding process with the matrix polymer leading to poor interfacial adhesion and interaction of composites resulting in low mechanical properties of the final products. The use of maleated polymer has been the most common method to improve interfacial adhesion due to MA-grafted polymer increasing the polarity leading to better adhesion with wood fiber [136, 137, 449]. Due to the Mw and MA% of MAPP varying according to MAPP type and processing method, the mechanical properties of MAPP-treated hybrids were affected by the Mw and MA% of MAPP [450]. Thus, three types of commercially used MAPP are investigated (see Table 2). With the hybrid prepared via fiber modification and via matrix modification with MAPP [317, 318], the effects of the level of MA graft of MAPP are also investigated by two roll-mill system by the conventional method shown in Schedule 7.1.

Figure 7.5-Figure 7.9 shows the impact strength and mechanical properties of homo-PP hybrid containing different MAPP contents in different MA% and Mw respectively. It can be clearly observed in Figure 7.5 that G3003 (high Mw with low MA%) results in hybrids with superior impact strength compared to G3216 with similar Mw with high MA grafting level. Moreover, it is concluded that excessively

high MA% of MAPP doesn't impart the hybrid with superior impact strength. On the contrary it even decreases the value at a certain polymer Mw because it holds the coupling agent too close to the hydrophilic surface and doesn't allows sufficient interaction with the continuous matrix phase [451, 452]. Due to saturation of reactive sites at the interface, excess compatibilizer behaves like a third phase rather than a compatibilized binary blend resulting in slippages. Similar behaviours of slippages caused by excess MAPE among nonpolar hydrophobic matrix had verified by GU and coworkers [453].

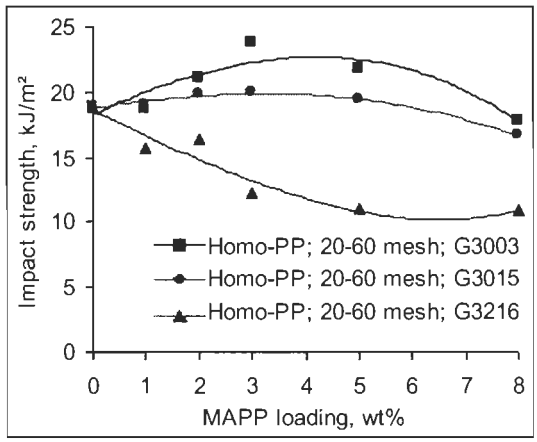

Figure 7.5 Effects of the type of MAPP on impact strength of homo-PP hybrids

The tensile strength of homo-PP hybrids is shown in Figure 7.6 as a function of MAPP loading. The tensile strength of the hybrid increases with increasing MAPP loading, regardless of Mw and MA% due to the improved interfacial adhesion and compatibility between the hydrophilic wood fiber and hydrophobic PP [319, 320, 454, 455]. With MAPP excess loading, the decreasing trend on tensile of homo-PP hybrids is confirmed with the previous statement with the same explanation [320, 456] regardless of their types and concentrations. The MAPP-treated composites with sufficient Mw and MA% show improved tensile strength, elongation and toughness, but without obvious improvement of modulus.

The enhanced tensile strength of the MAPP-treated composites has relationship with the amount of MA% and the Mw of MAPP. At low MAPP loading, e.g. less than 4wt%, MA% has no obvious difference on tensile strength between MAPP type in different Mw and MA%. However, as more MAPP is introduced, lower MA% (G3003) offers the composite with positive effects on tensile compared to higher MA graft MAPP at similar Mw (G3216) as shown in Figure 6 because higher MA grafted

MAPP employed results in sufficient MAPP chains coated on wood fiber closely less interaction and entanglements to the matrix [451, 452].

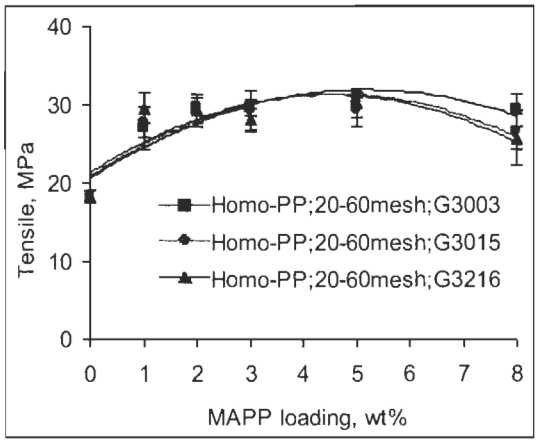

Figure 7.6 Effects of the type of MAPP on tensile strength of homo-PP hybrids

Excessively low or high Mw and MA grafted MAPP could diffuse into the matrix polymer and provides sufficient reactive sites for reaction between the hydroxyl groups of wood and carboxyl groups of MAPP. Therefore, the sufficient polymer backbone Mw of MAPP would sufficiently diffuse and entangle with the homo-PP matrix due to the moderately Mw of MAPP. High MA% provides the maleated polymer with excess sites for attachments leading to the maleated polymer chains too closely coated on the surface of wood fiber to weaken the polymer entanglement with the matrix resulting in lower tensile. Therefore, it is concluded that MAPP in different Mw has similar behaviour at the same highly MA graft, even inferior to lower MA grafted MAPP at similar Mw.

Our results are more significance than the report by Kim and coworkers [450] due to wide extend of MAPP loading as well as the selected Mw and high MA% of MAPP. Similar results are confirmed for tensile strength.

The increase in the elongation of the composites is expected due to the presence of maleated polymer both low or high Mw of MAPP as well MA%, and then slightly drops as excessive MAPP is introduced as seen in Figure 7.7. The result for the elongation as a function of different MAPP addition is agreement with the improvement of interfacial adhesion [195].

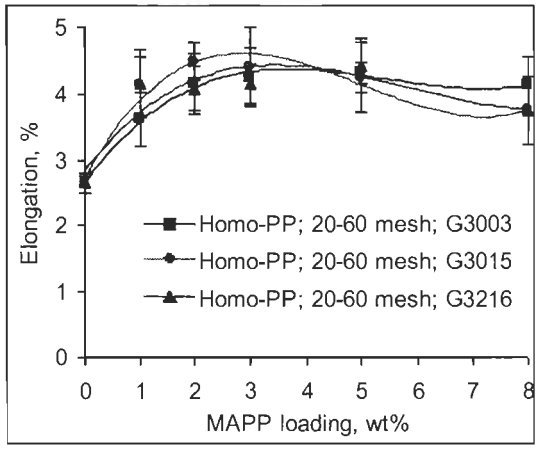

Figure 7.7 Effects of the type of MAPP on elongation of homo-PP hybrids

It is concluded that the trend of elongation and modulus diverges when 4wt% MAPP is incorporated. When the content of MAPP is less than 4wt%, higher MA% of MAPP provides the composite with higher elongation and lower modulus. The MA% controls the trends of the changes seen in Figure 7.7 and Figure 7.8. Moreover, at the same MA graft level, low Mw results in the composite with higher elongation by allowing the coupling agent easily reside at the interface between MAPP and homo-PP matrix. Lower MA grafted MAPP (G3003, 1.5% maleic acid) could offer sufficient interaction and hydrogen bonding between the anhydride group of MAPP and wood fiber restricting their deformation by forming networks being shown by their modulus too (Figure 7.8).

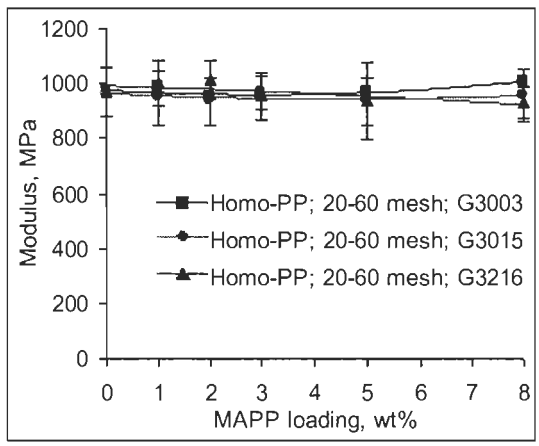

Figure 7.8 Effects of the type of MAPP on modulus of homo-PP hybrids

However, the lower MA grafted MAPP doesn't hurt the elongation and modulus as excessive MAPP introduced. But the elongation as well modulus of the composite coupled by excessively higher MA grafted MAPP is worsened.

The toughness of the composite is observed to be greatly improved by increasing the amount of maleated polymer (Figure 7.9) due to the improved wettability and the compatibility between the matrix and wood fiber. These results also being shown by values of elongation at break (Figure 7.7). The toughening mechanism of homo-PP hybrid by adding maleated polymer is caused by enhancing the interfacial adhesion to assist stretching of polymer fibrils from the wood fiber covering surface layer [140], diffusing shear yielding of maleated polymer chains from the matrix [140] and also exhibiting dowel failures at the grip end [457].

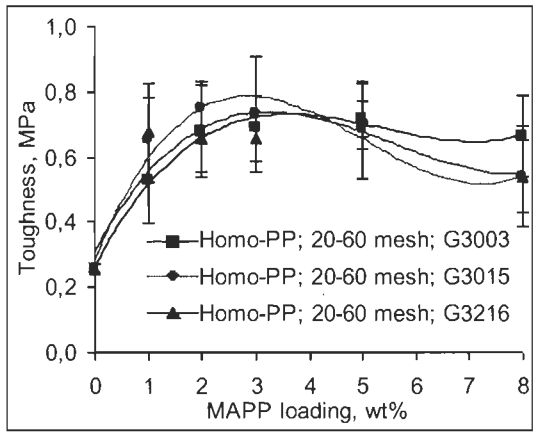

Figure 7.9 Effects of the type of MAPP on toughness of homo-PP hybrid

The difference of toughness comes from the difference in the interfacial adhesion and interaction by MAPP type. As MAPP in different MA graft level and similar Mw employed, e.g. G3003 versus G3216, the higher MA% provides the composites with enough bonding sites leading to superior toughness lowering 4wt% content. Above 4wt% content, excessively higher MA grafted MAPP resides on the surface of wood fiber easily which leads to slippages [450] and be deformed by pulling-out wood fiber from the matrix [138, 140].

When MAPP in different Mw and at the same MA% employed, e.g. G3015 versus G3216, the lower Mw MAPP (G3015) offers the composites with superior toughness due to low MAPP polymer chains penetrating and residing on wood fiber easily under the similar attaching sites [450] at low content. But as this type MAPP incorporated excessively, higher Mw MAPP would also reside on wood fiber enough to enhance the toughness by stretching and diffusing shear yielding due to sufficient polymer chains involved into the system. Meanwhile, the layer of lower Mw MAPP residing and covering on the surface of wood fiber maybe grow too thick to help

significant slippages when bearing impact due to the much lower molecules introduced leading to deforming plastically [140] without strong adhesion.

7.3.2.3 Effects of the morphological structure of the matrix on the properties of PP hybrids with or without MAPP

Mechanical properties are determined on the morphological structural of the matrix and the mean values of the properties are plotted against wood fiber content in Figure 7.10-Figure 7.14. Figure 7.10 shows the unnotched impact strength decreases significantly as incorporation of wood fiber without MAPP present comparing to virgin homo-PP and co-PP due to an unsatisfactory dispersion of wood fiber and poor formation of a durable interface in the hybrid from the chemical incompatibility causing failure in stress transfer from the matrix to wood fiber which is consistent with the result reported by Karmarkar and coworkers [84].

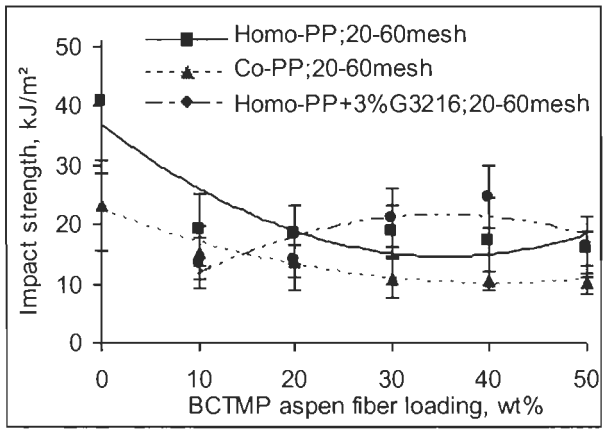

Figure 7.10 Effects of the morphological structure of PP on Impact strength

However, the different morphological structure between homo- and co-PP provides the composites with a little varied behaviour of impact. It is concluded that the impact behaviours of the reinforcement of birch fiber in homo-PP and co-PP are a little different in falling slopes seen from the curves in Figure 7.10. The impact of homo-PP hybrid is induced sharply, down to 53% comparing to virgin homo-PP by incorporation of 10wt% wood fiber, while the induction to co-PP composites is about 34% compared to virgin co-PP. However, the impact strength of co-PP hybrid could be worsened more rapidly with the changes of wood fiber content, down 34% from 10wt% to 50wt% while dropping 17% in the case of homo-PP. Conversely, impact strength of hybrids could achieve optimal value with the change of wood fiber

content in the presence of MAPP as described in Figure 10 due to the improved interfacial adhesion [320] and compatibility [455].

Since the tensile strength decreases by incorporating of wood fiber both homo-PP and co-PP due to poor interfacial adhesion, there is a difference in the decrease from the different morphological structure. It is seen from Figure 7.11 that tensile strength decreases 38% with 10wt% fiber employed compared to virgin homo-PP and then dropped 22% as wood fiber content increase to 50wt%. Correspondingly hybrid of co-PP reinforced with birch fiber showed tensile strength decrease by introduction of wood fiber, 31% with 10wt% fiber introduced and a little drop (4%) with 50wt% wood fiber. The larger decline in the composites based on homo-PP is represented in Figure 7.11, especially when wood fiber are incorporated at first. The result is different from the observation reported by Karmarkar and coworkers [84].

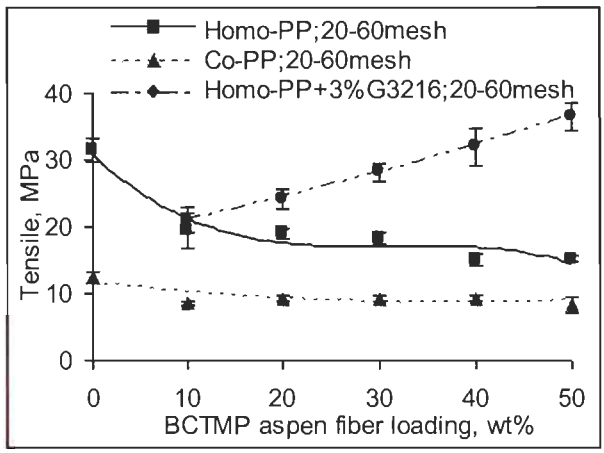

Figure 7.11 Effects of the morphological structure of PP on Tensile strength

As suitable coupling agent employed, the behaviour of tensile strength enhanced straight meaning the stress has been transferred from the matrix chains to wood fibers due to the interfacial adhesion and interracial bonding improved between wood fiber and the matrix which is in agreement with other author results [84].

The behaviors of the decreased elongation (Figure 7.12) and increased modulus (Figure 7.13) with the changes of wood fiber without coupling agent have been described in above section. There are significant differences in the declining slopes of the elongation and modulus of the composite based on homo-PP and co-PP. Conversely to the behaviors of impact and tensile, the steep decline in elongation immediately with wood fiber addition is obvious to co-PP hybrid, down 62% with 10wt% added and keeping similar descended trend, 60%, when going from 10wt%

fiber to 50wt%. In the case of homo-PP, the elongation is changed to 37% by incorporating of 10wt% fiber and dropping by 9% with fiber increasing from 10wt% to 50wt%. The difference of elongation behavior came from restricting soft co-PP chains more than relative stiff homo-PP chains and thus exhibiting a wide change in elongation of co-PP hybrid.

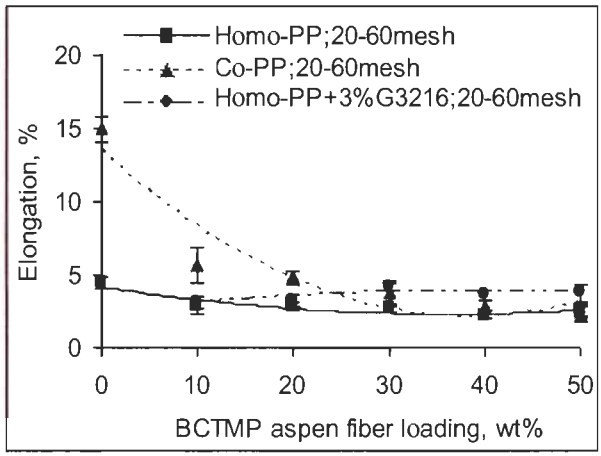

Figure 7.12 Effects of the morphological structure of PP on Elongation

In general, the tensile modulus increases with increasing wood fiber loading. The behavior of modulus is correlated with the decrease of elongation. Similar to elongation, there is obvious difference between homo-PP hybrid and co-PP hybrid. From Figure 7.13, the modulus of homo-PP hybrid increases 8% as fiber increased from 10phr to 50phr while co-PP hybrid is up 82% at the same range of fiber due to the difference in morphologies of the involved molecules. Although MAPP had effects on the modulus, the improvement of modulus was principally originated from the attribution of the morphology of wood fiber, i.e. high Modulus of rupture, and the changes of the crystal morphology [376]. The slight drop of modulus of homo-PP and co-PP hybrids comes from the deviation of the values.

Different to the nanocomposites, the elongation of the hybrids incorporating of 3phr coupling agent increases slightly due to the improvement of interfacial adhesion, from 3.1% up to 4.2% at 30wt% fiber loaded and reaches 3.8% with the reinforcement of 50wt% wood fiber. Moreover, modulus increases obviously comparing to the composites without the presence of coupling agent in Figure 7.13. Modulus increases from 945MPa to 1250MPa with the content of wood fiber changing from 10phr to 50phr which is related to the previous research by Bledzki and Faruk [195] as coupling agent in limited usage.

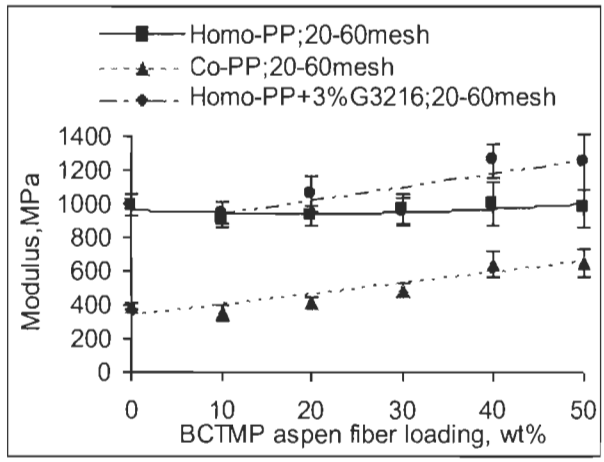

Figure 7.13 Effects of the morphological structure of PP on Modulus

The different morphological structure of the matrix leads different partly properties. The toughness is affected by their chemical structure as shown in Figure 7.14. The toughness of the hybrids based on both homo-PP and co-PP are declining with the fiber content increase. Due to the significant effects on co-PP by wood fiber, the scope of the decrease of toughness is higher, 85% for 10phr fiber compared to virgin polymer and 66% decrease for 50phr fiber loading. The observed changes in toughness are for the elongation behavior.

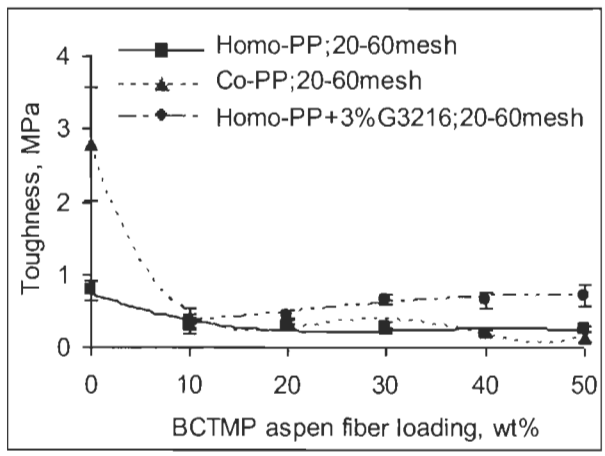

Figure 7.14 Effects of the morphological structure of PP on Toughness

Although the composite displays stiffer when G3216 is incorporated as indicated in Figure 7.13, it is also observed that coupling agent contributes the hybrids with a bit higher toughness with the help of improved wettability and compatibility noted in Figure 7.14which is in agreement to the changes of elongation. Thereby, MAPP

could provide hybrid composite with a higher modulus as well as highly elongation and highly toughness at the same time.

7.3.2.4 Effects of NC loading on the properties of homo-PP hybrids

The homo-PP nanocomposites and its hybrids were manufactured according to Schedule 7.1. The changes in the curves of the impact and tensile are presented in Figure 7.15 and Figure 7.16 respectively by NC increase. Figure 7.15 shows the effect of NC content on the impact strength of hybrids made with virgin homo-PP or with the additions of wood fiber, coupling agent as well DCP. With the more NC introduced, the curve of the nanocomposites gradually declines from 41kJ/m² to 17kJ/m² at 20wt% loading, down by 58%, because the exfoliation of MMT layers into the matrix was not strongly dependent on the NC loadings at high concentration due to the aggregates easily and intercalation of the polymer melt becoming difficult. Generally, the mechanical properties can be enhanced only in the case of intercalation or exfoliation [458].

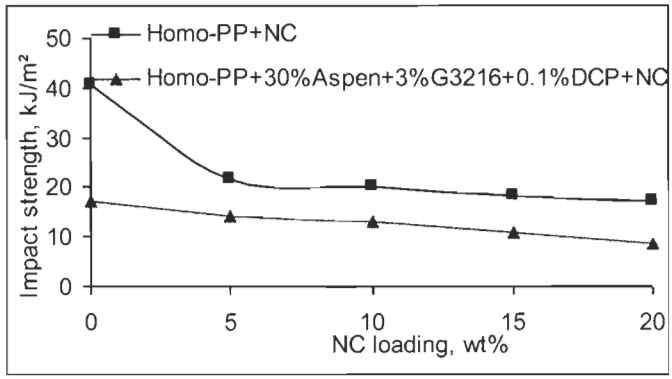

Figure 7.15 Effect of NC loading on the impact

However, high loading could prevent complete exfoliation of some of them leading to less influence by the effect of the intercalation and exfoliation layers. Thereby, this results mainly from the poor dispensability of NC in the nanocomposites and its ultrabad morphology lacking of compatibilizer in the system.

Although MAPP and DCP could improve the wettability [320] and the nucleating effect of NC could be strengthened by the addition of wood fiber and coupling agent by increasing the crystallization temperature and decreasing the crystalline enthalpy [459], impact strength of hybrids decreased down 50% versus those without NC due to the highly NC aggregation and low surface energy leading the hybrids into huge

viscosity which prohibits the movement of the molecular chains. This behaviour of impact is also observed by Yeh and coworkers [460].

The influence of NC content on the tensile strength of nanocomposites is shown in Figure 7.16 as well that of the hybrids. The curve of tensile strength of the nanocomposite decreases slightly by 17% for 20wt% NC incorporated compared to virgin homo-PP because the exfoliation is inefficient at high clay level as well as their dispersion leading to obvious aggregates among lesser interfacial adhesion system [233]. This result is opposite to the improvement of the tensile of the PP/MMT nanocomposites compatibilized with MAPP by Chen [233], Zhang [461] and acrylic acid modified PP with organically modified clay by Vu and coworkers [458].

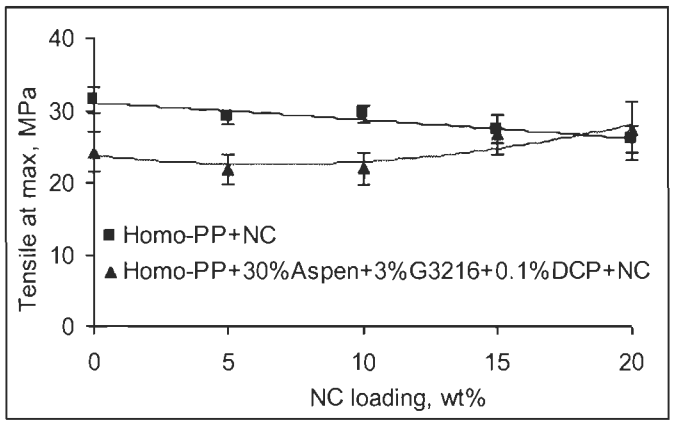

Figure 7.16 Effect of NC loading on the tensile

Conversely, the tensile strength of the hybrids decreases slightly by incorporation of NC at first due to the stress concentration as well as the poor NC dispersion. However, as more NC is introduced, the penetrated NC particles work as solid join-points after strongly driving force under the high viscosity which originates from the strong interfacial strength due to delamination and better dispersion. Even when an aggregation occurs, more points produced bear the stress, and lead to superior tensile strength, up 12% for homo-PP hybrids at 20% NC loading compared to the hybrid without NC added. The difference between the hybrids and the nanocomposites implies that the improvement of the tensile strength with high filled NC is related to the surface polarity. NC particles in the hybrids could be deposited on the surface of wood fiber and be dispersed along the direction of wood fibers [462] and even located in wood lumen [425, 462] to reduce its negative effects. The morphology of the matrix polymer as well as other additives act as interfacial bonding agents or

surface treatments of the fillers to give superior properties due to better compatibility in the system [463]. The behaviour of tensile strength in our research is in an agreement with the conclusion by Lee and coworkers [459], but is opposite to the studies by Yeh and coworkers [460].

Figure 7.17 and Figure 7.18 show the influence of NC content on the tensile modulus and elongation at maximum of the nanocomposies and the hybrids based on homo-PP. The modulus of the nanocomposites goes from 991MPa of virgin polymer to 1.5×10^3MPa filled with 20wt% NC while corresponding change in elongation is a reduction from 4.4% to 2.9%. The improvement of modulus is contributed from the greatly constrained mobility of the polymer chains by increasing the NC content according to Kojima and coworkers [441]. The performance of the hybrids is slightly different with the nanocomposites exhibiting an increasing trend of their modulus with slow steps which implies some particles are located in wood fiber lumen and thus not prohibiting the movements of the molecule chains [462].

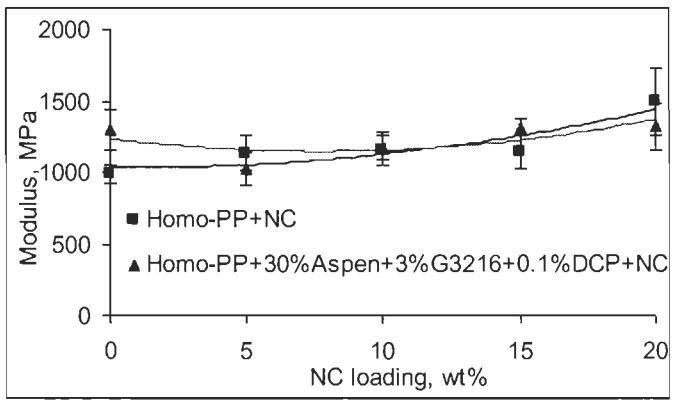

Figure 7.17 Effect of NC loading on the modulus

An observed decrease in the elongation at maximum load in the nanocomposites could be explained by the plastic deformation of the matrix which is greatly limited by an increase of the NC loading under poor interaction and interfacial adhesion between the hydrophilic-layered NC and the hydrophobic PP. This decreased extensibility is obviously detrimental in the case of the mechanical properties but could be beneficial in some applications of the materials. The decrease of extensibility implied increasing resistance to permeability [458]. But the tendency of the elongation of the hybrids is conversely as in Figure 7.18. With a slight increasing in modulus, the elongation of the hybrids is not reduced but extended, up 5%, from 2.56% to 2.69%. This obvious different behavior of modulus and elongation of the

hybrids maybe come from the location of NC particles being in wood lumen and deposited on the surface of wood fiber which makes NC loose the most of its contribution to stiffness. There is practically no effect on the elongation but improvement of the plasticity of the hybrids with the reinforcement by wood fiber.

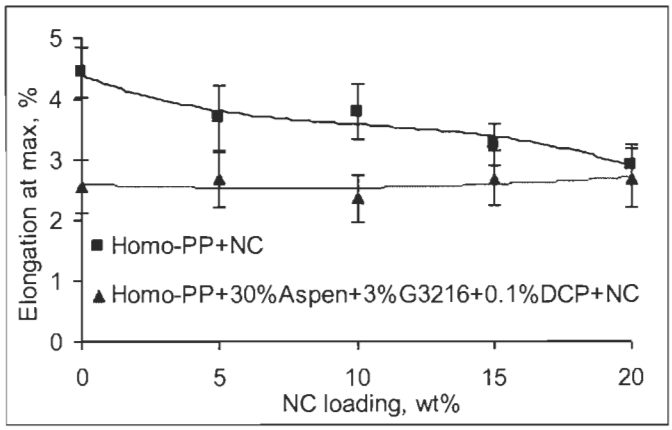

Figure 7.18 Effect of NC loading on the elongation

Figure 7.19 plots the fracture toughness resistance versus the NC content exhibiting a different performance as a function of the NC in nanocomposites and hybrids. There is a large enhancement of nearly 17% in toughness with 20phr NC comparing to the hybrids without NC. With the use of wood fiber, MAPP and DCP, the NC particles would prefer to interact with and modified by the functionalized PP and MAPP during the compounding processing to strengthen the interfacial adhesion and interactions to the matrix due to their similar polarity. They are also mostly distributed along the wood fiber due to the similar reasons. Better wetted NC particles leads to lubricated bundles of aggregates easily due to the particles bundled by polar polymeric materials resulting in mainly wood fiber pullout. Moreover, the NC particles generate numerous microcracks around the grafted molecules connecting with polymeric chains, wood fibers or other particles and which may propagate along the clay platelets resulting in a highly rough facture surface [464] while working as fixed joints too due to NC particles which are hard platelets.

Conversely to the hybrids, although amounts of NC particles in the nanocomposites work as joint-points by interacting or entangling themselves with wood fiber and the matrix molecule chains, less force is transferred due to poor adhesions as well as their aggregates and less slippages happen under the force due to incompatibility. All

the reasons mentioned above make the toughness of the nanocomposites without wood fiber and other additives decreased.

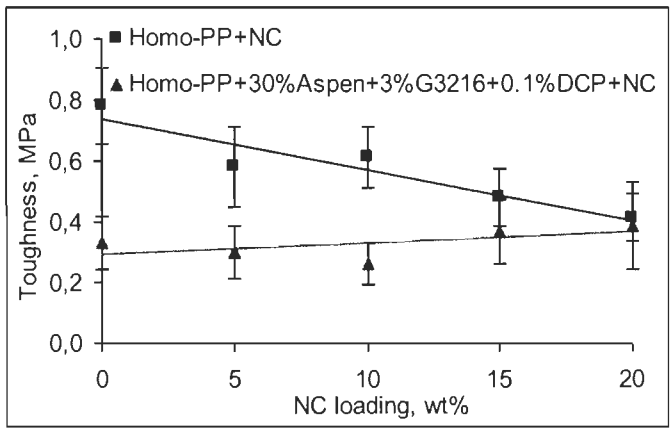

Figure 7.19 Effect of NC loading on the toughness

The performance of the toughness among the nanocomposites and hybrids is related to the changes of dominant toughening mechanisms which are proposed in high loading level with functions of modifiers.

7.3.2.5 Effect of DCP on the mechanical properties of hybrid composites

The behaviors of DCP effects on homo-PP hybrids with the reinforcement of 30wt% aspen BCTMP pulp fiber and 3wt% G3216 are summarized in Table 7.4. In the case of un-notched samples, the impact and tensile strength have decreased with the amount of DCP added in the presence of 30wt% aspen fiber, whicle impact strength decreases by 19% from 21kJ/m^2 for hybrids without DCP down to 17kJ/m^2 for hybrids in the present of 0.1-0.2wt% DCP because the impact strength depends on molecular weight directly [355]. The degradation of PP matrix [356, 357] and wood fiber [353] result in decrease of the resistance of the crack and limiting the contribution from the chains entanglements, even though DCP can enhance interfacial adhesion between wood fiber and the matrix.

The tensile strength of the hybrid is cut down when 0.2wt% DCP is incorporated compared to the hybrid without DCP in Table 7.4. Nachtigall and coworkers [465] reported that DCP hydrolyzed the chains of PP in order to graft anhydride acids during the incorporation of MAPP resulting in decreased molecular weight of the matrix which is agreement with the results of the degradation of the matrix by Huang [356] and Azizi [357]. The decrease in molecular weight implies less stress transferred from the matrix to wood fiber because of a lack of sufficient chains

entanglements would make wood fibers pullout more easy as well as prorogue the decomposition of wood fiber [353]. Therefore, the tensile strength of the hybrid decreases with the amount of DCP present down to 15MPa at 0.3wt% level from 28MPa without DCP present, down by 46%.

The declined elongation at maximum with the changes of DCP loading is observed in Table 7.4 which corresponds to severe scissions of the polymer chains and wood fiber resulting in limiting the amount of entanglements between the matrix molecules and MAPP, even among the matrix chains themselves. So the fiber fails and the propagation of the crack extends largely as well as less contribution from fibers pullout in the system to achieve more fragility with lower energy absorption at a critical strain.

Table 7.4 Effects of DCP on the mechanical properties of PP hybrids reinforced with 30wt% BCTMP aspen fiber and 3wt% G3216

Properties	DCP concentration, wt%		
	0	0.1	0.2
Impact strength, kJ/m²	21.11 (4.96)	17.03 (4.12)	17.33 (3.75)
Stress at Max. Load, MPa	28.1 (1.38)	24.24 (2.66)	14.98 (3.02)
Strain at max load, %	4.16 (0.29)	2.56 (0.45)	1.7 (0.17)
Modulus, MPa	9.5×10^2 (87)	1.3×10^3 (137)	1.2×10^3 (89)
Toughness, MPa	0.66 (0.07)	0.33 (0.13)	0.13 (0.03)
Plasticity†	1.02	1.06	1.15

† Plasticity is defined as the ratio of the *Energy to break point /Energy to yield point*

The enhancement of modulus in homo-PP hybrid is contributed from the acceleration of thermo-oxidation by DCP and high acidity as well the stronger degradation of wood fiber due to lower lignin content which stabilizes the materials against thermo-oxidation [466]. As mentioned above, whatever the amount of DCP added, the absorbed facture energy decreased by introduction of DCP leading to the decomposition of the matrix and fiber in Table 7.4. Due to serious degradation occurring in the presence of bleached fiber, the toughness decreased to 80% of initial value with 0.2wt% DCP addition. Furthermore, the plasticity of the hybrids reinforced with bleached fiber and high MA% MAPP increased dramatically up 13% as 0.3wt% DCP was introduced due to the strong degradation resulting in lower molecular mass components.

7.4 Conclusions

(1) The selected wood fiber weakens both impact strength and tensile strength of PP composites. However, the size of selected wood fiber has no effect on the mechanical properties of PP composites without coupling agent employed.

(2) With changes of the Mw of MAPP as well MA%, MAPP gives PP hybrids with superior tensile strength and toughness. There are different behaviors of impact strength with varying their Mw and MA graft level. It is concluded that MAPP with high Mw and low MA graft level could result in homo-PP hybrids with better performance.

(3) Both the impact strength and tensile strength of both homo-PP and co-PP hybrids without coupling agent decrease simultaneously with wood fiber incorporation. Both of them are enhanced by wood fiber increase when G3216 is presented. These enhancements are also confirmed by the increase of elongation and toughness in the presence of coupling agent.

(4) Inorganic NC enhances the tensile strength of PP hybrids slightly in the presence of coupling agent, but not with PP nanocomposites. It shows similar behavior of impaired values of the impact strength in both cases. In general, the decrease of elongation of PP hybrids is confirmed by the increase of modulus.

(5) In two-roller mill system, DCP decreases the impact/tensile strength of PP composites by the thermo-oxidation speed up at temperatures near 200 °C. The degraded PP composite exhibits higher deformation as well as higher plasticity.

7.5 Acknowledgements

The author would like to thank the NSERC, FQRNT and Auto 21 for their financial support.

Chapter 8 - Effects of Coupling agent, Initiator and Nanofiller on the Properties of Polyethylene Composites

Ruijun Gu and Bohuslav V. Kokta

Journal of Composite Materials

Abstract: Systematic studies of the effects of the concentrations of maleated polyethylene (MAPE), dicumyl peroxide (DCP) and Nanoclay (NC) were undertaken to study the effects on the mechanical properties of PE Nanocomposite and hybrid composite.

In addition the effect of compounding sequences on resulting wood fiber reinforced composites was also examined.

Keywords: Wood fiber, Aspen fiber, Polyethylene, Nanoclay, Composite, Nanocomposite

8.1 Introduction

Polyethylene (PE) is an important engineering polymer used widely while wood fiber being biodegradable, low cost and reusable is available worldwide [44, 82, 91, 135, 167, 467, 468]. There were lots of research on PE/Clay Nanocomposites and PE-wood fiber hybrid composites dealing with its mechanical properties [81, 92, 316, 334, 390, 469, 470, 471, 472, 473, 474, 475], flammability [332, 476, 477] and deformation behavior [400, 401].

Coupling agents in wood fiber reinforced polymer composites play a very important role in improving the weak adhesion, poor dispersion and incompatibility between the hydrophilic natural fibers and the hydrophobic polymer [314, 315, 478]. Poor composite strength results from the lack of stress transfer from the polymer matrix to the load bearing natural fibers [113]. So far, over forty coupling agents have been used in production and research. The popular coupling agents currently being used include isocyanates, anhydrides, silanes, and anhydride-modified copolymers. Coupling agents are usually coated on the surface of wood fiber, polymer or both by compounding, blending, soaking, spraying, or other methods. But the use of modified PE for wood fiber-reinforced PE composites is well know and widely practised due to their superior properties. Maleated PE was shown to be best in wood-fiber/HDPE composite by comparing the effectiveness of oxidized PE, MAPP and MAPE [92]. Meanwhile DCP is widely used as another important crosslinking agent [330, 348, 349, 380, 381, 382, 383, 479, 480, 481, 482, 483] being the most

utilized because of chemical bonding to both the wood fiber and the polymer matrix[321].

The aim of this article is to investigate the influence of MAPE, DCP and NC on the mechanical properties of PE Nanocomposite and Hybrid composite reinforced by cellulosic fibers.

8.2 Experimental and materials

8.2.1 Materials

Thermoplastics: Linear low density polyethylene was supplied by Novacor Chemicals Inc. in branded as NOVAPOL® HI-0753-H.

Wood fiber: Air-dried aspen fiber (CTMP, 20-60mesh) was prepared in Integrated Pulp and Paper Center laboratory.

Coupling agent: Maleated polyethylene (Eastman G-2010, Kingsport Tenn.) was supplied by Eastman chemical company and has an acid number of 2.

Initiator: Dicumyl peroxide (98% active DCP) whose halflife is 1 min at 171°C, supplied by Sigma Chemical Co. was used as an initiator as received.

Nanofiller: Cloisite® Na+ received from Southern Clay Products Inc. was used. The typical physical properties were shown in Table 8.1.

Table 8.1 Typical physical properties bulletin

Physical Properties		Cloisite® Na^+
Description		Natural montmorillonite
Treatment		None
Moisture, %		4-9%
Color		Off white
Density, g/cc		2.86
Dry particles size μm by volume	10%	<2
	50%	<6
	90%	<13
d_{001} X-Ray		11.7 Å

8.2.2 Experimental and compounding

8.2.2.1 Effect of the adding sequence of wood fiber on the mechanical properties of Aspen-PE composite

Aspen-PE composite blended with 3%MAPE, 3%NC (Cloisite® Na+) with or without 0.1%DCP at 30% content of fiber served as a reference to study the blending sequence of Aspen fiber. The addition sequence of fiber was defined as premixing

and no-premixing method depending on the sequence of fiber compounding which is illustrated in Schedule 8.1.

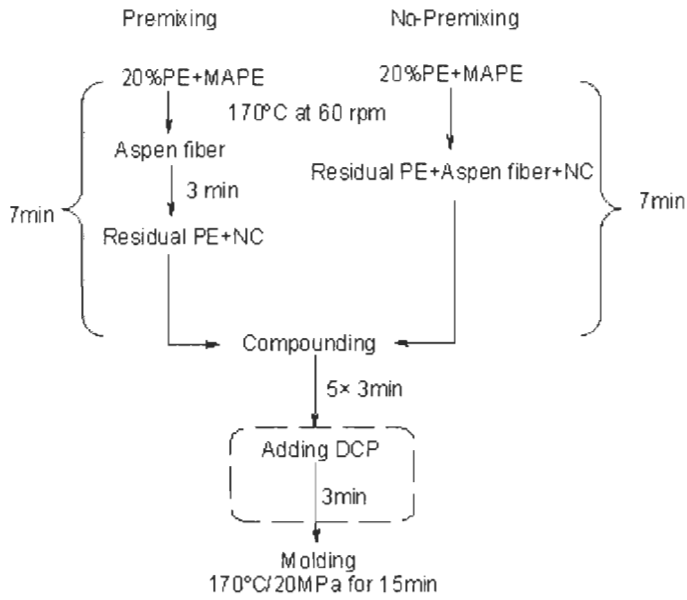

Schedule 8.1 Compounding and molding conditions

8.2.2.2 Effects of independent variables on the Mechanical Properties of PE composite

All composites were compounded in a two-roll C.W. Brabender according to the compositions listed on Table 8.2 to study the influence of NC, MAPE and DCP on the mechanical properties of PE Nanocomposite and Aspen-PE composite by No-premixing method in Schedule 8.1.

8.2.3 Compression molding

The composite strips were pressed into a dog-bone shaped mould (ASTM D638 Type V). 22 specimens (10 for tensile testing and 12 for impact testing) which were simultaneously prepared in the same mould. The mould was maintained at 170±2°C DAKE PRESS and held for 15 min under the pressure of 20MPa. After the high pressure stage, the mould was cooled below 60°C by circulating cold water in the platens. The approximate dimensions of tensile specimen were as follows: width 0.30-0.32cm and thickness 0.27-0.29cm. Width of impact sample was 0.28-0.30cm and thickness was 0.13-0.15cm.

8.2.4 Mechanical tests

All the specimens were conditioned in testing room overnight, and then the width and thickness were measured with micrometer after polishing. Tensile testing was

performed on an Instron tester (Model 4201) at 23°C and 50% level of relative humidity according to ASTM D638. PE with reinforcement of NC was broken down at 30mm extension due to its higher plastic characteristics.

8.2.5 Determination of tensile impact

Tensile impact strength (un-notched) was determined by a TMI impact tester (TMI No 43-01) according to ASTM D1822 at ambient temperature (23°C).

Table 8.2 Compositions of PE Nanocomposite and Aspen-PE composite

Composites	PE, g	Aspen, g	MAPE, g	DCP, g	Cloisite® Na^+, g
PE	100	—	—	—	0
PEN3	97.0	—	—	—	3
PEN10	90.0	—	—	—	10
PEN15	85.0	—	—	—	15
PEN20	80.0	—	—	—	20
PEN3D0.1	96.9	—	—	0.1	3
PEN3D0.2	96.8	—	—	0.2	3
PEN3D0.3	96.7	—	—	0.3	3
PEN3D0.5	96.5	—	—	0.5	3
PEN3M2	95.0	—	2	—	3
PEN3M3	94.0	—	3	—	3
PEN3M5	92.0	—	5	—	3
PEN3M8	89.0	—	8	—	3
PEF30M3N3	64.0	30	3	0.0	3
PEF30M3N3D0.1	63.9	30	3	0.1	3
PEF30M3N3D0.2	63.8	30	3	0.2	3
PEF30M3N3D0.3	63.7	30	3	0.3	3
PEF30M3N3D0.5	63.5	30	3	0.5	3

8.3 Results and Discussions

8.3.1 Effects of the mixing sequence of aspen fiber on the mechanical properties of the Aspen-PE composites

The influence of adding sequence of wood fiber on the impact and tensile properties of the reference composite are listed in Figure 8.1. The impact properties of the composite compounded with no-premixing method was superior to that of compounded with premixing. It was concluded from Figure 8.1 that the difference of increase was varied in presence of DCP. The increase of the impact strength of Aspen-PE composite with 0.1% DCP was up (42%, from 83kJ/m² to 118kJ/m²) greater than the composite without DCP (up 28%, from 57kJ/m² to 73kJ/m²). And the increase of the tensile strength of Aspen-PE

composite with DCP added was up 18%, from 38MPa to 45MPa while that of the composite without DCP was 8%, from 38MPa to 41MPa.

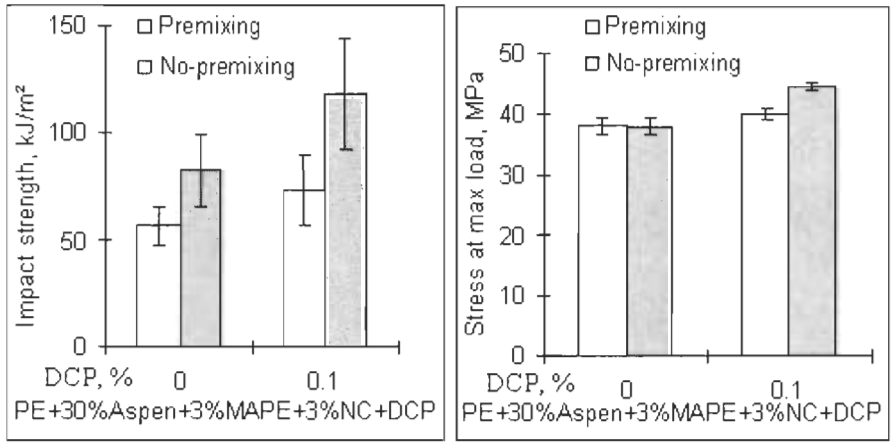

Figure 8.1 Effects of the adding sequence of fiber on impact and stress of Aspen-PE composite

The results indicated that with the higher ratio of MAPE to matrix, MAPE was coated on the surface of fibers leading to more anhydride groups being grafted with hydroxyl groups of fibers, but few structures of PE-MAPE-Fiber were formed. Moreover, the difference of influence was stronger with the presence of DCP due to a higher MAPE coating effect on the grafting reaction between fiber and matrix as well as fiber itself.

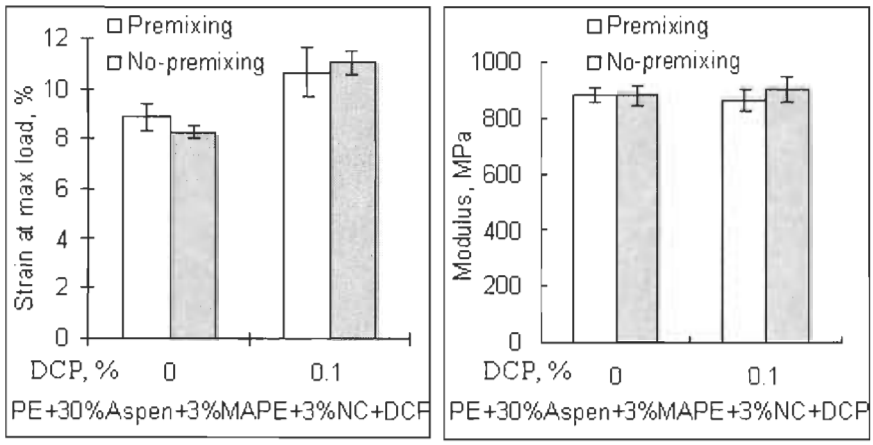

Figure 8.2 Effects of the adding sequence of fiber on strain and modulus of Aspen-PE composite

The modulus of Aspen-PE composite either with the addition of DCP or not varied from -2.3% to 2.5% in the range of standard deviation in Figure 8.2. So, there was no obvious effect on the modulus of the composite with DCP [353].

8.3.2 Effects of Cloisite® Na+ and MAPE on the mechanical properties of PE Nanocomposite

Figure 8.3 shows the effect of the impact and tensile strength of the composites with NC and MAPE loading on PE Nanocomposite. The impact strength decreased steadily as NC was introduced due to matrix fiber debonding, no reaction between matrix fiber and particulates, decreasing from 134kJ/m² of pure PE to 63kJ/m² at 20% of NC.

The results also showed that NC had a positive influence on the tensile strength of the composites which increased steadily up 16.5% from 25MPa to 29MPa but there was a decrease of 45% of the strain from 13.4% when compared to pure PE due to more conjoint points producing more physical interfacial adhesion.

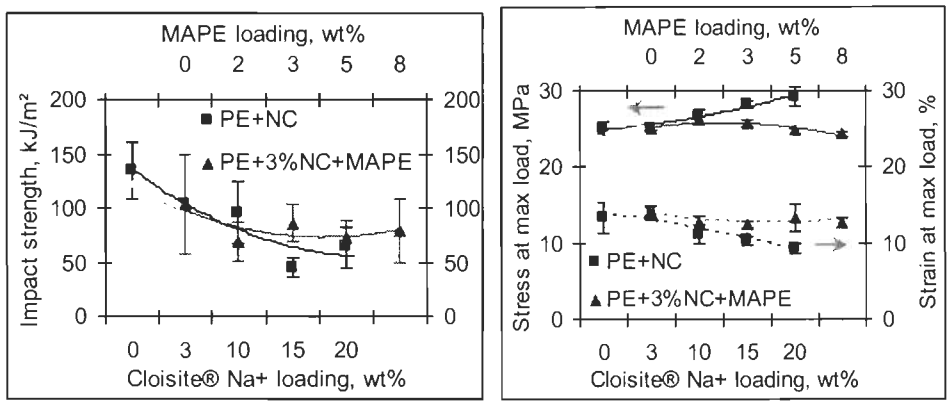

Figure 8.3 Effects of Cloisite® Na+ and MAPE on mechanical properties of Nanocomposite

It is possible that MAPE improved the tensile properties a bit as well as strain due to more interaction and adhesion between NC particles and matrix, and then these decreased slightly due to excess MAPE covering the particulates of NC forming plastic pellets with nuclear structure to saturate surface while without covalent bonding resulting in slippages among the matrix because Cloisite® Na+ was preferred to interact with polar matrix, such as MAPE. At other hand, excess MAPE resulted in self-entanglement rather than being entangled with PE matrix due to the difference of polarity.

The modulus increased significantly linearly with NC introduction, from 568MPa for pure PE to 793MPa for the nanocomposite with 20wt% NC as presented in Figure 8.4. As MAPE was introduced into the nanocomposite, the modulus increased slightly, up 12%, due to more interaction with a matrix and

stronger adhesion between NC particles and matrix while excess MAPE leads to slippages, acting as a lubricant.

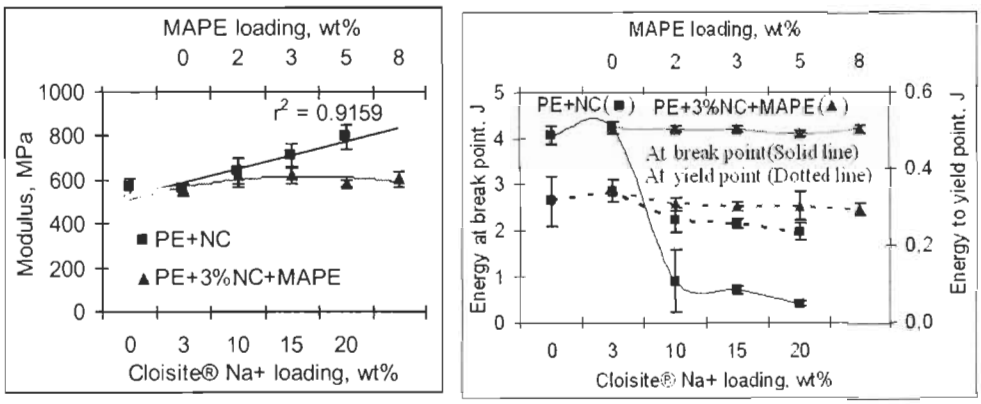

Figure 8.4 Effects of Cloisite® Na+ and MAPE loading on modulus and energy of Nanocomposite

Fracture energy of nanocomposite containing less NC increased a bit at lower content of NC and then decreased sharply with more NC introduced because the Nanocomposite with less NC has more plastic characteristics of the specimens, with more energy absorbtion at break and the efficiency of the interaction between matrix and the particles of NC was higher. Fracture energy dropped sharply upon more NC introduction due to excess particles of filler weakening the interfacial strength among fillers and matrix. The surface energy of the particles of NC was lower than that of reactive component. Moreover, the particles of NC absorbed less fracture energy which made the nanocomposite with more NC more fragile due to its harder phase and its restriction of matrix fiber entanglement.

Figure 8.5 showed that NC and MAPE loading on the difference between fracture energy and yield energy. It was concluded that nanocomposite filled with more NC would have improved deformation resistance while MAPE could enhance the plasticity leading a bit more deformation, and more MAPE leads to higher deformation.

The results from Figure 8.5 were consistent with the conclusions mentioned above. So it was concluded that MAPE couldn't improve but weaken the physical and mechanical properties of nanocomposites filled with NC while NC could improve the properties except impact strength.

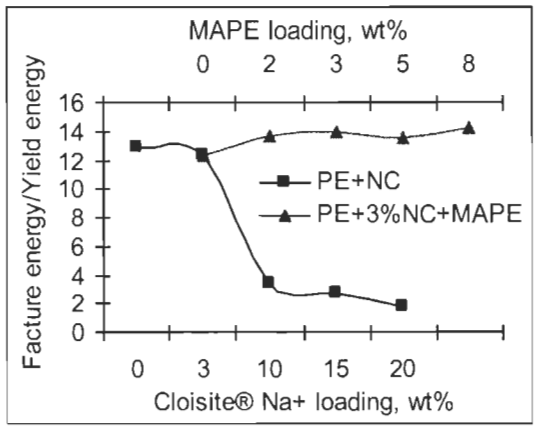

Figure 8.5 Effects of NC and MAPE loading on the energy difference of Aspen-PE composite and PE Nanocomposite

8.3.3 Effects of DCP loading on the properties of Aspen-PE composite and PE Nanocomposite

From Figure 8.6, DCP has positive influence on the impact and tensile strength of Aspen-PE composites from 56.7kJ/m² to 100kJ/m² and 38MPa to 42MPa because more wood fibers were involved in the reaction between wood fiber and PE by grafting and resulting in transferring more force onto wood fibers-MAPE-PE and fibers-PE networks.

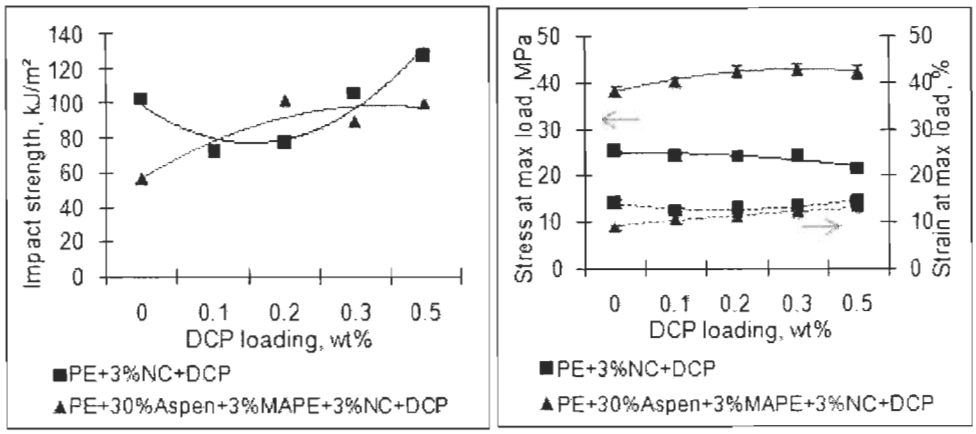

Figure 8.6 Effects of DCP loading on mechanical properties of Aspen-PE composite and PE Nanocomposite

For PE Nanocomposite, the decomposition of DCP was rapidly catalyzed by the basic NC resulting in excess radicals occurring at same time to initiate and terminate quickly, and the thermo-oxidization was speeded-up more than the oxidization in the composite with fiber in the presence of DCP resulting in impact and tensile strength decrease and increase of the modulus as shown in

Figure 8.6 and Figure 8.7. With more DCP added, more radicals of DCP were ready to radicalize and re-polymerize to form more cross-linked structures leading to improvement of the impact strength and modulus decrease. It was also concluded that the effect of DCP on impact strength of PE nanocomposite decreased it 43%, from 103kJ/m² to 72kJ/m², and then reaching 127kJ/m². For Aspen-PE composite, more impact strength could be transferred onto wood fibers by the etherification linkages, hydrogen bonding, polymer entanglement as well as mechanical interbonding. While for PE nanocomposite, the force was carried mainly by polymer chains, and would be transferred to the conjoints (NC particles) by mechanical interbonding by polar forces and physical linkages.

With more DCP added, the radicals principally radicalized and terminated PE which provided the composite with a stronger impact but weaker tensile property as well as lower strain due to the degradation of the matrices.

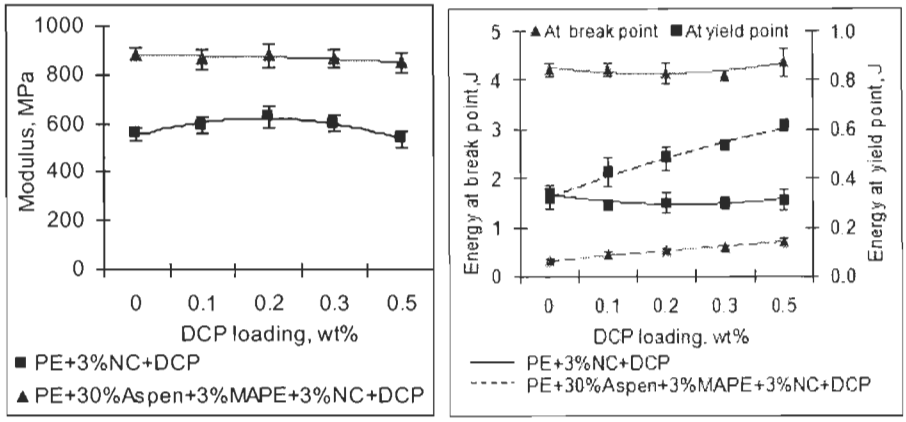

Figure 8.7 Effects of DCP loading on modulus and energy of Aspen-PE composite and PE Nanocomposite

The effects of DCP on break energy of PE nanocomposite and Aspen-PE composites filled with MAPE and NC are shown in Figure 8.7. Energy at break point of Aspen-PE composite increased steadily as DCP introduced to the matrix from 0.32J to 0.70J, up 120%, due to the formation of more matrix-wood fiber structures with radicalization.

It was also concluded that PE nanocomposite was more flexible exhibiting a high ratio of E_{Break}/E_{Yield} which is around 12-15, while for Aspen-PE composite it was near 1.00-1.16 due to the reinforcement of wood fiber and MAPE exhibiting higher stiffness resulting in almost no yield (see Figure 8.8). The material with higher ratio

of E_{Break}/E_{Yield} means higher plasticity. It was understood easily that the reinforcement of wood fiber could increase the stiffness of the matrix due to the characteristics of natural fiber leading to lower deformation.

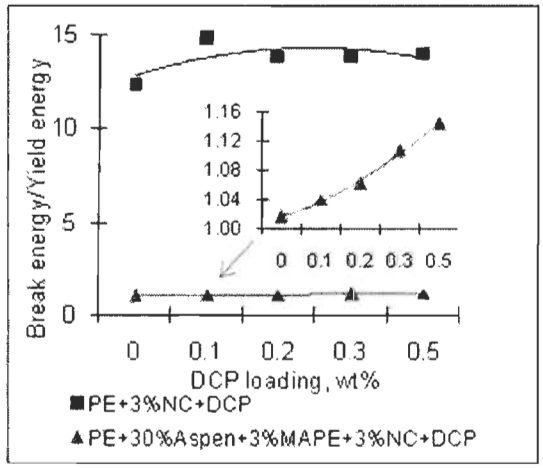

Figure 8.8 Effects of DCP loading on the energy difference of Aspen-PE composite and PE Nanocomposite

The results also revealed the nuances of the different elasticity of the composite filled with wood fiber was becoming better following the increase of DCP loading from the inserted figure in Figure 8.8 which confirmed that the introduction of DCP could improve both impact and tensile properties of the composite combined with wood fiber because DCP would perfect the stereo-structures of the composite while reducing the deformation resistance a bit.

8.4 Conclusions

The following conclusions were drawn from the above results:

(1) Wood plastic composite compounded with no-premixing, e.g. fiber, residual matrix and other fillers added at same time, could achieve the superior properties than wood fiber pre-covered by the mixture of coupling agent and small part of matrix.

(2) NC improved tensile and deformation properties of Nanocomposite except for impact strength; the modulus increased linearly following the content of NC, and MAPE visibly reduced the properties of Nanocomposite filled with NC without the reinforcement by wood fiber.

(3) DCP improved both impact and tensile strength of the composite with fiber but deteriorated them for nanocomposite. Even though DCP would improve the properties due to forming the stereo-structures, it also provided the

composite with better plasticity resulting in reducing the deformation resistance slightly.

8.5 Acknowledgements

The authors would like to thank the NSERC, Natural Centers of Excellence of Canada and Auto 21 (The Automobile of the 21st Century) for the financial support.

Chapter 9 - Antioxidant and Initiator on the Mechanical Properties of Polypropylene-Aspen Composites

Ruijun Gu and Bohuslav V. Kokta
Journal of Thermoplastic Composite Materials. 2008, 21(2):175-189.
DOI: 10.1177/0892705707086802
http://jtc.sagepub.com/cgi/content/abstract/21/2/175

Abstract: Studies on the effect of blending method, the introduction method of initiator (Dicumyl peroxide, DCP) and the blending time with antioxidant (Irganox) added on the mechanical properties of PP/Aspen composites with and without dicumyl peroxide respectively were undertaken. An optimum blending time for the composite with Irganox was obtained. The optimum content of Irganox as well as pre-mixing and the final-step feeding-method of DCP were compared to that of conventional method of blending in order to achieve the optimum values of impact and tensile strength properties.

Keywords: Composite, Polypropylene, Antioxidant, Irganox, DCP, Nanoclay, Wood fiber, Aspen, CTMP

9.1 Introduction

Wood plastic composites have become more popular due to their abundant availability, low cost, high relative strength and stiffness, low density, and renewable nature [135, 328, 329, 330, 331] as well as excellent machanical and physical properties. However, the problem of the compounding of wood fiber with a matrix may leads to poor mechanical properties of the composites due to (I) the poor compatibility between the polar hydrophilic wood fiber and the non-polar hydrophobic polypropylene may result in a weak interfacial adhesion and (II) poor dispersion of wood fiber in the polypropylene because of strong fiber-fiber interactions resluting from hydrogen bonding. Coulping agent [167, 332, 333, 334] such as maleated polyolefins [319, 328, 335, 336, 337, 338] is used to improve the adhsions between matrix and wood fiber. There are many references on dicumyl peroxide use as an initiator to graft the matrix itself or with fiber [348, 349]. On the other hand, the substantial thermal decomposition of matrix takes place at high processing temperature [356], especially the thermo-oxidative degradation which must be considered in open roll mills. Moreover, the presence and decomposition of DCP is speeding up the oxidation of matrix. So it is necessary to define a stabilizing system, especially the content of thermal antioxidants.

The purpose of this work was to find out the effect of an antioxidant on the degradation of matrice due to dicumyl peroxide addition alone or combined with a coupling agent by studying the effect on the mechanical properties.
Futhermore the influence of antioxidant and blending conditions were investigated in order to obtain optimum mechanical properties.

9.2 Experimental and materials

9.2.1 Materials

Homo-polypropylene was supplied by Montell Canada Inc. Air-dried wood fiber is aspen fiber (CTMP, 20-60 mesh) which was prepared in Centre de Recherche en Pâtes et Papiers laboratory of Centre Intégré en Pâtes et Papiers. Maleated polypropylene (MAPP) was supplied by Eastman chemical company as coupling agent under the name Epolene G-3003 polymer with 9% acid anhydride. Dicumyl peroxide (98% active DCP) was supplied by Sigma-Aldrich Chemical Co. and was used as the initiator, mp.39-41°C, and halftime 0.2 min at 190°C. Cloisite® Na^+ Nanoclay (NC) received from Southern Clay Products Inc. was used as filler. Irganox B561 (Irganox 1010/Irgafos 168, 1/4) received from Ciba was used as an antioxidant.

9.2.2 Experimental and compounding

All samples were compounded in a two-roll C.W.Brabender to study the influence of Irganox and DCP and their adding-method on the mechanical properties of PP-Aspen composite. The influence of blending time on the mechanical properties under antioxidant existence was also investigated.

9.2.2.1 Differences between pre-mixing and conventional blending method

In order to study the effect of blending method on the mechanical properties, PP-Aspen composite were blended with 3wt% MAPP and 3wt% NC at 30wt% fiber loading with pre-mixing and conventional method under the same processing time and temperature. The procedures were as follows: (I) **Conventional method:** Melting 20wt% PP with MAPP and NC at 190°C at 60 rpm, adding aspen fiber and residual PP within 7min, remixing for 5 times and each time for 5min to obtain a uniform composite sheet, then removing the composite sheet from the roller and transforming it into strips with knife according to the molder size. (II) **Pre-mixing method:** At first, coating aspen fiber with the mixture of 20wt% melting PP, MAPP

and NC before the residual PP is introduced (total time was limited in 7 min), followed by the same steps as described in (I).

9.2.2.2 Different addition-method of DCP with/without Irganox

PP-Aspen composite were prepared with different adding-method of antioxidant and initiator (PP reinforced with 20wt% fiber as reference, named PPF20). The procedures were same as follows except the feeding time of DCP. **A**: DCP was added after the residual PP and aspen fiber added with/without 1.0wt% Irganox addition within 10min from aspen fiber addition; **B**: DCP was added before peeling and molding. The composites were reblended with these steps for 5 times and each time for 5 min to obtain a uniform sheet, and the composite sheet was removed from the roller. Sample trips were made fitting the molder size with knife.

9.2.2.3 Different influences and functions of Irganox and blending time

PP-Aspen composites with 30wt% aspen fiber reinforcement and 3wt%MAPP and 3wt%NC (named PPF30M3N3) with 0, 0.2wt% DCP were used to explore the effects of Irganox with or without DCP.

Moreover we prepared PP composite reinforced with 30wt% fiber and 3wt%MAPP, 3wt%NC, 0.2wt%DCP and 1.0wt% Irganox (named PPF30M3N3D0.2I0.1) to study the effects of blending time on the mechanical properties varying from 25 to 60 min. The composites mentioned above were prepared with conventional method with DCP introduced at final step. It's important to note that Irganox was introduced as a component of the mixture of melted 20wt% PP, MAPP, NC at 190°C at 60 rpm before addition of the residual PP and aspen fiber.

9.2.3 Compression molding

The composite strips were molded to dog-bone shape specimens (ASTM D638 Type V). 24 specimens (12 for tensile testing and 12 for impact strength testing) were simultaneously put in a DAKE molder covered by metal plates on both sides, heated at 192±2°C, pressed for 15 min under a pressure of 20MPa (25-26 tons), and then cooled down to below 100°C by circulating cold water in the press. The approximate dimensions of tensile specimen were as follows: width 0.26-0.33cm and thickness 0.31-0.33cm. And the width of impact specimen was 0.28-0.30cm and thickness 0.15-0.17cm.

9.2.4 Mechanical tests

All the specimens were conditioned in testing room, and measured with micrometer after polishing. Mechanical measurements were made on an Instron tester (Model 4201) at 23°C and 50% level of relative humidity. Samples properties were automatically determined by the Series IX Automated Materials Testing system-Version5.20 under ASTM D638.

9.2.5 Determination of tensile impact

Tensile impact strength (un-notched) was measured at 23°C using a TMI impact tester (TMI No 43-01) which was equipped with a special fixture for test specimen according to ASTM D1822. The maximum energy of the pendulum was 2J. Test specimens were obtained from compression-molded plates.

9.3 Results and Discussions

9.3.1 Effect of blending method on the properties of PP/Aspen/MAPP/NC composites

PP-Aspen composite with 3%MAPP and 3%NC (PPF30M3N3) were prepared using either the conventional method or pre-mixing method respectively. The mechanical properties obtained by different method of blending were somewhat different in impact and tensile properties as shown in Table 9.1. Superior impact strength with conventional method was obtained (up 95% higher than from that of pre-mixing) due to the reaction of more PP and wood fiber with anhydride groups of MAPP leading to more branching linkages among matrix. On the other hand the pre-mixing leads to better adhesion between wood fiber and matrix which leads to slightly better tensile properties. The composite prepared with pre-mixing method had the most anhydride groups to react with wood fiber and a bit of PP which can't form big branched structures in whole matrix, and also had excessive PP/MAPP mixture coated on the fibers which made the fibers stiffer and encircled by residual PP in following processing. So, the bonds between anhydride groups of MAPP and hydroxyl groups of fiber were more dispersed non-uniformly in whole composite than with the conventional method which leads to a bit inferior impact strength. At same time, the adhesion between wood fiber and matrix was strengthened which leads to higher tensile properties which was the reasons that the impact strength was up 95% while the tensile strength was down 5%.

The following conclusion could be drawn from Table 9.1. The strain at different point of the composite blended with pre-mixing was superior to that of the composite prepared with conventional method as well as modulus and energy.

Table 9.1 Mechanical property of PP-Aspen composites with MAPP and DCP

Properties	PPF30M3N3			
	Pre-mixing		Conventional	
	Av.	s.d.	Av.	s.d.
Impact strength, kJ/m²	41.2	----	80.5	----
Stress at max load, MPa	45.8	0.67	43.5	2.74
Stress at auto break point, MPa	45.7	0.61	43.5	2.75
Stress at Z-slp yield point, MPa	45.7	----	44.0	----
Strain at max load, %	8.90	1.16	8.54	0.66
Strain at auto break point, %	8.98	1.364	8.57	0.65
Strain at Z-slp yield point,%	9.03	----	8.43	----
Modulus, MPa	974	46.5	921	56.6
Energy to yield point, J	0.41	0.09	0.36	0.05
Energy to break point, J	0.42	0.11	0.37	0.06

9.3.2 Effect of Irganox and DCP adding-method on the properties of PP/Aspen composites

The results of the effect of DCP introduction method on the impact and tensile properties of the composite (PPF20 as ref.) with/without Irganox are listed in Figure 9.1. The tensile properties of the composite initiated with DCP at final-step was superior to those of the composite added at early-step because the reaction time of DCP was longer, the degradation and oxidation on wood fiber and matrix was stronger. Moreover, very little residual DCP was left to crosslink the matrix when molding after longer compounding. It was also concluded that the properties of the composite with DCP were worse than the properties of composite without it and the antioxidant was more efficient in preventing the mechanical properties from worsening in longer compounding time. During longer compounding time in the presence of DCP, the effect of inhibitory action became clearer. The observed difference in strength properties of the composite with added DCP in final-step was attributed to the different function. It was assumed that the Irganox would work as an antioxidant when DCP was introduced at early-step while after that it would work mainly as a filler to reduce the adhesion between wood fiber and matrix. So, whenever DCP was added either at final or early-steps, the mechanical properties of the composite with DCP were inferior to that of the composite without DCP. Irganox worked more as an antioxidant when the compounding time with DCP was longer.

From Figure 9.1, it's obvious that the mechanical properties were weakened by DCP addition as presented in [357] while at near 200°C the rate of DCP decomposition is too high and yields high radical concentration at the beginning of the process [384] to lead to lower molecular weight which influences the impact strength [355]. These maximum amounts of radicals [385, 386] would abstract hydrogen atoms from matrix molecules to produce alkyl radicals which will be reformed with wood fiber and itself [387]. Unfortunately, lots of free radicals of DCP escaped and more free radicals of matrix were not formed, but reacted with matrix/fiber which leads to the decomposition of PP [356, 357, 484] as well as wood fiber [353] due to shortening their chains at an open-air roller. In consequence, in order to minimize matrix degradation we adopted method B in our following experiments meaning that samples were processed only 3 minutes with DCP on roll mills before molding. In addition, the DCP should be mixed with polymer and fiber under its decomposition temperature or an injection method should be used.

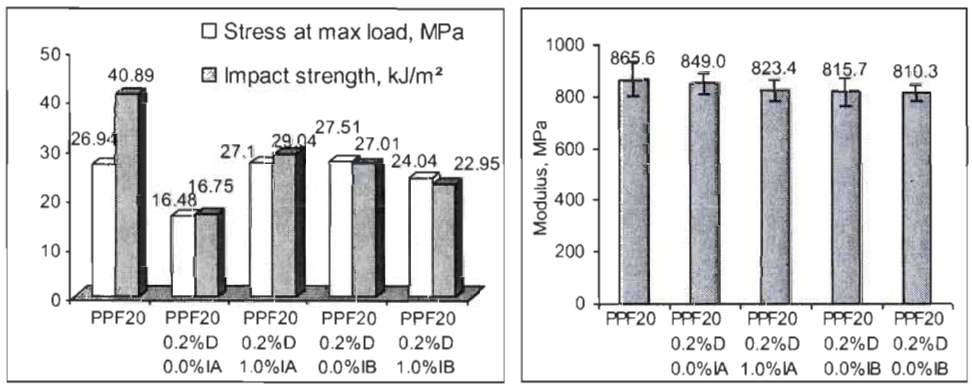

Figure 9.1 Effects of Irganox and DCP adding method on the impact/stress and modulus of the PP-Aspen composite at 20wt% level

Note: D-DCP; I-Irganox; A-DCP added by Method A and B-DCP added by Method B

The modulus of the controlled reference was slightly higher than the others due to the introduction of DCP. With DCP the modulus of the composite with Irganox was a bit higher (0.6-3.1%) when compared to the composite with no Irganox.

9.3.3 Effects of the anti-degradation of Irganox on the mechanical properties of the composites with or without DCP added

The effect of antioxidant on the mechanical properties of the PP-Aspen composites with MAPP and NC with or without DCP was studied. The mechanical properties were tested to evaluate the influence of Irganox on the composites as illustrated in Figure 9.2. The impact strength for the composite with DCP was inferior to that of

the composite without DCP because less free radical was available to crosslink due to the opening in processing vessel. DCP was also speeding up the oxidation of matrix. It's worthy to note that Irganox inhibits impact strength from being lowered as DCP is introduced.

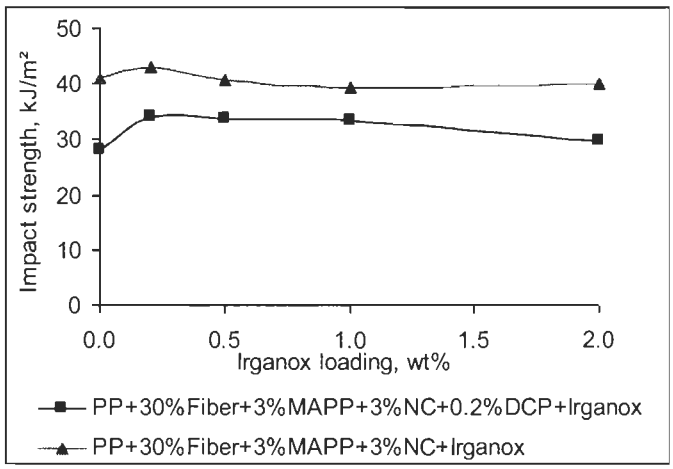

Figure 9.2 Effects of Irganox loading on the impact strength of the composites with or without DCP

There was an optimum value of Irganox to achieve highest impact strength of the composite with initiator around 0.2 wt% level. It was confirmed that antioxidants reacted preferentially with radicals yielded by decomposed DCP, retaining the crosslinking of matrix by increased antioxidant content [387]. The content of antioxidant at 0.2wt% level was just right to limit destructive oxidation induced by DCP. But in excess the residual Irganox works more as a filler same way as the antioxidant introduced into the composite without DCP and lead to the weakening of the impact properties.

The observed increase in the tensile strength properties of PP-Aspen with MAPP/NC added following the introduction of DCP was in agreement with the impact strength from Figure 9.3 as well as strain. The antioxidant worked as a filler no existence of initiator to block the adhesion of components among the matrix each other to lead to inferior properties.

So, it was concluded that optimum Irganox addition could prohibit initiator from lowering the mechanical properties of the composite, even though the properties were still inferior to the composite without DCP.

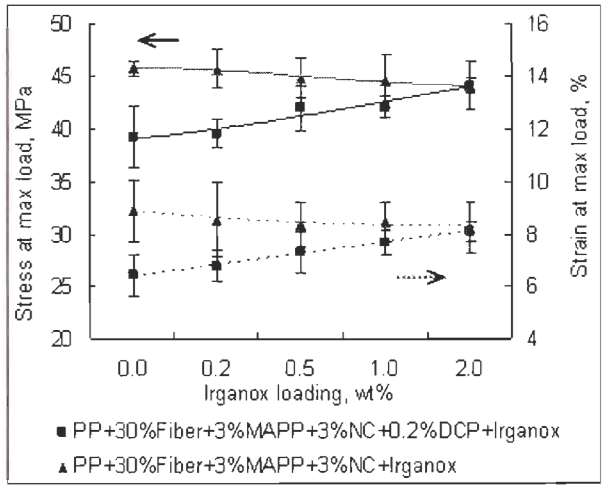

Figure 9.3 Effects of Irganox loading on the stress and strain at max of the composites with or without DCP

Figure 9.4 illustrates that the Irganox content (below 2.0wt %) has no noticeable impact on the modulus of the composite with or without DCP.

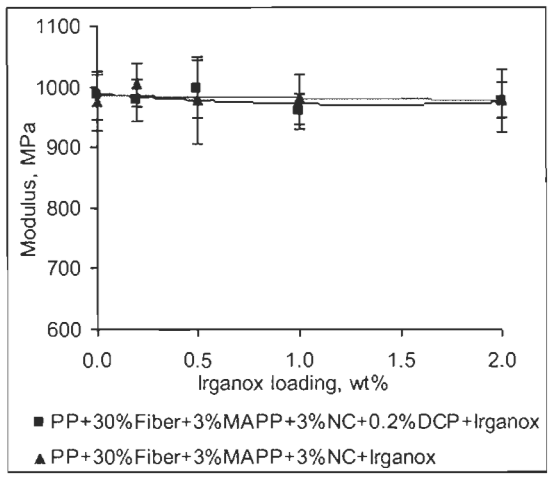

Figure 9.4 Effects of Irganox loading on the modulus of the composites with or without DCP

The changes of energy to break point due to DCP are presented in Figure 9.5. The energy to break point of the composite with DCP increased steadily (up 50%) with Irganox content increasing while the composite without DCP showed decrease of about 17.3%. In general, the composite without DCP has superior abilities to absorb more fracture energy at same content of Irganox loading. That is to say DCP has negative influence on the fracture properties which as similarly shown in previous research [357] when Brabender mill was used for compounding.

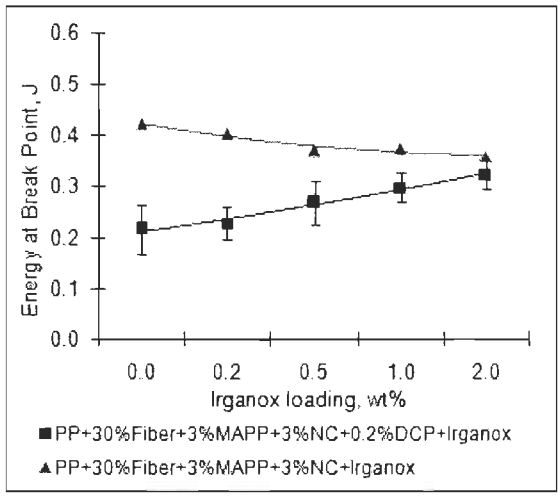

Figure 9.5 Effects of Irganox loading on the facture energy of the composites with or without DCP

9.3.4 Effects of the blending time on the mechanical properties of the composites with Irganox

Different blending time was used to study its influences on the mechanical properties of Aspen-PP composite (PPF30M3N3D0.2I0.1) as described in Figure 9.6-Figure 9.9.

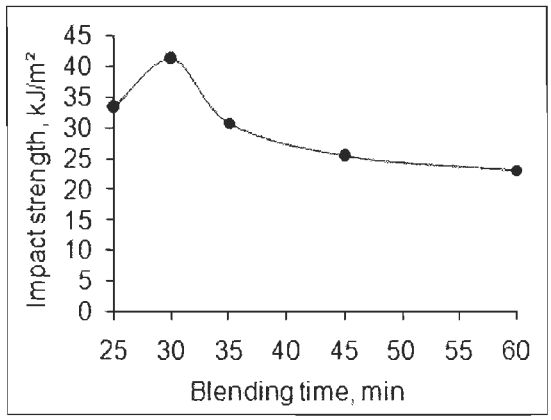

Figure 9.6 Effects of blending time on impact strength of the Aspen-PP composite

Figure 9.6 shows that the impact strength of the composite increased and then decreased as blending time extended and achieved an optimum value at 30mins due to the fact that an antioxidant compensated for the degradation due to DCP. As blending time extended longer, high operation temperature might heightened the degradation of the natural wood fibers and polymer matrices resulting in the inferior impact strength [356, 357, 484], though the impact properties benefited from the uniform distribution of additives.

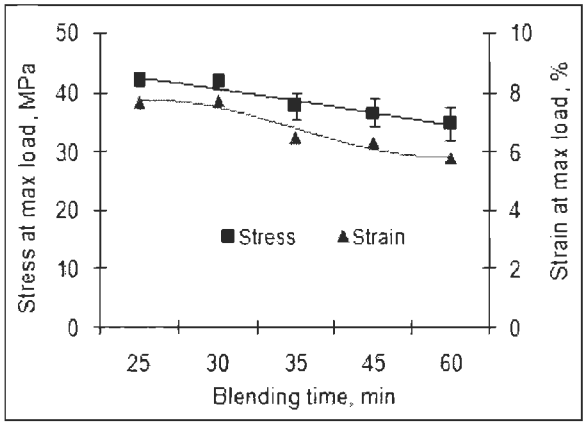

Figure 9.7 Effects of blending time on max stress and strain of the Aspen-PP composite

The tensile strength as well as strain decreased with the increase of blending time as indicted in Figure 9.7. Result indicated that the degradation of the matrix and wood fiber [356, 357, 484] would be heightened due to longer blending time during high procedure temperature, and it could also be fiber attrition. Irganox should react with free radicals of DCP and hinder free radicals from hurting the matrix and wood fiber. So there was an optimum time to protect the composite from degrading, mainly the matrix.

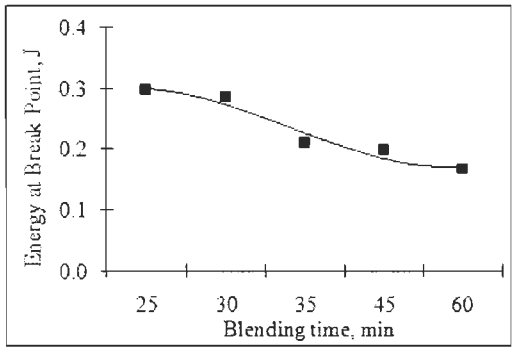

Figure 9.8 Effects of blending time on energy of the Aspen-PP composite

On the other hand, the results obtained from Figure 9.8 shows that the energy decreased due to the same reasons that either short fiber chains or decomposed matrix/wood fiber has no benefits of the mechanical properties [355]. More decomposed matrix and aged and shorten wood fiber would form during long-term procedure operation at high-temperature.

The modulus of the composites showed no changes as blending time extended as seen in Figure 9.9. It was concluded that the rate of DCP decomposition at 200°C was too high to yield high free radicals at beginning [384] and the degradation of

matrix and wood fiber occurred at beginning too. There were no free radicals from DCP, matrix or wood fiber as time passed because they either have escaped from the composite through persistent mixing or have terminated by Irganox or themselves.

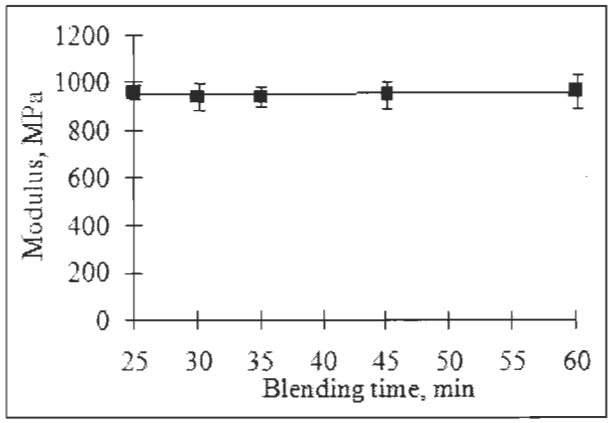

Figure 9.9 Effects of blending time on modulus of the Aspen-PP composite

Though there was an amount of antioxidant, a tiny amount of aging in wood fiber takes place and leads to a composite a bit stiffer at high processing temperature and long processing time. The degradation of polypropylene also leads to its chain scission to higher modulus in solid state due to an increase in crystallinity. On the other hand, the reformation of new chemical groups due to degradation leads to lower modulus because of a decrease in crystallinity. So the result shown in Figure 9.9 was the co-effect which was counteracting each other or the fine difference was difficult to be observed due to the potentially confusable functions of experimental errors. It was difficult to relate the degradation of matrix to the changes of modulus.

9.4 Conclusions

The introduction of DCP at final stage of compounding has a positive influence on impact strength of the composite due to the matrix grafting. The influence of DCP adding-method, Irganox and blending time on mechanical properties of the composite has been investigated in details.

Irganox has completely different influences on the mechanical properties of the composite with or without DCP. The mechanical properties of the composite with DCP were increasing because of the protection of Irganox. Even though under the protection of antioxidant, DCP still has weakened the mechanical properties of the composite with coupling agent and filler. In the composite without DCP, the mechanical properties were decreasing due to the decrease of the adhesion among matrix caused by particles of NC and Irganox.

Blending time has important influences not only on impact strength but also on tensile properties. There was a peak value in the trend of impact due to the balance between thermal oxidative degradation and the improvement of interfacial bonding from the finely distribution of components, especially natural wood fiber, NC, and Irganox.

The DCP amount and its additional type have a small influence on the modulus of the composite at different blending times as well as the Irganox content. As a blending time increased, the modulus showed no visible change compared to the experimental error. We drew a conclusion that modulus was related to the amount and type of the components.

9.5 Acknowledgment

The authors wish to thank the NSERC and National Centers of Excellence of Canada-Auto 21 for its financial support.

Chapter 10 - Water Behavior and Mechanical Characteristics of Wood Plastic Composites Reinforced with Organo-Nanoclays

Ruijun Gu and Bohuslav V. Kokta

Some parts were presented in Proceedings of the 96th EXFOR & PAPTAC Annual Meeting. Montreal, Quebec, Canada. 2-3 February 2010: D126-136
Full manuscript is to be published in Journal of Reinforced Plastics and Composites

Abstract: Nanomer and Cloisite are the popular commercial nanoclays (NC) available in the market. The mechanical properties of wood plastic composite (WPC) based on linear low density polyethylene with or without wood fiber are compared for different added nanoclays. In addition, the moisture uptakes at 23°C and 45% relative humidity (RH) and water uptake/loss after immersion in water are evaluated. I.34TCN type nanoclay as well as Cloisite Na+ lead to composites with superior mechanical properties and better water resistance behaviors compared to the other kind of nanoclays. Discoloration occurs to WPC reinforced with unmodified NC.

Keywords: Organo-nanoclay, Polyethylene, Water loss, Water uptake, Wood fiber, Wood plastic composite

10.1 Introduction

Wood fiber is available worldwide and biodegradable[82, 485]. WPC combines the performance and cost attributes of both wood and thermoplastics. Biodegradable wood fiber are low cost, abundant [45, 95] with low disposal cost [91, 485] which helps WPC with biodegradablity [486, 487, 488]. This green composite material gains an increasing niche in North America market [111, 117] because of its improved compatibilization and adhesion to hydrophobic polyolefin [81, 92, 314, 315, 316, 478] as well an initiator [330, 348, 349, 380, 381] by chemical bonding [321].

Surface modified NC are widely used in technological applications [489] because of their improvements of strength [490, 491], modulus[489], improved solvent resistance [28, 492], controlled biodegradability [44], and water vapor transmission resistance [493] which are dependent on the degree of dispersion of inorgnanic phase in polymeric matrix [494]. Wood fibers would also help in the decrease of the deposition due to its polarity [495, 496, 497, 498, 499], and even reinforce the polyolefin and replace the mineral fillers to reduce cost, enhance appearance, lower weight and improve properties [155, 398, 399] and help environmental recycling [81,

121, 403, 404]. In the recent years, numerous researchers, including our group, have already worked on the introduction of NC in WPC with PE matrix [388, 389, 405, 453, 500, 501, 502] leading to improvement in the mechanical properties of nanocomposite [503, 504, 505, 506].

WPC has been widely used to replace impregnated wood in many outdoor and neat plastics applications [99, 110], and also in biomedical field today [507, 508]. Water uptake has attracted attentions since wood particulates are hydrophilic. Water is absorbed from the atmosphere via hydrogen bonding by hydroxyl and oxygen containing groups [509] which results in fiber swelling and adverse dimensional changes and fungus growth [56]. Although some strength properties of maleated WPC were fully recovered after desorption [510], WPC materials could crack due to the pressure generated by the fiber swelling. Once WPC was cracked, which will decrease their tensile strength [511], it cannot recover even after desorption due to further penetration of water molecules within the composite structures. So, possible attempts to resist such effects are of interest when designing WPC for outdoor applications. An attempt to control the undesirable water uptake was done by removing lignin and hemicellulose [512] or fiber acetylation [511, 513]. However, there are no publications on water uptake and water loss as a function of different NC incorporated in wood fiber PE composites.

In this study, both bleached wood fibers and maleated polymer were employed to produce WPC with improved mechanical properties and water uptake resistance as well as a study on the effects of differently organically surface modified NC on the properties of PE composite which were carried out. An originally novel finding on the functions of NC particles was revealed by the water uptake and water loss behaviours.

10.2 Experimental

10.2.1 Materials

Thermoplastic: Linear low density polyethylene (Novacor® HI-0753-H) was donated by NOVA Chemicals. Its melting mass-flow rate is 1.0g/10min (ASTM D1238). Its specific density is 0.92g/cm^3 (ASTM D792).

Wood fibers: Industrial bleached chemi-thermo-mechanical pulp of aspen (BCTMP, Brightness 82-85% ISO) received as a gift from Temcell Inc (Temiscaming division) was used. The pressed bale wood pulp was air-dried and ground at our laboratory to

produce fine fibers after soaking and loosening. Particles that were passed through a 20-mesh but retained on a 60-mesh screen were employed in this studies. Bleached wood fiber in certain particle size helps us in finding out the effects on water resistance by lignin and fiber length.

Coupling agent: MAPE (maleated polyethylene, G2010) was supplied by Eastman chemical company (Kingsport Tenn.). The content of maleic acid grafts is 1.5% and the molecular weight is 15,000.

Initiator: Dicumyl peroxide (98% active DCP) supplied by Sigma Chemical Co. was used as an initiator. Its halftime is 1 min at 171°C.

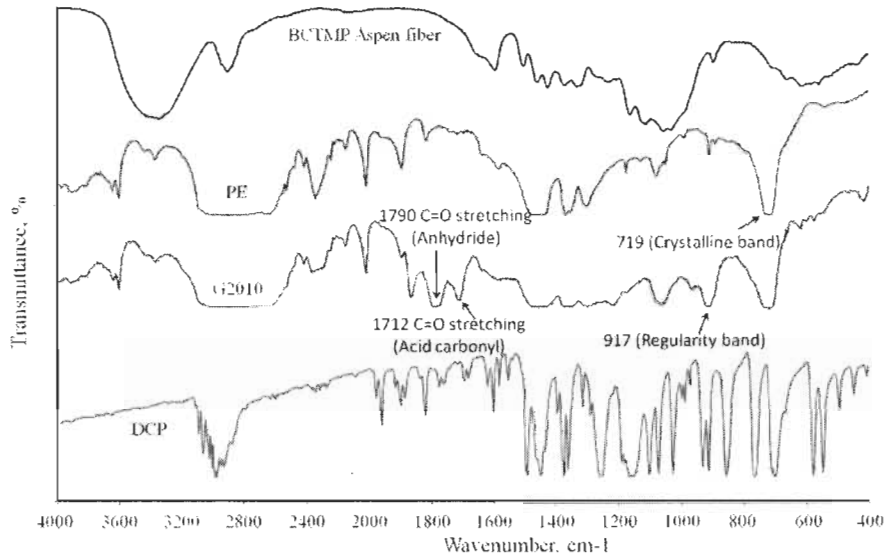

Figure 10.1 FTIR spectra of used materials in this study

Nanoclays: Seven commercial nanoclays received from Southern Clay Products Inc. and Nanocor Inc. were used in this study. Except for Cloisite Na+, the NCs were surface modified montmorillonites by surfactants with various molecular structures. The physical data are summarized in Table 10.1. The nanoclays can be divided into five families according to the structure of the surfactants. Cloisite 10A and I.28E are clays modified by ammonium salts with a single alkyl (tallow) tail. The surfactant used in I.34TCN is ammonium salts with two alkyl (tallow) tails. I.44P is modified by ternary amine with two alkyl (tallow) tails. I.30E is modified by primary amine with a single tail while I.31PS is modified by primary amine containing silane with a single tail. Surfactants in I.34TCN has hydroxyl group attached to either the tallow tail or the ammonium head. The hydroxyl group has crucial impacts on the properties and structure of the composites.

Table 10.1 Typical Physical Properties Bulletin of NC

Type	Physical properties			
	Surfactant†	Chemical chain Ramification, tail	Particle size μm	Density kg/m³
Closite® Na+	None	--	2-13	336
Closite® 10A	125meq/100g dimethyl benzyl hydrogenated tallow quaternary ammonium chloride	1	2-13	265
I.28E	25-30wt% trimethyl stearyl ammonium	1	8-10	420
I.34TCN	25-30% methyl dihydroxyethyl hydrogenated tallow ammonium chloride	2	16-22	300-360
I.44P	35-45wt% dimentyl dialkyl (C14-C18) amine	2	≤20	200-500
I.30E	25-30wt% octadecyl amine	1	8-10	410
I.31PS	15-35wt% octdecyl amine and 0.5-5wt% aminopropyltriethoxysilane	1	≤20	200-500

† Tallow (alkyl) consists of 65% C18, 30% C16, and 5% C14.

10.2.2 Preparation of WPC

All the sheets were prepared by a two-roll mill according to Schedule 10.1 to study the influence of wood fiber with the presence of the compatiblizers as well as the changes of NCs on the mechanical properties and their characteristics. 22 specimens (10 for tensile strength testing and 12 for tensile impact strength testing) were simultaneously pressed into sheet trips in a dog-bone shaped mould (ASTM D638 Type V for tensile strength and ISO 8256 Type II for tensile impact strength).

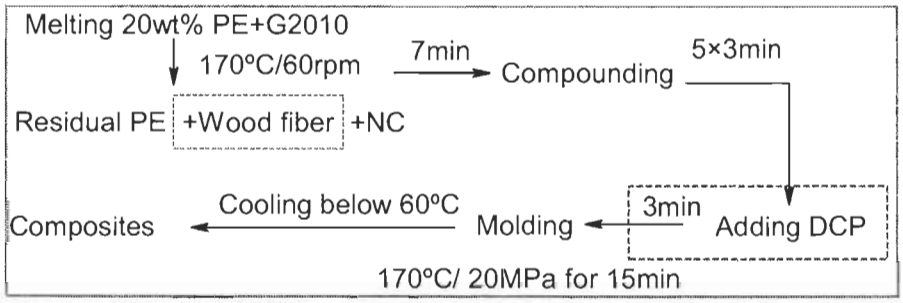

Schedule 10.1 Compounding and molding conditions

The approximate dimension of tensile specimen was 0.31-0.32cm in width and 0.28-0.32cm in thickness while the width of impact specimen was 0.29-0.35cm and the thickness was 0.14-0.15cm. The specifications of the two roll mill were: 30 cm length, 15 cm radius, 0.6 gear ratio and 60 rpm roll speed.

10.3 Characterization

10.3.1 Mechanical tests

All the specimens were conditioned at 23°C and 45% relative humidity, and then width and thickness were measured after being polished. The tensile test was performed using an Instron machine (Model 4201) according to ASTM D638.

10.3.2 Determination of tensile impact

Tensile impact strength (un-notched) was measured with Zwick tester at ambient temperature (23°C), which was equipped with a special fixture for test specimens according to DIN 53448. The maximum energy of the pendulum was 2J.

10.3.3 Fourier transform infrared analysis

FTIR is used to reveal the chemical structures of wood fiber and polymer as well as the nature of NC with different surfactants.

Sample preparation: 0.5mg of oven dried fraction of each sample are grinded with 100mg of KBr. 13mm KBr pellets are prepared in a standard device with 10MPa pressure for 5 min under 700mmHg vacuum. The thickness of the pellets is 200μm. Polymer films are prepared by casting melted polymers on the 13mm stainless pressed column, and then being pressed at the same condition to get 700μm films.

Spectra were rationed against pure KBr or blank on a Perkin Elmer spectrophotometer (System 2000 FTIR) at a resolution of $4cm^{-1}$ with a coaddition of 60 scans for each spectrum. Spectra normalization of NC was performed with Spectrum V3.02 software from Perkin Elmer at the peak of H-O-H (1650-1630 cm^{-1}). No baseline correction was used.

10.3.4 Dimensional stability

Tensile specimens were cut into $25\times8.6\times3mm^3$ pieces and used for the measurement of moisture uptake and water uptake. Three specimens from each sample were weighed after conditioning at 23°C and 45% RH for 1 week, and then all specimens were oven-dried at 105°C for 3 days to constant weight. The specimens were immersed in the bottles with distilled water and kept at 23°C for 10, 20, 30, 40 and 56 days for sorption of water. Mass of the samples was measured after removing them from the bottles at regular days. The samples were wiped with tissue paper to remove free water from surface before weighing within 0.5 min of removal from the water before re-immersing them back into the water. Finally, all specimens were

oven-dried at 105°C for 1 week. The water uptake at any times (Wt)) and the moisture uptake and the water loss were calculated according to the following equation:

$$\text{Water uptake } (\%) = \frac{(M_t - M_0)}{M_0} \times 100 \qquad \text{Equation 10.1}$$

$$\text{Moisture uptake } (\%) = \frac{(M_0 - M_D)}{M_D} \times 100 \qquad \text{Equation 10.2}$$

$$\text{Water loss } (\%) = \frac{(M_{D56} - M_D)}{M_D} \times 100 \qquad \text{Equation 10.3}$$

where

M_t: Mass of sample at exposure time t
M_0: Mass of conditioned sample t =0
M_D: Dried mass of sample before immersion
M_{D56}: Dried mass of sample after immersion 56days

10.4 Results and Discussions

10.4.1 Mechanical properties

10.4.1.1 Effect of wood fiber loading on the properties of WPC

Wood fiber was employed as reinforcement materials for thermoplastics industry due to its higher fiber aspect ratio compared to wood flour [341]. Generally, wood pulp fiber was typically used to improve strength as well as stiffness due to the stress transfer from the matrix to the fiber [87, 113, 114, 116] above a critical fiber length. This shortest pull-out length of fiber was called the critical fiber length leading load transfer length to reach its maximum value [442]. Stress transfer happens only if the bond between the matrix and fiber is good when the fibers are of finite length. Osswald reported [442] that if the fiber length is less than the critical length and the matrix can't effectively grip wood fiber to take the strain, it will slip, and be pulled out, instead of being broken under tension. So, the strong bond between the matrix and wood fiber should be built-up by chemical and physical means [444, 445] except the critical length to bear the load [443].

In the following discussion, the different mechanical properties of WPC were compared after the compatibility improvement by G2010 and DCP. The results of impact strength, tensile strength, elongation, and modulus tests on WPC made with different load of wood fiber are presented in Figure 10.2-Figure 10.5. Results show

that using different fiber proportions had an important effect throughout the WPC manufacturing processes.

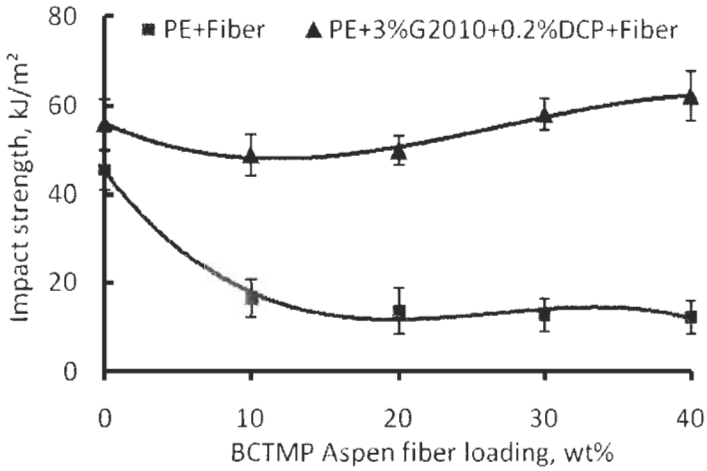

Figure 10.2 Effects of fiber loading on impact strength of WPC

Impact strength, tensile strength, modulus, and elongation at maximum load provide an excellent measure of the degree of reinforcement provided by the wood fiber to the composites [447]. Due to the incompatibility between the matrix and the wood fibers, impact strength of incompatibilized WPC decreases as a function of the content of wood fibers (see Figure 10.2). Impact strength decreases 73% from 45kJ/m² of neat PE down to 12kJ/m² as 40wt% of fibers were introduced. Upon the improvement of compatibility, impact strength is improved upward 11% from 56kJ/m² of virgin PE to 62kJ/m² for the composites with 40wt% of fibers. The introductions of wood fibers lead to more bridges formation via ester links which increased the efficiency of the impact force transfer.

Since the tensile strength depends on the weakest parts of the composites, the tensile strength of incompatiblized WPC decreases by incorporating bleached aspen fiber due to the poor adhesion between hydrophobic PE and hydrophilic wood fiber (see Figure 10.3). The tensile strength drops 24% from 25MPa for neat PE down to 19MPa for 40wt% fiber employed. The effect of fiber bundle content on the tensile strength is consistent with the results reported by Selke [91] and Raj [360].

As the compatibilizer is introduced, that is G2010 and DCP, the compatibility between wood fiber and the matrix must be improved [92], which leads to superior tensile strength. The tensile strength is also enhanced by forming more chemical bonding between the migration of maleated PE and wood fibers since enough fibers provide more active sites on surface for esterification, that is hydroxyl groups. Thus,

more ramified structures would be formed as more fibers combined which increase the tensile strength due to load transfer [87, 113, 114, 116] while limiting its deformation (see Figure 10.4), and also producing more bonds at fiber ends at the same time to maximize stress transfer [116]. On the other hand, more wood fiber introduced could eliminate the migration of maleated polymer and avoid slippages [92, 316, 453].

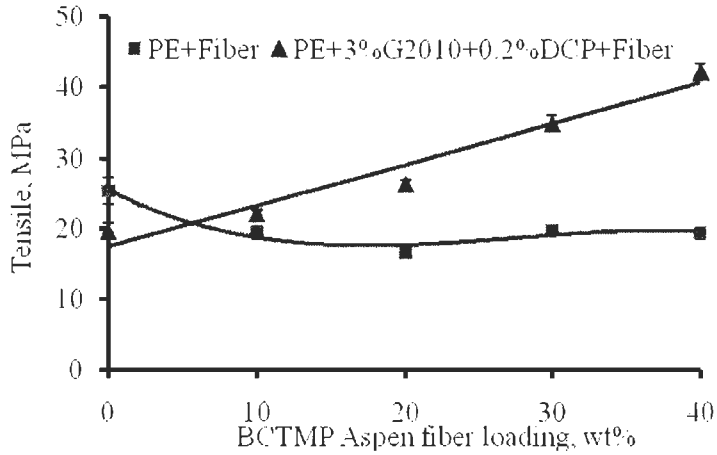

Figure 10.3 Effects of fiber loading on Tensile strength of WPC

Decreasing elongation and increasing modulus with increasing content wood fibers with and without a coupling agent are presented in Figure 10.4-Figure 10.5. The increase in elongation and decrease in tensile strength of PE modified by G2010/DCP originate from the addition of low MAPE molecules. The elongation of WPC increases 20% from 11% for virgin PE to 13% at 10wt% fiber content, the additional incorporation of wood fibers tends to decrease elongation and increase modulus due to higher modulus of wood fiber acting as backbones in the matrix [92, 202]. This significant elongation difference is in concordance with the improvement of interfacial adhesion. In general, wood fibers have low elongation and they restrict the polymer molecules flowing past one another, exhibiting better resistance to deformation which concords with the published results [56, 360]. However, the reticulated structures are formed in the composites after the addition of coupling agent/initiator which leads to high elongation as a function of wood fiber addition due to strong interactions and improved adhesion. This elongation behavior is typical of reinforced thermoplastic in general and has been reported by many researchers [56, 360].

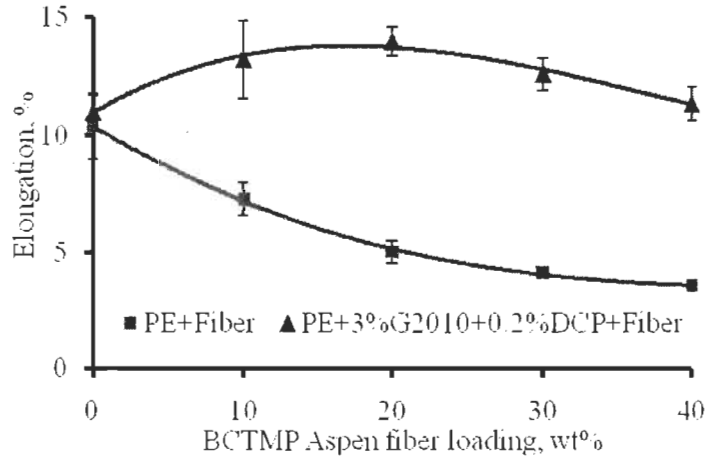

Figure 10.4 Effects of fiber loading on Elongation of WPC

The effect of fiber loading on the tensile modulus is shown in Figure 10.5. The modulus increases slightly which principally benefits from the attribution of the morphology of wood fiber, for example high modulus of rupture, and the changes of the crystal morphology [376] as well as the distribution of wood fiber. Similar results were also reported by Raj et al. [360] and Yuan et al. [202].

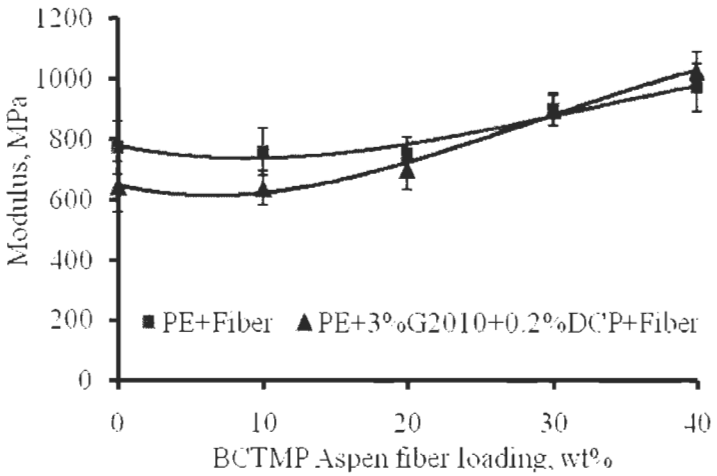

Figure 10.5 Effects of fiber loading on Modulus of WPC

Although the degradation of the matrix caused by the presence of DCP could hurt the modulus, it also makes wood fiber stiffer due to the thermal-oxidation [353]. The modulus of incompatiblized WPC is little higher than that of the composites with additives because the compatibility is improved by MAPE and DCP through grafting and crosslinking reactions. Referring to the works of Yin et al. [376], it was concluded that the crystallinity degree of PE around wood fiber was increased which helped in modulus augmentation [202] when 40wt% fiber was used.

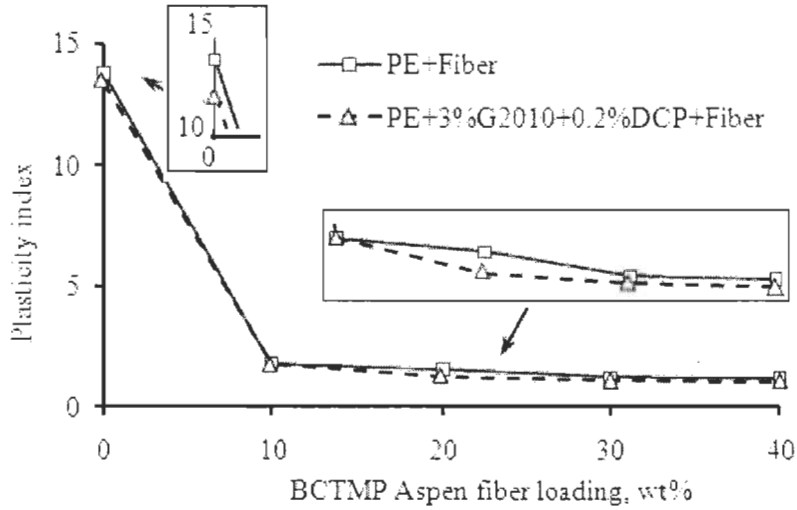

Figure 10.6 Effects of fiber loading on Plasticity of WPC

The ratio of the energy to break point to the energy to yield point is defined as the plasticity index to monitor the rheology of WPC in Figure 10.6. It is clearly seen that the value of plasticity index decreases dramatically with the increase of fiber content resulting in making WPC more brittle. Migneault et al. [446] reported that the torque would increase as more fiber presented leading to the decrease of the rheology of WPC. Hence, the fibers could produce strong frictional force during compounding, and exhibit high viscosity, to cut the fibers and form more over-refined fractures during processing. Obviously, the improvement of the compatibility could not yield the satisfied ductility of WPC. We could draw a conclusion that the characteristics of wood fiber dominate this contribution compared to that of other additives.

10.4.1.2 Effects of the changes of NC on the properties of the nanocomposites

Melt compounding is a versatile process to prepare PE nanocomposites. Melt intercalation enables the layered silicates to be mixed with the polymer matrix in molten state which requires the polymer to be compatible with the clays. However, hydrophilic clays and hydrophobic polymers are not compatible in their virgin states. Surface modification of clay has commonly been used to achieve a greater compatibility of the clay and polymer, which leads to an increase the d-spacing between silicate interlayers [489, 514]. The introduction of small molecular weight alkyl chain ions converts the clay surfaces from hydrophilic to organophilic [515]. FTIR spectra of the organo-NCs are summarized in Figure 10.7. The typical bands for oxydes are assigned to the peaks of Si-O-Si, Si-O-Al and Si-O-Mg stretching

around 1050cm^{-1} and the broad stretching peaks of the hydrates including Al-OH and Si-OH appear at 3600cm^{-1} [516, 517, 518]. The peaks at 1640cm^{-1} are associated with the bound H_2O due to its non-removal under the oven-drying [516]. The characteristic bands of MMT at 523cm^{-1} and 466cm^{-1} are the stretching vibration of Si-O bonds, the bending vibration of Si-O-Al and the Si-O-Si bending vibration, respectively [517].

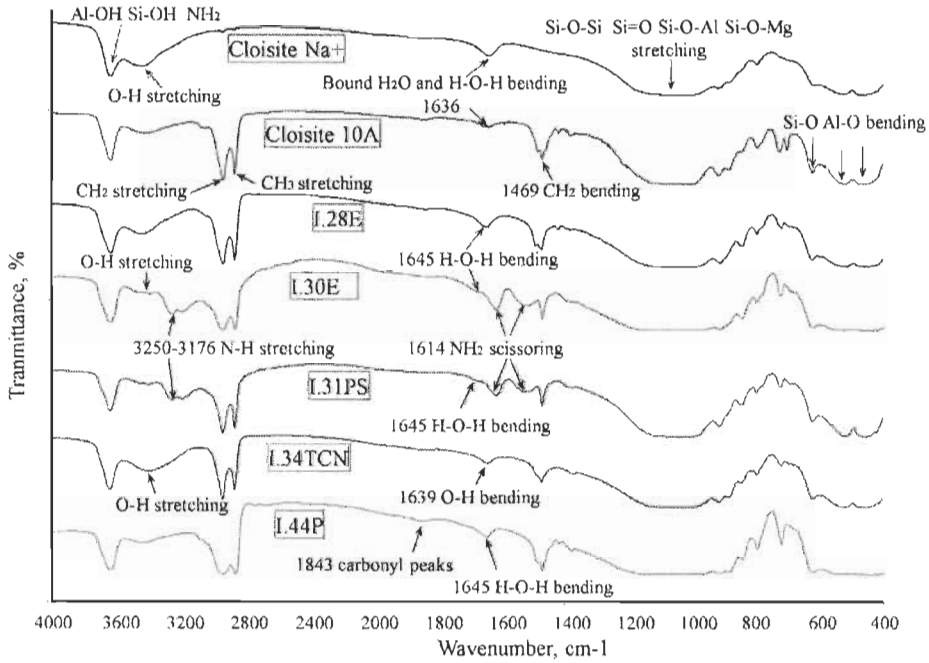

Figure 10.7 FTIR spectra of Organo-nanoclays with different surfactant

Modified NC exhibit intense peaks at 2924cm^{-1} and 2846cm^{-1} due to CH_2 and CH_3 symmetric and asymmetric stretching of the pendant HT chains, respectively [516, 519]. The distinct peak at 1469cm^{-1} corresponds to the CH_2 bending [516, 519]. The two small peaks in the spectra of I.30E and I.31PS near 3200cm^{-1} reflect the N-H stretching vibrations, an indication that the surfactant in the modified NC has amine groups [517]. However, the band of N-H of the ammonium salt (Cloisite 10A, I.28E and I.34TCN) and ternary amine (I.44P) is difficult to detect due to the weak vibration of N-H. So, the double peaks at 3200cm^{-1} could be used to distinguish the type of surfactant employed. Due to the HT tail of I.34TCN has 2 hydroxyl groups, the distinct peak at 1639cm^{-1} was intensified as indicated in Figure 10.7.

The impact behavior of polymeric nanocomposites made with different organo-nanoclay is presented in Figure 10.8 as a function of NC content. With the NC content increase, the fitted curves of the nanocomposites increase at 1wt% proportion

and then gradually decline. Although NC particles can't exfoliate in non-maleated nanocomposites [506], the nanocomposites benefit the contributions of the intercalated functions of small amount of silicates exhibiting an increase. This increase is varied according to the nature of the surfactant of NC, where from 45kJ/m² for neat PE up to 52-56kJ/m² after 1wt% NC reinforcement. Obviously, impact strength decreases as the amount of NC increased as it is deduced from Figure 10.8. However, the decreases are functions of nature of NC modified by the surfactants. It is found that the polymeric nanocomposites reinforced with Cloisite Na+ and I.34TCN could achieve better strength at the 10wt% level than I.44P. The I.44P is hindered by the two alkyl tails of the surfactants other than I.34TCN which has double dihydroxyethyl HT which provides an extra interaction.

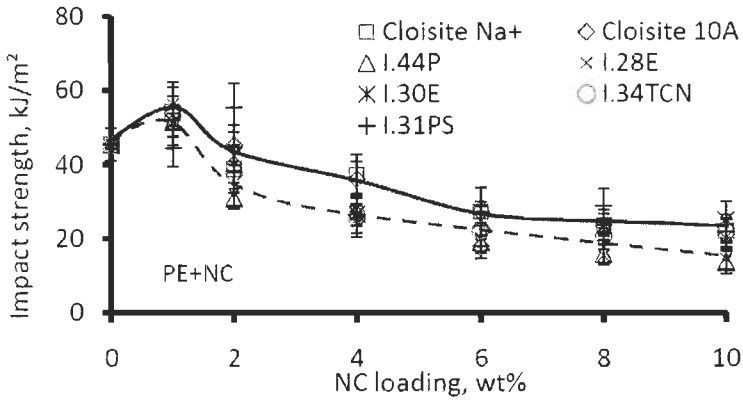

Figure 10.8 Effects of NC on Impact strength of polymeric nanocomposites

The tensile behavior is presented in Figure 10.9 as a function of NC concentration. With the NC increase, the plotted curves of the polymeric nanocomposites gradually decline. As mentioned above, only maleated olefins were found to intercalate in the galleries of the silicates at the first stage of the mixing process while no exfoliation was observed for non-maleated nanocomposites [506]. The tensile strength of the non-maleated nanocomposites decreases with clay loading from 25MPa for neat PE to 20MPa for the nanocomposites with 10wt% NC as shown in Figure 10.9. Similar to impact behaviors, the decreases are varied originating from the nature of NC. It is found to follow the sequence: Cloisite Na+>I.34TCN>I.30E=I.31PS>Cloisite 10A=I.28E>I.44P, such that the polymeric nanocomposites using 10wt% organoclays with single alkyl tail surfactants prevail in the gain over those nanocomposites using organoclays with two alkyl tail surfactants with an exception of I.34TCN because a single tallow amine appears to control the polymer-clay

miscibility more favorably than a ditallow amine [520]. I.34TCN leads to superior tensile strength due to its double pendent hydroxyl groups which provides extra affinities, possibly hydrogen bonding, leading to stronger interactions between the organoclays and the matrix and consequently better restriction of segments. It is also concluded that amine content has stronger interactions with the matrix than ammonium salt with a single tail.

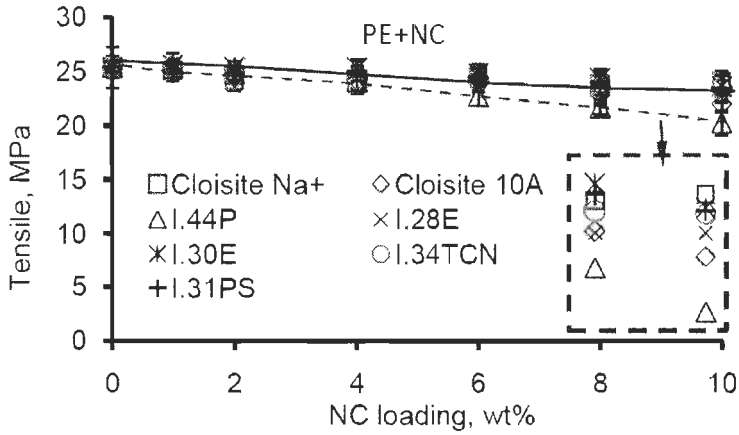

Figure 10.9 Effects of NC on tensile strength of polymeric nanocomposites

Although organoclays gain in d-spacing exhibiting more physical significances than the appreciation of the amount of a degree of intercalation because a higher d-spacing gain implies that more surfactants segments or chains reside in the galleries of the layer silicate while hydrophobic PE of high molecule weight has difficulty to replace the polarized surfactants leading to less interactions between the matrix and the particles of NC. That explains why pristine montmorillonites achieved the highest tensile with lower d-spacing.

The polymeric composites also show the different elongation and modulus with varying levels of the surfactants. The rheological properties are highly affected by the introduction of nanofiller to the polymer. With the addition of NC, the elongation decreases while the tensile modulus increases compared to neat PE as it is indicated in Figure 10.10 and Figure 10.11.

As mentioned above, the elongation decreases as the NC level increases. The nanocomposites with good compatibility could yield high elongation due to good adhesion. Conversely, poor interactions between the polymer and NC result in modulus increase at low content as shown in Figure 10.11. The tensile moduli of the nanocomposites containing organoclays show an improvement over that of the pure

PE. The nanocomposites with I.44P have the highest modulus. But we meet same problem as Yang [521] with moduli reproducibility.

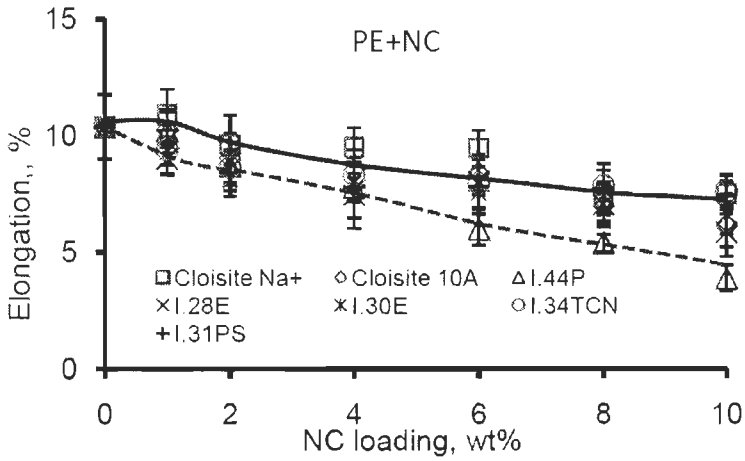

Figure 10.10 Effects of NC on Elongation of polymeric nanocomposites

The modulus increase could be attributed to the reinforcement of PE matrix by the nanoclays [522]. Moreover, the processing conditions have a strong influence of the crystallization of the nanocomposites, that is melting processing (isothermal crystallization) and cooling rate (non-isothermal crystallization) [515] while nanoclays play two roles in the crystallizations, that is a nucleating agent to facilitate the crystallization (1-5wt%) and a physical hindrance to retard the crystallization above 5wt% [523]. The enhanced crystallization of PE due to the clay additions to PE [390, 524] could also attribute modulus enhancement and elongation decrease.

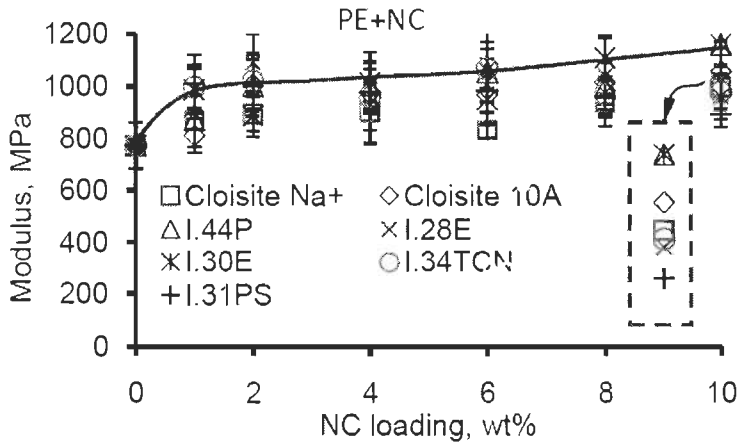

Figure 10.11 Effects of NC on Modulus of polymeric nanocomposites

10.4.1.3 Effects of the changes of NC on the properties of WPC

Wood fibers would help the particles of NC to reach good dispersion [453]. However, wood fiber had determined the properties and structures of the composites due to their amounts and their reactivity. It was noted that since NC could be completely exfoliated in pure MAPE [400], the particles of NC in WPC could be well dispersed and deposited on fiber surface or lumen [453] instead of exfoliated by MAPE molecules when a small amount is added.

The impact strength of the composites decreased with the addition of NC after improvement at low NC content as shown in Figure 10.12. With aforementioned similarities, a little improvement comes from the interactions between NC particles and the matrix. The decrease in impact strength originates from the strengthened nucleating effect of NC by the addition of wood fiber and coupling agent resulting in increase of the crystallization temperature and decrease of the crystalline formation [459].

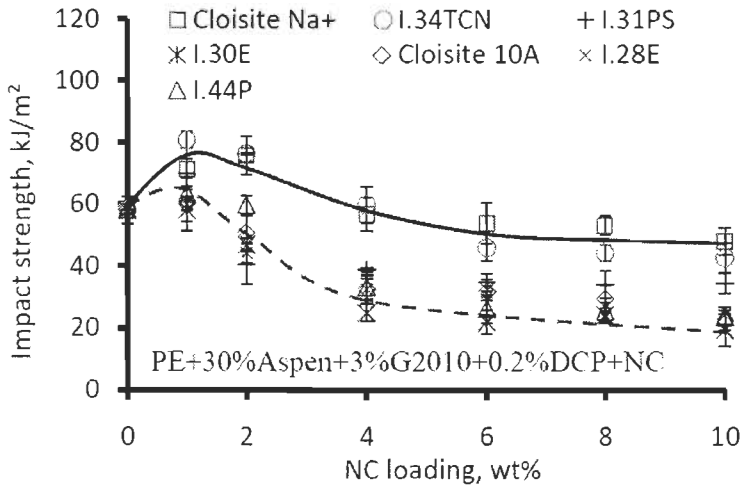

Figure 10.12 Effects of NC on Impact strength of WPC

As NC content increases, the higher NC aggregation and low surface energy gives wood composites high viscosity, which prohibits the movement of the molecular chains resulting in decreasing impact strength downward 40-70% respectively depending on which kind surfactant used in organo-NC. This behavior of impact strength was also observed by Yeh and coworkers [460]. It is clearly found that the composites reinforced with Cloisite Na+ and I.34TCN were on the level of 40% compared to the composites with the addition of I.30E, Cloisite 10A, I.28E and I.44P down by 65-70% while I.31PS is set at middle at 50%. Relative good performance of the composites filled with Cloisite Na+ and I.34TCN benefit from the strong

interactions from more polymer pendent chains entering the empty galleries of natural NC and the extra functions of hydroxyl groups in I.34TCN via maleic anhydride groups in MAPE.

The tensile strength of the composites is deteriorated by the addition of NC except for Cloisite Na+ and I.34TCN as presented in Figure 10.13. The esterification could happen between the hydroxyl groups in I.34TCN surfactant and maleic anhydride groups in MAPE. This esterification and the possible diffusion of polymer molecules in the galleries of the layer silicate may contribute to the composites tensile strength up 3-6%, and then the tensile properties decline with the additional NC loading.

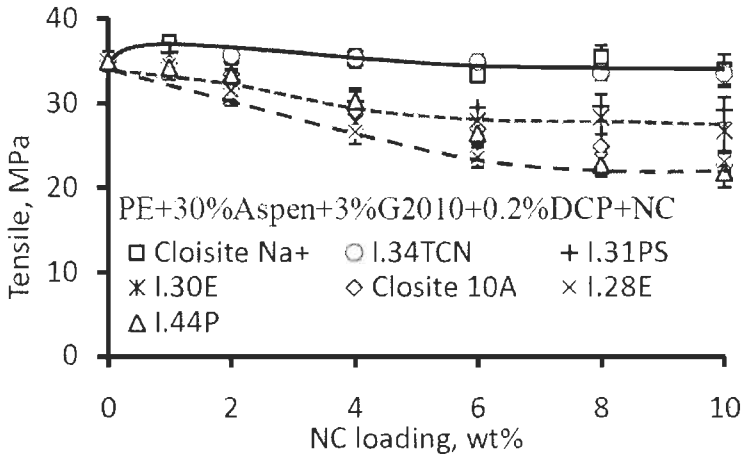

Figure 10.13 Effects of NC on Tensile strength of WPC

It is found that NC had similar role in the composites as in the non-wood nanocomposites. However, the effects of nanoclays gaining in d-spacing may have been enlarged after the matrix was functionlized with the addition of MAPE and DCP [525, 526]. It implies that more NC particles are intercalated due to the higher reactivity of the matrix. The sequence of the tensile decline is Cloisite Na+=I.34TCN<I.30E=I.31PS<Cloisite 10A=I.28E<I.44P, which is consistent with the nature of surfactants. This result also confirms that amines also have stronger interactions with the polarized PE/Aspen composites with coupling agent as well as initiator than with ammonium of the same molecular "tail".

The effect of incorporating NC on the elongation of WPC is summarized in Figure 10.14 : the elongation decreases with increasing NC content as expected [527]. Figure 10.14 indicates that the elongation of WPC decreases with the addition of NC and the changes become more obvious following the addition up to 10wt% of NC which decreases elongation up to 33% (Cloisite Na+ and I.34TCN) and 63% (I.44P),

respectively. This suggests that the interactions of NC with the composites are affected by the surfactants of NC.

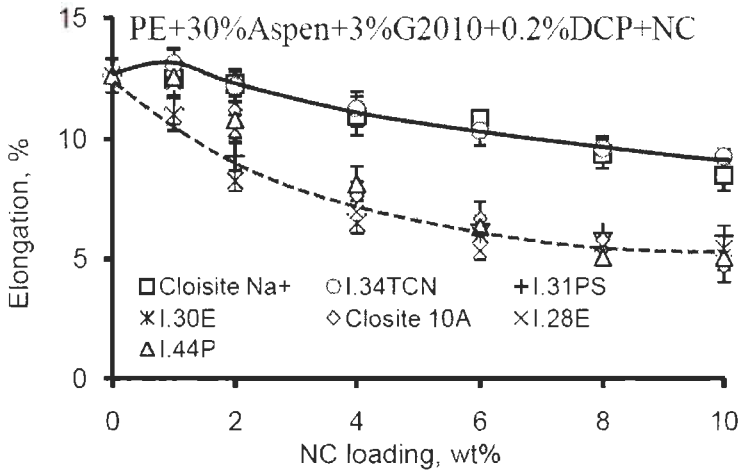

Figure 10.14 Effects of NC on Elongation of WPC

The elongation at maximum load of the composites containing NC modified with amine or ammonium salts is around 5% and 9% for the composites of NC treated by hydroxylated ammonium salt (I.34TCN) or untreated (Cloisite Na+) while the elongation for the composites without NC is up to 12.6%. The wood composites become more brittle with the addition of NC implying an increase of modulus in Figure 10.15.

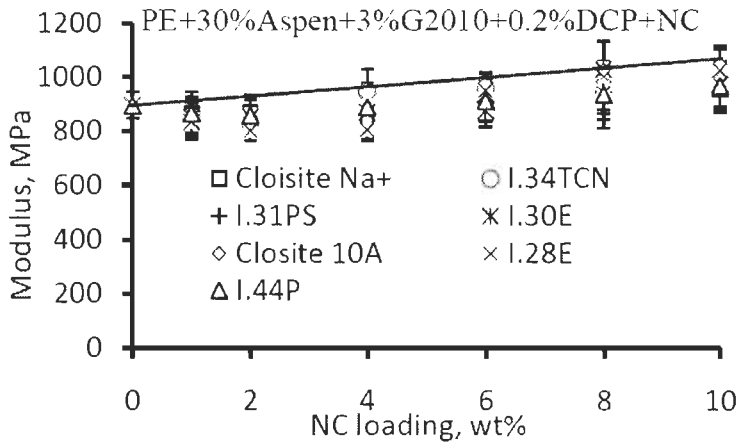

Figure 10.15 Effects of NC on Modulus of WPC

Figure 10.15 shows modulus as a function of NC loading. The tensile modulus changes a little with the addition of NC and rose to 1000MPa when the NC concentration reached 10wt%, which is higher than the value of WPC without NC (900MPa) due to the enhancement of torque as well as viscosity following the

addition of NC and presumably the contribution of the increased crystallinity caused by NC particles. The increase of modulus with the increase of NC is in an agreement with the conclusion reached by Zhong and coworkers [500].

10.4.2 Tensile behaviors

Figure 10.16 shows typical tensile properties of the polymeric nanocomposites. Stress–strain curves for PE only containing NC (Cloisite Na+) show the dramatic increase in elongation at max load at low content of NC (no more than 4wt%) and hold at 15MPa for larger extension (50% reachly, not broken). But the nanocomposites filled with a high content of NC (10wt%) are broken at 24.5% extension and at low stress 6MPa. It is clearly seen that the ratio of stress to strain increases by increasing NC content which implies an increase of modulus too.

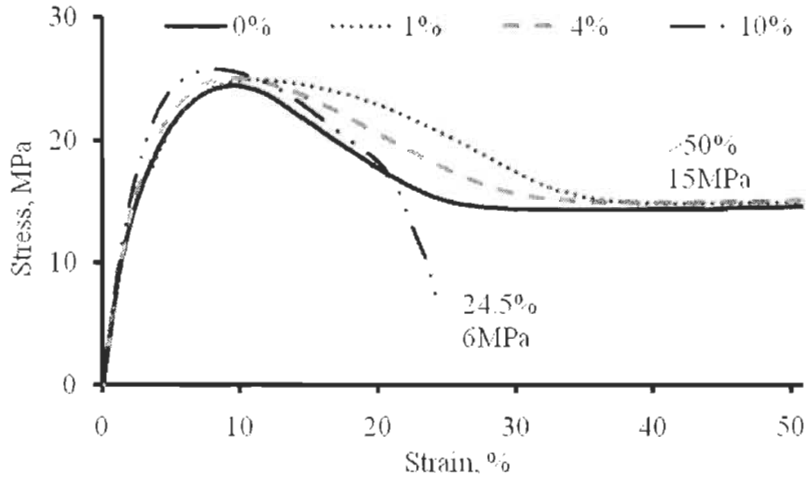

Figure 10.16 Tensile behaviors of PE/Cloisite Na+ nanocomposites

Figure 10.17 shows typical stress-strain curves for the materials based on different PE-based formulations. It is apparent that important yielding and necking occur in the materials without fiber being loaded during tensile deformation process. On the other hand, PE without the presence of fiber exhibits typical ductile fracture behavior under an essential work of fracture testing conditions while WPC displays a typical brittle fracture behavior. Pure PE and its nanocomposites fracture in ductile mode via craze formation and growth are expected and evidenced by a large increase of the strain-to-failure at more than 50% under 14MPa. However, the composites filled only with fiber display a brittle behavior as evidenced by low value of the strain-to-failure to 4.8%. As maleated PE and initiator are introduced, the strain-to-failure is

extended to 14.3% and fractured at 35MPa which is superior to the value of neat PE as it is demonstrated in Figure 10.17.

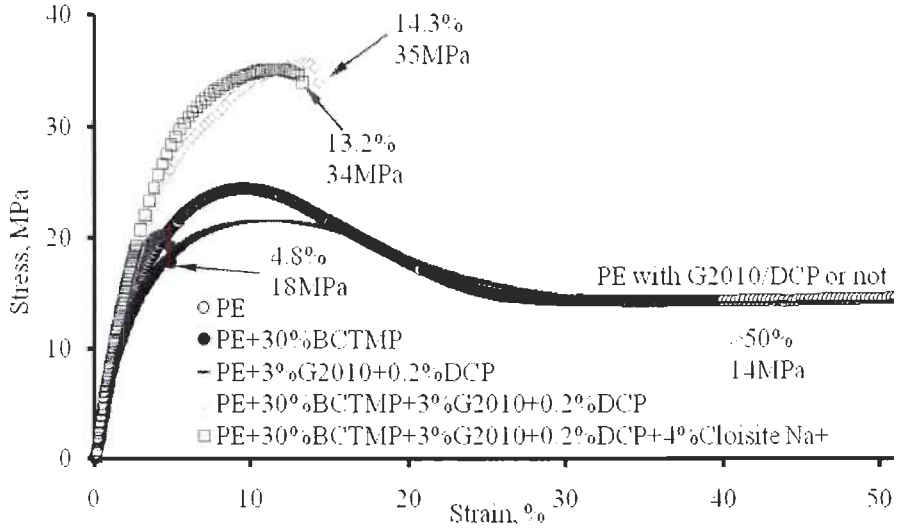

Figure 10.17 Tensile behaviors of PE composites

When NC is introduced into the composites, the strain-to-failure ratio decreases a little reaching 13.2% at 34MPa due to the reinforcement of NC. As mentioned above, the modulus of ductile polymer can be improved by the addition of a rigid material such as wood fiber and NC. The stress-strain curve of PE shows the gross yielding and necking behavior with the addition of 3%G2010 and 0.2%DCP exhibiting lower modulus resulting from the oxidation of DCP and the reaction of MAPE during process.

The ratio of stress to strain of the composites as coupling agent and DCP used is higher than that of the composites without compatibilizers due to the improved interfacial adhesion and interaction between plastic and wood fibers [393, 394, 405]. The increase of the ratio of stress to strain of the composites containing NC may come from the enhancement of crystallization and the inhibition of the motion of polymer chains by NC particles.

10.4.3 Water characterization

10.4.3.1 Moisture uptake

Moisture uptake gives us water absorption characteristics of the wood composites exposed at unsaturated humidity conditions. The moisture content of all the wood composites is illustrated in Figure 10.18 and Figure 10.19. Whether the coupling agent and initiator are used or not, the moisture uptake increases as a function of

wood fiber content increase due to presence of more hydroxyl groups with oxygen groups bonding with water molecules by hydrogen bonds [509]. In our case, most OH groups are localized in the cellulose phase, and only a small amount of water interact with the surface OH groups of the crystalline phase [334]. The characteristics of wood fiber play an important role when the fibers are incorporated in a matrix.

When a maleated polyolefin, MAPE, is used as a coupling agent, some kind of interactions, such as esterification, between the hydrophobic polymer and hydrophilic wood fiber occur and convert the hydroxyl groups into carbonyl groups which will weaken hydrogen bonding [314, 420]. It is shown that maleated polyolefin interacted with OH groups at the surface of wood fiber and chains entanglements between PE and maleated PE were also formed due to similar molecular structure which implies that some parts of hydrophobic PE will adhere to the surface of wood fiber by covalent bonds as well as physical entanglements. Fractionally coated wood fiber absorb less water because of the amount of surface OH decrease and the repellent actions from the hydrophobic segments of polyolefin as Figure 18 indicates.

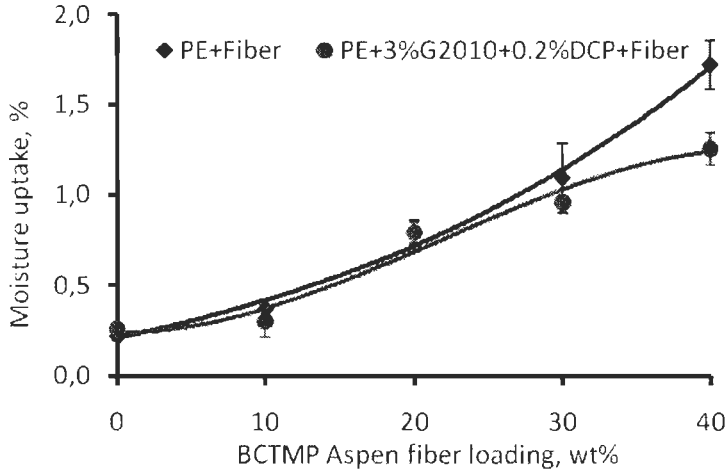

Figure 10.18 Moisture uptake behaviors of WPC made with the compatibilizer or not as function of fiber content at 23°C and 45% RH

Figure 10.19 shows us the moisture content in WPC as a function of NC. The moisture content varies depending upon the NC loading when they are exposed in air. Since PE absorbs moisture very slightly, the moisture is absorbed by wood component in the composites initially via porous tubular and lumen [528], and then occupies microvoids. It was known that NC particles lumen-loaded and deposited on the surface of wood fiber [453]. Thus the penetration of water molecules will be

limited by some low NC loading by the so-called capillary action into the deeper sections of the composites. This result was already reported by Nourbakhsh [529] where the value of 1% is exhibited in the composites without NC, which decreases to 0.5-0.6% with 1-10wt% NC loading as water is under unsaturated conditions.

The hydrophilic/organophilic NC particles absorb water molecules due to the formation of agglomerate [530] under saturated condition. The moisture differences originate from the different nature of NC surfactants.

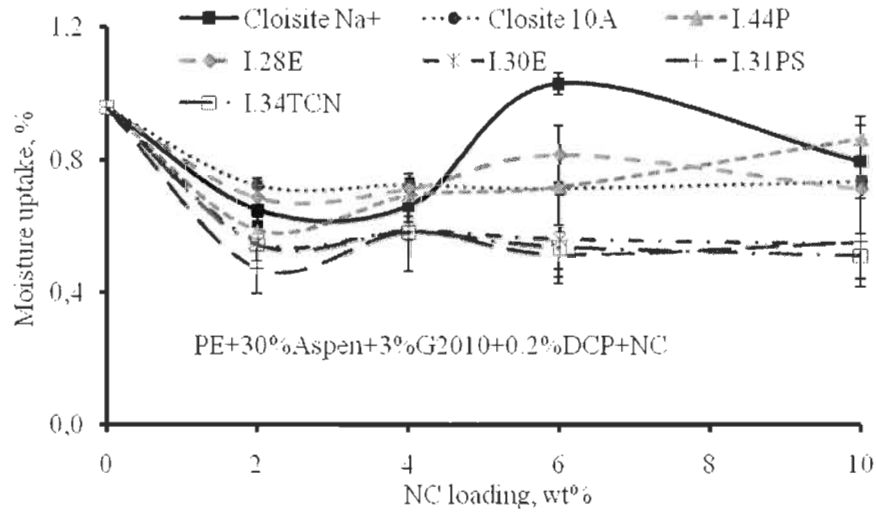

Figure 10.19 Moisture uptake behaviors of WPC made with different kinds NC as function of NC content at 23°C and 45% RH

10.4.3.2 Water uptake

Rather than the actions of hydroxyl groups of wood fiber during moisture up-taking, more potential channels will be expanded in water uptake. Without compabitilizers, the interfacial compatibility between wood fiber and the matrix is poor which results in some microvoids, which will speed the penetration of water into the depth of the composites. Due to the amounts of OH groups exposed on the fiber surface, WPC without coupling agent take up more water molecules as Figure 10.20 shown. In the composites with coupling agent employed, maleated PE builds up some interactions to eliminate the amounts of OH groups and also hold hydrophobic polymer chains around wood fiber surface leading to less water uptake.

The result of water uptake after 56 days water soaking test are also presented in Figure 10.20. The initial PE has the lowest water uptake due to its hydrophobic character while grafted PE has a little higher water absorption due to its hydrophobic surface changed into hydrophilic after coupling agent and imitator employed. The

soaking time has less impact on both of them. As wood fibers were introduced, WPC takes-up more water molecules as a function of the fiber content and the soaking time. It is same as moisture uptake, the so-called capillary action would be enlarged as excess water penetrated. Water molecules could mainly be combined with OH groups or other oxygen containing groups by hydrogen bonding with water. As a result, transportation of water molecules via capillary action to voids and water molecules accumulated at the interfacial voids contribute to the total amount of water uptake in excess water as is indicated in Figure 10.21a.

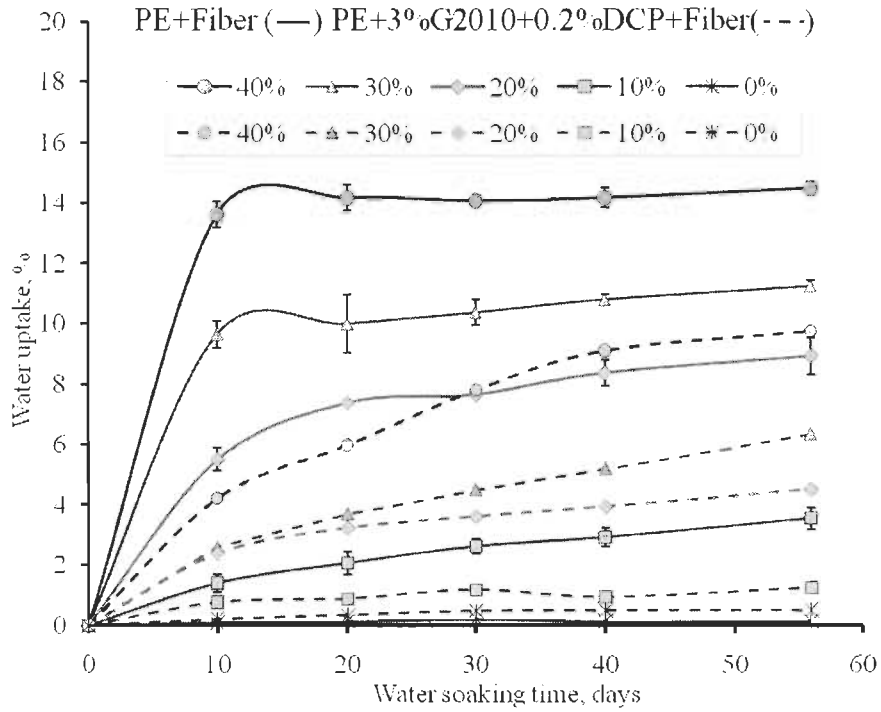

Figure 10.20 Water uptake behaviors of compatilized and incompatilized WPC as a function of fiber content immersed in distilled water at 23°C

All the samples of the coupled WPC have low water uptake but keeping absorbtion level compared to the unmodified WPC which takes short time to reach saturation, which indicates the unsaturated condition up to 56 days. Similar results were also presented by Yeh [531], San [423] and Viksne [510]. Without compatibilizers, more fiber loaded, less time (15 days) is needed to reach saturation because it undertakes water molecules by forming more penetrated channels leading to more capaillary action. On the other hand, less fiber provides less channels and decrease the chance for water molecules to contact wood fibers. The saturated points of WPC reiforced

with 20, 30, and 40wt% fiber are set at 8, 10, and 14%, respectively. Meanwhile, the coupled WPC employed 40wt% wood fiber only absorbs 9%.

Conversly to unmodified WPC, the water behavoirs of coupled WPC are quite different, which concern the absorption capacity and the saturation time. With the presence of coupling agent and initiator, less fiber was introduced and there was less water uptake because the absorption capacity of the functionlized wood fiber was weakened. This finding is a consequence of the attachment of hydrophobic polymer on fiber surface which changes the hydrophilic surface of initial fibes into the hydrophobic surface, which resists the attachment of water as indicated in Figure 10.21b. Moreover, the potential channels include pores, pits, and microcracks in fiber surface, which acted with capillary, and they could be improved after modification by improved compatibility as indicated in Figure 10.21c.

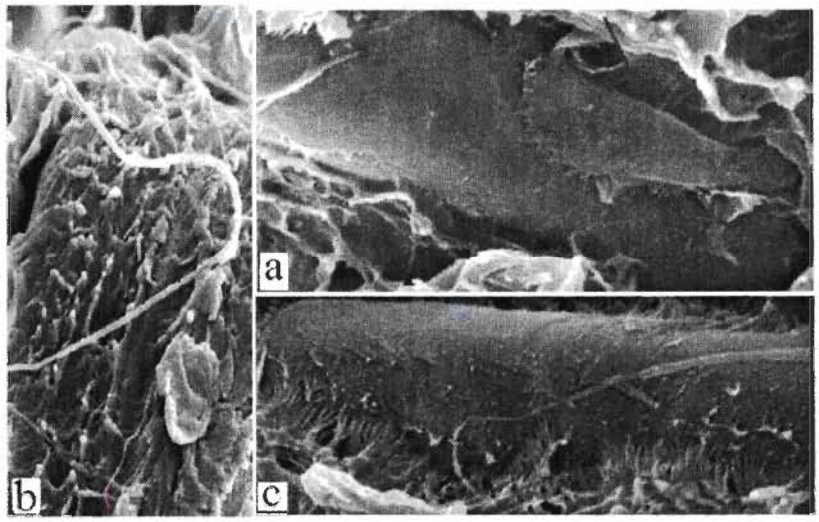

Figure 10.21 Illustrations of water penetration [453]

It should be also noted that less fibers are easy to be bonded entirely leading to the approach of the saturation in less time. As more fibers are introduced, more fibers are exposed to water molecules because less encapsulations occur in the composites, which have a higher content of wood fibers, and wood fibers are easily exposed on the surface [532]. The exposed wood fiber will make water penetrate from the unfilled pores, pits, and voids causing the incompatiblity between partly bonded wood fiber and the matrix in depth. That is the reason that the water uptake increases when more fiber is introduced. However, the absorption speed will be slowed down by the deposited hydrophobic polymer and the improvement of morphological structures which will increase the saturation time. As soaking time extends, water

uptake increases gradually. These conclusions are in accordance with the previous works [423, 533, 534]. It is of interest that the uptake speed will be accelerated by the swelling of cell wall, which could produce some cracks, twisting acting as water channels. It is assumed that more introduced fibers will shorten the saturated soaking time in the case where a limited amount of coupling agent is used.

Figure 10.22 illustrates the water uptake of the composites with different NC as a function of NC content. Statistical analysis has indicated that there were significant increases in water uptake with an increase in NC loading after the initial decrease which is similar to the results of Salmah [535]. As discussed above, the initial decreases come from the smoothened fiber surface by blocking pores, pits, and capillaries as is illustrated in Figure 10.23a. The following increase is attributed to the hydrophilic agglomerates of NC particles at high percentage [530]. Like the crystallization caused by NC, NC also plays two roles in water uptake, that is as a physical blocking agent to prevent water penetration at a low content and a bulking agent to absorb water at relatively high contents. The content is distinguished according to the characteristics of surfactants as summarized in Table 10.2. The course of water uptake is also different as a function of the characteristics of surfactants as indicated in Figure 10.22.

NC works as a blocking agent at low content and most NC particles will inlay the pores, pits and some lumens (Figure 10.23a) due to strong driving force shear and high viscosity during compounding, and some particles deposit on fiber surface (Figure 10.23b) due to opposite polarity between wood fiber and NC. Smoothened fiber surface, especially filled by hydrophobic surfactant, will decrease the water contact angle and lower the contact area and efficiency. This will lower the water absorption capacity of wood fiber similarly to the modification of coupling agent. Due to the difference of the characteristics of wood fiber and NC, water molecules favor to attack wood fibers through residual hydroxyl groups and the residual free lumen and pores (Figure 10.23d) prior to NC particles. The decreased absorption capability leads to low water absorption and gives WPC filled with NC a high water resistance.

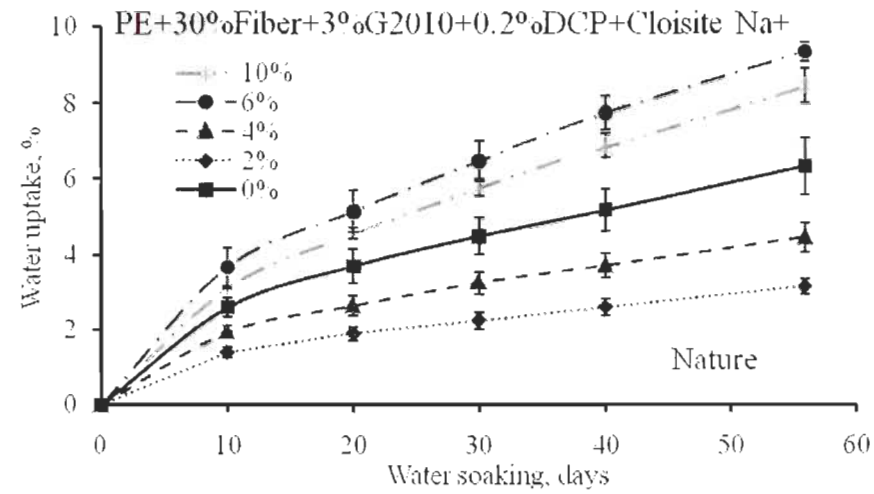
PE+30%Fiber+3%G2010+0.2%DCP+Cloisite Na+
10%
6%
4%
2%
0%
Water uptake, %
Water soaking, days
Nature

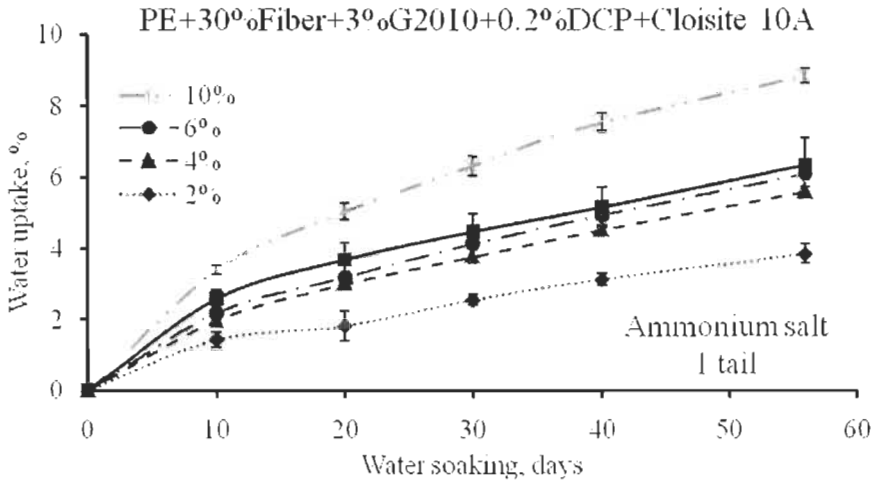
PE+30%Fiber+3%G2010+0.2%DCP+Cloisite 10A
10%
6%
4%
2%
Water uptake, %
Water soaking, days
Ammonium salt
1 tail

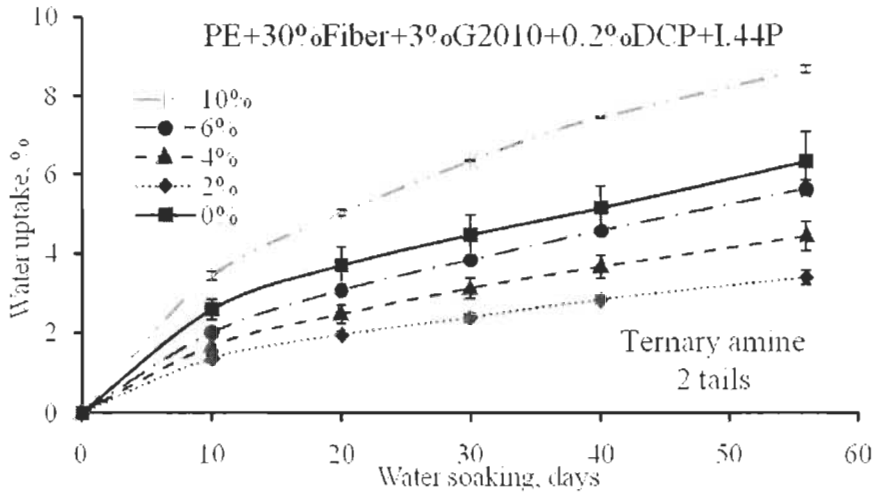
PE+30%Fiber+3%G2010+0.2%DCP+I.44P
10%
6%
4%
2%
0%
Water uptake, %
Water soaking, days
Ternary amine
2 tails

Continue……

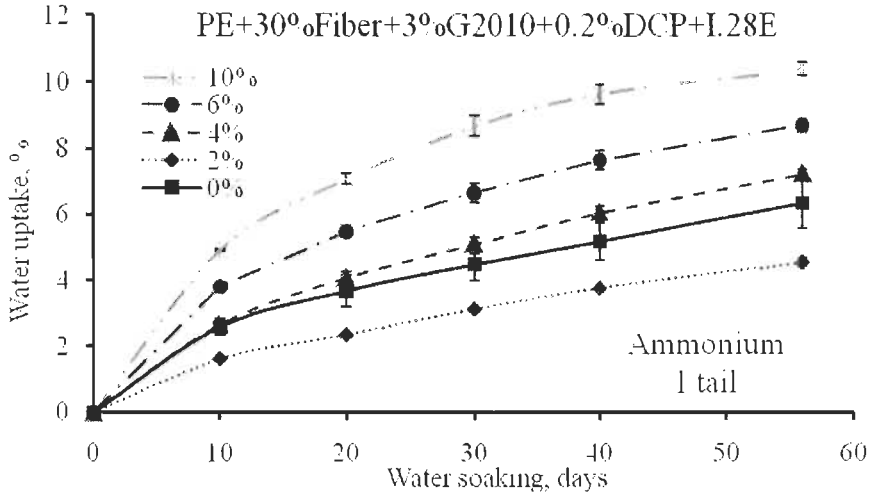
PE+30%Fiber+3%G2010+0.2%DCP+I.28E
10%
6%
4%
2%
0%
Ammonium
1 tail
Water uptake, %
Water soaking, days

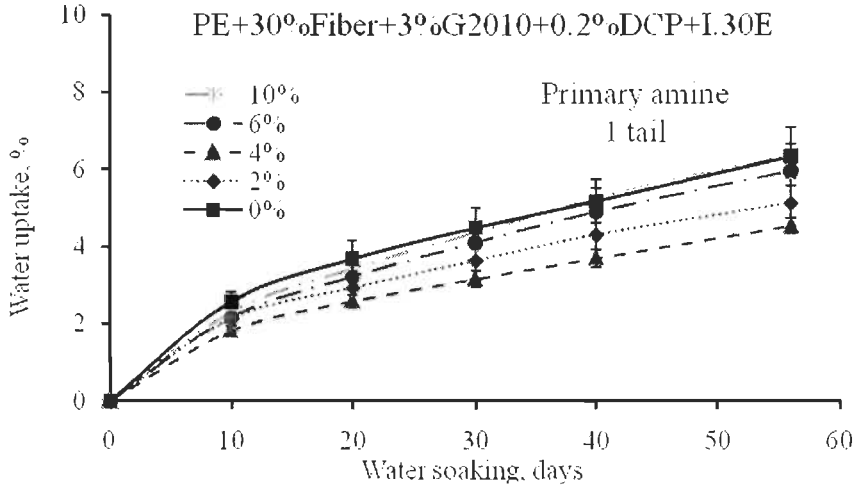
PE+30%Fiber+3%G2010+0.2%DCP+I.30E
10%
6%
4%
2%
0%
Primary amine
1 tail
Water uptake, %
Water soaking, days

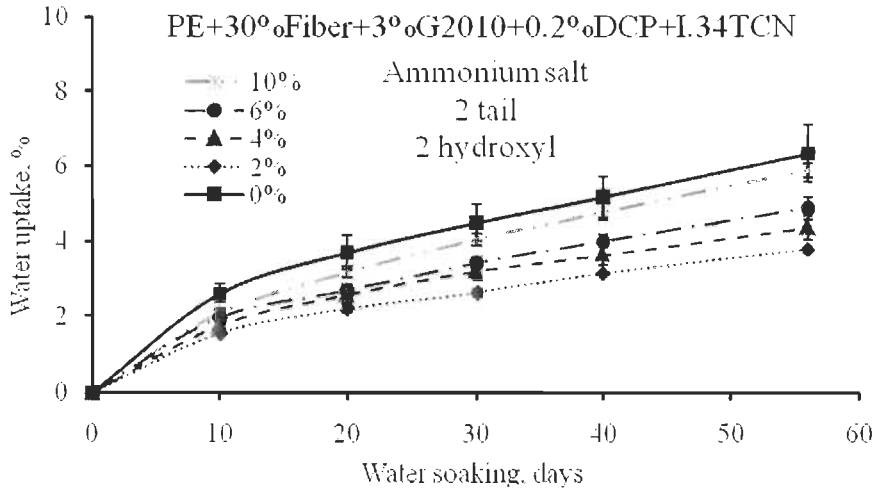
PE+30%Fiber+3%G2010+0.2%DCP+I.34TCN
10%
6%
4%
2%
0%
Ammonium salt
2 tail
2 hydroxyl
Water uptake, %
Water soaking, days

Continue……

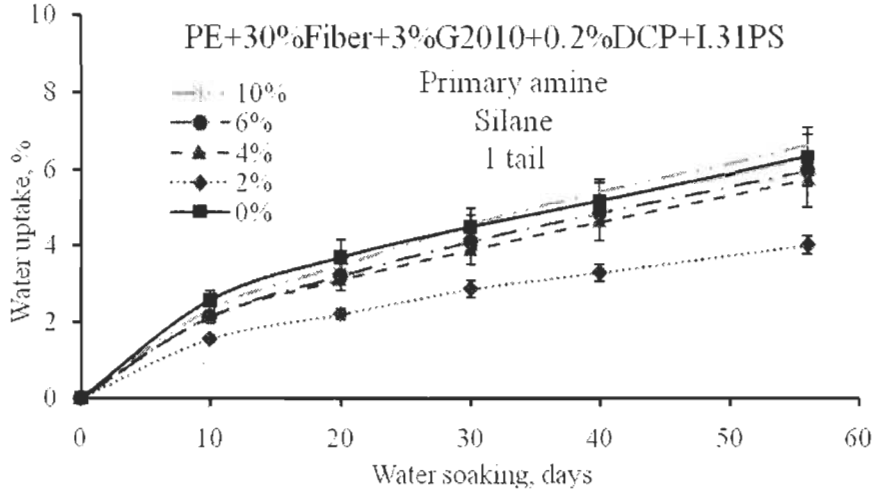

Figure 10.22 Water uptake behaviors of WPC made with different kinds NC subjected to different surfactant as a function of NC content immersed in distilled water at 23°C

As a result of NC content increase, the gain of water uptake would increase, following the increase of NC addition, resulting from the water incompatibility (Figure 10.23c) caused by the deposition of NC particles on fiber surface and the hydrophilic agglomerates strengthened by the hydration of NC particles along wood fibers. It was seen that the number of hydrated inserted NC particles will be increased after more NC particles were exposed to water and its attacks.

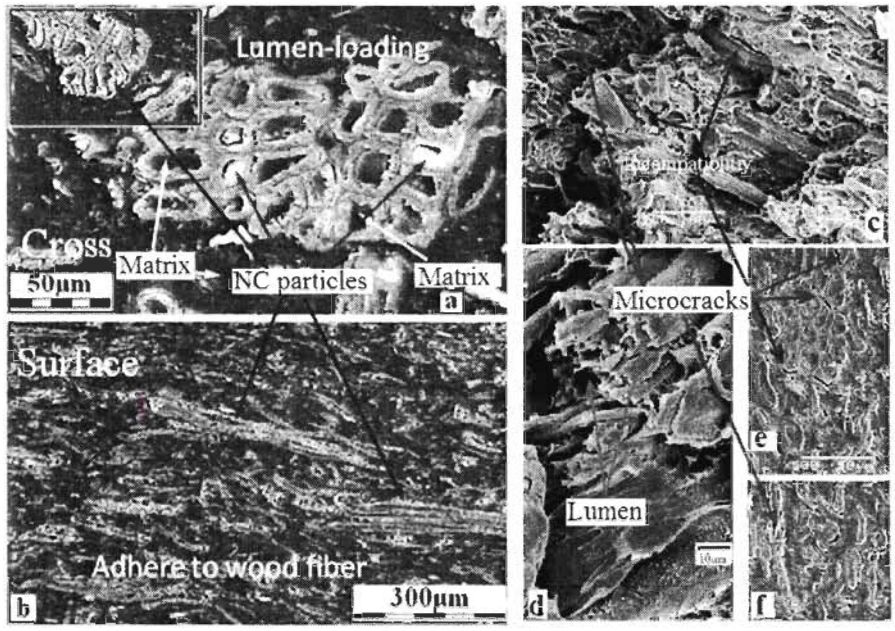

Figure 10.23 Illustrations of the functions of NC particles in WPC during soaking [453]

As a result of extended soaking time, wood fiber wall will be swelled, which will expand the existed microvoids and microcracks of the material body and deteriorate their compatibility. Moreover, NC particles will be fully hydrated. Thus, more water molecules will penetrate in depth along wood fiber and silicate layers (Figure 10.23c and d), the bulk faults caused by swelling (Figure 10.23e, and f) as well as the incompatible interfaces is enhanced by fiber wall swelling (Figure 10.23c, e, and f). With the aforementioned similarities to the compatibilizers, the addition of NC particles will retard the point of saturation compared to that of WPC without reinforcements. The addition of NC enhances water resistance of WPC even in soaking up to 56 days. However, the behaviors of modified NC are influenced by the nature of the surfactants, especially to the attached salt type and their pendant ride chain (Table 10.1). So the definite concentration of the roles as mentioned above will fluctuate according by NC types in Table 10.2.

Table 10.2 Water behaviors of WPC as functions of NC particles

NC type	Surfacant type	Functions of NC particles		Discoloration
		Blocking	Bulking	
Cloisite Na+	None	≤4%	≥6%	Irreversible Pink
Cloisite 10A	Ammonium 1 pendant chain	≤6%	≥10%	No change
I.44P	Ternary amine 2 pendant chains	≤6%	≥10%	No change
I.28E	Ammoniumm 1 pendant chain	≤2%	≥4%	No change
I.30E	Primary amine 1 pendant chain	≤10%	---	No change
I.34TCN	Ammonium salt 2 pendant chain 2 hydroxyl	≤10%	---	No change
I.31PS	Primary amine, Silane 1 pendant chain	≤10%	>10%	No change

At the same concentration of NC presented, it is clearly seen that water uptake behaviors of WPC could be improved if organo-NC modified with primary amine and/or silane with single pendant are used as surfactants, such as I.30E and I.31PS which provide the composites with low water uptake even up to 10wt% resulting in excellent dimensional stability compared to the composites without NC particles due to its high polymer hydrophobicity. However, the composites containing the modified NC with ammonium salt or ternary amine absorbed more water, such as Cloisite 10A, I.44P and I.28E except I.34TCN because of its dihydroxyethyl and

high polarity. For this kind of modified NC, the two roles of NC in water uptake behavior were entirely different which was indicated by their content in Table 10.2. Nonetheless, modified NC will help the composites absorb amounts of water at high loading exceeding 10wt%. Due to the hydroxyl groups of I.34TCN interaction with the matrix and wood fiber leading to superior compatibilty, I.34TCN imparts the composites with similar behaviors to NC treated by primary amine with a different mechanism. The contribution of I.34TCN comes from the improvement of interaction among NC particle, fibers, and the matrix while the presence of primary amines modified NC results in its relative high hydrophobicity. The increase of water absorption by Cloisite Na+ originates from its hydration of metal ions which indicates low organophilicity.

It is concluded that primary amine modified NC results in WPC with superior water resistance and gives the composites a high dimensional stability even loaded at 10wt%. In contrast to primary amines, ammonium salt or ternary amine chemical groups could be attacked easily by water molecules at the cationic sites. Following the increase of the content of this kind of NC, more water molecules are brought in leading to wood fiber swelling and distortion of the composites structures. The hygroscopic nature of montmorillonites results from the capillary action of the voids of silicate layer and the ionic attraction of un-exchanged cations, such as Si^{2+}, Na^{+}, Ca^{2+}, Al^{3+}, and Mg^{2+}. Considering the mechanical properties, the contributions of NC on both mechanical properties and water uptake are in the following sequence: I.34TCN>I.31PS=I.30E>Cloisite Na^{+}>Cloisite 10A>I.44P=I.28E. The employment of I.34TCN could lead to high-quality composites and Cloisite Na^{+} could lower the cost. The water uptakes of WPC with the reinforcement of NC can be split into three phases:

- Initial phase: water uptake is mainly contributed due to wood fibers and increases quickly in 20 days.
- Second phase: wood fibers continue absorbing leading to supersaturation and NC particles are hydrated and aggregated after 20days. The water uptaking speed is dramatically increased, which is supported by Figure 10.22.
- Final phase: NC particles, replacing wood fiber, become major compounds who absorb water. The water uptaking speed increases smoothly and steadily and takes long time to reach the saturated condition.

10.4.3.3 Discoloration during water soaking

It is an interesting finding that only natural montmorillonites (Cloisite Na^+) reinforced WPC discolored during water soaking. The color effect becomes irreversible and pink as functions of the soaking time and NC content as imaged in Figure 10.24. In our case, the discolored samples were scanned after soaking 56 days. The generated color palette was carried out by CSS Driver Palette (http://www.cssdrive.com/imagepalette/) using scanning images after removal of the marks caused by the crossheads during tensile testing. The generated colors are coded in Figure 10.24.

No records were found concerning the discoloration of WPC after water uptake. It is not exactly known why natural NC filled WPC is discolored rather than organo-NC. It certainly does seem that something in our process is interacting with the untreated NC typically this would be a cationic material due to the impossibility to be caused by cobalt which is less than 1ppm and it was also present in all products. It is noted that the discoloration only occurs in soaked samples and becoming a deep color as NC content is increased and the soaking time is extended to more than 20 days.

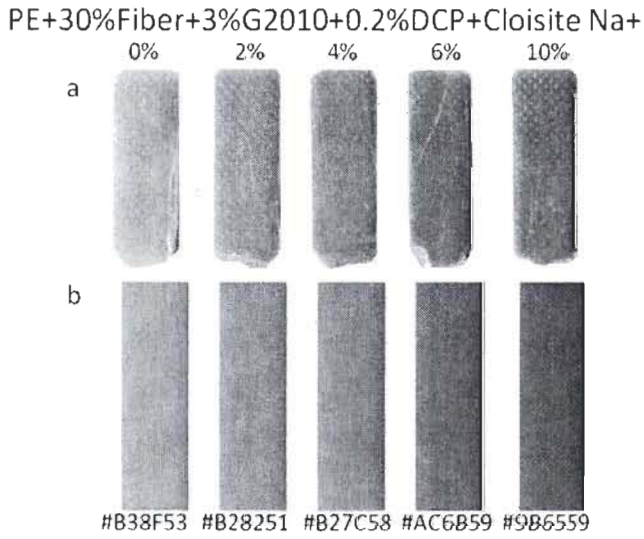

Figure 10.24 Discoloration of WPC filled with Cloisite Na+ after soaking 56days

a: scanning images; b: generated color palette by removal of the white marks (pressed by crosshead)

Hence, our guess is that water molecules interacted with the cation exchangeable sites on the Na^+. It is assumed that water molecules penetrated in the layers of NC particles easily and formed combined water by ionic covalents (such as $SiO_2 \cdot H_2O$ and $Al_2O_3 \cdot H_2O$, *etc*) due to the nature of NC having empty galleries and appreciable concentration of cations. These kind of hydrated structures could not be destroyed

even oven-drying at 105°C for 1 week because the mentioned structures are irreversiblly exfoliated dispersion caused by strong driving force during high viscosity blending. It is assumed that the discoloration of initial natural NC could be recovered after heat treatment. Unlike natural NC, the undiscoloration of WPC reinforced with organo-NC, the hydrated structures are hindered due to the organic surfactants entered into the galleries and most cations being replaced by cationic ammonium salt.

10.4.3.4 Water (weight) loss

Water loss gives us the changed characteristics of WPC as function of coupling agent/initiator and NC in Figure 10.25 and Figure 10.26. WPC with coupling agent/initiator present or not will lose some soluble compounds after 56days of soaking, including highly acidic on low Mw hemicelluloses, lignin, extractives, and some sucrose. With more fiber loading, more the water loss occurs. In the coupling agent/initiator presented, some low Mw chemicals might have combined with them and got attached on fiber surface leading to unremoval. The blockages of pores, pits, and lumens would also prevent some low chemical content inside from getting lost. So, the modified WPC has a somewhat lower water loss in comparison with the ungrafted WPC in Figure 10.25.

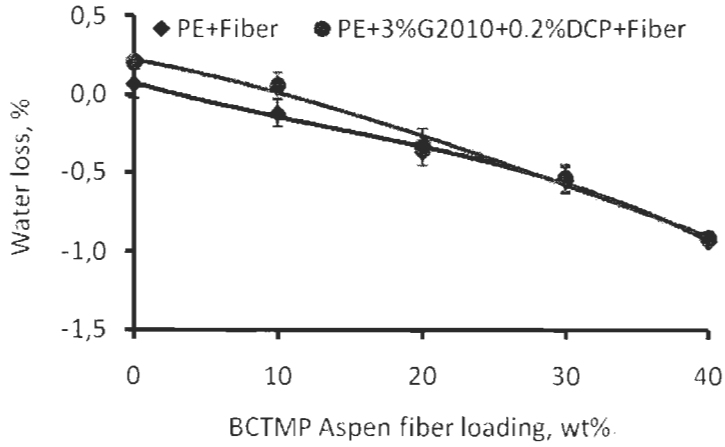

Figure 10.25 Water loss behaviors of compatibilized or incompatibilized WPC as a function of fiber content

Similar to moisture uptake behaviors, NC affects water loss properties of WPC as it is indicated in Figure 10.26. Although water loss becomes larger with the increase of NC, the total percentage was quite small (less 0.6wt%) and still lower than for WPC

without NC. It is concluded that the NC concentration has influence on water loss, from the different characteristics of surfactants, but this effect is negligible.

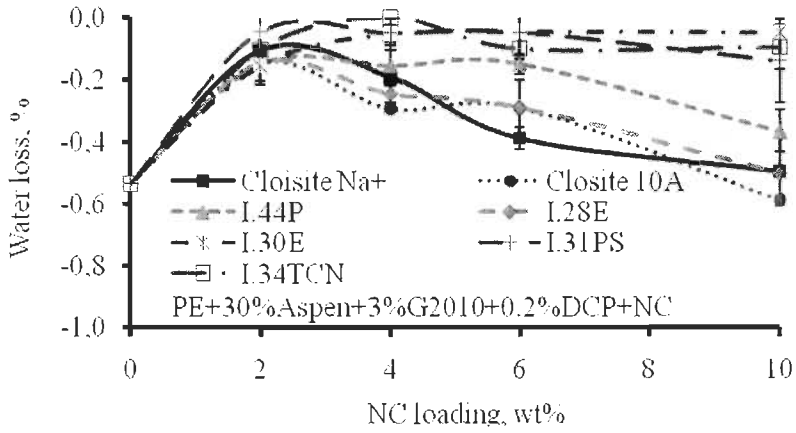

Figure 10.26 Water loss behaviors of WPC made with different kinds NC as a function of NC content

Considering the application environments of WPC, the soaking time has important impact on water behaviors of WPC in our experiment. However, the addition of NC could contribute to better performance of WPC in rainy and snowing environmental conditions, such as Canada. Obviously, the addition of NC could prolong the use life of outdoor products made by WPC, such as park benches and decking in natural parks, from swelling and loss.

10.5 Conclusions

MAPE compatibilization and incorporation of wood fiber and organoclay are investigated to evaluate the mechanical properties improvement and water uptake of WPC. The addition of wood fiber shows a different behavior of the tensile and elongation of LLDPE-based composites with the addition of the system of compatibilizers (MAPE, DCP). The compatibilization results in better polymer impregnation of the wood fiber, which significantly improves the tensile strength and elongation. Even more important is that the compatibilizers lower water uptake and water loss which improve deformation stability and performance.

The incorporation of NC in the composites further reduces the impact and tensile strength, lower elongation, and increase the modulus of both the nanocomposites and the composites with PE matrix. However, NC would improve the water absorption and water loss of PE composites. Surfactants play an important role in this function by their morphological structures as well as chemical reactions. It should be

mentioned that NC plays two roles during water uptakes which is related to its content and also influences on the discoloration of WPC. Considering the strength and water behaviors, I.34TCN modified by ammonium with 2 hydroxyl groups has superior contribution to the composites as well as Cloisite Na^+.

Stress-strain behaviors of the nanocomposites and the composites based on PE are also studied to confirm the morphologies of the nanocomposites. They become more brittle, absorb less fracture energy and exhibit high stiffness as the content of NC is increased. Comparing the changes of stress-strain curves of the based PE materials, the effects of each component on the morphologies are well ordered. PE compounding with maleated PE/DCP could weaken its tensile properties, but not change its ductile properties. Conversely, the morphological changes with the presence of wood fiber with coupling agent leads to short strain-to-failure. However, the maximum tensile strength could be strengthened when the interfacial adhesion is improved. The composites become more brittle with NC addition displaying modulus increase and tensile strength decrease.

10.6 Acknowledgements

The authors would like to thank the NSERC (Grand # 4160105), NCE Auto21 (C402-CGP), FQRNT (# 127387) and Ministry of Education, Youth and Sports of the Czech Republic (Grant # 2B06097) for the financial support. The authors would also thank Temcell Inc. and NOVA Chemicals for their donation. A version of small parts of this article was presented at 96th EXFOX & PAPTAC annual conference, Montreal, Canada. 2-3 February, 2010.

Chapter 11 - Morphological Structures and Functionalization of Wood fiber in Wood Plastic Composites

Ruijun Gu and Bohuslav V. Kokta

Journal of Applied Polymer Science

Abstract: Chemical bonding of maleated polymer at the interface in wood plastic composites (WPC) was investigated in this study. Fiber quality analysis (FQA) and Scanning electron microscope (SEM) illustrated the changes of morphological structures and the fracture modes of wood fiber during compounding. FQA also revealed the thickness of the coated polymer on fiber surface was affected by the Mw of coupling agent, where its high Mw leads to thicker surface layer.

FTIR analysis showed the evidence of a chemical bond between wood fiber and maleated polymer through esterification. The distinct peak of esterification occurred in the range between $1800cm^{-1}$ and $1650cm^{-1}$ at FTIR spectra. The mass concentration of chemical components coated on the surface of wood fiber was related to the type of coupling agent type including Mw and grafted maleic anhydride type (MA%), where higher Mw or higher MA% yielded more esterifications as shown by carbonyl index with both IR and XPS analysis. Unlike entirely bonded fibers, the FTIR spectra of the partly bonded wood fiber have obvious differences in the peak of ester links which could be maximized at 3wt% content which corresponded to the fiber width recorded by FQA. For both entirely and partly functionalized fiber, MAPE leads to more fines by shorter fiber length and exhibits fluffier surface of fibers analyzed by FQA, which is evidenced the SEM. According to the FTIR spectra, there were always differences in $1740cm^{-1}$ and $1053cm^{-1}$ region due to morphological surface changes and the attachments of maleated polymer.

XPS which measures the sample elemental composition of a very thin surface layer was used to assess the surface composition. The decreased elements intensities of modified fiber evidence the roughness of fiber surface. The variation of oxygen and carbon concentration was profiled in the sampling depth which corresponds to the structures of cell layer.

In addition, maleated wood fiber showed a remarkable change on C1s and O1s ratios when compared to the initial fiber. The detailed formation on the bonds is revealed with high resolution spectra by the relative increase of oxidized carbon, especially with C2, and the relative decrease of C1. Moreover, the attachment of maleated polymer shifts the deconvoluted carbon spectra downward but oxygen towards

higher energies. Meanwhile, the nature of the coupling agent, such as MAPP and MAPE has important impact on the atomic ratio of oxygen and carbon as well as the proportion of the deconvoluted carbons. In any case, high MA content could result in high ester content leading to high O/C ratio. However, the chemical morphological differences and coupling agents contributed by maleated fiber with different bonding formations major in the oxidized carbons are characterized by hydroxyl index, grafting index, carbonyl index as well as the ratio of oxidized carbon to unoxidized carbon. The difference in the mentioned parameters could be used to monitor the occurrences of ester linkages and their types, especially by the number of oxygen. Based on the data, MAPE could contribute to much superior reactivity compared to that of MAPP at the same MA% level which was confirmed by the IR analyses.

A simplified approach estimated surface coverage by lignin and extractives to be high on CTMP fiber surface due to the TMP processing and the WPC manufacturing, which will help the final materials to achieve lower thermo-degradation and smoother appearances.

Key words: Birch fiber, XPS, Esterification, FQA, FTIR, Maleated polymer, SEM, Wood fiber

11.1 Introduction

Wood fiber has drawn much attention for being biodegradable and renewable [82, 485], inexpensive and richable [45, 95], for low disposal cost [91, 485], and for plastic wood composites being bioproducts [486, 487, 488]. However, the interfacial compatibility between hydrophobic polymer and hydrophilic wood fiber should be improved to meet their applications [81, 92, 314, 315, 316, 405, 478].

XPS was used to characterize the surface chemical composition of wood fiber [137, 478, 536, 537, 538]. XPS provides a means of obtaining detailed characterization of the surface. It gives a quantitative elemental composition and identifies certain functional groups on the surface. FTIR was used to determine the chemical structures of WPC [66, 137, 355, 478, 536, 539, 540]. The signals strength of treated wood fiber could be amplified by extraction [536] to reduce the overlaps produced by free molecules.

Although several studies have been done on coupling mechanisms of WPC via IR signal and XPS [137, 478, 536], the mechanisms of adhesive bonding was not fully developed.

Maleated polyolefins react with wood particles through an esterification reaction which occurs between the maleated groups of the polyolefins and the hydroxyl groups on the wood particles surface. There are two models of esterification of MAPP treated wood fiber, including half-ester and diester structures, following IR signal of extracted fiber [337, 541, 542, 543]. MAPE has been proposed to be used in WPC based PE polymer due to its superior contribution to effectively improved interfacial bonding between the hydrophilic wood fiber and hydrophobic PE [92, 393]. Keener [92] and Yang [393] also concluded that maleated polyolefin contributed to optimal performance of WPC, for example MAPE is used as binding agent in PE system while MAPP is used in PP system. However, most of this previous work often indirect evidence due to the fiber modified through a solvent-based process [337, 541, 542, 543].

A more realistic process has been reported by Lu and coworkers utilizing a Haake blender to graft MAPE onto wood fiber to reform the esterificaton reaction [137]. However, conclusions were based on the assumption that the MAPE treatment followed the indirectly obtained previous results of MAPP treatement. Carlborn and Maruana elucidated the mechanism of the chemical reaction between wood particles and maleated polyolefins during maleation of wood particles produced via reactive extrusion [544]. They monitored the chemical changes on the surface of wood particles with the treatment of maleated polyolefins by studying the MAPE content, the extrusion conditions and the effect of Mw of MAPP on the grafting efficiency with FTIR and XPS spectra [544]. It was great investigation on maleated wood fiber, but it still cannot monitor the chemical and morphological changes after they were fed into real WPC. An effective process to monitor the maleated polyolefins grafting onto the surface of wood fiber still needs to be developed.

Whatever both reactive extrusion and reactive blender is used for chemical compounding, the initial wood fiber from real WPC system could be extracted to reveal the coupling mechanism and the morphological changes among the WPC system. There are no records on any systematic investigations on this yet. Therefore, it is important to investigate the coupling action of maleated polyolefins onto the surface of wood fiber and characterize the functionalized wood fiber with proven chemical analysis techniques. In this study, reactive blending was employed to completely or partly graft maleated polyolefins to wood fiber. Both Soxhlet extraction and hot-xylene dissolution were used to delaminate on unglue to obtain

functionalized wood fiber. Particular emphasis was placed on examining the efficiency of grafting of the surface modification, as chemical functions of materials compositions, such as maleated polyolefins contents and molecular weights. FQA, SEM, XPS and FTIR were used to identify chemical changes on the surface of the wood fiber and the morphologies of wood fiber during compounding with maleated polyolefins.

11.2 Experimental and materials

11.2.1 Materials

11.2.1.1 Thermoplastic

Linear low density polyethylene (NOVA® GF-0218-F) was received from NOVA Chemicals. Its melt mass-flow rate is 2.0g/10min. Its specify density is 0.922g/cm^3. Polypropylene homopolymer (Marlex® HGZ-1200) was donated by Phillips Sumika Polypropylene Company (The Woodlands, TX, USA.). Its melting mass-flow rate is 115g/10min. Its specify density is 0.907g/cm^3. The chemical characteristics are observed by IR spectra in Figure 11.1.

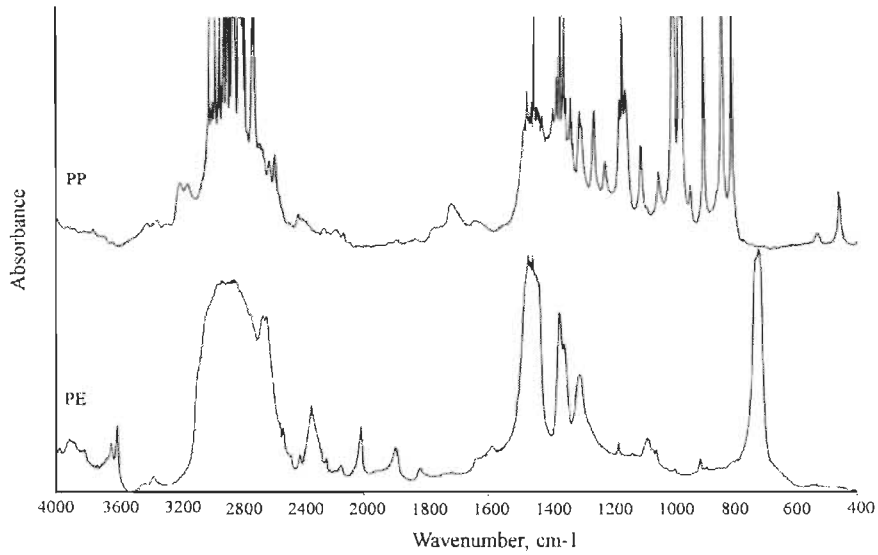

Figure 11.1 FTIR spectra of Polyolefins

11.2.1.2 Maleated polyolefin

Maleated polypropylene (Ma-PP, G2010 and G2608) and maleated polyethylene (Ma-PE) supplied by Eastman chemical company (Kingsport Tenn.) are used as binding agent. The typical IR chemical morphologies are shown in Figure 11.2 while the typical physical properties of maleated polyolefins are indicated in Table 11.1.

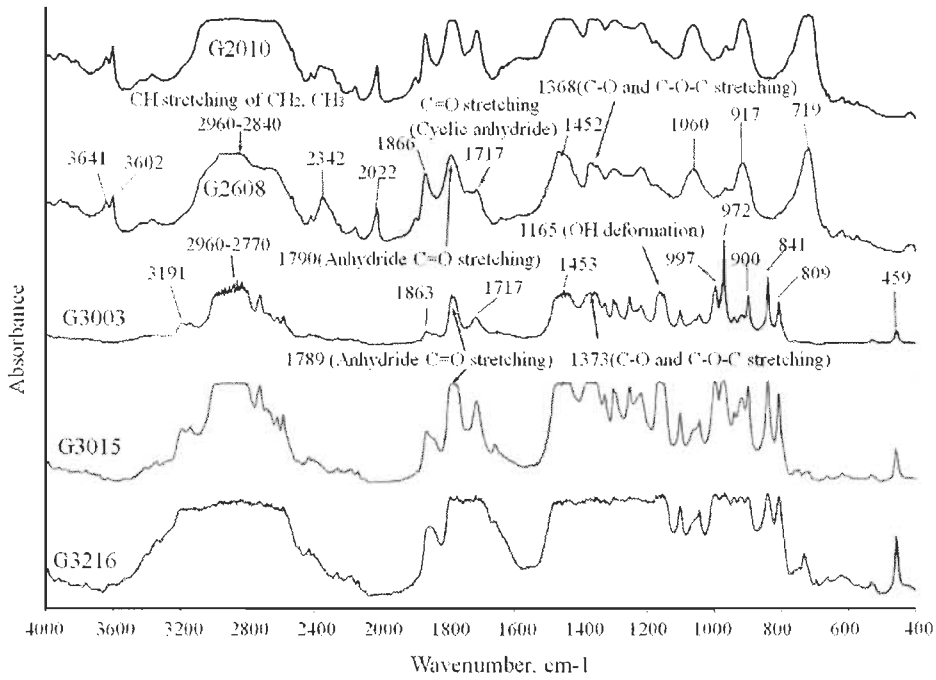

Figure 11.2 FTIR spectra of Maleated polyolefins

Table 11.1 Typical characteristics of Maleated Polyolefins

Physical properties	G2010/Epolene C-18	G2608	G3003	G3015	G3216
Polymer type	Ma-PE	Ma-PE	Ma-PP	Ma-PP	Ma-PP
Maleic anhydride graft, wt%	1.5	1.5	1.5	2.5	2.5
Melting point, °C†	---	122	158	156	142
Molecular mass, g/mol‡	15,000	65,000	52,000	47,000	60,000
Melt flow index at 190°C	---	8[a]	---	---	---
Viscosity at 190°C, cPa s	2,400-6,000[b]	---	60,000	18,000	18,000

†DSC Tm; ‡ Molecular weight measured via GPC using polystyrene standards.
[a] Melt index at 190°C, 2.16kg weight according to ASTM D1238;
[b] Viscosity at 150°C.

11.2.1.3 Wood fiber

Industrial chemi-thermo-mechanical pulp of yellow birch (Betula alleghaniensis) is employed. The wood pulp fibers were air-dried and ground at our laboratory to produce fine particles. Particles that passed through a 20-mesh but retained on a 80-mesh screen are employed in this study. The chemical properties of the extracted CTMP birch fiber with xylene and initial birch fiber are given in Figure 11.3.

11.2.1.4 Organic solvent

p-xylene (99.9%, ACS grade) and acetone (ACS grade) were used for Soxhlet extraction and hot solution separation.

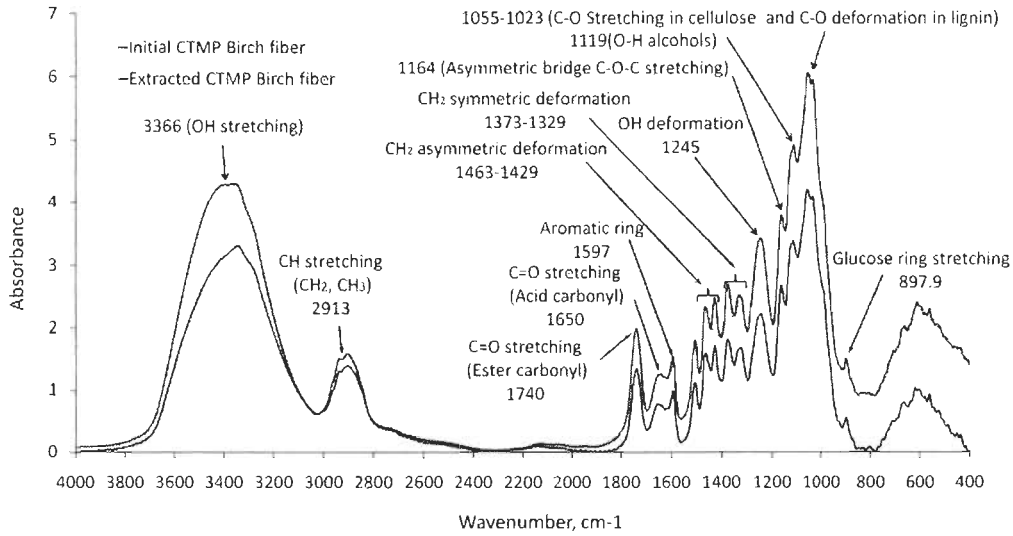

Figure 11.3 FTIR spectra of Initial and Extracted CTMP Birch fiber

11.2.2 Experimental

11.2.2.1 Preparation of wood plastic composites

Maleated polyolefin was compounded with 10, 20, 30, 40, 50 and 60wt% birch CTMP fiber to obtain entirely bonded wood fiber by Method 1 in Schedule 11.1. Polyolefin was compounded with 30wt% birch CTMP fiber in the presence of 0, 1, 2, 3, 5, 8 and 10wt% maleated polymer to get partly bonded wood fiber by Method 2 in Schedule 11.1. All the composites are prepared by a two-roll mill.

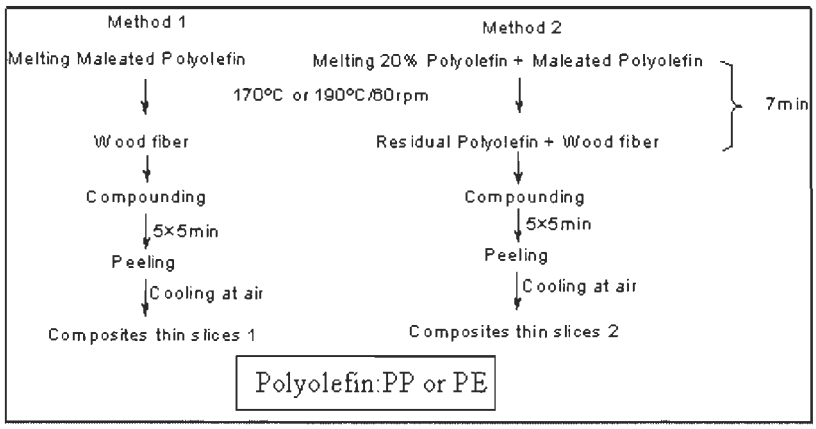

Schedule 11.1 Compounding conditions

The compounding temperature of the composites originated from PE and PP is 170°C and 190°C respectively. Thin slices are obtained after peeling from the roller and stored at the conditioned room for next steps. The specifications of the used two

roll mill (C.W. Brabender®) were: 30 cm length, 15 cm radius, 0.6 gear ratio and 60 rpm roll speed.

11.2.2.2 Preparation of coupled wood fiber

All the thin slices of the composites are dissolved in boiling xylene. The crude treated wood fibers are separated from the solution (polymer or maleated polymer mixture) by means of a small aperture wire mesh (100mesh) [545]. The resulting crude fibers are extracted by Soxhlet extractor with xylene for 48h in reflux [137, 546]. Treated wood fibers purified by acetone after extraction are coded as extracted treated wood fiber in Table 11.2. Concerning the composites based on PE with 30wt% fiber imported, it is hard to get enough fiber to perform the extraction. Thus the dissolving-filtering separation is used to remove free-polymer. The cycling separation is repeated 4 times due to its very high solution viscosity. Finally, the resulting crude treated wood fibers are dispersed in boiling xylene again and then poured into acetone to precipitate [547]. The purified treated wood fibers are dried in air as listed in Table 11.2. The separation procedure is illustrated in Schedule 11.2.

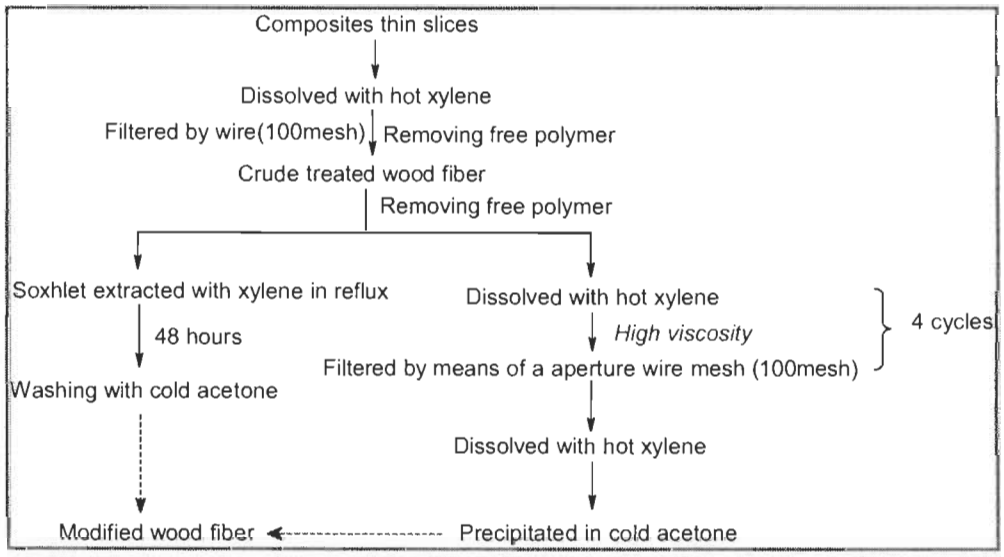

Schedule 11.2 Separation procedure of treated wood fiber

11.2.3 Characterization

11.2.3.1 Fiber quality analysis (FQA)

Physical characteristics of treated and extracted wood fiber were determined by the Fiber quality analyzer (LDA02090 HiRes) according to ISO 16065 and TAPPI T271.

5000 fibers were counted to determine an average fiber length, width, curl and kink of treated pulp fiber.

Table 11.2 Descriptions of modified wood fiber

Sample		Notes	
Birch fiber (20-80mesh)		Initial	
Extracted birch fiber (20-80mesh)		xylene extracted, acetone washed	
Bonded entirely			
G3015F10 G3015F20 G3015F30 G3015F40 G3015F50 G3015F60	Low Mw G3015 bonded Extraction	G3216F10 G3216F20 G3216F30 G3216F40 G3216F50 G3216F60	High Mw G3216 bonded Extraction
G2010F40 G2010F50 G2010F60	Low Mw G2010 bonded Extraction	G2608F40 G2608F50 G2608F60	High Mw G2608 bonded Extraction
Bonded partly			
PPF30G0 PPF30G1 PPF30G2 PPF30G3 PPF30G5 PPF30G8 PPF30G10	Matrix: PP G3003 bonded Extraction	PEF30G0 PEF30G1 PEF30G2 PEF30G3 PEF30G5 PEF30G8 PEF30G10	Matrix: PE G2010 bonded Dissolution

11.2.3.2 Scanning electron microscopy (SEM)

Sample preparation: Wood fiber were mounted on a substrate and cut to a proper size and fixed onto a microscope aluminum stub. Sample stub with fibers was surface metalized by means of a Polaron (Model SC 7620) sputter coater with evaporated Au metal (4nm in thickness).

The morphological studies on the fibers were carried out by SEM (JSM 5500, JEOL, Japan) at an acceleration voltage of 15kV, the spot size is 30 and the working distance is 19mm.

11.2.3.3 Fourier transform infrared analysis (FTIR)

Sample preparation: 0.5mg oven dried each treated wood fiber fraction are grinded with 100mg of KBr. 13mm KBr pellets were prepared in a standard device with 10MPa pressure for 5 min under 700mmHg vacuum. The thickness of the pellets was 200μm. Polymer films were prepared by casting melted polymers on the 13mm

stainless pressed stick, and then being pressed at the same condition to get 700μm films.

Spectra were acquired against a bare KBr or blank background spectrum on a Perkin Elmer spectrophotomer (System 2000 FTIR) at a resolution of $4cm^{-1}$ with a coaddition of 60 scans for each spectrum. All the data analyzes were performed with Spectrum V3.02 software from Perkin Elmer in the following sequence.

1. All spectra were viewed in absorbance;
2. Spectra baseline correction was calculated at $3900cm^{-1}$, $2000cm^{-1}$ and 1900 cm^{-1} points in limited range;
3. Spectra normalizations of fibers were performed at the peaks of the glucose ring stretching/vibration ($895\text{-}898cm^{-1}$);
4. All treated spectra were transferred as ASCII files and plotted by Excel.

Spectra of polymers were viewed at slip mode, no baseline correction and normalization was used. Grafting was the main surface characteristics of wood fiber during compounding. On the previous works [137, 536, 544, 548], the regions of interest in the FTIR spectra of wood fiber coupled with maleated polyolefins were the absorbance bands near $2852\text{-}2919cm^{-1}$ and $1710\text{-}1740cm^{-1}$, for the CH stretching of aliphatic carbon chains and carbonyl groups stretching, suggesting the formation of ester linkages, respectively. The carbonyl index could be calculated by the following equation:

$$\text{Carbonyl index}_{IR}(CI_{IR}) = \frac{A_{1740}}{A_{2900}} \times 100\% \qquad \textbf{Equation 11.1}$$

where A_{1740} represents the peak area at $1740cm^{-1}$ which corresponds to ester carbonyl and A_{2900} represents the peak area around $2900cm^{-1}$ due to the alkane CH stretching vibrations of methylene or ethylene groups. In addition, the peak intensity at $1740cm^{-1}$ could represent the grafting index.

11.2.3.4 X-ray photoelectron spectroscopy (XPS)

Prior to XPS analysis, all samples were oven-dried. Untreated and treated wood fiber was recorded with XPS by the Integrated Pulp and Paper Center, University of Quebec at Trois-Rivieres, Quebec, Canada. XPS was performed with a Kratos Axis Ultra (HIS 165) spectrometer (Kratos Analytical, Manchester, UK) at 3 locations using a monochromatic X-ray source and a dual Al-Kα anode (15mA, 1486.7eV) at 225W. The analyzer mode was hybrid mode. The surface sensitive analysis works to

a depth 10nm. The measured area at each point was $1\times2mm^2$. Due to the structure of wood fiber which is non homogeneous, core-level shift will vary sampling depth. So, the depth profile for each element measured was proposed in the complete sampling depth of about 5nm. The base pressure was less 2.5×10^{-9} Torr and the operating pressure was 1.8×10^{-9} Torr. For each sample, two spectra in the fixed analyzer mode were recorded.

(i) Survey spectra (0-1300eV and pass energy 160eV) were recorded to estimate composition. During the analysis, the electron takeoff angle was 45°, the emission angle was 90°, the dwell time was 100ms, the acquisition time was 130s, the step was 1000meV and the sweep time was 1. The survey spectra were used to determine the concentration of each element present on the surface of the samples. The O/C ratio used is very popular in pulp fibers. High resolution spectra of the C1s were obtained to further analyze the chemical bonding of the carbon atoms.

(ii) High-resolution spectra (within 20eV and pass energy 40eV) were recorded to obtain information on chemical bonds.

During the analysis, the electron take-off angle was 45°, the dwell time was 332ms, the acquisition time was 182s, the step was 100meV and the sweep time was 3.

The electron auger of carbon, nitrogen and oxygen were set at 1250eV, 1110eV and 980eV. The binding energy reference for the peak of C1s, N1s and O1s were set at 283.0eV, 398.0eV and 531.0eV. From the survey spectra, the atomic concentration ratio of oxygen to carbon was determined by integrating the area under the curve after removal of the linear background [549, 550, 551].

High-resolution analysis of the carbon chemical bonds was performed by iterative convolution, using a nonlinear least-squares procedure based on the Levenberg-Marquardt algorithm. The contributions show up in the same peak but the peak intensities at a given bending energy were deconvoluted with Gaussian-Lorentzian peak fit by CasaXPS with a Sun Sparc Station IPX computer (Vision 2). The Gaussian-Lorentzian ratio was set at 0.20 for all curve fittings corresponding to the distribution of O-C-O/C-O in a cellulose monomer [552].

The atoms analyzable by XPS in pure cellulosic fibers are carbon and oxygen. The chemical shifts for carbon (Cls) in pulp fibers can be deconvouluted into four components according to the number of oxygen atoms bonded to carbon [549, 553]. Relative amounts of them could be determined by deconvolution of high resolution

C1s spectra using symmetric Gaussians. Relative peak positions were fixed during the curve fitting process as described [554].

- The unoxidized C1 class corresponds to carbon atoms bonded only with carbon (C-C) or hydrogen atoms (C-H), and it is pointed out at binding energy of 283eV.
- The C2 class corresponds to the carbon atoms bonded with one oxygen atom (C-O) and it appears at a higher binding energy compared to C1 ($\Delta_{Binding\ energy}$=+1.5±0.2ev).
- The C3 class corresponds to the carbon atoms bonded to a carbonyl (C=O) or two non-carbonyl oxygen atoms (O-C-O) ($\Delta_{Binding\ energy}$=+2.8±0.2ev)
- Finally, the C4 class is associated with carbon atoms bonded to a carbonyl (C=O) and two non-carbonyl oxygen atoms (O-C=O) ($\Delta_{Binding\ energy}$=+3.75±0.2ev)

Maleated polyolefins are believed to be attached to the surfaces of wood fiber via ester links between the hydroxyl groups of wood fiber and the anhydride groups which led to the formation of a monoester with carboxylic groups pendant groups or a diester formation without carboxylic acid pendant groups at a single site reaction [338, 405, 478, 543, 544, 555]. For CTMP fibers, the C1 mainly arises from lignin. However, we assume that all extractives including fatty acids and glycerides were entirely removed after extraction. The presence of C1 class of C1s can be attributed to carbon chains of maleated polyolefins while the presence of C4 class comes from acetyl groups of hemicelluloses content [556] as well as the ester linkages of the esterification with maleated polyolefins. Thus, both the formation of monoester and the formation of diester contribute to the values of C4 class, and the molecular chains of maleated polyolefins contributes to the C1 class content. The deconvoluted carbon components for wood fibers were classified and presented in Table 11.3.

Table 11.3 Classification of deconvoluted carbons (C1s) [537, 550, 552, 557, 558]

C1s	Sources in the samples
C1	Terpene, Fatty acid, lignin, and aliphatic chains of polymer
C2	(OH) Cellulose, hemicelluloses, lignin, maleate groups
C3	Fatty acid and their esters, hemicelluloses, and lignin
C4	Resinic acid, hemicellulose, ester linkages

As mentioned above, the chemical reaction of maleated polyolefins and wood fibers takes place between the maleate groups of the polyolefin and hydroxyl groups. Since

C2 component only arises from atoms bonded to a single oxygen atom, other than carbonyl oxygen (C-OH), Carlborn and Matuana used hydroxyl index to quantify the changes in the content of C2 component to monitor the occurrence of the esterification between the maleated polyolefins and the wood fibers the by the following Equation [544].

$$\text{Hydroxyl index } (HI) = \frac{C2_{Modified}}{C2_{Unmodified}} \qquad \textbf{Equation 11.2}$$

where $C2_{Modified}$ and $C2_{Unmodified}$ are the relative amount of the C2 component in the deconvoluted high-resolution C1s spectrum of wood fiber sample with or without modification after extraction. Due to C1 and C4 bands which are assigned to the aliphatic chain or ester carbonyl groups come from the esterification reaction, the changes in content of C1 and C4 are employed as grafting index to evidence the occurrence of the ester links during compounding byEquation 11.3.

$$\text{Grafting index}_{\chi}(GI) = \frac{C_{\chi Modified}}{C_{\chi Unmodified}} \qquad \textbf{Equation 11.3}$$

where χ represents the deconvoluted C1 or C4 band of the modified wood fiber before and after modification after extraction.

In addition, C3 and C4 came from the vibration of ester carbonyl. Carbonyl index could be quantified by the changes in the ratio of the content of carbonyl groups to the C-C/C-H stretching vibration bands (C1) by the following Equation.

$$\text{Carbonyl index}_{IR}(CI_{IR}) = \frac{A_{1740}}{A_{2900}} \times 100\% \qquad \textbf{Equation 11.4}$$

According to previous reports [536, 298], to determine the types of oxygen–carbon bonds present, chemical bond analysis of carbon was accomplished by curve fitting the C1s peak from the high-resolution spectra and deconvoluting it into four subpeaks corresponding to an unoxidized carbon, C1, and various oxidized carbons, C2, C3, C4 and C5 if possible. An oxidized to unoxidized carbon ratio ($C_{ox/unox}$) was calculated with their integrated peak area to quantify the degree of surface oxidation evidencing the chemical reactions (Equation 11.5).

$$C_{ox/uox} = \frac{C_{Oxidized}}{C_{Unoxidized}} = \frac{(C2 + C3 + C4 + C5)}{C1} \qquad \textbf{Equation 11.5}$$

As previously described [544, 559, 560, 561, 562], quantitative analysis of surface lignin and extractives was performed using both the O/C ratio (Equation 11.6 and

Equation 11.7) and the intensity of the C1 carbon peak (Equation 11.8 and Equation 11.9) based the models of pure wood fibers. The percentage of surface lignin and surface extractives, calculated using the O/C ratio, are given by Equation 11.6 and Equation 11.7.

$$\emptyset_{Lignin} = \frac{O/C_{Extracted\ fiber} - O/C_{Cellulose}}{O/C_{Lignin} - O/C_{Cellulose}} \times 100\% \qquad \textbf{Equation 11.6}$$

$$\emptyset_{Extractives} = \frac{O/C_{Extracted\ fiber} - O/C_{Fiber}}{O/C_{Extracted\ fiber} - O/C_{Extractives}} \times 100\% \qquad \textbf{Equation 11.7}$$

where $O/C_{Extracted\ fiber}$ and O/C_{Fiber} are experimentally determined and O/C_{Lignin}, $O/C_{Cellulose}$ and $O/C_{Extractives}$ are the theoretical values 0.33, 0.83 and 0.11, respectively according to the studies of Mjöberg [563] (see Table 11.4). The percentage of surface lignin and surface extractives, calculated using the C1 value, are given by Equation 11.8 and Equation 11.9.

$$\emptyset_{Lignin} = \frac{C1_{Extracted\ fiber} - \alpha}{C1_{Lignin}} \times 100\% \qquad \textbf{Equation 11.8}$$

$$\emptyset_{Extractives} = \frac{C1_{Extracted\ fiber} - C1_{Fiber}}{C1_{Extracted\ fiber} - C1_{Extractives}} \times 100\% \qquad \textbf{Equation 11.9}$$

where $C1_{Extracted\ fiber}$ and $C1_{Fiber}$ are the relative amount of the C1 component in the deconvoluted high-resolution C1s spectrum of pulp sample after and before extraction, C1Lignin and C1Extractives are the theoretical value of 49 and 94 in Table 11.4. α was the contribution to the C1 peak from surface contamination. A value of 2% was used for α, which was the lowest relative amount of C1 peak detected on the surface of fully bleached standard pulp fibers (pure cellulose contains only C2 and C3 carbons, however a small C1 peak is routinely observed due to adsorbed hydrocarbon contaminants [564].

Table 11.4 Theoretical values of atomic composition and deconvoluted C1s

Sample	O/C	C1	C2	C3	C4
Cellulose	0.83	0	83	17	0
Lignin	0.33	49	49	2	0
Oleic acid	0.11	94	0	0	6

11.3 Results and Discussions

11.3.1 Characterizations for wood fiber by FQA and SEM

During the processing, the shear stress applied by the rollers will break the fibers under high viscosity resulting in the changes of the characteristics of wood fibers.

The final fibers are determined by FQA compared to the initial fibers to reveal the rheological and morphological changes.

11.3.1.1 Modified wood fiber bonded completely with maleated polyolefins in different Mw

The fines percentage, fiber length and width distribution are presented in Figure 11.4a-c. The fines content increases significantly due to fiber fracture as shown in Figure 11.4a. For MAPP modified wood fiber, either G3015 or G3216 have got more than 30% fines, even 65% as 30wt% fiber loading. Although the torque increases with the increase of fiber content [446], the fines content decreases probably due to the shear stress are shared by more fibers. While G3015, low Mw, could lead to the modified fiber to higher fines content resulting in the lower molecules weight polymer penetration, reaction and even to easier wood fiber peal compared to G3216, high Mw. Compared to MAPP, MAPE produces more fines during processing than either G2010 or G2608 due to more functional groups occurrence resulting in cutting and bruising (Figure 11.4d-f and Figure 11.5 to Figure 11.9) exhibiting higher viscosity, and the fines could reach 80% as G2010 employed. Similar to the mechanism of MAPP, low Mw MAPE achieves higher fines content.

So, the fines content in the final wood fiber will increase dramatically within the range of 30-80% compared to the initial fiber at the values of 12%.

As Awal and coworkers [565] described that the fibers would be cut during extrusion process, the fiber lengths in our case are also fractured seriously while the thickness increases due to the maleated polymer is coated on the surface of wood fiber as illustrated in Figure 11.4b-c. As fiber employed the torque in the system increases due to the increase of viscosity and functions between wood fiber and the binding polymer, the arithmetic length of wood fibers decreases and reaches a minimum value as 30wt% MAPP is loaded by cutting and bruising with strong driving force under high viscosity [566]. The resulting fiber length increases with wood fiber content is increased further resulting from the weakness of the shear impact of maleated polymer near the surface of wood fiber. Compared to the initial fiber length (0.95-0.98mm), the range of fiber length of MAPP treated wood fiber is 0.18-0.45mm while the fiber length of MAPE treated wood fiber is 0.19-0.23mm which is corresponding to the increase of fines and higher processing viscosity caused by MAPE which also confirmed by their SEM images in Figure 11.5-Figure 11.9.

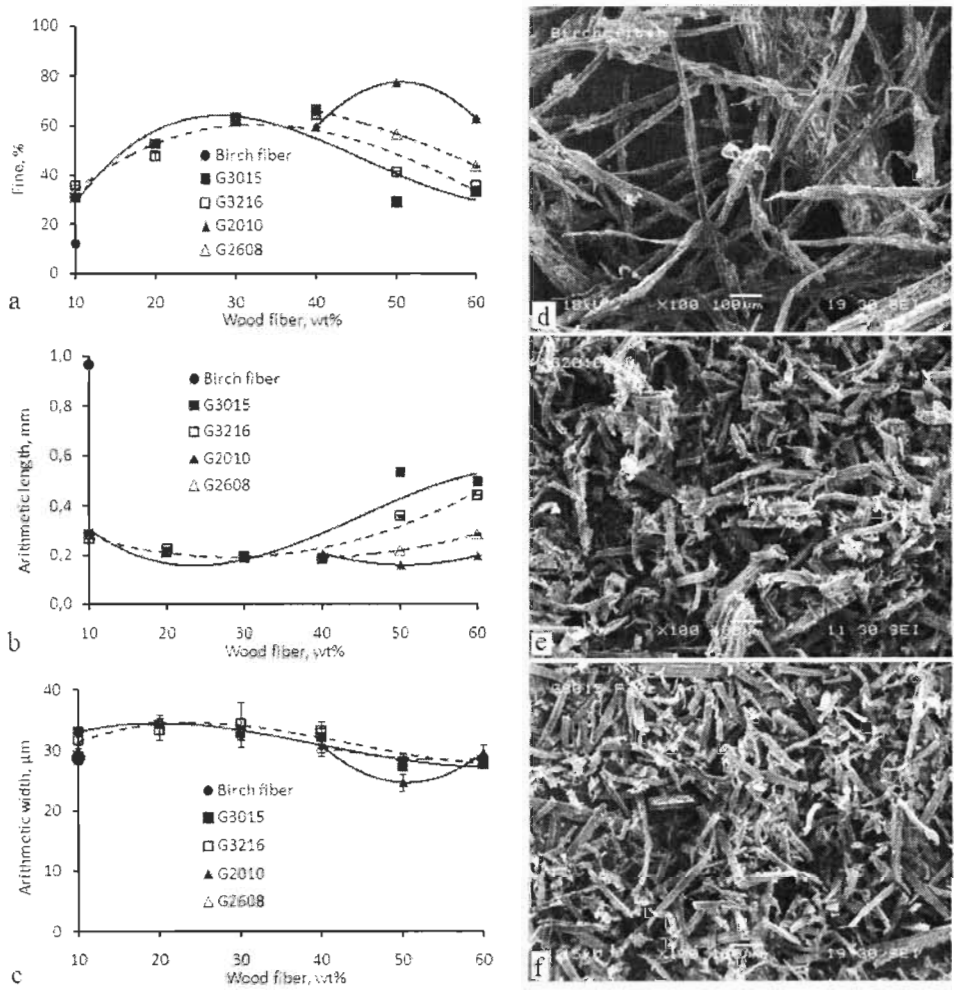

Figure 11.4 Characteristics of entirely bonded wood fiber

Initial fibers have smooth surfaces (Figure 11.5b-c) and clear rupture (Figure 11.5d) while most treated wood fibers are fractured and fibrillated (Figure 11.6 to Figure 11.9) due to the strong driving force and the shear stress originating from the interactions during processing.

Both MAPP and MAPE could react with the hydroxyl groups by ester linkages [337, 338, 478, 543, 544, 555], therefore the stronger driving force as well as the shear stress fractures wood fibers through the improved adhesion, exhibiting a rough surface & fiber-ends and fractured & cracked fibers leading to more fine pieces as shown in Figure 11.6-Figure 11.9. Maleated polyolefins with low molecular weight lead to shorter fiber due to higher wettability leading to stronger reactions which could be observed in their facture modes in Figure 11.6-Figure 11.9. As seen from the Figures, low Mw maleated polymer contributes the treated wood fiber with rougher surface and more facture models, especially to fibrillation.

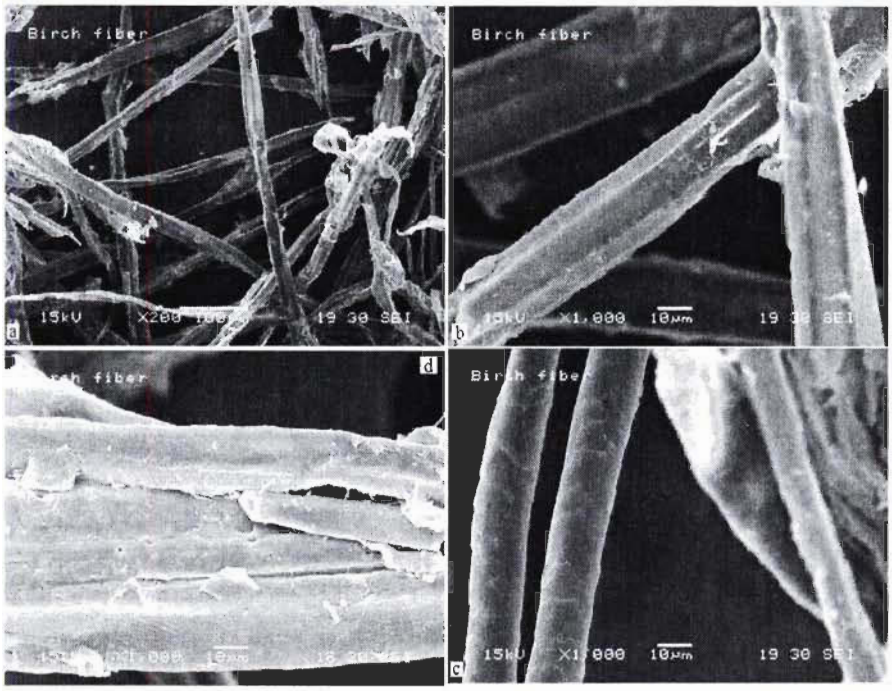

Figure 11.5 Characteristics of the initial birch fiber

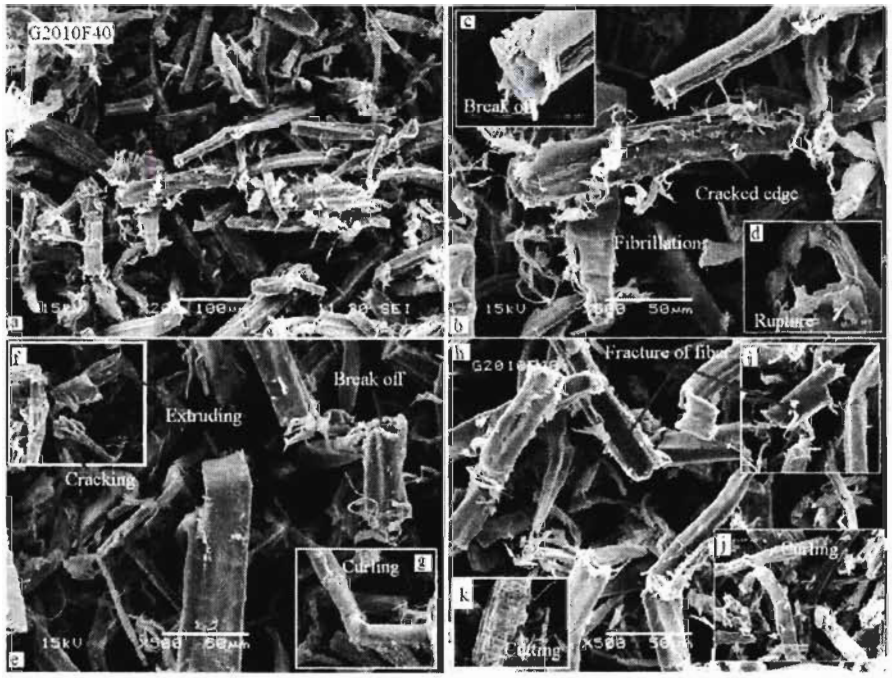

Figure 11.6 Fracture pictures of G2010F40

However, as maleated polyolefins are presented, the fiber width increases moderately although the width trend is to decrease with further wood fiber content increase. The increases originate from the coated polymer resulting in rough surface while the decreases come from fiber factures, such as cracking, pinwheel, peeling, and

extruding. The range of width of MAPP treated wood fiber is 27-34μm compared to its initial values of 29μm. So, the thickened fiber is estimated to increase 5μm at maximum. And Mw has little impact on the changes of width because Mw has less contribution to the thickness. As mentioned above, the fiber width of MAPE treated wood fiber decreases a little due to more factures, such as peeling and cracked, occurring (Figure 11.6c and Figure 11.7b).

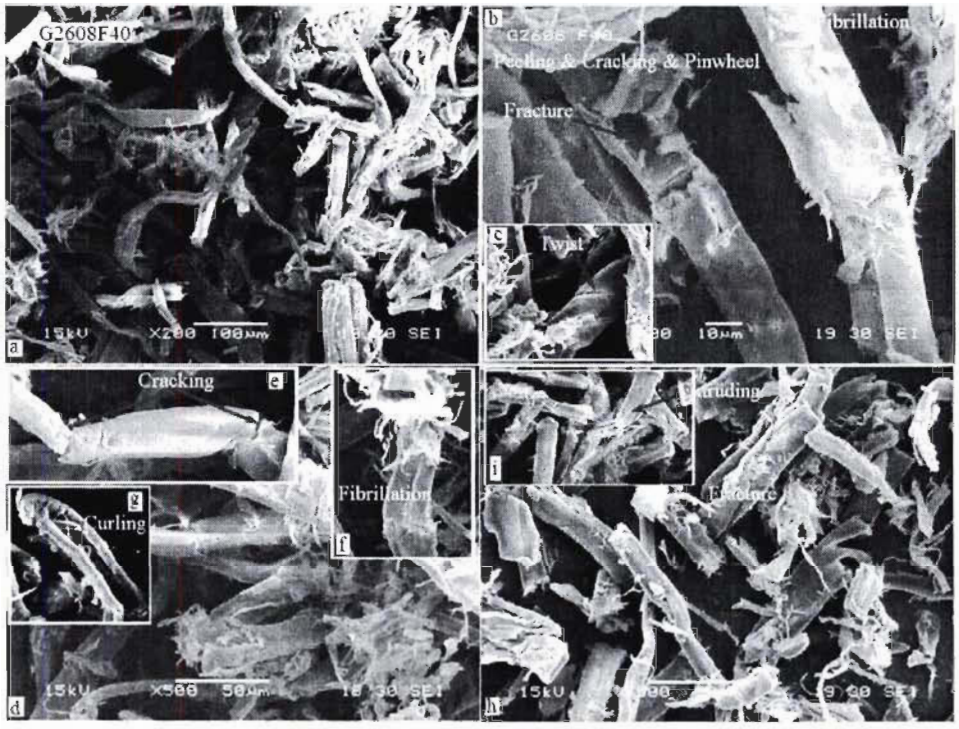

Figure 11.7 Fracture pictures of G2608F40

Due to the interactions occurring between wood fibers and binding polymer, the characteristics of wood fibers are changed before and after processing. The functionalized wood fibers exhibit complex morphologies as shown in Figure 11.10. As found out from FQA, the modified wood fibers have higher curls and kinks content as shown in Figure 11.10a-b. Compared to initial wood fiber, higher curls correspond to the fracture pictures of curling (Figure 11.6g, Figure 11.7g, Figure 11.8f and g, and Figure 11.9b and d) and extruding (Figure 11.6e and f, Figure 11.7i) by compounding driving force and shear stress on wood fibers. Meanwhile, kinks content increases with increasing wood fiber content which correspond to the fiber factures, such as cracks (Figure 11.6b, Figure 11.7b and h, Figure 11.8b, d and e, Figure 11.9b, c and d) and fibrillation (Figure 11.6b, Figure 11.7b and f, Figure 11.8b).

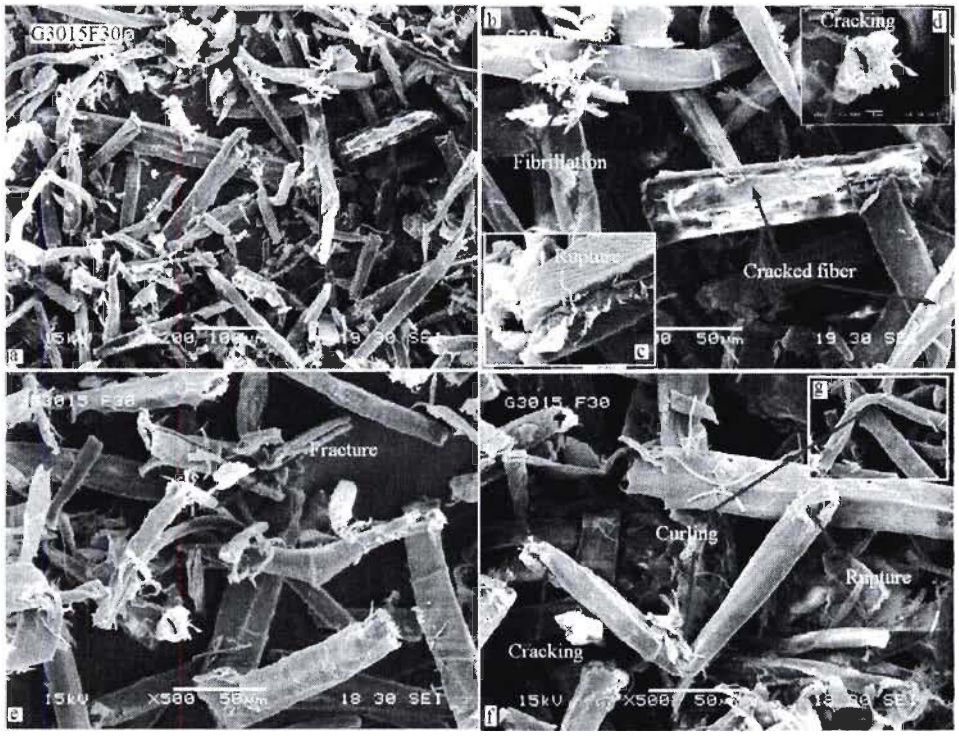

Figure 11.8 Fracture pictures of G3015F30

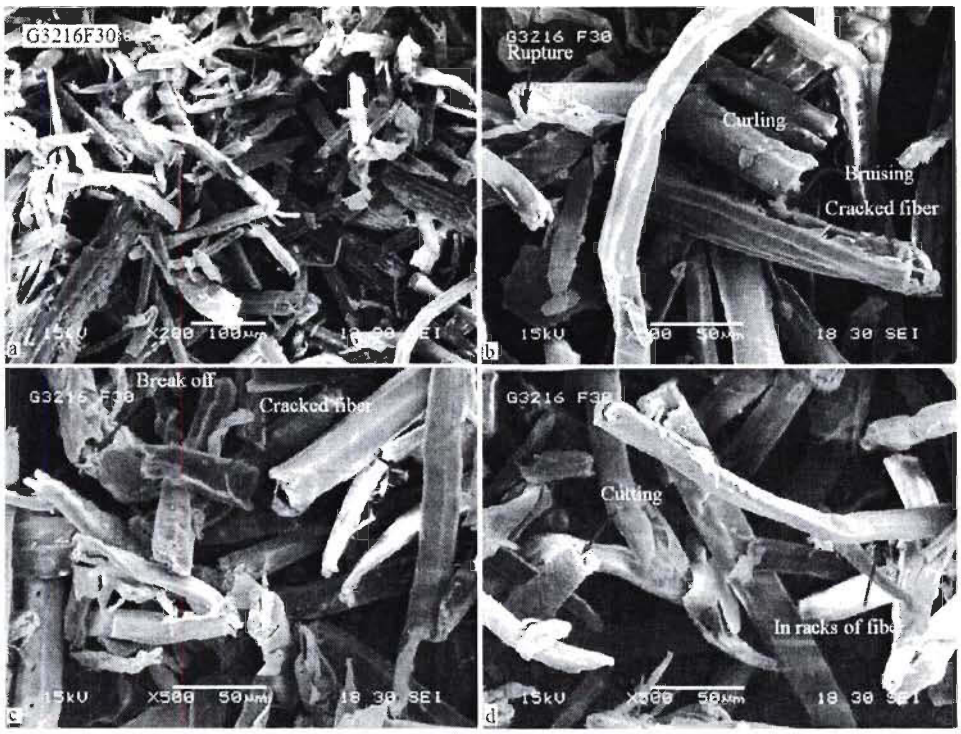

Figure 11.9 Fracture pictures of G3216F30

Due to the action of twist (Figure 11.7c) and curling (Figure 11.6g, Figure 11.7g, Figure 11.8f and g, and Figure 11.9b and d), the kink angles of the resulting wood

fibers are enlarged as described in Figure 11.10c. Because of much more kinks are formed, the kinks per mm are higher than that of initial fibers (Figure 11.10d).

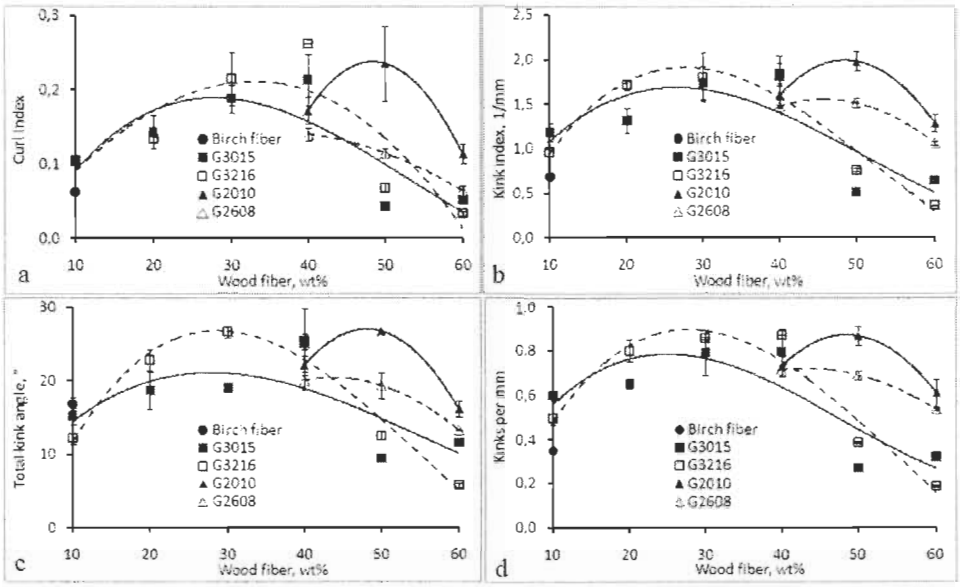

Figure 11.10 Characteristics of entirely bonded wood fiber

Opposite to the changes of the length and width, high Mw MAPP leads to wood fiber with higher curls and more kinks due to longer pendant polymer chains. But low MAPE content results in higher curls and kinks produced by the stronger reactions. It is concluded that the Mw has high impact on the curls and kinks under moderate interfacial reactions, such as with MAPP, while the changes occurred during the processing have more impact on the curls and kinks in stronger interactions occurring such as MAPE. The difference of the curls and kinks between MAPP treated wood fibers and MAPE treated wood fibers come from the reaction intensity at the same fiber loading. Obviously, MAPE could achieve high curls and more kinks content compared to MAPP which indicates that more facture occurred as seen in Figure 11.6-Figure 11.9.

11.3.1.2 Modified wood fiber bonded partly with G3003

MAPP treated wood fiber were studied to see the effect of coupling agent on the morphologies of resulted wood fiber. According to our previous works, use of MAPP could achieve optimal strength at 3wt% and slight deterioration occurred as excess MAPP employed due to slippages [378, 405]. In this case, we could point out this result by FQA following the increase of MAPP. Due to the limits of coupling agent employment, the fiber fractures mainly come from the shear force. The wettability is

another factor showing the morphological changes of wood fiber after the interfacial adhesion is improved by coupling agent.

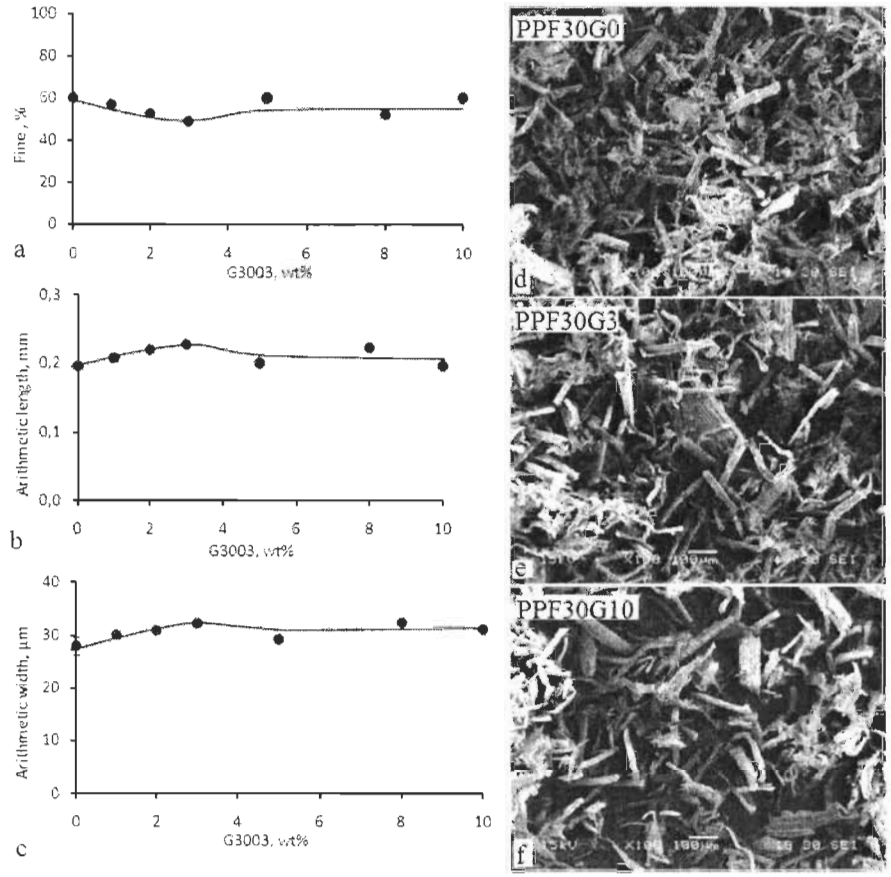

Figure 11.11 Characteristics of partly bonded wood fiber with G3003

The fines percentage, fiber length and width distribution for partly bonded wood fibers are presented in Figure 11.11a-c. The quantity of fines particles of the treated wood fiber without G3003 employed are 60% due to the incompatibility between wood fiber and the matrix. With incorporation of G3003, the fines content decreases steadily due to the improved compatibility. The fines percent reach the lowest value of 49% with 3wt% G3003 as presented in Figure 8a because this amount of G3003 yields best compatibility to prevent wood fiber from fracturing and also exhibit superior strength [378, 405]. However, when excess G3003 is employed, the proper wettability or compatibility will be converted into slippages because of the amount of G3003 molecules entangling on the surface of wood fiber (Figure 11.12c and Figure 11.12c'4) due to their polarities [453]. Thus the fracture of wood fiber could be modified by the shear force from the coated polymers other than the matrix which

leads to the increase of fines content again from 49% with the thinnest coat up to 60% with the thickest coater formed as 10wt% G3003 is incorporated.

Similar to the formation of fines, the fiber length as well as fiber width increases due to incorporated G3003 bonded on the surface of wood fiber forming a coat to improve the compatibility and wetability while the thickness could not produce shear stress. Therefore, both the optimal value of fiber length and width could be achieved at 3wt% G3003 (0.228mm for length and 32.3μm for width) compared to the treated wood fiber without G3003 (0.197mm for length and 28μm for width) which contributes from the fractured wood fiber as discussed. Thus it is easy to estimate the thickness of the bonded coat as less 4μm. It also indicates that the 3wt% G3003 is entirely bonded with 30wt% filled wood fibers and formed superior structures through the coated maleated PP.

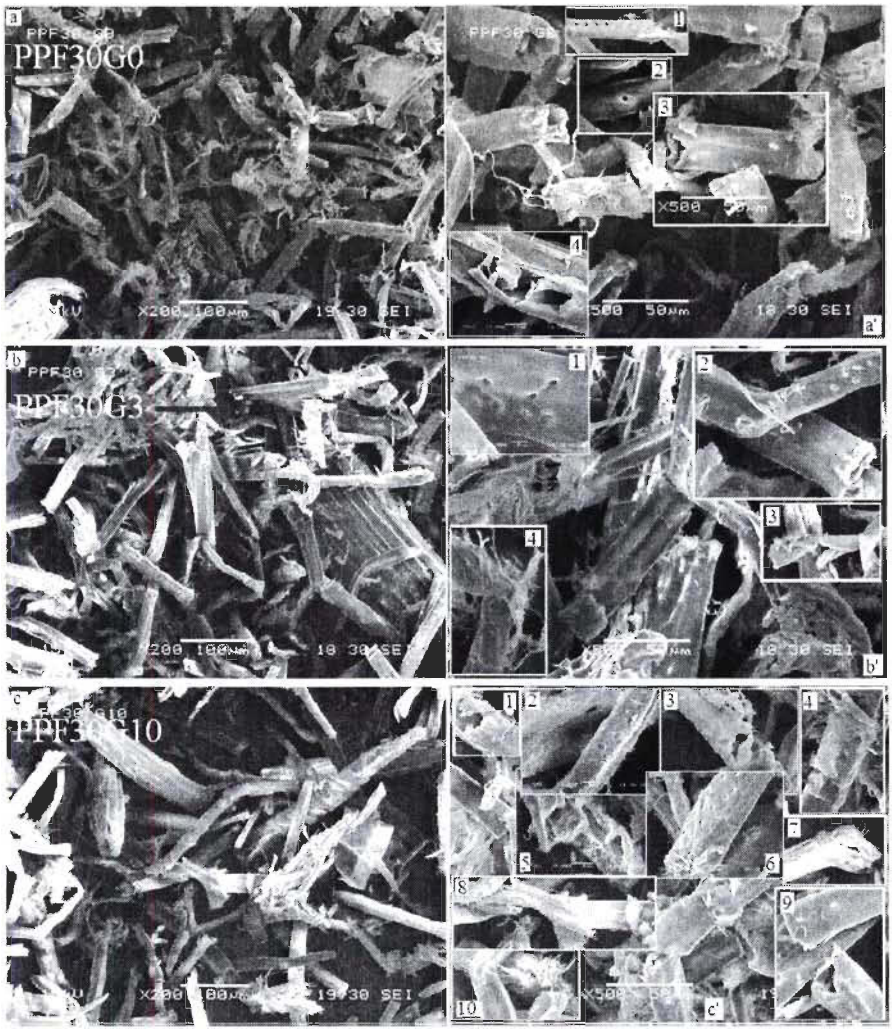

Figure 11.12 Fracture pictures of partly bonded wood fiber with G3003

Due to the differences of length and width are within thirty micrometers, it is difficult to be distinguished by SEM images in Figure 11.11d-f, but the functions are revealed in Figure 11.12. With additional coupling agent, both fiber length and width decreases slightly, but is still superior to wood fiber without the presence of coupling agent, because the thicker coated polymer could produce the interfacial shear stress resulting in more break off but less curling and fibrillations as shown in Figure 11.12b'-c'.

To summarize, the incompatibility could deteriorate wood fiber overwhelmingly by friction force coupled with shear stress from the matrix. As coupling agent is presented, the effects caused by friction force will be minimized with the improved interfacial compatibility and enhanced wetability. However, there is an optimal amount of coupling agent which not only improves interface by forming chemical bonding efficiently on the surface of wood fiber but also prevents filled wood fiber from weakening. The thickness of coated bonded polymer is an important factor, too thin would not be enough to improve the compatibility resulting in wood fiber being destroyed by the friction while too thick would lead to slippages and submit wood fibers to interfacial shear stress by producing more fines and exhibiting fiber size decreases due to the thicker coated polymer which results in additional shear stress along the fibers.

Due to the fact that the effective thickness of the coat is affected by the amount of maleated polymer introduced, the characteristics of the coated polymer has important impact on the bonded wood fibers which is related to the amount of the employed coupling agent. The characteristic of the modified wood fiber corresponding to the curls, kinks as well as the kink angle are shown in Figure 11.13. It is not same as the bonded completely type, the amount of the curls and kinks have hardly decreased. The data of FQA indicate that the amount of curls and kinks of modified wood fibers increase with the increase of G3003 from 0 to 3wt% in Figure 11.13a-b due to more fibers curling and fibrillating as shown in Figure 11.12b2-4. With excess G3003 is introduced, the curls and kinks content decrease a little due to less fibrillations and curling (Figure 11.12b'-c'). It is assumed that the dominant fracture mechanisms in wood fiber-based composites are changed following the coupling agent increasing.

However, the incorporation of coupling agent yields an increase the percent of the kinks per mm, and the ratio is kept as excess G3003 used in Figure 11.13d. This result may originate from the increase of break offs (Figure 11.12c'1 and 9) and

bonded molecules (Figure 11.12c'2 and 3) which do not contribute to the amount of kinks. Due to the functional groups of the coated polymer and the fibers' fractures, the kink angles are increased as described in Figure 11.13c.

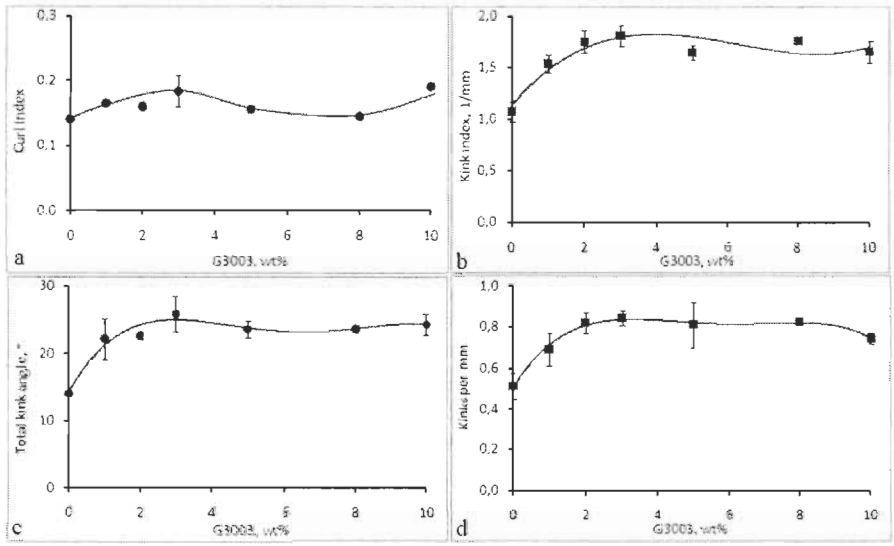

Figure 11.13 Characteristics of partly bonded wood fiber with G3003

Irrespective of wood fiber being bonded completely or partly, the increased width has an impact on the characteristics of wood fiber, such as curls and kinks. The proper amount of coupling agent would make fibers thicker which contributes to the modified wood fiber with high curls and kinks. The curls and kinks are related by fracture modes, especially to fibrillation and cracking while break offs and ruptures have little effects. It is important that the thickness of the coated polymer is determined by the incorporated amount of coupling agent exhibiting the change of the fracture modes.

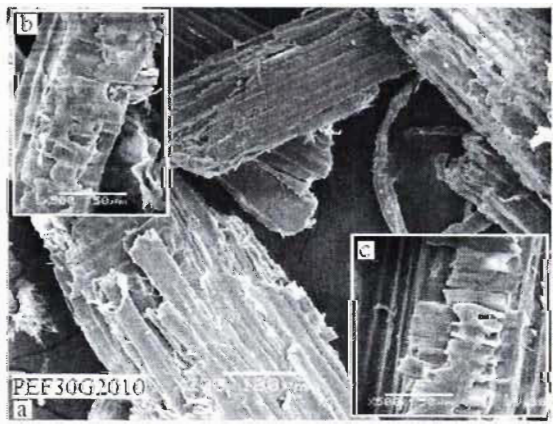

Figure 11.14 Oriented morphology and fracture pictures of partly bonded wood fiber with G2010

Except for the fractures mentioned above, it is also found that there are also pores or pits on the surface of wood fibers which are filled by incorporated the coupling agent (as Figure 11.12a'1-2, b'1 and c'6 show) and wood fiber are oriented and cut by strong driving force, especially for PE or MAPE as shown in Figure 11.14.

11.3.2 Surface and Interface Characterization by FTIR

FTIR spectroscopy was used to monitor and quantify changes that occurred on the surface of wood fibers after modification with maleated polyolefins. Infrared spectra of unmodified wood fibers and pure maleated polymer are shown in Figure 11.2-Figure 11.3. Infrared spectra of entirely and partly modified wood fibers are shown in Figure 11.15 to Figure 11.23. Obviously, there are many similarities and differences between wood fiber and modified wood fiber due to the small amount of coated polymer. Table 11.5 lists the wavenumbers of peaks found in these spectra, along with the assignments of corresponding functional groups.

11.3.2.1 FTIR spectra of entirely bonded wood fiber

Regardless of wood fiber content, evidence of the grafting of MAPE compound to the surface of wood fiber entirely is apparent in the spectra of modified wood fiber in Figure 11.15 and Figure 11.16. There are two large distinct peaks at 2919cm^{-1} and 2852cm^{-1} assigned to the C-H stretching vibrations of the MAPE backbone molecules [314, 544] which is different in appearance to that of unmodified birch fiber (Figure 11.3). Moreover, the distinct change is clearly seen near the absorption band at 1740cm^{-1} where three distinct peaks at 1866cm^{-1}, 1790cm^{-1} and 1717cm^{-1} associated with cyclic anhydride, anhydride C=O stretching and C=O stretching from maleic acid respectively have disappeared due to the anhydride groups reacting with the hydroxyl groups on wood fibers by ester linkages. Instead, the peak intensity of absorption bands at 1740cm^{-1} has significantly increased due to the increase of ester carbonyl, implying that the esterifications occurred [314, 337, 537, 544, 555].

Table 11.5 FTIR Absorption Bands and Assignments

Extracted fiber cm^{-1}	MAPE cm^{-1}	MAPP cm^{-1}	Modified fiber, cm^{-1}		Peak assignments	Reference
			MAPE	MAPP		
3366	3641, 3602	3191	3350	3400-3300	O-H stretching	314, 355, 478, 537, 544
2913	2960-2840	3000-2770	2924-2852	2913	C-H stretching (CH_2, CH_3)	314, 355, 478, 536, 537
---	2342, 2022	---	---	---	Crystalline and amorphous phase of PE	567, 568, 569
---	1866	1863	---	---	Cyclic anhydride	570
---	1790	1789	---	---	Anhydride C=O stretching	555
1737	---	---	1740	1740	C=O stretching (unconjugated) (ester carbonyl)	571 314, 337, 537, 544, 555
---	1717	1717	---	---	C=O stretching (acid carbonyl)	314, 337, 478, 537, 555
1650	1639	---	1653	1650	Conjugated C=O, C=C stretch vibration	572
1597,1504	1591	---	1597,1505	1597,1505	Aromatic ring vibration	355, 537, 572
1463,1424	1452	1453	1463-1427	1463-1424	CH_2 deformation (asymmetric)	572
1373,1329	1368	1373	1373,1329	1379,1326	CH_2 deformation (symmetric)	572
1245	1300-1220	1300-1250	1250	1245	C-O, C-O-C stretching	537, 544, 572
1164	1165	1165	1164	1161	OH deformation Propyl groups	337, 544, 555 314
1119	1113	1103	1110	1110	O-H association in holocellulose	478, 571
1055-1023	1060	1043	1054-1029	1055-1043	C-O in cellulose	161, 536, 539, 573, 574, 575
---	---	997-972	---	---	PP crystalline band (monomer units=10)	576, 577, 578
---	917	900	---	---	Regularity bands	578, 579, 580
898	---	---	895	892-898	Glucose ring frequency	355, 571, 572, 575, 581
	---	841-809	---	---	PP crystalline band (monomer units=12)	578
---	719	---	---	---	PE crystalline band	536, 582
---	---	459	---	---	Polymer backbone triple carbon bending	583

However, the changes of these interesting peaks are unnoticeable at birch fiber concentrations which are entirely bonded except the absorption around 3400cm^{-1} due to the OH stretching vibrations [314, 355, 478, 537, 544] other than H_2O from Figure 11.15-Figure 11.16. In the fingerprint region between 1600 and 400 cm^{-1}, many sharp and discrete absorption bands due to various functional groups present in the wood constituents are observed because most IR bands characteristics of esterifications and polymer molecules are not in the this range except the crystalline band at 719cm^{-1} originating from MAPE [582]. However, it is seen that most crystallinity of MAPE has vanished due to the chemical morphological changes at the amount as well as the interactions.

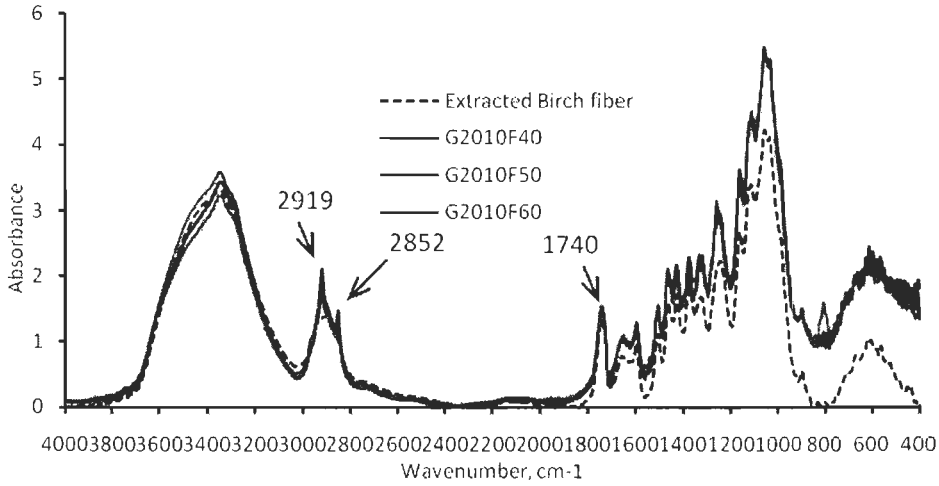

Figure 11.15 FTIR spectra of entirely bonded wood fiber with G2010

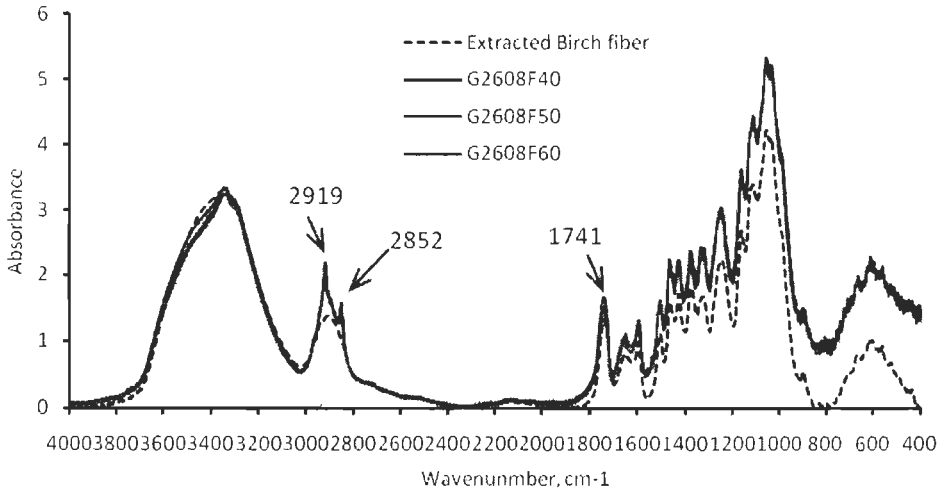

Figure 11.16 FTIR spectra of entirely bonded wood fiber with G2608

As expected, each type MAPE yields completed esterifications to the hydroxyl groups of wood fibers exhibiting same bands intensities associated with ester carbonyl stretching. By contrast, due to the increase of Mw, G2608 has very little left shift band of ester carbonyl at 1741cm^{-1}. The major differences between the FTIR spectra of the two MAPE modified wood fiber are seen at 2919, 2852 and 1741cm^{-1} from the difference of the intensities of reactions and the morphological molecules due to the different Mw (Figure 11.17).

It is indicated that G2608 having high Mw has increased intensities of absorption bands of CH stretching at 2919cm^{-1} and 2852cm^{-1} and the peaks at 1741cm^{-1} related to ester carbonyl resulting from the longer skeleton of molecular chains.

Other than the difference of the absorption bands due to the esterifications, there are also littile differences in the fingerprint region of wood fiber such as increase of the intensities of the peaks at 1362cm^{-1}, 1054cm^{-1} and 965cm^{-1} related to the CH_2 deformation and C-O activities in lignocelluloses that are contributed with the changes of the fiber size during processing. The increase of 1362cm^{-1} band results from the addition of CH structures by the grafting reaction [338, 478, 544, 555]. High Mw MAPE could provide more CH content as the grafting reaction occurred exhibiting high intensity near 1362cm^{-1}. Also use of G2608 yielded more fines (Figure 11.4) and could achieve a little intensity of nearly all major bands [571].

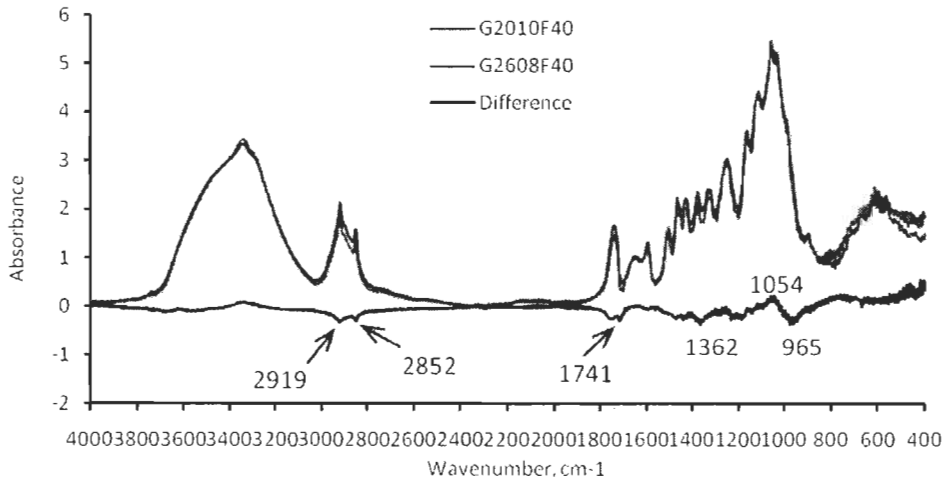

Figure 11.17 FTIR difference spectra of entirely bonded wood fiber with MAPE

Similar to MAPE, evidence of the grafting of MAPP bonding to the surface of wood fiber entirely is also revealed except the bands of C-H stretching occurred around 2900cm^{-1} where is single-banded in FTIR spectra of MAPP treated wood fiber. The

evidence supporting the chemical bonding of MAPP to the surfaces of wood fibers is confirmed by XPS results by increase of C/O ratio on the surface of wood fibers. Compounding wood fibers with MAPP causes a significant increase in the broad carbohydrate band at 3400cm^{-1} and 1600-400cm^{-1} due to the changes of the fiber morphologies which were confirmed by FQA (Figure 11.4 and Figure 11.10) and SEM (Figure 11.5 to Figure 11.9). As opposed to the changes of the IR bands of fibers, the changes of the salient peaks with the occurrences of esterification reaction with MAPP is unremarkable with increase in the birch fiber concentrations if the reactive maleic anhydrides is sufficient in the compounding system.

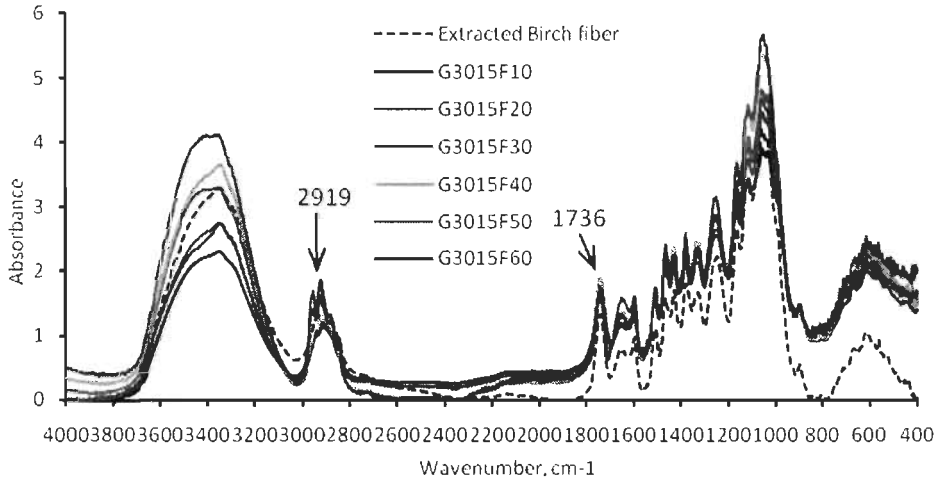

Figure 11.18 FTIR spectra of entirely bonded wood fiber with G3015

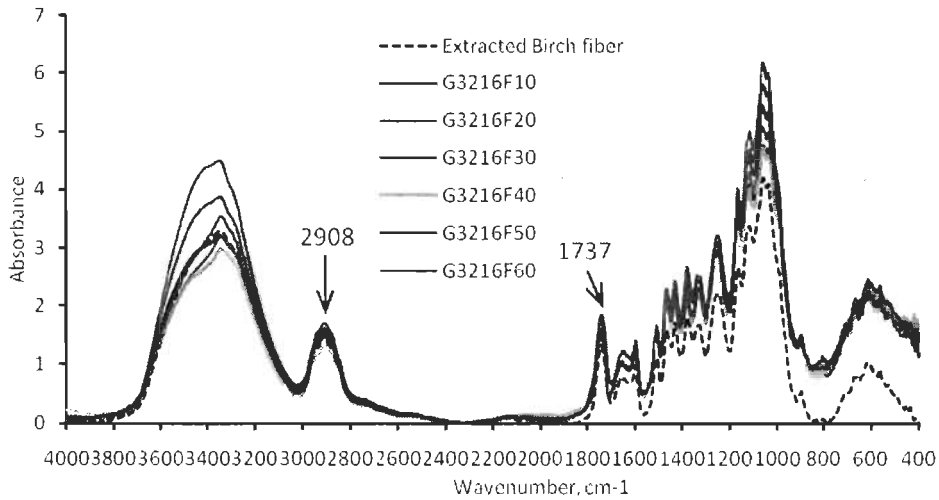

Figure 11.19 FTIR spectra of entirely bonded wood fiber with G3216

There are also two large distinct single-peaks at 2919cm^{-1} related to the C-H stretching vibrations of CH_2 and CH_3 of fibers and MAPP which shows same

appearance to unmodified birch fiber (Figure 11.3). These three kinds MAPP, G3003, G3015 and G3216, have same IR spectra, especially in the absorption bands related to anhydride groups and the crystalline peaks. By contrast to pure MAPP, the absorption bands at 1863cm^{-1}, 1789cm^{-1} and 1717cm^{-1} associated with cyclic anhydride, anhydride C=O stretching and C=O stretching from maleic acid groups respectively are converted into unconjugated ester carbonyl groups through esterifications reactions [337, 541, 542, 543, 544].

It was shown that high temperature melting could destroy the crystalline region of PP, but it could reappear after cooling [578]. Obviously, it is surely amorphous parts of MAPP coated on the fibers from the IR results of the modified wood fibers. The crystalline peaks of MAPP at 997cm^{-1} and 972cm^{-1} are assigned to PP helix in the length of 10 monomer unites while olefinic length of 12 monomer unites have absorption peaks at 841 cm^{-1} and 809 cm^{-1} [578]. Yin and coworkers [376] studied that the interactions between wood fibers and the maleic anhydride moiety could alter the nucleating ability of MAPP around wood fiber. However, the increased crystalline content of MAPP are not adhered to wood fiber which was removed by extraction in our case. The bonded MAPP on the surface of wood fibers was not studied. In addition, the crystalline regions of bonded MAPP are destroyed by the surface chemical changes including esterification reaction and fiber surface polarity shown by IR spectra in our studies.

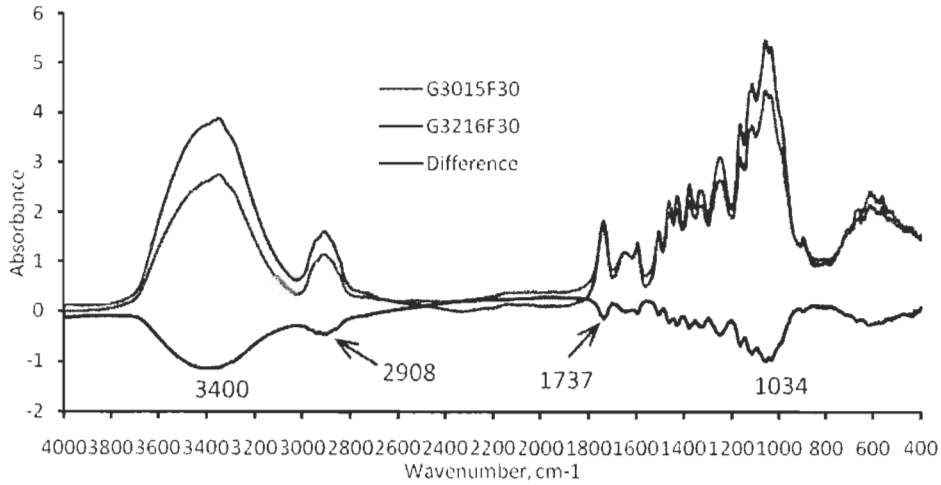

Figure 11.20 FTIR difference spectra of entirely coated wood fiber with MAPP

As expected each type MAPP react fully and consumes all exposed hydroxyl groups on fiber surface by ester linkages. The intensity would be changed depending on the

morphological changes caused by fracturing during processing. As analyzed in FQA, the fiber sizes of wood fiber modified with G3015 or G3216 are very close as seen from Figure 11.4, but modified wood fiber treated with G3216 (high Mw MAPP) has high curls and kinks index leading to bigger relative absorbance of the intense and broad carbohydrate band centered around 1111-1054 cm^{-1} and the OH band at 3400cm^{-1} [571]. This observation is supported by the difference spectra of G3015F30 by G3216F30 as recorded in Figure 11.20. It is also indicated that high Mw MAPP causes an increase in the intensity of the peaks of ester carbonyl (1737cm^{-1}) and the C-H stretching vibration (2908 cm^{-1}) of the pendant chains of MAPP.

It is a surprising finding that the intensity increase of the bands around 2900cm^{-1} and 1740cm^{-1} is overproportional when wood fiber is fully bonded with different Mw maleated polyolefins which is also supported by the calculating the grafting index. This result suggests that most of the maleated polymer is attached to the wood fibers surface via two acid groups from the cyclic anhydrides through disesterification reaction due to only single distinct peak in the range of 1700-1750cm^{-1} detection [544]. Otherwise, two distinct peaks in the range of 1700-1750cm^{-1} should be detected if the esterification reaction had occurred through monoester reaction [337, 543, 584]. One peak around 1710cm^{-1} is assigned to the nonreacted carboxylic acid (monoester formation) and another peak near 1740cm^{-1} is caused by the ester carbonyl absorption (diester formation) [337, 543, 584]. As seen in Figure 11.15-Figure 11.20, all the spectra of completely modified wood fibers show only single peak at 1740cm^{-1}, and be absence of bands at 1710cm^{-1} which clearly proved that there were no free carboxylic acid groups in these samples, thus confirming that only diester formation occurred.

In addition, the band intensities deviate from 3400cm^{-1} and the fingerprint region of carbohydrate band apparently from the changes of resultant fiber size and their interfacial morphologies apparently. The increase in carbonyl groups concentration (calculated from Equation 11.1) over Mw of the coupling agent is showed in Figure 11.21.

Initially, the carbonyl index was higher for modified wood fiber with high Mw maleated polymer. This supports the analysis of Figure 11.17 and Figure 11.20. Higher carbonyl index indicates the increase of oxidized carbon. Therefore, carbonyl index could be used to monitor the esterification reactions during the roller compounding.

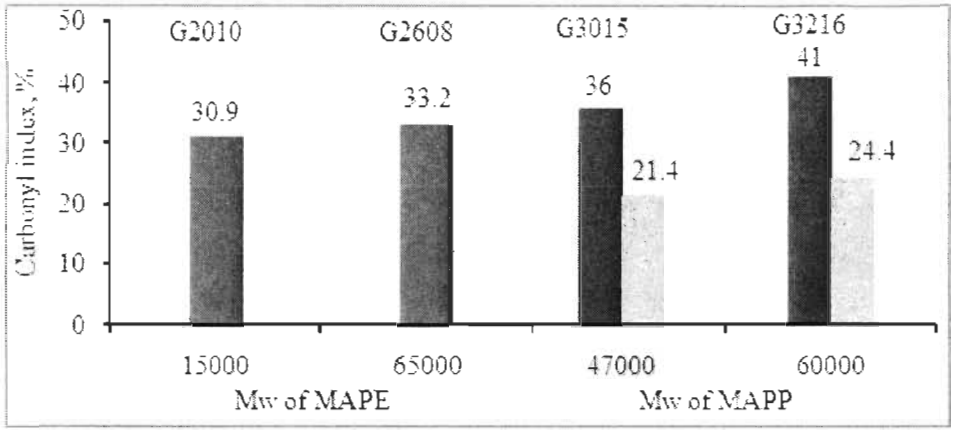

Figure 11.21 Effect of Mw and MA% on carbonyl index for entirely bonded wood fiber

Obviously, a difference in carbonyl index is observed between MAPE and MAPP-modified wood fibers. Since MAPP used in this section has higher maleic anhydride content (2.5%), it provides more reactive sites to attack wood fiber than MAPE (1.5%) leading to higher carbonyl index in Figure 11.21 which was supported by the increased the O/C ratio in Table 11.6 and high carbonyl index determined by XPS in Table 11.7. The normalized values are represented by gray bars at the same maleic anhydride content (1.5%) in Figure 11.21. Conversely, MAPE-modified wood fiber has significantly higher carbonyl concentration. This result tells us MAPE has high degree of reaction with wood fiber compared to MAPP, forming more ester carbonyl links during the processing. This reaction is always accompanied by severe fractures which were already shown in Figure 11.4 and in Figure 11.6-Figure 11.9.

11.3.2.2 FTIR spectra of partly bonded wood fiber

Although new absorption bands are appeared around 2919cm^{-1}, 2851cm^{-1} and 1740cm^{-1} which are attributed to the different CH_2 vibrations modes characteristic of the aliphatic hydrocarbon chain of the coupling agents [585, 586, 587, 588] and the evidence of the chemical bonding through ester linkages [337, 543, 584] after compounding by roller blender, it is necessary to monitor their changes by varying the coupling agent concentration.

Unlike entirely bonded wood fiber, the FTIR spectra of partly bonded wood fibers display the mentioned interesting bands too and it is important that the intensity of these bands vary following the changes of the amount of coupling agent employed which is shown in Figure 11.22 and Figure 11.23. However, the successful attachments to wood fibers entirely or partly have the same aforementioned

similarities except the intensities of the peaks associated with the ester links and the aliphatic pendant chains. It implies that the amount of coupling agent on the surface of wood fibers is varied following their loaded amount which is also quantified by their intensities at 1740cm^{-1} after normalization in Figure 11.24.

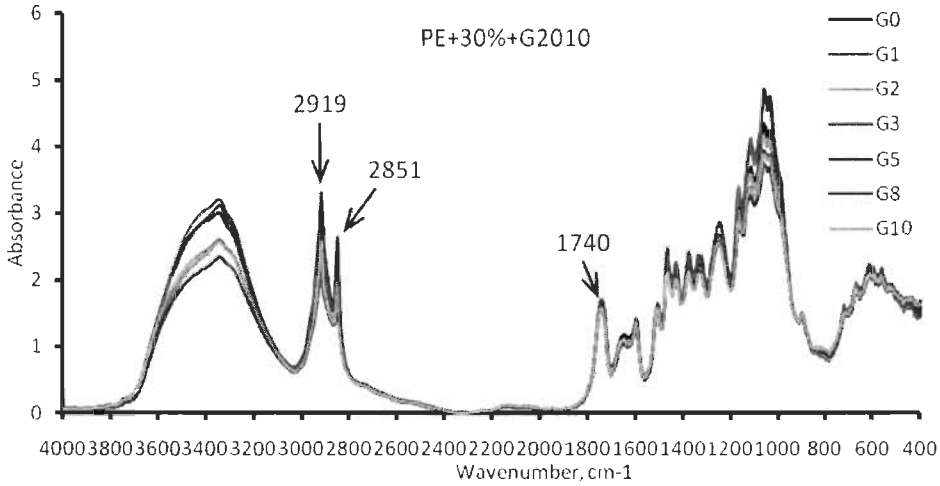

Figure 11.22 FTIR spectra of partly bonded wood fiber with G2010

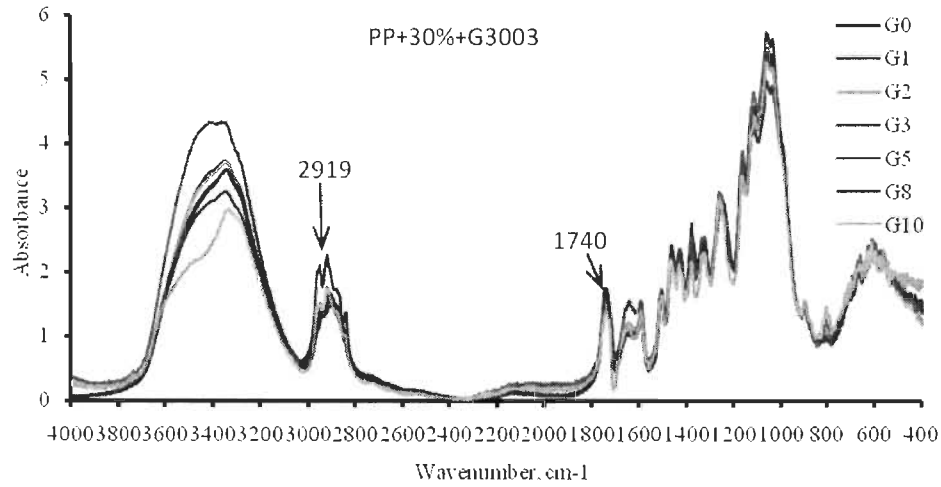

Figure 11.23 FTIR spectra of partly bonded wood fiber with G3003

As shown previously, wood fibers modified with inefficient coupling agent are also esterified by diester formation as seen in single band occurring at 1740cm^{-1} without the absorbance of monoester formation at 1710cm^{-1} [544]. It is also clear that 3wt% coupling agent could achieve optimal intensity of diester formation and moderate intensity of the band of CH_2 vibrations bands at 2900cm^{-1}. Furthermore, the bands of wood fibers bonded with 3wt% coupling agent are deviated to higher band

carbohydrate band intensities in the range of 1500-400cm^{-1} and around 3400cm^{-1} due to their rough surface which supported by FQA analysis in Figure 11.13.

So, superior chemical surface structures could be achieved by employing appreciable amount of coupling agent exhibiting surface roughening and rising including curls and kinks, and gaining higher content of carbonyl ester via increase of grafting index in Figure 11.24 while maintaining fiber length and width as imaging in Figure 11.13. It is possible to relate the changes of the ester content in the modified wood fiber with the changes of coupling agent attached.

Both use of MAPE and MAPP could significantly increase the carbonyl concentration as discussed in Figure 11.21. The peak intensity at 1740cm^{-1} is used to monitor the grafting index in the esterification reaction in Figure 11.24. As expected at the same maleic anhydride content, G2010 has superior interactions with wood fiber compared to G3003 which exhibits higher peak intensity at 1740cm^{-1} as shown in Figure 11.24. Therefore, it could be confirmed that whether bonded completely or not, MAPE seems to have superior interactions with wood fiber compared to MAPP containing the same concentration of reactive groups in their own blending system. So, the interfacial morphologies are mostly related to the nature of the matrix including flow viscosity and functional groups to produce the roughening surface and fractured structures. This finding was supported by the observations of SEM images. Nevertheless, it seems that modified wood fiber could achieve optimal carbonyl concentration at 3wt% exhibiting excellent strength [378, 405] and more fibrillated fibers as shown in Figure 11.12.

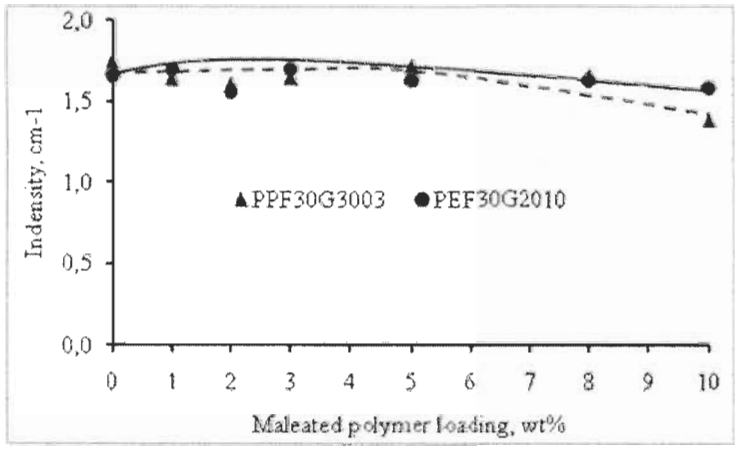

Figure 11.24 Intensity of ester carbonyl at 1740cm^{-1} for partly bonded wood fiber

11.3.3 Surface and Interface Characterization by XPS

11.3.3.1 Effect of the sampling depth on the binding position and the elemental concentration

Survey spectra of all samples are run to determine the percentages of the elements present at the surface. The main elements detected using XPS were oxygen and carbon. Small amounts of nitrogen are detected in unmodified wood fiber which required a change of resolution to observe them in Figure 11.25. The N1s core-level spectra for CTMP birch fiber has been curve-fitted with components arising from the nitrogen containing structure at binding energy of 398eV [589] which originates from protein in pulp fibers [590]. Most of this kind of extractives could be lipophilic extractives because it can be extracted mostly by *p*-xylene resulting in very low nitrogen content (0.69%), down from 1.51% of nitrogen content of initial fiber. However, the residual extractives, mainly hydrophilic, was removed completely after the functions by high temperature compounding and followed by hot-xylene treatment including Soxhlet extraction leading to the N1s bands loss in XPS spectra within the complete scanning depth of 5nm.

The background in all XPS survey spectra has similar shapes as indicated in Figure 11.25. Similarities in the background in shapes imply that all tested fibers have similar chemical and physical morphologies. However, there are differences in the intensity among the chosen samples. The intensity of initial birch fiber was a little high which could be used to evidence the extracted and modified fiber surface roughening by etching the surface and attaching fractional polymer leading to the sampling depth increased to 5nm, which comes from the core-level shifts. It is noted that the background of initial fiber has a very high intensity (16×10^3 a.u.) at very surface (0nm) and then intensities are weakened which are around (7×10^3 a.u.) following the increased sampling depth to 2nm. Unlike the initial birch fiber, the background of both extracted and modified birch fiber is indeed exactly similar in shapes and intensity.

It is clearly seen that extracted birch fiber has higher oxygen concentration compared to the initial fiber due to the exposure of oxygen on the fiber surface which was also confirmed by the increased the ratio of O/C in Table 11.6. Conversely to extracted fiber, the fibers with modification are rich in carbon because sample surface of modified wood fibers undergo chemical esterification leading to the attachments of

carbon-rich polymer on fiber surface within the detected depth as fitted in Figure 11.25 and Figure 11.26.

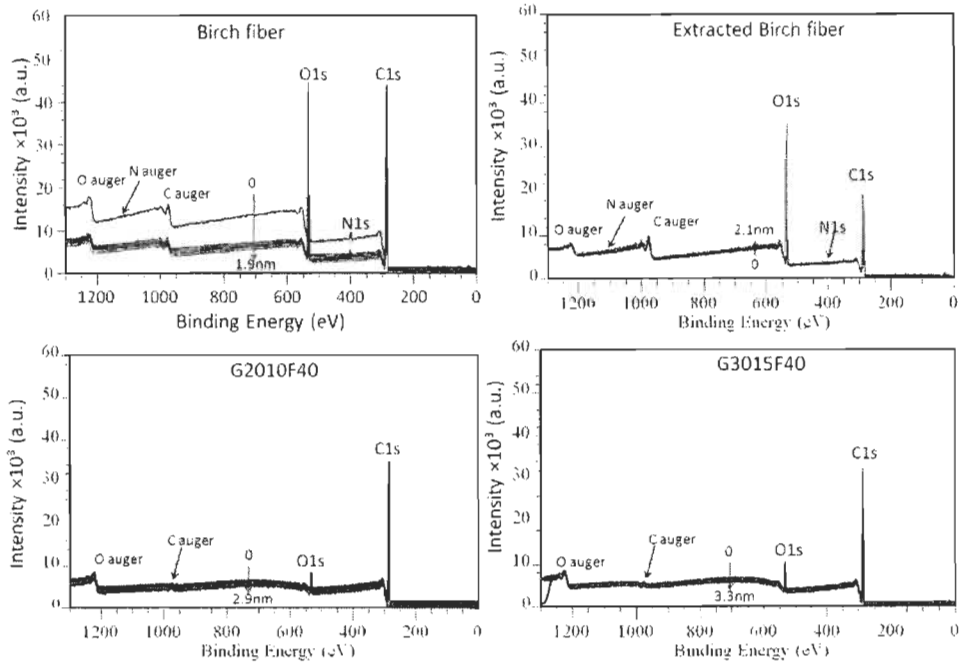

Figure 11.25 Survey spectra as function of sampling depth

As an indication that the penetration of the X-rays in the sample to the elements at deeper depth, X-rays would lose the intensity, which as mentioned above, where the intensity of elements in modified wood fiber would exhibit comparative weakness than the initial fiber with the increase of the sampling depth (core-level) from the roughening surface [591].

It is observed that the detected surface elements atomics referring to carbon, oxygen and nitrogen are varied as a function of the sampling depth in Figure 11.27. Obviously, the O1s concentration increase with the increase of the sampling depth while both C1s and N1s elements decrease to the level of initial and extracted birch fiber which is agreement with the distribution of the principal chemical constitutes in the various layers of the cell wall [309] due to the CTMP processing which almost did not destroy the cell wall except middle lamella [310, 592]. This result indicates that carbon-rich constituents are bonded on fiber surface including lignin and extractives, and the oxygen-rich structures are centered in the depth of cell wall, such as holocellulose. The changes of the concentration of oxygen, carbon and nitrogen evidence that the structure of wood fiber is inhomogeneous too, in line with the formation of cell layer.

In addition, it is easily found that the deconvoluted C2 signal increases greatly after extraction and modification in Figure 11.26. The changes of the deconvoluted carbons signals are shown in Table 11.7. It is due to potential errors that the sampling depth has no effects on the shifts in their survey spectra (Figure 11.25). It should be admitted, nonetheless, this conclusion represents the imposition of the prejudices of the experimenter onto the experimental data. In this case the shifts of binding energy could be clarified by the high resolution spectra showing a little difference in the C1s, O1s and N1s envelope in Figure 11.31 and Figure 11.28 respectively. It is noted that this kind shifts are also observed in the C1s components as summarized in Figure 11.29.

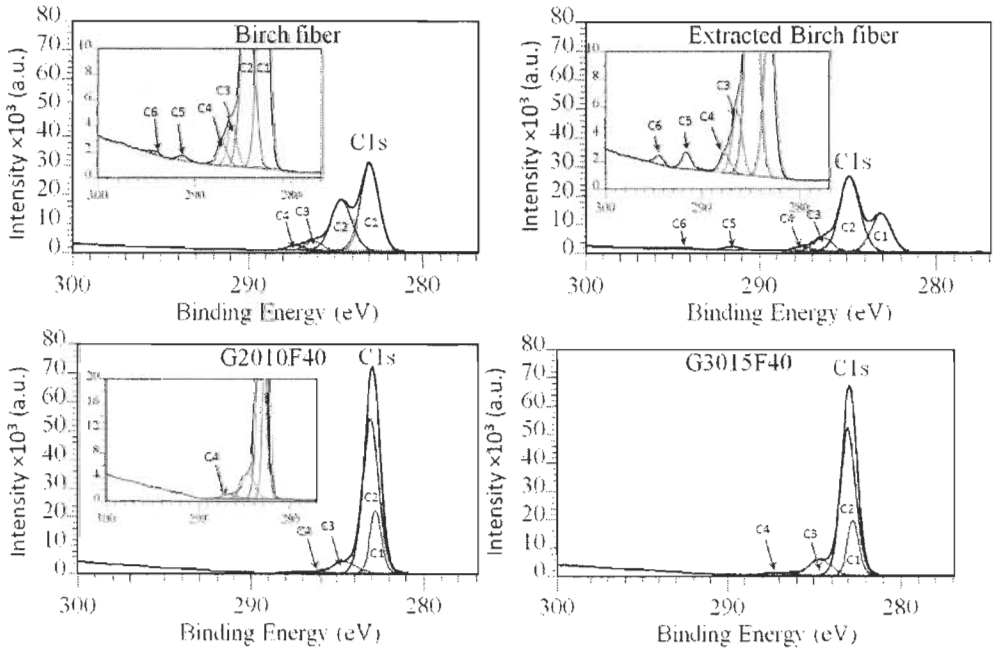

Figure 11.26 High resolution C1s peaks spectra at the maximum sampling depth

In our experiment, the XPS analysis probes much deeper to detect the complete oxygen and carbon profiles and mix in a contribution from deeper down, returning an apparent oxygen and carbon concentration, in an analysis made normal to the sample surface as indicated in Figure 11.27. The variations of carbon and oxygen concentration are observed clearly, and also clarified use the fractional bonded polymers (MAPP or MAPE molecules) on the wood fiber with very bad surface leading to important inhomogenity. This finding was identified by the increased complete sampling depth to detect the oxygen and carbon profiles to 5nm rather than 3.4nm, where the unmodified birch fiber is detectable in the complete sampling

depth to 3.4nm and became non-detectable at more than that depth. Even so, the sampling depth in our measurements is related to the photoelectron attenuation length on the order of 2-5nm. This means that 95% of the information could be obtained from the samples [593].

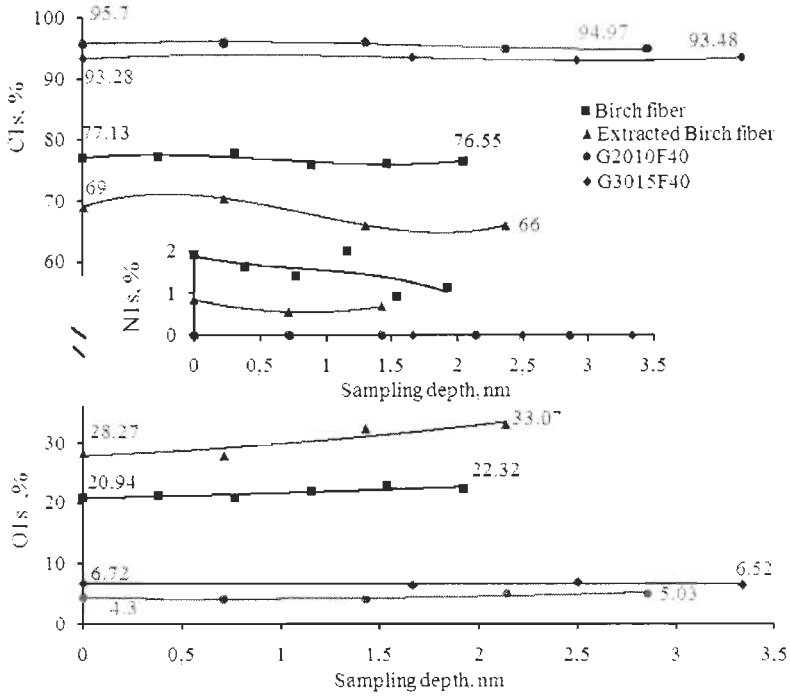

Figure 11.27 The concentration depth profile for the elements

The oxygen and nitrogen bands emerge in same shapes with an upward chemical shifts in line with the probing depth in Figure 11.28. Extraction could increase the surface amount and intensity of oxygen by the exposure with high resolution spectra of O1s in Figure 11.28. However, the amount and the intensity of oxygen on the surface are drastically decreased after the surface treatments rather than initial and extracted birch fibers due to the depositions of the maleated polymer. G3015F40 displays higher O1s concentration compared to G2010F40 due to the high content maleate groups leading to presence of more carbonyl groups as stated in Table 11.7.

The N1s concentration will be attenuated by the extractives removal and may disappear completely after the modification procedure. It is assumed that the hydrophilic extractives containing nitrogen could move to the surface of modified fibers and disappear at higher temperature from the fiber surface [594].

Unlike oxygen and nitrogen bands, the C1s bands show different shapes which are centered in the overlayers of C1 and C2 component due to the reciprocal change in

their proportions as shown in Figure 11.26. The changes of the proportion of deconvoluted C1s are indicated in Table 11.7.

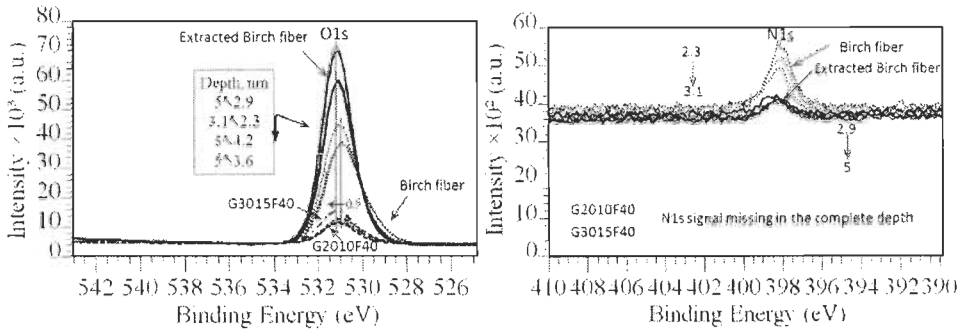

Figure 11.28 High resolution spectra of O1s and N1s as function of modification and depth

11.3.3.2 Effect of the grafted maleated polymers on the chemical shifts and the elemental concentration

Although the chemical shift caused by the sampling depth is very small and even neglected, it is a notable finding that the fixation of maleated polymer shifts the detected oxygen and carbon bands upward which is already described in Figure 11.28-Figure 11.30, especially to the deconvoluted C1s (Figure 11.29).

As aforementioned above, the comparative intensities of oxygen decrease compared to that of carbons after maleated polymer attachment, due to maleated polymers are rich in carbons and poor in oxygen atoms as seen in Figure 11.25-Figure 11.26.

Not only the sampling depth affects on the elemental concentration, but the maleated polymer has influence on the complete elemental profile which is plotted in Figure 11.27. This finding is quantized by the substantially increased C1s concentration and the decreased O1s concentration after modification in contrast to the unmodified wood fiber. All these observations confirm the importance of the polymeric structure in the fixation mechanism [595]. As concluded above, the O1s, N1s and C1s signals for the initial birch fibers are detectable within 3.4nm and become non-detectable exceeding this depth which is different to the extracted and modified birch fiber. Thereby, it is assumed that the complete sampled depth of the initial fiber including holocellulose, surface lignin and surface extractives is around 3.4nm which proved the models assumptions of the calculations of the surface coverage of lignin and extractives in Equation11.6-Equation 11.9, showing these were absolutely right [554, 559, 560, 561, 562].

The behaviours of the deconvoluted components provide more detailed information of the formation of bonding occurrences. The influences of the grafted maleated polymers on the deconvoluted C1s behaviours in modified wood fiber are stated in Figure 11.29 and Figure 11.30. Due to the functions of maleated polymer on fiber surface producing ester carbonyl and adding more C-H structures by the grafting reaction [338, 478, 544, 555], the influences mainly on C1 and C4 component will first be described.

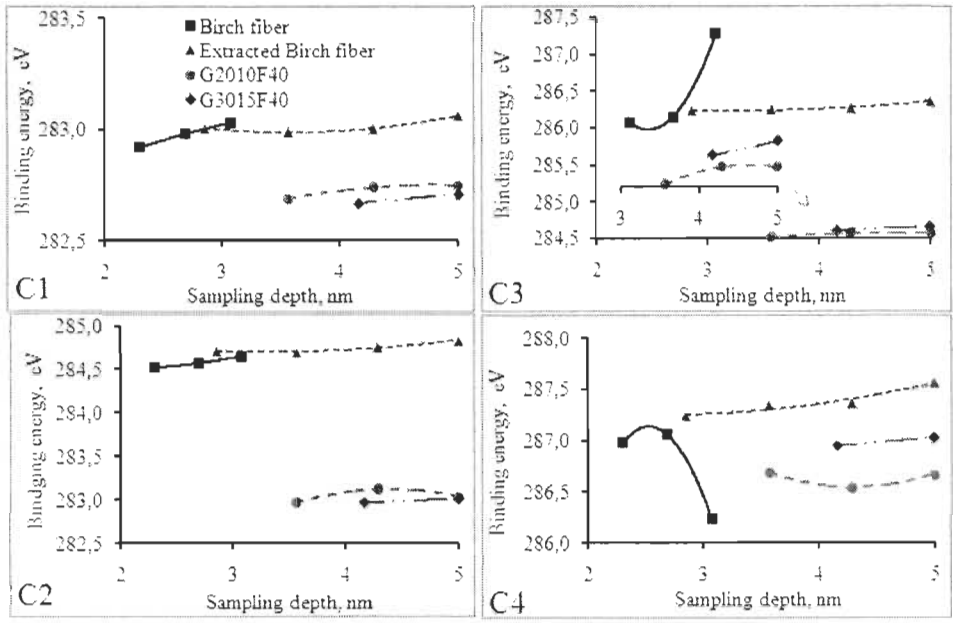

Figure 11.29 The depth profile for the deconvoluted C1s in binding energy

The deconvoluted C1s have small shifts downward in C1, C2 and C3 except C4 compared to extracted birch fiber in Figure 11.29. The C1 component band is caused by the internal molecular vibrations we have explicitly included those due to the C-H and C-C vibrations. As mentioned above, the grafting reaction could add more C-H to fiber surface, at the other side shoot up the C-C proportion due to its long olefinic molecular length. Thereof, rich C-C vibrations in the fixed maleated polymers could cause small downward shifts to C1 band because C-C is low energy models [596]. Concerning the changes of C2 and C3 components, they were caused by the combined effects of insufficient resolution and the substrate overlayer from low-energy vibrational models including C-C stretch vibrations [596] and the fractional overlayer from the irregular coated maleated polymer referring as the roughening surface [597]. The differences of binding energy between modified birch fiber with MAPP and MAPE originate from the inherent different molecular structures and the

different maleic anhydride contained. Obviously, the extraction has no effects on the chemical shifts of C1 and C2 compared to the initial birch fiber but has truly impact on the shifts of C3 and C4 due to the removals of lipophilic extractives.

As aforementioned in Figure 11.29, although the concentration of the deconvoluted C1s components of modified fiber varied by the sampling depth, the complete concentration is well located for each C1s component. Since the C2 and C3 concentration would be affected by the processing both compounding and hot solvent treatment due to high temperature, the following thermal degradation will contribute to high content of C=O groups by decreasing COOH groups content [598]. However, this thermal oxidation has less impact on the results of modified fiber due to their same background including their shapes and intensity in Figure 11.25. IR indicated that there was no existence of COOH in the modified birch fiber by the absence of the peaks of 1710cm^{-1}such as in Table 11.5, where the C4 band would not be influenced. Hence, it comes from the inherent and formed ester carbonyl by grafting.

It is also concluded that G3010F40 could lead to highly oxidized carbon proportion increase (C2, C3 and C4) compared to G2010F40 which comes from the high maleic anhydride groups content with higher esterification degree as shown in Figure 11.30 and also summarized in Table 11.7. Due to the fact that the C1 and C4 bands were assigned to absolutely not and completely oxidized carbons which are immune to the thermo-degradation, the changes of C1 and C4 content are forceful evidence to monitor the esterification reaction happening between fiber surface and the maleate groups as grafting index (Equation 11.3) in Table 11.7.

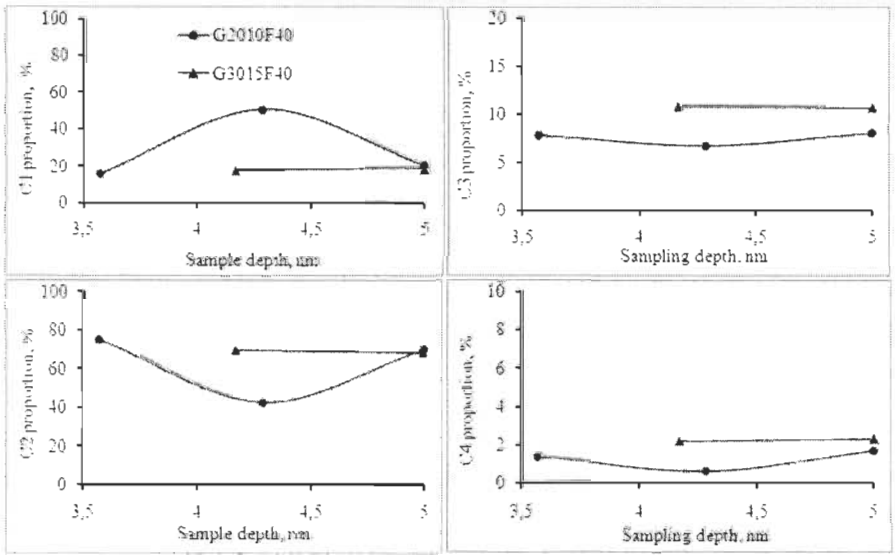

Figure 11.30 The depth profile for the proportion of the deconvoluted C1s

Since the elemental concentration varies along the sampling depth, the average value at full detected depth was chosen to determine the ratio of O/C in Table 11.6 thereof. The relative elemental compositions of the samples are presented in Table 6 as well as their surface coverage of lignin and extractives calculated by Equation 11.6-Equation 11.9.

The O/C ratios of modified birch fibers decrease significantly from 0.448 of extracted fiber down to 0.047 and 0.071 of G2010 and G3015 modified birch fiber respectively which corresponds to the results in Figure 26 and the investigation shown in Figure 11.30. It was also found that the xylene extraction increases the O/C ratio from 0.282 of the initial fiber to 0.448 due to removal of the lipophilic extractives from wood fiber which would ameliorate the exposure of oxygen on the fiber surface which is in line with the previous findings [549, 564, 599, 600, 601, 602]. Whether extracted or not, the remove of the extractives would not contribute to the decrease of the O/C ratio of modified fiber.

In addition, WPC were produced by wood fiber compounding with thermoplastic under high temperature and strong driving forces at high viscosity. During this processing, wood fiber was fractured (as IR and SEM results supported) and unavoidably thermal oxidized [353, 603]. As studied, the decrease of fiber size during compounding processing has similar effects to extraction exhibiting the increase of the O/C ratio [604]. However, the functions induced by thermal degradation were more complex. It was well known that heating treatment was very popular in wood preservation under the protection of nitrogen to decrease the O/C ratio [605]. Conversely, there are no nitrogen protection in our case where all the processing were exposed to air which is similar to weathering or photooxidation by increasing in signal intensities of carbon-oxygen bonds and oxygen-carbon-oxygen bonds (or unsaturated carbon oxygen bond) and oxygen-to-carbon ratio, and decreasing in carbon-carbon and carbon-hydrogen bonds of weathered and UV-irradiated wood surfaces which suggests that wood surface was oxidized [606]. Eastman and coworkers showed that thermally degraded wood fiber contains high percentages of oxygen [607]. Thermal degradation of wood is greater in the presence of air by oxidation by atmosphere oxygen. Acid formed builds up in concentration and hence can catalyze hydrolysis due to the nature of CTMP fiber which is rich in extractives before extraction [608]. Röder and Sixta reported that the COOH groups

content decrease while C=O groups increase in wood fiber [598] exhibiting the increase of C3 value supported by Figure 11.26 and Table 11.7.

As mentioned above, the fractures and the thermal degradation could occur to some degrees. Nevertheless, both of them lead to wood fiber with increased O/C ratio. So, the contributions of the O/C ratio come only from the coated maleated polymer-amount of maleated polymer bonded with wood fiber providing rich-C1s content as shown in Table 11.6 and Figure 11.31. Of course, the surface contamination affecting the measurements is difficult to avoid [609].

The chemical composition of the fiber surface can vary dramatically from that of the bulk materials, especially during the manufacturing of wood plastic composites by interfacial esterification. The hydrophobic materials present on the fiber surface and fines including lignin and extractives have an impact on the strength of the composites. The phenolic hydroxyl groups on lignin have higher reactity than hydroxyl groups in celluloses, even though the amounts are small [600]. Extractives also affected the fiber wettability [610] and influenced on the mechanical and physical properties [611].

Table 11.6 shows that the amounts of estimated surface lignin and extractives on air-dried CTMP fibers using the C1 carbon and the ratio of O/C. Both methods which give similar result in surface coverage by lignin of CTMP fibers, which containing a high total amount of lignin were employed. It is not exactly known why fiber material with a low amount of lignin is sensitive to the methods used. However, it is proven that the O/C and C1 carbon are more sensitive to interference from contamination and extractives in fibers with a low amount of lignin [612]. CTMP fiber surfaces are rich in lignin (more 57%) than the bulk of the fiber due to air-dried samples which showed a higher amount of lignin on the fiber surface [612].

Unlike surface lignin, the amount of extractives on the fiber surface shows a different result calculated by two methods exhibiting the value calculated by O/C was higher than the value calculated by C1 as a result of a small amount of low Mw lignin extracted. It was well known that the models used to calculate the surface coverage of lignin and extractives from either the amount of C1 carbon or the O/C ratio assume that the extracted surface consists only lignin and carbohydrates, where low Mw extractable organic extractives in unextracted fiber reside on the top of the carbohydrates and lignin, and the thickness of each component exceeds the analyzing depth [554, 559, 560, 561, 562]. It should be mentioned that the lignin was

unextractable in these models. However, Öestenson reported that some small amount of low Mw lignin could be extracted by organic solvent actually [602] and leads to relative low C1 concentration [600] but high O/C ratio [564]. This variation can not affect the calculation of surface lignin due to its large amount, but could overestimate the amount of surface extractives by O/C while underestimating the value by C1. This opposite trend will widen the difference among these two calculations. In fact that calculation based on O/C ratio can be precise, and calculation based on C1 is not precise because deconvolution is not precise compared to O/C determination. Nonetheless, the surface concentration of extractives is higher with more than 37% resulting from the release and redistribution of extractives onto the CTMP fiber surfaces during TMP processing [613].

As mentioned previously, the bast fiber in presence of extractives can help in internal lubrication during the blending process [614], especially since the migration of extractives to surface is favored by the high temperature [594], and may improve the wettability of polyolefins due to its hydrophobicity [420]. It was also found that lignin and other extractives in wood fibers act as antioxidants through resonance stabilization of free radicals [615, 616]. Clearly, high surface coverage by lignin and extractives could smooth the processing and protect wood fiber from serious thermal oxidation. In addition, the presence of residual extractives also has a substantial effect on fiber wettability, where high extractives content leads to low wettability [617]. Therefore, WPC made with initial wood fibers would also show lower moisture sorption and thickness swelling characteristics [618, 619]. According to our experiences, CTMP fibers are fed easily and dispersed more uniformly than BCTMP fiber because CTMP fibers are richer in lignin [620], especially on the fiber surface [613].

As mentioned, the chemical reaction of maleated polyolefins and wood particles takes place between the maleate groups of the polyolefin and hydroxyl groups on the surface of wood which was already proved by IR results. Like FTIR, both MAPE and MAPP modified birch fiber lead to a significant increase of C1s, meaning a higher amount of maleated polymer bonded on the surface of wood fiber as shown in Figure 11.31 and Table 11.6.

The modified birch fiber with low O/C ratio, such as G2010F40 (O/C 0.047) and G3015F40 (O/C 0.071) have a strong reducing effect on the wettability compared to lignin (O/C 0.39) but similar hydrophobicity of the extractives (O/C 0.08) [621].

Thus, WPC made with maleated wood fiber referring to the grafting with maleated polymer will achieve low water absorption [423, 510, 538]. The surface of maleated wood fibers show high roughness which will cause hysteresis of the contact angle [622]. Moreover, any amount of hydrophobic grafted fiber will lower the advancing contact angle leading to more sensitivity to high energy components on the surface [620].

Table 11.6 Average Values of the Elemental Surface Composition and the O/C ratio

Samples	Extraction	Average			O/C	Φ_{Lignin}, %		$\Phi_{Extractives}$, %	
		O1s	C1s	N1s		O/C	C1	O/C	C1
Birch fiber	No	21.69	76.81	1.51	0.282	76.5	75.3	49.0	37.0
Extracted fiber	Yes	30.39	67.88	0.69	0.448	---	---	---	---
G2010F40	Yes	4.48	95.52	0	0.047	---	---	---	---
G3015F40	Yes	6.67	93.33	0	0.071 (0.043†)	---	---	---	---

† The normalized value of G3015 at 1.5% maleic anhydride as G2010.

It is also seen that G3015 modified fibers have superior level of oxidized carbons than those modified with G2010 originating from the functions of higher maleate groups exhibiting high O/C ratio in Table 11.6 and high proportion of C4 in Table 11.7. It is also found that the normalized values of O/C ratio of G3015F40 is 0.043 are little lower than G2010F40 with the same maleic anhydride level. It implies that MAPE has superior grafting efficiency than MAPP. All the above results were correlated with the IR analysis by carbonyl index as in Figure 11.21 and also shown by the SEM observation in Figure 11.6 to Figure 11.9.

Since the C1s signal is usually deconvoluted into four components according to oxidation level (Figure 11.26), the choice of chemical groups used in the peak fitting is classified and sourced as summarized in Table 11.3. The formation of the following chemical groups by modification is used to explain the enhanced intensity in the C1s envelope in Figure 11.26. However, the high resolution spectra of C1s peaks for the initial and extracted birch fiber have two additional bands, C5 and C6. Although they are very weak, it shows the different nature of the treated fibers.

The C5 peak at 291eV is assigned to the carbonate type (O-C(=O)-O) [623], carbamate type (O-C(=O)-N, O-C(=C)-O) and/or urea formation (N-C(=O)-N) [589, 624] due to the chemical shift caused by fourth oxygen or nitrogen atom [589, 623, 624, 625] from the extractives containing protein. The C6 peak at 294eV is invoked by the shake-up satellite peak due to π-π^* transitions in aromatic rings [600, 626, 627]. The π-π^* shake-up at 294.6eV suggests significant aromatic character on the

initial and extracted fiber surface and implies the higher surface coverage of phenyl monomer structures [627]. Due to the removal of surface extractives, the surface coverage by lignin is rich on the surface leading to higher π-π* function as shown in Figure 11.26 and increased C5 band as noted in Table 11.7.

It was reported that xylene, the solvent used for PP and PE removals, with its aromatic ring also allows a clear signal around 292eV binding energy due to π-π* bonding of carbons in the benzene ring via XPS [628]. However, no peaks were detected around this binding energy in all XPS spectra, which indicated that acetone replacement and oven treatment were adequate to fully remove the solvent. These structures must be destroyed after extraction and the deposition of maleated polymers due to prior to reaction with anhydride to eliminate the radical leading to blocking the transition in aromatic rather extensive π-polyconjugated systems [629].

Curve fitted C1s high resolution spectra of the extracted fiber and modified fiber are shown in Figure 11.31. As illustrated in Figure 11.31, the peak intensity corresponding to C1 decreased dramatically while an increase in C2 and C3 was observed as a shoulder peak, where extracted fiber is lower in C1 band and higher in C2 and C3 band in Table 11.7. This trend is a result of the amount of ether carbon (C2) presented on fiber surface. The reduction of C1 bonds in the xylene-extracted fiber was correlated to the removal of non-carbohydrates [630] including extractives [600, 631] and some low molecular weight lignin [602] while the greater contribution of C3 and C2 in extracted fiber is caused by an increased content of carbohydrates at the surface [602].

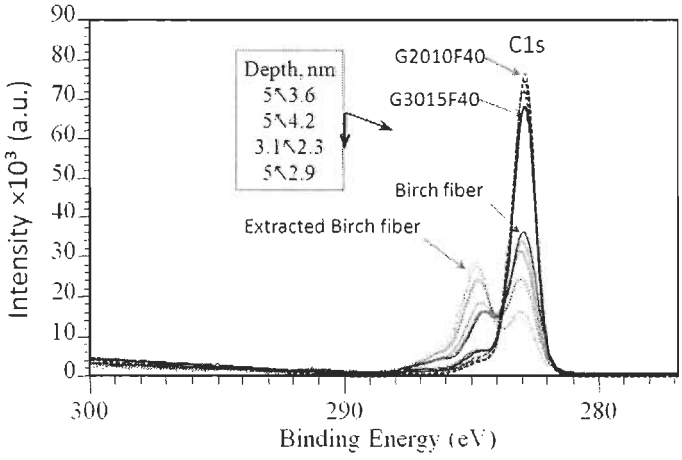

Figure 11.31 XPS C1s peak spectra for unextracted, extracted and modified birch fiber

Unlike the extracted fiber, the amount of alkyl carbon (C1) in maleated fiber indicates that some materials, which are rich in aliphatic carbon that does not originate from the extractives, are present in the outermost surface of fibers. Although extraction will decrease the amount of C1 [600, 602], the decrease of C1 in maleated fiber originates from the amounts of bonded polymer molecules. The difference in the C1 band between the fibers treated with G2010 and G3015 is from the chains of olefinic molecules of G3015 with $-CH_3$ side chains leading to a little high C1 proportion in G3015F40 while the higher C3 and C4 content of MAPP-modified birch fiber also resulted in its higher ester content as discussed earlier.

Like FTIR, which clearly showed a qualitative increase of carbonyl index as a function of maleated polymer, both G2010 and G3015 shows an increasing trend in complete concentration which quantifies the evidences of the occurrence of esterification reactions same found by IR results. Wood fiber modified with MAPP could be characterized by higher ester carbonyl index (CI 0.72) originating from its higher maleate groups content (G3015, 2.5%) compared to that (CI 0.52) yielded with MAPE (G2010, 1.5%), even though MAPE has higher reactive efficiency with providing more reactive sites to fix onto wood fiber forming more ester links as IR results showed in Figure 11.21. In fact, the normalized CI (CI 0.43) and the grafting index could be used to monitor the grating efficiency and corresponds to the results found by IR.

As stated in Table 11.7, the greater contributions of C3 in maleated fiber is caused by an increased content of carbonyl compounds on the fiber surface compared to the initial and extracted fiber from the generated ester links. Due to the high temperature compounding processing and overall extraction, the removal of extractives in modified fiber goes father than extraction. Less residual extractives in the modified fibers will decrease the C1 peak while increasing the proportion of C3 and C2 in the spectra [602]. However, with the increase of the contribution of carbonyl groups, both G2010F40 and G3015F40 has high CI value in contrast to extracted fiber implying more carbonyl groups rather than COOH were formed as enough maleated polymer was deposited. The total of carbonyl groups in G3015F40 is higher than G2010F40, which comes from the high anhydride content. However, the normalized CI content of G3015F40 shows that MAPP has a lower reactivity than MAPE if having same maleic anhydride level, which is related with the grafting index by C4. It is very hard to understand why modified fibers have a low amount of ester

carbonyl (C4) but a high amount of ether carbon (C2). In theory, maleated polymer could only contribute to the proportion of C4 and C1 from their maleate groups and the alkyl molecular chains. However, maleated polyolefins may also contain unbound oligomeric maleic anhydride and free maleic anhydride [632] which contributes to the C2 and C3 proportion on fiber surface. Whatever, C4 would contribute to the increase of the ratio of the oxidized carbon to unoxidized carbon by the Equation 11.5 [298, 536], even though the proportion of C4 is rather small as shown in Table 11.7.

Table 11.7 High Resolution C1s Peaks of Wood Fibers Determined by XPS

Samples	Analysis of C1s peak, % (Average value)					HI	GI		CI	$C_{ox/unox}$
	C1	C2	C3	C4	C5†		C1	C4		
Birch fiber	58.05	33.28	3.32	4.39	0.75	---	---	---	0.13	0.72
Extracted fiber	36.91	51.17	7.52	3.07	1.84	1.00	1.00	1.00	0.29	1.72
G2010F40	17.96	72.62	7.9	1.52	--	1.42	0.487	0.50	0.52	4.57
G3015F40	18.08	68.97	10.7	2.26	--	1.35	0.490	0.74 (0.44‡)	0.72 (0.43‡)	4.53

† C5 used as carbonate groups when CI calculated. ‡ The normalized value of G3015 at 1.5% maleic anhydride as G2010.

As mentioned above, the chemical reaction of maleated polyolefins and wood fibers takes place between the maleate groups of the polyolefin and hydroxyl groups. Since the change of C1 was mainly related to the alkyl groups which is qualified as grafting index by C1 to reflect the amount of bonded polymer on fiber surface. It is noted that C1 could reflect the reaction directly but is affected by the molecular length, where high Mw maleated polymer could achieve high grafting index. For the Mw effect on the grafting efficiency we refer the reader to the in-situ work of Carlborn and Matuana [544], which was not normalized the maleic anhydride level. Concerning our studies, low Mw G2010 achieves similar GI by C1 to high Mw G3015 showing G2010 having high reactivity grafting which is line with the conclusions made by the normalized CI, GI by C4 and the IR analysis.

Esterification of wood fibers with anhydride groups in maleated polyolefins provides a certain degree of hydrophobicity by blocking the hydroxyl groups which induces the change of C2 component. It clearly illustrates that the HI level is up 1.35 and 1.42 corresponding to G3015 and G2010 which were fed at excessive amount in order to bond wood fiber as entirely bonded. The leveled-off extracted fiber might be attributed to the unbound maleate groups in the grafted maleated polymer which indicates that a full level of maximum grafting efficiency has been reached. It is interesting finding that the difference among the fullly grafted wood fibers exhibits

the different grafting efficiency between these two kinds maleated polymer based on different matrices at same maleic anhydride grafted level. High HI value of G2010 indicates a high grafting efficiency, where low Mw makes more molecules close to the fiber surface and reacts easily. Oppositely, high Mw G3015 might not allow residing on the wood fiber which will decrease the chance of anhydride groups to contact wood fiber.

In summary, all the reactions will form oxidized carbon. Stark and Matuana reported that the formation of a saddle peak implied the surface oxidation and quantified by the ratio of oxidized carbon to unoxidized carbon ($C_{ox/unox}$) [536]. Clearly, it is reasonable for extracted birch fiber having high $C_{ox/unox}$ (2.19) due to the removal of non-carbohydrates, which is rich in carbon [630]. However, the above description should be viewed with some caution due to the small shoulder occurred to the modified fibers. The $C_{ox/unox}$ of modified fibers is presented in Table 11.7. Differences in the oxidized-unoxidized carbon ratio for the modified fiber are apparent higher than that for the initial fiber, even higher than maleated fibers which are evidence the new formation of oxygen-carbon bonds. The attachment of G2010 and G3015 on the fiber surface increases the $C_{ox/unox}$ by 2.6 times more than that of extracted fiber reaching 4.57 and 4.53 respectively from the original value of 1.72 of extracted fiber. So, the esterification reaction is a process leading to the formations of oxygen-carbon bonds.

11.4 Conclusions

This study examined the chemical reactions between maleated polyolefins and birch fibers in a blender process. The effects of maleated polyolefins content and their Mw and maleic anhydride were studied, with the goal of determining their grafting efficiency of modification and the formation on ester linkages using FTIR and XPS analysis. The chemical surface morphologies and the physical morphologies of modified fiber were also investigated. From the experimental results, the following conclusions can be drawn.

(1).The fluffy and fractured surface was formed as maleated polyolefins were introduced. MAPE use could result in more fines by decreasing fiber length and increasing fibrillations compared to MAPP which increases fibrillations. Mw of maleated polymer has a slight impact on the changes of fiber size, but a great difference on the surface morphologies. Highly Mw MAPP achieved

high curl and kink content of fiber which was opposite to the effect of MAPE. Moreover, the morphologies of modified fiber have changed during roll blending as a function of MAPP concentration, where the optimal concentration was determined at 3% to gain the modified fiber with maximum length and width at minimal fines proportion while exhibiting high curls and kinks content. All the mentioned changes of fibers were confirmed by SEM observations.

(2). The esterification reaction between wood fibers and maleated polymers occurred as a function of their concentration (bonded completely or partly). Both methods show no difference in the grafting reaction which produced mostly diester linkages from wood fiber. The bonding formation was identified by the distinct peaks profiles between 1800 and 1650cm^{-1} other than 1710cm^{-1} which was assigned to ester carbonyl. However, distinct trend was observed between Mw of maleated polymers and carbonyl index determinated by IR through a blending process, where highly Mw maleated polymer formed relatively high content diester linkages both with MAPE and MAPP. MAPP and MAPE were also compared to find MAPE having superior reactivity after normalization. Besides, partly bonded fiber was used to optimize the esterificated performance, where 3wt% MAPP would be ideal to achieve the best results.

(3). Wood fiber with modification or extraction has similar background in shapes and intensity compared to initial wood fiber, which implies their similarities in surface morphology. The carbon and oxygen concentration of initial and extracted fiber was varied as a function of the sampling depth which came from core-level shift, and indicated inhomogeneous structures. A little difference among modified fiber was found in the concentration of oxygen and carbon as function of depth profiles resulting from the chemical structure of binding agent. Significant difference in the surface elemental compositions evidences the occurrences of ester bonds by increasing the ratio of O/C. The high resolution spectra of C1s give us more information on the type of bonding formed which was used to determinate hydroxyl index, carbonyl index, grafting index as well as $C_{ox/unox}$. The depositions of maleated polymers result in an upward chemical shift of oxygen and all deconvoluted C1s downward. The difference in maleic anhydride content gives modified

fiber with different kinds of oxygen-carbon bonds. High MA% G3015 achieves high oxygen-carbon bonds compared to low MA% G2010 feathered by grafting index with C4 and carbonyl index. However, MAPE could reach superior reactivity contrast to MAPP after compromise at the same level by higher hydroxyl index directly.

(4). Regardless the type and MA% of maleated polymer, the investigated maleated polymer eliminated the shake-up effects of surface lignin. The extractives on the fiber surface could migrate during high temperature processing, and then were destroyed as witnessed by missing nitrogen band.

(5). CTMP birch fiber was found to be a suitable material to be modified with maleated polyolefins and compounded into WPC due to rich surface coverage by lignin and extractives which acted as internal lubricant and natural antioxidant leading to good performance.

11.5 Acknowledgements

The authors would like to thank the NSERC, NCE Auto21 and FQRNT for the financial support. We would appreciate Agnès Lejeune for her help with the SEM and XPS measurement, and also thank Phillips Sumika Polypropylene Company for their donation.

Chapter 12 - Bacterial cellulose reinforced thermoplastic composites: Fabrication and performance evaluation

Ruijun Gu and Bohuslav V. Kokta
BioResources. #1071 Accepted

Abstract: During this study, the mechanical properties behaviors of PE composites were discovered with the addition of bacterial cellulose (BC). It was found that BC could improve the mechanical properties of the composites with the combination of traditional wood fiber. In addition, the improvements were affected by its after-treatment method. The nanofifiber confirmation had an impact on impact strength. It seems that the pellicle BC was able to achieve superior impact strength compared to the fluffy one, but had similar effects on the tensile strength in comparsion to the composites with pellicle BC.

Keywords: Bacterial cellulose, Nanofiber, Maleated polyethylene, Polyethylene, Wood fiber, Wood composite

12.1 Introduction

Cellulose is the most abundant biopolymer on earth as the major component of plant cell wall, and it also is a representative of microbial extracellular polymers. Some bacteria produce cellulose (called biocellulose or bacterial cellulose) [633, 634, 635]. Wood fiber and BC have identical chemical structure, but different physical and chemical properties [636, 637, 638]. Nanofiber or microfibrillated/ nanofibrillated celluloses are prinicipally produced by mechanical disintegration of fiber bundles into submicron nanofibril bundles (10-50nm in diameter) with the help of enzymatic pre-treatment, which is applied before mechanical procedures in order to ease the delaminaiton and to decrease the energy consumption [639, 640, 641]. But nano-scaled BC is mainly produced by an acetic acid-producing bacterium, *Gluconacetobacter xylinum* due to its most efficient strain [642, 643, 644].

BC has some special physical and chemical properties such as high crystallinity and hydrophilicity, ultrafine network architecture, purity (free of lignin and hemicelllose), and moldability during formation [637, 638]. Because of the unique properties, resulting from the ultrafine reticulated structure from the nascent chains of BC with a width of approximately 50nm. BC has found a multitude of applications in paper [645, 646], food industries [647], as a biomaterial in enzyme immobilization [648, 649], and biomedical applications [650 , 651]. BC has a high capacity of

reinforcement agent potential to obtain a new class of truly green composites due to its high Young's modulus, up to 134GPa [652], and the fact it is derived from renewable resources. The incompatibility problem between hydrophobic matrix and hydrophilic fibers applies to the hydrophilic BC as well. So, the interfacial compatibility should be improved by use of a coupling agent [92, 316, 405, 478] as well as an initiator [330, 380, 381, 405], resulting in the formation of chemical bonding between the WF and the matrix [314, 544].

In this study, bacterial cellulose composites were fabricated to study the reinforcement behaviors of BC on the mechanical properties. The effect of BC reinforcement was also investigated with the addition of CTMP fiber or not. In addition, the after-treatment method of BC was also evaluated based on the studies of the reinforcement of BC in different formation.

12.2 Experimental

12.2.1 Materials

Thermoplastic: Linear low density polyethylene (Novacor® HI-0753-H) was donated by NOVA Chemicals. Its melting mass-flow rate is 1.0g/10min. Its specify density is 0.92g/cm^3.

Wood fiber: Industrial chemi-thermo-mechanical pulp (CTMP) of yellow birch (*Betula alleghaniensis*) was employed. The wood pulp fibers were air-dried and ground at our laboratory to produce fine particles. Particles that passed through a 20-mesh but were retained on a 60-mesh screen were employed in this study.

Bacterial cellulose: Bacterial cellulose materials were donated by Research Center of Medical Technology and Biotechnology (fzmb GmbH-*Forschungszentrum für Medizintechnik und Biotechnologie*, Geranienweg 7, 99947 Bad Langensalza, Germany), which were produced by *Gluconacetobacter xylinum* AX 5 (culture collection fzmb GmbH) in classical Schramm/Hestrin (SH)-medium [653] at the University of Jena, which contains glucose as described in previous report [654, 655, 656]. BC sheets were produced by static fermentation, and washed with water after fermentation and cut as shown in Figure 12.1. In order to study the effect of after-treatment method on the mechanical properties of PE composites as well as the assistance of wood fiber, original BC was mechanically treated by different after-treatment method after it is harvested, and achieved different physical formations, that is fluffy and pellicle formation as shown in Figure 12.2. Fluffy sample 1 (B1)

was treated by a cutting mill in its wet form before freeze drying, and then milled by a centrifugal mill after the drying process. Pellicle sample 2 (B2) was first freeze-dried in its original wet form, and then milled in a dry form by a centrifugal mill. The particle sizes of B1 and B2 were not examined in our work. However, the diameter of them is similar, 50-100nm in diameter as shown in Figure 12.3. Still, BC is different from the nanofibrillated cellulose. BC has higher denser networks than wood fiber as indicated in Figure 12.3A, and also has a highly branched, three dimensional, and reticulated structure as shown in Figure 12.3B. Oppositely, wood fiber is un-branched as shown in Figure 12.4.

Figure 12.1 Picture of original BC made by static fermentation (the source: fzmb GmbH)

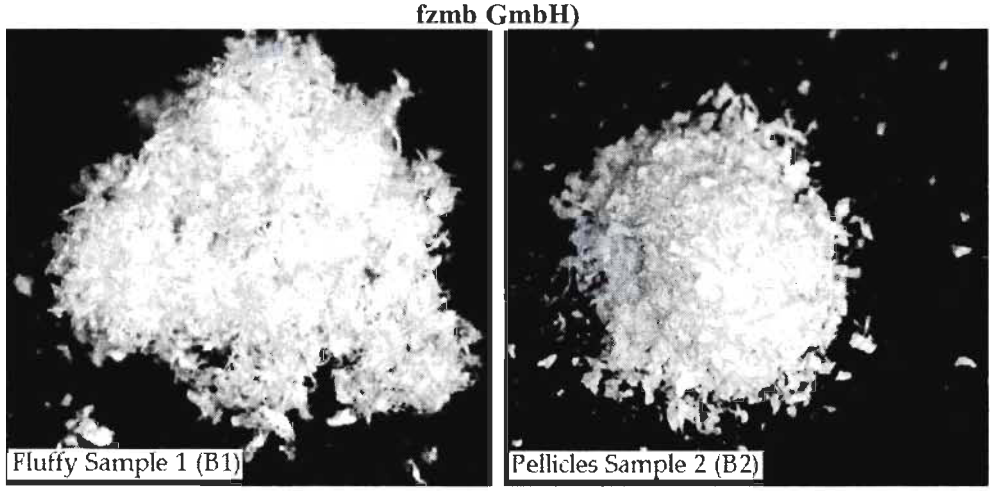

Figure 12.2 Pictures of fluffy (left, B1) and pellicle (right, B2) BC after treatments

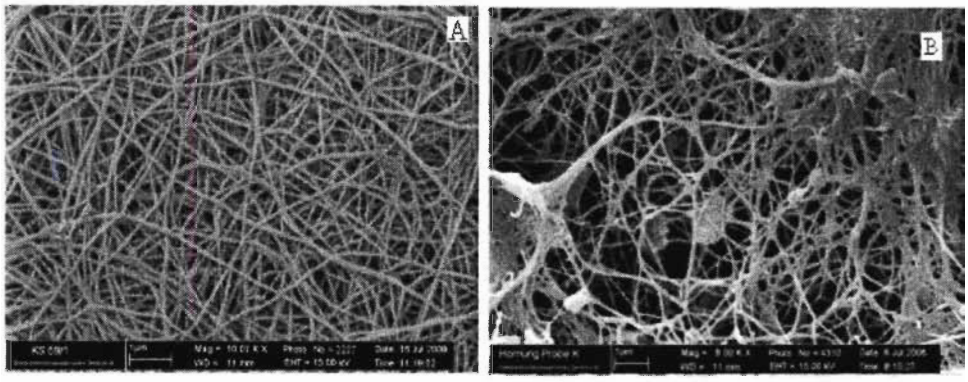

Figure 12.3 SEM of the general structure of original BC (the source: fzmb GmbH)

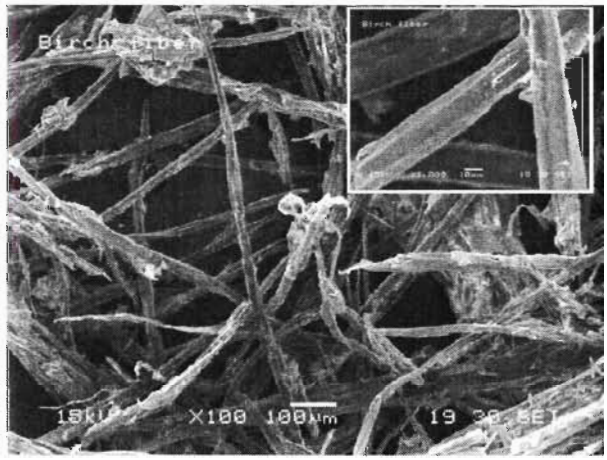

Figure 12.4 SEM of CTMP birch fiber (the source: chapter 11)

Coupling agent: MAPE (G2010) was supplied by Eastman chemical company (Kingsport Tenn.). Its maleic acid graft content is 1.5wt% and the molecular weight is 15,000.

Initiator: Dicumyl peroxide (98% active DCP) supplied by Sigma Chemical Co. was used as an initiator. Its halftime is 1min at 171°C.

12.2.2 Preparation of PE composites

All of the sheets were prepared by a two-roll mill (CWB Instruments Inc. Model T-303) according to Schedule 12.1 to study the influence of wood fiber with the presence of the compatiblizers as well as the bacterial cellulose on the mechanical properties as formulated in Table 12.1.

22 specimens (10 for tensile strength testing and 12 for tensile impact strength testing) for each sample were simultaneously obtained by pressing the sheet trips into a dog-bone shaped mould (ASTM D638 Type V for tensile strength and ISO 8256

Type II for tensile impact strength). The approximate dimension of tensile specimen was 0.30-0.32cm in width and 0.27-0.33cm in thickness, while the width of impact specimen was 0.29-0.36cm and the thickness was 0.17-0.18cm. The specifications of the use of two-roll mill were: 30cm length, 15 cm radius, 0.6 gear ratio, and 60 rpm roll speed.

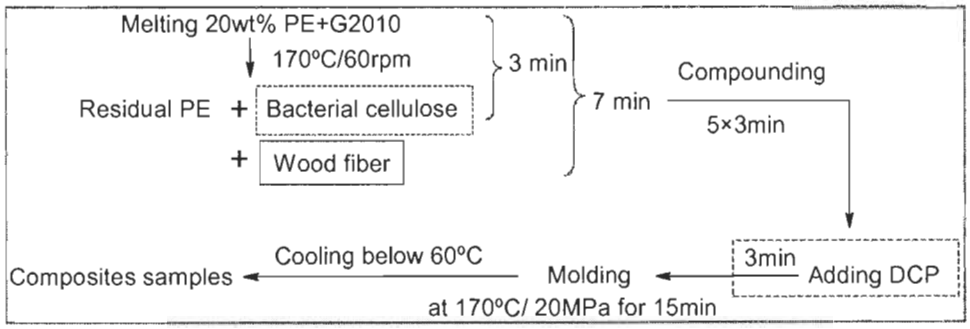

Schedule 12.1 Compounding and molding conditions

12.2.3 Mechanical tests

All of the specimens were conditioned at 23°C and 45% RH, and then width and thickness were measured after polishing. The tensile test was performed using an Instron machine (Model 4201) according to ASTM D638 while tensile impact strength testing was carried out by means of a Zwick tester following the DIN 53448 method.

12.3 Results and Discussions

The characteristics of B1 and B2 are differed from their observations, which are fluffy and pellicle form. This difference comes from its physical formation. However, their chemical functions should be same when BC is well dispersed in the composites, in fact, that it is difficult to achieve an uniform distribution during a melting compounding. The interpretation of the distribution of BC is discernible due to its fibril-like aggregations in particular for hydrophobic system, even in cellulose acetate butyrate composites [657]. Obviously, the planar B2 was dispersed easily than 3-D conformation B1 when BC chains were exposed to high driving shear force during compounding because there were more large fibril-like spots of B1 compared to B2 by our observation.

In the following discussion, the different behaviors of the mechanical properties of the composites are compared after the addition of wood fiber and BC in presence of coupling agent and initiator as depicted in Table 12.1. Like in our previous report

(chapter 10), coupling agent and initiator could deteriorate the tensile strength, increase the elongation, and lower their modulus (Sample B). But it is worth noting that it could improve the impact strength by 23% from 45.4 kJ/m² for neat PE up to 55.8kJ/m² for compatibilized PE. There was an indication that a small amount of BC nanofibers improved the interaction between the wood fibers and the synthetic polymer matrix due to its branched structure, which enhanced tensile strength by 5-7% compared to coupled PE (Sample B). Unlike tensile strength, the impact strength of compatibilized PE decreased as a small amount of BC was introduced, as shown in Table 12.1. Neither B1 nor B2 addition could achieve superior impact strength compared to virgin PE (Sample A) or compatibilized PE (Sample B) due to their fibril-like aggregations from their denser networks and their reticulated structure. It is important that the bacterial cellulose composite reinforced with B2 (Sample C2 44.9kJ/m²) had relative high impact strength in contrast to B1 (Sample C1 26.4kJ/m²) resulting from its relatively uniform dispersion due to their physical formation.

Table 12.1 Composition and Mechanical Properties of the Composites

Code	Compositions, g						Impact	Tensile	Elongation	Modulus
	PE	Wood fiber	B1	B2	G2010	DCP	kJ/m²	MPa	%	MPa
A	100	--	--	--	--	--	45.4(4.4)	25.4(1.9)	10.4(1.4)	771(90)
B	96.8	--	--	--	3	0.2	55.8(5.8)	19.7(1.2)	11(0.7)	644(83)
C1	95.8	--	1	--	3	0.2	26.4(2.2)	20.6(1.3)	8(0.8)	962(68)
C2	95.8	--	--	1	3	0.2	44.9(4.4)	21.1(0.8)	8.4(0.9)	1011(87)
D	70	30	--	--	--	--	12.5(2.9)	18.1(1.2)	2.5(0.3)	1188(108)
E	66.8	30	--	--	3	0.2	40.9(3.9)	34.6(1.3)	9.1(0.7)	900(85)
F1	65.8	30	1	--	3	0.2	42.3(1.8)	36.9(1.3)	9.3(0.7)	951(101)
F2	65.8	30	--	1	3	0.2	54.3(1.9)	36.8(0.8)	9.5(0.7)	893(44)

Due to BC addition resulting in high modulus [652], the composites reinforced with 1wt% BC had high modulus, which was increased by 20-30% compared to neat PE and 50-60% compared to compatiblized PE without any wood fiber added. Obviously, the improvement of elongation was significant from 11% of the coupled PE down to 8-8.4% as 1wt% BC employed. It seems that both pellicle and fluffy BC yielded similar improvements in tensile strength, modulus, and elongation. So, the contributions come from the chemical bonding, not being related to physical morphology if they are in the same scale as well as distributed well. The direct evidence of chemical bonds between bacterial cellulose and the matrix has not been

proved, but the interfacial adhesion among the composites was surely improved due to BC making up the wood fiber structures [658].

In fact, two after-treatment methods of BC showed no influence on their chemical composition due to their being generated by same bacteria, but in different morphologies. Thus, it would also be evaluated indirectly due to its chemical structure same to wood fiber. Whatever, in the absence of assistance by traditional wood fiber, with a small amount of BC addition it could be difficult to obtain superior strength higher than neat PE due to the fact that excess maleated polymer could form a thick attached hydrophobic layer around wood fiber leading to slippages among the hydrophobic matrix. Considering the high manufacturing cost of BC, an amount of wood fiber was introduced to investigate the changes in the mechanical properties.

It was observed that the composite with 30wt% wood fiber added had the weakest tensile strength and impact strength (Sample D with 18.1MPa and 12.5kJ/m^2) respectively if there was no the compatibilizer used, including coupling agent or initiator, due to the poor adhesion. It is also well known that coupling agent and initiator could improve both impact strength and tensile strength of the composite (Sample E with 34.6MPa and 40.9kJ/m^2, respectively) when wood fiber is presented by forming ester linkages [314, 544].

Due to the fact that BC attachment in situ to wood fiber via strong adhesion caused by the high self-affinity of cellulose through hydrogen bonding [659] as well as their similar polarities, the introduction of BC in small amounts could increase the impact and tensile strength of the composites (Sample F1 and F2) compared to the composite without wood fiber presented (Sample E). Moreover, with the assistance of wood fiber, BC not only improved the tensile strength of PE-wood composites (Sample F1 and F2), but also enhanced their impact strength, which differed to its functions in PE composites employed with BC only (Sample C1 and C2). Juntaro et al. reported that the interfacial adhesion between PLA and the sisal fiber was enhanced when BC attaching onto fiber surface implying a relative high apparent interfacial adhesion [658]. Although this attachment occurred in culturing, it shows us that there exists a way of BC depositing on wood fiber surface, even by compounding, at least it could disperse better than those without the presence of wood fiber. Still, their similar polarities also contribute BC with better dispersion accompanying the distribution of wood fiber, in particular under strong driving and

shear force. Although a low concentration of BC is given, the dominant effect is almost certainly improved in the apparent interfacial shear strength, which allows wood fiber to contribute more effectively to the overall composites performance. So, both impact and tensile strength were improved after small amounts of B1 and B2 were presented in the composites F1 and F2, which also contributed with a little high strain as indicated in Table 12.1.

The difference of impact and tensile strength of F1 and F2 came from their physical formation. It is an interesting finding that B1 raised the impact strength by 60% from 26.4kJ/m^2 of the bacterial cellulose composite (C1) up to 42.3 kJ/m^2 of the composite with 30wt% birch fiber present (Sample F1). As a flipside to the improvement of the dispersion of B1 in the composite, B2 enhanced impact strength by 21% from 44.9kJ/m^2 of C2 up to 42.3 kJ/m^2 of F2. It is quite clear that the distribution of fluffy BC (B1) was improved significantly with the help of traditional wood fiber compared to pellicle BC (B2). Benefiting from this contribution, the tensile strength was also improved by feeding a small amount of BC in addition, which resulted in more grafted structures. However, a little difference contribution on tensile of the composites with the reinforcement of BC helping with additional dispersion via wood fiber was observed, where B1 addition could achieve 79% enhancement from 20.6MPa of C1 up to 36.9MPa of F1 while B2 addition was increased 75% from the value at 21.1MPa of the composite without wood fiber (Sample C2) up to the value at 36.8MPa of the composites with wood fiber (Sample F2). So, it is concluded that wood fiber could help BC achieve a more uniform dispersion. The improved distribution of BC will optimize the distribution of the networks of coupling agent and cellulose chains (wood fiber and BC), which results in superior interfacial adhesion to achieve enhanced impact and tensile strength.

In case of the biofiber composites including BC and wood fiber, more fibers introduced could induce the molecules of maleated polymer to cover on the fiber surface with a thin hydrophobic layer, leading to embedding them into the PE matrix and preventing slippages from occurring [92, 316, 453]. Although very small amounts of BC were introduced, as long as they were embedded and well combined with traditional wood fiber, it was possible to increase the impact strength of the composites by 3% and 33% through reinforcement with B1 and B2 compared to the composites without BC (Sample E), respectively. In contrast to impact strength, the tensile strength of F1 had nearly the same change as F2 after a small amount of BC

was added, where both of them were increased in the range of 6% compared to wood composites without the presence of BC (Sample E). B1 and B2 had different effect on impact strength, but less on tensile strength, elongation and modulus due to its different reinforcement mechanism. The contribution of impact strength comes from the formation of networks in wood composites. Obviously that more uniform distribution of pellicle BC (B2) could produce more networks than fluffy BC (B1) leading to improved impact resistance, increased elongation, and decreased modulus even though slightly. But for tensile strength, the contribution mainly depends on the amount of bonds formed which was limited by the amount of exposed BC.

The decreased elongation and increased modulus of incompatibilized composites was discovered, which attributed of the high modulus of wood fiber acting as backbones in the matrix [92, 202] as well as a remarkably high modulus of elasticity of BC due to its super-molecular structure [660]. The elongation difference was attributed to the improved interfacial adhesion. Improved compatibility could allow coated wood fiber to flow past on another in a very small range, which exhibiting a bit increase of elongation. This elongation behavior is typical of reinforced thermoplastic in general and has been reported by many researchers [56, 360]. However, the macrophysical modulus is still dominated by the contributions of the backbone fibers, such as high modulus of rupture, which is little affected by the addition of nanofiber due to its small amount.

12.4 Conclusions

A small amount of BC introduced into the composites, in combination with addition of traditional wood fiber, was able to improve impact strength, tensile strength and their deformations. The after-treatment of BC had great impact on impact strength, both in the presence and absence of wood fiber. Impact strength was much more sensitive to the distribution of biofibers compared to tensile strength. It seems that BC without mill cutting exhibits greater improvement that pellicle BC is better than fluffy BC. But the difference could be reduced with the assistance of wood fiber in good dispersion of nanofiber. In addition, the elongation results showed similar trends to tensile strength. However, modulus originates from the contributions of the backbone of wood fiber reinforcement, leading to a reduced effect. It is concluded that pellicle BC can provide superior improvements to mechanical properties of a reinforced plastic composite.

12.5 Acknowledgements

The authors would like to thank the NSERC, NCE Auto21, and FQRNT for the financial support. The authors truly appreciate Dr. Ivan Fortelny for the impact measurement at the Institute of Macromolecular Chemistry, Czech Republic. We would also thank NOVA chemical for its donation, and fzmb GmbH for their works on bacterial cellulose.

Chapter 13 - General Conclusions & Recommendations

In recent years, wood fibers are used to produce green materials. Coupling agents play an important role in improving interfacial affinity and adhesion between hydrophilic wood fiber and hydrophobic polymer matrix. The most popular coupling agents presently being used include anhydride-modified polymer, e.g. MAPE and MAPP.

At the interface, primary bonding forces include covalent bonding, secondary bonding (such as van der Waals's forces & hydrogen bonding), macromolecular chain entanglement, and mechanical interblocking which was indicated in Table 13.1. Among of them, covalent bonding between coupling agent and the polymer matrix is mainly carbon-oxygen bonding by grafting & coupling function forming mainly ester bridges to maleated polymer resulting in main contributions to strengthened networks. Sometimes, wood fiber and the polymer may be strongly connected with carbon-carbon bonding by copolymerizing and crosslinking (entanglement) structures in the presence of initiator.

Table 13.1 Coupling mechanism of wood composites [420]

Coupling type	Structure at the interface			
Covalent bonding (~50 Kcal/mol)	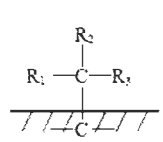	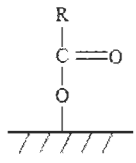	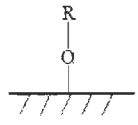	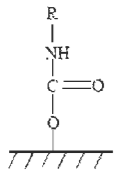
	Carbon-carbon bonding	Esterification	Etherfication	Carbamation
Secondary bonding (~10 Kcal/mol)	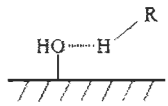	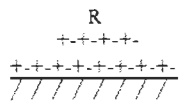		
	Hydrogen bonding (~5 Kcal/mol)	van der Waals forces (<4 Kcal/mol)		
Mechanical adhesion	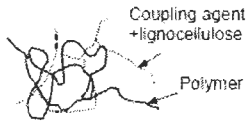	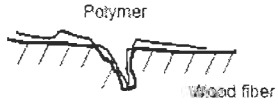		
	Molecular chain entanglement	Mechanical interlocking		

The pendant chains of maleated polymer entangle with the polymer matrix at naturally due to similar backbones. The free ends of the polymer penetrate into pores, pits, and fractures on the fiber surface and hold wood fibers by lumen-loading which

resulted in interblocking structures. Therefore, the interface is integrated with these mechanisms.

13.1 General conclusions

In this study, we focus on the esterification due to its importance. Prior to the coupling mechanisms, the compounding conditions of both wood composites and polymeric nanocomposites were optimized which were described in section 1-4.

1. The total blending time was established to be around 30-35min to achieve optimum impact strength without weakening tensile strength.
2. The bulk mixing method (no-premixing method) could lead to superior impact and tensile strengths compared to pre-mixing method where wood fiber was pre-coated by the mixture of the maleated polymer and small amount of the polymer matrix.
3. The addition sequence of DCP at final-step achieves higher impact strength without the decrease in tensile strength due to the difference in the oxidation and grafting reaction in presence of initiator.
4. Antioxidant agent prevents wood composites from thermal oxidation & degradation in the presence of DCP. In absence of DCP, it acted as an inorganic filler leading to inferior impact and tensile properties. It was concluded that DCP speeded the thermal oxidation & degradation of the composites based PP.

Secondly, after polymeric nanocomposites and wood composites prepared with optimized conditions, the effects of wood fiber, coupling agent, nanofiller and DCP were investigated. According to the studies on the changes of each component, some conclusions were made as follows (5-9).

5. Wood fiber showed different strength behaviors in incompatibilized and compatiblized composites. Both impact and tensile strength decreased with the increase of wood fiber content without compatibilizer presented due to poor interface adhesion. However, the strengths were improved as the compatibilizer were employed as a function of wood fiber concentration increase due to the improved compatibilities accompanying the increase amounts of bonding, because more wood fiber provided more reactive sites. In addition, it was shown that the size of selected wood fiber (20-60mesh, 60-80mesh, and 80+mesh) has no effect on the mechanical properties of PP

composites without coupling agent employed. This finding was confirmed by the FQA results, showing the employed wood fiber could be fractured during compounding. As 1wt% bacterial cellulose was added into wood composites, the interfacial interactions were extended and the impact and tensile strength were improved because bacterial cellulose could attach in situ to wood fiber via strong inherence caused by the high self-affinity of cellulose through hydrogen bonding.

6. It was shown that the mechanical properties of wood composites were significantly enhanced by employment of coupling agents and affected by their characteristics, where high Mw low MA% MAPP could contribute the homo-PP hybrids with better performance. However, it should be noted that the properties deteriorated after excess coupling agent was used due to its entanglements and slippages which was observed by SEM images. It is important that the optimum concentration for coupling agent were found to be 3wt% for maleated polyolefin of wood composites with 30wt% wood fiber and 0.2% DCP.
7. It was an interesting finding that the introduction of NC at low content (<2wt%) could increase impact and tensile strengths, but weaken the strength at high content (up to 20wt%). Different organo-NC exhibited different behaviors due to the different nature of attached surfactants, and the differences were enlarged when the system was compatibilized with coupling agent and initiator. Although NC-concentrates could give uniform sheets easily, NC-natural led to better mechanical performance than NC-concentrates as well as other modified NC except I.34TCN which has reactive pendant groups -OH ready to react with coupling agent, where NC-concentrates has no extensive interactions with the polymer matrix.NC-natural was deposited on the surface of wood fiber, and even loaded in wood lumen. The strong interactions between NC-natural and polarized polymer were verified by SEM images of PE nanocomposites.
8. In two-roller mill system, DCP decreased the impact/tensile strength of PP composites by the thermo-oxidation speed up at temperatures near 200°C. However, DCP showed a positive effect on PE composites implying that the degradation of PE polymer and wood fiber was over-ridden by its copolymerization and crosslinking.

9. Through the systemical studies via CCD, the concentrations of additives were optimized to maximize both the impact strength as well as tensile properties. The relative effect of each component was revealed, where coupling agent has positive effect, NC has two roles on the properties upon its content, and DCP has positive effect for PE composites but negative one for PP composites.

Thirdly, the moisture uptake, water uptake and water loss of the composites were evaluated to meet its outdoor application. The results of water behaviors as functions of the changes of wood fiber and NC were shown in section 10-12.

10. The moisture uptake, water uptake and water loss of the composites decreased with employment of coupling agent due to the interfacial adhesion improvement and hydrophobic polymer deposition on fiber surface leading to the decrease of void fractions and penetration channels blocking, including elimination of the amounts of OH groups leading to increase hydrophobicity. As the soaking time extended, water uptake increased due to the water molecules penetration in-depth along the weaknesses of wood fiber. Moreover, the uptaking speed will be acceleted by the swelling cell wall, which could produce some cracks which act as water channels. Conversly, the absorption speed will be slow down by the deposited hydrophobic polymer leading to a longer saturated time for compatibilized composites compared to incompatibilized ones.
11. The moisture uptake, water uptake and water loss of the composites increased with the increase of wood fiber loading. As more fiber were introduced, more fiber could be exposed to water molecules, which will make water penetrates to the unfilled pores, pits, voids and even between partly bonded wood fiber and the matrix in depth. Meanwhile, more fibers provided more hydrophilic groups to combine with water. It was also estimated that more fiber introduced will shorten the saturated soaking time with the limited amount of coupling agent thereof.
12. In the studies of water behaviors, it was found that NC would improve the water resistance and water loss of wood composites via the actions of blocking and bulking, which was a function of NC amount and its surface modification by surfactant. It should be noted that surfactants play an important role by their morphological structures as well as chemical

reactions, and are also a source of wood composites anti-discoloration. It was novel finding that the color reactions of wood composites filled with NC-natural. It was also the first report to show the effect of NC content on their water behaviors.

Fourthly, the stress-strain behavior of the polymeric nanocomposites based PE was studied. NC-natural made the polymeric nanocomposites more brittle as its content increased. Comparing the changes of stress-strain curves of the based PE materials, the effects of wood fiber, coupling agent, initiator on the morphologies were well-ordered. Normally, the compatibilized composites became more brittle as wood fiber and NC were introduced while the compatibilizer showed converse effect in the presence of wood fiber, showing high Possion's ratio with fiber employment. Preferred to superior strength and better water behaviors, I.34TCN modified by ammonium with 2 hydroxyl groups as well as natural NC were the best ones.

Finally, coupling mechanisms were established both for MAPP and MAPE for different Mw. Surface treatments of wood fibers were carried out with two kinds of maleated polyolefins (MAPE and MAPP) via melt blending. FQA and SEM were used to monitor the morphological changes of wood fiber and their fracture modes. In addition, FTIR and XPS analyses revealed the decrease in hydrophilicity of wood fiber with maleated polyolefin treatments and new bond formation with employment of coupling agent because of chemical bonding occurred at the interface. The chemical changes were systematically illustrated by FQA, SEM, FT-IR and XPS in section 13-18.

13. In entirely bonded experiments, the interfacial morphologies of modified wood fiber were illustrated with the break-off, cracking, curling, extruding, twisting, fibrillations, and pinwheels models. The changes of the morphologies were mainly related to the characteristics of the matrix and maleated polymer, where PE or MAPE could make wood fiber shorter with serious fractures contrary to PP or MAPP. It should be noted that the morphologies were also related to the Mw of maleatd polymer and their amounts which were evidenced by FQA and SEM analyses. Opposite to the changes of fiber size, high Mw MAPP lead to wood fiber with higher curls and more kinks due to longer pendant polymer chains while low Mw MAPE obtains higher curls and kinks driven by the stronger reactions. It is concluded that the Mw has high impact on the curls and kinks under

moderate interfacial reactions to MAPP. However, the Mw has high impact on the curls and kinks following stronger interactions happened if the functions occurred during wood fiber compounded with MAPE. Obviously, MAPE could achieve high curls and more kinks compared to MAPP which indicates more facture occurred.

14. In partly bonded experiments, the optimum fiber length and width could be achieved at an optimal concentration of coupling agent employed. FQA results were shown that 3wt% MAPP could be set to wood composites with 30wt% fiber loaded, which also produced more complex fractures, i.e. fibrillations exhibiting max curls and kinks by FQA data and confirmed by SEM images.
15. Based on the entirely bonded experimental results, maleic anhydride graft has an important impact on the esterification, where high MA% maleated polymers produced more chemical bonding shown by FTIR spectra and formed high carbonyl index calculated by the peaks areas. Moreover, the reactivity of MAPE was higher than MAPP after normalization at the same MA% level. Unlike in entirely bonded experiments, the results of partly bonded experiments indicated that the amount of coupling agent had an impact on the formation of chemical bonding at an optimal concentration of 3wt%. For both MAPP and MAPE, the reactive efficiency decreased if excess coupling agent were employed which lead to a decrease of the intensity of carbonyl band.
16. XPS was used to evaluate the grafting efficiency and the formation of ester links between wood fiber and maleated polymer in a blender process. The modified fibers were similar compared to extracted or initial fiber shown by their survey spectra. However, the changes of the carbon and oxygen concentration varied as a function of the sampling depth which indicated its inhomogeneous structures-fractional coated structure. A little difference of binding energy as well as the concentration of oxygen and carbon among bonded fiber was found as a function of depth profiles. Significant difference in the surface elemental compositions of the bonded fibers evidenced the occurrences of ester bonds by increased ratio of O/C, where the O/C ratio of extracted fiber at 0.448 decreased to 0.047 and 0.071 of MAPE and MAPP-modified fibers respectively. Moreover, the high resolution spectra of C1s

gave us more information on the type of bonding formed and also used to determinate hydroxyl index, carbonyl index, grafting index as well as $C_{ox/unox}$ effect on the reactive efficiency, even the depositions of maleated polymer lead to the chemical shifts of oxygen upward and all deconvoluted C1s downward. XPS results also proved the difference in maleic anhydride resulted in the modified fiber with different kind of oxygen-carbon bonds identified by the changes of the area of the deconvoluted carbon leading to the $C_{ox/unox}$ ratio from 1.72 of extracted fiber up to 4.57 and 4.53 of MAPE and MAPP modified fiber respectively. High MA% MAPP achieved high oxygen-carbon bonds compared to low MA% MAPE by increasing the C3 and C4 concentration. Whatever, MAPE could accomplish superior reactivity contrast to MAPP after normalization of hydroxyl index, grafting index as well as carbonyl index calculated by XPS at the same level.

17. It was an exciting finding that the shake-up effect of surface lignin was eliminated after maleated polymer were employed regardless their type and MA% used as well as the nitrogen band was missing due to the removal of nitrogen-contained extractives after the modification procedure, which made the hydrophilic extractives containing nitrogen moved to the surface of modified fibers and then disappeared at higher temperature from the fiber surface.
18. As an engineering material enduring high temperature and high pressure during process, wood composites reinforced with CTMP wood fiber could achieve good performance due to rich surface coverage by lignin (75-76%) and the extractives (37-49%) which act as internal lubricant and natural antioxidant during their manufacturing.

13.2 Recommendations for future work

Based on our current studies, future works are suggested as follows:

1. For compounding process, the two-roll blender was open to air. So, the pilot experimental results should be performed.
2. The thickness of coated maleated polymer on fiber surface would be measured by single-fiber extraction. The morphology fractional distribution and structures of coating should be identified.

3. Compared to imbedded wood fiber from wood composites by dissolution and extraction, infrared imaging microscope (IIM) could be used to reveal fiber surface chemical structures with incredible details to collect high-resolution spectra while obtain molecular information on a microscopic scale of the original materials without damages.
4. The energy consumed during compounding should be evaluated and related to the fractures of initial fibers to improve the energy efficiency.
5. The acceleration of the thermal degradation of wood composites by DCP should be given a detailed study.
6. The relationship between the inhomogeneous structures of cell wall and the sampling depth should be explored further. It is assumed that the changes of depth profiles could be related to the cell layers.

Appendix 1 Refereed Journals & Proceedings

Journal of Thermoplastic Composite Materials

http://jtc.sagepub.com

Effect of Independent Variables on Mechanical Properties and Maximization of Aspen Polypropylene Composites

Ruijun Gu and Bohuslav V. Kokta
Journal of Thermoplastic Composite Materials 2008; 21; 27
DOI: 10.1177/0892705707085347

The online version of this article can be found at:
http://jtc.sagepub.com/cgi/content/abstract/21/1/27

Published by:
SAGE
http://www.sagepublications.com

Journal of Thermoplastic Composite Materials

http://jtc.sagepub.com

Effects of Antioxidant and Initiator on the Mechanical Properties of Polypropylene Aspen Composites

Ruijun Gu and Bohuslav V. Kokta
Journal of Thermoplastic Composite Materials 2008; 21; 175
DOI: 10.1177/0892705707086802

The online version of this article can be found at:
http://jtc.sagepub.com/cgi/content/abstract/21/2/175

Published by:
SAGE
http://www.sagepublications.com

Journal of Thermoplastic Composite Materials

http://jtc.sagepub.com

Effect of Variables on the Mechanical Properties and Maximization of Polyethylene Aspen Composites by Statistical Experimental Design

Ruijun Gu, Bohuslav V. Kokta and Gabriela Chalupova

Journal of Thermoplastic Composite Materials 2009; 22; 633 originally published online Jun 19, 2009;
DOI: 10.1177/0892705709105965

The online version of this article can be found at:
http://jtc.sagepub.com/cgi/content/abstract/22/6/633

Published by:
SAGE
http://www.sagepublications.com

Journal of Thermoplastic Composite Materials

http://jtc.sagepub.com

Maximization of the Mechanical Properties of Birch-Polypropylene Composites with Additives by Statistical Experimental Design

Ruijun Gu and Bohuslav V. Kokta

Journal of Thermoplastic Composite Materials 2010; 23; 239 originally published online Jul 28, 2009;
DOI: 10.1177/0892705708103402

The online version of this article can be found at:
http://jtc.sagepub.com/cgi/content/abstract/23/2/239

Published by:
SAGE
http://www.sagepublications.com

Journal of Thermoplastic Composite Materials

http://jtc.sagepub.com/

Mechanical Properties of PP Composites Reinforced with BCTMP Aspen Fiber

Ruijun Gu and B.V. Kokta

Journal of Thermoplastic Composite Materials 2010 23: 513 originally published online 16 December 2009
DOI: 10.1177/0892705709355232

The online version of this article can be found at:
http://jtc.sagepub.com/content/23/4/513

Published by:
SAGE
http://www.sagepublications.com

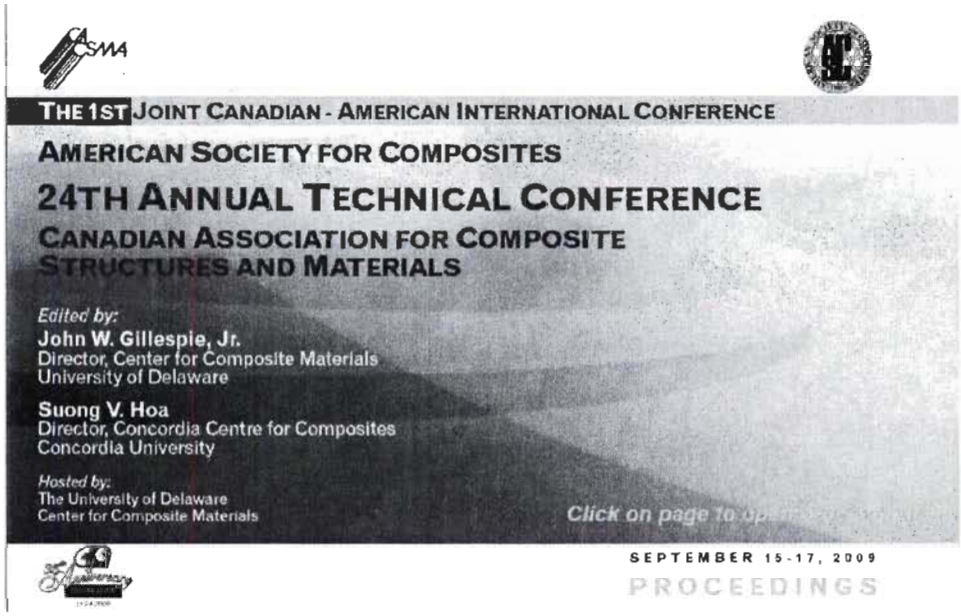

978-0-9812879-2-8

EXFOR & Annual Meeting
EXFOR et le Congrès annuel
2010

Papers presented February 2 & 3, 2010
Communications présentées les 2 et 3 février 2010

PAPTAC / ATPPC

Preprints courtesy of Natural Resources Canada
Prétirés : gracieuseté de Ressources naturelles Canada

Natural Resources Canada | Ressources naturelles Canada

Canada

PREPRINTS
PRÉTIRÉS

Papers presented
Wednesday February 3 AM

Communications présentées
Mercredi le 3 février - avant-midi

Research I / Recherche I

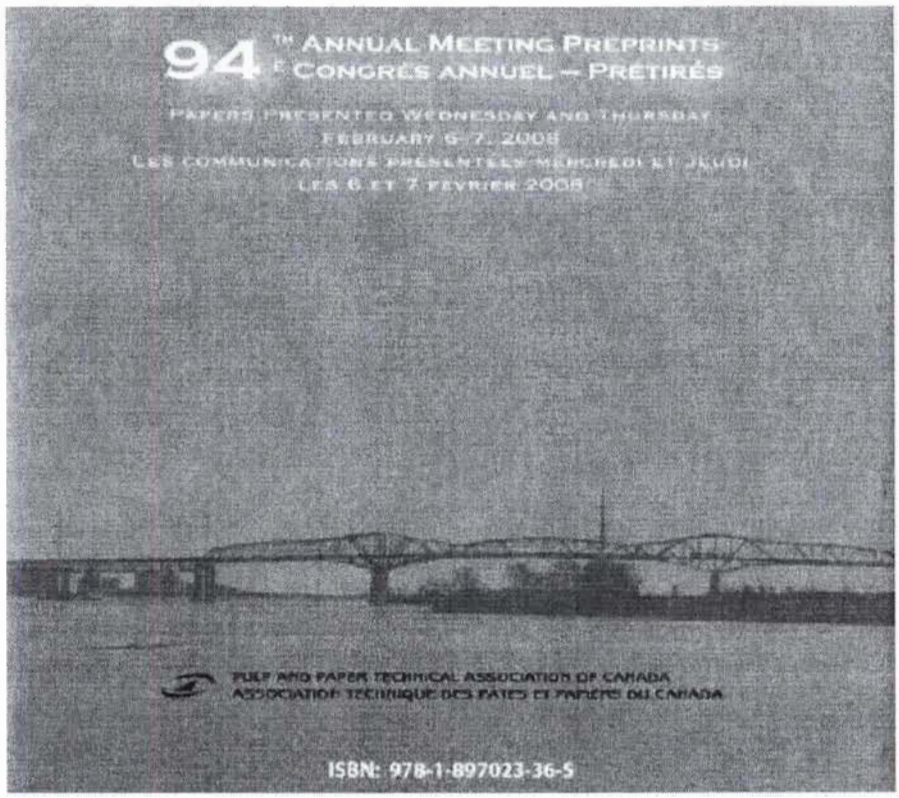

Appendix 2 Refereed Posters

APMA-AUTO21 Annual Conference and Exhibition 2009 & 24th ASC

C403-CGP: Optimization of Mechanical Properties of PE Composites via CCD and Deposition Formation of Nanofiller

Ruijun GU, B.V. KOKTA and K. LAW
Integrated Pulp and Paper Center
University of Quebec at Trois-Rivieres
E-mail: Ruijun@uqtr.ca

Introduction

Wood plastic composites (WPC) are becoming cost-competitive in automotive applications [1]. Naturally reinforced plastic composites are going to remain a competitive technology to replace oil-based and inorganic materials due to the prices of natural fiber which are renewable and high biodegradable resources[2-3].

The current penetration of WPC in the automotive segment is going for 1/3 [4] with further potential to increase after great improvement in quality while driving by the environmental and cost competitiveness of WPC. PE is the dominant resin used in the production of WPC, with about 90% of the composites being produced using virgin or recycled PE [5].

The present studies were focused on the optimization of the mechanical properties via central composite design by optimizing each composition, i.e. MAPE, Nanofiller and DCP as a function of wood fiber content. The improvement of interfacial adhesion grafting/crosslinking by MAPE and DCP and the depositions of nanofiller particles on the surface of wood fiber as well as inside fiber lumen and their formations were confirmed by SEM microscopy. In addition, the differences between natural NC and nano-concentrates were also compared.

Experiment

Materials

Plastic: LLDPE (Novacor® HI-0735-H, MFI=1.0g/min), Novacor Chemicals Ltd.
Wood fiber: Air-dried CTMP birch fiber (*Betula papyrifera* Marsh, 28-60mesh) was prepared and screened in Integrated Pulp and Paper Center laboratory.
MAPE: G2010 containing 1.5% maleic acid and its Mw is 15,000, Eastman.
Initiator: DCP with its halftime being 1min at 171°C, Sigma Chemical Co.
Nanofiller: NC-natural (Cloisite® Na+), Southern Clay Products Inc.
NC-concentrates (MB2001), PolyOne Corporation.

Schematic of a Central composite design-2⁴+star design

Table 1. Factor levels in experiments

Coded levels / Actual levels	-1.682	-1	0	1	+1.682
†Nanofiller, wt%	0(0) ‡	0.81(2)	2(5)	3.19(8)	4(10)
G2010, wt%	0	1.01	2.5	3.99	5
DCP, wt%	0	0.041	0.1	0.16	0.2

† Cloisite® Na+ or MB2001; ‡ Figures in brackets are wt% for MB2001

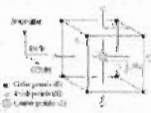

Processing

- The changes in morphology of NC-natural and NC-concentrates in PE nanocomposites.
- Effects of birch fiber loading on the mechanical properties of PE composites via CCD.
- Effect of NC-natural and NC-concentrates on the mechanical properties of PE composites and their depositions formations.

Compression Molding and Mechanical Tests:

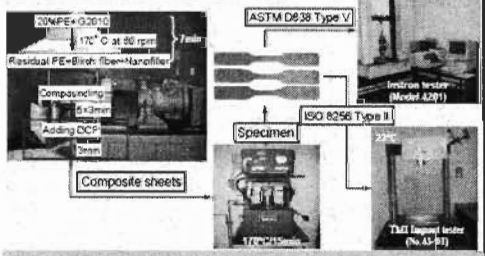

Results

Mechanical properties

Increase fiber loading via CCD compared to virgin PE	
Cloisite® Na+	MB2001
+Impact	-Impact
++Tensile	+Tensile
+++Modulus	++Modulus

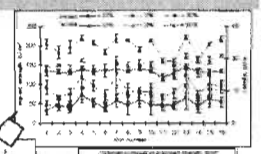

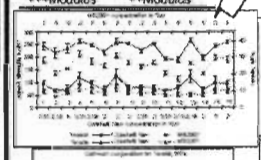

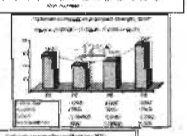

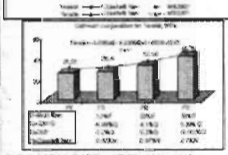

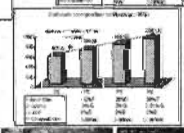

SEM (JSM 6400, JEOL, Japan)

Conclusions

- NC-concentrates achieves an exfoliated plaque easily, but weaker interacting to the matrix; NC-natural also achieves micro/nanosize distribution from macrosize, and has stronger interactions to the matrix.
- Birch fiber plays a remarkable role in enhancing the properties of PE composites in the presence of MAPE, DCP and NC. The loading of 30% birch fiber yields better results when compared to the lower charges.
- Both impact and tensile of the composites filled with NC-natural are superior to the composites prepared with NC-concentrates due to NC-natural depositing on the surface of wood fiber, even locates in wood lumen than NC-concentrates. Meanwhile, the nature and particles formation of NC have influence on the functions by MAPE and DCP.
- The strong interactions between NC-natural and polarized polymer is also verified by SEM images of PE nanocomposites.

References

1. Frost&Sullivan. European Markets for Naturally-Reinforced Plastic Composites. May 2008.
2. V.K. Mathur. Composite materials from local resources. Construction and Building Materials. 2006, 20(7): 470-477.
3. Geoffrey Pritchard. Plastic reinforced with natural fibers. Plastics, Additives and Compounding. 2007, 9(4): 40-43.
4. Alireza Aaroni. Wood-plastic composites as promising green-composites for automotive industries? Bioresource Technology. 2008, 99(11): 4661-4667.
5. Nexant's ChemSystems. PERP Program-Thermoplastic Wood Composites (05/06S2). July 2007.

Acknowledgement

Thank the NSERC, FORINT and Auto 21 for their financial support.

Scientific contest of posters of UQTR 2007 & 6th International Symposium "Materials made of Renewable Resources"

Effect of Independent Variables on Mechanical Properties and Maximization of Aspen-Polypropylene Composites

Effet des variables indépendantes sur les propriétés mécaniques et de la maximisation des Composites des Polypropylènes et Trembles

Ruijun GU and Bohuslav V. KOKTA
Centre Intégré en Pâtes et Papier
Université du Québec à Trois-Rivières
3351 boul. des Forges, C.P.500
Trois-Rivières, Québec, Canada G9A 5H7

SUMMARY| RÉSUMÉ

Study on the effect of concentration of maleated polypropylene, dicumyl peroxide, nanoclay and aspen fiber loading on the mechanical properties of PP/Aspen composites was undertaken with the objective to protect or increase the impact strength without losing or weakening tensile strength. The central composite design of *Statgraphic plus* was used to determine the optimum concentration of additives and to maximize both the impact as well as tensile strength properties to be superior to that of pure polypropylene .
Finally the material price of PP-composites with an optimal composition of filler (aspen fiber and NC), coupling agent (MAPP) and DCP were compared to that of pure PP and PP reinforced with glass fibers.

L'étude des effets des concentrations de polypropylène maléaté, du dicumyl peroxyde, des nano-argile et des fibres des trembles sur les propriétés mécaniques des composites à base de PP renforcés avec les fibres des trembles a été entrepris avec l'objectif de protéger ou augmenter la résistance aux chocs sans perdre ou affaiblir les renforts des résistances à la traction. CCD de *Statgraphic plus* fait possible a déterminer les concentrations optimales des additifs et maximiser en même temps l'impact aussi bien que les propriétés des tensions pour être supérieures que PP vierge.
Enfin les prix matériels des PP-composites avec une composition optimale de remplisseur (fibres des trembles et des nano-argiles), les agents d'accouplement (MAPP) et les DCP ont été comparés à celui des PP vierge et des PP renforcés avec les fibres des verres.

INTRODUCTION

Wood plastic composites are used to replace impregnated wood in many outdoor and other plastics applications, and also in biomedical due to their abundant availability, low cost, high relative strength and stiffness, low density and renewable nature. The wood fibers are natural and renewable resources which will provide the composites with an excellent biodegradability helping to reduce waste disposal burdens as well as excellent mechanical and physical properties, such as low cost/high volume etc. In general the compatibility between composite components should be improved using either physical or chemical modification of the thermoplastics or wood fiber using coupling agent. The popular coupling agent like maleated polyolefins could improve the linkage between matrix and fiber. Coupling agents like maleated polypropylene, maleated polyethylene and silane [or sodium benzoate] and dicumyle/benzoyl peroxide [as a nucleating agent are the most utilized. Wood fiber could be treated with some chemicals, such as alkali, isocyanate and peroxide] to create more reactive point. The properties of composite materials are also determined by the characteristics of the polymer matrices themselves, together with reinforcement, and the adhesion fiber/matrix interface that mainly depends on voids and the bonding strength at the interface. Moreover, wood fibers are rich in lignin with abundance of hydroxide groups which could react with carboxyl groups to form branched structures and thus improve the strength of the composites. Because lignin is a solid polymer with big molecules, lignocelluloses fiber may produce more solid point in matrix to lead to superior impact strength to the composite .

EXPERIMENTAL

Materials

Polypropylene was supplied by Montell Canada Inc. Air-dried wood fiber is aspen fiber (CTMP, 20-60 mesh) and were prepared at CRPP. MAPP was supplied by Eastman chemical company as coupling agent named Epolene G-3003 was a PP with 9% acid anhydride. DCP, 98% supplied by Sigma, was used as an initiator, mp.39-41°C, decomposed rapidly at 120-125°C. Cloisite®10Å Nanoclay received from Southern Clay Products Inc. was used as a nano-filler

RESULTS AND DISCUSSIONS

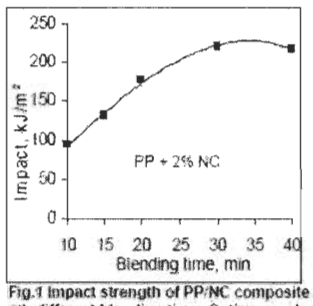

Fig.1 Impact strength of PP/NC composite with different blending time; Optimum value (216.83-220.63 kJ/m²) at 35 min

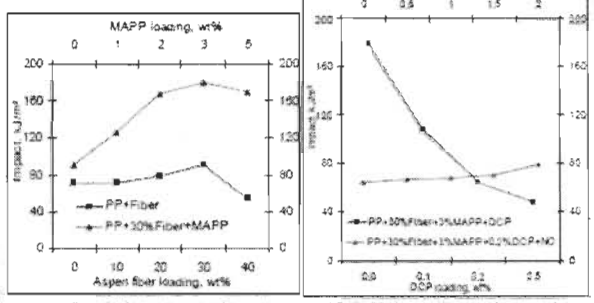

Fig.2 Effect of aspen fiber, MAPP, DCP and NC loading on the impact strength of the composites

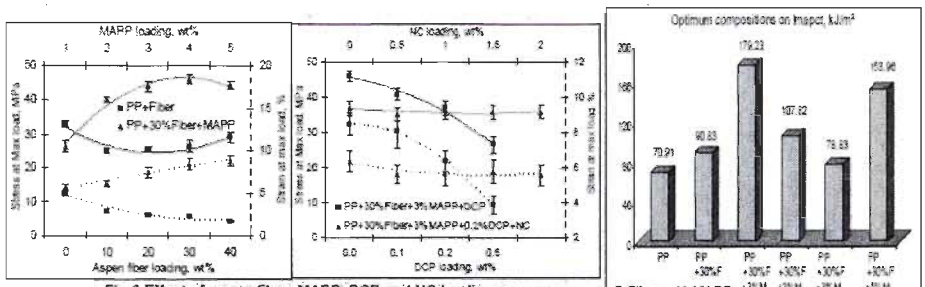

Fig.3 Effect of aspen fiber, MAPP, DCP and NC loading on max Stress/Strain of the composites

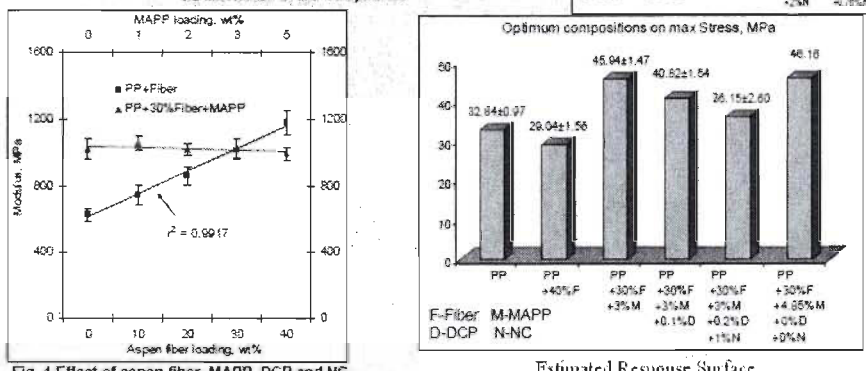

Fig. 4 Effect of aspen fiber, MAPP, DCP and NC loading on Modulus of composites

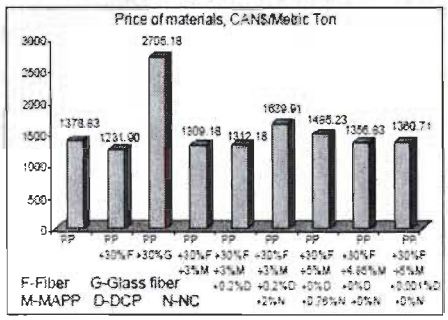

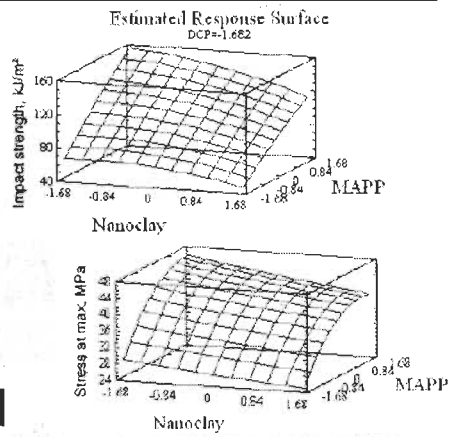

CONCLUSIONS

- 35 min was an optimum blending time to achieve optimum mechanical properties as well as the uniformity of additives.
- Modulus of PP-Aspen composite shows increasing linear relationship with the content of fiber loaded.
- A systematic study of the effect of concentration of aspen fiber, MAPP, DCP and NC content on the mechanical properties of PP/Aspen composite with the objective to protect/increase the impact strength without losing tensile strength realized using the Central Composite Design lead to the optimum concentrations of additives best both for the impact as well as tensile strength properties, as listed in Table 1.

Table 1 Optimizations of mechanical properties of the PP composites

Properties	The increase of physical properties of composites compare to virgin PP.		
	30% Fiber	30% Fiber+3%MAPP	CCD with 30% Fiber loading
Impact	28.1%	152.8%	117.1%
Stress at max load	-19.7%	39.9%	40.6%
Strain at max load	-54.4%	-33.0%	-19.6%
Modulus	61.5%	62.4%	63.6
Toughness	-72.8%	-41.8%	-32.4%

- The economic calculations present a clear decrease of price for composites with high amount of aspen fiber in comparison with that of glass fiber reinforced composites as well as pure polypropylene.

Acknowledgment

The authors wish to thank the NSERC and National Centers of Excellence of Canada–Auto 21 for its financial support.

10th International Conference on Wood & Biofiber Plastic Composites FPS2009

Mechanical Properties of PP Hybrid Nanocomposites Reinforced with Bleached Aspen CTMP Fiber

Ruijun GU and Bohuslav V. KOKTA
Integrated Pulp and Paper Center, University of Quebec at Trois-Rivieres, Quebec, Canada
E-mail: Ruijun@uqtr.ca

Introduction

PP is a typical polyolefin materials used in biofiber plastic composite [1]. The present studies were focused on the effect of incorporating wood fibers on the properties of a composite material with/without MAPP to indicate the improvement of the interfacial adhesion made by MAPP [2]. The effects of the molecular weight (Mw) and maleic acide grafts (MA%) of MAPP were also studied to evaluate the improvements of mechanical properties [3]. Due to the degradation of PP [4, 5] and wood fiber [6], DCP has typical negative effects on PP composite which is opposite to PE composites [7]. In addition, the mechanical behaviours of highly filled NC PP composites were investigated in comparison to PP nanocomposites without wood fiber reinforcement.

Experiment

Materials

Plastic: Homo-PP (Martex-HGZ-1200, MFI=115g/10min), Philips Sumika
Co-PP (Pro-fax SB842, MFI=22g/10min), Ashland.
Fiber: Air-dried BCTMP aspen fiber (20-60, 60-80 and 80+mesh) were prepared and screened in Integrated Pulp and Paper Center laboratory.
Coupling agent: G3003, G3015 and G3216 containing 1.5, 2.6 and 2.6% maleic acid respectively. Eastman (Kingsport, Tenn.)
Initiator: Dicumyl peroxide(98% active DCP) with its halftime is 0.2 min at 190°C, Sigma Chemical Co.
Nanofiller: Cloisite® Na+ NC, Southern Clay Products Inc.

Processing

- Effects of inorganic NC loading on the properties of PP Nanocomposites
- Effect of independent variables on the mechanical properties of PP hybrids

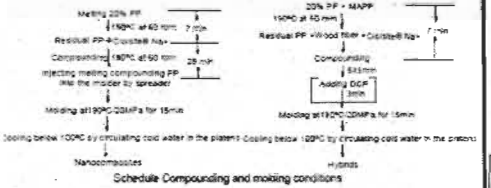

Schedule Compounding and molding conditions

Compression Molding

Dog-bone shaped specimens (ASTM D638 Type V for tensile and ISO 8256 Type II for impact testing were prepared.

Mechanical Tests

Tensile testing was performed on the Instron tester (Model 4201) at 23°C and 50% RH according to ASTM D638. Tensile impact strength (un-notched) was determined by a TMI impact tester (TMI No 43-01) according to ASTM D1822 at ambient temperature (23°C).

Results

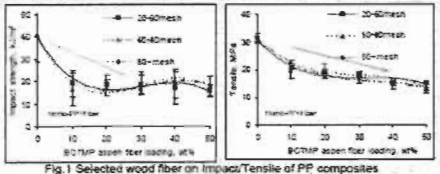

Fig.1 Selected wood fiber on Impact/Tensile of PP composites

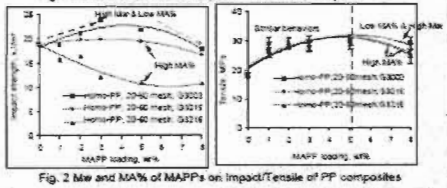

Fig. 2 Mw and MA% of MAPPs on Impact/Tensile of PP composites

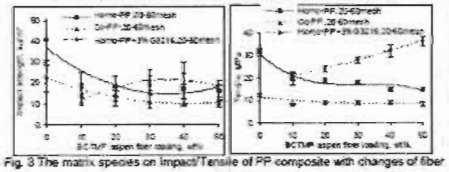

Fig. 3 The matrix species on Impact/Tensile of PP composite with changes of fiber

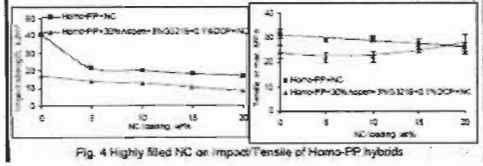

Fig. 4 Highly filled NC on Impact/Tensile of Homo-PP hybrids

Table. The mechanical properties of PP composites reinforced with 30wt% BCTMP aspen fiber and 3wt% G3216: the effect of DCP

Properties	DCP concentration, wt%		
	0	0.1	0.2
Impact strength, kJ/m²	21.11 (4.96)	17.03 (4.12)	17.33 (3.75)
Stress at Max. Load, MPa	28.1 (1.38)	24.24 (2.66)	14.98 (3.02)
Strain at max load, %	4.158 (0.292)	2.562 (0.449)	1.7 (0.168)
Modulus, MPa †	953.9 (87.2)	1299 (137)	1185 (89)
Toughness, MPa †	0.6572 (0.0723)	0.3329 (0.1334)	0.133 (0.0343)
Plasticity†	1.016	1.057	1.145

† Plasticity is defined as the ratio of the E_{break}/E_{max}

Conclusions

- Impact/tensile decrease as selected wood fiber are employed without coupling agent.
- Whatever the Mw of MAPP as well MA%, MAPP gives PP composites with superior tensile. However, there are differences in impact strength with varying Mw and MA% level. It is concluded that MAPP with high Mw and low MA graft level could result in the homo-PP composites with better properties.
- The behaviors on impact/tensile of both homo-PP and co-PP composites without coupling agent decrease simultaneously with wood fiber addition in different descended trend. As G3216 is added, both impact and tensile are enhanced with wood fiber increase. These enhancements are also confirmed by the increase of elongation in the presence of coupling agent.
- In two-roller mill system, DCP impaired impact/tensile of PP composites due to the thermo-oxidation by DCP at 200°C. The degradation by DCP of PP composites resulted in shorter elongation as well as higher plasticity.

References

1. Principia Consulting. Principia Partners September 2005, 4 (9): 1.
2. Yang, Han-Seung *et al.* Composite Structure. 2007, 77(1): 45-55.
3. Kim, Hee-Soo *et al.* Composites Part A. 2007, 38(6): 1473-1482.
4. Huang, H. *et al.* Journal of Applied Polymer Science. 2000, 78(6): 1233-1238.
5. Aziz, Hamed *et al.* Polymer Testing. 2004, 23(2): 137-143.
6. Karimi, Alinaghi *et al.* Journal of Applied Polymer Science. 2006, 102:4759-4763.
7. Gu, Ruijun *et al.* J. of Thermoplastic Composite Materials. Submitted JTCM 2008-24.
8. Gu, Ruijun *et al.* J. of Thermoplastic Composite Materials. 2008, 21(1):27-50.

Acknowledgement

Thank the NSERC, FQRNT and Auto 21 for their financial support. Thank Philips Sumika for donated materials.

Scientific contest of posters of UQTR 2008

Effects of Coupling agent, Initiator and Nanofiller on the Properties of Polyethylene Composites

Ruijun GU and Bohuslav V. KOKTA

Integrated Pulp and Paper Center, University of Quebec at Trois-Rivieres
3351 boul. des Forges C.P.500 Trois-Rivieres, Quebec, Canada G9A 5H7

Resume

Systematic studies of the effects of the concentrations of maleated polyethylene (MAPE), dicumyl peroxide (DCP) and Nanoclay (NC) were undertaken to study the effects on the mechanical properties of PE Nanocomposite and hybrid composite.
In addition the effect of compounding sequences on resulting properties of wood fiber reinforced composites was also examined.

Introduction

PE is an important engineering polymer used widely while wood fiber being biodegradable, low cost and reusable is available worldwide. There were lots of research on PE Nanocomposite and PE hybrid composite. Coupling agents in wood plastic composite (WPC) play a very important role in improving the weak adhesion, poor dispersion and incompatibility between the hydrophilic natural fibers and the hydrophobic polymer. Maleated PE was shown to be the best in wood fiber-reinforced PE composites due to its superior properties by comparing the effectiveness of oxidized PE, MAPP and MAPE. Meanwhile DCP is widely used as another important nucleating agent being the most utilized because of chemical bonding to both the wood fiber and the polymer matrix. The aim of this work is to investigate the influence of MAPE, DCP and NC on the mechanical properties of PE Nanocomposite and Hybrid composite reinforced by cellulose fibers.

Materials

Thermoplastic: Linear low density polyethylene (NOVAPOL® HI-0753-H) was supplied by Novacor Chemicals Inc.
Fiber: Air-dried aspen fiber (CTMP, 20-60mesh) was prepared and screened in Integrated Pulp and Paper Center laboratory.
Coupling agent: Maleated polyethylene (MAPE, Eastman G-2010) was supplied by Eastman chemical company (Kingsport, Tenn.) and contains 6% acid anhydride.
Initiator: Dicumyl peroxide (98% active DCP) with its halftime is 1min at 171°C, supplied by Sigma Chemical Co.
Nanofiller: Cloisite® Na+ received from Southern Clay Products Inc.

Conclusions

1. WPC compounded with non-premixing could achieve the superior properties than wood fiber pre-covered by the mixture of coupling agent and small part of matrix.
2. NC improved tensile and deformation properties of Nanocomposite except impact strength; modulus increased linearly following the content of NC, and MAPE visibly reduced the properties of Nanocomposite filled with NC without the reinforcement by wood fiber.
3. DCP improved both impact and tensile strength of the composite with fiber but deteriorated them for Nanocomposites. Even though DCP would perfect the properties due to forming the stereo-structures, it also provided the composite with better plasticity resulting in reducing the deformation resistance slightly.

Experimental

1. Compounding
- Effect of the adding sequence of wood fiber
- Effects of independent variables

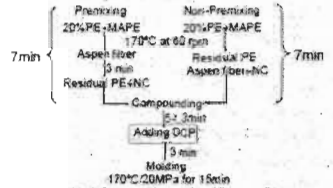

Schedule 1 Compounding and molding conditions

2. Compression Molding
Dog-bone shaped specimens (ASTMD638 Type V) were prepared.
3. Mechanical Tests
Tensile testing was performed on an Instron tester (Model 4201) at 23°C and 50% RH according to ASTM D638.
4. Determination of Tensile Impact
Tensile impact strength (un-notched) was determined by a TMI impact tester (TMI No 43-01) according to ASTM D1822 at ambient temperature (23°C).

Results and Discussions

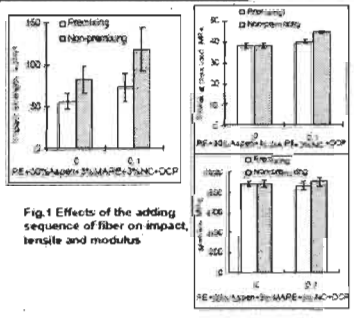

Fig.1 Effects of the adding sequence of fiber on impact, tensile and modulus

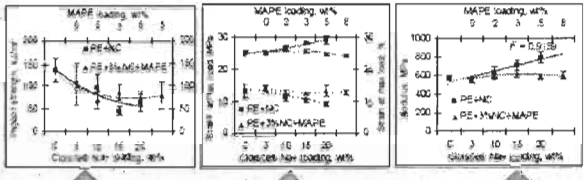

Fig.2 Effects of Cloisites Na+, MAPE and DCP on impact, tensile/strain and modulus (—— Stress ..... Strain)

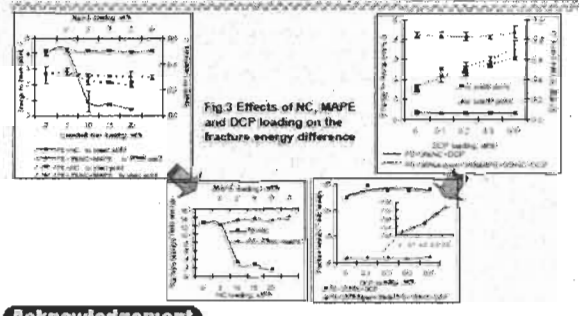

Fig.3 Effects of NC, MAPE and DCP loading on the fracture energy difference

Acknowledgement

The authors wish to thank the NSERC and National Centers of Excellence of Canada–Auto 21 for its financial support.

Natural Sciences and Engineering Research Council of Canada

Appendix 3 Equiments& Instruments

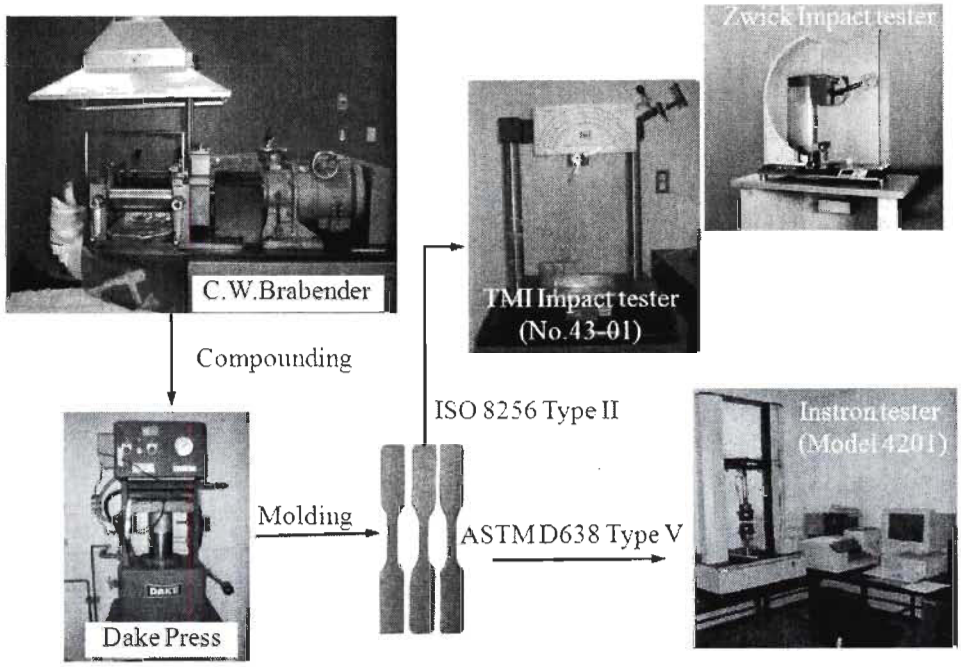

Main equipments used in experimental

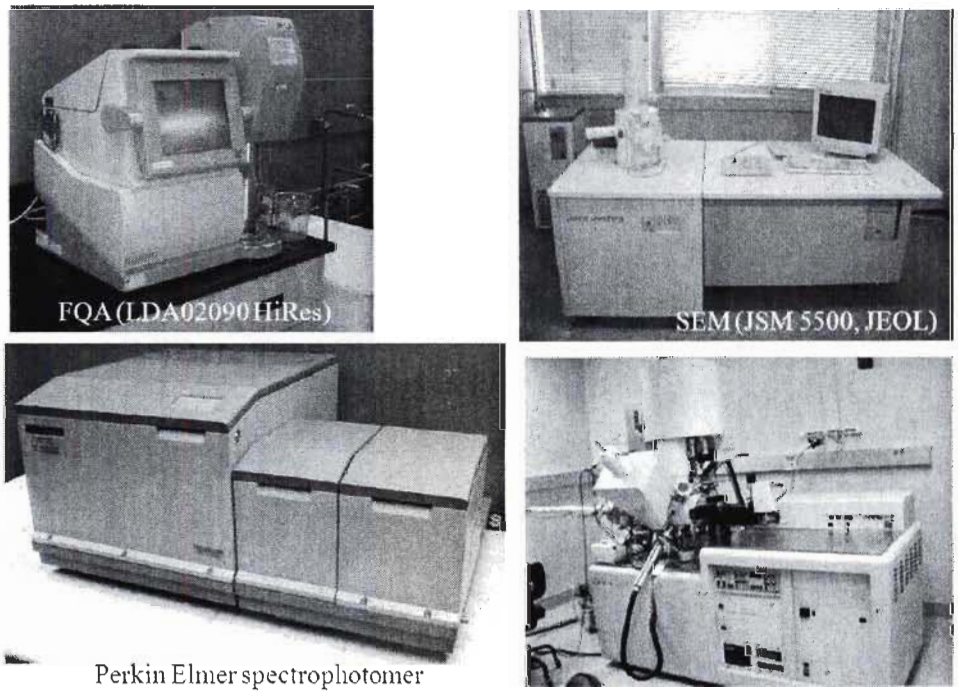

Perkin Elmer spectrophotomer
(System 2000 FTIR)

Kratos Axis Ultra (HIS 165)

Instruments for characterization

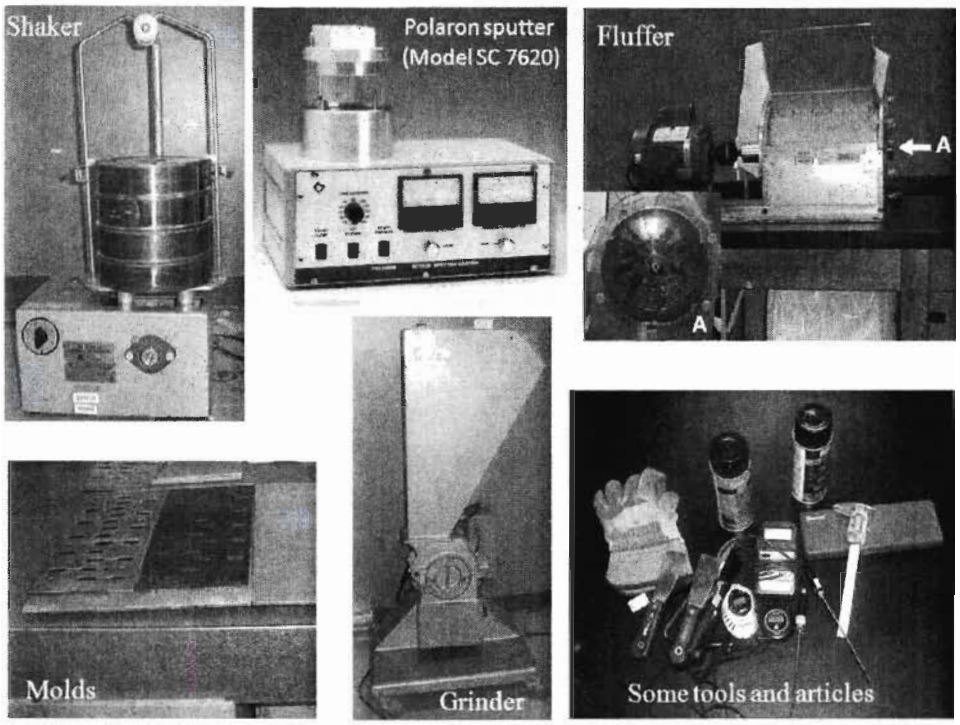

Additional equiments

Bibliography

1 E.T. Thostenson, C. Li and T-W. Chou. Nanocomposites in context. Composites Science and Technology. 2005, 65(3-4): 491-516.

2 Y. Zhou, V. Rangari, H. Mahfuz, S. Jeelani and P.K. Mallick. Experimental study on thermal and mechanical behavior of polypropylene, talc/polypropylene and polypropylene/clay nanocomposites. Materials Science and Engineering: A. 2005, 402(1-2): 109-117.

3 L-P. Cheng, D-J. Lin and K-C. Yang. Formation of mica-intercalated-Nylon 6 nanocomposite membranes by phase inversion method. Journal of Membrane Science. 2000, 172(1-2): 157-166.

4 J-H. Chang, Y.U. An, D. Cho and E.P. Giannelis. Poly(lactic acid) nanocomposites: comparison of their properties with montmorillonite and synthetic mica (II). Polymer. 2003, 44(13):3715-3720.

5 L. Böger, M.H.G. Wichmann, L.O. Meyer and K. Schulte. Load and health monitoring in glass fibre reinforced composites with an electrically conductive nanocomposite epoxy matrix. Composites Science and Technology. 2008, 68(7-8): 1886-1894.

6 E. Bozkurt, E. Kaya and M. Tanoğlu. Mechanical and thermal behavior of non-crimp glass fiber reinforced layered clay/epoxy nanocomposites. Composites Science and Technology. 2007, 67(15-16): 3394-3403.

7 J. Chandradass, M.R. Kumar and R. Velmurugan. Effect of nanoclay addition on vibration properties of glass fibre reinforced vinyl ester composites. Materials Letters. 2007, 61(22):4385-4388.

8 X. Kornmann, M. Rees, Y. Thomann, A. Necola, M. Barbezat and R. Thomann. Epoxy-layered silicate nanocomposites as matrix in glass fibre-reinforced composites. Composites Science and Technology. 2005, 65(14):2259-2268.

9 D.P.N. Vlasveld, P.P. Parlevliet, H.E.N. Bersee and S.J. Picken. Fibre–matrix adhesion in glass-fibre reinforced polyamide-6 silicate nanocomposites. Composites Part A: Applied Science and Manufacturing. 2005, 36(1):1-11.

10 S.M. Zebarjad and S.A. Sajjadi. On the strain rate sensitivity of HDPE/CaCO3 nanocomposites. Materials Science and Engineering: A. 2008, 475(1-2):365-367.

11 L. Jiang, J. Zhang and M.P. Wolcott. Comparison of polylactide/nano-sized calcium carbonate and polylactide/montmorillonite composites: Reinforcing effects and toughening mechanisms. Polymer. 2007, 48(26):7632-7644.

12 C. Deshmane, Q. Yuan and R.D.K. Misra. On the fracture characteristics of impact tested high density polyethylene–calcium carbonate nanocomposites. Materials Science and Engineering: A. 2007, 452-453:592-601.

13 K. Yang, Q. Yang, G. Li, Y. Sun and D. Feng. Morphology and mechanical properties of polypropylene/calcium carbonate nanocomposites. Materials Letters. 2006, 60(6): 805-809.

14 V.P. Cyras, L.B. Manfredi, M-T. Ton-That and A. Vázquez. Physical and mechanical properties of thermoplastic starch/montmorillonite nanocomposite films. Carbohydrate Polymers. 2008, 73(1):55-63.

15 A. Ammala, C. Bell and K. Dean. Poly(ethylene terephthalate) clay nanocomposites: Improved dispersion based on an aqueous ionomer. Composites Science and Technology. 2008, 68(6):1328-1337.

16 M.N. Muralidharan, S.A. Kumar and S. Thomas. Morphology and transport characteristics of poly(ethylene-co-vinyl acetate)/clay nanocomposites. Journal of Membrane Science. 2008, 315(1-2):147-154.

17 K. Saminathan, P. Selvakumar and N. Bhatnagar. Fracture studies of polypropylene/nanoclay composite. Part I: Effect of loading rates on essential work of fracture. Polymer Testing. 2008, 27(3):296-307.

18 E. Picard, J.-F. Gérard and E. Espuche. Water transport properties of polyamide 6 based nanocomposites prepared by melt blending: On the importance of the clay dispersion state on the water transport properties at high water activity. Journal of Membrane Science. 2008, 313(1-2):284-295.

19 A.D. Drozdov, E.A. Jensen and J. deC. Christiansen. Viscoelasticity of polyethylene/montmorillonite nanocomposite melts. Computational Materials Science. 2008, 43(4): 1027-1035.

20 G. Diaconu, M. Paulis and J.R. Leiza. Towards the synthesis of high solids content waterborne poly(methyl methacrylate-co-butyl acrylate)/montmorillonite nanocomposites. Polymer. 2008, 49(10):2444-2454.

21 Q-X. Jia, Y-P. Wu, Y-Q. Wang, M. Lu and L-Q. Zhang. Enhanced interfacial interaction of rubber/clay nanocomposites by a novel two-step method. Composites Science and Technology. 2008, 68(3-4):1050-1056.

22 M.I.B. Tavares, R.F. Nogueira, R.A. da Silva San Gil, M. Preto, E.O. da Silva, M.B.R. Silva and E. Miguez. Polypropylene–clay nanocomposite structure probed by H NMR relaxometry. Polymer Testing. 2007, 26(8): 1100-1102.

23 W. Dong, X. Zhang, Y. Liu, H. Gui, Q. Wang, J. Gao, Z. Song, J. Lai, F. Huang and J. Qiao. Effect of rubber on properties of nylon-6/unmodified clay/rubber nanocomposites. European Polymer Journal. 2006, 42(10):2515-2522.

24 S.R. Ha, K.Y. Rhee, H.C. Kim and J.T. Kim. Fracture performance of clay/epoxy nanocomposites with clay surface-modified using 3-aminopropyltriethoxysilane. Colloids and Surfaces A: Physicochemical and Engineering Aspects. 2008, 313-314:112-115.

25 S. Kim, E. Hwang, Y. Jung, M. Han and S. Park. Ionic conductivity of polymeric nanocomposite electrolytes based on poly(ethylene oxide) and organo-clay materials. Colloids and Surfaces A: Physicochemical and Engineering Aspects. 2008, 313-314: 216-219.

26 C.I.W. Calcagno, C.M. Mariani, S.R. Teixeira and R.S. Mauler. The effect of organic modifier of the clay on morphology and crystallization properties of PET nanocomposites. Polymer. 2007, 48(4):966-974.

27 J.K. Mishra, J-H. Ryou, G-H. Kim, K-J. Hwang, I. Kim and C-S. Ha. Preparation and properties of a new thermoplastic vulcanizate (TPV)/organoclay nanocomposite using maleic anhydride functionalized polypropylene as a compatibilizer. Materials Letters. 2004, 58(27-28):3481-3485.

28 M. Mravčáková, K. Boukerma, M. Omastová and M.M. Chehimi. Montmorillonite/polypyrrole nanocomposites. The effect of organic modification of clay on the chemical and electrical properties. Materials Science and Engineering: C. 2006, 26(2-3):306-313.

29 K.S. Katti, D. Sikdar, D.R. Katti, P. Ghosh and D. Verma. Molecular interactions in intercalated organically modified clay and clay–polycaprolactam nanocomposites: Experiments and modeling. Polymer. 2006, 47(1):403-414.

30 A. Dasari, Z-Z. Yu, Y-W. Mai, G-H. Hu and J. Varlet. Clay exfoliation and organic modification on wear of nylon 6 nanocomposites processed by different routes. Composites Science and Technology. 2005, 65(15-16): 2314-2328.

31 S. Peeterbroeck, M. Alexandre, R. Jérôme and P. Dubois. Poly(ethylene-co-vinyl acetate)/clay nanocomposites: Effect of clay nature and organic modifiers on morphology, mechanical and thermal properties. Polymer Degradation and Stability. 2005, 90(2):288-294.

32 B. Minisini and F. Tsobnang. Molecular mechanics studies of specific interactions in organomodified clay nanocomposite. Composites Part A: Applied Science and Manufacturing. 2005, 36(4):531-537.

33 B. Minisini and F. Tsobnang. Molecular dynamics study of specific interactions in grafted polypropylene organomodified clay nanocomposite. Composites Part A: Applied Science and Manufacturing. 2005, 36(4):539-544.

34 W. Loyens, P. Jannasch and F.H.J. Maurer. Effect of clay modifier and matrix molar mass on the structure and properties of poly(ethylene oxide)/Cloisite nanocomposites via melt-compounding. Polymer. 2005, 46(3):903-914.

35 Y. Kojima, A. Usuki, M. Kawasumi, A. Okada, T. Kurauchi and O. Kamigaito. Synthesis of nylon 6-clay hybrid by montmorillonite intercalated with ε-caprolactam. Journal of Polymer Science Part A: Polymer Chemistry. 1993, 31(4): 983-986.

36 J.W. Gilman. Flammability and thermal stability studies of polymer layered-silicate (clay) nancomposites. Applied Clay Science. 1999, 15(1-2): 31-49.

37 J. Zhu, F.M Uhl, A.B. Morgan and C.A. Wilkie. Studies on the Mechanism by which the formation of Nanocomposites Enhances Thermal Stabiliry. Chemistry of Materials. 2001, 13(12): 4649-4654

38 S. Bourbigot, J.W. Gilman and C.A. Wilkie. Kinetic analysis of the thermal degradation of polystyrene–montmorillonite nanocomposite. Polymer Degradation and Stability. 2004, 84(3):483-492.

39 K. Yano, A. Usuki, A. Okada, T. Kurauchi and O. Kamigaito. Synthesis and properties of polyimide-clay hybrid. Journal Polymer Science Part A: Polymer Chemistry. 1993, 31(10): 2493-2498.

40 S.D. Burnside and E.P. Giannelis. Synthesis and properties of new poly(dimethylsiloxane) nanocomposites. Chemistry of Materials. 1995, 7(9): 1597-1600.

41 D. Porter, E. Metcalfe and M.J.K. Thomas. Nanocomposite Fire Retardants-A Review. Fire and Materials. 2000, 24(1):45-52.

42 R.A. Vaia, S. Vasudevan, W. Krawiec, L.G. Scanlon and E.P.Giannelis. New polymer electrolyte nanocomposites: Melt intercalation of poly(ethylene oxide) in mica-type silicates. Advance Materials. 1995, 7(2): 154-156.

43 E. Ruiz-Hitzky. Conducting Polymers Intercalated in Layered Solids. Advance Materials. 1993, 5(5): 334-340.

44 S.S. Ray, K. Yamada, M. Okamoto and K. Ueda. Control of Biodegradability of Polylactide via Nanocomposite Technology. Macromolecular Materials and Engineering. 2003, 288(3): 203-208.

45 G. Pritchard. Plants move up the reinforcement agenda. Plastics, Additives and Compounding. 2007, 9(4): 40-43.

46 R.M. Rowell. Agro-fiber based composites: Exploring the limits. In: S.I. Andersen, P.Brøndsted, H.Liholt, Aa. Lystrup, J.T. Rheinländer, B.F. Sørensen and H.Toftegaard. Proceedings of the 18th Risø International Symposium on Materials Science: Polymeric Composites-Expanding the limits, Roskilde, Denmark, 1997: 127-133.

47 A.K. Pramanick and M. Sain. Nonlinear Viscoelastic Creep Prediction of HDPE-Agro-fiber Composites. Journal of Composite Materials. 2006, 40(5): 417-431.

48 R.M. Rowell, D.F. Caulfield, G. Chen, W.D. Ellis, R.E. Jacobson, S.E. Lange and R. Schumann. Recent advances in agro-fiber/thermoplastic composites. In: LHC Mattoso, E. Frollini, A. Leao, editors. Proceedings of the second international symposium on natural polymers and composites, Atibaia, Brazil, May 1998: 11–20.

49 Y. Habibi, W.K. El-Zawawy, M.M. Ibrahim and A. Dufresne. Processing and characterization of reinforced polyethylene composites made with lignocellulosic fibers from Egyptian agro-industrial residues. Composites Science and Technology. 2008, 68(7-8): 1877-1885.

50 H.P.S.A. Khalil, A.M. Issam, M.T.A. Shakri, R. Suriani and A.Y. Awang. Conventional agro-composites from chemically modified fibres. Industrial Crops and Products. 2007, 26(3): 315-323.

51 Suhara Panthapulakkal and Mohini Sain. Agro-residue reinforced high-density polyethylene composites: Fiber characterization and analysis of composite properties. Composites Part A: Applied Science and Manufacturing. 2007, 38(6): 1445-1454.

52 N. Reddy and Y. Yang Biofibers from agricultural byproducts for industrial applications. Trends in Biotechnology. 2005, 23(1): 22-27.

53 K.K. Asthana, R. Lakhani and L.K. Aggarwal. Expanded polystyrene composite door shutters —an alternative to wooden door shutters. Construction and Building Materials. 1996, 10(6): 475-480.

54 P. Zou, H. Xiong and S. Tang. Natural weathering of rape straw flour (RSF)/HDPE and nano-SiO2/RSF/HDPE composites. Carbohydrate Polymers. 2008, 73(3): 378-383.

55 H-S. Yang, D-J. Kim and H-J. Kim. Rice straw–wood particle composite for sound absorbing wooden construction materials. Bioresource Technology. 2003, 86(2): 117-121.

56 A.K. Bledzki and J. Gassan. Composites reinforced with cellulose based fibres. Progress in Polymer Science. 1999, 24(2): 221-274.

57 M. Morreale, R. Scaffaro, A. Maio and F.P. La Mantia. Effect of adding wood flour to the physical properties of a biodegradable polymer. Composites Part A: Applied Science and Manufacturing. 2008, 39(3):503-513.

58 A.K. Mishra and A.S. Luyt. Effect of sol–gel derived nano-silica and organic peroxide on the thermal and mechanical properties of low-density polyethylene/wood flour composites. Polymer Degradation and Stability. 2008, 93(1): 1-8.

59 K.B. Adhikary, S. Pang and M.P. Staiger. Dimensional stability and mechanical behaviour of wood-plastic composites based on recycled and virgin high-density polyethylene (HDPE). Composites Part B: Engineering. 2008, 39(5): 807-815.

60 L. Dányádi, T. Janecska, Z. Szabó, G. Nagy, J. Móczó and B. Pukánszky. Wood flour filled PP composites: Compatibilization and adhesion. Composites Science and Technology. 2007, 67(13): 2838-2846.

61 Z. Dominkovics, L. Dányádi and B. Pukánszky. Surface modification of wood flour and its effect on the properties of PP/wood composites. Composites Part A: Applied Science and Manufacturing. 2007, 38(8): 1893-1901.

62 S.M.B. Nachtigall, G.S. Cerveira and S.M.L. Rosa. New polymeric-coupling agent for polypropylene/wood-flour composites. Polymer Testing. 2007, 26(5): 619-628.

63 T. Li and N. Yan. Mechanical properties of wood flour/HDPE/ionomer composites. Composites Part A: Applied Science and Manufacturing. 2007, 38(1): 1-12.

64 Y. Zhao, K. Wang, F. Zhu, P. Xue and M. Jia. Properties of poly(vinyl chloride)/wood flour/montmorillonite composites: Effects of coupling agents and layered silicate. Polymer Degradation and Stability: 2006, 91(12): 2874-2883.

65 N.M. Stark and L.M. Matuana. Influence of photostabilizers on wood flour–HDPE composites exposed to xenon-arc radiation with and without water spray. Polymer Degradation and Stability. 2006, 91(12): 3048-3056.

66 C-F. Kuan, H-C. Kuan, C-C.M. Ma and C-M. Huang. Mechanical, thermal and morphological properties of water-crosslinked wood flour reinforced linear low-density polyethylene composites. Composites Part A: Applied Science and Manufacturing. 2006, 37(10): 1696-1707.

67 M. Bengtsson and K. Oksman. The use of silane technology in crosslinking polyethylene/wood flour composites. Composites Part A: Applied Science and Manufacturing. 2006, 37(5): 752-765.

68 M. Bengtsson, P. Gatenholm and K. Oksman. The effect of crosslinking on the properties of polyethylene/wood flour composites. Composites Science and Technology. 2005, 65(10): 1468-1479.

69 S-Y. Lee, H-S. Yang, H-J. Kim, C-S. Jeong, B-S. Lim and J-N. Lee. Creep behavior and manufacturing parameters of wood flour filled polypropylene composites. Composite Structures. 2004, 65(3-4): 459-469.

70 D.P. Kamdem, H. Jiang, W. Cui, J. Freed and L.M. Matuana. Properties of wood plastic composites made of recycled HDPE and wood flour from CCA-

treated wood removed from service. Composites Part A: Applied Science and Manufacturing. 2004, 35(3): 347-355.

71 M.N. Ichazo, C. Albano, J. González, R. Perera and M.V. Candal. Polypropylene/wood flour composites: treatments and properties. Composite Structures. 2001, 54(2-3): 207-214.

72 H. Ismail and R.M. Jaffri. Physico-mechanical properties of oil palm wood flour filled natural rubber composites. Polymer Testing. 1999, 18(5): 381-388.

73 R. Umer, S. Bickerton and A. Fernyhough. Modelling the application of wood fibre reinforcements within liquid composite moulding processes. Composites Part A: Applied Science and Manufacturing. 2008, 39(4): 624-639.

74 X. Xu, K. Jayaraman, C. Morin and N. Pecqueux. Life cycle assessment of wood-fibre-reinforced polypropylene composites. Journal of Materials Processing Technology. 2008, 198(1-3): 168-177.

75 R.K. Johnson, A. Zink-Sharp, S.H. Renneckar and W.G. Glasser. Mechanical properties of wetlaid lyocell and hybrid fiber-reinforced composites with polypropylene. Composites Part A: Applied Science and Manufacturing. 2008, 39(3): 470-477.

76 J. Aurrekoetxea, M. Sarrionandia and X. Gómez. Effects of microstructure on wear behaviour of wood reinforced polypropylene composite. Wear. 2008, 265(5-6): 606-611.

77 D. Pasquini, E. de Morais Teixeira, A.A. da Silva Curvelo, M.N. Belgacem and A. Dufresne. Surface esterification of cellulose fibres: Processing and characterisation of low-density polyethylene/cellulose fibres composites. Composites Science and Technology. 2008, 68(1): 193-201.

78 M. Bengtsson, M.L. Baillif and K. Oksman. Extrusion and mechanical properties of highly filled cellulose fibre–polypropylene composites. Composites Part A: Applied Science and Manufacturing. 2007, 38(8): 1922-1931.

79 B.S. Gupta, I. Reiniati and M-P.G. Laborie. Surface properties and adhesion of wood fiber reinforced thermoplastic composites. Colloids and Surfaces A: Physicochemical and Engineering Aspects. 2007, 302(1-3): 388-395.

80 A. Wechsler and S. Hiziroglu. Some of the properties of wood–plastic composites. Building and Environment. 2007, 42(7): 2637-2644.

81 Y. Lei, Q. Wu, F. Yao and Y. Xu. Preparation and properties of recycled HDPE/natural fiber composites. Composites Part A: Applied Science and Manufacturing. 2007, 38(7): 1664-1674.

82 S. Singh and A.K. Mohanty. Wood fiber reinforced bacterial bioplastic composites: Fabrication and performance evaluation. Composites Science and Technology. 2007, 67(9): 1753-1763.

83 L. Augier, G. Sperone, C. Vaca-Garcia and M-E. Borredon. Influence of the wood fibre filler on the internal recycling of poly(vinyl chloride)-based composites. Polymer Degradation and Stability. 2007, 92(7): 1169-1176.

84 A. Karmarkar, S.S. Chauhan, J.M. Modak and M. Chanda. Mechanical properties of wood-fiber reinforced polypropylene composites: Effect of a novel compatibilizer with isocyanate functional group. Composites Part A: Applied Science and Manufacturing. 2007, 38(2): 227-233.

85 S.Q. Shi and D.J. Gardner. Hygroscopic thickness swelling rate of compression molded wood fiberboard and wood fiber/polymer composites. Composites Part A: Applied Science and Manufacturing. 2006, 37(9): 1276-1285.

86 A.K. Bledzki and O. Faruk. Injection moulded microcellular wood fibre–polypropylene composites. Composites Part A: Applied Science and Manufacturing. 2006, 37(9): 1358-1367.

87 A. Sretenovic, U. Müller and W. Gindl. Mechanism of stress transfer in a single wood fibre-LDPE composite by means of electronic laser speckle interferometry. Composites Part A: Applied Science and Manufacturing. 2006, 37(9): 1406-1412.

88 B.P. Smith. Maguire develops auxiliaries with special advantages for wood-fibre composites. Plastics, Additives and Compounding. 2005, 7(5): 18-19.

89 A.K. Bledzki, M. Letman, A. Viksne and L. Rence. A comparison of compounding processes and wood type for wood fibre-PP composites. Composites Part A: Applied Science and Manufacturing. 2005, 36(6): 789-797.

90 V.N. Hristov, R. Lach and W. Grellmann. Impact fracture behavior of modified polypropylene/wood fiber composites. Polymer Testing. 2004, 23(5): 581-589.

91 S.E. Selke and I. Wichman. Wood fiber/polyolefin composites. Composites Part A: Applied Science and Manufacturing. 2004, 35(3): 321-326.

92 T.J. Keener, R.K. Stuart and T.K. Brown. Maleated coupling agents for natural fibre composites. Composites Part A: Applied Science and Manufacturing. 2004, 35(3): 357-362.

93 D. Bhattacharyya, M. Bowis and K. Jayaraman. Thermoforming woodfibre–polypropylene composite sheets. Composites Science and Technology. 2003, 63(3-4): 353-365.

94 L. Lundquist, B. Marque, P-O. Hagstrand, Y. Leterrier and J-A.E. Månson. Novel pulp fibre reinforced thermoplastic composites. Composites Science and Technology. 2003, 63(1): 137-152.

95 V.K. Mathur. Composite materials from local resources. Construction and Building Materials. 2006, 20 (7): 470-477.

96 G. Pritchard. Plants move up the reinforcement agenda. Plastics, Additives and Compounding. 2007, 9(4): 40-43.

97 A. Jacob. WPC industry focuses on performance and cost. Reinforced Plastics. 2006, 50(5): 32-33.

98 I.-W. Chen, E.J. Winn and M. Menon. Application of deformation instability to microstructural control in multilayer ceramic composites. Materials Science and Engineering A. 2001, 317(1-2): 226-235.

99 A. Ashori. Wood–plastic composites as promising green-composites for automotive industries!. Bioresource Technology. 2008, 99(11): 4661-4667.

100 E. Badel, C. Delisee and J. Lux. 3D structural characterisation, deformation measurements and assessment of low-density wood fibreboard under compression: The use of X-ray microtomography. Composites Science and Technology. 2008, 68(7-8): 1654-1663.

101 F. Yao, Q. Wu, Y. Lei, W. Guo and Y. Xu. Thermal decomposition kinetics of natural fibers: Activation energy with dynamic thermogravimetric analysis. Polymer Degradation and Stability. 2008, 93(1): 90-98.

102 R.R.N. Sailaja. Mechanical and thermal properties of bleached kraft pulp–LDPE composites: Effect of epoxy functionalized compatibilizer. Composites Science and Technology. 2006, 66(13): 2039-2048.

103 M.Q. Zhang, M.Z. Rong and X. Lu. Fully biodegradable natural fiber composites from renewable resources: All-plant fiber composites. Composites Science and Technology. 2005, 65(15-16): 2514-2525.

104 U. Råberg and J. Hafrén. Biodegradation and appearance of plastic treated solid wood. International Biodeterioration & Biodegradation. 2008, 62(2): 210-213.

105 M.D.H. Beg, K.L. Pickering and S.J. Weal. Corn gluten meal as a biodegradable matrix material in wood fibre reinforced composites. Materials Science and Engineering: A. 2005, 412(1-2): 7-11.

106 P. Fratzl and R. Weinkamer. Nature's hierarchical materials. Progress in Materials Science. 2007, 52(8): 1263-1334.

107 A. G. Facca, M.T. Kortschot and N. Yan. Predicting the tensile strength of natural fibre reinforced thermoplastics. Composites Science and Technology. 2007, 67(11-12): 2454-2466.

108 F.M. B. Coutinho and T.H.S. Costa. Performance of polypropylene–wood fiber composites. Polymer Testing. 1999, 18(8): 581-587.

109 Principia Partners September 2005. Natural & Wood Fiber Composites Newsletter. 2005, 4 (9): 1.

110 Optimat Ltd and MERL Ltd. Wood plastic composite study-Technologies and UK market Opportunities. Published by The Waste and Resources Action Programme, August 2003.

111 Anon. While strong WPC growth continues in the USA. Additives for Polymers. 2006, 5:10-11

112 Chelsea Center for Recycling and Economic Development, University of Massachusetts. Technical report #19: An investigation of the potential to expand the manufacture of recycled wood-plastic composite products in Massachusetts, April 2000.

113 B.Z. Jang. Advanced Polymer Composites: Principles and Applications. ASM international, USA, 1994: 1-20.

114 K. Almgren. Licentiate thesis: Stress-transfer mechanisms in wood-fibre composites. Stockholm, KTH Solid Mechanics, Royal Institute of Technology, 2007, Sweden.

115 A. Sretenovica, U. Müllera and W. Gindl. Mechanism of stress transfer in a single wood fibre-LDPE composite by means of electronic laser speckle interferometry. Composites Part A: Applied Science and Manufacturing. 2006, 37(9): 1406-1412.

116 C-H. Hsueh. Analytical analyses of stress transfer in fibre-reinforced composites with bonded and debonded fibre ends. Journal of Materials Science, 1989, 24: 4475-4482.

117 S. Mazumdar. Composites Growth Realizing Its Global Potential. In: Global Composite Market Report: Opportunities, Market and Technologies. E-Composites Inc. 2005: 459 pages.

118 Anon. While strong WPC growth continues in the USA. Additives for Polymers, Volume 2006, Issue 5, May 2006, Pages 10-11.

119 M.J. Smith, H. Dai and K. Ramani. Wood–thermoplastic adhesive interface—method of characterization and results. International Journal of Adhesion and Adhesives. 2002, 22(3): 197-204.

120 E.R. Coats, F.J. Loge, M.P. Wolcott, K. Englund and A.G. McDonald. Production of naural fiber reinforced thermoplastic composites through the use of polyhydroxybutyrate-rich biomass. Bioresource Technology. 2008, 99(7): 2680-2686.

121 Y. Cui, S. Lee, B. Noruziaan, M. Cheung and J. Tao. Fabrication and interfacial modification of wood/recycled plastic composite materials. Composites Part A: Applied Science and Manufacturing. 2008, 39(4): 655-661.

122 O. Faruk and L.M. Matuana. Nanoclay reinforced HDPE as a matrix for wood-plastic composites. Composites Science and Technology. 2008, 68(9): 2073-2077.

123 O. Rothlin. Processing wood-plastic composites places new demands on feeders. Plastics, Additives and Compounding. 2007, 9(4): 36-39.

124 M. Bengtsson and K. Oksman. Silane crosslinked wood plastic composites: Processing and properties. Composites Science and Technology. 2006, 66(13): 2177-2186.

125 J. Zhao, X. Wang, J. Chang and K. Zheng. Optimization of processing variables in wood–rubber composite panel manufacturing technology. Bioresource Technology. 2008, 99(7): 2384-2391.

126 M. Abdelmouleh, S. Boufi, M.N. Belgacem and A. Dufresne. Short natural-fibre reinforced polyethylene and natural rubber composites: Effect of silane coupling agents and fibres loading. Composites Science and Technology. 2007, 67(7-8): 1627-1639.

127 V.G. Geethamma, G. Kalaprasad, G. Groeninckx and S. Thomas. Dynamic mechanical behavior of short coir fiber reinforced natural rubber composites. Composites Part A: Applied Science and Manufacturing. 2005, 36(11): 1499-1506.

128 H. Ismail, S. Shuhelmy, M.R. Edyham. The effects of a silane coupling agent on curing characteristics and mechanical properties of bamboo fibre filled natural rubber composites. European Polymer Journal. 2002, 38(1): 39-47.

129 H. Ismail, M.R. Edyham and B. Wirjosentono. Bamboo fibre filled natural rubber composites: the effects of filler loading and bonding agent. Polymer Testing. 2002, 21(2): 139-144.

130 K. Boustany R.L. Arnold. Short Fibers Rubber Composites: the Comparative Properties of Treated and Discontinuous Cellulose Fibers. Journal of Elastomers and Plastics. 1976, 8(2): 160-176.

131 N.E. Marcovich, M.I. Aranguren, M.M. Reboredo. Modified woodflour as thermoset fillersPart I. Effect of the chemical modification and percentage of filler on the mechanical properties. Polymer. 2001, 42(2): 815-825.

132 N.E. Marcovich, M.M. Reboredo and M.I. Aranguren. Modified woodflour as thermoset fillers: II. Thermal degradation of woodflours and composites. Thermochimica Acta. 2001, 372(1-2): 45-57.

133 J. Duanmu, E.K. Gamstedt, A. Rosling. Hygromechanical properties of composites of crosslinked allylglycidyl-ether modified starch reinforced by wood fibres. Composites Science and Technology. 2007, 67(15-16): 3090-3097.

134 R.G. Schmidt and C.E. Frazier. Network characterization of phenol-formaldehyde thermosetting wood adhesive. International Journal of Adhesion and Adhesives. 1998, 18(2): 139-146.

135 A.K. Bledzki, S. Reihmane and J. Gassan. Thermoplastics Reinforced with Wood Fillers: A Literature Review. Polymer-Plastics Technology and Engineering. 1998, 37(4): 451-468.

136 Q. Li and L.M. Matuana. Effectiveness of Maleated and Acrylic Acid-Functionalized Polyolefin Coupling Agents for HDPE-Wood-Flour Composites. Journal of Thermoplastic Composite Materials. 2003, 16(6): 551-564.

137 J.Z. Lu, I.I. Negulescu and Q. Wu. Maleated wood-fiber/high-density-polyethylene composites: Coupling mechanisms and interfacial characterization. Composite Interfaces. 2005, 12(1-2): 125-140.

138 B. Nyström, R. Joffe and R. Långström. Microstructure and Strength of Injection Molded Natural Fiber Composites. Journal of Reinforced Plastics and Composites. 2007, 26(6): 579-599.

139 T-W. Chou. Microstructural Design for Fiber Composites. Cambridge Solid State Science Series, ISBN-13: 9780521354820 | ISBN-10: 052135482X, 1992: 169-230.

140 V.N. Hristov, S.T. Vasileva, M. Krumova, R. Lach and G.H. Michler. Deformation Mechanisms and Mechanical Properties of Modified Polypropylene/Wood Fiber Composites. Polymer Composites. 2004, 25 (5): 521-526.

141 B.J. Lee, A.G. McDonald and B. James. Influence of fiber length on the mechanical properties of wood-fiber/polypropylene prepreg sheets. Materials Research Innovations. 2001, 4(2-3) : 97-103.

142 S.H. Zeronian, H. Kawabata and K.W. Alger. Factors affecting the tensile properties of nonmercerized and mercerized cotton fibers. Textile Research Journal. 1990, 60(3): 179-183.

143 N.M. Stark. Wood fiber derived from scrap pallets used in polypropylene composites. Composites and Manufactured Products. Forest Products Journal. 1999, 49(6):39-46.

144 Level of Toughness. Impact Modifiers center-Functional ethylene copolymers. SpecialChem-Polymer Additices&Colors.

145 C. Klason, J. Kubát; H.-E. Strömvall. The Efficiency of Cellulosic Fillers in Common Thermoplastics. Part 1. Filling without Processing Aids or Coupling Agents. International Journal of Polymeric Materials. 1984, 10(3):159-187.

146 R.T. Woodhams, G. Thomas and D.K. Rodgers. Wood Fibers as Reinforcing Fillers for Polyolefins. Polymer Engineering and Science. 1984, 24(15):1166-1171.

147 S. Andersson, R. Serimaa, T. Paakkari, P. SaranpÄÄ and E. Pesonen. Crystallinity of wood and the size of cellulose crystallites in Norway spruce (*Picea abies*). Journal of Wood Science. 2003, 49(6) :531-537.

148 A.A. Ibrahem, M.A. Yousef and S.A. EL-Meadawy. Effect of Beating on Fibre Crystallinity and Physical Properties of Paper Sheets. Journal of Islamic Academy of Sciences. 1989, 2(4):295-298.

149 M.J. Deaner, S. Godavarti and R.K.Willams. Polyolefin wood fiber composite. US Patent 6680090 Issued on January 20 2004.

150 A. Amash and P. Zugenmaier. Study on cellulose and xylan filled polypropylene composites. Polymer Bulletin. 1998, 40: 251-258.

151 J.Z. Lu, Q. Wu and H.S. McNabb. Chemical Coupling in Wood Fiber and Polymer Composites: A Review of Coupling agents and Treatments. Wood Fiber and Science. 2000, 32(1): 88-104.

152 Dupont Dow introduces impact modifier line. Additives for Polymers. 2002, 5:3-4.

153 M.A. Semsarzadeh. Fiber matrix interactions in jute reinforced polyester resin. Polymer Composites. 1986, 7(1): 23-25.

154 P.K. Ray, A.C. Chakravarty and S.B. Bandyopadhaya. Fine structure and mechanical properties of jute differently dried after retting. Journal of Applied Polymer Science. 1975, 20(7) : 1765-1767.

155 P.J. Herrera-Franco and A. Valadez-González. Mechanical properties of continuous natural fibre-reinforced polymer composites. Composites Part A: Applied Science and Manufacturing. 2004, 35(3): 339-345.

156 S. Abe, M. Tsutsumi, M. Yosshikama and Y. Sakaguchi. Effects of Water-Pretreatment on Tensile Strength of Crosslinked Cottn Fibers. Journal of Textile Engineering. 2001, 47(1): 13-22.

157 V. D. Gupta. An x-ray study of crystallite orientation in jute treated with caustic soda solution. Journal of Polymer Science. 1957, 26(112): 110-112.

158 P.K. Ray. On the crystallite orientation in jute and mesta fibers under different moisture conditions. Journal of Applied Polymer Science. 1967, 11(10):2021-2028.

159 C. Pouteau, B. Cathala, P. Dole, B. Kurek and B. Monties. Structural modification of Kraft lignin after acid treatment: characterisation of the apolar

extracts and influence on the antioxidant properties in polypropylene. Industrial Crops and Products. 2005, 21(1): 101-108.

160 S. Wampole and P. Glenn. Treatment of wood, wood fiber products, and porous surfaces with periodic acid and iodic acid. United States Patent 6537357. Pubilication date: 2003.

161 G. Gardea-Hernández, R. Ibarra-Gómez, S.G. Flores-Gallardo, C.A. Hernández-Escobar, P. Pérez-Romo and E.A. Zaragoza-Contreras. Fast wood fiber esterification. I. Reaction with oxalic acid and cetyl alcohol. Carbohydrate Polymers. 2008, 71(1): 1-8.

162 P.A. Ahlgren, J.R. Wood and D.A.I. Goring. The fiber saturation point of various morphological subdivisions of Douglas-fir and aspen wood. Wood Science and Technology. 1972, 6(2) :81-84.

163 J.R. Speaks, R.O. Campbell, M.A. Veal. Composite wood products from solvent extracted wood raw materials. United States Patent 5665798. Publication date: 1997.

164 B-G. Lee, H-J. Lee and D-Y. Shin. Effect of Solvent Extraction on Removal of Heavy Metal Ions Using Lignocellulosic Fiber. Materials Science Forum. 2005, 486-487: 574-577.

165 A.G. Kravtsov, H. Brünig and S.F. Zhandarov. Analysis of the polarization state of melt-spun polypropylene fibers. Journal of Materials Processing Technology. 2002, 124(1-2): 160-165.

166 A. Akhtarkhavari, M.T. Kortschot and J.K. Spelt. Adhesion and durability of latex paint on wood fiber reinforced polyethylene. Progress in Organic Coatings. 2004, 49(1): 33-41.

167 M.N. Belgacem, P. Bataille and S. Sapieha. Effect of corona modification on the mechanical properties of polypropylene/cellulose composites. Journal of Applied Polymer Science. 1994, 53(4): 379-385.

168 S. Abe, M. Tsutsumi, M. Yoshikawa and Y. Sakaguchi. Effects of Water-Pretreatment on Tensile Strength of Crosslinked Cotton Fibers. Journal of Texitile Engineering. 2001, 47(1): 13-22.

169 I. Sakata, M. Morita, N. Tsuruta and K. Morita. Activation of wood surface by corona treatment to improve adhesive bonding. Journal of Applied Polymer Science. 1992, 49(7): 1251-1258.

170 Q. Wang, S. Kaliaguine and A. Ait-Kadi. Catalytic grafting: A new technique for polymer-fiber composites. III. Polyethylene-plasma-treated KevlarTM fibers composites: Analysis of the fiber surface. Journal of Applied Polymer Science. 1992, 48(1): 121-136.

171 S. Dong, S. Sapieha, H. P. Schreiber. Rheological properties of corona modified cellulose/polyethylene composites. Polymer Engineering and Science. 1992, 32(22):1734-1739.

172 K.L. Mittal. Silanes and other coupling agents-Festschrift in Honor of the 75th Birthday of Dr. Edwin P. Plueddemann, VSP BV, Utrecht, Netherlands. 1992: 1-19.

173 M.D.H. Beg. Doctoral thesis: The improvement of interfacial bonding weathering and recycling of wood fibre reinforced polypropylene composites. The University of Waikato, Hamilton, New Zealand. March 2007.

174 A.K. Bledzki , S. Reihmane and J. Gassan. Properties and modification methods for vegetable fibers for natural fiber composites. Journal of Applied Polymer Science. 1996, 59(8) : 1329-1336.

175 M. Stehr and I. Johansson. Weak boundary layers on wood surfaces. Journal of Adhesion Science and Technology. 2000, 14(10): 1211-1224.

176 S. Shokoohi, A. Arefazar and R. Khosrokhavar. Silane Coupling Agents in Polymer-based Reinforced Composites: A Review. Journal of Reinforced Plastics and Composites. 2008, 27(5): 473-485.

177 A.P. Yakovlev. Experimental investigation of the damping properties of composite coatings. Strength of Materials. 1977, 9(12) : 1504-1509.

178 J.Z. Lu, Q. Wu and I.I. Negulescu. The Influence of Maleation on Polymer Adsorption and Fixation, Wood Surface Wettability, and Interfacial Bonding Strength in Wood-PVC Composites. Wood and Fiber Science. 2002, 34(3): 434-459.

179 P. Ehrburger, J.B. Donnet, A.R. Ubbelohde, J.W. Johnson, M.O. W. Richardson and R.A.M. Scott. Interface in Composite Materials. Philosophical Transactions of the Royal Society of London. Series A, Mathematical and Physical Sciences. 1980, 294(1411): 495-505

180 L.M. Matuana, R.T. Woodhams, J.J. Balatinecz and C.B. Park. Influence of interfacial interactions on the properties of PVC/cellulosic fiber composites. Polymer Composites. 1998, 19(4): 446-455.

181 B.V.Kokta, D. Maldas, C. Daneault and P. Béland. Composites of Polyvinyl chloride-wood fiber. I-Effect of Isocyante as a bonding agent. Polymer-plastics Technology Engineering. 1990, 29(1-2):87-118.

182 R.G. Raj, B.V. Kokta and C. Daneault. Effect of Fiber Treatment on Mechanical Properties of Polypropylene-Wood Fiber Composites. Die Makromolekulare Chemie. Macromolecular Symposia. 1989, 28:187-202.

183 D. Maldas and B.V. Kokta. Effect of fiber treatment on the mechanical properties of hybrid fiber reinforced polystyrene composites. Part II. Use of

glass fiber and wood pulp as hybrid fiber. Journal of Adhesion Science and Technology. 1990, 4(2):89-97.

184 D. Maldas and B.V. Kokta. Effects of coating treatments on the Mechanical Behavior of Wood-fiber-filled Polystyrene Composites. I. Use of Polyethylene and Isocyanate as Coating Components. Journal of Applied Polymer Science. 1990, 40(5-6): 917-928.

185 D. Maldas, B.V. Kokta and C. Daneault. Thermoplastic Composites of Polystyrene: Effect of Different Wood Species on Mechanical Properties. Journal of Applied Polymer Science. 1989, 38:413-439.

186 B.V.Kokta, D. Maldas, C. Daneault and Z. Koran. Effect of Extreme Conditions on the Mechanical Properties of Wood Fiber-Polystyrene Composites. I. Chemithermomechamical Pulp as Reinforcing filler. Drevársky Výskum. 1990, 125: 1-39.

187 D. Maldas, B. V. Kokta and C. Daneault. Influence of coupling agents and treatments on the mechanical properties of cellulose fiber-polystyrene composites. Journal of Applied Polymer Science. 1989, 37(3): 751-775.

188 A. Nourbakhsh, B.V. Kokta, A. Ashori, and A. Jahan-Latibari. Effect of a Novel Coupling Agent, Polybutadiene Isocyanate, on Mechanical Properties of Wood-Fiber Polypropylene Composites. Journal of Reinforced Plastics and Composites. 2008, 27(16-17): 1679-1687.

189 B.V. Kokta, D. Michalkova, I. Fortelny and Z. Krulis. Poly(propylene)/aspen/liquid polybutadiene composites: maximization of impact strength, tensile and modulus by statistical experimental design. Polymers for Advanced Technologies. 2007, 18(2): 106-111.

190 M. Hejda, K. Kong, R.J. Young and S.J. Eichhorn. Deformation micromechanics of model glass fibre composites. Composites Science and Technology. 2008, 68(3-4): 848-853.

191 J-M. Park, P-G. Kim, J-H. Jang, Z. Wang, B-S. Hwang and K.L. DeVries. Interfacial evaluation and durability of modified Jute fibers/polypropylene (PP) composites using micromechanical test and acoustic emission. Composites Part B: Engineering. 2008, 39(6):1042-1061.

192 M. Bengtsson, N.M. Stark and K. Oksman. Durability and mechanical properties of silane cross-linked wood thermoplastic composites. Composites Science and Technology. 2007, 67(13): 2728-2738.

193 PERP Program-Thermoplastic Wood Composites (05/06S2). New Report Alert by Nexant's ChemSystems. June 2007.

194 Y. Lei, Q. Wu, C.M. Clemons, F. Yao and Y. Xu. Influence of Nanoclay on properties of HDPE/Wood Composites. Journal of Applied Polymer Science. 2007, 106(6): 3958-3966.

195 A.K. Bledzki and O. Faruk. Wood Fibre Reinforced Polypropylene Composites: Effect of Fibre Geometry and Coupling Agent on Physico-Mechanical Properties. Applied Composite Materials. 2003, 10(6): 365-379.

196 B.P. Morin, I.P. Breusova and Z.A. Rogovin. Structural and chemical modifications of cellulose by graft copolymerization. Advances in Polymer Science. 1982. 42 : 139-166.

197 J.L. Garnett and L-T. NG. Additive effects common to Radiation grafting and Wood Plastic Composite Formation. Radiation Physics and Chemistry. 1996, 48(1): 217-230.

198 M.L. Leza, I. Casinos and G.M. Guzman. Graft copolymerization of 4-vinylpyridine onto cellulosics: effect of temperature. European Polymer Journal. 1989, 25(12): 1193-1196.

199 M. Román-Aguirre, A. Márquez-Lucero and E.A. Zaragoza-Contreras. Elucidating the graft copolymerization of methyl methacrylate onto wood-fiber. Carbohydrate Polymers. 2004, 55(2): 201-210.

200 L. Chotirat, K. Chaochanchaikul and N. Sombatsompop. On adhesion mechanisms and interfacial strength in acrylonitrile–butadiene–styrene/wood sawdust composites. International Journal of Adhesion and Adhesives. 2007, 27(8): 669-678.

201 D. Maldas, B.V. Kokta, R.G. Raj and C. Daneault. Improvement of the mechanical properties of sawdust wood fibre—polystyrene composites by chemical treatment. Polymer, 1988, 29(7): 1255-1265.

202 Q. Yuan, D. Wu, J. Gotama and S. Bateman. Wood fiber reinforced Polyethylene and Polypropylene Composites with high modulus and impact strength. Journal of Thermoplastic Composites Materials. 2008, 21(3): 195-208.

203 R. Li, L. Ye and Y-W. Mai. Application of plasma technologies in fibre-reinforced polymer composites: a review of recent developments. Composites Part A: Applied Science and Manufacturing. 1997, 28(1): 73-86.

204 N. Olaru, L. Olaru and GH. Cobiliac. Plasma-Modified Wood fiber as Fillers in Polymeric Materials. Romanian Journal of Physics. 2005, 50(9-10):1095-1101.

205 S. Tajima and K. Komvopoulos. Surface of Low-Density Polyethylene by Inductively Coupled Argon Plasma. Journal of Physical Chemistry B. 2005, 109: 17623-17629.

206 R. M. Rowell. A new generation of composite materials from agro-based fiber. In: P.N. Prasa, E. James, Ting Joo Fai eds. Polymers and other advanced materials: emerging technologies and business opportunities. Proceedings of the 3rd international conference on frontiers of polymers and advanced

materials. Kuata Lumpur, Malaysia, New York, NY USA. 1995 January 16-20: 659-665.

207 X. Yuan, K. Jayaraman and D. Bhattacharyya. Effects of plasma treatment in enhancing the performance of woodfibre-polypropylene composites. Composites Part A: Applied Science and Manufacturing. 2004, 35(12): 1363-1374.

208 J.H. Coleman. Method of Grafting Ethylenically Unsaturated Monomer to a Polymeric Substrate. U.S. Patent 3600122, 1971.

209 S. Gaur, G. Vergason and V. Etten. Plasma Polymerization:Theory and Practice. 43rd Annual Technical Conference Proceedings, April 15–20, 2000 ISSN 0737-5921, Denver, CO, USA.

210 F.D. Alsewailem and R.K. Gupta. Effect of Impact modifier types on Mechanical Properties of Rubber-Toughened Glass-Fiber Reinforced Nylon 66. The Canadian Journal of Chemical Engineering. 2006, 84(12): 693-703.

211 Arkema Company http://www.arkema.com

212 Toughening method. Impact Modifiers Center-Acrylic based. SpecialChem-Polymer Additives &Colors

213 Core shell impact modifer. Impact modifier center-Acrylic based. SpecialChem-Polymer Additives &Colors.

214 Toughening mechanism. Impact Modifiers Center-Acrylic based . SpecialChem-Polymer Additives &Colors

215 L.J. Lee, C. Zeng, X. Cao, X. Han, J. Shen and G. Xu. Polymer nanocomposite foams. Composites Science and Technology. 2005, 65(15-16): 2344-2363.

216 Y. Fujimoto, S.S. Ray, M. Okamoto, A. Ogami, K. Yamada and K. Ueda. Well-Controlled Biodegradable Nanocomposite Foams: From Microcellular to Nanocellular. Macromolecular Rapid Communications. 2003, 24(7): 457-461.

217 Q. Zhou and C-B. Cong. Exo-endothermic Blowing Agent and its Foaming Behavior. Journal of Cellular Plastics. 2005, 41 (3): 225-234.

218 J. Markarian. Wood-plastic composites: current trends in materials and processing. Plastics, Additives and Compounding. 2005, 7(5): 20-26.

219 M. Reedy. New chemical foaming agents expand wood/plastic composite market. Plastics, Additives and Compounding. 2002, 4(5): 24-26.

220 O. Faruk, A.K. Bledzki and L.M. Matuana. Microcellular Foamed Wood-Plastic Composites by Different Processes: a Review. Macromolecular Materials and Engineering. 2007, 292(2): 113-127.

221 A.K. Bledzki and O. Faruk. Microcellular Injection Molded Wood Fiber-PP Composites: Part I-Effect of Chemical Foaming Agent Content on Cell Morphology and Physico-mechanical Properties. Journal of Cellular Plastics. 2006, 42(1):63-76.

222 A.K. Bledzki and O. Faruk. Microcellular Injection Molded Wood Fiber-PP Composites: Part II-Effect of Wood Fiber Length and Content on Cell Morphology and Physico-mechanical Properties. Journal of Cellular Plastics. 2006, 42(1):77-88.

223 A.K. Bledzki and O. Faruk. Microcellular Wood Fiber Reinforced PP Composites: Cell Morphology, Surface Roughness, Impact and Odor Properties. Journal of Cellular Plastics. 2005, 41(6): 539-550.

224 R. Gosselin, D. Rodrigue and B. Riedl. Injection Molding of Postconsumer Wood–Plastic Composites II: Mechanical Properties. Journal of Thermoplastic Composite Materials. 2006, 19(6): 659-669.

225 G. Lin, X-J. Zhang, L. Liu, J-C. Zhang, Q-M. Chen and L-Q. Zhang. Study on microstructure and mechanical properties relationship of short fibers/rubber foam composites. European Polymer Journal. 2004, 40(8): 1733-1742.

226 L.M. Matuana, C.B. Park and J.J. Balatinecz. Cell morphology and property relationships of microcellular foamed pvc/wood-fiber composites. Polymer Engineering and Science. 1998, 38(11) : 1862-1872.

227 G.M. Rizvi, R. Pop-Iliev and C.B. Parky. A Novel System Design for Continuous Processing of Plastic/Wood-Fiber Composite Foams with Improved Cell Morphology. Journal of Cellular Plastics. 2002, 38(5) : 367-383.

228 G.M. Rizvi, C.B. Park and G. Guo. Strategies for Processing Wood Plastic Composites with Chemical Blowing Agents. Journal of Cellular Plastics. 2008, 44(2):125-137.

229 S. Zhang, D. Rodrigue and B. Riedl. Preparation and Morphology of Polypropylene/Wood Flour Composite Foams via Extrusion. Polymer Composites. 2005, 26(6): 731-738.

230 H. Zhang, G.M. Rizvi, W.S. Lin, G. Guo and C.B. Park. Development of an Extrusion System for Fine-Celled Foaming of Wood-Fiber Composites Using a Physical Blowing Agent. SPE, ANTEC, Technical Papers. 2001, 47: 1746-1758.

231 G.M. Rizvi, C.B. Park, W.S. Lin, G. Guo and R. Pop-Iliev. Expansion mechanisms of plastic/wood-flour composite foams with moisture, dissolved gaseous volatiles, and undissolved gas bubbles. Polymer Engineering and Science. 2003, 43(7): 1347-13601.

232 G. Rizvi, L.M. Matuana and C.B. Park. Foaming of PS/wood fiber composites using moisture as a blowing agent. Polymer Engineering and Science. 2000, 40(10): 2124-2143.

233 L. Chen, S-C. Wong and S. Pisharath. Fracture Properties of Nanoclay-Filled Polypropylene. Journal of Applied Polymer Science. 2003, 88(14):3298-3305

234 R.C. Neagu, E.K. Gamstedt and F. Berthold. Stiffness Contribution of Various Wood Fibers to Composite Materials. Journal of Composite Materials. 2006, 40(8):663-699

235 S.B. Mishra, A.K. Mishra, N.K. Kaushik and M.A. Khan. Study of performance properties of lignin-based polyblends with polyvinyl chloride. Journal of Materials Processing Technology. 2007, 183(2-3):273-276.

236 A.N. Shebani, A.J. van Reenen and M. Meincken. The effect of wood extractives on the thermal stability of different wood species. Thermochimica Acta. 2008, 471(1-2):43-50.

237 K.L. Pickering, G.W. Beckermann, S.N. Alam and N.J. Foreman. Optimising industrial hemp fibre for composites. Composites Part A: Applied Science and Manufacturing. 2007, 38(2):461-468.

238 A. Gregorová, Z. Cibulková, B. Košíková and P. Šimon. Stabilization effect of lignin in polypropylene and recycled polypropylene. Polymer Degradation and Stability. 2005, 89(3):553-558.

239 J. Yu, G. Wang, J. Chen, X. Zeng and W. Wang. Toughening of polypropylene combined with nanosized CaCO3 and styrene-butadiene-styrene. Polymer Engineering and Science. 2007, 47(3):201-206.

240 Z.A. Kusmono, M. Ishak, W.S. Chow, T. Takeichi and Rochmadi. Influence of SEBS-g-MA on morphology, mechanical, and thermal properties of PA6/PP/organoclay nanocomposites. European Polymer Journal. 2008, 44(4);1023-1039.

241 K. Saminathan, P. Selvakumar and N. Bhatnagar. Fracture studies of polypropylene/nanoclay composite. Part II: Failure mechanism under fracture loads. Polymer Testing. 2008, 27(4):453-458.

242 B-W. Jo, S-K. Park and D-K. Kim. Mechanical properties of nano-MMT reinforced polymer composite and polymer concrete. Construction and Building Materials. 2008, 22(1):14-20.

243 M.S. Lakshmi, B. Narmadha and B.S.R. Reddy. Enhanced thermal stability and structural characteristics of different MMT-Clay/epoxy-nanocomposite materials. Polymer Degradation and Stability. 2008, 93(1):201-213.

244 C. Deshmane, Q. Yuan and R.D.K. Misra. High strength–toughness combination of melt intercalated nanoclay-reinforced thermoplastic olefins. Materials Science and Engineering: A. 2007, 460-461:277-287.

245 C. Deshmane, Q. Yuan, R.S. Perkins and R.D.K. Misra 176. On striking variation in impact toughness of polyethylene–clay and polypropylene–clay nanocomposite systems: The effect of clay–polymer interaction. Materials Science and Engineering: A. 2007, 458(1-2):150-157.

246 E. Ruiz-Hitzky and A. Van Meerbeek. Chapter 10.3 Clay Mineral– and Organoclay–Polymer Nanocomposite. Developments in Clay Science. 2006, 1:683-621.

247 C-S. Chou, E.E. LaFleur, D.P. Lorah, R.V. Slone and K.D. Neglia. Aqueous nanocomposite dispersions: process, composition, and uses. United States Patent 6838507 Issued on January 4 2005.

248 R.O. James, L.A. Rowley, D.F. Hurley and J.N. Border. Method of manufacturing a nanocomposite article. World intellectual property organization, Pubilished No.: WO/2005/019326 on March 3 2005.

249 Natural Resources Canada. http://atlas.nrcan.gc.ca/site/english/maps/environment/forest/forestcanada/forestedecozones

250 Tree book. http://www.for.gov.bc.ca/hfd/library/documents/treebook/treebook.pdf p.126.

251 Steve Nix. http://forestry.about.com/b/2007/08/26/canadas-provincial-and-territorial-trees.htm

252 Global Forest Pure Science. http://www.globalforestscience.org

253 Herbarium, Cofrin Center for Biodiversity, University of Wisconsin-Green Bay. http://www.uwgb.edu/biodiversity/herbarium/trees/betall01.htm

254 R.B. Miller. Wood Handbook-Wood as an engineering material. Chapter 1: Characteristics and Availability of Commercially Important Woods. Forest Products Laboratory. Gen. Tech. Rep.FPL-GTR-113. May 1999, Madison, WI, U.S.

255 Britannica Concise Encyclopedia. Wood technology http://www.britannica.com/ebc/art-66141/Cross-section-of-a-tree-trunk

256 Mechanical pulping process. http://individual.utoronto.ca/abdel_rahman/paper/fpmp.html

257 Chemical pulping process.
http://www.metsopaper.com/paper/MPwHome.nsf/FR?ReadForm&ATL=/paper/MPwGeneral.nsf/WebWID/WTB-061129-2256F-CEECE

258 N. Gierlinger and M. Schwanninger. Chemical Imaging of Poplar Wood Cell Walls by Confocal Raman Microscopy. Plant Physiology. 2006, 140(4):1246–1254.

259 Proceeding: 47th FAO Advisory Committee on Paper and Wood Products. Item 4: The role of emerging countries in the paper and forest products world markets: China, Russia and India. Rome, Italy, 6 June 2006.

260 E. Sjöström. Wood chemistry: fundamentals and applications. Academic Press Inc., 2nd edition, San Diego, CA, USA, 1993: 120.

261 M. Blomstedt. Doctoral thesis: Modification of cellulosic fibers by carboxymethyl cellulose-effects on fiber and sheet properties. Department of Forest Products Technology, Helsinki University of Technology. 2007, Espoo, Finland.

262 H. Goyal. PaperOnWeb-Properties of Wood:
http://www.paperonweb.com/wood.htm

263 D.A. I. Goring and T. E. Timell. Molecular weight of native cellulose. TAPPI. 1962, 45: 454–460.

264 R. Wathén. Doctoral thesis: Studies on fiber strength and its effect on paper properties. Department of Forest Products Technology, Helsinki University of Technology. 2006, Espoo, Finland.

265 Chemical Composition of Wood. Institute of Paper Science and Technology, Georgia Institute of Technology.
http://www.ipst.gatech.edu/faculty_new/faculty_bios/ragauskas/technical_reviews/Chemical%20Overview%20of%20Wood.pdf

266 P. Maijala. Doctoral thesis: Heterobasidion annosum and wood decay: Enzymology of cellulose, hemicellulose, and lignin degradation. Department of Bioscience, University of Helsinki. 2000, Helsinki, Finland

267 R. Gu, Y. Xie, S. Zeng, H. Wu and S. Yasuda. Carbon-13 enrichment of rice stalk lignin traced by solid state ^{13}C NMR spectroscopy, Chemical Journal of Chinese Universities (Natural Science Edition). 2002, 23(6):1073-1076.

268 R. Gu, Y. Xie and H. Wu. Carbon 13-enrichment of dehydrogenation polymers of monolignols traced by solid ^{13}C nuclear magnetic resonance, Chemistry and Industry of Forest Products. 2002, 22(1):1-6.

269 Q. Su, Y. Xie, R. Gu, Z. Hu, H. Wu and H. Yang. Studies on lignin and carbohydrate complex of monolignols (II) —synthesized DHP from

microcrystalline cellulose and coniferins, Paper Science and Technology. 2002, 21(5):9-11.

270 R. Gu and Y. Xie. Studies on lignin and carbohydrate complex of monolignols (I)—synthesized DHP from holocellulose and coniferins, Paper Science and Technology. 2001(5):1-6.

271 H. Wikberg. Doctoral thesis: Advanced solid state NMR spectroscopic techniques in the study of Thermally modified wood. Department of Chemistry, University of Helsinki. 2005, Helsinki Finland.

272 R.C. Pettersen. The Chemical composition of wood-Chapter 2: The Chemistry of Solid Wood (Ed: R.M. Rowell). American Chemical Society, Wsshington DC, USA, 1984: 76-81.

273 A. Gutiérrez, J.C. del Río, M.J. Martínez-Íñigo, M.J. Martínez and Á.T. Martínez. Production of New Unsaturated Lipids during Wood Decay by Ligninolytic Basidiomycetes. Applied and Environmental Microbiology. 2002, 68(3): 1344-1350.

274 A. Gutiérrez, J.C. del Río, M.J. Martínez and A.T. Martínez. Fungal Degradation of Lipophilic Extractives in Eucalyptus globulus Wood. Applied and Environmental Microbiology. 1999, 65(4): 1367-1371.

275 Á.T. Martínez. Wood Extracts in Pulp and Paper Manufacture, Technical and Environmental Implications and Biological Removal. "Wood Extractives Biocontrol" Project (European Project FAIR CT95-560), 1999: http://www.biomatnet.org/secure/Fair/S341.htm

276 R. Peters. Woodworker's Guide to Wood. 2000, Sterling Publishing Co. Inc. ISBN 0-8069-3687-8

277 Value Created Resources http://www.valuecreatedreview.com. Wood Science-Hardwoods and Softwoods.

278 B.H. Bond. Wood Identification for Hardwood and Softwood Species Native to Tennessee (PB1692). The University of Tennessee Institute of Agriculture, US Department of Agriculture.

279 S. Cook. Steve's Place V6.3> Science >Plant Growth http://www.steve.gb.com/science/plant_growth.html

280 Molecular Expressions: Tress Collection-Bitternut hickory. http://micro.magnet.fsu.edu/trees/pages/bitternuthickory.html

281 H. Liholt and M. Lawther. Natural Organic Fibers. Comprehensive Composite Materials. Vol.1: Fiber Reinforcements and General Theory of Composites. Wiley-VCH 2003, Vol.1, Chapter 1.10: 1-23.

282 J. Gassan and A.K. Bledzki. Influence of Adhesion Mediators on Damp Hold Back Natural Fibres. Die Angewandte Makromolekulare Chemie. 1996, 236(1): 129–134.

283 H.P. Fink, J. Ganster and J. Fraatz. Akzo-Nobel viskose Chemistry Seminar Challenges in Cellulosic Man-made Fibres 1994. Stockholm, 30 May–3 June.

284 A.J. Michell. Wood cellulose organic polymer composites. Composite Asia Pacific 1989. Adelaide, Vol. 89, 19–21 June.

285 J. Guillichsen and H. Paulapuro. Papermaking Science and Technology. Book 5: Mechanical pulping. Published y Fapet Oy. 1999.

286 Domtar Company-Pulp products technical data. www.domtar.com

287 R.A. Horn. Morphology of wood pulp fiber from softwoods and influence on paper strength. USDA Forest service research paper, FPL 242. 1974, Forest Products Laboratory, Madison, WI, USA.

288 R.A. Horn. Morphology of pulp fiber from hardwoods and influence on paper strength. 1978, USDA Forest service research paper, FPL 312. Forest Products Laboratory, Madison, WI, USA.

289 R.A. Horn and V.C. Setterholm. Fiber morphology and new crops. In: J. Janick and J.E. Simon (eds.), Advances in new crops. Timber Press, Portland, OR. 1990:270-275.

290 M.D. Canpbell and R.S.P. Coutts. Wood fibre-reinforced cement composites. Journal of Materials Science. 1980, 15(8): 1962-1970.

291 Top Analytic Ltd. Lignin and carbohydrates on pulp fibre surfaces. 1992 file data.

292 Y.W. Mai, M.I. Hakeem and B. Cotterell. Effects of water and bleaching on the mechanical properties of cellulose fibre cements. Journal of Materials Science. 1983, 18(7): 2156–2162.

293 D.G. Briggs. Forest Products Measurements and Conversion Factors: with special emphasis on the U.S. Pacific Northwest. Chapter 8: Pulp and Paper. College of Forest Resources, University of Washington. 1994.

294 D.F. Caulfield, R.E. Jacobson, K.D. Sears and J.H. Underwood. Woodpulp fibres as reinforcements for high-melting engineering thermoplastics for "under-the-hood" automotive applications. In: Proceedings, Polymer Processing Society, 17th annual meeting. 2001 May 21-24. Montreal, Canada. Montreal, Canada.

295 C.N. Zárate, M.I. Aranguren and M.M. Reboredo. Thermal degradation of a phenolic resin, vegetable fibers, and derived composites. Journal of aApplied Polymer Science. 2007, 107(5): 2977-2985.

296 N.M. Stark and L.M. Matuana. Ultraviolet Weathering of Photostabilized Wood-Flour-Filled High-Density Polyethylene Composites. Journal of Applied Polymer Science. 2003, 90(10): 2609-2617.

297 R. Seldén, B. Nyström and R. Langström. UV Aging of Poly(propylene)/Wood-Fiber Composites. Polymer Composite. 2004, 25(5): 543-553.

298 L.M. Matuana and D.P. Kamdem. Accelerated Ultraviolet Weathering of PVC/Wood-Flour Composites. Polymer Engineering and Science. 2002, 42(8): 1657-1666.

299 C. Pouteau, P. Dole, B. Cathala, L. Averous and N. Boquillon. Antioxidant properties of lignin in polypropylene. Polymer Degradation and Stability. 2003, 81(1):9-18.

300 B. Košíková and A. Gregorová. Sulfur-free lignin as reinforcing component of styrene-butadiene rubber. Journal of Applied Polymer Science. 2005, 97(3): 924-929.

301 B. Košíková, A. Gregorová, A. Osvald and J. Krajčovičová. Role of lignin filler in stabilization of natural rubber-based composites. Journal of Applied Polymer Science. 2007, 103(2): 1226-1231.

302 A. Gregorová, Z. Cibulková, B. Košíková and P. Šimon. Stabilization effect of lignin in polypropylene and recycled polypropylene. Polymer Degradation and Stability. 2005, 89(3): 553-558.

303 A. Gregorová, B. Košíková and R. Moravčík. Stabilization effect of lignin in natural rubber. Polymer Degradation and Stability. 2006, 91(2): 229-233.

304 T.A. Lehtinen, T.M. Ruffin, J.P. Walsh and A.R. Hill. Method of making cellulosic composite articles. US patent 6030562. Issued on 29 February 2000.

305 H. Goyal. PaperOnWeb-Grades of Pulp: http://www.paperonweb.com/gradepl.htm

306 D.K. Shen, M.X. Fang, Z.Y. Luo and K.F Cen. Modeling pyrolysis of wet wood under external heat flux. Fire Safety Journal. 2007, 42(3): 210-217.

307 AIKAWA Group. FINEBAR refining technology. Introduction to Stock Prep Refining training manual 2001. Shizuoka, Japan. 2001: 1-63. Page: 10. http://www.aikawagroup.com/Training_Manual.pdf.

308 ThermoWood Handbook. Finnish Thermowood Association c/o Wood Focus Oy. FIN-00171, 8 April 2003, Helsinki, Finland. http://www.thermowood.fi/data.php/200312/795460200312311156_tw_handbook.pdf

309 A. Karnis, D. Atack and M. I. Stationwala. What Happens in Refining. Part II. Pulp & Paper Canada. 1986, 87(11):54-62.

310 R. Franzén. General and selective upgrading of mechanical pulps. Nordic Pulp Paper Research Journal. 1986, 1(3):4-13.

311 The Macrogalleria. Level 2: http://www.pslc.ws/mactest/floor2.htm

312 The Macrogalleria. Level 3: http://www.pslc.ws/mactest/floor4.htm

313 Blueridge films Inc. Plastics for Industry. http://www.blueridgefilms.com/page2.htm

314 J.Z. Lu, Qinglin Wu and H.S. McNabb. Chemical coupling in wood fibre and polymer composites: a review of coupling agents and treatments. Wood and Fiber Science. 2000, 32(1):88-104.

315 F. Zhang, T. Endo, W. Qiu, L. Yang and T. Hirotsu. Preparation and Mechanical Properties of Composite of Fibrous Cellulose and Maleated Polyethylene. Journal of Applied Polymer Science, 2002, 84(11):1971–1980.

316 S. Mohanty, S.K. Verma and S.K. Nayak. Dynamic mechanical and thermal properties of MAPE treate jute/HDPE composites. Composites Science and Technology. 2006, 66(3-4): 538-547

317 A. Arbelaiz, B. Fernández, J.A. Ramos, A. Retegi, R. Llano-Ponte and I. Mondragon. Mechanical properties of short flax fibre bundle/polypropylene composites: Influence of matrix/fibre modification, fibre content, water uptake and recycling. Composites Science and Technology. 2005, 65(10):1582-1592.

318 C. Chuai, K. Almdal, L. Poulsen and D. Plackett. Conifer fibers as reinforcing materials for polypropylene-based composites. Journal of Applied Polymer Science. 2001, 80(14): 2833-2841.

319 K. Oksman and C. Clemons. Mechanical properties and morphology of impact modified polypropylene-wood flour composites. Journal of Applied Polymer Science. 1998, 67(9): 1503-1513.

320 M. Khalid, S. Ali, L.C. Abdullah, C.T. Ratnam and S.Y.T. Choong. Effect of MAPP as coupling agent on the mechanical properties of Palm fiber empty fruit bunch and cellulose Polypropylene Biocomposites. International Journal of Engineering and Technology. 2006, 3(1): 79-84.

321 H.D. Rozman, C.Y. Lai, H. Ismail and Z.A.M. Ishak. The effect of coupling agents on the mechanical and physical properties of oil palm empty fruit bunch-propylene composites. Polymer International. 2000, 49(11): 1273-1278.

322 P. Jandura, B.V. Kokta and B. Riedl. Cellulose Fibers/Polyethylene Hybrid Composites: Effect of Long Chain Organic Acid Cellulose Esters and Organic

Peroxide on Rheology and Tensile Properties. Journal of Reinforced Plastics and Composites. 2001, 20(8): 697-717.

323 D. Jarus, J. DeWerth and J. Qian. Polyolefin Nanocomposite in TPOs. Automotive TPO Conference Detroit, MI, USA October 2005.

324 C. Bélanger and B. Labrecque. 2006 Technology Group on Polymer Nanocomposites – PNC-Tech. Industrial Materials Institute. National Research Council Canada, 75 de Mortagne Blvd. Boucherville, Québec, J4B 6Y4.

325 Nanocomposites-from research to reality. Provided by Omnexus.com, 3 Nov 2004.

326 PolyOne launches nanoclay materials, appoints new distributor. Additives for Polymers. 2003, 9: 10.

327 E. Salernitano and C. Migliaresi. Composite materials for biomedical application: a review. Journal of Applied Biomaterials & Biomechanics. 2003, 1:3-18.

328 H. Dalaväg, C. Klason, and H.E. Strömvall. The Efficiency of Cellulosic Fillers in Common Thermoplastics. Part II. Filling with Processing Aids and Coupling agent. International Journal of Polymeric Materials. 1985, 11(1):9-38.

329 B-D. Park and J.J. Balatinecz. Effects of Impact Modification on the Mechanical Properties of Wood-Fiber Thermoplastic Composites with High Impact Polypropylene (HIPP). Journal of Thermoplastic Composite Material. 1996, 9(4) : 342-364.

330 Z. Nogellova, B.V. Kokta and I. Chodak. A Composite LDPE/WOOD Flour Crosslinked by Peroxide. Journal of Macromolecular Science, Part A. 1998, 35(7):1069-1077.

331 P. Zadorecki and A.J. Michel. Future prospects for wood cellulose as reinforcement in organic polymer composites. Polymer Composites. 1989, 10(2):69-77.

332 P.H. Winfield, A.F. Harris and A.R. Hutchinson. The use of flame ionisation technology to improve the wettability and adhesion properties of wood. International Journal of Adhesion and Adhesives. 2001, 21(2):107-114.

333 W. Qiu, F. Zhang, T. Endo and T. Hirotsu. Preparation and characteristics of composites of high-crystalline cellulose with polypropylene: Effects of maleated polypropylene and cellulose content. Journal of Applied Polymer Science. 2003, 87(2): 337-345.

334 R. Gauthier, C. Joly, A. C. Coupas, H. Gauthier and M. Escoubes. Interfaces in polyolefin/cellulosic fiber composites: Chemical coupling, morphology, correlation with adhesion and aging in moisture. Polymer Composites. 1998, 19(3): 287-300.

335 S-M. Lai, F-C. Yeh, Y. Wang, H-C. Chan and H-F. Shen. Comparative study of maleated polyolefins as compatibilizers for polyethylene/wood flour composites. Journal of Applied Polymer Science. 2003, 87(3):487–496.

336 D. Maldas and B.V. Kokta. Role of coupling agents on the performance of wood flour-filled polypropylene composites, International of Journal Polymer Materials. 1994, 27(1–2):77–88.

337 J.M. Felix and P. Gatenholm. The nature of adhesion in composites of modified cellulose fibers and polypropylene. Journal of Applied Polymer Science.1991 42(3): 609-620.

338 M. Kazayawoko, J.J. Balatinecz and L.M. Matuana. Surface modification and adhesion mechanisms in woodfiber-polypropylene composites. Journal of Materials Science. 1999, 34(24):6189–6199.

339 S. Dez-Gutierrez, M.A. Rodrguez-Perez, J.A. De Saja, and J.I. Velasco. Dynamic mechanical analysis of injection-moulded discs of polypropylene and untreated and silane-treated talc-filled polypropylene composites. Polymer. 1999, 40(19): 5345-5353.

340 Y.X. Pang, D.M. Jia, H.J. Hua, D.J. Hourston and M. Song. Effects of a compatibilizing agent on the morphology, interface and mechanical behaviour of polypropylene/poly(ethylene terephthalate) blends. Polymer. 2000, 41(1):357-365.

341 N.M. Stark and R.E. Rowlands. Effects of wood fiber characteristics on mechanical properties of wood/polypropylene composites, Wood and Fiber Science. 2003, 35(2): 167-174.

342 A.C. Karmaker and J.A. Youngquist. Injection molding of polypropylene reinforced with short jute fibers. Journal of Applied Polymer Science. 1996, 62(8): 1147-1151.

343 B.V. Kokta, R.G. Raj and C. Daneault. Use of wood flour as filler in polypropylene: studies on mechanical properties. Polymer-plastics technology and engineering. 1989, 28(3):247–259.

344 R.G. Raj, B.V. Kokta, D. Maldas and C. Daneault. Use of wood fibers in thermoplastics. VII. The effect of coupling agents in polyethylene-wood fiber composites. Journal of Applied Polymer Science. 1989, 37(4):1089–1103.

345 H-C. Kuan, J-M Huang, C-C.M. Ma and F-Y. Wang. Processability, morphology and mechanical properties of wood flour reinforced high density polyethylene composites. Plastics, Rubber and Composites. 2003, 32(3):122-126.

346 T.L. Smith, D. Masilamani, L.K. Bui, R. Brambilla, Y.P. Khanna and K.A. Garbriel. Acetals as nucleating agents for polypropylene. Journal of Applied Polymer Science. 1994, 52(5):591-596.

347 J.O. Iroh and J. P. Berry. Mechanical properties of nucleated polypropylene and short glass fiber-polypropylene composites. European Polymer Journal. 1996, 32(12):1425-1429.

348 K. Joseph and S. Thomas and C. Pavithran. Effect of chemical treatment on the tensile properties of short sisal fibre-reinforced polyethylene composites. Polymer. 1996, 37(23):5139-5149.

349 J. George, R. Janardhan, J.S. Anand, S.S. Bhagawan and S. Thomas. Melt rheological behaviour of short pineapple fibre reinforced low density polyethylene composites, Polymer. 1996, 37(24):5421-5431.

350 M.M. Sain and B.V. Kokta. Effect of solid-state modified polypropylene on the physical performance of sawdust-filled polypropylene composites. Advances in Polymer Technology. 1993, 12(2):167-183.

351 B.V. Kokta. Mechanical properties of polypropylene composites reinforced with switch-grass. XXII Reinforced Plastic Conference, Karlovy Vary, Czech Republic, on May 20-22 2003: 8.

352 B.V. Kokta. Polypropylene Composites Reinforced with Cellulosic Fibers, ModPol2003, Stara Lesna, Slovakia, on October 5-8 2003: 22.

353 A. Karimi, S. Nazari, I. Ghasemi, M. Tajvidi and G. Ebrahimi. Effect of the delignification of wood fibers on the mechanical properties of wood fiber-polypropylene composites. Journal of Applied Polymer Science. 2006, 102(5):4759-4763.

354 K.L. Fung, R.K.Y. Li and S.C. Tjong. Interface modification on the properties of sisal fiber- reinforced polypropylene composites Interface modification on the properties of sisal fiber- reinforced polypropylene composites. Journal of Applied Polymer Science. 2002, 85(1):169-176.

355 A.O. Ibhadon. Fracture mechanics of polypropylene: Effect of molecular characteristics, crystallization conditions, and annealing on morphology and impact performance. Journal of Applied Polymer Science. 1998, 69(13):2657-2661.

356 H. Huang, H. H. Lu and N. C. Liu. Influence of grafting formulations and extrusion conditions on properties of silane-grafted polypropylenes. Journal of Applied Polymer Science. 2000, 78(6):1233-1238.

357 H. Azizi and I. Ghasemi. Reactive extrusion of polypropylene: production of controlled-rheology polypropylene (CRPP) by peroxide-promoted degradation. Polymer Testing. 2004, 23(2):137-143.

358 A.R. Sanadi, D.F. Caulfield, R.E. Jacobson and R.M. Rowell. Renewable Agricultural Fibers as Reinforcing Fillers in Plastics: Mechanical Properties of Kenaf Fiber–Polypropylene Composites. Industrial and Engineering Chemistry Research. 1995, 34(5):1889-1896.

359 A.K. Rana, A. Mandal, B.C. Mitra, R. Jacobson, R. Rowell and A. N. Banerjee. Short jute fiber-reinforced polypropylene composites: Effect of compatibilizer. Journal of Applied Polymer Science. 1998, 69(2):329-338.

360 R.G. Raj, B.V. Kokta and C. Daneault. Effect of chemical treatment of fibers on the mechanical properties of polyethylene-wood fiber composites. Journal of Adhesion Science and Technology. 1989, 3(1):55-64.

361 X. Yuan, Y. Zhang and X. Zhang. Maleated polypropylene as a coupling agent for polypropylene-waste newspaper flour composites. Journal of Applied Polymer Science. 1999, 71(2): 333-337.

362 J-M. Park, S.T. Quang, B-S. Hwang and K.L. DeVries. Interfacial evaluation of modified Jute and Hemp fibers/polypropylene (PP)-maleic anhydride polypropylene copolymers (PP-MAPP) composites using micromechanical technique and nondestructive acoustic emission. Composites Science and Technology. 2006, 66(15):2686-2699

363 A.R. Sanadi, D. F. Caulfield and R.M. Rowell. Reinforcing polypropylene with natural fibers. Plastics Engineering. 1994, 50(4):27-28.

364 S. Morlat, B. Mailhot, D. Gonzalez and J-L. Gardette. Photo-oxidation of Polypropylene/Montmorillonite Nanocomposites. 1. Influence of Nanoclay and Compatibilizing Agent. Chemistry of Materials. 2004, 16 (3):377–383.

365 A.K. Ghosh and E.M. Woo. Analyses of crystal forms in syndiotactic polystyrene intercalated with layered nano-clays. Polymer. 2004, 45(14):4749-4759.

366 K. Oksman. Improved interaction between wood and synthetic polymers in wood/polymer composites. Wood Science and Technology. 1996, 30(3):197-205.

367 K. Oksman and H. Lindberg. The Influence of a SBS Compatibilizer in Polyethylene-Wood Flour Composites. Holzforschung. 1998, 52(6):661–666.

368 K. Oksman, H. Lindberg and A. Holmgren. The nature and location of SEBS-MA compatibilizer in polyethylene-wood flour composites. Journal of Applied Polymer Science. 1998, 69(1): 201-209.

369 T. Peijs, H.G.H. van Melick, S.K. Garkhail, G.T. Pott and C.A. Baillie. Natural-fibre-mat-reinforced thermoplastics based on upgraded flax fibres for improved moisture resistance. In Crivelli Visconti (Edotor), Processing of the 8th European Conference on Composite Materials: Science, Technologies and Applications, ECCM-8 conference, Naples (Italy), 3-6 June 1998, Vol.2: 119-126. Woodhead Publishing, Cambridge, England.

370 W.D. Brouwer. Natural fibre composites: Where can flax compele with glass? SAMPLE Journal. 2000, 36:18-23.

371 A.K. Mohanty, M. Misra and G. Hinrichsen. Biofibres, biodegradable polymers and biocomposites: An overview. Macromolecular Materials and Engineering. 2000, 276-277(1):1-24.

372 J.C.M. de Bruijn. Natural Fibre Mat Thermoplastic Products from a Processor's Point of View. Applied Composite Materials. 2000. 7(5-6):415-420.

373 T.H.S. Costa, D.L. Carvalho, D.C.S. Souza, F.M.B. Coutinho, J.C. Pinto and B.V. Kokta. Statistical experimental design and modeling of polypropylene-wood fiber composites. Polymer Testing. 2000, 19(4):419-428.

374 M. Sain and B.V. Kokta. Response Surface Methodology-A Useful Tool for the Optimization of Molecular Adhesion and Mechanical Properties of PP Composites. Journal of Reinforced Plastics and Composites. 1994, 13(1):38-53.

375 N. Othman, H. Ismail and M. Mariatti. Effect of compatibilisers on mechanical and thermal properties of bentonite filled polypropylene composites. Polymer Degradation and Stability. 2006, 91(8):1761-1774.

376 S. Yin, T.G. Rials and M.P. Wolcott. Crystallization behavior of polypropylene and its effect on woodfiber composite properties. In 15th international conference on wood fiber-plastic composites. Madison WI, USA. 26-26 May 1999:139-146.

377 A.R. Sanadi, D.F. Caulfield and R.E. Jacobson. Agro-fiber/thermoplastic composites. In: R.M. Rowell, R.A.Yound, J.K. Rowell, editiors. Paper and composites from agro-based resources, Boca Roton: CRC Lewis Publishers, chapter 12: 377-401.

378 R. Gu and B.V. Kokta. Effect of Independent Variables on Mechanical Properties and Maximization of Aspen-Polypropylene Composites, Journal of Thermoplastic Composite Materials. 2008, 21(1): 27-50.

379 D. Maldas, and B.V. Kokta. Role of Coupling Agents and Treatment on the Performance of Wood Fiber-Thermoplastic Composites. In: "*Wood-Fiber/Polymer Composites: Fundamental Concepts, Processes and Material Options*", Editor: M.P. Wolcott, Forest Products Society: Madison, WI, USA. 1994: 112-119.

380 I. Krupa and A. S. Luyt. Mechanical properties of uncrosslinked and crosslinked linear low-density polyethylene/wax blends. Journal of Applied Polymer Science. 2001, 81(4): 973-980.

381 M. Gaboyard, J-J. Robin, Y. Hervaud and B. Boutevin. Free-radical graft copolymerization of phosphonated methacrylates onto low-density polyethylene. Journal of Applied Polymer Science. 2002, 86(8):2011–2020.

382 T.H. Kim, H-K. Kim, D.R. Oh, M.S. Lee, K.H. Chae and S. Kaang. Melt free-radical grafting of hindered phenol antioxidant onto polyethylene. Journal of Applied Polymer Science. 2000, 77(13):2968–2973.

383 S.K. Isac and K.E. George. Reactive processing of polyethylenes on a single screw extruder. Journal of Applied Polymer Science. 2001, 81(10):2545–2549.

384 A.K. Sen, B. Mukherjee, A.S. Bhattacharyya, P. P. De and A.K. Bhowmick. Functionalization of polyethylene and ethylene propylene diene terpolymer in the bulk through dibutyl maleate grafting. Angewandte Makromolekulare Chemie. 1991, 191(1):15-30.

385 S.S. Pesetskii, B. Jurkowski, Y.M. Krivoguz and K. Kelar. Free-radical grafting of itaconic acid onto LDPE by reactive extrusion: I. Effect of initiator solubility. Polymer. 2001, 42(2):469-475.

386 V.M. Zakoshansky. Method for the decomposition of cumene hydroperoxide by acidic catalyst to phenol and acetone. United States Patent 5254751. Published on October 19, 1993.

387 T. Yamazaki and T. Seguchi. ESR study on chemical crosslinking reaction mechanisms of polyethylene using a chemical agent. IV. Effect of sulfur- and phosphorous-type antioxidants. Journal of Polymer Science Par A: Polymer Chemistry. 2000, 38(17):3092-3099.

388 M. Tanniru, Q. Yuan and R.D.K Misra. On significant retention of impact strength in clay-reinforced high-density polyethylene (HDPE) nanocomposites. Polymer. 2006, 47(6): 2133-2146.

389 H. Zhai, W. Xu, H. Guo, Z. Zhou, S. Shen and Q. Song. Preparation and characterization of PE and PE-g-MAH/montmorillonite nanocomposites. European Polymer Journal. 2004, 40(11): 2539-2545.

390 T.G. Gopakumar, J.A. Lee, M. Kontopoulou and J.S. Parent. Influence of clay exfoliation on the physical properties of montmorillonite/polyethylene composites. Polymer. 2002, 43(20):5483-5491.

391 J.K. Sameni, S.H. Ahmad and S. Zakaria. Effect of mape on the mechanical properties of rubber wood fiber/thermoplastic natural rubber composites. Advance in Polymer Technology. 2004, 23(1):18-23.

392 K.S. Anderson, S.H. Lim and M.A. Hillmyer. Toughening of polylactide by melt blending with linear low-density polyethylene. Journal of Applied Polymer Science. 2003, 89(14): 3757-3768.

393 H-S. Yang, M.P. Wolcott, H-S. Kim, S. Kim and H-J. Kim. Effect of different compatibilizing agents on the mechanical properties of lignocellulosic material filled polyethylene bio-composites. Composite Structures. 2003, 79(3): 369-375.

394 F. Mengeloglu and A. Kabakci. Determination of Thermal Properties and Morphology of Eucalyptus Wood Residue Filled High Density Polyethylene Composites. International Journal of Molecular Sciences. 2008, 9(2):107-119.

395 Y. Wang, F-C. Yeh, S-M. Lai, H-C. Chan and H-F. Shen. Effectiveness of functionalized polyolefins as compatibilizers for polyethylene/wood flour composites. Polymer Engineering and Science. 2003, 43(4): 933-945.

396 Southern Clay Products-Nanoclay. Available at: http://www.nanoclay.com/selection_chart.asp, Accessed: 19 November 2007.

397 M. Maiti and A.K. Bhowmick. Structure and properties of some novel fluoroelastomer/clay nanocomposites with special reference to their interaction. Journal of Polymer Science: Part B: Polymer Physics. 2006, 44(1): 162-176.

398 C. Eckert. Opportunities for natural fibers in plastic composites. Proceedings of the 5th Progress in Woodfibre-Plastic Composites Conference, Toronto, Canada. May 25-26 2000.

399 K. Jayaraman and D. Bhattacharyya. Mechanical performance of woodfibre–waste plastic composite materials. Resources, Conservation and Recycling. 2004, 41(4):307-319.

400 K.H. Wang, I.J. Chung, M.C. Jang, J.K. Keum and H.H. Song. Deformation Behavior of Polyethylene/Silicate Nanocomposites As Studied by Real-Time Wide-Angle X-ray Scattering. Macromolecules. 2002, 35(14):5529–5535

401 A. Mudaliar , Q. Yuan and R.D.K. Misra. On surface deformation of melt-intercalated polyethylene-clay nanocomposites during scratching. Polymer Engineering and Science. 2006, 46(11):1625-1634.

402 R. Endo, K. Kamei, I. Iida and Y. Kawahara. Dimensional stability of waterlogged wood treated with hydrolyzed feather keratin. Journal of Archaeological Science. 2008, 35(5): 1240-1246.

403 R. Siddiquea, J. Khatib and I. Kaur. Use of recycled plastic in concrete: A review. Waste Management. 2008, 28(10):1835-1852.

404 J.M. Encinara and J.F. González. Pyrolysis of synthetic polymers and plastic wastes. Kinetic study. . Fuel Processing Technology. 2008, 89(7):678-686.

405 R. Gu, B.V. Kokta and G. Chalupova. Effect of Variables on the Mechanical Properties and Maximization of Polyethylene-Aspen Composites by Statistical Experiment Design. Journal of Thermoplastic Composite Materials. 2009, 22(6): 633-649.

406 H-M. Park, W-K. Lee, C-Y. Park, W-J. Cho and C-S. Ha. Environmentally friendly polymer hybrids Part I Mechanical, thermal, and barrier properties of thermoplastic starch/clay nanocomposites. Journal of Material Science. 2003, 38(5):909-915.

407 M. Pramanik, S.K. Srivastava, B.K. Samantaray and A.K. Bhowmick . Synthesis and characterization of organosoluble, thermoplastic elastomer/clay nanocomposites. Journal of Polymer Science Part B: Polymer Physics. 2002, 40(18):2065-2073.

408 T.J. Pinnavaia and G. W. Beall. Polymer-clay nanocomposites. February 2001. Wiley Publishing Inc., New York.

409 B.M. Novak. Hybrid Nanocomposite Materials - between inorganic glasses and organic polymers. Advanced Materials. 1993, 5(6):422-433.

410 J.A. Méndez, F. Vilaseca, M.A. Pèlach, J.P. López, L. Barberà, X. Turon, J. Gironès, P. Mutjé. Evaluation of the reinforcing effect of ground wood pulp in the preparation of polypropylene-based composites coupled with maleic anhydride grafted polypropylene. Journal of Applied Polymer Science. 2007, 105(6): 3588-3596.

411 P.B. Messersmith and S.I. Stupp. Synthesis of nanocomposites: Organoceramics. Journal of Materials Research. 1992, 7(9):2599-2611.

412 A. Okada and A. Usuki. The chemistry of polymer-clay hybrids. Materials Science and Engineering: C. 1995, 3(2):109-115.

413 J-X. Li, J. Wu, C-M. Chan. Thermoplastic nanocomposites. Polymer. 2000, 41(18):6935-6939.

414 L.M. Sherman. Nanocomposites: A little goes a long way-From auto parts to barrier packaging, the race is on to commercialize nano-clay thermoplastic composites. Plastics Technology. 1999, 45(6):52-59.

415 C. Becker, B. Kutsch, H. Krug and H. Kaddami. SAXS and TEM Investigations on Thermoplastic Nanocomposites Containing Functionalized Silica Nanoparticles. Journal of Sol Gel Science and Technology. 1998, 13 (1):499-503.

416 D.C. Montgomery. Design and Analysis of Experiments, 6th Edition. Published by John Wiley&Sons Inc in December 2004. New York.

417 R.H. Myers and D.C. Montgomery. Response surface methodology: Process and Product Optimization Using Designed Experiments, 2nd Edition. Published by Wiley-Interscience in August 1995. New York.

418 A.I. Khun and J.A. Cornell. Response surface: Designs and Analysis, 2nd Edition. Published by Narcel Dekker Inc. in 1996. New York.

419 B.V. Kokta, K.N. Law, I. Fortelny, F. Lednicky and Z. Krulis. Hybrid composite of PE with Birch fiber and nanoclay. Chemické listy. 2007, 101:S23-S25.

420 Z. Lu. Doctoral dissertation: Chemical Coupling in Wood-Polymer Composites. Louisiana State University, Baton Rouge, LA, USA, December 2003.

421 P.W. Balasuriya, L. Ye, Y.-W. Mai and J. Wu. Mechanical properties of wood flake-polyethylene composites. II. Interface modification. Journal of Applied Polymer Science. 2002, 83(12): 2505-2521.

422 M. Botros. Development of new generation coupling agents for wood-plastic composites. The Global Outlook for Natural and Wood Fiber Composites. New Orleans, LA, USA. December 3-5 2003.

423 H.P. San, L.A. Nee and H.C. Meng. Physical and Bending Properties of Injection Moulded Wood Plastic Composites Boards. ARPN Journal of Engineering and Applied Sciences. 2008, 3(5):13-19.

424 C. Xiong, R. Qi and W. Gong. The preparation and properties of wood flour/high density polyethylene composites by *in-situ* reaction extrusion. Polymers advanced technologies. 2009, 20(3): 273-279.

425 X. Cai, B. Riedl, S.Y. Zhang and H. Wan. The impact of the nature of nanofillers on the performance of wood polymer nanocomposites. Composites Part A: Applied Science and Manufacturing. 2008, 39(5): 727-737.

426 H.C. Kim. Toughening Mechanisms of Long-Fiber-Reinforced Thermoplastics. SAE Special Publications. 1998, 1340: 167-171.

427 J.M. Crosby and T.R. Drye. How Fibers Affect Fracture Behavior of Nylon-66 Composites. Modern Plastics. 1986, 63(11): 74-84.

428 W. Liu, M. Misra, P. Askeland, L.T. Drzal and A.K. Mohanty. 'Green' composites from soy based plastic and pineapple leaf fiber: fabrication and properties evaluation. Polymer. 2005, 46(8): 2710-2721.

429 A.K. Mohanty, P. Tummala, W. Liu, M. Misra, P.V. Mulukutla and L.T. Drzal. Injection Molded Biocomposites from Soy Protein Based Bioplastic and Short Industrial Hemp Fiber. Journal of Polymers and the Environment. 2005, 13(3):279-285.

430 Nexant Inc. New Industry Outlook for Polyethylene and Polypropylene. ChemSystems-News archive, published on 24 May 2008.

431 Q. Yuan and R.D.K. Misra. Impact fracture behavior of clay–reinforced polypropylene nanocomposites. Polymer. 2006, 47(12): 4421-4433.

432 R.R. Thridandapani, A. Mudaliar, Q. Yuan and R.D.K. Misra. Near surface deformation associated with the scratch in polypropylene–clay nanocomposite: A microscopic study. Materials Science and Engineering: A. 2006, 418(1-2): 292-302.

433 Y. Dong and D. Bhattacharyya. Effects of clay type, clay/compatibiliser content and matrix viscosity on the mechanical properties of polypropylene/organoclay nanocomposites. Composites Part A: Applied Science and Manufacturing. 2008, 39(7): 1177-1191.

434 E. Bodrosa, I. Pillin, N. Montrelay and C. Baley. Could biopolymers reinforced by randomly scattered flax fibre be used in structural applications? Composites Science and Technology. 2007, 67(3-4): 462-470.

435 D.J. Gardner, N.C. Generalla, D.W. Gunnells and M.P. Wolcott. Dynamic wettability of wood. Langmuir. 1991, 7(11):2498-2502.

436 R.A. Ryntz. Adhesion to Plastics: Molding and Paintability. Global Press, Minnisota, USA. 1998:255pp.

437 W.D. Ellis, R.M. Rowell and S.L. LeVan. Thermal Degradation Properties of Wood Reacted with Diethylchlorophosphate or Phenylphosphonic dichloride as Potential Flame Retardants. Wood and Fiber Science. 1987, 19(4): 439-445.

438 H.-S. Kim, H.-S. Yang, H.-J. Kim and H.-J. Park. Thermogravimetric analysis of rice husk flour filled thermoplastic polymer composites. Journal of Thermal Analysis and Calorimetry. 2004, 76(2): 395-404.

439 H.-S. Kim, H.-S. Yang, H.-J. Kim, B.-J. Lee and T.-S. Hwang. Thermal properties of agro-flour-filled biodegradable polymer bio-composites. Journal of Thermal Analysis and Calorimetry. 2005, 81(2): 299-306.

440 R. Gu and B.V. Kokta. Effects of Antioxidant and Initiator on the Mechanical Properties of Polypropylene Aspen Composites. Journal of Thermoplastic Composite Materials. 2008, 21(2): 175-189.

441 Y. Kojima, A. Usuki, M. Kawasumi, A. Okada, Y. Fukushima, T. Kurauchi and O. Kamigaito. Mechanical properties of nylon 6-clay hybrid. Journal of Material Research. 1993, **8**(5)**:**1185–1189.

442 T.A. Osswald. Fundamental principles of polymer composites: processing and design. In: Proceedings of the 5th International Conference of Wood fiber–Plastic Composites. Forest Products Society, Madison, WI, May 26–27 1999.

443 D. Roylance. Mechanics of materials (Wiley ISBN 0-471-59399-0). Module in Tensile response of materials: Introduction to composites materials. MIT, MA, USA.2000:1-7.

444 R. Kohler and K. Nebel. Cellulose-Nanocomposites: Towards High Performance Composite Materials. Macromolecular Symposia, 2006, 244(1):97-106.

445 R.H. Gauthier and C. Joly. Compatibilization between lignocellulosic fibers and polyolefin matrix. In: Proceedings of the 5th International Conference on

Wood fiber–Plastic Composites, Forest Products Society, Madison, WI, May 26–27, 1999: 153–164.

446 S. Migneault, A. Koubaa, F. Erchiqui, A. Chaala, K. Englund, C. Krause and M. Wolcott. Effect of fiber length on processing and properties of extruded wood-fiber/HDPE composites. Journal of Applied Polymer Science. 2008, 110(2): 1085-1092.

447 D.H. Mueller and A. Krobjilowski. New Discovery in the Properties of Composites Reinforced with Natural Fibers. Journal of Industrial Textiles. 2003, 33(2): 111-130.

448 P.V. Joseph, Z. Oommen, K. Joseph and S. Thomas. Melt Rheological Behaviour of Short Sisal Fibre Reinforced Polypropylene Composites. Journal of Thermoplastic Composite Materials. 2002, 15(2):89-114.

449 H-S. Yang, H-J. Kim, H-J. Park, B-J. Lee and T-S. Hwang. Effect of compatibilizing agents on rice-husk flour reinforced polypropylene composites. Composite Structure. 2007, 77(1): 45-55.

450 H. Kim, B. Lee, S. Choi, S. Kim and H. Kim. The effect of types of maleic anhydride-grafted polypropylene (MAPP) on the interfacial adhesion properties of bio-flour-filled polypropylene composites. Composites Part A: Applied Science and Manufacturing. 2007, 38(6): 1473-1482.

451 S. Panthapulakkal, M Sain and S Law. Effect of coupling agents on rice-husk-filled HDPE extruded profiles. Polymer International. 2005, 54(1): 137-142.

452 G. Canché-Escamilla, J.I. Cauich-Cupul, E. Mendizábal, J.E. Puig, H. Vázquez-Torres and P.J. Herrera-Franco. Mechanical properties of acrylate-grafted henequen cellulose fibers and their application in composites. Composites Part A: Applied Science and Manufacturing. 1999, 30(3): 349-359.

453 R. Gu, B.V. Kokta and K.N. Law. Optimization of Mechanical Properties of PE Composites using Central Composite Design and Deposition Formation of Nanofiller. 24th Annual Technical Conference on Composites, Newark, DE, USA. 15-17 September 2009: Paper #312.

454 R. Mahlberg, L. Paajanen, A. Nurmi, A. Kivistö, K. Koskela and R.M. Rowell. Effect of chemical modification of wood on the mechanical and adhesion properties of wood fiber/polypropylene fiber and polypropylene/veneer composites. Holz als Roh-und Werkstoff. 2001, 59(5): 319-326.

455 K.V. Pochiraju, G.P. Tandon and N.J. Pagano. Analyses of single fiber pushout considering interfacial friction and adhesion. Journal of the Mechanics and Physics of Solids. 2001, 49(10): 2307-2338.

456 G. Pritchard. Quick reference guide. In: Plastics Additives-An A-Z reference (Polymer Science and Technology Series). Ed. G. Pritchard. Published in July 1998. Publisher: Chapman and Hall: New York. Page 12.

457 C. Hwang, C. Hse and T.F. Shupe. Effects of raw materials on the properties of wood fiber-polyethylene composites--part 3: effect of a compatibilizer and wood adhesive on the interfacial adhesion of wood/plastic composites. Forest Products Journal. 2008, 59(5):66-72.

458 Y.T. Vu, G.S. Rajan, J.E. Mark and C.L. Myers. Reinforcement of elastomeric polypropylene by nanoclay fillers. Polymer International. 2004, 53(8):1071-1077.

459 S. Y. Lee, I.A. Kang, G.H. Doh, W.J. Kim, J.S. Kim, H.G. Yoon and Q. Wu. Thermal, mechanical and morphological properties of polypropylene/clay/ wood flour nanocomposites. eXpress Polymer Letters. 2008, 2(2): 78-87.

460 S-K. Yeh, D. Ortiz, A. Al-Mulla and R.K. Gupta. Mechanical and Thermal Properties of Wood/Layered Silicate/Plastic Composites. 8th International Conference on Woodfiber-Plastic Composites (and other natural fibers). Madison, Wisconsin, USA. 23-25 May 2005.

461 Q. Zhang, Q. Fu, L. Jiang and Y. Lei. Preparation and properties of polypropylene/montmorillonite layered nanocomposites. Polymer International. 2000, 49(12): 1561-1564.

462 B.V. Kokta and G.A. Chalupova. Birch fibre-reinforced hybride nanocomposites of polyethylene. Polymeric Materials P2008. Halle, Germany, September 24-26 2008.

463 K.S. Chan, Y.-D. Lee, D.P. Nicolella, B.R. Furman, S. Wellinghoff and R. Rawls. Improving fracture toughness of dental nanocomposites by interface engineering and micromechanics. Engineering Fracture Mechanics. 2007, 74(12):1857-1871.

464 N. Juan. Review on impact and fracture toughness properties of nanoclay. Research report 2006. Pittsburg State University. **KS66762**. 9 August 2006.

465 S.M.B. Nachtigall, R.B. Neto and R.S. Mauler. A factorial design applied to polypropylene functionalization with maleic anhydride. Polymer Engineering and Science. 1999, 39(4):630-637.

466 M. Canetti, F. Bertini, A.De Chirico and G. Audisio. Thermal degradation behaviour of isotactic polypropylene blended with lignin. Polymer Degradation and Stability. 2006, 91(3): 494-498.

467 R. Chandra and R. Rustgi. Biodegradation of maleated linear low-density polyethylene and starch blends. Polymer Degradation and Stability. 1997, 56(2): 185-202.

468 M. Rusu and N. Tudorachi. Biodegradable Composite Materials Based on Polyethylene and Natural Polymers. I. Mechanical and Thermal Properties. Journal of Polymer Engineering. 1999, 19(5):355-369.

469 M. Alexandre, P. Dubois, T. Sun, J.M. Garces and R. Jérôme. Polyethylene-layered silicate nanocomposites prepared by the polymerization-filling technique: synthesis and mechanical properties. Polymer. 2002, 43(8):2123-2132.

470 G. Liang, J. Xu, S. Bao and W. Xu. Polyethylene/maleic anhydride grafted polyethylene/organic-montmorillonite nanocomposites. I. Preparation, microstructure, and mechanical properties. Journal of Applied Polymer Science. 2004, 91(6):3974-3980.

471 Z. Zhou, H. Zhai, W. Xu, H. Guo, C. Liu and W-P. Pan. Preparation and characterization of polyethylene-g-maleic anhydride-styrene/montmorillonite nanocomposites. Journal of Applied Polymer Science. 2006, 101(2):805-809.

472 F. Bergaya, T. Mandalia and P. Amigouët. A brief survey on CLAYPEN and Nanocomposites based on unmodified PE and organo-pillared clays. Colloid Polymer and Science. 2005, 283(7):773-782.

473 A. Ranade, K. Nayak, D. Fairbrother and N.A. D'Souza. Maleated and non-maleated polyethylene–montmorillonite layered silicate blown films: creep, dispersion and crystallinity. Polymer. 2005, 46(18):7323-7333.

474 P.J. Herrera-Franco and A. Valadez-González. A study of the mechanical properties of short natural-fiber reinforced composites. Composites Part B: Engineering. 2005, 36(8):597-608.

475 J.A. Lee, M. Kontopoulou and J.S. Parent. Time and shear dependent rheology of maleated polyethylene and its nanocomposites. Polymer. 2004, 45(19):6595-6600.

476 B. Li and J. He. Investigation of mechanical property, flame retardancy and thermal degradation of LLDPE–wood-fibre composites. Polymer Degradation and Stability. 2004, 83(2): 241–246.

477 H. Lu, Y. Hu, J. Xiao, Q. Kong, Z. Chen and W. Fan. The influence of irradiation on morphology evolution and flammability properties of maleated polyethylene/clay nanocomposite. Materials Letters. 2005, 59(6): 648-651.

478 Q. Li and L.M. Matuana. Surface of cellulosic materials modified with functionalized polyethylene coupling agents. Journal of Applied Polymer Science. 2003, 88(2):278-286.

479 B.C. Jang, S.Y. Huh, J.G. Jang and Y.C. Bae. Mechanical properties and morphology of the modified HDPE/starch reactive blend. Journal of Applied Polymer Science. 2001, 82(13): 3313–3320.

480 MA.P. Muñoz P., M.D. Vargas, M.M. Werlang, I.V.P. Yoshida and R.S. Mauler. High-density polyethylene modified by polydimethylsiloxane. Journal of Applied Polymer Science. 2001, 82(14): 3460–3467.

481 G. Wang, P. Jiang, Z. Zhu and J. Yin. Structure-property relationships of LLDPE-highly filled with aluminum hydroxide. Journal of Applied Polymer Science. 2002, 85(12): 2485–2490.

482 S. Abe and M. Yamaguchi. Study on the foaming of crosslinked polyethylene. Journal of Applied Polymer Science. 2001, 79(12): 2146–2155.

483 F. Li, Y. Chen, W. Zhu, X. Zhang and M. Xu. Shape memory effect of polyethylene/nylon 6 graft copolymers. Polymer. 1998, 39(26): 6929-6934.

484 N.C. Liu, G.P. Yao and H. Huang. Influences of grafting formulations and processing conditions on properties of silane grafted moisture crosslinked polypropylenes. Polymer. 2000, 41(12): 4537-4542.

485 C-S. Wu. Renewable resource-based composites of recycled natural fibers and maleated polylactide bioplastic: Characterization and biodegradability. Polymer Degradation and Stability. 2009, 94(7): 1076-1084.

486 M.J. John and S. Thomas. Biofibres and biocomposites. Carbohydrate Polymer. 2008, 71(3):343-364.

487 J.K. Pandey, K.R. Reddy, A.P. Kumar and R.P. Singh. An overview on the degradability of polymer nanocomposites. Polymer Degradation and Stability. 2005, 88(2): 234-250.

488 K.G. Satyanarayana, G.G.C. Arizaga and F. Wypych. Biodegradable composites based on lignocellulosic fibers-An overview. Progress in Polymer Science. 2009, 34(9): 982-1021.

489 M. Hetzer and D.De Kee. Wood/polymer/nanoclay composite, environmentally friendlly sustainable technology: A review. Chemical Enginnering and Design. 2008, 86(10): 1083-1093.

490 M. Song, C.W. Wong, J. Jin, A. Ansarifar, Z.Y. Zhang and M. Richardson. Preparation and characterization of poly(styrene-co-butadiene) and polybutadiene rubber/clay nanocomposites. Polymer International. 2005, 54(3):560-568.

491 S. Wu, D. Jiang, X. Ouyang, F. Wu and J. Shen. The structure and properties of PA6/MMT nanocomposites prepared by melt compounding. Polymer Engineering and Science. 2004, 44(11): 2070-2074.

492 M. Pramanik, H. Acharya and S.K. Srivastava. Exertion of Inhibiting Effect by Aluminosilicate Layers on Swelling of Solution Blended EVA/Clay Nanocomposite. Macromolecular Materials and Engineering. 2004, 289(6): 562-567.

493 M.A. Osman, V. Mittal, M. Morbidelli and U.W. Suter. Epoxy-Layered Silicate Nanocomposites and Their Gas Permeation Properties. Macromolecules. 2004, 37(19): 7250-7257

494 D. Majumdar, N. Dontula, T.N. Blanton and G.S. Freedman. Smectite clay intercalated with polyether block polyamide copolymer. European Patent 1312582, published on 21 May 2003.

495 M.D.H. Beg and K.L. Pickering. Mechanical performance of Kraft fibre reinforced polypropylene composites: Influence of fibre length, fibre beating and hygrothermal ageing. Composites Part A: Applied Science and Manufacturing. 2008, 39(11):1748-1755.

496 N.K. Bhardwaj, S. Kumar and P.K. Bajpai. Effects of processing on zeta potential and cationic demand of kraft pulps. Colloids and Surfaces A: Physicochemical and Engineering Aspects. 2004, 246(1-3): 121-125.

497 C. Bellmann, A. Caspari, T.T.L. Doan, E. Mäder, T. Luxbacher and R. Kohl. Electrokinetic Properties of Natural Fibres. International Electrokinetics Conference 2004. Pittsburgh Pennsylvania, USA. 13-17 June 2004. Paper 59.

498 M.T. Goulet. Doctor's Dissertation: The Effect of Pulping, Bleaching, and Refining Operations on the Electrokinetic Properties of Wood Fiber Fines. Lawrence University, Appleton, Wisconsin, USA. June 1989.

499 A. Baltazar-y-Jimenez and A. Bismarck. Wetting behaviour,moisutre p-take and electrokinetic properties of lignocellulosic fibers. Cellulose. 2007, 14(2): 115-127.

500 Y. Zhong, T. Poloso, M. Hetzer and D.De Kee. Enhancement of Wood/Polyethylene Composites via Compatibilization and Incorporation of Organoclay Particle. Polymer Engineering and Science. 2007, 47(6): 797-803.

501 F. Mengeloglu and K. Karakus. Some Properties of Eucalyptus Wood Flour Filled Recycled High Density Polyethylene Polymer-Composites. Turkish Journal of Agriculture and Forestry. 2008, 32(6):537-546.

502 L.M. Matuana and O. Faruk. Hybrid HDPE/Wood-Flour/Montmorillonite Nanocomposites. 9th Wood & Biofiber Plastic Composites, Madison, USA, 21-23 May 2007.

503 C. Zhao, H. Qin, F. Gong, M. Feng, S. Zhang and M. Yang. Mechanical, thermal and flammability properties of polyethylene/clay nanocomposites. Polymer Degradation and Stability. 2005, 87(1): 183-189.

504 J.H. Park and S.C. Jana. The relationship between nano- and micro-structures and mechanical properties in PMMA–epoxy–nanoclay composites. Polymer. 2003, 44(7): 2091-2100.

505 R. Qi, X. Jin and C. Zhou. Preparation and Properties of Polyethylene-Clay Nanocomposites by an In Situ Graft Method. Journal of Applied Polymer Science. 2006, 102(5): 4921-4927.

506 M. Kato, H. Okamoto, N. Hasegawa, A. Tsukigase and A. Usuki. Preparation and properties of polyethylene-clay hybrids. Polymer Engineering and Science. 2003, 43(6):1312-1316.

507 W.K. Czaja, D.J. Young, M. Kawecki and R.M. Brown. The future prospects of microbial cellulose in biomedical applications. Biomacromolecules. 2007, 8(1):1-12.

508 Z. Cai and J. Kim. Bacterial cellulose/poly(ethylene glycol) composite: characterization and first evaluation of biocompatibility. Cellulose. 2010, 17(1):83-91.

509 T. Kondo. Hydrogen bonds in regioselectively substituted cellulose derivatives. Journal of Polymer Science Part B: Polymer Physics. 1994, 32(7): 1229-1236.

510 A. Viksne, A.K. Bledzki, L. Rence, and R. Berzina. Water Uptake and Mechanical Characteristics of Wood Fiber-Polypropylene Composites. Mechanics of Composite Materials. 2006, 42(1): 73-82.

511 R. Mat Taib, S. Ramarad, Z.A. Mohd Ishak and H.D. Rozman. Effect of Immersion Time in Water on the Tensile Properties of Acetylated Steam-exploded Acacia mangium Fibers-Filled Polyethylene Composites. Journal of Thermoplastic Composite Materials. 2009, 22(1); 83-98.

512 W.G. Glasser, R. Taib, R.K. Jain and R. Kander. Fiber-Reinforced Cellulosic Thermoplastic Composites. Journal Applied Polymer Science. 1999, 73(7): 1329-1340.

513 M.N. Anglès, J. Salvadó and A. Dufresne. Steam-exploded residual softwood-filled polypropylene composites. Journal of Applied Polymer Science. 1999, 74(8):1962-1977.

514 T.D. Fornesa, P.J. Yoona, D.L. Hunterb, H. Keskkulaa and D.R. Paul. Effect of organoclay structure on nylon 6 nanocomposite morphology and properties. Polymer. 2002, 43(22):5915-5933.

515 S.C. Tjong. Structural and mechanical properties of polymer nanocomposites. Materials Science and Engineering: Reports. 2006, 53(3-4):73-197.

516 D.J. Frankowski, M.D. Capracotta, J.D. Martin, S.A. Khan and R.J. Spontak. Stability of Organically Modified Montmorillonites and Their Polystyrene Nanocomposites After Prolonged Thermal Treatment. Chemistry of Materials. 2007, 19(11):2757-2767.

517 C-H. Wang, Y-T. Shieh and S. Nutt. The Effects of Soft-Segment Molecular Weight and Organic Modifier on Properties of Organic-Modified MMT-PU Nanocomposites. Journal of applied polymer science. 2009, 11(2) :1025-1032.

518 Z. Wu, C. Zhou and R. Qi. The Preparation of Phenolic Resin/Monmorillonite Nanocomposites by Suspension Condensation Polymerization and Their Morphology. Polymer Composites. 2002, 23(3):634-646.

519 S-J. Park, K. Li and S-K. Hong. Preparation and Characterization of Layered Silicate-modified Ultrahigh-Molecular-Weight Polyethylene Nanocomposites. Journal of Industrial and Engineering Chemistry. 2005, 11(4):561-566.

520 S. Kumar, J.P. Jog and U. Natarajan. Preparation and Characterization of Poly(methyl methacrylate)-Clay Nanocomposites via Melt Intercalation: The Effect of Organoclay on the Structure and Thermal Properties. Journal of Applied Polymer Science. 2003, 89(5): 1186-1194.

521 I-K. Yang and P-H. Tsai. Preparation and Characterization of Polyether-Block-Amide Copolymer/Clay Nanocomposites. Polymer Engineering and Science. 2007, 47(3):235-243.

522 T. Liu, K.P. Lim, W.C. Tjiu, K.P. Pramoda and Z-K. Chen. Preparation and characterization of nylon 11/organoclay nanocomposites. Polymer. 2003, 44(12): 3529-3535.

523 G. Zhang and D. Yan. Crystallization kinetics and melting behavior of nylon 10,10 in nylon 10,10-montmorillonite nanocomposites. Journal of Applied Polymer Science. 2003, 88(9):2181-2188.

524 S.C. Tjong and S.P. Bao. Crystallization regime characteristics of exfoliated polyethylene/vermiculite nanocomposites. Journal of Polymer Science Part B: Polymer Physics. 2005, 43(3):253-344.

525 S. Hotta and D.R. Paul. Nanocomposites formed from linear low density polyethylene and organoclays. Polymer. 2004, 45(22):7639-7654.

526 K.H. Wang, M.H. Choi, C.M. Koo, Y.S. Choi and I.J. Chung. Synthesis and characterization of maleated polyethylene/clay nanocomposites. Polymer. 2001, 42(24): 9819–9826.

527 J-H. Lee, D. Jung, C-E. Hong, K.Y. Rhee and S.G. Advani. Properties of polyethylene-layered silicate nanocomposites prepared by melt intercalation with a PP-g-MA compatibilizer. Composites Science and Technology. 2005, 65(13):1996-2002.

528 S. Das, A. K. Saha, P. K. Choudhury, R.K. Basak, B.C. Mitra, T. Todd, S. Lang and R.M. Rowell. Effect of steam pretreatment of jute fiber on dimensional stability of jute composite. Journal of Applied Polymer Science. 2000, 76(11): 1652-1661.

529 A. Nourbakhsh and A. Ashori. Influence of Nanoclay and Coupling Agent on the Physical and Mechanical Properties of Polypropylene/Bagasse Nanocomposite. Journal of Applied Polymer Science. 2009, 112(3):1386-1390.

530 H. Ardhyananta, H. Ismail and T. Takeichi. Effects of Organoclay Loading and Ethylene Glycol on Mechanical, Morphology and Thermal Properties of Ethylene Vinyl Acetate/Organoclay Nanocomposites. Journal of Reinforced Plastics and Composites. 2007, 26(8):789-806.

531 S-K. Yeh and R.K. Gupta. Improved wood–plastic composites through better processing. Composites: Part A. 2008, 39(11): 1694–1699.

532 N. Stark. Influence of Moisture Absorption on Mechanical Properties of Wood Flour-Polypropylene Composites. Journal of Thermoplastic Composite Materials. 2001, 14(5): 421-432.

533 N. Islam, M. Haque and M. Huque. Mechanical and Morphological Properties of Chemically Treated Coir-Filled Polypropylene Composites. Industrial &Engineering Chemistry Research. 2009, 48(23):10491-10497.

534 M. Tajvidi, S.K. Najafi and N. Moteei. Long-Term Water Uptake Behavior of Natural Fiber/Polypropylene Composites. Journal of Applied Polymer Science. 2006, 99(5):2199-2203.

535 A.G. Supri, H. Salmah and K. Hazwan. Low Density Polyethylene-Nanoclay Composites: The Effect of Poly(acrylic acid) on Mechanical Properties, XRD, Morphology Properties and Water Absorption. Malaysian Polymer Journal. 2008, 3(2):39-53.

536 N.M. Stark and L.M. Matuana. Surface chemistry changes of weathered HDPE/wood-flour composites studied by XPS and FTIR spectroscopy. Polymer Degradation and Stability. 2004, 86(1):1-9.

537 H. Bouafif, A. Koubaa, P. Perré, A. Cloutier and B. Riedl. Analysis of Among-Species Variability in Wood Fiber Surface Using Drifts and XPS: Effects on Esterification Efficiency. Journal of Wood Chemistry and Technology. 2008, 28(4):296-315.

538 M. Sain and P. Eng. Spectroscopic Characterization of Engineered Lignocellulosic Fibers with Mono-Substituted Polysiloxane Films. Applied Spectroscopy Reviews. 2001, 36(1): 119-137.

539 J.S. Fabiyi, A.G. McDonald, M.P. Wolcott and P.R. Griffiths. Wood plastic composites weathering: Visual appearance and chemical changes. Polymer Degradation and Stability. 2008, 93(8):1405-1414.

540 N.M. Stark and L.M. Matuana. Characterization of weathered wood–plastic composite surfaces using FTIR spectroscopy, contact angle, and XPS. Polymer Degradation and Stability. 2007, 92(10) :1883-1890.

541 H. Kishi, M. Yoshioka, A. Yamanoi, N. Shiraishi. Composites of Wood and Polypropylenes I. 1988, 34(2):133-139.

542 M. Kazayawoko, J. J. Balatinecz, R. T. Woodhams and S. Law. Effect of Ester Linkages on the Mechanical Properties of Wood Fiber-Polypropylene Composites. Journal of Reinforced Plastics and Composites. 1997 16(15): 1383-1406.

543 L.M. Matuana, J.J. Balatinecz, R.N.S. Sodhi and C.B. Park. Surface characterization of esterified cellulosic fibers by XPS and FTIR Spectroscopy. Wood Science and Technology. 2001, 35(3): 191-282.

544 K. Carlborn and L.M. Matuana. Functionalization of Wood Particles through a Reactive Extrusion Process. Journal of Applied Polymer Science. 2006, 101(5): 3131-3142.

545 G.W. Beckermann and K.L. Pickering. Engineering and evaluation of hemp fibre reinforced polypropylene composites: Fibre treatment and matrix modification. Composites Part A: Applied Science and Manufacturing. 2008, 39(6):979-988.

546 W. Qiu, F. Zhang, T. Endo and T. Hirotsu. Effect of Maleated Polypropylene on the Performance of Polypropylene/Cellulose Composite. Polymer Composites. 2005, 26(4): 448-453.

547 S.C. Tjong and Y. Meng. The Effect of Compatibilization of Maleated Polypropylene on a Blend of Polyamide-6 and Liquid Crystalline Copolyester. Polymer International. 1997, 42(2):209-217.

548 K. Carlborn and L.M. Matuana. Composite materials manufactured from wood particles modified through a reactive extrusion process. Polymer Composites. 2005 26(4) : 534-541.

549 G.M. Dorris and D.G. Gray. The surface analysis of paper and wood fibres by ESCA (I). Application to cellulose and lignin, Cellulose Chemistry and Technology. 1978, 12(1):9-23.

550 G.M. Dorris and D.G. Gray, The surface analysis of paper and wood fibers by ESCA (II). Surface composition of mechanical pulps, Cellulose Chemistry and Technology. 1978, 12(6):721–734.

551 L-S. Johansson, J. Campbell, K. Koljonen, M. Kleen and J. Buchert. On surface distributions in natural cellulosic fibres. Surface and interface analysis. 2004, 36(8):706-710.

552 E.J. Kontturi. Surface Chemistry of Cellulose: from natural fibres to model surfaces. Doctoral dissertation. Eindhoven University of Technology. 2005.

553 C.M.G. Carlsson and G. Ström. Adhesion between plasma-treated cellulosic materials and polyethylene. Surface and Interface Analysis. 1991, 17(7):511–515.

554 K. Koljonen, M. Österberg, L.-S. Johansson and P. Stenius. Surface chemistry and morphology of different mechanical pulps determined by ESCA and AFM. Colloids and Surfaces A: Physicochemical and Engineering Aspects. 2003, 228(1-3):143-158.

555 M. Kazayawoko, J.J. Balatinecz and R.T. Woodhams. Diffuse reflectance Fourier transform infrared spectra of wood fibers treated with maleated polypropylenes. Journal of Applied Polymer Science. 1997, 66(6):1163-1173.

556 M. Jaić, R. Živanović, T. Stevanović-Janežsć and A. Dekanski. Comparison of surface properties of beech- and oakwood as determined by ESCA method. European Journal of Wood and Wood Products. 1996, 54(1): 37-41.

557 D. P. Kamdem, B. Riedl, A. Adnot and S. Kaliaguine. ESCA spectroscopy of poly(methyl methacrylate) grafted onto wood fibers. Journal of Applied Polymer Science. 1991, 43(10):1901–1912.

558 X. Hua, S. Kaliaguine, B.V. Kokta and A. Adnot. Surface analysis of explosion pulps by ESCA Part 1. Carbon (1s) spectra and oxygen-to-carbon ratios. Wood Science and Technology. 1993, 27(6) : 449-459.

559 J. Buchert, G. Carlsson, L. Viikari and G. Ström. Surface characterization of unbleached kraft pulps by enzymatic peeling and ESCA. Holzforschung. 1996, 50(1), 69–74.

560 N. Maximova, M. Österberg, K. Koljonen and P. Stenius. Lignin adsorption on cellulose fibre surfaces: Effect on surface chemistry, surface morphology and paper strength. Cellulose. 2001, 8(2): 113–125.

561 P. Stenius and J. Laine. Studies of cellulose surfaces by titration and ESCA. Applied Surface Science. 1994, 75(1-4):213–219.

562 G. Ström and G. Carlsson. Wettability of kraft pulps-effect of surfacecomposition and oxygen plasma treatment. Journal of Adhesion Science and Technology. 1992, 6(6):745–761.

563 P.J. Mjöberg. Chemical surface analysis of wood fibres by means of ESCA. Cellulose Chemistry and Technology. 1981, 15(5): 481-486.

564 Q. Zhou, M.J. Baumann, H. Brumer and T.T. Teeri. The influence of surface chemical composition on the adsorption of xyloglucan to chemical and mechanical pulps. Carbohydrate Polymers. 2006, 63 (4) 449–458.

565 A. Awal, S. B. Ghosh and M. Sain. Development and morphological characterization of wood pulp reinforced biocomposite fibers. Journal of Materials Science. 2009, 44(11): 2876-2881.

566 P.F. Vena. Master's Dissertation. Thermomechanical Pulping (TMP), Chemithermomechanical Pulping (CTMP) and Biothermomechanical Pulping

(BTMP) of Bugweed (*Solanum Mauritianum*) and Pinus Patula. Stellenbosch University December 2005.

567 F-W. Shen, Y-J. Yu and H. McKellop. Potential errors in FTIR measurement of oxidation in ultrahigh molecular weight polyethylene implants. Journal of Biomedical Materials Research Part B: Applied Biomaterials. 1999, 48(3):203-210.

568 S. M. Kurtz, O. K. Muratoglu, R. Gsell, K. Greer, F.W. Shen, C. Cooper, F.J. Buchanan, S. Spiegelberg, S. S. Yau and A. A. Edidin. Interlaboratory validation of oxidation-index measurement methods for UHMWPE after long-term shelf aging. Journal of Biomedical Materials Research Part B: Applied Biomaterials. 2002, 63(1) :15-23.

569 A. Solti, D.O. Hummel and P. Simak. Computer-supported infrared spectrometry of polyethylene, ethene copolymers, and amorphous poly(alkyl ethylene)s. Die Makromolekulare Chemie. Macromolecular symposia. 1986, 5(5):105–133.

570 M.N. Khalaf, A.H. Al-Mowali and G.A. Adam. Rheological Studies of Modified Maleated Polyethylene/Medium Density Polyethylene Blends. Malaysian Polymer Journal. 2008, 3(2):54-64.

571 O. Faix and J. H. Böttcher. The influence of particle size and concentration in transmission and diffuse reflectance spectroscopy of wood. European Journal of Wood and Wood Products. 1992, 50(6):221-226.

572 M.A. Tshabalala. Handbook of Wood Chemistry and Wood Composites-Chapter 8: Surface Characterization. Roger M. Rowell (Editor). CRC Press. 2005: 187-211.

573 E. Kontturi, P.C. Thüne and J.W. Niemantsverdriet. Cellulose Model Surfaces-Simplified Preparation by Spin Coating and Characterization by X-ray Photoelectron Spectroscopy, Infrared Spectroscopy, and Atomic Force Microscopy. Langmuir. 2003, 19 (14):5735–5741.

574 K.K. Pandey. A study of chemical structure of soft and hardwood and wood polymers by FTIR spectroscopy. Journal of Applied Polymer Science. 1999, 71(12):1969–1975.

575 R. Chen and K. A. Jakes. Effect of pressing on the infrared spectra of single cotton fibers. Applied Spectroscopy. 2002, 56(5), 646–650.

576 T. Semba, K. Kitagawa, S. Endo, K. Maeda and H. Hamada. In situ fiber-reinforced composites from blends containing polypropylene and polycaprolactone. Journal of Applied Polymer Science. 2004, 91(2):833-840.

577 N. Kawamoto, H. Mori, K. Nitta, N. Yui and M. Terano. Characterization of the differences in the crystallinity from surface to bulk of compression-molded polypropene sheets using attenuated total reflection fourier-transform IR

spectroscopy. Macromolecular Chemistry and Physics. 1996, 197(11):3523-3530.

578 X. Zhu, D. Yan and Y. Fang. In Situ FTIR Spectroscopic Study of the Conformational Change of Isotactic Polypropylene during the Crystallization Process. The Journal of Physical Chemistry. B.2001, 105(50):12461-12463.

579 S.A. Jabarin and E.A. Lofgren. Photooxidative effects on properties and structure of high-density polyethylene. Journal of Applied Polymer Science. 1994, 53(4):411-423.

580 P. Pagès, F. Carrasco, J. Saurina and X. Colom. FTIR and DSC study of HDPE structural changes and mechanical properties variation when exposed to weathering aging during Canadian winter. Journal of Applied Polymer Science. 1996, 60(2):153-159.

581 A. Naumann, M. Navarro-González, S. Peddireddi, U. Kües and A. Polle. Fourier transform infrared microscopy and imaging: Detection of fungi in wood. Fungal Genetics and Biology. 2005, 42(10):829-835.

582 G. Zerbi, G. Gallino, N. Del Fanti and L.Baini. Structural depth profiling in polyethylene films by multiple internal reflection infrared spectroscopy. Polymers. 1989, 30(12):2324–2327.

583 B.M. Dorscht and C. Tzoganakis. Reactive extrusion of polypropylene with supercritical carbon dioxide: Free radical grafting of maleic anhydride. Journal of Applied Polymer Science. 2003, 87(7):1116–1122.

584 M.I. Arnguren, N.E. Marcovich and M.M. Reboredo. Sawdust and Woodflour: Its esterification and Use in the Formulation of Polymer Composites. Proceeding of an International Foundation for Science Workshop on Recent Advances in Biotechnology for Tree Conservation and Management. Florianopolis, Brazil, 15-19 September 1998:180-197.

585 L.J. Bellamy. The Infrared Spectra of Complex Molecules. Wiley: New York. 1958.

586 S.H. Nahm. Direct Evidence for Covalent Bonding Between Ketene Dimer Sizing Agents and Cellulose. Journal of Wood Chemistry and Technology. 1986, 6(1):89-112.

587 M.A. Khan, K.M.I. Ali and S.C. Basu. IR studies of wood plastic composites. Journal of Applied Polymer Science. 1993, 49(9) :1547-1551.

588 S.K. Dirlikov and J.L. Koenig. Assignment of the Carbon-Hydrogen Stretching and Bending Vibrations of Poly(Methyl Methacrylate) by Selective Deuteration. Applied Spectroscopy. 1979, 33(6): 555-561.

589 G. Beamson and D. Briggs. High resolution XPS of organic polymers: the Scienta ESCA300 database. Wiley New York: Wiley, 1992: 110, 188, 208.

590 S. Chen and H. Tanaka. Surface analysis of paper containing polymer additives by X-ray photoelectron spectroscopy I: Application to paper containing dry strength additives. Journal of Wood Science. 1998, 44(4):303-309.

591 O.A. Baschenko and V.I. Nefedov. Relative intensities in x-ray photoelectron spectra. Part VII. The effect of elastic scattering in a solid on the angular distribution of photoelectrons escaping from samples covered with thin films of various thicknesses. Journal of Electron Spectroscopy and Related Phenomena. 1980, 22: 153-169.

592 M. Htun and L. Salmen. Die Bedeutung der physikalischen und chemischen Holzeigenschaften für einen effizienten Energieeinsatz bei der (Refiner-) Holzstofferzeugung. Wochenblatt für Papierfabrikation. 1996, 124(6):232-235.

593 C.J. Powell, A. Jablonski, I.S. Tilinin, S. Tanuma and D.R. Penn. Surface sensitivity of Auger-electron spectroscopy and X-ray photoelectron spectroscopy. Journal of Electron Spectroscopy and Related Phenomena. 1999, 98-99:1-15.

594 M. Nuopponen, T. Vuorinen, S. Jämsä and P. Viitaniemi. The effects of a heat treatment on the behaviour of extractives in softwood studied by FTIR spectroscopic methods. Wood Science and Technology. 2003, 37(2):109-115.

595 D. Montplaisir, C. Daneault and B. Chabot. Surface Composition of Grafted Thermomechanical Pulp Through XPS Measurement. Bioresources. 2008, 3(4):1118-1129.

596 J.N. Andersen, A. Beutler, S. L. Sorensen, R. Nyholm, B. Setlik and D. Heskett. Vibrational fine structure in the C1s core level photoemission of chemisorbed molecules: ethylene and ethylidyne on Rh(111). Chemical Physics Letters. 1997, 269(3-4) :371-377.

597 D.T. Clark, M.M. Abu-Shbak. Surface aspects of the heat treatment of polyethylene terephthalate as revealed by ESCA. Polymer Degradation and Stability. 1984, 9(4) : 225-237.

598 T. Röder and H. Sixta. Thermal treatment of cellulose pulps and its influence to cellulose reactivity. Lenzinger Berichte, 2004, 83:79-83

599 K-N. Law, X. Song and C. Daneault. X-ray photoelectron spectroscopy (XPS) study on chemical pulps. (ACS PacificChem 2005, Honolulu, Hawaii, December 15-20, USA.

600 J. Laine and P. Stenius. Surface characterization of unbleached kraft pulps by means of ESCA. Cellulose. 1994, 1(2): 145-160.

601 P. Widsten, J.E. Laine, P. Qvintus-Leino and S. Tuominen. Effect of High-Temperature Defibration on the Chemical Structure of Hardwood. Holzforschung. 2002, 56 (1) 51–59.

602 M. Öestenson, P. Gatenholm and G.Toriz. Effects of Extractives on the Surface Chemistry and Wettability of High Temperature Chemithermomechanical Pulps. Nordic Pulp and Paper Research Journal. 2004, 19(1):53-58.

603 A. de Ruvo and M. Htun. Fundamental and practical aspects of paper-making with recycled fibers. The Role of Fundamental Research in Papermaking. Transactions of the 1981 Fundamental Research Symposium, Cambridge, Editor J. Brander. 1981:195-225.

604 B. Dale, S.P.S. Chundawat and B. Venkatesh. Enzyme Synergies in the Hydrolysis of Afex Pretreated Biomass. The AIChE Annual Meeting 2005. Cincinnati, OH, USA. 30 October-4 November 2005.

605 P. Gérardin, M. Petrič, M. Petrissans, J. Lambert and J.J. Ehrhrardt. Evolution of wood surface free energy after heat treatment. Polymer Degradation and Stability. 2007, 92(4):653-657.

606 D.N.-S. Hon. ESCA study of oxidized wood surfaces. Journal of Applied Polymer Science. 1984, 29(9):2777-2784.

607 S.A. Eastman, A.J. Lesser and T.J. McCarthy. Supercritical CO2-assisted, silicone-modified wood for enhanced fire resistance. Journal of Materials Science. 2009, 44(5):1275-1282.

608 A.J. Stamm. Thermal Degradation of Wood and Cellulose. Industrial and Engineering Chemistry. 1956, 48(3):413-417.

609 K. Li and D.W. Reeve. Sample Contamination in Analysis of Wood Pulp Fibers with X-ray Photoelectron Spectroscopy . Journal of Wood Chemistry and Technology. 2005, 24(3):183-200.

610 R.M. Nussbaum and M. Sterley. The Effect of Wood Extractive Content on Glue Adhesion and Surface Wettability of Wood. Wood and Fiber Science. 2002, 34(1) :57-71.

611 A. Ashori and A. Nourbakhsh. Reinforced polypropylene composites: Effects of chemical compositions and particle size. Bioresource Technology. 2010, 101(7):2515-2519.

612 D. Fernando, J. Hafrén, J. Gustafsson and G. Daniel. Micromorphology and topochemistry of extractives in Scots pine and Norway spruce thermomechanical pulps: a cytochemical approach. Journal of Wood Science. 2008, 54(2) :134-142.

613 A.H. Hultén, J. Basta, P. Larsson and M. Ernstsson. Comparison of different XPS methods for fiber surface analysis. Holzforschung. 2006, 60(1):14-19.

614 A. Sanadi, D. Caulfield and R. Rowell. Lignocellulosic/Plastic Composites. Technology summaries. August 1998:8-12.

615 S.H. Renneckar. Doctoral dissertation. Modification of Wood Fiber with Thermoplastics by Reactive Steam-Explosion Processing. Virginia Polytechnic Institute & State University, Blacksburg, VA, USA. June 2004.

616 T.P. Schultz and D.D. Nicholas. Lignin: Historical, Biological, and Materials Perspectives (V.742). Chapter 8: Lignin Influence on Angiosperm Sapwood Susceptibility to White-Rot Fungal Colonization: A Hypothesis. ACS Symposium Series. Editor: Wolfgang G. Glasser, Robert A. Northey and Tor P. Schultz. American Chemistry Society Publication. November 1999:205–213.

617 G.I. Mantanis and R.A. Young. Wetting of wood. Wood Science and Technology. 1997, 31(5): 339-353.

618 J-W. Kim, D.P. Harper and A.M. Taylor. Effect of Extractives on Water Sorption and Durability of Wood-Plastic Composites. Wood and Fiber Science. 2009, 41(3) :279-290.

619 S.K. Najafi, A. Kiaefar and M. Tajvidi. Effect of bark flour content on the hygroscopic characteristics of wood-polypropylene composites. Journal of Applied Polymer Science. 2008, 110(5) :3116-3120.

620 Å. Henriksson and P. Gatenhalm. Surface properties of CTMP fibers modified with xylans. Cellulose. 2002, 9(1) :55-64.

621 C.M.G. Carlsson, G. Stroem, I. Eriksson, and E. Lindstroem. Improved wettability of chemithermomechanical pulp by oxygen plasma treatment. Nordic Pulp and Paper Research Journal. 1994, 9(2): 72–75, 83.

622 J.C. Berg. The use of single fiber wetting measurements in the assessment of absorbency. In: A.F. Turbak and T.L.Vigo (editors), Nonwovens, An Advanced Tutorial. TAPPI Press, Atlanta, GA. USA. 1989:219–239.

623 R. Paynter. Case study-plasma oxidation of polystyrene. INRS-EMT, University Of Quebec. Course CHM634.

624 R.M. Petoral. XPS manual: Photoelectron Spectroscopy applied to molecular surface science. Linköping University. November 2005. Page 18.

625 S.C. Yoon and B.D. Ratner. Surface Structure of Segmental Poly(ether urethanes) and Poly(ether urethane ureas) with Various Perfluoro Chain Extenders. An X-ray Photoelectron Spectroscopic Investigation. Macromolecules. 1986, 19(4): 1068-1079.

626 C.M. Whelan, F. Cecchet, R. Baxter, F. Zerbetto, G.J. Clarkson, D.A. Leigh and P. Rudolf. Adsorption of a Benzylic Amide Macrocycle on a Solid Substrate: XPS and HREELS Characterization of Thin Films Grown on Au(111). Journal of Physical Chemistry B. 2002, 106 (34): 8739–8746.

627 L.F. de Castro. Doctoral Dissertation. Surface modification of polymers by plasma polymerization techniques for tissue engineering. Ramon Llull University. Barcelona, Catalonia, Spain. June 2008.

628 O.J. Rojas. Boundary Lubrication and Molecular Assembly in Fiber Processing. National Textile Center Annual Report on project C05-NS09: November 2008.

629 T. Dizhbite, G. Telysheva, V. Jurkjane and U. Viesturs. Characterization of the radical scavenging activity of lignins-natural antioxidants. Bioresource Technology. 2004, 95(3):309-317.

630 L. Börås and P. Gatenholm. Surface Composition and Morphology of CTMP Fibers. Holzforschung. 1999, 53(2):188–194.

631 G. Carlsson. Licentiate Dissertation. Plasma treatment of pulp and paper: ESCA characterization, water wettability, and adhesion to polyethylene. Royal Institute of Technology, Stockholm, Sweden. 1991.

632 S.M. Hacker. Not all maleated polyolefins are created equal. In: Proceedings of the Society of Plastics Engineers Annual Technical Conference. Vol. 1. Paper #0172. Dallas, Texas, USA. May 6-10, 2001:2673-2676.

633 R.M. Brown. Biogenesis of Natural Polymer Systems with Special Reference to Cellulose Assembly and Deposition. The Third Philips Morris Science Symposium. 1978: 52-123.

634 K. Watanabe, H. Takemura, M. Tabuchi, N. Tahara, H. Toyosaki, Y. Morinaga, T. Tsuchida, H. Yano and F. Yoshinaga. Cellulose-producing bacteria. US Patent 6818434. issued on November 6, 2004.

635 J.I. Morán, V.A. Alvarez, V.P. Cyras and A. Vázquez. Extraction of cellulose and preparation of nanocellulose from sisal fibers. Cellulose. 2008, 15(1):149-159.

636 C-F. Chau, P. Yang, C-M. Yu and G-C. Yen. Investigation on the Lipid- and Cholesterol-Lowering Abilities of Biocellulose. Journal of Agricultural and Food Chemistry. 2008, 56(6):2291-2295.

637 A.S. Kumar, K. Mody and B. Jha. Bacterial exopolysaccharides - a perception. Journal of Basic Microbiology. 2007, 47(2) :103-117.

638 U. Udhardt, S. Hesse and D. Klemm. Analytical Investigations of Bacterial Cellulose. Macromolecular Symposia. 2005, 223(1) :201 – 212.

639 D. Klemm, D. Schumann, F. Kramer, N. Heßler, D. Koth and B. Sultanova . Nanocellulose Materials-Different Cellulose, Different Functionality. Macromolecular Symposia. 2009, 280(1) :60 – 71.

640 M. Ankerfors and T. Lindström. Method for providing a nanocellulose involving modifying cellulose fibers. International patent. Published no. WO/2009/126106. Published on 15 October 2009.

641 M. Ankerfors and T. Lindström. On the Manufacture and Use of Nanocellulose. 9th International Conference on Wood & Biofiber Plastic Composites. Madison, Wisconsin, USA. May 21-23, 2007.

642 Y. Yamasa, K. Hoshino and T. Ishikawa. The Phylogeny of Acetic Acid Bacteria Based on the Partial Sequences of 16S Ribosomal RNA : The Elevation of the Subgenus Gluconoacetobacter to the Generic Level. Bioscience, Biotechnology, and Biochemistry. 1997, 61(8) :1244-1251.

643 Y. Yamada. Transfer of Acetobacter oboediens Sokollek et al. 1998 and Acetobacter intermedius Boesch et al. 1998 to the genus Gluconacetobacter as Gluconacetobacter oboediens comb. nov. and Gluconacetobacter intermedius comb. nov. International Journal of Systematic and Evolutionary Microbiology. 2000, 50(6):2225-2227.

644 Y. Chao, Y. Sugano, T. Kouda, F. Yoshinaga and M. Shoda. Production of bacterial cellulose by Acetobacter xylinumwith an air-lift reactor. Biotechnology Techniques. 1997, 11(11) : 829-832.

645 B. Surma-Ślusarska, S. Presler and D. Danielewicz. Characteristics of Bacterial Cellulose Obtained from Acetobacter Xylinum Culture for Application in Papermaking. Fiber & Textiles in Eastern Europe. 2008, 16(4):108-111.

646 A.H. Basta and H. El-Saied. Performance of improved bacterial cellulose application in the production of functional paper. Journal of Applied Microbiology. 2009, 107(6) : 2098-2107.

647 A. Okiyama, M. Motoki and S. Yamanaka. Bacterial cellulose. IV: Application to processed foods. Food hydrocolloids. 1993, 6(6) : 503-511.

648 S-C. Wu and Y-K. Lia. Application of bacterial cellulose pellets in enzyme immobilization. Journal of Molecular Catalysis B: Enzymatic. 2008, 54(3-4) :103-108.

649 Rainer Jonas and Luiz F. Farah. Production and application of microbial cellulose. Polymer Degradation and Stability. 1998, 59(1-3) :101-106

650 W.K. Wan, J.L. Hutter, L. Milton and G. Guhados. Bacterial Cellulose and Its Nanocomposites for Biomedical Applications. Cellulose Nanocomposites: Chapter 15. American Chemical Society Symposium Series Vol. 938. July 13 2006:221-241.

651 J. Kim, Z. Cai and Y. Chen. Biocompatible Bacterial Cellulose Composites for Biomedical Application. Journal of Nanotechnology in Engineering and Medicine. 2010, 1(1): 011006 (7 pages) doi:10.1115/1.4000062

652 D. Klemm, D. Schumann, F. Kramer, N. Heßler, Michael Hornung, Hans-Peter Schmauder and Silvia Marsch. Nanocelluloses as Innovative Polymers in Research and Application. Advances in Polymer Science. 2006, 205: 49-96.

653 M. Schramm and S. Hestrin. Factors affecting production of cellulose at the air/liquid interface of a culture of Acetobacter xylinum. Journal of general microbiology. 1954, 11(1): 123-129.

654 M. Hornung, M. Ludwig, A.M. Gerrard and H.P. Schmauder. Optimizing the Production of Bacterial Cellulose in Surface Culture: Evaluation of Substrate Mass Transfer Influences on the Bioreaction (Part 1). Engineering in Life Sciences. 2006, 6(6), 537-545.

655 M. Hornung, M. Ludwig, A.M. Gerrard and H.P. Schmauder. Optimizing the Production of Bacterial Cellulose in Surface Culture: Evaluation of Product Movement Influences on the Bioreaction (Part 2). Engineering in Life Sciences. 2006, 6(6), 546-551.

656 M. Hornung, M. Ludwig and H.P. Schmauder. Optimizing the Production of Bacterial Cellulose in Surface Culture: A novel Aerosol Bioractor Working on a Fed Batch Principle (Part 3). Engineering in Life Sciences. 2007, 7(1), 35-41.

657 W. Gindl and J. Keckes. Tensile properties of cellulose acetate butyrate composites reinforced with bacterial cellulose. Composites Science and Technology. 2004, 64(15): 2407-2413.

658 J. Juntaro, M. Pommer, G. Kalinka, A. Mantalaris, M.S.P. Shaffer and A. Bismarck. Creating Hierarchical Structures in Renewable Composites by Attaching Bacterial Cellulose onto Sisal Fibers. Advanced Materials. 2008, 20(16): 3122-3126.

659 M. Pommet, J. Juntaro, J.Y.Y. Heng, A. Mantalaris, A.F. Lee, K. Wilson, G. Kalinka, M.S.P. Shaffer and A. Bismarck. Surface Modification of Natural Fibers Using Bacteria: Depositing Bacterial Cellulose onto Natural Fibers To Create Hierarchical Fiber Reinforced Nanocomposites. Biomacromolecules. 2008, 9(6):1643–1651.

660 S. Yamanada, K. Watanabe, N. Kitamura, M. Iguchi, S. Mitsuhashi, Y. Nishi and M. Uryu. The structure and mechanical properties of sheets prepared from bacterial cellulose. Journal of Materials Science. 1989, 24(9): 3141-3145.